COMPUTER METHODS FOR SOLVING DYNAMIC SEPARATION PROBLEMS

Charles D. Holland

Texas A&M University

Athanasios I. Liapis

University of Missouri

McGraw-Hill Book Company

New York St. Louis San Francisco Auckland Bogotá Hamburg
Johannesburg London Madrid Mexico Montreal New Delhi
Panama Paris São Paulo Singapore Sydney Tokyo Toronto

PREFACE

Because of the availability of high-speed computers the time is fast approaching when the engineer will be expected to be as conversant with the unsteady state solutions to process systems as was expected for the steady state solutions in the past.

In this book a combination of the principles of separation processes, process modeling, process control, and numerical methods is used to produce the dynamic behavior of separation processes. That is, this book "puts it all together." The appropriate role of each area is clearly demonstrated by the use of large realistic systems.

The order of presentation of the material was selected to correspond to the order of the anticipated difficulty of the numerical methods. Two-point methods for solving coupled differential and algebraic equations are applied in Part 1 while multipoint methods are applied in Part 2, and selected methods for solving partial differential equations are applied in Part 3. Also, the presentation of the material within each section is in the order of increasing difficulty. This order of presentation is easily followed by the student or practicing engineer who has had either no exposure or little exposure to the subject.

Techniques for developing the equations for the description of the models are presented, and the models for each process are developed in a careful way that is easily followed by one who is not familiar with the given separation process.

In general, the best possible models that are compatible with the data commonly available are presented for each of the separation processes. The reliability of the proposed models is demonstrated by the use of experimental data and field tests. For example, the dynamic behavior predicted by the model for the system of evaporators was compared with the observed behavior of the system of evaporators at the Freeport Demonstration Unit. Experimental data as well as field tests on the Zollar Gas Plant for distillation columns, absorbers,

and batch distillation columns were used for comparison purposes. Experimental results were used to make the comparisons for adsorption and freeze-drying.

The development and testing of the models presented in this book required the combined efforts of many people to whom the authors are deeply indebted. In particular, the authors appreciate the support, assistance, and encouragement given by J. H. Galloway and M. F. Clegg of Exxon; W. E. Vaughn, J. W. Thompson, J. D. Dyal, and J. P. Smith of Hunt Oil Company; D. I. Dystra and Charles Grua of the Office of Saline Water, U.S. Department of Interior; J. P. Lennox, K. S. Campbell, and D. L. Williams of Stearns–Rogers Corporation. Support of the research, upon which this book is based, by David L. Rooke, Donald A. Rikard, Holmes H. McClure, and Bob A. Weaver (all of Dow Chemical Company), and by the National Science Foundation is appreciated. Also, for the support provided by the Center for Energy and Mineral Resources and the Texas Engineering Experiment Station, the authors are most thankful. The authors acknowledge with appreciation the many contributions made by former and present graduate students, particularly those by A. A. Bassyoni, J. W. Burdett, J. T. Casey, An Feng, S. E. Gallun, A. J. Gonzalez, E. A. Klavetter, Ron McDaniel, Gerardo Mijares, P. E. Mommessin, and N. J. Tetlow.

The authors gratefully acknowledge the many helpful suggestions provided by Professors L. D. Durbin, T. W. Fogwell, and R. E. White of the Department of Chemical Engineering, Texas A&M University, and O. K. Crosser, T. W. Johnson, and J. M. Marchello of the Department of Chemical Engineering, University of Missouri-Rolla. A. I. Liapis thanks especially Professor D. W. T. Rippin of E. T. H. Zuuch, who encouraged his investigations in the field of separation processes, and stimulated his interest in the application of mathematics.

The senior author is deeply indebted to his staff assistant, Mrs. Wanda Greer, who contributed to this book through her loyal service and assistance in the performance of departmental administrative responsibilities; to his daughter, Mrs. Charlotte Jamieson, for typing this manuscript; and to his wife, Eleanore, for her understanding and many sacrifices that helped make this book a reality.

Charles D. Holland
Athanasios I. Liapis

COMPUTER METHODS FOR SOLVING DYNAMIC SEPARATION PROBLEMS

CHAPTER

ONE

INTRODUCTION— MODELING AND NUMERICAL METHODS

An in-depth treatment of both the modeling of dynamic separation processes and the numerical solution of the corresponding equations is presented in this book.

After the models which describe each of the separation processes at unsteady state operation have been formulated, the corresponding equations describing each of these models are solved by a variety of numerical methods, such as the two-point implicit method, Michelsen's semi-implicit Runge–Kutta method, Gear's method, collocation methods, finite-difference methods, and the method of characteristics. The ability to solve these equations permits the engineer to effect an integrated design of the process and of the instruments needed to control it. The two-point implicit method (or simply implicit method) is applied in Part 1; Michelsen's semi-implicit Runge–Kutta method and Gear's method in Part 2; and the collocation method, finite-difference methods, and the method of characteristics are applied in Part 3. To demonstrate the application of the numerical methods used in Parts 1 and 2, the use of these methods is demonstrated in this chapter by the solution of some relatively simple numerical examples. The methods used in Part 3 are developed in Chap. 10 and their application is also demonstrated by the solution of relatively simple numerical examples.

The techniques involved in the formulation of models of processes is best

demonstrated by the consideration of particular processes. A wide variety of processes including evaporation, distillation, absorption, adsorption, and freeze-drying are considered. Both stagewise processes such as distillation columns equipped with plates and continuous processes such as adsorption processes are treated. All of these models are based on the following fundamental principles:

1. Conservation of mass or material balances
2. Conservation of energy or energy balances
3. Transfer of mass

In order to demonstrate the techniques suggested for the formulation of the equations representing the mass and energy balances, several different types of systems at unsteady state operation are presented in Sec. 1-1. These techniques are further demonstrated in subsequent chapters by the development of the equations for particular process models.

In order to solve the equations describing the model of a given process, a variety of numerical methods may be used. Representative of these are the methods listed above. An abbreviated presentation of selected methods and their characteristics are given in Sec. 1-2.

1-1 FORMULATION OF THE EQUATIONS FOR SELECTED MATERIAL AND ENERGY-BALANCE MODELS

Material Balances

Let the particular part of the universe under consideration be called the *system* and the remainder of the universe the *surroundings*. A material balance for a system is based on the *law of conservation of mass*. For purposes of application, a convenient statement of this law follows: *Except for the conversion of mass to energy and conversely, mass can neither be created nor destroyed.* Consequently, for a system in which the conversion of mass to energy and conversely is not involved, it follows that during the time period from $t = t_n$ to $t = t_n + \Delta t$,

$$\begin{pmatrix}\text{Input of material}\\ \text{to the system}\\ \text{during the time}\\ \text{period } \Delta t\end{pmatrix} - \begin{pmatrix}\text{output of material}\\ \text{from the system}\\ \text{during the time}\\ \text{period } \Delta t\end{pmatrix} = \begin{pmatrix}\text{accumulation of}\\ \text{material within}\\ \text{the system during}\\ \text{the time period } \Delta t\end{pmatrix}$$

The accumulation term is defined as follows:

$$\begin{pmatrix}\text{Accumulation of material}\\ \text{within the system}\\ \text{during the time period } \Delta t\end{pmatrix} = \begin{pmatrix}\text{amount of material}\\ \text{in the system at}\\ \text{time } t_n + \Delta t\end{pmatrix} - \begin{pmatrix}\text{amount of}\\ \text{material in the}\\ \text{system at time } t_n\end{pmatrix}$$

In the analysis of systems at unsteady state, the statement of the material balance given above is more easily applied when restated in the following form:

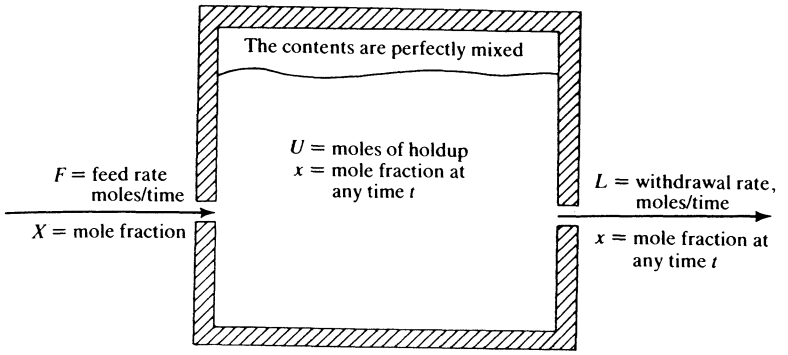

Figure 1-1 Sketch of a perfect mixer.

$$\int_{t_n}^{t_n+\Delta t}\left[\begin{pmatrix}\text{input of material}\\ \text{per unit time}\end{pmatrix} - \begin{pmatrix}\text{output of material}\\ \text{per unit time}\end{pmatrix}\right] dt = \begin{pmatrix}\text{amount of material}\\ \text{in the system}\end{pmatrix}\Bigg|_{t_n+\Delta t} - \begin{pmatrix}\text{amount of material}\\ \text{in the system}\end{pmatrix}\Bigg|_{t_n} \tag{1-1}$$

To illustrate the formulation of material balances, consider the perfect mixer shown in Fig. 1-1, and let it be required to obtain the differential equation representing the total material balance at any time t after an upset in the feed has occurred. Suppose that the upset in the feed occurs at time $t = 0$. The component-material balance over the time period from t_n to $t_n + \Delta t$ is given by

$$\int_{t_n}^{t_n+\Delta t}(FX_i - Lx_i)\,dt = (Ux_i)\Big|_{t_n+\Delta t} - (Ux_i)\Big|_{t_n} \tag{1-2}$$

where F = feed rate, mol/h (or mass/h) (note that in the absence of chemical reactions, the number of moles is conserved)
L = product rate, mol/h (or mass/h)
U = holdup, moles (or mass)
x_i = mole (or mass) fraction of component i in the mixer at any time t
X_i = mole (or mass) fraction of component i in the feed at any time t

(In the application of the two-point implicit method, Euler's method, and the trapezoidal rule, the numerical method may be applied directly to Eq. (1-2) as demonstrated in subsequent chapters.)

The differential equation corresponding to Eq. (1-2) may be obtained by use of the mean-value theorems. First, apply the *mean-value theorem of integral calculus* (App. 1A) to the left-hand side of Eq. (1-2) to obtain

$$\int_{t_n}^{t_n+\Delta t}(FX_i - Lx_i)\,dt = \left[(FX_i - Lx_i)\Big|_{t_n+\alpha\,\Delta t}\right]\Delta t \tag{1-3}$$

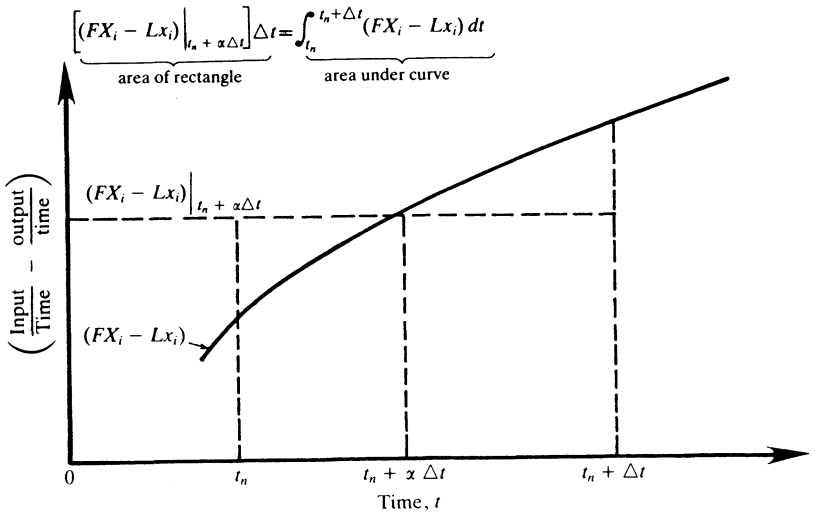

Figure 1-2 Geometrical interpretation of the mean-value theorem of integral calculus.

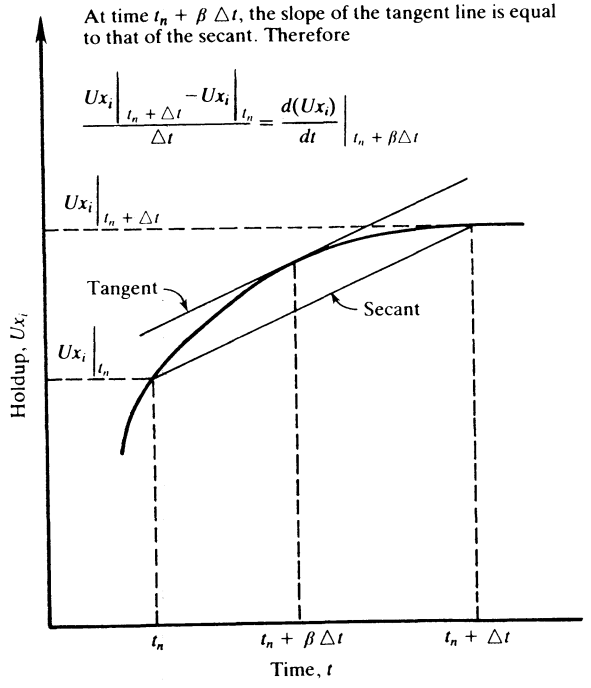

Figure 1-3 Geometrical interpretation of the mean-value theorem of differential calculus.

where $0 \le \alpha \le 1$. The geometrical representation of Eq. (1-3) is that there exists a rectangle having the height $(FX_i - Lx_i)|_{t_n+\alpha\,\Delta t}$ and the base Δt which has an area exactly equal to that under the curve of $(FX_i - Lx_i)$ versus t over the time interval from t_n to $t_n + \Delta t$; see Fig. 1-2.

Application of the *mean-value theorem of differential calculus* to the right-hand side of Eq. (1-2) yields

$$(Ux_i)\Big|_{t_n+\Delta t} - (Ux_i)\Big|_{t_n} = \Delta t\,\frac{d(Ux_i)}{dt}\Big|_{t_n+\beta\,\Delta t} \tag{1-4}$$

where $0 < \beta < 1$. The geometrical picture of Eq. (1-4) is that there exists a tangent line having a slope, $d(Ux_i)/dt|_{t_n+\beta\,\Delta t}$, which is exactly equal to that of the secant line connecting the points at t_n and $t_n + \Delta t$ on the curve of (Ux_i) versus t; see Fig. 1-3.

After the right-hand sides of Eqs. (1-3) and (1-4) have been equated and the resulting expression divided by Δt, one obtains

$$(FX_i - Lx_i)\Big|_{t_n+\alpha\,\Delta t} = \frac{d(Ux_i)}{dt}\Big|_{t_n+\beta\,\Delta t} \tag{1-5}$$

In the limit as Δt is allowed to go to zero, Eq. (1-5) reduces to

$$(FX_i - Lx_i)\Big|_{t_n} = \frac{d(Ux_i)}{dt}\Big|_{t_n} \tag{1-6}$$

Since t_n was arbitrarily selected, Eq. (1-6) holds for all $t_n > 0$, and thus the final result is

$$FX_i - Lx_i = \frac{d(Ux_i)}{dt} \qquad (t > 0) \tag{1-7}$$

Energy Balances

Energy balances are based on the first law of thermodynamics which asserts that the energy of the universe is a constant. Thus, the total amount of energy entering minus that leaving a particular part of the *universe*, called the *system*, must be equal to the accumulation of energy within the system. The following formulation of the energy balance is easily applied to systems at unsteady state operation:

$$\int_{t_n}^{t_n+\Delta t}\left[\begin{pmatrix}\text{input of energy to the}\\ \text{system per unit time}\end{pmatrix} - \begin{pmatrix}\text{output of energy from the}\\ \text{system per unit time}\end{pmatrix}\right]dt$$
$$= \begin{pmatrix}\text{amount of energy}\\ \text{within the system}\end{pmatrix}\Big|_{t_n+\Delta t} - \begin{pmatrix}\text{amount of energy}\\ \text{within the system}\end{pmatrix}\Big|_{t_n} \tag{1-8}$$

In order to account for all of the energy entering and leaving a system, the energy equivalents of the net heat absorbed by the system and the net work done by the system on the surroundings must be taken into account. *Heat* and

work represent energy in the state of transition between the system and its surroundings. A system that has work done on it experiences the conversion of mechanical energy to internal energy. In the following analysis, a basis of one pound-mass (one lb_m) is selected. Thus, the symbols KE, PE, and E denote kinetic, potential, and internal energies, respectively, in British thermal units per pound-mass of fluid. The total energy possessed by 1 lb_m of fluid is denoted by E_T, that is,

$$E_T = E + KE + PE \tag{1-9}$$

The enthalpy H of 1 lb_m of fluid is defined by

$$H = E + Pv \tag{1-10}$$

where P = pressure lb_f/ft^2, where lb_f means pounds force
v = specific volume, ft^3/lb_m

In the interest of simplicity, the mechanical equivalent of heat (778 ft lb_f/Btu) has been omitted as the divisor of the Pv product in Eq. (1-10) and other equations which follow. For convenience, let

$$H_T = E_T + Pv \tag{1-11}$$

For a flow system at *steady state* operation (a process in which the variables do not change with respect to time), Eq. (1-8) reduces to the well-known expression $\Delta H = Q$, where no work is done by the system on the surroundings, and where the kinetic and potential energy changes are negligible. For an unsteady state process, however, the expression for the energy balance is not quite so simple. Two types of systems are considered in the following development which are characteristic of the systems considered in subsequent sections.

Fluids Flowing In Pipes

In the development which follows, it is supposed that the pipe is flowing full and that perfect mixing occurs in the radial direction and that no mixing occurs in the axial direction z (see Fig. 1-4). Let z_j, z_{j+1}, t_n, and t_{n+1} be arbitrarily selected within the time and space domains of interest, that is,

$$0 < z_j < z_{j+1} < z_T \qquad t > 0$$

where $\Delta z = z_{j+1} - z_j$
$\Delta t = t_{n+1} - t_n$

The energy balance on the element of fluid contained in the volume from z_j to z_{j+1} over the time period from t_n to t_{n+1} is formulated in the following manner. The energy in the fluid which enters the element of volume at z_j per unit time is given by

$$\begin{pmatrix}\text{Input of energy per}\\ \text{unit time by flow}\end{pmatrix} = wE_T\Big|_{z_j,\,t} \tag{1-12}$$

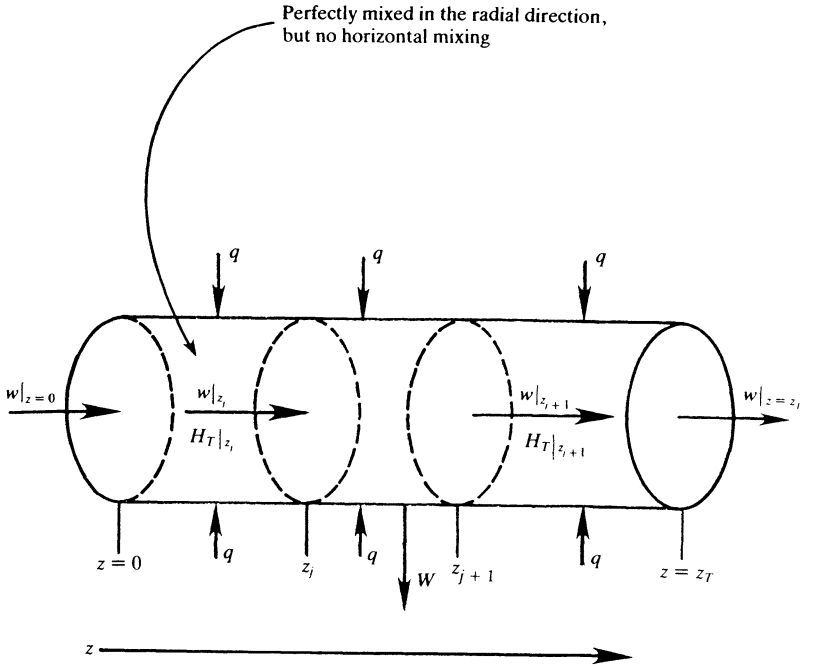

Figure 1-4 Energy balance on an element of volume from z_j to z_{j+1} for a flow system.

at any time t ($t_n \le t \le t_{n+1}$). The work required to force one pound mass of fluid into the element of volume at z_j at any time t ($t_n \le t \le t_{n+1}$) is given by

$$\begin{pmatrix}\text{Work per}\\ \text{unit mass}\end{pmatrix} = \int_0^v P\,dv\Big|_{z_j,\,t} = Pv\Big|_{z_j,\,t} \tag{1-13}$$

Observe that this work, Pv, may vary with time throughout the time period Δt. At any time t

$$\begin{pmatrix}\text{Rate at which work is done on the}\\ \text{element of volume by the entering fluid}\end{pmatrix} = (wPv)\Big|_{z_j,\,t} \tag{1-14}$$

Suppose that heat is transferred continuously from the surroundings to the system at each z along the boundary as shown in Fig. 1-4. Let this rate of heat transfer be denoted by q [Btu/(h·ft)]. Then at each z ($z_j \le z \le z_{j+1}$) and any $t > 0$

$$\begin{pmatrix}\text{Heat transferred across the boundary of}\\ \text{the element of volume per unit time}\end{pmatrix} = \int_{z_j}^{z_{j+1}} q\,dz \tag{1-15}$$

Two cases where the system does work (commonly called shaft work) on the surroundings are considered. In the first case, the work is done by the system (energy leaves the system) on the surroundings at a point z lying between z_j and z_{j+1} as shown in Fig. 1-4, and the rate at which work is done is denoted by W (ft lb_f/unit time). In the second case, work is done by the system in a continuous manner at each point z along the boundary, and the rate at which work is done at each point is denoted by $\mathscr{W}$ [ft lb_f/(ft unit time)]. In this case,

$$\begin{pmatrix}\text{Shaft work done by the element of volume}\\ \text{on the surroundings per unit time}\end{pmatrix} = \int_{z_j}^{z_{j+1}} \mathscr{W}\, dz \qquad (1\text{-}16)$$

The integral-difference equation is formulated for the first case, and the final result for the second case is readily obtained therefrom. The input terms of Eq. (1-8) are as follows:

$$\begin{pmatrix}\text{Input of energy to}\\ \text{the element of volume}\\ \text{over the time period } \Delta t\end{pmatrix} = \int_{t_n}^{t_{n+1}} \left[(wE_T)\Big|_{z_j,\,t} + (wPv)\Big|_{z_j,\,t} + \int_{z_j}^{z_{j+1}} q\, dz \right] dt \qquad (1\text{-}17)$$

The output terms are

$$\begin{pmatrix}\text{Output of energy from}\\ \text{the element of volume}\\ \text{over the time period } \Delta t\end{pmatrix} = \int_{t_n}^{t_{n+1}} \left[(wE_T)\Big|_{z_{j+1},\,t} + (wPv)\Big|_{z_{j+1},\,t} + W \right] dt \qquad (1\text{-}18)$$

The accumulation of energy within the element of volume over the time period Δt is given by

$$\begin{pmatrix}\text{Accumulation of energy within the element}\\ \text{of volume over the time period } \Delta t\end{pmatrix} = \int_{z_j}^{z_{j+1}} (\rho S E_T)\Big|_{t_{n+1},\,z}\, dz - \int_{z_j}^{z_{j+1}} (\rho S E_T)\Big|_{t_n,\,z}\, dz \qquad (1\text{-}19)$$

where ρ is the mass density (lb_m/ft^3) of the fluid and S is the cross-sectional area of the element of volume as shown in Fig. 1-4. The cross-sectional area S is generally independent of z, and it will be considered constant throughout the remainder of this development. Since $\rho = 1/v$, Eq. (1-11) may be used to give

$$\rho E_T = \rho H_T - \rho(Pv) = \rho H_T - P \qquad (1\text{-}20)$$

and this expression may be used to restate Eq. (1-19) in the following form:

$$\begin{pmatrix}\text{Accumulation of energy}\\ \text{during the time period } \Delta t\end{pmatrix} = \int_{z_j}^{z_{j+1}} \left(\rho H_T\Big|_{t_{n+1},\,z} - \rho H_T\Big|_{t_n,\,z} \right) S\, dz - \int_{z_j}^{z_{j+1}} \left(P\Big|_{t_{n+1},\,z} - P\Big|_{t_n,\,z} \right) S\, dz \qquad (1\text{-}21)$$

Through the use of Eq. (1-11) to state the inputs and outputs in terms of H_T, the final expression for the energy balance may be restated in the form

$$\int_{t_n}^{t_{n+1}} \left[(wH_T)\Big|_{z_j,\,t} - (wH_T)\Big|_{z_{j+1},\,t} + \int_{z_j}^{z_{j+1}} q\, dz - W \right] dt$$

$$= \int_{z_j}^{z_{j+1}} \left[(\rho H_T)\Big|_{t_{n+1},\,z} - (\rho H_T)\Big|_{t_n,\,z} \right] S\, dz - \int_{z_j}^{z_{j+1}} \left(P\Big|_{t_{n+1},\,z} - P\Big|_{t_n,\,z} \right) S\, dz \qquad (1\text{-}22)$$

Examination of the second integral on the right-hand side of Eq. (1-22) shows that it has the physical significance of being the difference between the amount of work required to sweep out the element of volume at times t_{n+1} and t_n. In most processes this is negligible relative to the enthalpy differences appearing on the right-hand side.

If the element of volume does shaft work continuously on the surroundings at each point z along the boundary, then W in Eq. (1-22) is replaced by the expression given by Eq. (1-16).

Development of the Partial Differential Equation Corresponding to the Energy Balance

Beginning with the following form of the energy balance for the flow of a fluid through a pipe

$$\int_{t_n}^{t_{n+1}} \left[(wH_T)\Big|_{z_j,\,t} - (wH_T)\Big|_{z_{j+1},\,t} + \int_{z_j}^{z_{j-1}} q\, dz - W \right] dt$$

$$= \int_{z_j}^{z_{j-1}} \left[(\rho E_T S)\Big|_{t_{n+1},\,z} - (\rho E_T S)\Big|_{t_n,\,z} \right] dz \qquad (1\text{-}23)$$

the corresponding partial differential equation may be obtained by the proper application of the mean-value theorems (App. 1A, Theorems 1A-1 and 1A-2) followed by the limiting process wherein Δz and Δt are allowed to go to zero. However, in order to apply the *mean-value theorem of integral calculus* to the left-hand side of Eq. (1-23), the integrand must be continuous throughout the interval $z_j < z < z_{j+1}$. If the point at which the system does work W on the surroundings is z_k, then the integrand has a point of discontinuity at z_k, since

$$\begin{aligned} W &= 0 \qquad (0 < z < z_k,\ t > 0) \\ W &= W \qquad (z = z_k,\ t > 0) \\ W &= 0 \qquad (z_k < z < z_T,\ t > 0) \end{aligned} \qquad (1\text{-}24)$$

Thus, if the mean-value theorem is to be applied in any subsequent operation, it is necessary to pick the interval $(z_j < z < z_{j+1})$ such that it does not contain z_k, that is, the interval $(z_j < z < z_{j+1})$ may be either to the left or right of z_k. (Note that if $z_k = z_j$, the differential equation will fail to exist in the limit as Δz goes to zero.) Consequently, the equation to be considered is of the same form as Eq. (1-23) except that it does not contain W, and it is to be applied over the time period from t_n to t_{n+1} and over the distance $z_{j-2} < z < z_{j-1} < z_k$ or $z_k < z_j < z < z_{j+1}$.

Consider first the left-hand side of Eq. (1-23) (with the point z_k excluded) and let it be denoted by "L.H.S." Application of the *mean-value theorem of differential calculus* (Theorem 1A-1) to the first two terms and the *mean-value theorem of integral calculus* (Theorem 1A-2) to the third term yields

$$\text{L.H.S.} = \Delta z \int_{t_n}^{t_{n+1}} \left[\left. \frac{\partial (wH_T)}{\partial z} \right|_{z_j + \alpha_1(t) \cdot \Delta z,\, t} + q \Big|_{z_j + \alpha_2(t) \cdot \Delta z,\, t} \right] dt \tag{1-25}$$

where

$$0 < \alpha_1(t) < 1 \qquad 0 \le \alpha_2(t) \le 1.$$

Since all terms appearing under the integral sign depend upon time alone, the *mean-value theorem of integral calculus* may be applied to Eq. (1-25) to give

$$\text{L.H.S.} = \Delta z\, \Delta t \left[\left. \frac{\partial (wH_T)}{\partial z} \right|_{①} + q \Big|_{②} \right] \tag{1-26}$$

where ① $= z_j + \alpha_1(t_p) \cdot \Delta z,\ t_p$

② $= z_j + \alpha_2(t_p) \cdot \Delta z,\ t_p$

$t_p = t_n + \gamma_1 \Delta t \qquad 0 \le \gamma_1 \le 1$

Consider next the right-hand side of Eq. (1-23) and let it be denoted by "R.H.S." Application of the *mean-value theorem of differential calculus* to the integrand followed by the application of the *mean-value theorem of integral calculus* to the integral yields

$$\text{R.H.S.} = \Delta z\, \Delta t \left. \frac{\partial (\rho E_T S)}{\partial t} \right|_{③} \tag{1-27}$$

where ③ $= t_n + \beta(z_p) \cdot \Delta t,\ z_p$

$z_p = z_j + \gamma_2 \Delta z$

$0 < \beta(z_p) < 1$

$0 \le \gamma_2 \le 1$

Thus

$$\left. \frac{\partial (wH_T)}{\partial z} \right|_{①} + q \Big|_{②} = \left. \frac{\partial (\rho E_T S)}{\partial t} \right|_{③} \tag{1-28}$$

In the limit as Δz and Δt are allowed to go to zero in any manner whatsoever, Eq. (1-28) reduces to

$$\frac{\partial (wH_T)}{\partial z} + q = \frac{\partial (\rho E_T S)}{\partial t} \qquad (0 < z < z_k,\ z_k < z < z_T,\ t > 0) \tag{1-29}$$

where it is understood that z_j and t_n were arbitrarily selected with the point z_k excluded. Since Eq. (1-23) applies over any interval $0 < z_j < z_{j+1} < z_T$ which may contain z_k, it is evident that the set of partial differential equations is a subset of the set of integral-difference equations.

If ρ and S are independent of time and w is independent of z, Eq. (1-29) reduces to

$$w \frac{\partial H_T}{\partial z} + q = \rho S \frac{\partial E_T}{\partial t} \tag{1-30}$$

Since

$$\frac{\partial H_T}{\partial z} = \frac{\partial H_T}{\partial P} \frac{\partial P}{\partial z} + \frac{\partial H_T}{\partial T} \frac{\partial T}{\partial z} \tag{1-31}$$

$$\frac{\partial E_T}{\partial t} = \frac{\partial E_T}{\partial v} \frac{\partial v}{\partial t} + \frac{\partial E_T}{\partial T} \frac{\partial T}{\partial t} \tag{1-32}$$

it follows that if pressure-volume (Pv) effects as well as potential and kinetic energy effects are negligible, then Eq. (1-30) reduces to

$$wC_p \frac{\partial T}{\partial z} + q = SC_v \frac{\partial T}{\partial t} \tag{1-33}$$

where

$$C_p = \left(\frac{\partial H}{\partial T} \right)_P \qquad C_v = \left(\frac{\partial E}{\partial T} \right)_v$$

Liquid Flowing Through a Perfect Mixer With An Open Boundary

For the perfect mixer shown in Fig. 1-5, the energy balance on the fluid contained in the mixer over the time period from t_n to $t_n + \Delta t$ is given by

$$\int_{t_n}^{t_{n+1}} [w_i H_{Ti} - w_o H_{To} - (w_i - w_o) P_s v_s + Q - W]\, dt = ME_{Ts} \Big|_{t_{n+1}} - ME_{Ts} \Big|_{t_n} \tag{1-34}$$

where the subscripts i and o denote the inlet and outlet values of the variables, respectively, and M denotes the mass contained in the system at any time t

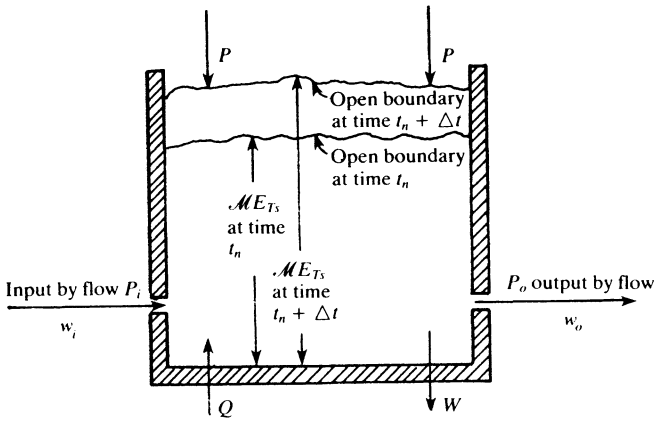

Figure 1-5 Sketch of a variable-mass, variable-energy system with an open boundary.

$(t_n < t < t_{n+1})$. Note that the rate at which the expanding boundary does work on the surroundings is equal to $(w_i - w_o)P_s v_s$. Since

$$w_i - w_o = \frac{dM}{dt} \tag{1-35}$$

$$ME_{Ts}\Big|_{t_{n+1}} - ME_{Ts}\Big|_{t_n} = \int_{t_n}^{t_{n+1}} \frac{d(ME_{Ts})}{dt}\, dt \tag{1-36}$$

and $H_{Ts} = E_{Ts} + P_s v_s$, it is possible to restate Eq. (1-34) in the following equivalent form:

$$\int_{t_n}^{t_{n+1}} (w_i H_{Ti} - w_o H_{To} + Q - W)\, dt = MH_{Ts}\Big|_{t_{n+1}} - MH_{Ts}\Big|_{t_n} - \int_{t_n}^{t_{n+1}} M \frac{d(P_s v_s)}{dt}\, dt \tag{1-37}$$

Use of the mean-value theorems followed by the limiting process whereby Δt is allowed to go to zero yields the following differential equation:

$$w_i H_{Ti} - w_o H_{To} + Q - W = \frac{d(MH_{Ts})}{dt} - M \frac{d(P_s v_s)}{dt} \tag{1-38}$$

In most processes, the second term on the right-hand side of Eq. (1-38) is negligible relative to the first term on the right-hand side.

1-2 SELECTED NUMERICAL METHODS— THEIR APPLICATION AND CHARACTERISTICS

Euler's method, the trapezoidal rule, the two-point implicit method, the fourth-order Runge–Kutta method, the semi-implicit Runge–Kutta method, and Gear's

method are used to solve a single differential equation. To explain the behavior of these methods, a stability analysis is presented. Developments of the Runge–Kutta and Gear's methods are presented in Chap. 9.

Euler's Method

Consider the differential equation

$$\frac{dy}{dt} = f(t, y) \tag{1-39}$$

for which a solution (a set of sensed pairs (t, y) which satisfy both the initial conditions $y = y_0$ when $t = t_0$ and the differential equation) is sought. The initial value of the first derivative is found by substituting t_0 and y_0 in the differential equation to give

$$y'_0 = f(t_0, y_0) \tag{1-40}$$

Let the independent variable to be changed be an incremental amount, denoted by $h (h = \Delta t)$. The step size h may be either preselected or changed during the course of the calculation. On the basis of this set of values t_0, y_0, and y'_0, it is desired to predict the value of y at time t_1 $(t_1 = t_0 + h)$. This value of y is denoted by y_1. One of the simplest methods for doing this is Euler's method which may be thought of as consisting of the first two terms of a Taylor series expansion of y, namely,

$$y_1 = y_0 + hy'_0$$

This process is continued by substitution of (t_1, y_1) in the differential equation to obtain y'_1. Then y_2 is found by use of Euler's predictor

$$y_2 = y_1 + hy'_1$$

Continuation of this process yields the numerical solution in terms of the sensed pairs (t, y). Euler's method may be represented as follows:

Predictor:

$$y_{n+1} = y_n + hy'_n \qquad T_{n+1} = \frac{h^2}{2} y_n^{(2)}(\xi) \qquad (t_n < \xi < t_{n+1}) \tag{1-41}$$

Differential equation:

$$y'_n = f(t_n, y_n) \tag{1-42}$$

The symbol T_{n+1} denotes the truncation error in the formula for the predictor. The truncation error is defined by

$$T_{n+1} = y(t_{n+1}) - y_{n+1} \tag{1-43}$$

where $y(t_{n+1})$ is the correct value of y at time t_{n+1}, and y_{n+1} is the predicted value of y at time t_{n+1}. If the predicted value of y at time t_{n+1} is computed by

use of the correct value of y at time t_n, then the value of T_{n+1} obtained by use of Eq. (1-43) is commonly referred to as the *local truncation error.*

Euler's method is classified as a predictor because the value of y_n at t_n may be used to predict the value of y_{n+1}, the value of y at time t_{n+1}; that is, a predictor is an explicit expression in y. Euler's method is demonstrated by use of the following example:

Example 1-1 For the perfect mixer shown in Fig. 1-5, obtain a numerical solution corresponding to the following conditions. At $t = 0$, $X = 0.9$, $x = 0.1$, $U = 50$ moles, and for all t, $F = L = 100$ mol/h. For $X = 0.9$ for all $t \geq 0$, find the solution by use of Euler's method at values of $h = 0.2$, 0.4, 0.5, and 0.6.

SOLUTION Since it is given that the holdup U remains constant, Eq. (1-7) reduces to

$$FX - Lx = U\frac{dx}{dt} \tag{A}$$

where the subscript i has been dropped in the interest of simplicity. After the numerical values of F, L, X, and U given in the statement of the problem have been substituted into Eq. (A), the following result is obtained

$$x' = 1.8 - 2x \tag{B}$$

where $x' = dx/dt$. In the notation for the mixer, Euler's predictor becomes

$$x_{n+1} = x_n + hx'_n \tag{C}$$

For $h = 0.2$ h and $x_0 = 0.1$, the differential equation gives

$$x'_0 = 1.8 - 2(0.1) = 1.6$$

Then by use of the predictor

$$x_1 = 0.1 + (0.2)(1.6) = 0.42$$

To compute x_2, the process is repeated. First

$$x'_1 = 1.8 - 2(0.42) = 0.96$$

Then

$$x_2 = 0.42 + (0.2)(0.96) = 0.612$$

Continuation of this process gives the points displayed in Fig. 1-6 for $h = 0.2$ h. The points shown for other values of h were obtained in the same manner as that demonstrated for $h = 0.2$ h. The numerical solutions are shown as broken lines and the analytical solution is represented by the smooth curve. The analytical solution is obtained by integration of Eq. (A) at constant U, F, L, and X to give

$$x = X - (X - x_0)e^{-Lt/U} \tag{D}$$

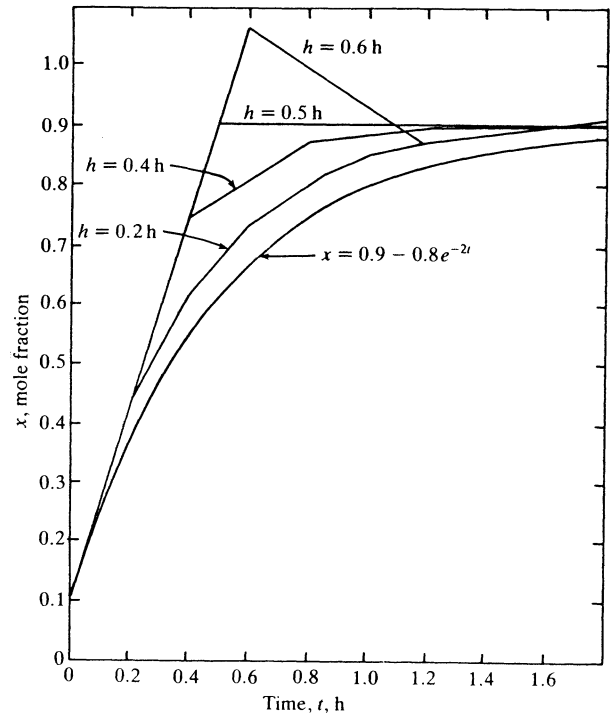

Figure 1-6 Solution of Example 1-1 by use of Euler's method.

or

$$x = 0.9 - 0.8e^{-2t}$$

and at $t = 0.2$ h, $x = 0.363\,74$.

Another predictor similar to Euler's but more accurate is called the *point-slope predictor.*

Predictor:

$$y_{n+1} = y_{n-1} + 2hy'_n \qquad T_{n+1} = \frac{h^3}{3}y_n^{(3)}(\xi) \qquad (t_{n-1} < \xi < t_{n+1}) \tag{1-44}$$

Since only one point, y_{n-1}, and the slope, y'_n, are required to predict y_{n+1}, this method is sometimes referred to as the point-slope predictor (Ref. 12).

While this method is more accurate than Euler's for any one time step, it has the disadvantage that some scheme is required to initiate the process. Although the starting y_0 is known, the value y'_1, needed in the point-slope predictor to compute y_2, is generally unknown. Since y'_1 may be computed from the

differential equation, a starting method reduces to a scheme for finding y_1. Two methods commonly used to find y_1 are (1) Euler's method (the first two terms of a Taylor's series) and (2) the first three terms of a Taylor's series. The starting procedures are demonstrated by use of Example 1-1 for the case where $h = 0.2$ h. When Euler's method is used, the value

$$x_1' = 0.96$$

is obtained as shown in the solution of Example 1-1. Next, x_2 may be computed by the point-slope predictor as follows:

$$x_2 = x_0 + 2hx_1' = 0.1 + (2)(0.2)(0.96) = 0.484$$

After the solution procedure has been initiated, the remainder of the calculational procedure is analogous to that demonstrated for Euler's method.

When the first three terms of a Taylor series are used to initiate the process, a formula for $x^{(2)}$, the second derivative (d^2x/dt^2) is needed. This formula is obtained from the differential equation. Differentiation of Eq. (B) of Example 1-1 gives

$$x^{(2)} = -2x'$$

Then

$$x_1 = x_0 + hx_0' + \frac{h^2}{2}x_0^{(2)} = (0.1) + (0.2)(1.6) + \frac{(0.2)^2}{2}(-2)(1.6)$$

$$= 0.356$$

Next the differential equation is used to obtain x_1' as follows:

$$x_1' = 1.8 - 2(0.356) = 1.088$$

Application of the point-slope predictor yields

$$x_2 = 0.1 + (2)(0.2)(1.088) = 0.5352$$

Fourth-order Runge–Kutta Method

This method, named for its principal authors, Runge and Kutta, was one of the earliest methods developed. It is classified as a predictor type because it makes use of the value of y_n at t_n to predict y_{n+1} at t_{n+1} by means of Taylor's series expansion of y about t_n. The evaluation of higher-order derivatives is, however, not required by the final formulas. Instead, one substitution in the differential equation is required for each of the derivatives in the original expansion. For expansions of order greater than four, the number of substitutions exceeds the order. The fourth-order Runge–Kutta method is developed in a manner analogous to that shown in Chap. 9 for the second-order Runge–Kutta method. The formula for the fourth-order predictor follows:

Predictor:

$$y_{n+1} = y_n + \frac{k_1 + 2k_2 + 2k_3 + k_4}{6} \qquad T_{n+1} = O(h^5) \tag{1-45}$$

where $k_1 = hf(t_n, y_n)$

$$k_2 = hf\left(t_n + \frac{h}{2}, y_n + \frac{k_1}{2}\right)$$

$$k_3 = hf\left(t_n + \frac{h}{2}, y_n + \frac{k_2}{2}\right)$$

$$k_4 = hf(t_n + h, y_n + k_3)$$

This method is sometimes given a separate classification because it differs from a conventional predictor in that it contains values of the function at intermediate times and positions, say $t_n + h/2$, $y_n + k_1/2$. The truncation error of the fourth-order predictor is of order h^5, denoted by $O(h^5)$. The following modified form of the fourth-order Runge–Kutta method which reduces the storage requirement over that required by Eq. (1-45) was proposed by Gill(10). This predictor, called the Runge–Kutta–Gill method follows:

Predictor:

$$y_{n+1} = y_n + \frac{1}{6}\left[k_1 + 2\left(1 - \frac{1}{\sqrt{2}}\right)k_2 + 2\left(1 + \frac{1}{\sqrt{2}}\right)k_3 + k_4\right] \tag{1-46}$$

where $k_1 = hf(t_n, y_n)$

$$k_2 = hf\left(t_n + \frac{h}{2}, y_n + \frac{1}{2}k_1\right)$$

$$k_3 = hf\left[t_n + \frac{h}{2}, y_n + \left(-\frac{1}{2} + \frac{1}{\sqrt{2}}\right)k_1 + \left(1 - \frac{1}{\sqrt{2}}\right)k_2\right]$$

$$k_4 = hf\left[t_n + h, y_n - \frac{1}{\sqrt{2}}k_2 + \left(1 + \frac{1}{\sqrt{2}}\right)k_3\right]$$

The fourth-order Runge–Kutta method (Eq. (1-45)) is applied in essentially the same way as that shown for Euler's method. To illustrate, the calculations for the first increment for $h = 0.2$ h for Example 1-1 follow:

$$k_1 = 0.2[1.8 - (2)(0.1)] = 0.32$$

$$k_2 = 0.2\left[1.8 - (2)\left(0.1 + \frac{0.32}{2}\right)\right] = 0.256$$

$$k_3 = 0.2\left[1.8 - (2)\left(0.1 + \frac{0.256}{2}\right)\right] = 0.2688$$

$$k_4 = 0.2[1.8 - (2)(0.1 + 0.2688)] = 0.2125$$

Thus

$$x_1 = 0.1 + [0.32 + (2)(0.256) + (2)(0.2688) + 0.2125]/6$$
$$= 0.3637$$

Although this value of x_1 is more accurate than that given by Euler's method for $h = 0.2$ h, the number of computational steps is seen to be equal to four times the number required by Euler's method. However, the Runge–Kutta method is the more accurate of the two since the truncation of Euler's method is proportional to h^2 and that of the Runge–Kutta is proportional to h^5.

Semi-Implicit Runge–Kutta Methods

Although the predictor methods are easily applied, they become unstable for large values of h as discussed in a subsequent section. Implicit methods, such as the trapezoidal rule discussed below, are more difficult to apply but they tend to remain stable at large values of h. However, before considering these implicit methods, it is appropriate to present a recent extension of the Runge–Kutta methods, called the semi-implicit Runge–Kutta methods. The initial developers of the semi-implicit Runge–Kutta methods were Rosenbrock(13), Calahan(3), Allen(1), and Butcher(2). A review of a number of other methods which have been proposed has been presented by Seinfeld et al.(14). The third-order method was originally proposed by Caillaud and Padmanabhan(4) and subsequently modified by Michelsen(11). The formula for Michelsen's formulation of this method for a system of differential equations follows:

$$\mathbf{y}_{n+1} = \mathbf{y}_n + R_1\mathbf{k}_1 + R_2\mathbf{k}_2 + R_3\mathbf{k}_3 \tag{1-47}$$

where $\mathbf{k}_1 = h[\mathbf{I} - ha\mathbf{J}(\mathbf{y}_n)]^{-1}\mathbf{f}(\mathbf{y}_n)$

$\mathbf{k}_2 = h[\mathbf{I} - ha\mathbf{J}(\mathbf{y}_n)]^{-1}\mathbf{f}(\mathbf{y}_n + b_2\mathbf{k}_1)$

$\mathbf{k}_3 = [\mathbf{I} - ha\mathbf{J}(\mathbf{y}_n)]^{-1}[b_{31}\mathbf{k}_1 + b_{32}\mathbf{k}_2]$

In the above expressions, $\mathbf{J}(\mathbf{y}_n)$ denotes the jacobian matrix of the functional part of each differential equation of the form

$$\frac{dy}{dt} = f(y) \tag{1-48}$$

For a single differential equation

$$\mathbf{J}(\mathbf{y}_n) = \left.\frac{\partial f(y)}{\partial y}\right|_{y_n} \tag{1-49}$$

A development of the semi-implicit Runge–Kutta method is given in Chap. 9, and by use of the formulas given there the constants were evaluated to four significant figures to give

$$a = 0.4358 \qquad b_2 = 3/4 \qquad b_{31} = -0.6302 \qquad b_{32} = -0.2423$$
$$R_1 = 1.038 \qquad R_2 = 0.8349 \qquad R_3 = 1$$

To demonstrate the application of this method, x_1 is computed for Example 1-1 for $h = 0.2$ h.

$$k_1 = 0.2[1 - (0.2)(0.4358)(-2)]^{-1}(1.6) = 0.2725$$

$$k_2 = 0.2[1 - (0.2)(0.4358)(-2)]^{-1}\{1.8 - 2[0.1 + (0.75)(0.2725)]\}$$
$$= 0.2029$$

$$k_3 = [1 - (0.2)(0.4358)(-2)]^{-1}[(-0.6302)(0.2725) + (-0.2423)(0.2029)]$$
$$= -0.1881$$

Thus

$$x_1 = 0.1 + (1.038)(0.2725) + (0.8349)(0.2029) + (-0.1881) = 0.3642$$

The parameters listed above were selected such that the method is A stable as discussed in Chap. 9. The application of the semi-implicit Runge–Kutta method to systems of differential and algebraic equations and the selection of a step size in agreement with a specified accuracy are presented in Chap. 6.

The Trapezoidal Corrector

The "pure" implicit method commonly known as the trapezoidal rule is considered next. The trapezoidal rule is commonly referred to as a corrector. With each corrector, a predictor is usually employed and the method is referred to as a predictor-corrector method. The predictor is used to obtain the first approximation of y when $t = t_n$. This value of y, denoted by y_n, is then used to initiate the iterative process between the corrector and the differential equation. Generally, predictor-corrector pairs are picked that have truncation errors of approximately the same degree in h but with a difference in sign. One of the simplest pairs consists of the point-slope predictor and the trapezoidal corrector which follows:

Predictor:

$$y_{n+1} = y_{n-1} + 2hy'_n \qquad T_{n+1} = \frac{h^3}{3}y_n^{(3)}(\xi_1) \qquad (t_{n-1} < \xi_1 < t_{n+1}) \tag{1-50}$$

Corrector:

$$y_{n+1} = y_n + \frac{h}{2}(y'_{n+1} + y'_n) \qquad T_{n+1} = \frac{-h^3}{12}y_n^{(3)}(\xi_2) \qquad (t_n < \xi_2 < t_{n+1}) \tag{1-51}$$

The first step of the calculational procedure is the use of the predictor to compute y_2 on the basis of the known value of y_0. The value of y'_1, needed in the predictor formula, is found by one of the starting procedures previously described for the point-slope predictor. After the procedure has been initiated, previously computed values of y_{n-1} and y'_n are used in the predictor to predict y_{n+1}, and this value of y_{n+1} is then used in the differential equation to compute y'_{n+1}. This value y'_{n+1} is used in the corrector to compute y_{n+1}, which may be

further improved by iteration between the corrector and the differential equation. For example, suppose it is required to compute x for Example 1-1 by use of the above predictor-corrector method. Again as in Example 1-1, $x_0 = 0.1$ and $x'_0 = 1.6$. Take x_1 to be equal to 0.356, the value found by use of the first three terms of Taylor's series expansion as shown below Eq. (1-44). Then as shown there, the differential equation gives

$$x'_1 = 1.088$$

and the trapezoidal corrector gives

$$x_1 = 0.1 + \frac{0.2}{2}(1.088 + 1.6) = 0.3688$$

Substitution of this value of x_1 into the differential equation yields $x'_1 = 1.062$ and the next value for x_1 is

$$x_1 = 0.1 + \frac{0.2}{2}(1.062 + 1.6) = 0.3662$$

Repeated iteration gives the correct value $x_1 = 0.3667$.

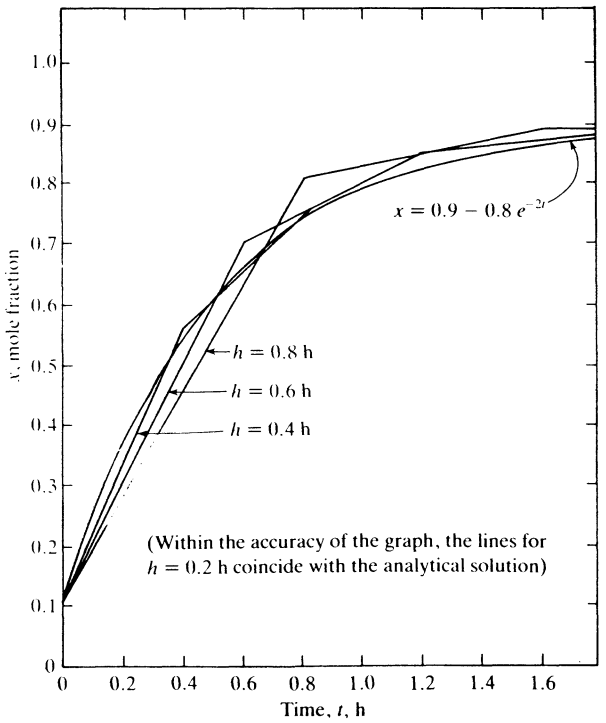

Figure 1-7 Solution of Example 1-1 by use of the trapezoidal rule.

Calculations for the next time step are carried out in the following manner. The number $x_1 = 0.3667$ is used to compute x'_1 by use of the differential equation

$$x'_1 = 1.8 - (2)(0.3667) = 1.067$$

The predicted value of x_2 for the next time step is found by use of the predictor

$$x_2 = 0.1 + (2)(0.2)(1.067) = 0.5268$$

and the corresponding value of x'_2 is found as follows:

$$x'_2 = 1.8 - (2)(0.5268) = 0.7464$$

On the basis of these values, the corrector is used to compute the first trial value of x_2, namely,

$$x_2 = 0.3667 + \frac{0.2}{2}(0.7464 + 1.067)$$

$$x_2 = 0.548$$

Continued iteration on the corrector gives $x_2 = 0.5445$. (In this case, it is possible to solve the corrector explicitly for x_{n+1} since the differential equation $x'_{n+1} = f(t_{n+1}, x_{n+1})$ is linear in x_{n+1}.) The behavior of this method for Example 1-1 is shown in Fig. 1-7.

Two-Point Implicit Method

The two-point implicit method (or simply the implicit method) contains an adjustable parameter which may be selected such that the method reduces either to the Euler predictor or to a corrector. The method may be applied to either an integral-difference equation such as Eq. (1-2) or to a differential equation. Consider

$$\int_{t_n}^{t_{n+1}} f(t, y)\,dt = y_{n+1} - y_n \tag{1-52}$$

which may be reduced to the differential equation

$$\frac{dy}{dt} = f(t, y)$$

When applied to Eq. (1-52), the implicit method consists of approximating the integral by use of a weighted value of the integrand based on its values at t_{n+1} and t_n as follows:

$$[\phi f(t_{n+1}, y_{n+1}) + (1 - \phi) f(t_n, y_n)]h = y_{n+1} - y_n \tag{1-53}$$

where $0 \leq \phi \leq 1$, and the truncation error is given by

$$T_{n+1} = \frac{h^2}{2}(1 - 2\phi)y^{(2)}(t_n) + \frac{h^3}{6}(1 - 3\phi)y^{(3)}(t_n) + O(h^4) \tag{1-54}$$

This formula may be developed as described in Prob. 1-2. Observe that when $\phi = 0$, Eq. (1-53) reduces to Euler's predictor and when $\phi = \frac{1}{2}$, Eq. (1-53) reduces to the trapezoidal corrector.

For $\phi = 0.6$ and $h = 0.2$ h, application of the implicit method to Eq. (1-2), the integral-difference form of Eq. (A) of Example 1-1 yields

$$[0.6(1.8 - 2x_{n+1}) + (1 - 0.6)(1.8 - 2x_n)](0.2) = x_{n+1} - x_n$$

For $x_{n+1} = x_1$ and $x_n = x_0$, this equation may be solved for x_1 at $x_0 = 0.1$ and $h = 0.2$ to give

$$x_1 = 0.3581$$

Gear's Predictor-Corrector Methods (Refs. 8, 9)

Gear's predictor-corrector methods consist of multipoint methods which are developed in Chap. 9. The corrector is implicit in that it contains the derivative of the variable to be evaluated at the end of the time step under consideration. However, instead of carrying the customary variables

$$\mathbf{Y}_n = [y_n, hy'_n, y_{n-1}, y_{n-2}, \ldots, y_{n-k}]^T \tag{1-55}$$

for a kth-order Gear method, the corresponding terms of the Taylor series are carried in a vector called the Nordsieck vector, $\mathbf{Z}_n$, where

$$\mathbf{Z}_n = \left[y_n, hy'_n, \frac{h^2}{2!} y_n^{(2)}, \frac{h^3}{3!} y_n^{(3)}, \ldots, \frac{h^k}{k!} y_n^{(k)} \right]^T \tag{1-56}$$

The predicted values of the variables are carried in the vector, $\tilde{\mathbf{Z}}_n$, where

$$\tilde{\mathbf{Z}}_n = \left[\tilde{y}_n, h\tilde{y}'_n, \frac{h^2\tilde{y}_n^{(2)}}{2!}, \frac{h^3\tilde{y}_n^{(3)}}{3!}, \ldots, \frac{h^k\tilde{y}_n^{(k)}}{k!} \right]^T \tag{1-57}$$

The algorithm is applied as follows:

Step 1 On the basis of the most recent set of values of the variables for the last time step, $\mathbf{Z}_{n-1}$, the predicted values for the next time step are found as follows:

$$\tilde{\mathbf{Z}}_n = \mathbf{D}\mathbf{Z}_{n-1} \tag{1-58}$$

where $\mathbf{D}$ is the Pascal triangle matrix, and for a third-order Gear method ($k = 3$)

$$\mathbf{D} = \begin{bmatrix} 1 & 1 & 1 & 1 \\ 0 & 1 & 2 & 3 \\ 0 & 0 & 1 & 3 \\ 0 & 0 & 0 & 1 \end{bmatrix}$$

The nonzero element $d_{i+1,j+1}$ in the $(j + 1)$st column and $(i + 1)$st row of the Pascal triangle matrix is given by

$$d_{i+1,j+1} = \frac{j!}{(j - i)!\, i!}$$

Step 2 Use the first two elements of $\tilde{\mathbf{Z}}_n$ to determine the b that makes

$$G(y_n, y'_n, t_n) = 0$$

where

$$G(y_n, y'_n, t_n) = hf(\tilde{y}_n + \beta_{-1} b, t_n) - (h\tilde{y}'_n + b)$$
$$y_n = \tilde{y}_n + \beta_{-1} b$$
$$hy'_n = h\tilde{y}'_n + b$$

Step 3 Compute the value of $\mathbf{Z}_n$ at time t_n as follows:

$$\mathbf{Z}_n = \tilde{\mathbf{Z}}_n + b\mathbf{L} \tag{1-59}$$

and return to step 1.

The values of β_{-1}, for algorithms of order $k = 1, 2, 3, \ldots, 6$, are 1, 2/3, 6/11, 12/25, 60/137, and 60/147. The values of the elements of $\mathbf{L}$ for algorithms of order $k = 1, 2, \ldots, 6$ are presented in Table 9-3 of Chapter 9.

Example 1-2 To illustrate the application of Gear's method, let it be required to find x_1 at $t_1 = 0.2$ h (or $h = 0.2$) and $x_0 = 0.1$ for Example 1-1 by use of Gear's second-order method.

SOLUTION

$$x'_0 = 1.8 - 2x_0 = 1.8 - 2(0.1) = 1.6$$

$$x^{(2)} = \frac{d(1.8 - 2x)}{dx}\frac{dx}{dt} = -2x'$$

$$x_0^{(2)} = (-2)(1.6) = -3.2$$

For Gear's second-order method, $\beta_{-1} = 2/3$ and $\mathbf{L} = [2/3, 3/3, 1/3]^T$; see Tables 9-1 and 9-3. The elements of $\mathbf{Z}_0$ are $x_0 = 0.1$ and

$$hx'_0 = (0.2)(1.6) = 0.32$$

$$\frac{h^2}{2!} x_0^{(2)} = \frac{(0.2)^2(-3.2)}{2} = -0.064$$

Step 1

$$\tilde{\mathbf{Z}}_1 = \mathbf{D}\mathbf{Z}_0 = \begin{bmatrix} 1 & 1 & 1 \\ 0 & 1 & 2 \\ 0 & 0 & 1 \end{bmatrix} \begin{bmatrix} x_0 \\ hx_0' \\ \dfrac{h^2}{2!} x_0^{(2)} \end{bmatrix}$$

$$= \begin{bmatrix} 1 & 1 & 1 \\ 0 & 1 & 2 \\ 0 & 0 & 1 \end{bmatrix} \begin{bmatrix} 0.1 \\ 0.32 \\ -0.064 \end{bmatrix} = \begin{bmatrix} 0.356 \\ 0.192 \\ -0.064 \end{bmatrix}$$

Step 2

$$x_1 = \tilde{x}_1 + \beta_{-1} b = 0.356 + \frac{2b}{3}$$

$$hx_1' = h\tilde{x}_1' + b = 0.192 + b$$

$$G(x_1, x_1', t_1) = (0.2)\left[1.8 - 2\left(0.356 + \frac{2b}{3}\right)\right] - (0.192 + b)$$

The b that makes $G = 0$ is

$$b = 0.0202$$

Step 3

$$\mathbf{Z}_1 = \tilde{\mathbf{Z}}_1 + b\mathbf{L} = \begin{bmatrix} 0.356 \\ 0.192 \\ -0.064 \end{bmatrix} + (0.0202) \begin{bmatrix} 2/3 \\ 3/3 \\ 1/3 \end{bmatrix} = \begin{bmatrix} 0.369 \\ 0.212 \\ -0.0573 \end{bmatrix}$$

Thus,

$$x_1 = 0.369$$

The simultaneous change of the order and step size is described in Chap. 6. Also presented is the application of Gear's method to the solution of systems composed of both differential and algebraic equations.

1-3 STABILITY OF NUMERICAL METHODS

Even when the truncation and roundoff errors are negligible, numerical methods are subject to instabilities which cause the error $[y(t_{n+1}) - y_{n+1}]$ to become unbounded as the number of time steps is increased without bound. Symbols y_{n+1} and $y(t_{n+1})$ are used to denote the calculated and the exact values of the variables at time t_{n+1}, respectively.

These instabilities arise because the solutions of equations for the numerical methods differ from those of the differential equations which they are used to approximate. Numerical methods are difference equations which have solutions of the form $C\mu^n$, where C is an arbitrary constant, n the number of time steps, and μ is a root of the reduced equation. Numerical methods are used to approximate the solution of differential equations which generally have solutions of the form $Ce^{\mu t}$.

Instabilities of numerical methods arise from two causes: (1) the difference in forms of the solutions of the numerical method and the differential equation, and (2) the use of numerical methods characterized by second- and higher-difference equations to represent the solution of a first-order differential equation.

Stability of Numerical Methods Characterized by First-Order Difference Equations

In this case a first-order numerical method is used to represent a first-order differential equation. Consider first the use of Euler's method

$$y_{n+1} = y_n + hy_n'$$

for the integration of the linear differential equation with the constant coefficient λ

$$\frac{dy}{dt} = \lambda y \tag{1-60}$$

Instead of considering specific differential equations such as the one for Example 1-1, it has become customary to investigate the behavior of various integration techniques through the use of Eq. (1-60) whose solution is given by

$$y(t) = y(0)e^{\lambda t} \tag{1-61}$$

For $y(0)$ finite and $\lambda < 0$, it is evident that

$$\lim_{t \to \infty} y(t) = 0 \tag{1-62}$$

When Euler's method is used to integrate Eq. (1-60), one obtains the following difference equation

$$y_{n+1} - (1 + \lambda h)y_n = 0 \tag{1-63}$$

Assume a trial solution of the form $y_n = C\mu^n$. Substitution of the trial solution into Eq. (1-63) yields

$$C\mu^{n+1} - (1 + \lambda h)C\mu^n = 0 \tag{1-64}$$

Thus, $\mu = 1 + \lambda h$, and the solution is of the form

$$y_n = C(1 + \lambda h)^n \tag{1-65}$$

In order for the numerical method to remain stable as n increases without bound

$$\lim_{n\to\infty} y_n = 0 \tag{1-66}$$

it is necessary that $|1 + \lambda h| < 1$. Thus it is necessary that

$$\lambda < 0$$
$$|h\lambda| < 2 \tag{1-67}$$

where h is of course greater than zero.

Any method which has a finite general stability boundary is said to be *conditionally stable.* Thus, Euler's method is conditionally stable, that is,

$$|\mu(h\lambda)| \leq 1 \qquad \text{for} \qquad |h\lambda| < 2 \tag{1-68}$$

In general, explicit methods are *conditionally stable.* Although such methods are very easy to use, they may become uneconomical because of the necessity to use small step sizes in order to maintain stability.

The Trapezoidal Rule

When Eq. (1-60) is integrated by use of the trapezoidal rule

$$y_{n+1} = y_n + \frac{h}{2}(y'_{n+1} + y'_n) \tag{1-69}$$

one obtains the following difference equation for any one time step:

$$\left(1 - \frac{h\lambda}{2}\right)y_{n+1} - \left(1 + \frac{h\lambda}{2}\right)y_n = 0 \tag{1-70}$$

Substitution of the trial solution, $y_n = C\mu^n$, into Eq. (1-70) yields the following result upon solving for μ:

$$\mu = \mu(h\lambda) = \left(1 + \frac{h\lambda}{2}\right)\Big/\left(1 - \frac{h\lambda}{2}\right) \tag{1-71}$$

Thus, the solution is

$$y_n = C\left(\frac{1 + h\lambda/2}{1 - h\lambda/2}\right)^n \tag{1-72}$$

In order for the trapezoidal rule to remain stable as the number of time steps is increased indefinitely (Eq. (1-66)), it is necessary that

$$\lambda < 0$$

A numerical method is called *absolutely stable* or *A stable* if

$$|\mu(h\lambda)| < 1 \qquad -\infty < \lambda < 0 \tag{1-73}$$

A method is said to be *strongly A stable* if

$$\lim_{h\lambda\to\infty} |\mu(h\lambda)| = 0 \tag{1-74}$$

Thus, the trapezoidal rule is A stable but not strongly A stable.

Relatively few methods can be classified as A stable. Dahlquist(6,7) has proved two important theorems pertaining to A stability. First, he showed that an explicit k step method cannot be A stable. Secondly, he showed that the order of an A stable linear method cannot exceed 2, and that the trapezoidal rule has the smallest truncation error of these second-order methods.

Stability of Multistep Methods

Multistep methods are characterized by second-, third-, and higher-order difference equations which give rise to multiple roots while the reduced equation of the corresponding differential equation has only one root. Since one root of the difference equation can be generally identified as representing the differential equation, the remaining extraneous roots may lead to instabilities.

To illustrate the occurrence of an extraneous root, suppose that the simple point-slope predictor

$$y_{n+1} = y_{n-1} + 2hy'_n \tag{1-75}$$

is used to integrate Eq. (1-60). The corresponding difference equation is

$$y_{n+1} - 2h\lambda y_n - y_{n-1} = 0 \tag{1-76}$$

which is readily solved by assuming a solution of the form $y_n = C\mu^n$ to give

$$\mu^{n+1} - 2h\lambda\mu^n - \mu^{n-1} = 0 \tag{1-77}$$

or

$$\mu^2 - 2h\lambda\mu - 1 = 0$$

Thus, the solution of Eq. (1-76) is

$$y_n = C_1\mu_1^n + C_2\mu_2^n \tag{1-78}$$

where

$$\mu_1 = h\lambda + \sqrt{(h\lambda)^2 + 1}$$
$$\mu_2 = h\lambda - \sqrt{(h\lambda)^2 + 1}$$

The solution of the difference equation is now compared with the exact solution of the differential equation. Recall that for $\lambda < 0$ and $y(0)$ finite, the exact solution to the differential equation has the property that $y(t)$ approaches zero as t approaches infinity; see Eqs. (1-61) and (1-62). For $\lambda < 0$, $0 < \mu_1 < 1$, and $|\mu_2| > 1$ for all $h > 0$. Thus, the second root μ_2 leads to instability and y_n is unbounded for all $h > 0$ as n approaches infinity. The first root, μ_1, called the

principal root, is the root which makes it possible to represent the solution of the differential equation by the solution of the difference equation. Although C_2 may be set equal to zero to eliminate the effect of the extraneous root μ_2 on the analytical solution of the difference equation, the behavior of the numerical method in the integration of the differential equation is determined by both the principal root and the extraneous root. As a consequence of the extraneous root, the method will eventually fail regardless of how small h ($h > 0$) is made because in the limit as the number of time steps n is increased indefinitely, y_n becomes unbounded. This result is obtained by taking the limit of Eq. (1-78) as n approaches infinity.

Instead of only one extraneous root, multistep methods are characterized by numerous extraneous roots. The general expression for any linear multistep method is

$$y_{n+1} = \alpha_1 y_n + \alpha_2 y_{n-1} + \cdots + \alpha_k y_{n+1-k} + h(\beta_{-1} y'_{n+1} + \beta_0 y'_n + \cdots + \beta_{k-1} y'_{n+1-k}) \quad (1\text{-}79)$$

where $\{\alpha_i\}$ and $\{\beta_i\}$ are constants for any given numerical method, and all of the points are, of course, equidistant, $t_n = t_0 + nh$.

When the numerical integration of Eq. (1-60), with the initial condition $y(0) = 1$, is effected with Eq. (1-79), one obtains

$$y_{n+1} - \alpha_1 y_n - \alpha_2 y_{n-1} - \cdots - \alpha_k y_{n+1-k} - h(\beta_{-1} \lambda y_{n+1} + \beta_0 \lambda y_n + \cdots + \beta_{k-1} \lambda y_{n+1-k}) = 0 \quad (1\text{-}80)$$

After a solution of the form $y_n = C\mu^n$ has been assumed, Eq. (1-80) is readily reduced to

$$\mu^k - \alpha_1 \mu^{k-1} - \alpha_2 \mu^{k-2} - \cdots - \alpha_k - h(\beta_{-1} \lambda \mu^k + \beta_0 \lambda \mu^{k-1} + \cdots + \beta_{k-1} \lambda) = 0 \quad (1\text{-}81)$$

which is seen to be a polynomial of degree k in μ. The solution of this difference equation is given by

$$y_n = C_1 \mu_1^n + C_2 \mu_2^n + \cdots + C_k \mu^n \quad (1\text{-}82)$$

Thus, the difference equation has one principal root which corresponds to the solution of the differential equation (Eq. (1-60)) and $k - 1$ extraneous roots. If $|\mu_i| < 1$ for each of the k roots of Eq. (1-81), it is evident that

$$\lim_{n \to \infty} y_n = \lim_{n \to \infty} (C_1 \mu_1^n + C_2 \mu_2^n + \cdots + C_k \mu_k^n) = 0 \quad (1\text{-}83)$$

A multistep method is called *A stable* if

$$|\mu_i| < 1 \qquad (i = 1, 2, \ldots, k) \quad (1\text{-}84)$$

and *relatively stable* if

$$|\mu_i| < |\mu_1| \qquad (i = 2, 3, \ldots, k) \quad (1\text{-}85)$$

The terms *absolutely stable* and *A stable* are used interchangeably. If the second condition is satisfied, then any errors introduced into the computations will decay as n increases; whereas, if any of the extraneous roots μ_i are greater than unity in magnitude, the errors will grow as n increases. Methods which satisfy the condition given by Eq. (1-85) are also called *strongly stable*, and a method whose stability depends upon the sign of λ is sometimes called *weakly unstable*. Note, the definitions given by Eqs. (1-84) and (1-85) are frequently stated to include $|\mu_i| = 1$, in which case the zero on the right-hand side of Eq. (1-83) is replaced by a finite constant.

Any method which has an infinite general stability boundary is said to be *unconditionally stable*, or *A stable*. Thus, in a multistep method represented by Eq. (1-82), y_n tends to zero as n approaches infinity where $h > 0$ and $|\lambda| < 0$ or $|\mathrm{Re}\,(\lambda)| < 0$.

Seinfeld et al.(14) have shown that in the case of systems of coupled linear differential equations it is sufficient, in the examination of a multistep numerical method, to consider the method as applied to the single scalar equation $y' = \lambda_i y$, where λ_i takes on the values of the eigenvalues of each of the differential equations.

However, at this time no general theory of the stability of linear multistep methods applied to nonlinear differential equations exists.

Stability of Numerical Methods in the Integration of Stiff Differential Equations

Quite often systems are encountered with widely different time constants, which give rise to both long-term and short-term effects. The corresponding ordinary differential equations have widely different eigenvalues. Differential equations of this type have come to be called *stiff systems*. Use of the explicit Runge–Kutta methods or other explicit methods in the numerical integration of these equations results in instability and excessive computation time. For example, suppose the eigenvalues are λ_1 and λ_2, where $\lambda_1 \ll \lambda_2 < 0$. The most rapidly decaying component, or the stiff component, corresponds to the larger eigenvalue in absolute value λ_2, and this eigenvalue determines the step size to be used in the integration. That is, in order to ensure numerical stability, the stiff component requires the use of small step sizes. Since one is usually interested in the nonstiff component of the solution, the use of very small step sizes consumes too much computer time to be of any practical value.

In general, most all of the explicit methods are neither A stable nor strongly A stable. Consequently, they are completely unsuitable for solving systems of stiff differential equations. The implicit and semi-implicit methods are suitable for solving systems of stiff differential equations.

Of the large number of semi-implicit methods reported in the literature (Refs. 1, 2, 12, 13), the three most widely used are the semi-implicit Runge–Kutta methods proposed by Rosenbrock(13), Caillaud and Padmanabhan(4) and Michelsen(11). One of the principal competitors of the semi-implicit Runge–Kutta methods is Gear's method (Ref. 8).

An alternate to requiring A stability was proposed by Gear(8). It was suggested that stability was not necessary for values of $h\lambda$ close to the imaginary axis but not close to the origin. These correspond to oscillating components that will continue to be excited in nonlinear problems. Methods that were stable for all values $h\lambda$ to the left of Re $(h\lambda) = -D$, where D was some positive constant and accurate close to the origin, were said to be *stiffly stable* (Ref. 9). The multistep methods of Gear were shown to be stiffly stable for orders $k \leq 6$ (Ref. 9).

NOTATION

$\mathbf{D}$ = Pascal triangle matrix; see Eq. (1-58)
E = internal energy per unit mass (or per mole) of material
E_T = total energy per unit mass (or per mole) of material; $E_T = E + KE + PE$
E_{Ts} = total energy per unit mass (or per mole) of material in the system at any given time
F = flow rate of the feed in pounds-mass per hour (lb_m/h) (or moles per hour)
h = incremental change of the independent variable t, $h = t_{n+1} - t_n = \Delta t$; herein h is taken to be positive
H = enthalpy per unit mass (or per mole) of material; $H = E + Pv$
H_T = total enthalpy per unit mass (or per mole) of material; $H_T = E_T + Pv$
$\mathbf{I}$ = identity matrix
$\mathbf{J}$ = jacobian matrix; see Eq. (1-49) for the applications of this chapter
KE = kinetic energy per unit mass (or per mole) of material
lb_f = pound-force
lb_m = pound-mass
L = flow rate, lb_m/h (or mol/h)
$\mathbf{L}$ = column vector appearing in Gear's method
M = total mass of system at any time t
P = pressure, lb_f (pounds-force) per unit area
PE = potential energy per unit mass (or per mole) of material
q = rate of heat transfer (energy per unit time per unit length)
Q = rate of heat transfer from the surroundings to the system (energy per unit time)
S = cross-sectional area
t = independent variable; t_n = a particular value of t, the value of t at the end of the nth time increment
Δt = incremental change of the independent variable; also denoted by h; $t_{n+1} = t_n + \Delta t = t_n + h$
T_{n+1} = truncation error in the value of y_{n+1}

U = holdup, lb_m (pound-mass) or moles
v = volume per unit mass (or per mole) of material
w = mass flow rate
W = shaft work done by the system on the surroundings per unit time
$\mathscr{W}$ = shaft work done by the system on the surroundings per unit time per unit length of boundary
y = the dependent variable in the description of the methods of numerical analysis
$y^{(n)}(t) = d^n y/dt^n$
$y'(t) = dy/dt$
y_n = calculated value of the variable y at time t_n
$y(t_n)$ = correct value of the variable y at time t_n
X_i = mole fraction of component i in the feed
$\mathbf{Y}$ = a vector defined by Eq. (1-55)
$\mathbf{Z}$ = a vector defined by Eq. (1-56)
$\tilde{\mathbf{Z}}$ = a vector defined by Eq. (1-57)

Subscripts

i = component number; also inlet value of the variable
o = outlet value of the variable

Greek letters

α = constant
β = constant
ρ = mass density, mass per unit volume

REFERENCES

1. R. H. Allen: "Numerically Stable Explicit Integration Techniques Using a Linearized Runge–Kutta Extension," Boeing Scientific Res. Lab. Document *D1-82-0929* (October, 1969).
2. J. C. Butcher: "On Runge–Kutta Processes of High Order," *J. Aust. Math. Soc.*, **4**: 179 (1964).
3. D. A. Calahan: "Numerical Solution of Linear Systems with Widely Separated Time Constants," *Proc. IEEE (Letters)*, **55**: 2016 (1967).
4. J. B. Caillaud and L. Padmanabhan: "An Improved Semi-Implicit Runge–Kutta Method for Stiff Systems," *Chem. Eng. J.*, **2**: 227 (1971).
5. S. D. Conte and C. de Boor: *Elementary Numerical Analysis*, McGraw-Hill Book Company, 2d ed., 1972.
6. G. Dahlquist: "A Special Stability Problem for Linear Multistep Methods," *BIT* **3**: 27 (1963).
7. G. Dahlquist: "Convergence and Stability in the Numerical Integration of Ordinary Differential Equations," *Math. Scan.* **4**: 33 (1956).
8. C. W. Gear: *Numerical Initial Value Problems in Ordinary Differential Equations*, Prentice-Hall, Inc., Englewood Cliffs, N.J., 1971.
   Trans. Circuit Theory, **C1-18**(1): 89 (1971).
10. S. Gill: "A Process for Step-by-Step Integration of Differential Equations in an Automatic Digital Computing Machine," *Proc. Cambridge Philos. Soc.* **47**: 96 (1951).
11. M. L. Michelsen: "An Efficient General Purpose Method for the Integration of Stiff Ordinary Differential Equations," *AIChEJ*, **22**: 594 (1976).

12. W. E. Milne: *Numerical Solution of Differential Equations*, John Wiley & Sons, New York, 1960.
13. H. H. Rosenbrock: "Some General Implicit Processes for the Numerical Solution of Differential Equation," *Comput. J.* **5**:329 (1963).
14. J. H. Seinfeld, L. Lapidus, and M. Hwang: "Review of Numerical Integration Techniques for Stiff Ordinary Differential Equations," *Ind. Eng. Chem. Fundam.*, **8**(2):266 (1970).

PROBLEMS

1-1 Develop the formula for the point-slope predictor. It may be assumed that $y(t)$ is continuous and has continuous first, second, and third derivatives.

Hint: Begin by expanding $y(t)$ in a Taylor series expansion over the interval from t_n to $t_n + h$.

$$y(t_n + h) = y(t_n) + hy'(t_n) + \frac{h^2}{2!} y^{(2)}(t_n) + \frac{h^3}{3!} y^{(3)}(\xi) \qquad (t_n < \xi < t_{n+1})$$

Next expand $y(t)$ by a Taylor series over the interval from t_n to $t_n - h$.

1-2 Obtain the expression given in Eq. (1-54) for the truncation error $y(t_{n+1}) - y_{n+1}$ for the two-point implicit method.

Hint: Expand $y(t_{n+1})$ and y'_{n+1} in a Taylor series. Also note that the implicit method may be stated in the form

$$y_{n+1} = y_n + h[y'_n + \phi(y'_{n+1} - y'_n)]$$

and that the truncation error $[y(t_{n+1}) - y_{n+1}]$ is computed with respect to a correct point $[y(t_n), t_n]$ on the correct curve, that is,

$$y_n = y(t_n),\ y'_n = y'(t_n),\ \ldots,\ y_n^{(3)} = y^{(3)}(t_n)$$

1-3 (*a*) Repeat Example 1-1 with $h = 2$.

(*b*) Show that the unstable behavior obtained should be expected.

Hint: see Eq. (1-67).

APPENDIX 1A-1 THEOREMS

DEFINITION 1A-1

Continuity of $f(x)$ at x_0 The function $f(x)$ is said to be continuous at the point x if, for every positive number ε, there exists a δ, depending upon ε such that for all x of the domain for which

$$|x - x_0| < \delta_\varepsilon$$

then

$$|f(x) - f(x_0)| < \varepsilon$$

DEFINITION 1A-2

Continuity of $f(x)$ in an interval A function which is continuous at each point in an interval is said to be continuous in the interval.

THEOREM 1A-1

Mean-value theorem of differential calculus If the function $f(x)$ is continuous in the interval $a \le x \le b$ and differentiable at every point in the interval $a < x < b$, then there exists at least one value of ξ such that

$$\frac{f(b) - f(a)}{(b - a)} = \left.\frac{df(x)}{dx}\right|_{x = a + \xi(b-a)}$$

where $0 < \xi < 1$.

THEOREM 1A-2

Mean-value theorem of integral calculus If the function $f(x)$ is continuous in the interval $a \le x \le b$, then

$$\int_a^b f(x)\,dx = f(\xi)(b - a)$$

where $a \le \xi \le b$.

THEOREM 1A-3

Generalized theorem of integral calculus If $f(x)$ and $p(x)$ are continuous functions in the interval $a \le x \le b$, and $p(x) \ge 0$, then

$$\int_a^b f(x)p(x)\,dx = f(\xi) \int_a^b p(x)\,dx$$

where $a \le \xi \le b$.

THEOREM 1A-4

If the function $f(x)$ is continuous in the interval $a \le x \le b$ and $f(z) \lessgtr k \lessgtr f(b)$, then there exists a number c in the interval $a < c < b$ such that

$$f(c) = k$$

THEOREM 1A-5

Taylor's theorem If the functions $f(x), f'(x), \ldots, f^{(n)}(x)$ are continuous for each x in the interval $a \le x \le b$, and $f^{(n+1)}(x)$ exists for each x in the interval $a < x < b$, then there exists a ξ in the interval $a < x < b$ such that

$$f(a + h) = f(a) + hf'(a) + \frac{h^2}{2!} f^{(2)}(a) + \frac{h^3}{3!} f^{(3)}(a) + \cdots + \frac{h^n}{n!} f^{(n)}(a) + R_n$$

where $h = b - a$, and the remainder R_n is given by the formula

$$R_n = \frac{h^{n+1}}{(n+1)!} f^{(n+1)}(\xi) \qquad (a < \xi < b)$$

DEFINITION 1A-3

A function $f(x_1, x_2, \ldots, x_n)$ of n variables $x_1, x_2, \ldots, x_n$ is said to be homogeneous of degree m if the function is multiplied by λ^m when the arguments $x_1, x_2, \ldots, x_n$ are replaced by $\lambda x_1, \lambda x_2, \ldots, \lambda x_n$, respectively. That is, if $f(x_1, x_2, \ldots, x_n)$ is homogeneous of degree m, then

$$f(\lambda x_1, \lambda x_2, \ldots, \lambda x_n) = \lambda^m f(x_1, x_2, \ldots, x_n)$$

THEOREM 1A-6

Euler's theorem If the function $f(x_1, x_2, \ldots, x_n)$ is homogeneous of degree m and has continuous first partial derivatives, then

$$x_1 \frac{\partial f}{\partial x_1} + x_2 \frac{\partial f}{\partial x_2} + \cdots + x_n \frac{\partial f}{\partial x_n} = mf(x_1, x_2, \ldots, x_n)$$

PART ONE

SOLUTION OF STAGED SEPARATION PROBLEMS BY USE OF THE TWO-POINT IMPLICIT METHOD

CHAPTER

TWO

INTRODUCTION TO THE DYNAMIC BEHAVIOR OF EVAPORATOR SYSTEMS

Evaporation, one of the oldest of the unit operation processes, is commonly used to separate a nonvolatile solute from a volatile solvent. Since energy is transferred in an evaporator from a condensing vapor to a boiling liquid, evaporation may be regarded as a special case of the unit operation called *heat transfer*. On the other hand, evaporation may be regarded as a special case of the unit operation called *distillation* because a solvent is separated from a solute by virtue of the differences in their vapor pressures.

First the fundamental principles of evaporation are reviewed in Sec. 2-1. Then the equations required to describe an evaporator system at unsteady state operation are developed in Sec. 2-2. In Sec. 2-3, the two-point form of the implicit method is used to solve a numerical problem involving a single-effect evaporator. Numerical techniques such as Broyden's method and scaling procedures are also presented in Sec. 2-3.

2-1 FUNDAMENTAL PRINCIPLES OF EVAPORATION

Evaporators are commonly used for the special separation process wherein a volatile solvent is separated from a nonvolatile solute. Evaporators are commonly found in the inorganic, organic, paper, and sugar industries. Typical applications include the concentration of sodium hydroxide, brine, organic colloids, and fruit juices. Generally, the solvent is water.

Mode of Operation and Definitions

Three commercially available evaporators shown in Figs. 2-1, 2-2, and 2-3 are described briefly.

In the Swenson single-effect, long-tube vertical (LTV) rising-film evaporator shown in Fig. 2-1, evaporation occurs primarily inside the tubes, so it is used primarily to concentrate nonsalting liquors. As shown, the liquor is introduced at the bottom of the liquor chamber, is heated and partially vaporized as it climbs up through the tubes, and attains its maximum velocity at the tube exit. The outlet mixture impinges upon a deflector where gross, initial separation of the liquor and vapor occurs. Additional vapor is separated from the liquid by gravity as the vapor rises through the vapor body.

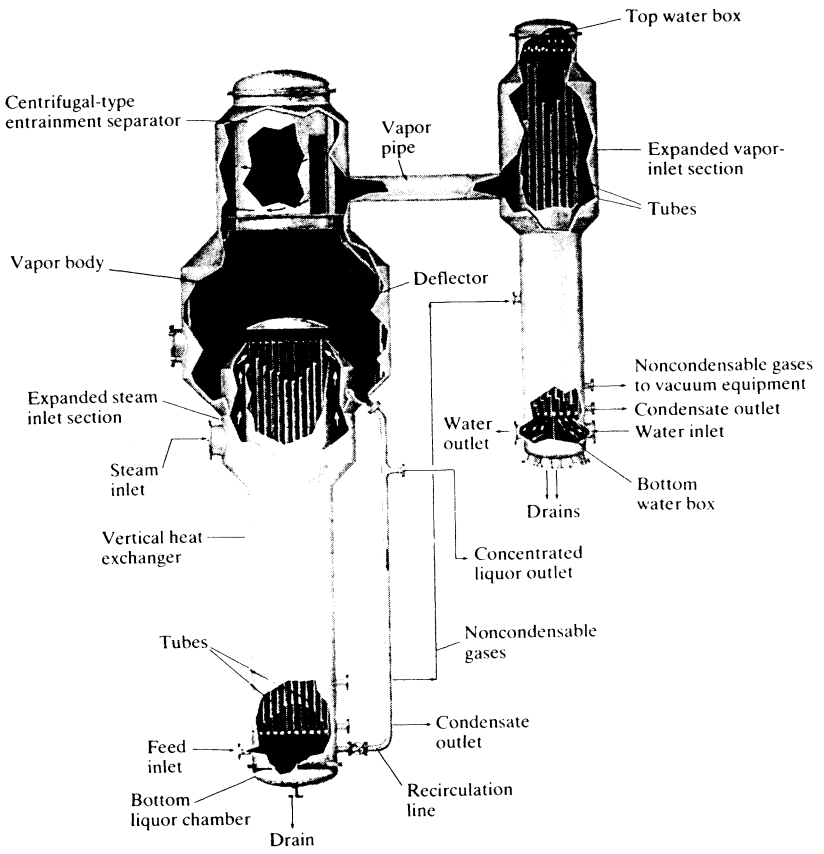

Figure 2-1 Swenson LTV rising-film evaporator with vertical-tube surface condenser. (*Courtesy Swenson Division, Whiting Corporation.*)

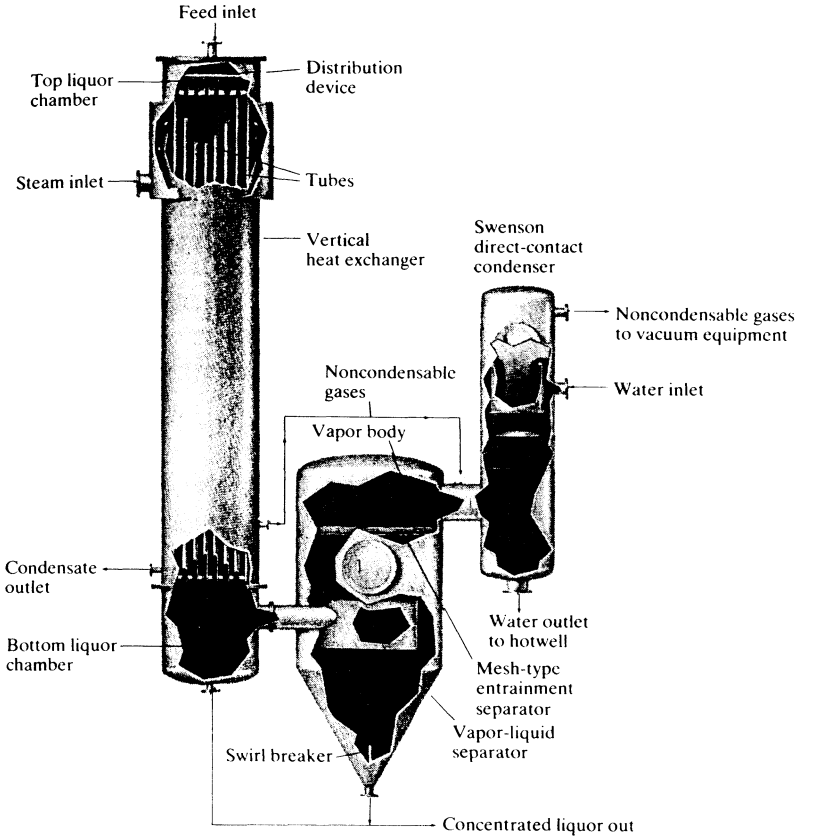

Figure 2-2 Swenson LTV falling-film evaporator. (*Courtesy Swenson Division, Whiting Corporation.*)

The Swenson single-effect, LTV falling-film evaporator shown in Fig. 2-2 has a separate vaporizer and heat exchanger. Liquor is fed into the top liquor chamber of the heat exchanger where it is distributed to each tube. The liquor accelerates in velocity as it descends inside the tubes. Liquid is separated from the vapor in the bottom liquor chamber and with a skirt-type baffle in the vapor body.

In the forced-circulation evaporator shown in Fig. 2-3, liquor is pumped through the tubes to minimize tube scaling or salting when precipitates are formed during evaporation. The Swenson forced-circulation evaporator shown in Fig. 2-3 has a submerged feed inlet, a single-pass vertical heat exchanger, an elutriating leg, a cyclone, and a barometric condenser.

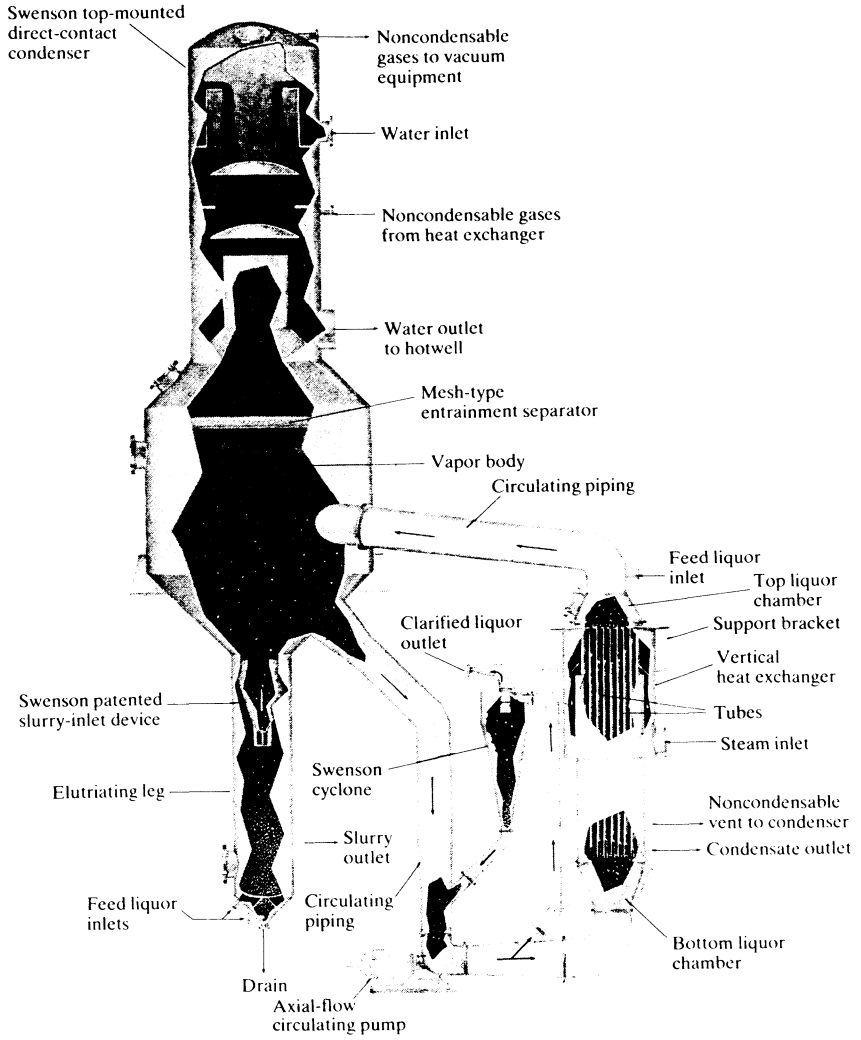

Figure 2-3 Swenson forced-circulation, submerged-inlet, vertical-tube evaporator. (*Courtesy Swenson Division, Whiting Corporation.*)

In *single-effect* operation, as the name implies, only one evaporator is employed. The feed upon entering this effect must be heated to the boiling point temperature of the effect at the operating pressure. Then the solvent, generally water, is evaporated and removed as a vapor. (Since water is the most common solvent, it is for definiteness regarded as the solvent in the development of the

equations. The final equations apply, however, for any solvent.) To evaporate one pound of water from, say, a sodium hydroxide solution, about 1200 Btu are needed, and this requires more than one pound of steam. The concentrated solution withdrawn from the evaporator is known as the *thick liquor* or *process liquid.*

In *multiple-effect* operation, several evaporators are connected in series. The vapor or steam produced in the first effect is introduced to the steam chest of the second effect and thus becomes the heating medium for the second effect. Similarly, the vapor from the second effect becomes the steam for the third effect. In the case of series operation with *forward feed*, depicted in Fig. 2-4, the thick liquor leaving the first effect becomes the feed for the second effect. For each effect added to the system, approximately one additional pound of solvent is evaporated per pound of steam fed to the first effect. This increase in the pounds of solvent evaporated per pound of steam fed is achieved at the expense of the additional capital outlay required for the additional effects.

To provide the temperature potential required for heat transfer to occur in each effect, it is necessary that each effect be operated at a successively lower pressure. The operating pressure of the last effect is determined by the condensing capacity of the condenser following this effect. The pressure distribution throughout the remainder of the system is determined by the design specifications for the system. The term *evaporator system* is used to mean either one evaporator or any number of evaporators that are connected in some prescribed manner. Unless otherwise noted, it will be supposed that the evaporators are connected in series with forward feed.

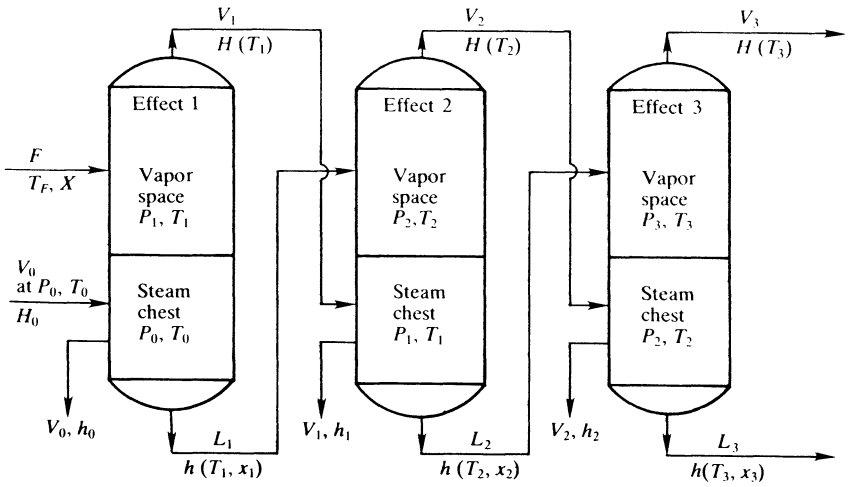

Figure 2-4 A triple-effect evaporator system with forward feed. The temperature distribution shown is for a system with negligible boiling point elevations.

To describe evaporator operation the three terms, *capacity*, *economy*, and *steam consumption* are commonly employed. By *capacity* of the evaporator system is meant the number of pounds of solvent evaporated per hour. The *economy* of an evaporator system is the total number of pounds of solvent vaporized per pound of steam fed to the system per hour. Note that the *economy* is the ratio of capacity to steam consumption.

If a true state of equilibrium existed between the vapor and the liquid phases in an evaporator, then the temperature and pressure in each phase would be equal and the temperature would be called the boiling point temperature of the evaporator. However, in an actual evaporator, the temperature of the vapor and liquid streams leaving an evaporator may be measurably different from each other and from other temperatures measured within the evaporator. Thus, the boiling point of an evaporator is commonly taken to be the boiling point temperature of the thick liquor (leaving the evaporator) at the pressure in the vapor space within the evaporator. Because of the effect of hydrostatic head, the pressure—and consequently the corresponding boiling point of the liquid at the bottom of the liquid holdup within an evaporator—is greater than it is at the surface of the liquid. However, because of the turbulent motion of the liquid within an evaporator, there exists no precise quantitative method in the analysis of evaporator operation for taking into account the effect of hydrostatic head.

Generally, the pure vapor above a solution is superheated because at a given pressure it condenses at a temperature below the boiling point temperature of the solution. The difference between the boiling point temperature of the solution and the condensation temperature of the vapor at the pressure of the vapor space is called the *boiling point elevation* of the effect. That an elevation of boiling point should be expected follows immediately by consideration of the equilibrium relationship between the two phases.

Equilibrium Relationships

As enumerated by Denbigh(6) the necessary conditions for a state of equilibrium to exist between a vapor and liquid phase of a multicomponent mixture are as follows:

$$\begin{aligned} \hat{f}_i^V &= \hat{f}_i^L \\ T^V &= T^L \\ P^V &= P^L \end{aligned} \tag{2-1}$$

where the superscripts V and L refer to the vapor and liquid phases, respectively, and where

$\hat{f}_i^V = f_i^V(P, T, \{y_i\})$, the fugacity of component i in the vapor phase of a mixture at the temperature T and pressure P of the mixture

$\hat{f}_i^L = \hat{f}^L(P, T, \{x_i\})$, the fugacity of component i in the liquid phase at the temperature T and pressure P of the mixture

T^V, T^L = temperature of the vapor and liquid phases, respectively

P^V, P^L = pressure of the vapor and liquid phases, respectively

The fugacity of any component i in a vapor mixture may be expressed in terms of the fugacity of the pure component at the same temperature T and total pressure P of the mixture as follows:

$$\hat{f}_i^V = \gamma_i^V f_i^V y_i \tag{2-2}$$

where f_i^V = fugacity of pure component i at the total pressure P and temperature T of the mixture

y_i = mole fraction of component i in the vapor phase

$\gamma_i^V = \gamma_i^V(P, T, \{y_i\})$, the activity coefficient of component i in the vapor phase

Similarly, for the fugacity $\hat{f}_i^L$ of component i in the liquid phase,

$$\hat{f}_i^L = \gamma_i^L f_i^L x_i \tag{2-3}$$

where $f_i^L = f_i^L(P, T)$

$\gamma_i^L = \gamma_i^L(P, T, \{x_i\})$

and x_i is the mole fraction of component i in the liquid phase. Use of Eqs. (2-2) and (2-3) permit Eq. (2-1) to be restated in the following form:

$$f_i^V \gamma_i^V y_i = \gamma_i^L f_i^L x_i \tag{2-4}$$

Next consider the distribution of the solvent such as water between the vapor phase and a liquid phase such as a sodium hydroxide solution at reasonably low temperatures and pressures. Since the sodium hydroxide is nonvolatile, the mole fraction of water vapor in the vapor phase is equal to unity ($y_{\text{solv}} = 1$), and since the vapor phase consists of a pure component, water vapor, $\gamma_{\text{solv}}^V = 1$. At reasonably low pressures, the volumetric behavior of the vapor approaches that of a perfect gas and its fugacity is equal to the pressure ($f_{\text{solv}}^V = P$). The fugacity of the solvent in the liquid phase at the pressure P and temperature T may be expressed in terms of its value at its vapor pressure P_{solv} at the temperature T as follows:

$$f_{\text{solv}}^L\Big|_{P,\,T} \cong f_{\text{solv}}^L\Big|_{P_{\text{solv}},\,T} = f_{\text{solv}}^V\Big|_{P_{\text{solv}},\,T} \cong P_{\text{solv}} \tag{2-5}$$

The final approximation is based on the assumption that the water vapor behaves as a perfect gas at the temperature T. Thus, Eq. (2-4) reduces to

$$P = \gamma_{\text{solv}}^L P_{\text{solv}} x_{\text{solv}} \tag{2-6}$$

A treatment of the thermodynamics of multicomponent mixtures is presented in Ref. 11.

The expressions for the Dühring lines are determined experimentally. Their existence may be deduced as follows. For any given pressure P, there is a temperature T such that the vapor pressure of the pure solvent is equal to the total pressure P, that is, there exists a T such that for solvent,

$$P = P_{\text{solv}}(T) \tag{2-7}$$

For a liquid mixture having a solvent mole fraction x_{solv}, there exists a temperature $\mathscr{T}$ such that the mixture will exert a pressure P equal to the vapor

pressure P_{solv} of the pure solvent at the temperature T, that is,

$$P = \gamma^L_{solv}(P, \mathscr{T}, x_{solv}) \cdot P_{solv}(\mathscr{T}) \cdot x_{solv} \tag{2-8}$$

Thus, it is seen that for every P and x_{solv}, there exists corresponding values of T and $\mathscr{T}$ which satisfy the above expressions.

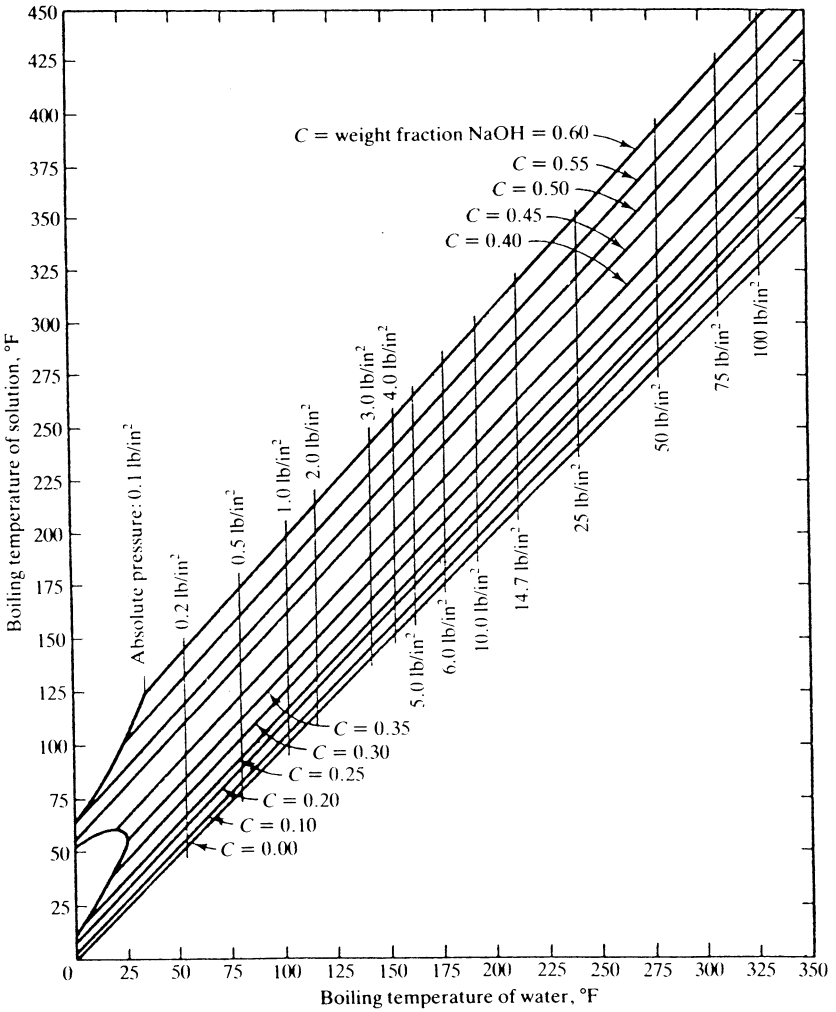

Figure 2-5 Dühring lines for solutions of sodium hydroxide in water. (*W. L. McCabe, "The Enthalpy Concentration Chart—A Useful Device for Chemical Engineering Calculations," Trans. Am. Inst. Chem. Engrs., vol. 31, p. 129 (1935), Courtesy American Institute of Chemical Engineers.*)

In view of the fact that the mole fraction of the solvent in the solution decreases as the mole fraction of the solute is increased

$$x_{solv} = 1 - x_{solute} \tag{2-9}$$

it follows that at a given pressure P, the vapor pressure P_{solv} (or more precisely the product $\gamma^L_{solv} P_{solv}$) is generally an increasing function of temperature, the total pressure P may be maintained constant as the concentration of the solute is increased by increasing the temperature $\mathscr{T}$ of the solution. This property of solutions containing dissolved nonvolatile solutes gives rise to the term *boiling point elevation.* The boiling point temperatures of many aqueous solutions containing dissolved solids follow the Dühring rule in that the boiling point temperature $\mathscr{T}$ of the solution is a linear function of the boiling point temperature T of pure water, that is,

$$\mathscr{T} = m(x)T + b(x) \tag{2-10}$$

It is customary to express x in Eq. (2-10) in terms of the mass fraction of the solute. When the straight-line relationship given by Eq. (2-10) is followed, the solution is said to obey the Dühring rule.

A typical Dühring plot for sodium hydroxide is shown in Fig. 2-5. The data were taken from the work of Gerlack(8). Observe that each concentration of dissolved solute yields a separate Dühring curve which is approximated with good accuracy by the straight line given by Eq. (2-10).

Reduction of the Rate of Heat Transfer by Boiling Point Elevation

As discussed above, the presence of the solute gives rise to an elevation in the boiling point by $(\mathscr{T} - T)$. The effect of boiling-point elevation on the rate of heat transfer is demonstrated as follows. If there were no boiling point elevation, then the rate of heat transfer Q (Btu/h) in a single-effect evaporator operating at the total pressure P would be given by

$$Q = UA(T_0 - T) \tag{2-11}$$

With boiling point elevation, the rate of heat transfer becomes

$$Q = UA(T_0 - \mathscr{T}) \tag{2-12}$$

Since $\mathscr{T} > T$, the rate of heat transfer is decreased by a decrease in the temperature potential for heat transfer of an amount equal to the boiling point elevation, namely,

$$(T_0 - T) - (T_0 - \mathscr{T}) = \mathscr{T} - T \tag{2-13}$$

In multiple-effect evaporator systems in which the evaporators are connected in series, the boiling point elevations of the individual effects are cumulative. This characteristic is a significant factor in the determination of the optimum number of effects for a given system.

2-2 DYNAMIC BEHAVIOR OF A SINGLE-EFFECT EVAPORATOR

The treatment of a system of evaporators at unsteady state operation is initiated by the formulation of the dynamic model for a single-effect evaporator for which the boiling point elevation is not negligible. By use of this evaporator example and a system of such evaporators, the role of inherited error in the solution of unsteady state problems of this type is demonstrated.

The mixture to be separated consists of a liquid mixture of a volatile solvent and a nonvolatile solute. The system of equations that describe a system of evaporators at unsteady state operation contains several integral-difference equations which are formulated below.

Formulation of the Equations of the Dynamic Model for a Single-Effect Evaporator

The equations describing the dynamic model of a single-effect evaporator are formulated on the basis of the following suppositions:

1. The process liquid in the holdup of the evaporator is perfectly mixed.
2. The mass of solvent in the vapor space is negligible relative to the mass of holdup of thick liquor in the evaporator.
3. The mass of steam in the steam chest is negligible relative to the other terms that appear in the energy balance for this portion of the system.
4. The holdup of energy by the walls of the metal tubes is negligible.
5. Heat losses to the surroundings are negligible.

For definiteness, suppose that at time $t = 0$, the evaporator is at steady state operation, and that at time $t = 0+$, an upset in some operating variable, say the composition X of the feed, occurs. The material and energy balances as well as the rate expressions follow. A total material balance on the thick liquor has the following form:

$$\int_{t_n}^{t_{n+1}} (F - V_1 - L_1)\, dt = \mathscr{M}_1\Big|_{t_{n+1}} - \mathscr{M}_1\Big|_{t_n} \tag{2-14}$$

where all symbols are defined in the Notation. From this integral-difference equation as well as those which follow, the corresponding differential equations are obtained through the use of the mean-value theorems of differential and integral calculus followed by appropriate limiting processes. The left-hand side of Eq. (2-14) may be restated in the following form through the use of the *Mean-Value Theorem of Integral Calculus* (see Theorem 1A-2, App. 1A).

$$\int_{t_n}^{t_{n+1}} (F - V_1 - L_1)\, dt = (F - V_1 - L_1)\Big|_{t_n + \alpha\,\Delta t}\,\Delta t \tag{2-15}$$

where $0 \le \alpha \le 1$. The *Mean-Value Theorem of Differential Calculus* (see Theorem 1A-1, App. 1A) may be used to restate the right-hand side of Eq. (2-14) in the form:

$$\mathscr{M}_1\Big|_{t_{n+1}} - \mathscr{M}_1\Big|_{t_n} = \Delta t\, \frac{d\mathscr{M}_1}{dt}\Big|_{t_n + \beta\,\Delta t} \tag{2-16}$$

where $0 < \beta < 1$. After these results have been substituted into Eq. (2-14) and the expression so obtained has been divided by Δt, one obtains

$$(F - V_1 - L_1)\Big|_{t_n + \alpha\,\Delta t} = \frac{d\mathscr{M}_1}{dt}\Big|_{t_n + \beta\,\Delta t} \tag{2-17}$$

In the limit as Δt approaches zero, Eq. (2-17) reduces to

$$(F - V_1 - L_1)\Big|_{t_n} = \frac{d\mathscr{M}_1}{dt}\Big|_{t_n} \tag{2-18}$$

Since t_n was selected arbitrarily in the time domain $t_n > 0$, Eq. (2-18) holds for all $t > 0$, and thus Eq. (2-18) becomes

$$F - V_1 - L_1 = \frac{d\mathscr{M}_1}{dt} \qquad (t > 0) \tag{2-19}$$

The integral-difference equation representing a component-material balance on the solute over the time period from t_n to t_{n+1} is given by

$$\int_{t_n}^{t_{n+1}} (FX - L_1 x_1)\, dt = \mathscr{M}_1 x_1\Big|_{t_{n+1}} - \mathscr{M}_1 x_1\Big|_{t_n} \tag{2-20}$$

The corresponding differential equation (obtained as shown above Eq. (2-19)) is

$$FX - L_1 x_1 = \frac{d(\mathscr{M}_1 x_1)}{dt} \tag{2-21}$$

The integral-difference equation representing an energy balance on the thick liquor is given by

$$\int_{t_n}^{t_{n+1}} [Fh(T_F, X) + Q_1 - V_1 H(\mathscr{T}_1) - L_1 h(\mathscr{T}_1, x_1)]\, dt = \mathscr{M}_1 h(\mathscr{T}_1, x_1)\Big|_{t_{n+1}} - \mathscr{M}_1 h(\mathscr{T}_1, x_1)\Big|_{t_n} \tag{2-22}$$

and the corresponding differential equation is

$$Fh(T_F, X) + Q_1 - V_1 H(\mathscr{T}_1) - L_1 h(\mathscr{T}_1, x_1) = \frac{d[\mathscr{M}_1 h(\mathscr{T}_1, x_1)]}{dt} \qquad (t > 0) \tag{2-23}$$

Since the holdup of steam in the steam chest is negligible relative to the other holdups of the system, the enthalpy balance on the steam is given by

$$\int_{t_n}^{t_{n+1}} (V_0 H_0 - V_0 h_0 - Q_1)\, dt = 0 \tag{2-24}$$

Since this integral is equal to zero for any choice of the upper and lower limits, it follows that the integrand is identically equal to zero for all t in the time domain of interest, that is,

$$V_0(H_0 - h_0) - Q_1 = 0 \qquad (t > 0) \tag{2-25}$$

or

$$V_0 \lambda_0 = Q_1 \tag{2-26}$$

Also, since the holdup of energy by the metal through which the energy is transferred is regarded as negligible, it follows that the expression

$$Q_1 = U_1 A_1(T_0 - \mathscr{T}_1) \tag{2-27}$$

is applicable for each t in the time interval ($t_n \le t \le t_{n+1}$) under consideration. Equation (2-26) may be used to eliminate Q_1 wherever it appears in the above expressions.

In summary, the complete set of equations required to describe the unsteady state operation of a single-effect evaporator follows:

Enthalpy balance:

$$Fh(T_F, X) + V_0 \lambda_0 - V_1 H(\mathscr{T}_1) - L_1 h(\mathscr{T}_1, x_1) = \frac{d[\mathscr{M}_1 h(\mathscr{T}_1, x_1]}{dt}$$

Heat transfer rate:

$$U_1 A_1(T_0 - \mathscr{T}_1) - V_0 \lambda_0 = 0$$

Mass equilibrium:

$$m(x_1)T_1 + b(x_1) - \mathscr{T}_1 = 0 \tag{2-28}$$

Component-mass balance:

$$FX - L_1 x_1 = \frac{d(\mathscr{M}_1 x_1)}{dt}$$

Total-mass balance:

$$F - V_1 - L_1 = \frac{d\mathscr{M}_1}{dt}$$

The variable Q_1 was eliminated wherever it appeared in the above equations through the use of Eq. (2-26).

Solution of a Steady State Evaporator Problem

Since the initial condition of the unsteady state evaporator problem considered in a subsequent section is the steady state solution, it is informative to examine the steady state equations which are obtained by setting the time derivatives in Eq. (2-28) equal to zero. The following example illustrates the use of the steady state equations.

Example 2-1 A single-effect evaporator is to be designed to concentrate a 20 percent (by weight) solution of sodium hydroxide to a 50 percent solution (see Fig. 2-6). The dilute solution (the feed) at 200°F is to be fed to the evaporator at the rate of 50 000 lb/h. For heating purposes, saturated steam at 350°F is used. Sufficient condenser area is available to maintain a pressure of 0.9492 lb/in^2 (absolute) in the vapor space of the evaporator. On the basis of an overall heat transfer coefficient of 300 Btu/(h · ft^2 · °F), compute (*a*) the heating area required, and (*b*) the steam consumption and the steam economy.

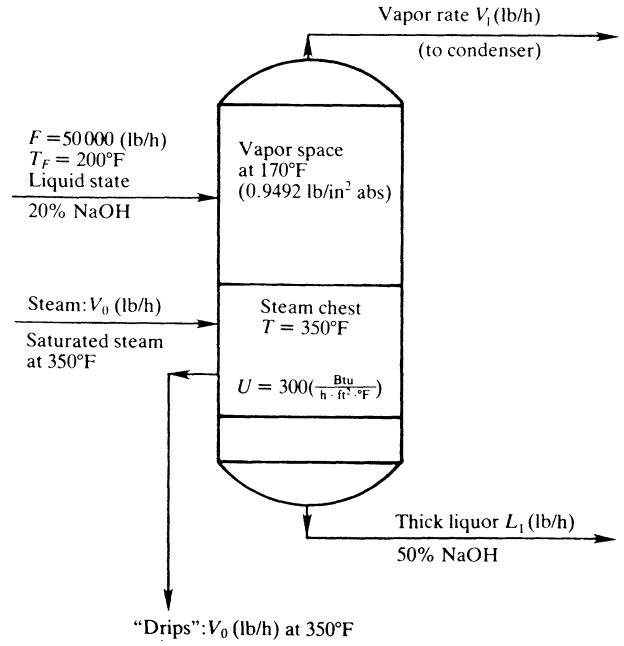

Figure 2-6 Design specifications for Example 2-1.

SOLUTION The rate L_1 at which the thick liquor leaves the evaporator is computed by use of the component-material balance on the solute NaOH

$$L_1 = \frac{FX}{x_1} = \frac{(50\,000)(0.2)}{(0.5)} = 20\,000 \text{ lb/h}$$

The vapor rate V_1 follows by use of the total-material balance

$$V_1 = F - L_1 = 50\,000 - 20\,000 = 30\,000 \text{ lb/h}$$

The boiling point of water at 0.9492 lb/in^2 (abs) is 100°F; see, for example, Keenan and Keyes(12). Use of this temperature and Fig. 2-5 gives a boiling point temperature of 170°F for a 50 percent NaOH solution.

The following enthalpies were taken from Fig. 2-7.

h_F (at 200°F and 20% NaOH) = 145 Btu/lb

h (at 170°F and 50% NaOH) = 200 Btu/lb

From Keenan and Keyes(12)

H (at 170°F and 0.9492 lb/in^2 (abs)) = 1136.94 Btu/lb

λ_0 (saturated at 134.63 lb/in^2 (abs)) = 870.7 Btu/lb at $T_0 = 350$°F

(*a*) Calculation of the heat transfer area A required The rate of heat transfer Q_1 is computed by Eq. (2-23). Solution of the steady state version of Eq. (2-23) for Q_1 gives

$$Q_1 = -Fh_F + V_1 H + L_1 h$$

Elimination of the liquid rate L_1 by use of the material balance $L_1 = F - V_1$ gives the following result upon rearrangment

$$Q_1 = V_1(H - h) - F(h_F - h)$$

Thus

$$Q_1 = (30\,000)(1136.94 - 200) - 50\,000(145 - 200)$$
$$= 30.858 \times 10^6 \text{ Btu/h}$$

Then by use of Eq. (2-27), the area A_1 is computed as follows:

$$A_1 = \frac{Q_1}{U_1(T_0 - \mathscr{T}_1)} = \frac{30.858 \times 10^6}{(300)(350 - 170)} = 571.45 \text{ ft}^2$$

(*b*) Calculation of the steam economy Since $Q_1 = V_0 \lambda_0$, the steam consumption is given by

$$V_0 = \frac{Q_1}{\lambda_0} = \frac{30.858 \times 10^6}{(870.7)} = 35\,440 \text{ lb/h}$$

Then

$$\text{Steam economy} = \frac{V_1}{V_0} = \frac{30\,000}{35\,440} = 0.847$$

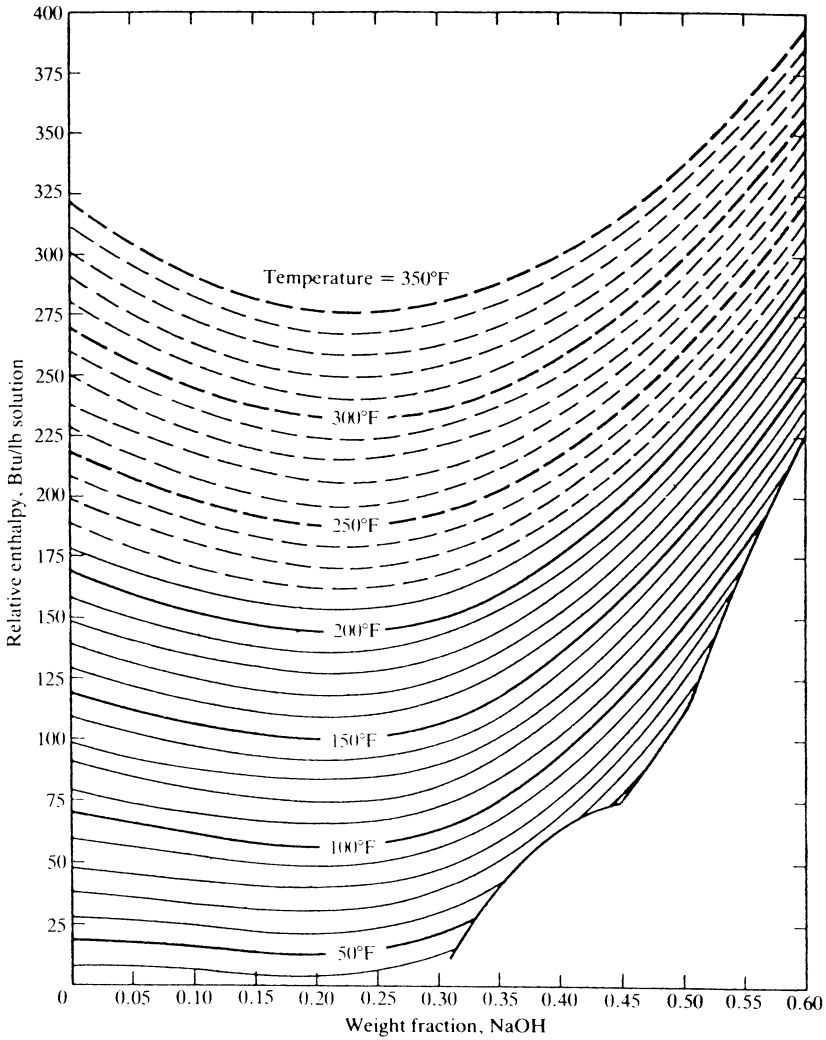

Figure 2-7 Enthalpy concentration chart for solutions of sodium hydroxide in water. (*W. L. McCabe, "The Enthalpy Concentration Chart—A Useful Device for Chemical Engineering Calculations," Trans. Am. Inst. Chem. Engrs., vol. 31, p. 129 (1935), Courtesy American Institute of Chemical Engineers.*)

2-3 SOLUTION OF TRANSIENT EVAPORATOR PROBLEMS BY USE OF THE TWO-POINT IMPLICIT METHOD

This method is applied to each of the integral-difference equations in a manner analogous to that demonstrated for the total material balance, Eq. (2-14). By approximation of the integral of Eq. (2-14) through the use of the two-point implicit method (see Chap. 1), the following result is obtained:

$$F - V_1 - L_1 + \sigma[F - V_1 - L_1]^0 = \frac{\mathscr{M}_1}{\phi\,\Delta t} - \frac{\mathscr{M}_1^0}{\phi\,\Delta t} \tag{2-29}$$

where $\sigma = (1-\phi)/\phi$ and $[\,]^0$ means that all variables contained within the brackets are to be evaluated at the beginning of the time step under consideration. Equation (2-29) is readily rearranged and restated in functional form to give the function f_5 of Eq. (2-30). Functions f_1 and f_4 of Eq. (2-30) were obtained in the same manner as described for the function f_5. The variable Q_1 was eliminated from the functions f_1 and f_2 through the use of the equality, $Q_1 = V_0\lambda_0$ (Eq. (2-26)). Thus

Enthalpy balance:

$$f_1 = Fh(T_F, X) + V_0\lambda_0 - V_1H(\mathscr{T}_1) - L_1h(\mathscr{T}_1, x_1) - \frac{\mathscr{M}_1h(\mathscr{T}_1, x_1)}{\phi\,\Delta t}$$

$$+ \sigma[Fh(T_F, X) + V_0\lambda_0 - V_1H(\mathscr{T}_1) - L_1h(\mathscr{T}_1, x_1)]^0 + \frac{\mathscr{M}_1^0h(\mathscr{T}_1^0, x_1^0)}{\phi\,\Delta t}$$

Heat transfer rate:

$$f_2 = U_1A_1(T_0 - \mathscr{T}_1) - V_0\lambda_0$$

Mass equilibrium:

$$f_3 = m(x_1)T_1 + b(x_1) - \mathscr{T}_1 \tag{2-30}$$

Component-mass balance:

$$f_4 = FX - L_1x_1 - \frac{\mathscr{M}_1x_1}{\phi\,\Delta t} + \sigma[FX - L_1x_1]^0 + \frac{\mathscr{M}_1^0x_1^0}{\phi\,\Delta t}$$

Total-mass balance:

$$f_5 = F - V_1 - L_1 - \frac{\mathscr{M}_1}{\phi\,\Delta t} + \sigma[F - V_1 - L_1]^0 + \frac{\mathscr{M}_1^0}{\phi\,\Delta t}$$

Since the system is described by five independent equations, all of the variables at t_{n+1} must be fixed except for five. It is, of course, supposed that the values of all variables are known at the beginning of the time period under consideration. A problem may be formulated in terms of the values of the variables which are fixed and those which are to be found at time t_{n+1} in the following manner.

Specifications:

$$F,\ X,\ T_F,\ T_0,\ P_1 \text{ (or } T_1\text{), and } \mathscr{M}_1 \text{ at time } t_{n+1}$$

To find:

$$V_1,\ V_0,\ x_1,\ L_1, \text{ and } \mathscr{T}_1 \text{ at time } t_{n+1}$$

This set of specifications corresponds to the case where the variables F, X, T_F, T_0, P_1, and $\mathscr{M}_1$ are either controlled or fixed at some prescribed value at time t_{n+1}. These specified values may differ from those at time t_n. In this analysis, it is also supposed that the overall heat transfer coefficient is a known constant.

The functional expressions (see Eq. (2-30)) may be solved by the Newton–Raphson method for the values of the variables at the end of the time period under consideration. The Newton–Raphson method is represented by

$$\mathbf{J}_k\,\Delta\mathbf{x}_k = -\mathbf{f}_k \tag{2-31}$$

The elements of the column vectors $\mathbf{x}_k$ and $\mathbf{f}_k$ are for convenience displayed in terms of their respective transposes

$$\Delta\mathbf{x}_k = [\Delta V_1\ \ \Delta V_0\ \ \Delta\mathscr{T}_1\ \ \Delta x_1\ \ \Delta L_1]^T \qquad \mathbf{f}_k = [f_1\ \ f_2\ \ f_3\ \ f_4\ \ f_5]^T \tag{2-32}$$

and the jacobian matrix $\mathbf{J}_k$ consists of five rows

$$[\partial f_j/\partial V_1,\ \partial f_j/\partial V_0,\ \ldots,\ \partial f_j/\partial L_1,\ (j = 1, 2, \ldots, 5)]$$

of functional derivatives

$$\mathbf{J}_k = \begin{bmatrix} -H(\mathscr{T}_1) & \lambda_0 & b_{13} & b_{14} & -h(\mathscr{T}_1, x_1) \\ 0 & -\lambda_0 & -U_1A_1 & 0 & 0 \\ 0 & 0 & -1 & b_{34} & 0 \\ 0 & 0 & 0 & -L_1\rho_1 & -x_1 \\ -1 & 0 & 0 & 0 & -1 \end{bmatrix} \tag{2-33}$$

where

$$\rho_1 = 1 + \tau_1/\phi \qquad \tau_1 = \frac{\mathscr{M}_1/L_1}{\Delta t}$$

$$b_{13} = -V_1\frac{\partial H(\mathscr{T}_1)}{\partial\mathscr{T}_1} - L_1\rho_1\frac{\partial h(\mathscr{T}_1, x_1)}{\partial\mathscr{T}_1}$$

$$b_{14} = -L_1\rho_1\frac{\partial h(\mathscr{T}_1, x_1)}{\partial x_1}$$

$$b_{34} = T_1\frac{\partial m(x_1)}{\partial x_1} + \frac{\partial b(x_1)}{\partial x_1}$$

Application of the Newton–Raphson Method

For each time period under consideration (say from t_n to t_{n+1}), the Newton–Raphson procedure consists of the repeated application of the above equations

until the solution set $\mathbf{x}_{n+1}$ at time t_{n+1} has been found. The solution set $\mathbf{x}_{n+1}$ at t_{n+1} becomes the initial set for the next time period (t_{n+1} to t_{n+2}), and the Newton–Raphson procedure is applied successively to determine the solution set $\mathbf{x}_{n+2}$ at time t_{n+2}.

However, before solving a numerical problem involving a single-effect evaporator at unsteady state operation, a simple numerical example is presented in order to demonstrate the application of the Newton–Raphson method (Refs. 5,11).

Example 2-2 Make one trial by the Newton–Raphson method for the set of positive roots which make $f_1(x, y) = f_2(x, y) = 0$.

$$f_1(x, y) = x^2 - y^2 + 1$$

$$f_2(x, y) = x^2 + y^2 - 5$$

For the first set of assumed values of the variables, take $x_1 = 1$, $y_1 = 1$.

SOLUTION

$$f_1(1, 1) = 1 - 1 + 1 = 1$$

$$f_2(1, 1) = 1 + 1 - 5 = -3$$

$$\frac{\partial f_1}{\partial x} = 2x \qquad \frac{\partial f_1}{\partial y} = -2y$$

$$\frac{\partial f_2}{\partial x} = 2x \qquad \frac{\partial f_2}{\partial y} = 2y$$

Then at $x_1 = 1$, $y_1 = 1$, the Newton–Raphson equations, $\mathbf{J}_1 \, \Delta\mathbf{x}_1 = -\mathbf{f}_1$

$$\frac{\partial f_1}{\partial x} \Delta x_1 + \frac{\partial f_1}{\partial y} \Delta y_1 = -f_1$$

$$\frac{\partial f_2}{\partial x} \Delta x_1 + \frac{\partial f_2}{\partial y} \Delta y_1 = -f_2$$

reduce to

$$2\Delta x_1 - 2\Delta y_1 = -1$$

$$2\Delta x_1 + 2\Delta y_1 = 3$$

Solution of these equations for Δx_1 and Δy_1 gives

$$\Delta x_1 = 1/2 \qquad \Delta y_1 = 1$$

Thus, the values of x and y to be used for the next trial are as follows:

$$x_2 = x_1 + \Delta x_1 = 1 + 1/2 = 3/2$$

$$y_2 = y_1 + \Delta y_1 = 1 + 1 = 2$$

On the basis of the assumed values $x_2 = 3/2$ and $y_2 = 2$, the process is repeated to determine x_3 and y_3. Repeated application of this process gives (to within the desired degree of accuracy)

$$x = \sqrt{2} \qquad y = \sqrt{3}$$

Next, an unsteady state evaporator problem is solved by use of the two-point implicit method. The specifications are taken to be the set stated above.

Example 2-3 Initially (at time $t = 0$), the evaporator described in Example 2-1 is at steady state operation at the conditions stated for this example. At time $t = 0+$ an upset in the mass fraction in the feed occurs. The upset consists of a step change in the feed concentration from $X = 0.2$ to $X = 0.24$. It is desired to find the transient values of the variables provided that the steam temperature T_0 is maintained at 350°F and the condenser temperature T_1 is maintained at 100°F. The holdup $\mathcal{M}_1$ is held fixed at 5000 pounds throughout the course of the upset. The heat transfer area A of the evaporator is 475.15 ft^2.

SOLUTION The functional expressions identified as Eq. (2-30) were solved simultaneously for each time period. A value of $\Delta t = 0.001$ h was used for the first 10 time periods. At the end of each set of 10 periods, the value of Δt was doubled. A value of $\phi = 0.6$ was employed. The flow rates were stated relative to the feed rate and the temperature relative to the steam temperature.

Selected transient values of the variables are shown in Table 2-1. The

Table 2-1 Solution of Example 2-3

Values of scaled variables (*Note:* $F = 50\,000$ lb/h, $T_0 = 350$°F)

Cumulative time (h)	V_1/F	V_0/F	$\mathcal{T}_1/T_0$	x_1	L_1/F
0.0	0.599 999	0.708 216	0.486 200	0.499 999	0.400 000
0.001	0.576 702	0.708 068	0.486 307	0.499 925	0.423 298
0.002	0.575 045	0.707 826	0.486 483	0.400 147	0.424 955
0.003	0.575 174	0.707 587	0.486 656	0.500 367	0.424 826
0.010	0.573 934	0.705 956	0.487 840	0.501 863	0.426 066
0.020	0.572 451	0.703 743	0.489 446	0.503 887	0.427 549
0.030	0.570 984	0.701 660	0.490 957	0.505 785	0.429 016
0.050	0.568 349	0.697 864	0.493 710	0.509 224	0.431 651
0.070	0.566 017	0.694 513	0.496 141	0.512 241	0.433 983
0.090	0.564 010	0.691 565	0.498 280	0.514 882	0.435 990
0.180	0.557 534	0.682 150	0.505 111	0.523 227	0.442 466
0.36	0.552 054	0.674 163	0.510 905	0.530 205	0.447 946
0.73	0.549 967	0.671 117	0.513 116	0.532 843	0.450 087
1.68	0.549 782	0.670 849	0.513 309	0.533 074	0.450 218
Final Steady State	0.549 782	0.670 848	0.513 310	0.533 075	0.450 218

values of some of the variables shown at time $t = 0$ differed slightly from those for Example 2-1 because the solution set in this table was obtained by use of curve fits of the data, and seven digits were carried throughout the course of the calculations.

The reciprocal of the τ represents the number of times the holdup $\mathscr{M}_1$ could be swept out at the liquid rate L_1 during a given time period Δt. At the conditions at the end of the first time period

$$1/\tau = \frac{\Delta t}{\mathscr{M}_1/L_1} = \frac{(0.001)(0.423 \times 50\,000)}{5000} = \frac{1}{236}$$

During the last sequence of time steps which contained $t = 1.68$ h (see Table 2-1), a $\Delta t = 0.1$ h was used for which

$$\frac{1}{\tau} \cong \frac{1}{2.2}$$

In the solution of Example 2-3, the Dühring lines shown in Fig. 2-5 were represented by Eq. (2-10) by taking

$$m(x) = 1.0 + 0.141\,952\,6x$$

$$b(x) = 271.3627x^2 - 9.419\,608x$$

Stability Characteristics of the Two-Point Implicit Method for Evaporator Problems

From the stability analysis of systems of linear differential equations, the two-point implicit method is shown to be A stable in Chap. 1, provided that a value of ϕ lying between 1/2 and 1 is used. Also, for $\phi > 1/2$, the two-point implicit method converged for the system of nonlinear differential and algebraic equations required to describe a single-effect evaporator.

If the values of the dependent variables are bounded as the number of time steps is increased indefinitely, the inherited error is also bounded. The inherited error is defined as the correct value of the dependent variable minus the calculated value of the variable at the end of the time period under consideration.

In order to investigate the general case where all of the equations and variables are taken into account, a wide variety of examples were solved for several different types of upsets such as step changes in the feed composition, feed rate, steam temperature, and different combinations of ϕ and Δt. Typical of the results obtained for various types of upsets in the operating conditions were those obtained when Example 2-3 was solved for a variety of combinations of ϕ and Δt.

In the problems in which the inherited error was unbounded, it was characteristic for the liquid rate to commence to oscillate first. For $\phi < 1/2$, all variables were highly unstable as shown by the lower graph in Fig. 2-8. (In these

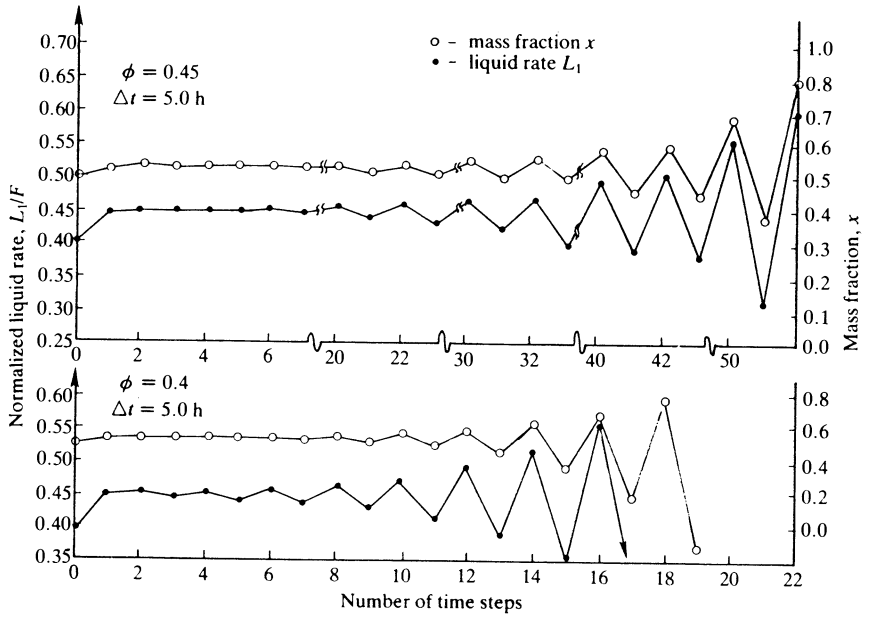

Figure 2-8 Variation of the inherited error for $\phi < 1/2$ for Example 2-3.

graphs the value of τ was computed on the basis of the steady state value of L_1.) However, for this condition ($\phi < 1/2$) the composition x had generally converged to its steady state value before the inherited error in L_1 became unbounded as demonstrated in Figs. 2-8 and 2-9.

The upper graph in Fig. 2-9 is typical of the stability of all variables for all examples for which $1/2 \leq \phi \leq 1$.

Scaling Procedures

Two types of scaling are presented below: (1) variable scaling and row scaling and (2) column scaling and row scaling. The first of these two procedures was used by Burdett(3,4) in the solution of a 17-effect evaporator system described in Chap. 3. The purpose of scaling is to reduce the elements of the jacobian matrix to the same order of magnitude. Also, it is desirable that the functions be of the same order of magnitude in order that the euclidean norm of the functions will represent a measure of how well all functions have been satisfied by the set of assumed values of the variables. For example, consider the equation

$$0 = x - 1$$

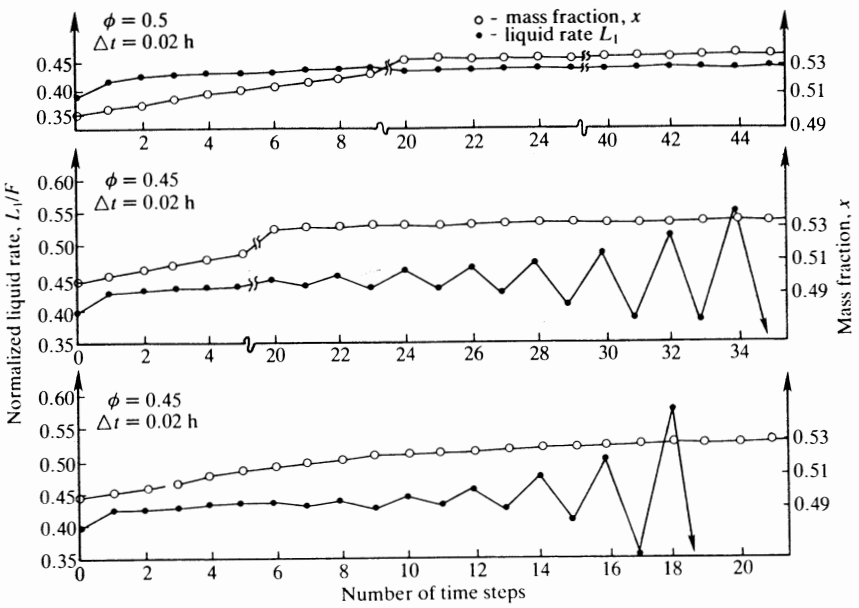

Figure 2-9 Variation of the inherited error for $\phi \leq 1/2$ for Example 2-3.

and let $f_1(x)$ denote the function

$$f_1(x) = x - 1$$

For $x = 1.1$

$$f_1(1.1) = 1.1 - 1 = 0.1$$

Now consider the function

$$0 = y - 1$$

After each side of this equation has been multiplied by 10^6, let $F(y)$ denote the function

$$F(y) = 10^6 y - 10^6$$

For $y = 1.1$

$$F(1.1) = 10^6(1.1) - 10^6 = 0.1 \times 10^6$$

In order to obtain a meaningful comparison of the functional values, it is evident that they should both be normalized, which may be effected in the

above case by division of $F(y)$ by 10^6 followed by the definition of the new function

$$g(y) = F(y)/10^6$$

This procedure amounts to row scaling as described in a subsequent section.

In order to reduce the size of the elements of the jacobian matrix relative to one another, row scaling must be combined with variable scaling. To illustrate variable scaling, reconsider Example 2-3, and let the new scaled variables be defined

$$\begin{aligned} v_0 &= V_0/F \qquad v_1 = V_1/F \qquad l_1 = L_1/F \\ u_1 &= T_1/T_0 \qquad \alpha_1 = \mathscr{T}_1/T_0 \end{aligned} \tag{2-34}$$

such that they lie approximately in the range 0 to 1. Next, make this change of variables in the functions $f_1, f_2, \ldots, f_5$, and then divide f_1 by $F\lambda_0$, f_2 by $F\lambda_0$, f_3 by T_0, f_4 by F, and f_5 by F. Then let

$$\begin{aligned} g_1 &= \frac{h(T_F, X)}{\lambda_0} + v_0 - \frac{v_1 H(\mathscr{T}_1)}{\lambda_0} - \frac{l_1 h(\mathscr{T}_1, x_1)}{\lambda_0} \\ &\quad - \frac{\mathscr{M}_1 h(\mathscr{T}_1, x_1)}{F\lambda_0 \phi\, \Delta t} + \sigma\left[\frac{h(T_F, X)}{\lambda_0} + v_0 - \frac{v_1 H(\mathscr{T})}{\lambda_0} - \frac{l_1 h(\mathscr{T}_1, x_1)}{\lambda_0}\right]^0 \\ &\quad + \frac{\mathscr{M}_1^0 h(\mathscr{T}_1^0, x_1^0)}{F\lambda_0 \phi\, \Delta t} \\ g_2 &= \frac{U_1 A_1 T_0}{F\lambda_0}(1 - \alpha_1) - v_0 \\ g_3 &= m(x_1)u_1 + \frac{b(x_1)}{T_0} - \alpha_1 \\ g_4 &= X - l_1 x_1 - \frac{\mathscr{M}_1 x_1}{F\phi\, \Delta t} + \sigma[X - l_1 x_1]^0 + \frac{\mathscr{M}_1^0 x_1^0}{F\phi\, \Delta t} \\ g_5 &= 1 - v_1 - l_1 - \frac{\mathscr{M}_1}{F\phi\, \Delta t} + \sigma[1 - v_1 - l_1]^0 + \frac{\mathscr{M}_1^0}{F\phi\, \Delta t} \end{aligned} \tag{2-35}$$

Note that several of the above functions could have been reduced to the precise form of $f(x)$ and $g(y)$. For example, g_2 could have been divided by the variable v_0 and g_3 by the variable u_1. However, the resulting functions become undefined when the assumed values for v_0 and v_1 are taken equal to zero, and generally functions possessing such characteristics are to be avoided.

When the functions are given by Eq. (2-35) and the new variables are taken to be

$$\mathbf{x} = [v_1 \quad v_0 \quad \alpha_1 \quad x_1 \quad l_1]^T$$

the jacobian matrix becomes

$$\mathbf{J} = \begin{bmatrix} \dfrac{-H(\mathscr{T}_1)}{\lambda_0} & 1 & b_{13} & b_{14} & \dfrac{-h(\mathscr{T}_1, x_1)}{\lambda_0} \\ 0 & -1 & \dfrac{-U_1 A_1 T_0}{F\lambda_0} & 0 & 0 \\ 0 & 0 & -1 & b_{34} & 0 \\ 0 & 0 & 0 & -l_1\rho_1 & -x_1 \\ -1 & 0 & 0 & 0 & -1 \end{bmatrix} \tag{2-36}$$

where

$$\rho_1 = 1 + \tau_1/\phi \qquad \tau_1 = \frac{\mathscr{M}_1/L_1}{\Delta t}$$

$$b_{13} = \frac{1}{\lambda_0}\left[-v_1 \frac{\partial H(\mathscr{T}_1)}{\partial \mathscr{T}_1} - l_1\rho_1 \frac{\partial h(\mathscr{T}_1, x_1)}{\partial \mathscr{T}_1}\right]\frac{\partial \mathscr{T}_1}{\partial \omega_1}$$

$$\frac{\partial \mathscr{T}_1}{\partial \omega_1} = T_0$$

$$b_{14} = \frac{-l_1\rho_1}{\lambda_0}\frac{\partial h(\mathscr{T}_1, x_1)}{\partial x_1}$$

$$b_{34} = u_1 \frac{\partial m(x_1)}{\partial x_1} + \frac{1}{T_0}\frac{\partial b(x_1)}{\partial x_1}$$

To demonstrate the effect of variable scaling followed by row scaling on the relative size of the elements of **J**, the following elements are evaluated at the solution values of the variables

Unscaled	*Variable and row scaling*
$U_1 A_1 = (300)(457.15)$	$\dfrac{U_1 A_1 T_0}{F\lambda_0} = \dfrac{(300)(457.15)(350)}{(50\,000)(870.7)}$
$= 137\,145$	$= 1.102$
$H(\mathscr{T}_1) = 1140$	$\dfrac{H(\mathscr{T}_1)}{\lambda_0} = \dfrac{1140}{870.7} = 1.309$

The above procedure may be generalized and stated in matrix notation as shown below.

Variable Scaling and Row Scaling

Consider the general case in which n independent functions $f_1, f_2, \ldots, f_n$ in n independent variables $x_1, x_2, \ldots, x_n$ are to be solved by the Newton–Raphson method. Let the Newton–Raphson equations for the kth trial be represented by

$$\mathbf{J}_k\,\Delta\mathbf{x}_k = -\mathbf{f}_k \tag{2-37}$$

where

$$\mathbf{J}_k = \begin{bmatrix} \dfrac{\partial f_1}{\partial x_1} & \cdots & \dfrac{\partial f_1}{\partial x_n} \\ \vdots & & \vdots \\ \dfrac{\partial f_n}{\partial x_1} & \cdots & \dfrac{\partial f_n}{\partial x_n} \end{bmatrix}$$

$$\Delta\mathbf{x}_k = [\Delta x_1 \;\; \Delta x_2 \;\cdots\; \Delta x_k]^T \qquad \Delta\mathbf{x}_k = \mathbf{x}_{k+1} - \mathbf{x}_k$$

$$\mathbf{f}_k = [f_{1k} \;\; f_{2k} \;\cdots\; f_{nk}]^T$$

Although the subscript k is not shown on the elements in $\mathbf{J}_k$, these elements as well as the functions $\mathbf{f}_k$ are to be evaluated at $\mathbf{x} = \mathbf{x}_k$.

Let $\mathbf{R}_k$ denote the square $n \times n$ diagonal matrix whose diagonal elements r_{ii} are equal to or just greater than the absolute value of the corresponding row elements of $\mathbf{x}_k$, that is,

$$r_{11} \geq |x_{1k}| \qquad r_{22} \geq |x_{2k}|, \ldots, r_{nn} \geq |x_{nk}| \tag{2-38}$$

(Except for the restriction that r_{ii} must never be set equal to zero, the inequality given by Eq. (2-38) need not be applied precisely in practice; that is, the r_{ii}'s need to be only approximately equal to the corresponding x_{ik}'s.) The row operations required to scale $\Delta\mathbf{x}_k$ may be represented by the matrix multiplication $\mathbf{R}_k^{-1}\,\Delta\mathbf{x}_k$. Thus, Eq. (2-37) may be restated in the following equivalent form:

$$\mathbf{J}_k\mathbf{R}_k\mathbf{R}_k^{-1}\,\Delta\mathbf{x}_k = -\mathbf{f}_k \tag{2-39}$$

or

$$\mathbf{D}_k\,\Delta\mathbf{Y}_k = -\mathbf{f}_k \tag{2-40}$$

where

$$\Delta\mathbf{Y}_k = \mathbf{R}_k^{-1}\,\Delta\mathbf{x}_k$$

$$\mathbf{D}_k = \mathbf{J}_k\mathbf{R}_k$$

Observe that $\mathbf{J}_k\mathbf{R}_k$ corresponds to the set of column operations in which column 1 is multiplied by r_{11}, column 2 by r_{22}, ..., and column n by r_{nn}. After these column operations have been performed, form the diagonal matrix $\mathbf{M}_k$ whose elements m_{ii} are selected such that for each row

$$m_{ii} = \text{maximum } |d_{ij}| \text{ over all elements of row } i$$

Premultiplication of each side of Eq. (2-40) by $\mathbf{M}_k^{-1}$ yields

$$\mathbf{M}_k^{-1}\mathbf{D}_k\,\Delta\mathbf{Y}_k = -(\mathbf{M}_k^{-1}\mathbf{f}_k) \tag{2-41}$$

or

$$\mathbf{E}_k \, \Delta\mathbf{Y}_k = -\mathbf{F}_k \tag{2-42}$$

where

$$\mathbf{E}_k = \mathbf{M}_k^{-1}\mathbf{D}_k$$

$$\mathbf{F}_k = \mathbf{M}_k^{-1}\mathbf{f}_k$$

Observe that the matrix multiplication $\mathbf{M}_k^{-1}\mathbf{D}_k$ corresponds to the set of row operations in which row 1 is divided by m_{11}, row 2 is divded by m_{22}, ..., and row n is divided by m_{nn}. Likewise, $\mathbf{M}_k^{-1}\mathbf{f}_k$ represents a set of row operations in which the first element is divided by m_{11}, ..., and the nth element is divided by m_{nn}.

Although the development of the above scaling procedure was presented in terms of matrix multiplications, one always obtains the final results in practice by carrying out the appropriate row or column operations rather than the matrix multiplications.

Column Scaling and Row Scaling

In this scaling procedure, the first step consists of the column scaling of the jacobian matrix in which the elements of each column are divided by the element of the respective column which is greatest in absolute value. Let $\mathbf{D}_k$ denote the diagonal matrix which contains the reciprocals of the elements of the respective columns which are largest in absolute value, and let $\{a_{ij}\}$ denote the elements of $\mathbf{J}_k$. The elements $\{d_{ii}\}$ of $\mathbf{D}_k$ are as follows:

$$d_{11} = 1/[\text{maximum } |a_{i1}| \text{ of column 1 of } \mathbf{J}_k]$$

$$d_{22} = 1/[\text{maximum } |a_{i2}| \text{ of column 2 of } \mathbf{J}_k]$$

$$\vdots \qquad\qquad \vdots$$

$$d_{nn} = 1/[\text{maximum } |a_{in}| \text{ of column } n \text{ of } \mathbf{J}_k]$$

Thus

$$(\mathbf{J}_k \mathbf{D}_k)(\mathbf{D}_k^{-1} \, \Delta\mathbf{x}_k) = -\mathbf{f}_k \tag{2-43}$$

Next row scaling is performed on the matrix $\mathbf{J}_k\mathbf{D}_k$. Let $\mathbf{E}_k$ denote the diagonal matrix which contains the reciprocals of the elements of the respective rows which are largest in absolute value, and let b_{ij} denote the elements of $\mathbf{J}_k\mathbf{D}_k$. The elements $\{e_{ii}\}$ of $\mathbf{E}_k$ are as follows:

$$e_{11} = 1/(\text{maximum } b_{1j} \text{ of row 1 of } \mathbf{J}_k\mathbf{D}_k)$$

$$e_{22} = 1/(\text{maximum } b_{2j} \text{ of row 2 of } \mathbf{J}_k\mathbf{D}_k)$$

$$\vdots \qquad\qquad \vdots$$

$$e_{nn} = 1/(\text{maximum } b_{nj} \text{ of row } n \text{ of } \mathbf{J}_k\mathbf{D}_k)$$

Thus, the row scaling of $\mathbf{J}_k\mathbf{D}_k$ is represented by

$$(\mathbf{E}_k\mathbf{J}_k\mathbf{D}_k)(\mathbf{D}_k^{-1} \, \Delta\mathbf{x}_k) = -\mathbf{E}_k\mathbf{f}_k \tag{2-44}$$

and

$$\Delta\mathbf{x}_k = -\mathbf{D}_k(\mathbf{E}_k\mathbf{J}_k\mathbf{D}_k)^{-1}\mathbf{E}_k\mathbf{f}_k \tag{2-45}$$

In a problem solved by Mommessin(15), variable scaling followed by row scaling was unsatisfactory, and it was necessary to use column scaling followed by row scaling.

Application of Broyden's Method

In many applications, the programming of the analytical expressions for the partial derivatives appearing in the jacobian matrix of the Newton–Raphson method becomes a cumbersome task, and the numerical evaluation of these derivatives for each trial becomes too time-consuming. In order to reduce the time requirement Broyden's method (Refs. 2, 11), which seldom requires more than one numerical evaluation of the partial derivatives, may be used. The development of this method is presented in Ref. 11, and the steps to be followed in the application of the method are enumerated below.

For the general case of n independent equations in n unknowns, the Newton–Raphson method is represented by Eq. (2-31) where

$$\mathbf{J}_k = \begin{bmatrix} \dfrac{\partial f_1}{\partial x_1} & \dfrac{\partial f_1}{\partial x_2} & \cdots & \dfrac{\partial f_1}{\partial x_n} \\ \vdots & \vdots & & \vdots \\ \dfrac{\partial f_n}{\partial x_1} & \dfrac{\partial f_n}{\partial x_2} & \cdots & \dfrac{\partial f_n}{\partial x_n} \end{bmatrix} \tag{2-46}$$

$$\mathbf{x}_k = [x_1 \quad x_2 \quad \cdots \quad x_n]^T \tag{2-47}$$

$$\mathbf{f}_k = [f_1 \quad f_2 \quad \cdots \quad f_n]^T \tag{2-48}$$

The steps of the algorithm are as follows:

Step 1 Assume an initial set of values of the variables $\mathbf{x}_0$, and compute $\mathbf{f}_0(\mathbf{x}_0)$.

Step 2 Approximate the elements of $\mathbf{H}_0$ where $\mathbf{H}_0$ is defined as follows:

$$\mathbf{H}_0 = -\mathbf{J}_0^{-1}$$

Broyden obtained a first approximation of the elements of $\mathbf{J}_0$ by use of the formula

$$\frac{\partial f_i}{\partial x_j} \cong \frac{f_i(x_j + h_j) - f_i(x_j)}{h_j}$$

where h_j was taken to be equal to $0.001x_j$.

Step 3 On the basis of the most recent values of $\mathbf{H}$ and $\mathbf{f}$, say $\mathbf{H}_k$ and $\mathbf{f}_k$, compute

$$\Delta\mathbf{x}_k = \mathbf{H}_k\mathbf{f}_k$$

Step 4 Find the s_k such that the euclidean norm of $\mathbf{f}(\mathbf{x}_k + s_k\,\Delta\mathbf{x}_k)$ is less than that of $\mathbf{f}(\mathbf{x}_k)$. First try $s_{k,1} = 1$ and if the following inequality is satisfied

$$\left[\sum_{i=1}^{n} f_i^2(\mathbf{x}_k + s_k\,\Delta\mathbf{x}_k)\right]^{1/2} < \left[\sum_{i=1}^{n} f_i^2(\mathbf{x}_k)\right]^{1/2}$$

proceed to step 5. Otherwise, compute $s_{k,2}$ by use of the following formula which was developed by Broyden:

$$s_{k,2} = \frac{(1+6\eta)^{1/2} - 1}{3\eta}$$

where

$$\eta = \frac{\sum_{i=1}^{n} f_i^2(\mathbf{x}_k + s_k\,\Delta\mathbf{x}_k)}{\sum_{i=1}^{n} f_i^2(\mathbf{x}_k)}$$

If the norm is not reduced by use of $s_{k,2}$ after a specified number of trials through the complete procedure, return to step 2 and reevaluate the partial derivatives of $\mathbf{J}_k$ on the basis of $\mathbf{x}_k$. As pointed out by Broyden, other methods for picking s_k may be used. For example, s_k may be picked such that the euclidean norm is minimized.

Step 5 In the course of making the calculations in step 4, the following vectors will have been evaluated:

$$\mathbf{x}_{k+1} = \mathbf{x}_k + s_k\,\Delta\mathbf{x}_k$$
$$\mathbf{f}_{k+1} = \mathbf{f}(\mathbf{x}_{k+1})$$

Test $\mathbf{f}_{k+1}$ for convergence. If convergence has not been achieved, compute

$$\mathbf{Y}_k = \mathbf{f}_{k+1} - \mathbf{f}_k$$

Step 6 Compute

$$\mathbf{H}_{k+1} = \mathbf{H}_k - \frac{(\mathbf{H}_k\mathbf{Y}_k + s_k\,\Delta\mathbf{x}_k)\,\Delta\mathbf{x}_k^T\mathbf{H}_k}{\Delta\mathbf{x}_k^T\mathbf{H}_k\mathbf{Y}_k}$$

and return to step 3.

Example 2-4 consists of a simple algebraic example which illustrates the application of this method.

Example 2-4 (Hess et al.(9), by courtesy *Hydrocarbon Processing*). It is desired to find the pair of positive roots that make $f_1(x, y) = 0$ and $f_2(x, y) = 0$, simultaneously

$$f_1(x, y) = x^2 - xy^2 - 2$$
$$f_2(x, y) = 2x^2 - 3xy^2 + 3$$

Take $x_0 = 1$ and $y_0 = 1$, and make one complete trial calculation as prescribed by steps 1 through 6.

SOLUTION

Step 1 Since $x_0 = 1$, $y_0 = 1$

$$\mathbf{x}_0 = [1, 1]^T$$

and

$$f_{1,0} = f_1(\mathbf{x}_0) = f_1(1, 1) = 1 - 1 - 2 = -2$$
$$f_{2,0} = f_2(\mathbf{x}_0) = f_2(1, 1) = 2 - 3 + 3 = 2$$

Step 2 Take the increment h for computing the derivatives with respect to x to be

$$h = (0.001)x_0 = 0.001$$

Then

$$\frac{\partial f_1}{\partial x} = \frac{f_1(1.001, 1) - f_1(1, 1)}{0.001} = 1.001$$

For computing the derivatives with respect to y, take

$$h = (0.001)y_0 = 0.001$$

Then

$$\frac{\partial f_1}{\partial y} = \frac{f_1(1, 1.001) - f_1(1, 1)}{0.001} = -2.001$$

and

$$\frac{\partial f_2}{\partial x} = \frac{f_2(1.001, 1) - f_2(1, 1)}{0.001} = 1.002$$

$$\frac{\partial f_2}{\partial y} = \frac{f_2(1, 1.001) - f_2(1, 1)}{0.001} = -6.003$$

Then

$$\mathbf{J}_0 = \begin{bmatrix} 1.001 & -2.001 \\ 1.002 & -6.003 \end{bmatrix}$$

The inverse of $\mathbf{J}_0$ is found by gaussian elimination as follows. Begin with

$$\begin{bmatrix} 1.001 & -2.001 \\ 1.002 & -6.003 \end{bmatrix} \Bigg| \begin{bmatrix} 1 & 0 \\ 0 & 1 \end{bmatrix}$$

and carry out the necessary row operations to obtain

$$\begin{bmatrix} 1 & 0 \\ 0 & 1 \end{bmatrix} \Bigg| \begin{bmatrix} 1.499\,2 & -0.499\,75 \\ 0.250\,23 & -0.250\,00 \end{bmatrix}$$

Then

$$\mathbf{J}_0^{-1} = \begin{bmatrix} 1.499\,2 & -0.499\,75 \\ 0.250\,23 & -0.250\,00 \end{bmatrix}$$

and

$$\mathbf{H}_0 = -\mathbf{J}_0^{-1} = \begin{bmatrix} -1.499\,2 & 0.499\,75 \\ -0.250\,23 & 0.250\,00 \end{bmatrix}$$

Step 3 On the basis of the most recent values $\mathbf{H}$ and $\mathbf{f}$, the correction $\Delta\mathbf{x}$ is computed as follows:

$$\Delta\mathbf{x}_0 = \mathbf{H}_0\mathbf{f}_0 = \begin{bmatrix} -1.499\,2 & 0.499\,75 \\ -0.250\,23 & 0.250\,00 \end{bmatrix} \begin{bmatrix} -2 \\ 2 \end{bmatrix} = \begin{bmatrix} 3.9979 \\ 1.0005 \end{bmatrix}$$

Step 4 Take $s_{0,1} = 1$. Then

$$\mathbf{x}_0 + \Delta\mathbf{x}_0 = \begin{bmatrix} 1 \\ 1 \end{bmatrix} + \begin{bmatrix} 3.9979 \\ 1.0005 \end{bmatrix} = \begin{bmatrix} 4.9979 \\ 2.0005 \end{bmatrix}$$

and

$$f_1(\mathbf{x}_0 + \Delta\mathbf{x}_0) = f_1(4.9979,\ 2.0005) = 2.9774$$

$$f_2(\mathbf{x}_0 + \Delta\mathbf{x}_0) = f_2(4.9979,\ 2.0005) = -7.0468$$

Since

$$(2.9774)^2 + (-7.0468)^2 > (-2)^2 + (2)^2$$

compute

$$\eta = \frac{f_1^2(\mathbf{x}_0 + \Delta\mathbf{x}_0) + f_2^2(\mathbf{x}_0 + \Delta\mathbf{x}_0)}{f_1^2(\mathbf{x}_0) + f_2^2(\mathbf{x}_0)} = \frac{(2.9774)^2 + (-7.0468)^2}{(-2)^2 + (2)^2} = 7.315\,29$$

and

$$s_{0,2} = \frac{(1 + 6\eta)^{1/2} - 1}{3\eta} = 0.259\,74$$

Then

$$\mathbf{x}_0 + 0.259\,74\,\Delta\mathbf{x}_0 = \begin{bmatrix} 1 \\ 1 \end{bmatrix} + \begin{bmatrix} 1.038\,39 \\ 0.259\,865 \end{bmatrix} = \begin{bmatrix} 2.038\,39 \\ 1.259\,865 \end{bmatrix}$$

and

$$f_1(\mathbf{x}_0 + s_{0,2}\,\Delta\mathbf{x}_0) = f_1(2.038\,39,\ 1.259\,865) = -1.080\,40$$

$$f_2(\mathbf{x}_0 + s_{0,2}\,\Delta\mathbf{x}_0) = f_2(2.038\,39,\ 1.259\,865) = 1.603\,72$$

Thus, the criterion on $\mathbf{f}_k$, namely,

$$(-1.080\,40)^2 + (1.6037)^2 < (-2)^2 + (2)^2$$

has been satisfied.

Step 5 If the convergence criterion is taken to be that the sum of the squares of f_1 and f_2 is to be reduced to some small preassigned number ε, say $\varepsilon = 10^{-10}$, then this criterion has not been satisfied by $x = 2.0384$ and $y = 1.259\,86$. Then compute

$$\mathbf{Y}_0 = \mathbf{f}_1 - \mathbf{f}_0 = \begin{bmatrix} -1.080\,40 \\ 1.603\,72 \end{bmatrix} - \begin{bmatrix} -2 \\ 2 \end{bmatrix} = \begin{bmatrix} 0.919\,60 \\ -0.396\,28 \end{bmatrix}$$

Step 6 Compute the following products which are needed to find $\mathbf{H}_1$:

$$\mathbf{H}_0\mathbf{Y}_0 = \begin{bmatrix} -1.499\,2 & 0.499\,75 \\ -0.250\,23 & 0.250\,00 \end{bmatrix} \begin{bmatrix} 0.919\,60 \\ -0.396\,28 \end{bmatrix} = \begin{bmatrix} -1.576\,5 \\ -0.329\,18 \end{bmatrix}$$

$$\Delta\mathbf{x}_0^T\mathbf{H}_0 = [3.9979,\ 1.0005] \begin{bmatrix} -1.499\,2 & 0.499\,75 \\ -0.250\,23 & 0.250\,00 \end{bmatrix} = [-6.2440,\ 2.2481]$$

$$\mathbf{H}_0\mathbf{Y}_0 + s_{0,2}\,\Delta\mathbf{x}_0 = \begin{bmatrix} -1.576\,7 \\ -0.329\,18 \end{bmatrix} + \begin{bmatrix} 1.038\,39 \\ 0.259\,865 \end{bmatrix} = \begin{bmatrix} -0.538\,31 \\ -0.069\,31 \end{bmatrix}$$

$$\Delta\mathbf{x}_0^T\mathbf{H}_0\mathbf{Y}_0 = [-6.2440,\ 2.2481] \begin{bmatrix} 0.919\,60 \\ -0.396\,28 \end{bmatrix} = -6.6328$$

Since

$$\mathbf{H}_1 = \mathbf{H}_0 - \frac{(\mathbf{H}_0\mathbf{Y}_0 + s_0\,\Delta\mathbf{x}_0)\,\Delta\mathbf{x}_0^T\mathbf{H}_0}{\Delta\mathbf{x}_0^T\mathbf{H}_0\mathbf{Y}_0}$$

it follows that

$$\mathbf{H}_1 = \begin{bmatrix} -1.499\,2 & 0.499\,75 \\ -0.250\,23 & 0.250\,00 \end{bmatrix} - \begin{bmatrix} -0.506\,74 & 0.182\,45 \\ -0.065\,25 & 0.023\,491 \end{bmatrix}$$

$$= \begin{bmatrix} -0.992\,46 & 0.317\,30 \\ -0.184\,98 & 0.226\,51 \end{bmatrix}$$

and the next trial is commenced by returning to step 3 with $\mathbf{H}_1$.

A modest improvement of Broyden's method may be achieved by combining it with Bennett's method (Ref. 1) as described by Holland(11).

2-4 EQUATIONS FOR A TRIPLE-EFFECT EVAPORATOR SYSTEM

A typical triple-effect evaporator system with forward feed is shown in Fig. 2-10. Multiple-effect evaporator systems are attractive because in an idealized system of N evaporators in which all of the latent heats are equal and boiling point elevations and sensible heat differences are negligible, N pounds of water may be evaporated per pound of steam fed to the system.

The equations describing the triple-effect system shown in Fig. 2-10 are formulated in a manner analogous to those shown for the single-effect system.

1st effect:

(see the five equations given by Eq. (2-28))

2nd effect:

$$L_1 h(\mathscr{T}_1, x_1) + V_1[H(\mathscr{T}_1) - h(T_1)] - V_2 H(\mathscr{T}_2) - L_2 h(\mathscr{T}_2, x_2) = \frac{d[\mathscr{M}_2 h(\mathscr{T}_2, x_2)]}{dt}$$

$$U_2 A_2(T_1 - \mathscr{T}_2) - V_1[H(\mathscr{T}_1) - h(T_1)] = 0$$

$$m(x_2)T_2 + b(x_2) - \mathscr{T}_2 = 0$$

$$L_1 x_1 - L_2 x_2 = \frac{d(\mathscr{M}_2 x_2)}{dt}$$

$$L_1 - V_2 - L_2 = \frac{d\mathscr{M}_2}{dt}$$

3rd effect:

$$L_2 h(\mathscr{T}_2, x_2) + V_2[H(\mathscr{T}_2) - h(T_2)] - V_3 H(\mathscr{T}_3) - L_3 h(\mathscr{T}_3, x_3) = \frac{d[\mathscr{M}_3 h(\mathscr{T}_3, x_3)]}{dt}$$

$$U_3 A_3(T_2 - \mathscr{T}_3) - V_2[H(\mathscr{T}_2) - h(\mathscr{T}_2)] = 0$$

$$m(x_3)T_3 + b(x_3) - \mathscr{T}_3 = 0$$

$$L_2 x_2 - L_3 x_3 = \frac{d(\mathscr{M}_3 x_3)}{dt}$$

$$L_2 - V_3 - L_3 = \frac{d\mathscr{M}_3}{dt}$$

The dynamic equations for a multiple-effect evaporator system may be solved by a variety of methods such as the two-point implicit method, Michelsen's semi-implicit Runge–Kutta method (Ref. 14), and Gear's method (Ref. 7). The two-point implicit method is demonstrated for a 17-effect system in the next chapter. The application of Michelsen's method and Gear's methods to distillation problems are presented in Chaps. 6, 7, and 8.

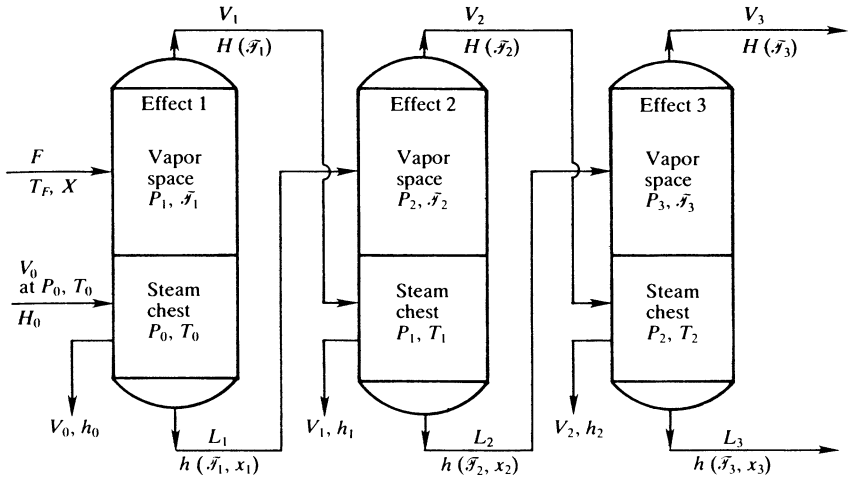

Figure 2-10 A triple-effect evaporator with forward feed. The temperature distribution is shown for a system with boiling point elevations.

In summary, the integral difference equations for evaporators may be solved by use of the two-point implicit method. To solve the system of equations for this process, either the Newton–Raphson method or the Broyden modification of it may be used. Scaling of these equations will generally be necessary and two scaling procedures have been presented for this purpose. As demonstrated by a simple example, the implicit method is stable provided that the weight factor $\phi \geq 1/2$.

NOTATION

$b(x_j)$ = intercept of that Dühring line having as its concentration parameter the variable x_j

$\mathbf{f}_k$ = column vector of the N functions $f_1, f_2, \ldots, f_N$

F = feed rate to the evaporator system, lb/h

$h(T_j)$, $h(\mathscr{T}_j)$ = enthalpy of the pure solvent in the liquid state at the temperatures T_j and $\mathscr{T}_j$, respectively, and pressure P_j, Btu/lb (where boiling point elevations are negligible, the notation h_j, which is equal to $h(T_j)$, is used)

$H(T_j)$, $H(\mathscr{T}_j)$ = same as above except the capital H denotes the vapor state

$h(\mathscr{T}_j, x_j)$ = enthalpy of the thick liquid at temperature $\mathscr{T}_j$, composition x_j and pressure P_j, Btu/lb

$h(T_F, X)$ = enthalpy of the feed at its entering temperature, pressure, and composition, Btu/lb (where boiling point elevations are negligible, the enthalpy of the feed is denoted by h_F)

$\mathbf{H}$ = $-\mathbf{J}^{-1}$

$\mathbf{J}$ = jacobian matrix; defined beneath Eq. (2-37).

l_j = L_j/F

$m(x_j)$ = slope of that Dühring line having as its concentration parameter the variable x_j

$\mathscr{M}_j$ = mass holdup of liquid in evaporator effect j, lb

P_j = total pressure in evaporator j

Q_j = rate of heat transfer for evaporator effect j, Btu/h

t_n = time at the end of the nth time period; $\Delta t = t_{n+1} - t_n$

T_F, T_0 = temperature of the feed and steam, respectively, to an evaporator

T_j = saturation temperature at the pressure P_j of the vapor leaving the jth effect of a multiple-effect evaporator system

$\mathscr{T}_j$ = temperature of the thick liquor leaving the jth effect

$\mathscr{u}$ = $\mathscr{T}/T_0$

u = T/T_0

v_j = V_j/F

V_j = mass flow rate of the vapor from the jth effect of a multiple-effect evaporator system

x_j = mass fraction of the solute in the thick liquor leaving effect j

$\mathbf{x}_k$ = column vector of the values of the variables used to make kth trial

$\Delta\mathbf{x}_k$ = column vector; $\Delta\mathbf{x}_k = \mathbf{x}_{k+1} - \mathbf{x}_k$

$\mathbf{x}^T$ = transpose of the column matrix $\mathbf{x}$

Subscripts

j = evaporator effect j

k, n = counting integers

Greek letters

γ = thermodynamic activity coefficient

ρ_j = $1 + \tau_j/\phi$

σ = $(1 - \phi)/\phi$

λ_j = $H_i - h_j$, latent heat of vaporization of the pure solvent at its saturation temperature T_j and pressure P_j

ϕ = weight factor of the two-point implicit method

r = $\dfrac{\mathscr{M}_j/L_j}{\Delta t}$

REFERENCES

1. J. M. Bennett: "Triangular Factors of Modified Matrices," *Numerische Mathematik*, **7**:217 (1965).
2. C. G. Broyden: "A Class of Methods for Solving Nonlinear Simultaneous Equations," *Math. Comput.*, **19**:577 (1965).
3. J. W. Burdett and C. D. Holland: "Dynamics of a Multiple-Effect Evaporator System," *AIChE J.*, **17**(5):1080 (1971).
4. J. W. Burdett: Ph.D. dissertation, Texas A&M University, College Station, TX, 1970.
5. B. Carnahan, H. A. Luther, and J. O. Wilkes: *Applied Numerical Methods*, John Wiley & Sons, New York, 1969.
6. Kenneth Denbigh: *The Principles of Chemical Equilibrium*, Cambridge University Press, New York, 1955.
7. C. W. Gear: "Simultaneous Numerical Solution of Differential-Algebraic Equations," *IEEE Trans. Circuit Theory*, **18**(1):89 (1971).
8. A. Gerlack: "Ueber Siedetemperaturen der Salzosungeen and Vergleiche der Eihohung der Siedetemperaturen Mit der Ubrigen Eigenschafter der Salzosungen," *Z. Anal. Chem.*, **26**:412 (1887).
9. F. E. Hess, C. D. Holland, Ron McDaniel, and N. J. Tetlow: "Solve More Distillation Problems, Part 8—Which Method to Use," *Hydrocarbon Process.*, **56**(6):181 (1977).
10. C. D. Holland: *Fundamentals and Modeling of Separation Processes: Absorption, Distillation, Evaporation, and Extraction*, Prentice-Hall, Inc., Englewood Cliffs, N.J., 1974.
11. C. D. Holland: *Fundamentals of Multicomponent Distillation*, McGraw-Hill Book Company, New York, 1981.
12. J. H. Keenan and F. G. Keyes: *Thermodynamic Properties of Steam*, John Wiley & Sons, New York, 1936.
13. W. L. McCabe: "The Enthalpy Concentration Chart—A Useful Device for Chemical Engineering Calculations," *Trans. Am. Inst. Chem. Eng.*, **31**:129 (1935).
14. M. L. Michelsen: "Application of the Semi-implicit Runge-Kutta Methods for Integration of Ordinary and Partial Differential Equations," *Chem. Eng. J.*, **14**:107 (1977).
15. P. E. Mommessin, G. W. Bentzen, and C. D. Holland: "Solve More Distillation Problems, Part 10—Another Way to Handle Reactions," *Hydrocarbon Process.*, **59**(7):144 (1980).

PROBLEMS

2-1 Consider the triple-effect evaporator system shown in Fig. 2-4 in which the boiling point elevations are negligible. The system is at steady state operation.

(*a*) If the sensible heat effects are negligible, $h_0 = h_1 = h_2 = h_3$ and $H_0 = H_1 = H_2 = H_3$, show that

$$V_0 = V_1 = V_2 = V_3$$

$$Q_1 = Q_2 = Q_3$$

(*b*) If in addition to part (*a*), $A_1 = A_2 = A_3$ and $U_1 = U_2 = U_3$, show that the *steam economy* is equal to 3.

2-2 Verify the expressions given for the elements appearing in the jacobian matrix given by Eq. (2-33).

2-3 Repeat Prob. 2-2 for the jacobian matrix given by Eq. (2-36).

2-4 If in the procedure called *variable scaling and row scaling* the elements of diagonal matrix $\mathbf{R}$ are taken to be $r_{11} = F$, $r_{22} = F$, $r_{33} = T_0$, $r_{44} = 1$, $r_{55} = F$, and if instead of using the elements of $\mathbf{D}$ which are largest in absolute value the following elements are used in the diagonal matrix $\mathbf{M}$, $m_{11} = F\lambda_0$, $m_{22} = F\lambda_0$, $m_{33} = T_0$, $m_{44} = F$, $m_{55} = F$, show that if one carries out the matrix operations on Eq. (2-31) one obtains the results given by Eqs. (2-34) through (2-36).

CHAPTER

THREE

DYNAMICS OF A MULTIPLE-EFFECT EVAPORATOR SYSTEM

The formulation and testing of a model for a relatively large process, a 17-effect evaporator system, is given in this chapter. The model proposed for each part of this system is presented and the corresponding equations are developed. Modeling techniques utilized in the modeling of a large process are developed and examined. For example, the proposed model for certain heat transfer processes makes it possible to replace the partial differential equations describing these processes by ordinary differential equations.

Although the equations for the model are solved by use of the two-point implicit method, it should be noted that other methods such as the semi-implicit Runge–Kutta method and Gear's method could be used as shown in Sec. 3-2. A comparison of the dynamic behavior predicted by the model with that observed in the field tests run on the system of evaporators is effected by solving the equations describing the model. An objective of this investigation was to develop a suitable model of the process on the basis of the fundamentals of heat transfer, mass transfer, fluid flow, and the information commonly available from the design prints. The model predicts not only the dynamic behavior of the system to an upset in any of the operating variables but also the new steady state solution.

The field tests were made on the Freeport Demonstration Unit, located at Freeport, Texas. This plant was constructed under the direction of the Office of Saline Water, U.S. Department of the Interior. The details of the construction, operation, and successes achieved by this plant are well documented (Refs. 9, 11, 13, 25).

One of the methods for producing fresh water from seawater or brackish water is evaporation (Refs. 8, 9, 14, 23, 24, 25). Of the technical effort expended on evaporation, most of it has been devoted to reducing the cost of construction (Refs. 9, 11, 13); some of it has been spent on the optimization of the process variables as required to minimize all cost factors (Refs. 8, 18, 19). Although numerous investigations on the dynamics of heat transfer and distillation processes have been reported (Refs. 6, 12, 21, 22), Burdett (3) appears to have been the first to study the dynamics of a multiple-effect evaporator process.

In 1945 Bonilla(1) presented a calculational procedure for minimizing the area required to achieve a specified separation. Highly approximate assumptions were necessary, however, in order to keep the iterative procedure manageable for the hand-calculation requirement of that day. Haung et al.(17) developed a procedure for optimizing plants equipped with LTV falling-film evaporators at steady state operation. Itahara and Stiel(18) applied dynamic programming to establish optimal design procedures for systems of multiple-effect evaporators. Their model allowed for the preheat of the feed through heat exchange with the condensate and vapor bleeds, and it was applicable to the design of evaporator systems at steady state operation. Recently, accurate thermodynamic and heat transfer data have become available (Refs. 2, 10, 23).

Description of the Desalination Plant

A photograph of the plant is shown in Fig. 3-1, a sketch of a typical evaporator in Fig. 3-2, and a simplified flow diagram of the process in Fig. 3-3. The design capacity of the plant was one million gallons per day, with a steam consump-

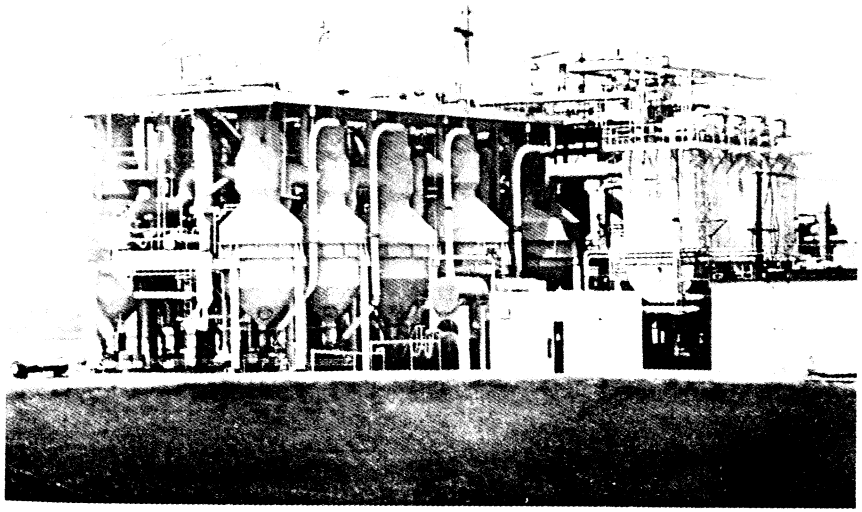

Figure 3-1 Freeport demonstration plant: multiple-effect LTV evaporator. (*Courtesy of the U.S. Department of Interior.*)

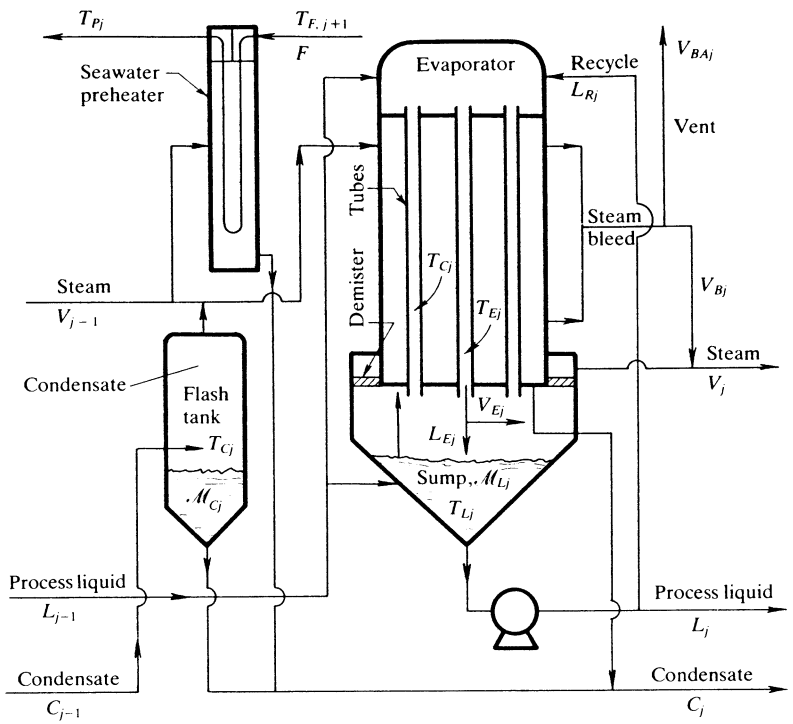

Figure 3-2 Flow diagram of a long-tube vertical evaporator and auxiliary equipment. (*J. W. Burdett and C. D. Holland: "Dynamics of a Multiple-Effect Evaporator System," AIChE J., vol. 17, p. 1080 (1971). Courtesy of the American Institute of Chemical Engineers.*)

tion of less than 0.08 pounds of supply steam per pound of gross product (Ref. 25). The plant consisted of 17 effects of the long-tube vertical (LTV) type of evaporator. The falling-film version of the LTV evaporator was used. As shown in Figs. 3-2, 3-3, and 3-4, a portion of the energy possessed by the condensate leaving each effect was recovered by allowing the condensate to flash in each of the condensate flash-tanks.

The first twelve effects of the plant were built as separate units, and each effect was sized according to its particular requirements. The last five effects were constructed in a single module. The feed preheater and condensate flash-tank were located within the "shell" of the effect with which they were associated.

Each evaporator consisted of a vertical shell-and-tube heat exchanger, which was mounted over a vapor–liquid separator. Noncondensables were removed continuously from each effect through the use of vapor bleeds which were vented to the atmosphere, to the vapor space of the next effect, to the feed

treater, or to the vacuum system. Most of the evaporators were equipped with 2-inch by 22-feet, 16-gauge tubes. The total areas for heat transfer varied from 3000 to 4000 square feet per effect. As shown in Fig. 3-2, demister mats were used to prevent the entrainment of process liquid in the vapor leaving the sump of each evaporator. The process liquid entered the evaporator tubes through a suitably designed distributor at the top of each evaporator.

The feed (seawater) was heated slightly before it entered the acid treater (see Fig. 3-3). Carbon dioxide and dissolved air were removed from the feed in the acid treater by first acidifying, followed by steam stripping, and then neutralizing with caustic. The feed was then preheated in a series of heat exchangers before it was introduced to the first effect (see Figs. 3-2 and 3-3).

In forward-feed operation, the pretreated, preheated feed and steam from the supply line were charged to the first effect. Slightly concentrated process liquid was withdrawn from the sump of the first effect and charged as feed to

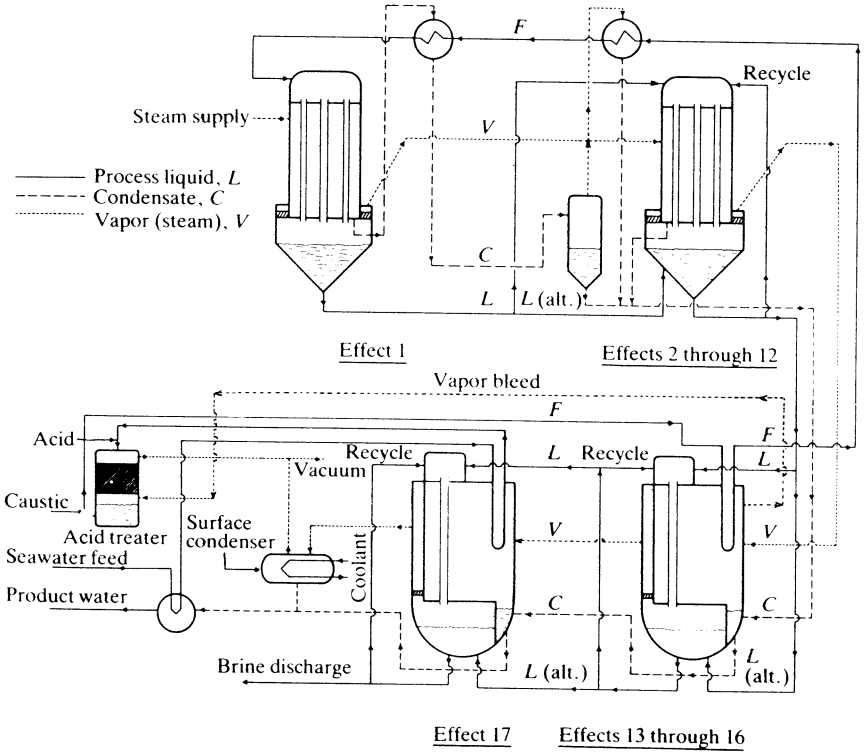

Figure 3-3 Simplified flow diagram of the evaporator system. (*J. W. Burdett and C. D. Holland: "Dynamics of a Multiple-Effect Evaporator System," AIChE J., vol. 17, p. 1080 (1971). Courtesy of the American Institute of Chemical Engineers.*)

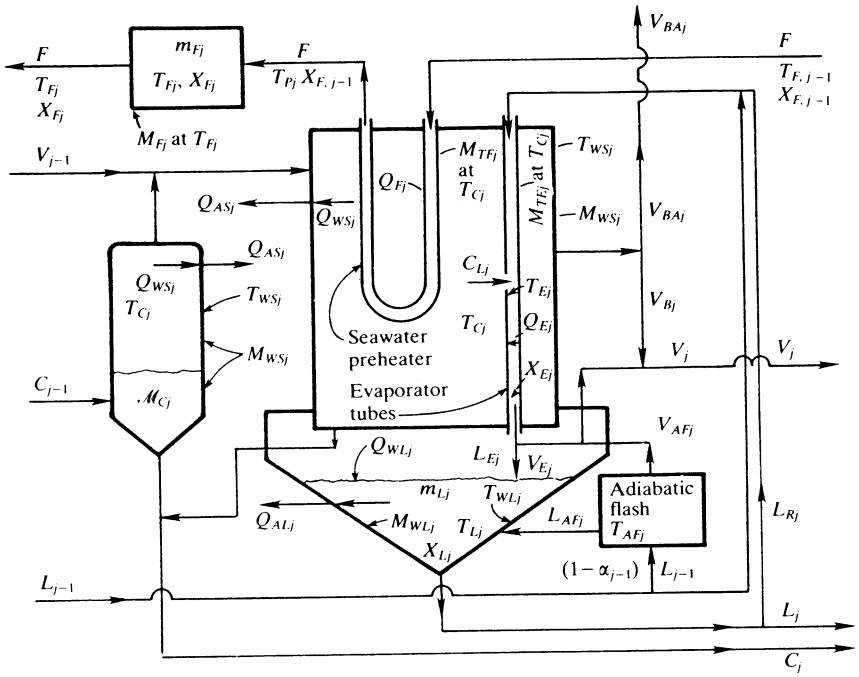

Figure 3-4 Composite model for evaporator effect j and its associated auxiliary equipment. (*J. W. Burdett and C. D. Holland: "Dynamics of Multiple-Effect Evaporator System," AIChE J., vol. 17, p. 1080 (1971). Courtesy of the American Institute of Chemical Engineers.*)

the second effect. The condensate leaving each effect was, of course, the desired product; however, it contained sensible heat which was recovered in part by use of a heat exchanger at the first effect and by flashing in the condensate flash-tank at the subsequent effects.

As the brine process liquid passed through the system, it became more concentrated, and its flow rate diminished. Effects 10 through 17 had provisions for recycling liquid from the sumps of these effects to increase the liquid loading on the walls of the tubes. Effects 11 through 14 had alternate feed inlets which permitted sump-to-sump flow. Both of these options are shown in Figs. 3-3 and 3-4 for effects 2 through 17, since these options were included in the mathematical model for all effects except the first.

Feed preheaters 1 through 12 were of the shell-and-tube type of heat exchangers. These preheaters were mounted vertically and adjacent to the evaporators (see Figs. 3-2 and 3-4). Since the flow of steam to each preheater was unrestricted, the steam chest of each evaporator and the shell of its associated preheater were at the same pressure. Due to the piping configuration, condensate removal was self-regulating. Venting of noncondensables was set by hand valves in the vent line provided for each effect. Effects 2, 3, and 6 each had two preheaters with parallel steam flow and serial feed flow. In the model, each pair was treated as a single preheater. The feed preheaters for effects 13 through 17 were located within the steam chests of the respective effects, together with the evaporator tubes as indicated in Figs. 3-3 and 3-4.

The condensate flash-tanks for effects 2 through 12 were located adjacent to the respective evaporator sumps at an elevation low enough to permit complete drainage of the condensate from the steam chest. Piping between the flash-tanks was located below the bottom level of the tanks in order to provide a water seal for the self-regulation of the condensate flow rates. The condensate flash-tanks for effects 13 through 17 were built into the wall of the module on the side of the respective sumps as indicated in Fig. 3-3.

The acid treater (see Fig. 3-3) consisted of a tower which was six feet in diameter and 43 feet high. The tower was packed with 16 feet of 3-inch by 3-inch stoneware Raschig rings. Seawater feed, acidified with sulfuric acid, entered the top of the tower through a full-cone spray nozzle. Steam from the steam bleed of effect 16 was introduced below the packing at a fixed flow rate. The vapor flow rate from the tower was controlled manually at a flow rate that was greater than the inlet vapor flow rate by an amount which would cause a temperature drop in the flashing feed of about 1°F.

A detailed description of this plant, its equipment, and its operations (prior to the addition of the 5-effect module) was given by Dykstra(9) in 1965. Additional details pertaining to both the 12-effect and the 17-effect operations of the plant are available from the annual reports by the operating company, Stearns–Roger Corporation, to the Office of Saline Water, U.S. Department of the Interior (Ref. 13).

Section 3-1 is devoted to the formulation and analysis of the heat transfer models. In Sec. 3-2 the assumptions for the process model are first stated and then the equations required to describe the proposed process model are enumerated. The analysis of the results of the field tests and a comparison of the experimental results with those calculated by use of the model of the plant are presented in Sec. 3-3.

3-1 DEVELOPMENT AND ANALYSIS OF THE HEAT TRANSFER MODELS

The relatively large mass of metal contained in the evaporators represented an appreciable capacity for the storage of energy. This capacitance cannot be neglected in any realistic analysis of the dynamics of the process. However, the use of the classical equation for conduction (see Eq. (3-11)) in the analysis would result in a tremendous task. To reduce the amount of effort required in the analysis, an approximation called the "heat transfer model for large cylindrical walls" was employed.

Formulation of the Heat Transfer Model for Large Cylindrical Walls

The proposed model not only transforms a partial differential equation into an ordinary differential equation but it also gives the correct rate of heat transfer at steady state as well as the correct heat content of the metal walls. The model makes use of the fact that at steady state, the mean temperature T_m at which the heat content of a large cylindrical wall should be evaluated is approximately equal to T_{av}, the arithmetic average of the internal and external wall temperatures. Large cylindrical walls such as those of the evaporator shells have an appreciable thickness, although the ratio of the external and internal radii is approximately equal to unity. Such walls are further characterized by the fact that the length L along the cylindrical axis is large enough so that heat transfer by conduction along the cylindrical axis may be neglected.

First, it is shown that the variation of the temperature with the radius of a large cylindrical wall is linear. The rate of heat transfer Q (Btu/h) by conduction through a large cylindrical wall of length L and radii r_1 and r_2 is given by

$$Q = -k2\pi rL\frac{dT}{dr} \qquad (r_1 < r < r_2) \tag{3-1}$$

where a temperature gradient exists only in the direction r. Integration of Eq. (3-1) for the case where r_1 may be taken approximately equal to r_2 in the calculation of the surface area $2\pi r_1 L$ (or $2\pi r_2 L$) yields

$$r - r_1 = \frac{k2\pi r_1 L}{Q}(T_1 - T) \tag{3-2}$$

where the thermal conductivity k (Btu/(h · ft · °F)) is taken to be independent of temperature. Elimination of $k2\pi r_1 L/Q$ by use of the boundary condition that at $r = r_2$, $T = T_2$, gives

$$T = T_1 - \left(\frac{T_1 - T_2}{r_2 - r_1}\right)(r - r_1) \tag{3-3}$$

This expression shows that at $r = r_{av}$, $T = T_{av}$, that is, at

$$r = r_{av} = \left(\frac{r_1 + r_2}{2}\right) \qquad T = \left(\frac{T_1 + T_2}{2}\right) = T_{av}$$

It will now be shown that the mean temperature T_m for computing the heat content of the metal wall of an evaporator or the heat content of the metal wall of the flash-tank is approximately equal to the corresponding arithmetic average temperature T_{av}. The total heat content of a cylindrical wall having a temperature gradient in the radial direction alone is given by

$$\text{Heat content} = \int_{r_1}^{r_2} E\rho L(2\pi r\, dr) \tag{3-4}$$

where E is the internal energy (Btu/lb) and ρ is the density (lb/ft^3) of the metal. Then by use of the *generalized theorem of integral calculus* (App. 1A) the right-hand side of Eq. (3-4) may be restated in the following form

$$\int_{r_1}^{r_2} E\rho L(2\pi r\, dr) = E_m \rho 2\pi L \int_{r_1}^{r_2} r\, dr \tag{3-5}$$

where the change in density with temperature is taken to be negligible. Since r_1 may be taken approximately equal to r_2 in the calculation of the surface area of large cylindrical walls, Eq. (3-5) reduces to

$$\int_{r_1}^{r_2} E\, dr = E_m \int_{r_1}^{r_2} dr \tag{3-6}$$

The internal energy above any arbitrary datum temperature, say T_1, is given by $E = C_v(T - T_1)$ and the mean value of E by $E_m = C_v(T_m - T_1)$, where the variation of C_v with temperature over the range from T_1 to T_2 can be neglected. On the basis of these suppositions, Eq. (3-6) may be reduced to

$$\int_{r_1}^{r_2} (T - T_1)\, dr = (T_m - T_1)(r_2 - r_1)$$

After the integrand $(T - T_1)$ has been replaced by its equivalent as given by Eq. (3-3) and the indicated integration has been carried out, the following result is obtained:

$$T_m = T_{av} \tag{3-7}$$

The proposed model was formulated such that the condition given by Eq. (3-7) is satisfied at steady state operation. In particular, let one half of the thermal resistance of the metal wall be concentrated at $r = r_1$ and the other half at $r = r_2$. These thermal resistances are called "effective thermal conductivity films," and they are assigned zero masses. Then the thermal resistance per film is given by

$$\begin{pmatrix}\text{Resistance per effective}\\ \text{thermal conductivity film}\end{pmatrix} = \frac{1}{h_e A} = \frac{1}{2}\left(\frac{r_2 - r_1}{k2\pi r_1 L}\right) \tag{3-8}$$

Thus, the corresponding equivalent film coefficient is given by

$$h_e = \frac{2k}{r_2 - r_1} \tag{3-9}$$

All of the mass of the actual wall is taken to be at the mean temperature $T_m = T_{av}$. The heat transfer model and its corresponding temperature profile at

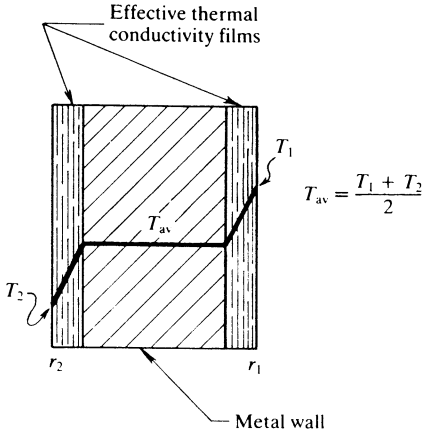

Figure 3-5 Temperature profile predicted for large cylindrical walls ($r_2/r_1 \simeq 1$ and the length along the cylindrical axis is large) at steady state. (*J. W. Burdett and C. D. Holland: "Dynamics of a Multiple-Effect Evaporator System," AIChE J., vol. 17, p. 1080 (1971). Courtesy of the American Institute of Chemical Engineers.*)

steady state are shown in Fig. 3-5. Examination of this model shows that at steady state, it provides the correct wall temperatures T_1 and T_2 needed in the formulation of the rates of heat transfer to and from the wall as well as the correct heat content of the metal wall.

For the case where no approximation is made with respect to the relative sizes of r_1 and r_2, appropriate expressions for T_m and the effective thermal conductivity films are developed as outlined in Prob. 3-2.

There follows an analysis in which a comparison is made between the temperatures predicted by the proposed heat transfer model and those obtained by solving the corresponding boundary-value problems. The results of this analysis support the use of the proposed heat transfer model in the modeling of the heat transfer through large cylindrical walls. The relationships developed in this analysis are also used in the justification of the use of a heat transfer model for thin metal walls under the heat transfer conditions such as those of the steam-heated heat exchangers of the evaporator system.

Analysis of the Heat Transfer Model for Large Cylindrical Walls

The primary purpose of the analysis that follows is to obtain an approximation of the errors in the temperatures predicted by use of the heat transfer model. Formulas for predicting these errors are obtained by solving the boundary-value problems corresponding to two different sets of boundary conditions.

Consider first the boundary-value problem having the boundary conditions depicted in Fig. 3-6. This problem corresponds to the case of a metal wall in contact with steam at $x = l$ and the surroundings at $x = 0$. At $x = l$, the steam film coefficient is denoted by h_2 and the steam temperature by T_S. At $x = 0$, an effective film resistance is used to represent the combined resistance offered by

the insulation and the air film to heat transfer. The effective film resistance is denoted by $1/h_1$ and defined by

$$\frac{1}{h_1} = \frac{l_{ins} A}{(kA)_{ins}} + \frac{A}{(hA)_{air}} \tag{3-10}$$

where A is the internal surface of the cylindrical section of the metal wall. The subscript "ins" refers to the insulation, the subscript "air" refers to the air film, and l_{ins} denotes the thickness of the insulation.

At time $t = 0$, the metal wall is at the uniform temperature T_A of the surroundings, and at time $t = 0+$, the steam (with the saturation temperature T_S) is turned on. The corresponding partial differential equation is given by

$$\frac{\partial T}{\partial t} = \alpha \frac{\partial^2 T}{\partial x^2} \qquad (0 < x < l,\ t > 0) \tag{3-11}$$

where

$$\alpha = \frac{k}{\rho C_v}$$

The boundary conditions are as follows:

$$\begin{aligned} k\frac{\partial T}{\partial x} - h_1(T - T_A) &= 0 \qquad (x = 0,\ t > 0) \\ k\frac{\partial T}{\partial x} + h_2(T - T_S) &= 0 \qquad (x = l,\ t > 0) \\ T &= T_A \qquad (t = 0, \text{ for all } x) \end{aligned} \tag{3-12}$$

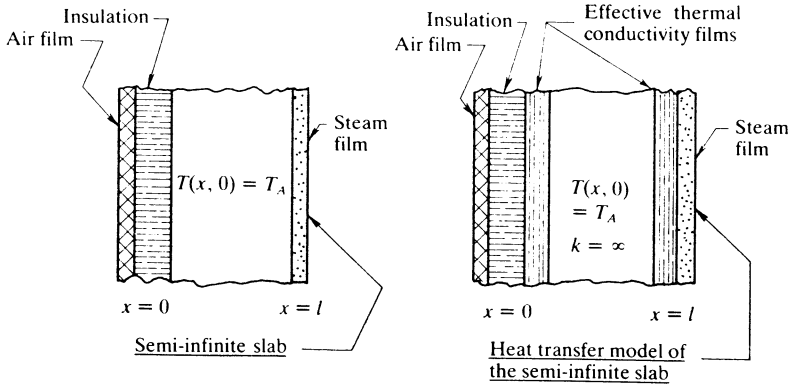

Figure 3-6 Heat transfer model of a semi-infinite slab in contact with air on the insulated side and steam on the other side. (*J. W. Burdett and C. D. Holland: "Dynamics of a Multiple-Effect Evaporator System," AIChE J., vol. 17, p. 1080 (1971). Courtesy of the American Institute of Chemical Engineers.*)

Equations (3-11) and (3-12) may be developed by following the outline given in Prob. 3-3. The following solution to this problem may be deduced from the result given by Carslaw and Jaeger(5) in case IV on page 126.

$$\frac{T(x,\,t) - T_A}{T_S - T_A} = a\left(x + \frac{1}{H_1}\right) - \sum_{n=1}^{\infty} C_n D_n Y_n(x) e^{-\alpha\beta_n^2 t} \tag{3-13}$$

where

$$a = \frac{1}{1/H_1 + 1/H_2 + l} \qquad (H_1 = h_1/k,\ H_2 = h_2/k)$$

$$C_n = \frac{[2(\beta_n^2 + H_2^2)]^{1/2}}{\beta_n\{(\beta_n^2 + H_1^2)[l(\beta_n^2 + H_2^2) + H_2] + H_1(\beta_n^2 + H_2^2)\}^{1/2}}$$

$$D_n = H_2(\cos \beta_n l)\,\frac{\beta_n^2 + H_1^2}{\beta_n^2 - H_1 H_2}$$

$$Y_n(x) = \beta_n C_n(\beta_n \cos \beta_n x + H_1 \sin \beta_n x)$$

$\beta_1, \beta_2, \ldots, \beta_n$ = first n positive roots of

$$(\beta^2 - H_1 H_2) \sin \beta l - \beta(H_1 + H_2) \cos \beta l = 0$$

An outline of the method of solution is given in Probs. 3-4 and 3-5. The result given by Eq. (3-13) may be used to determine the mean temperature which is required to give the correct heat content of a finite section of the slab at any time $t > 0$. The following expression for the determination of this mean temperature $T_m(t)$ is formulated in a manner similar to that shown for Eq. (3-5):

$$T_m(t) - T_A = \frac{1}{l}\int_0^l [T(x,\,t) - T_A]\,dx \tag{3-14}$$

When the integrand $[T(x, t) - T_A]$ is replaced by its equivalent as given by Eq. (3-13) and the indicated integration is carried out, the result so obtained may be rearranged to give

$$\frac{T_m(t) - T_A}{T_S - T_A} = a\left(\frac{1}{H_1} + \frac{l}{2}\right) - \frac{1}{l}\sum_{n=1}^{\infty} C_n^2 D_n(D_n + H_1) \exp(-\alpha\beta_n^2 t) \tag{3-15}$$

For the boundary-value problem under consideration, the corresponding heat transfer model is also shown in Fig. 3-6. The differential equation for the heat transfer model is given by

$$U_2(T_S - T) - U_1(T - T_A) = l\rho C_v \frac{dT}{dt} \tag{3-16}$$

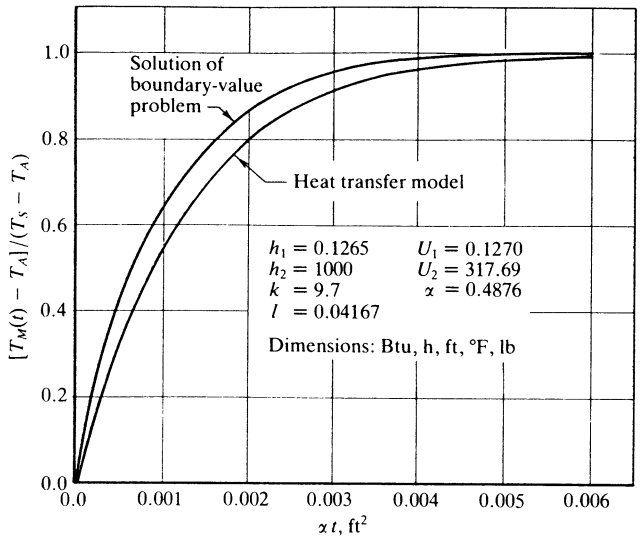

Figure 3-7 Comparison of the results given by the heat transfer model with those given by the solution of the corresponding boundary-value problem (see Fig. 3-6). (*J. W. Burdett and C. D. Holland: "Dynamics of a Multiple-Evaporator System," AIChE J., vol. 17, p. 1080 (1971). Courtesy of the American Institute of Chemical Engineers.*)

where

$$\frac{1}{U_1} = \frac{l_{\text{ins}} A}{(kA)_{\text{ins}}} + \frac{A}{(hA)_{\text{air}}} + \frac{l}{2k}$$

$$\frac{1}{U_2} = \frac{1}{h_{\text{steam}}} + \frac{l}{2k}$$

Separation of the variables in Eq. (3-16) followed by integration and rearrangement yields

$$\frac{T(t) - T_A}{T_S - T_A} = \left(\frac{U_2}{U_1 + U_2}\right)\left\{1 - \exp\left[-\left(\frac{U_1 + U_2}{l\rho C_v}\right)t\right]\right\} \tag{3-17}$$

A comparison of the values of $T(t)$ predicted by the heat transfer model as given by Eq. (3-17) with the theoretical values given by Eq. (3-15) is presented in Fig. 3-7. The heat transfer coefficients and other parameters used to compute the results shown in this figure were of the same order of magnitude as those for the system of evaporators under consideration.

A limiting case for the heat transfer model The boundary-value problem corresponding to an evaporator shell with a perfect insulator on one side and steam

with an infinite film coefficient on the other side is depicted in Fig. 3-8. The postulate of an infinite value of the steam film coefficient amounts to taking the surface temperature of the wall on the steam side equal to the saturation temperature T_S of the steam. The partial differential equation is again given by Eq. (3-11) and the boundary conditions are as follows:

$$\begin{aligned} T(x, 0) &= T_A \qquad (0 < x < l) \\ \frac{\partial T(0, t)}{\partial x} &= 0 \qquad (t > 0) \\ T(l, t) &= T_S \qquad (t > 0) \end{aligned} \tag{3-18}$$

The solution satisfying both the partial differential equation and the boundary conditions may be stated in terms of either a Fourier series of cosines or a series of complementary error functions (Refs. 5, 7). Of these two forms of the solution, only the latter is given because it is said to converge (Ref. 5) more rapidly for small values $\alpha t/l^2$

$$\frac{T_S - T(x, t)}{T_S - T_A} = 1 - \sum_{n=0}^{\infty} (-1)^n \left[\operatorname{erfc} \frac{(2n + 1)l - x}{2(\alpha t)^{1/2}} + \operatorname{erfc} \frac{(2n + 1)l + x}{2(\alpha t)^{1/2}} \right] \tag{3-19}$$

where

$$\operatorname{erfc} z = \frac{2}{\sqrt{\pi}} \int_z^{\infty} e^{-\lambda^2} \, d\lambda$$

the complementary error function.

The result given by Eq. (3-19) may be used to determine that mean temperature which is required to give the correct heat content of a finite section of

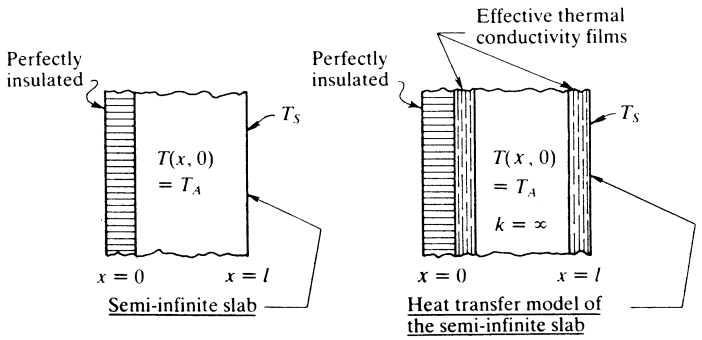

Figure 3-8 Heat transfer model of a semi-infinite slab which is perfectly insulated at one end and the temperature is constant at the other. (*J. W. Burdett and C. D. Holland: "Dynamics of a Multiple-Effect Evaporator System," AIChE J., vol. 17, p. 1080 (1971). Courtesy of the American Institute of Chemical Engineers.*)

the slab in a manner analogous to that demonstrated for Eq. (3-15). The corresponding result is given by

$$\frac{T_m(t) - T_A}{T_S - T_A} = 2\left(\frac{\alpha t}{l^2}\right)^{1/2} \left[\pi^{-1/2} + 2 \sum_{n=1}^{\infty} (-1)^n \operatorname{ierfc} \frac{nl}{(\alpha t)^{1/2}} \right] \tag{3-20}$$

where

$$\operatorname{ierfc} z = \int_z^{\infty} \operatorname{erfc} \xi \, d\xi = \frac{e^{-z^2}}{\sqrt{\pi}} - z \operatorname{erfc} z$$

Values of ierfc z have been tabulated by Carslaw and Jaeger(5).

For the boundary-value problem under consideration, the corresponding heat transfer model is also shown in Fig. 3-8. The differential equation for the heat transfer model is given by

$$\frac{2k}{l} (T_S - T) = l\rho C_v \frac{dT}{dt} \tag{3-21}$$

Separation of the variables followed by integration and rearrangement yields

$$\frac{T(t) - T_A}{T_S - T_A} = 1 - e^{-2\alpha t/l^2} \tag{3-22}$$

A comparison of the predicted values of the temperature ratio given by Eq. (3-22) with the theoretical values found by use of Eq. (3-20) appears in Fig. 3-9.

Errors in the mean temperatures predicted by the heat transfer model for large cylindrical walls The solutions given by Eqs. (3-15) and (3-17) correspond to a situation in which conditions are far more severe than any which ever existed during the test runs. The boundary conditions (see Eq. (3-12)) suppose that the initial temperature of the metal at the time of the upset is equal to the temperature T_A of the surroundings. To obtain some idea of the difference in the mean temperatures of the wall given by the solution of the boundary-value problem (see Eq. (3-15)) and the heat transfer model (Eq. (3-17)), consider the case where $T_A = 80°F$ and $T_S = 250°F$. That is, the initial temperature of the metal and the surroundings is 80°F at time $t = 0$, one side of the metal wall is suddenly exposed to saturated steam at 250°F. The initial time step used in the program for the system was 0.5 min. Then for $t = 1/120$ h, the following results are obtained from Fig. 3-9, that is, the solution of the boundary-value problem gives

$$T_m = 248°F$$

and the solution of the heat transfer model gives

$$T = 243°F$$

Although the boundary conditions given by Eq. (3-18) are closer to those which occurred during the test runs than the conditions given by Eq. (3-12),

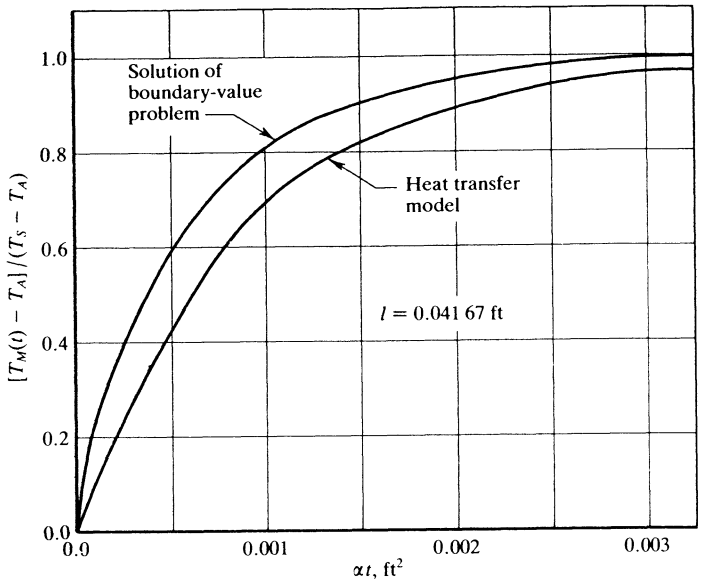

Figure 3-9 Comparison of the results given by the heat transfer model with those given by the solution of the corresponding boundary-value problem (see Fig. 3-8). (*J. W. Burdett and C. D. Holland: "Dynamics of a Multiple-Effect Evaporator System," AIChE J., vol. 17, p. 1080 (1971). Courtesy of the American Institute of Chemical Engineers.*)

they are also more severe than those which existed during the test run. For purposes of illustration, consider the case where the initial temperature T_A of the metal is 240°F and the temperature T_S of the steam in contact with one side of the wall is suddenly changed to 270°F. At the end of 1/120 h, the mean temperature given by the solution of the boundary value problem is

$$T_m = 269.90°\text{F}$$

and by the solution of the heat transfer model is

$$T = 269.72°\text{F}$$

These results may be obtained by use of Eqs. (3-20) and (3-22).

Heat Transfer Model for the Tubing of the Steam-Heated Heat Exchangers

The model proposed for these thin metal walls consists of a further simplification of the model proposed for the representation of the heat transfer through large cylindrical walls. The proposed mode for these thin metal walls consists simply of taking the mean temperature of the walls equal to the steam temperature. In the case of thin metal walls such as those found in the steam-heated heat exchangers, the mean temperature found by solving the boundary-value problem is almost exactly equal to the wall temperature predicted by use of the heat transfer model. In other words, the heat transfer model proposed in the previous section approaches an exact representation of the thin metal walls. Thus, for a heat transfer situation represented by Eq. (3-16), it is evident that the temperature of the wall is approximately equal to the steam temperature at the end of the first time step provided both of the following conditions are satisfied simultaneously:

$$\frac{U_2}{(U_1 + U_2)} \cong 1$$

and

$$\frac{l\rho C_v}{U_1 + U_2} \ll \Delta t$$

where U_2 contains the steam film coefficient. In a typical steam-heated heat exchanger, $U_2/(U_1 + U_2) \cong 0.825$, and $(l\rho C_v)/(U_1 + U_2)$ was equal to 0.000 157 while Δt was equal to 0.008 33 h.

Thus, in summary, the proposed heat transfer model is seen to apply provided (1) the "time constant" $l\rho C_v/(U_1 + U_2)$ is much less than the time step Δt used in the numerical solution of the evaporator problem (that is, the time constants for other units of the system are large relative to the one for the thin walls of the exchanger) and (2) the heat transfer coefficient for the steam side is much greater than the heat transfer coefficient for the other side. The use of the proposed model is further strengthened by the fact that energy balances involve differences in heat content of the walls at the beginning and end of each time period, and these differences are generally more accurate than the predicted wall temperatures.

The heat transfer model used for the metal walls of the tubes of the liquid–liquid feed-preheater associated with the first evaporator effect was essentially the same as the one described above except that the mass of the tubes was prorated to be at the temperatures assigned to the mass of each liquid according to the coefficient of heat transfer of each liquid. Similarly, well-insulated process piping was taken to be at the temperature of the process fluid adjacent to it.

Heat Transfer Model for the Liquid in the Feed Preheaters

The proposed model for the liquid in the feed preheaters consists of the use of the steady state relationships to describe the rate of heat transfer occurring at the beginning and at the end of any time period during the transient analysis of the process model. Support for this model is the fact that the process fluid undergoes plug flow through the tubes with little axial mixing and the fact that the residence time of the fluid in the exchanger was short compared with the time intervals used in the numerical solution for the system of evaporators.

All process liquid flowing through the tubes was taken to be concentrated in a perfect mixer following each exchanger. The heat content of the metal piping associated with each exchanger was taken to be at the temperature of the process liquid in the perfect mixer. The assumptions for the feed-preheaters and the liquid–liquid feed-preheaters are listed below.

3-2 FORMULATION OF THE MODEL FOR THE SYSTEM OF EVAPORATORS AT THE FREEPORT DEMONSTRATION UNIT

The proposed process model for the system of evaporators is obtained by dividing the plant into components which are describable by the fundamental relationships common to chemical engineering. First the assumptions upon which the model is based are presented, and then the equations required to describe the model are presented.

Assumptions Made in Modeling the System of Evaporators

There follows a statement of the assumptions upon which the mathematical model for the system of evaporators is based.

1. The masses of metal in evaporator tubes and in the feed preheaters are denoted by M_{TEj} and M_{TFj}, respectively. These masses of metal are taken to be at the temperature T_{Cj} of the condensing steam in effect j. This approximation is based on the fact that the steam film coefficient was relatively large compared with the liquid film coefficient, and the fact that the tube walls were relatively thin. The tubes and the heat transfer model are displayed in Figs. 3-2, 3-4, and 3-10.
2. The mass of metal M_{WSj} of each evaporator effect j which is exposed to condensing steam or condensate on one side and the surroundings on the other is assigned the temperature T_{WSj}. The rates of heat transfer to and

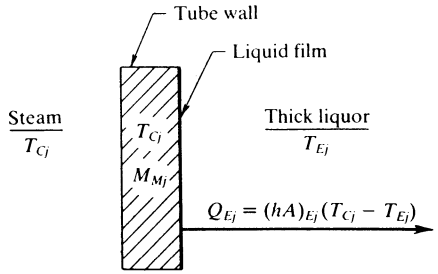

Figure 3-10 Heat transfer model for the metal tubes in contact with steam and thick liquor.

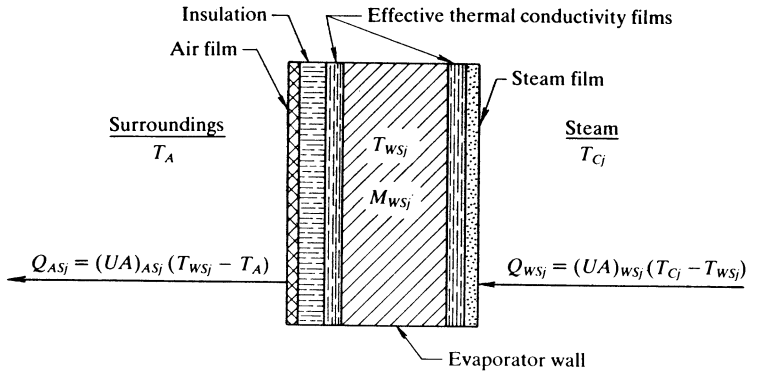

Figure 3-11 Heat transfer model for the evaporator wall in contact with steam and the surroundings.

from this mass of metal are given by the expressions shown in Fig. 3-11. One-half of the thermal resistance of the metal wall is assigned to an equivalent film on each side of the wall.

3. The holdup of energy by the insulation is taken to be negligible relative to the feed, process liquid, condensate, and metal in the evaporator system. This approximation rests primarily on the fact that the actual mass of the insulation was relatively small.
4. The mass of metal M_{WLj} of each effect j which is in contact with the process liquid on one side and the surroundings on the other is taken to be at the temperature T_{WLj}. The heat transfer model is displayed in Fig. 3-12.

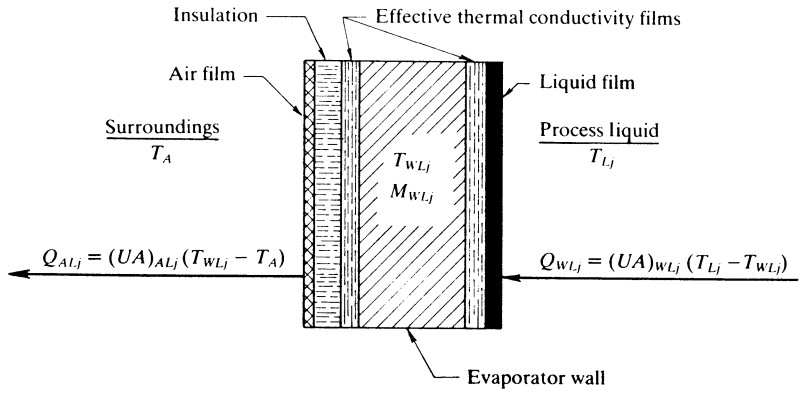

Figure 3-12 Heat transfer model for the evaporator wall in contact with process liquid and the surroundings.

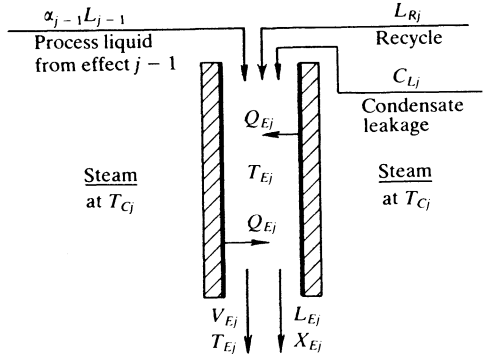

Figure 3-13 Model for the tubes of evaporator effect j.

5. The discharge temperature T_{Ej} of the process liquid from the tubes is computed by use of Dühring lines based on the condensate temperature of the next effect and the mass fraction X_{Ej} of salt in the liquid discharged from the tubes of evaporator effect j (see Fig. 3-13).
6. The pressure drop between the sump of one effect and the steam chest of the next effect is taken to be negligible.
7. In the rate expression for the transfer of heat from the condensing steam at temperature T_{Cj} to the process liquid flowing down through each evaporator tube, the discharge temperature T_{Ej} of the process liquid is used in the potential term $(T_{Cj} - T_{Ej})$ for heat transfer. This approximation is consistent with the fact that the heat transfer coefficient U_{Ej} employed was calculated at steady state operation on the basis of the discharge temperature.

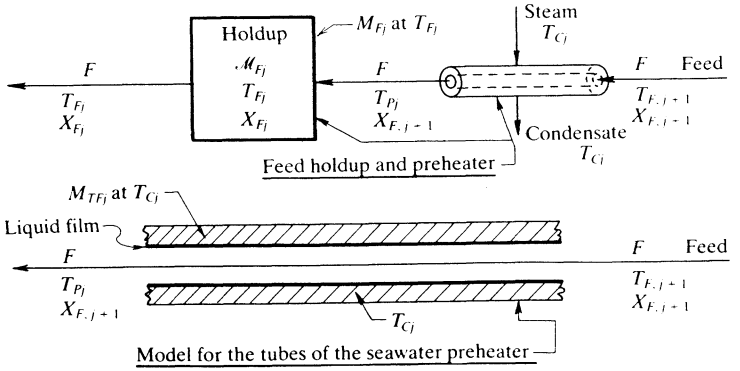

Figure 3-14 Models for the seawater preheater and holdup of the feed associated with an evaporator.

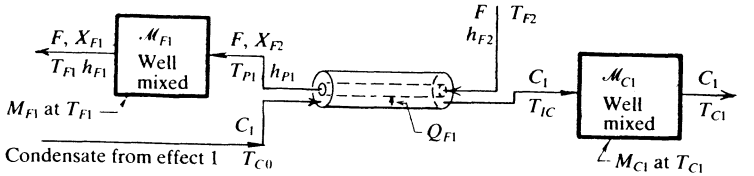

Figure 3-15 Models for the condensate holdup and feed preheater for the first effect. (*J. W. Burdett and C. D. Holland: "Dynamics of a Multiple-Effect Evaporator System," AIChE J., vol. 17, p. 1080 (1971). Courtesy of the American Institute of Chemical Engineers.*)

8. The accumulations of mass and energy of process liquid in the evaporator tubes are taken to be negligible relative to the accumulation of mass and energy of process liquid in the sump of effect j.
9. The total amount of steam condensate associated with each effect is denoted by $\mathcal{M}_{Cj}$ (see Figs. 3-4 and 3-15). Except for the first effect the mass of condensate $\mathcal{M}_{Cj}$ is taken to be at the saturation temperature of steam T_{Cj}, at the pressure in the steam chest. For the first effect, the mass of condensate $\mathcal{M}_{C1}$ in the preheater and in the line between the steam chest of the first effect and the condensate flash-tank of the second effect is taken to be concentrated in a perfect mixer following the preheater, as shown in Fig. 3-15. In all rate-of-heat-transfer calculations, the steam in the first effect is taken to be at the temperature T_{Cj} except for the first effect where it is taken to be at the saturation temperature T_{C0} of the supply steam. However, any superheat present in the steam entering the steam chest of a given effect, is taken into account in the energy balances.
10. The effect of noncondensables on the operation of the system of evaporators is taken to be insignificant because of the venting of the steam chest of each effect.
11. The mass of vapor (steam) in the steam chest in the evaporator and in the feed preheater as well as the vapor in the condensate flash-tank is taken to be negligible relative to the mass of condensate associated with each effect.
12. The mass of seawater feed in the preheater and preheater feedlines between effects j and $j-1$ is taken to be concentrated as the mass $\mathcal{M}_{Fj}$ of a perfect mixer as shown in Figs. 3-4, 3-14, 3-15, and 3-16. For all effects except the last one, wherein the holdup is associated with the acid treater, the masses of the holdups are taken to be independent of time. This assumption is based on the fact that the feedlines between effects were full at all times. The masses of metal in the feedlines associated with effect j are taken to be concentrated in the mass M_{Fj} at the temperature T_{Fj} of the perfect mixer. In the first effect, mass M_{F1} includes part of the mass of metal of the preheater. For the last effect, mass M_{F17} includes part of the mass of metal of the acid treater. This assumption is based on the fact that a change in temperature at a given point in the piping has a magnitude and a time response similar to that predicted by the temperature T_{Fj}.

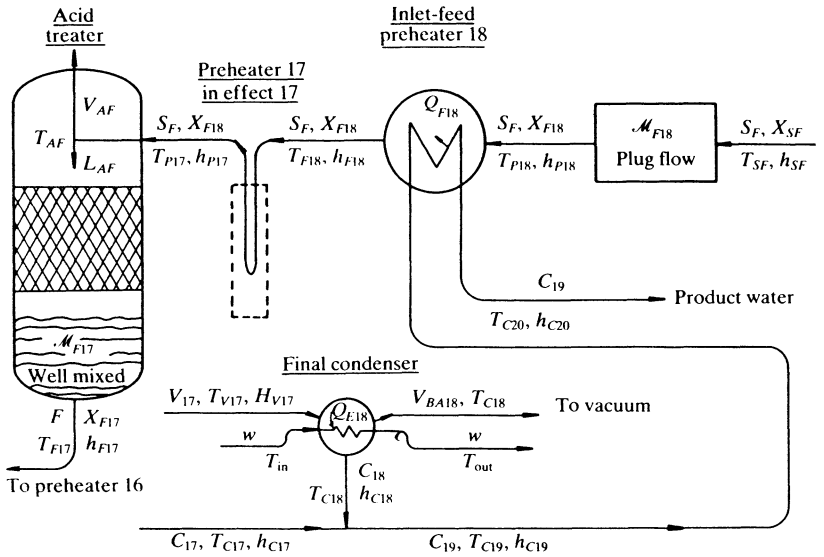

Figure 3-16 Composite model of peripheral equipment of the evaporator system. (*J. W. Burdett and C. D. Holland: "Dynamics of a Multiple-Effect Evaporator System," AIChE J., vol. 17, p. 1080 (1971). Courtesy of the American Institute of Chemical Engineers.*)

13. The dynamic behavior of the feed preheaters may be represented at any instant by the equations describing the steady state behavior of heat exchangers.
14. The mass of process liquid in the sump and in the lines associated with effect j is taken to be concentrated in the sump with a mass denoted by $\mathcal{M}_{Lj}$. This mass of liquid is taken to be perfectly mixed at the temperature T_{Lj} but not necessarily in thermal equilibrium with the vapor stream V_{Ej}.
15. For sump-to-sump flow, the process liquid stream $(1-\alpha_{j-1})L_{j-1}$ is assumed to flash adiabatically at the pressure in the sump of effect j, as displayed in Fig. 3-4. The liquid L_{Fj} formed by the flash is assumed to mix perfectly with the liquid in the sump. The vapor V_{Fj} formed by the flash is assumed to flow directly to the exit vapor line from effect j without loss or gain of energy.
16. The flow rate C_j of condensate from the flash-tank of effect j to the flash-tank of effect $j+1$ is taken to be regulated by a proportional controller that regulates the mass holdup of condensate $\mathcal{M}_{Cj}$ in the flash-tank. Although most of the flash-tanks did not actually have controllers, the assumption is justified on the basis that the response behavior for self-regulating systems of this type can be approximated by asuming that proportional controllers do exist. The gains of the assumed controllers are set to match the responses calculated with the model to the responses derived from theory or measured experimentally. Response ranges of the assumed controllers are limited to the cylindrical section above the cone in the flash-tanks of effects 2 to 12 and to the rectangular section in the flash-tanks of effects 13 to 17 in the module. In these regions changes in condensate holdup $\mathcal{M}_{Cj}$ are linear with changes in level. The mass of condensate associated with the first effect $\mathcal{M}_{C1}$ is taken to be constant due to the absence of a flash-tank for the first effect. Thus, the flow rate C_1 of the condensate may be determined by the material balance and energy balance equations for the steam chest of the first effect.

17. The masses of the metal components associated with the preheater of the first effect are taken to be concentrated in mass M_{C1} at temperature T_{C1} and in mass M_{F1} at T_{F1}. Mass M_{C1} includes the condensate piping from the steam chest of the first effect to the flash-tank of effect 2 and a portion of the preheater shell-and-tube mass. Mass M_{F1} includes the seawater feed piping from the preheater to the inlet for the first evaporator and a portion of the preheater shell-and-tube mass. The concentrated masses are taken to be located in the perfect mixers of the model for the preheater as shown in Fig. 3-15.
18. The dynamic values of the variables for the final condenser and feed preheater 18 (seawater feed to product-water heat exchanger) are assumed to be related by the conventional steady state equations as discussed for the heat exchanger model. The model for the final condenser is shown in Fig. 3-16.
19. The holdup of energy in the metal masses associated with the final condenser and feed preheater 18 is assumed to be constant. This assumption is based on the fact that large upsets in the major process variables produced only small changes in the temperatures in the final condenser and in preheater 18.
20. The acid treater is represented in the process model as an adiabatic flash process wherein the amount of seawater flashed is determined by the difference in flow rates of the stripping steam entering and leaving the tower. For the evaluation of steady state conditions, the amount of seawater flashed is regulated to achieve a preassigned drop in temperature of the vapor leaving relative to the feed entering the flash process. For the evaluation of the transient behavior following an upset, the amount of seawater flashed is assumed to be constant at the value established during the steady state period preceding the upset. The holdup of liquid in the acid treater is taken to be concentrated in a perfect mixer in the sump of the tower. The amount of this holdup $\mathcal{M}_{F17}$ is taken to be regulated by a proportional controller. A sketch of the model of the acid treater is shown in Fig. 3-16.
21. Flow rates of process liquid between evaporators are taken to be regulated by proportional controllers that detect changes in the mass holdup $\mathcal{M}_{Lj}$. Due to the noncylindrical shapes of the sumps, the mass $\mathcal{M}_{Lj}$ is not linear with the level measurement. Therefore, the proportionality factor of each controller is made a function of $\mathcal{M}_{Lj}$ in the numerical solution in order to correct for this nonlinearity.

22. To allow for the holdup of the feed in the piping between the feed pump (where the upsets in the feed composition occurred) and the evaporator module, a plug-flow section with holdup $\mathscr{M}_{F18}$ is assumed to exist as indicated in Fig. 3-16. This holdup is positioned before the preheater since most of the estimated holdup actually occurs there.
23. If any holes develop in the evaporator tubes of an effect, leakage of condensate and vapor occurs from the steam chest into the evaporator tubes. Provision for setting condensate leakage rate C_{Lj} is provided in the model as shown in Figs. 3-4 and 3-13. Allowance for vapor leakage is made by adding any estimated leakage to the estimate for vapor bleed V_{Bj}. Both of these leakage parameters were estimated from an analysis of steady state data.

Statement of the Equations Required to Describe the Model for the Evaporator System

Based on the assumptions stated, the equations required to describe each part of the evaporator system are presented in Table 3-1. The superscript zero is used to denote the values of the variables at the beginning of the time period under consideration, and the absence of a superscript is used to denote the values of the variables at the end of the time period under consideration. When the holdup of mass or energy of a particular part of the system cannot be neglected, the corresponding integral-difference equation is reduced to algebraic form by use of the implicit method. When the holdup of mass or energy of a given part of the system is negligible, the instantaneous form of the corresponding steady state equations evaluated at the end of the time period under consideration are given.

In the development that follows, the independent equations are assigned equation numbers. The subscript j is used to denote the number of the evaporator effect ($j = 1, 2, 3, \ldots, 17$). Streams as well as the properties of streams treated by peripheral equipment carry identifying subscripts $j = 18$, 19, and 20. Also, in the development that follows, the assumptions stated in the previous section are referred to by number.

In order to demonstrate the formulation of the equations shown in Table 3-1, the equations are formulated below for each of five different types of models which are used in the description of each evaporator; namely, (1) the heat transfer model, (2) processes which have negligible mass holdup, (3) processes which have negligible energy holdup, (4) equilibrium relationships, and (5) process controllers.

Energy balance on the walls of the evaporator The energy balances on the metal walls of the evaporators which are in contact with steam on one side and the surroundings on the other side are based on assumptions 2 and 3 and on the models displayed in Figs. 3-4 and 3-11. In particular, the resistance $1/(UA)_{WSj}$ and $1/(UA)_{ASi}$ to heat transfer are represented graphically in Fig. 3-11 and

Table 3-1 Equations required to describe the evaporator system

1. Energy balances on the walls of the evaporators

$$Q_{WSj} - Q_{ASj} + \sigma[Q_{WSj} - Q_{ASj}]^0 - \frac{M_{WSj}C_{pWSj}(T_{WSj} - T^0_{WSj})}{\phi\,\Delta t} = 0 \qquad (1 \le j \le 17) \qquad (1)$$

where

$$\sigma = (1 - \phi)/\phi$$

$$Q_{WS1} = (UA)_{WSL}(T_{C0} - T_{WS1})$$

$$Q_{WSj} = (UA)_{WSj}(T_{Cj} - T_{WSj}) \qquad (2 \le j \le 17)$$

$$Q_{ASj} = (UA)_{ASj}(T_{WSj} - T_A) \qquad (1 \le j \le 17)$$

$$Q_{WLj} - Q_{ALj} + \sigma[Q_{WLj} - Q_{ALj}]^0 - \frac{M_{WLj}C_{pWLj}(T_{WLj} - T^0_{WLj})}{\phi\,\Delta t} = 0 \qquad (1 \le j \le 17) \qquad (2)$$

where

$$Q_{WLj} = (UA)_{WLj}(T_{Lj} - T_{WLj}) \qquad (1 \le j \le 17)$$

$$Q_{ALj} = (UA)_{ALj}(T_{WLj} - T_A) \qquad (1 \le j \le 17)$$

2. Material and energy balances on the contents in the evaporator tubes

$$FX_{F1} - L_{E1}X_{E1} = 0 \qquad (3)$$

$$\alpha_{j-1}L_{j-1}X_{L,j-1} + L_{Rj}X_{Lj} - L_{Ej}X_{Ej} = 0 \qquad (2 \le j \le 17) \qquad (4)$$

$$F - L_{E1} - V_{E1} + C_{L1} = 0 \qquad (5)$$

$$\alpha_{j-1}L_{j-1} + L_{Rj} - L_{Ej} - V_{Ej} + C_{Lj} = 0 \qquad (2 \le j \le 17) \qquad (6)$$

$$Fh_{F1} + Q_{E1} - L_{E1}h_{E1} - V_{E1}H_{E1} + C_{L1}h_{CL1} = 0 \qquad (7)$$

$$\alpha_{j-1}L_{j-1}h_{L,j-1} + L_{Rj}h_{Lj} + Q_{Ej} - L_{Ej}h_{Ej} - V_{Ej}h_{Ej} + C_{Lj}h_{CLj} = 0 \qquad (2 \le j \le 17) \qquad (8)$$

where

$$Q_{E1} = (UA)_{E1}(T_{C0} - T_{E1})$$

$$Q_{Ej} = (UA)_{Ej}(T_{Cj} - T_{Ej}) \qquad (2 \le j \le 17)$$

$$mT_{C,j+1} + b - T_{Ej} = 0 \qquad (1 \le j \le 17) \qquad (9)$$

where

$$m = m(T_{C,j+1}, X_{Ej}),\ b = b(X_{Ej})$$

3. Adiabatic flash of the process liquid leaving effect $j - 1$ and entering effect j

$$(1 - \alpha_{j-1})L_{j-1} - L_{AFj} - V_{AFj} = 0 \qquad (2 \le j \le 17) \qquad (10)$$

$$(1 - \alpha_{j-1})L_{j-1}X_{L,j-1} - L_{AFj}X_{AFj} = 0 \qquad (2 \le j \le 17) \qquad (11)$$

$$(1 - \alpha_{j-1})L_{j-1}h_{L,j-1} - L_{AFj}h_{AFj} - V_{AFj}H_{AFj} = 0 \qquad (2 \le j \le 17) \qquad (12)$$

$$mT_{C,j+1} + b - T_{AFj} = 0 \qquad (2 \le j \le 17) \qquad (13)$$

(*Continued over*)

Table 3-1 Equations required to describe the evaporator system—*Continued*

where

$$m = m(X_{AFj},\ T_{C,j+1})$$
$$b = b(X_{AFj})$$

4. Material and energy balances on the contents of the steam chest of the first effect and the mass of metal in the evaporator tubes

$$V_0 - C_1 - V_{B1} - V_{BA1} - C_{L1} = 0 \quad (14)$$

$$V_0 H_0 - (C_0 + C_{L1})h_{C0} - (V_{B1} + V_{BA1})H_{C0} - Q_{E1} - Q_{WS1} + \sigma[V_0 H_0 - (C_0 + C_{L1})h_{C0} - (V_{B1} + V_{BA1})H_{C0} - Q_{E1} - Q_{WS1}]^0 - \frac{M_{TE1} C_{pTE1}(T_{C0} - T_{C0}^0)}{\phi\ \Delta t} = 0 \quad (15)$$

where

$$Q_{E1} = (UA)_{E1}(T_{C0} - T_{E1})$$
$$Q_{WS1} = (UA)_{WS1}(T_{C0} - T_{WS1})$$

5. Energy balances and rate equations for the preheater and condensate holdup associated with the first effect

$$C_1(h_{IC} - h_{C1}) + \sigma[C_1(h_{IC} - h_{C1})]^0 - \left[\frac{\mathscr{M}_{C1}(h_{C1} - h_{C1}^0) + M_{C1}(C_{pMC1})(T_{C1} - T_{C1}^0)}{\phi\ \Delta t}\right] = 0 \quad (16)$$

$$C_1 C_{pC1}(T_{C0} - T_{IC}) - FC_{pP1}(T_{P1} - T_{F2}) = 0 \quad (17)$$

$$(T_{C0} - T_{P1}) \exp\left[(UA)_{F1}\left(\frac{1}{FC_{pP1}} - \frac{1}{C_1 C_{pC1}}\right)\right] - (T_{IC} - T_{F2}) = 0 \quad (18)$$

6. Energy balances and rate expressions for the feed preheaters for evaporator effects $2 \geq j \leq 17$

$$(T_{Cj} - T_{Pj})\left[\exp\left(\frac{(UA)_{Fj}}{FC_{pPj}}\right)\right] - (T_{Cj} - T_{F,j+1}) = 0 \qquad (2 \leq j \leq 16) \quad (19)$$

$$(T_{C17} - T_{P17})\left[\exp\left(\frac{(UA)_{F17}}{S_F C_{pP17}}\right)\right] - (T_{C17} - T_{F18}) = 0 \quad (20)$$

7. Material and energy balances on the contents of the steam chests and flash-tanks, and on the mass of metal in the evaporator and preheater tubes for evaporator effects $2 \leq j \leq 17$

$$V_{j-1} + C_{j-1} - C_j - C_{Lj} - V_{Bj} - V_{BAj} + \sigma[V_{j-1} + C_{j-1} - C_j - C_{Lj} - V_{Bj} - V_{BAj}]^0 - \frac{(\mathscr{M}_{Cj} - \mathscr{M}_{Cj}^0)}{\phi\ \Delta t} = 0 \qquad (2 \leq j \leq 17) \quad (21)$$

$$V_{j-1} H_{V,j-1} + C_{j-1} h_{C,j-1} - Q_{Ej} - Q_{Fj} - (C_j + C_{Lj})h_{Cj} - Q_{WSj} - (V_{Bj} + V_{BAj})H_{Cj} + \sigma[V_{j-1} H_{V,j-1} + C_{j-1} h_{C,j-1} - Q_{Ej} - Q_{Fj} - Q_{WSj} - (C_j + C_{Lj})h_{Cj} - (V_{Bj} + V_{BAj})H_{Cj}]^0 - \frac{(\mathscr{M}_{Cj} h_{Cj} - \mathscr{M}_{Cj}^0 h_{Cj}^0)}{\phi\ \Delta t} - \frac{(M_{TEj} C_{pTEj} + M_{TFj} C_{pTFj})(T_{Cj} - T_{Cj}^0)}{\phi\ \Delta t} = 0 \qquad (2 \leq j \leq 17) \quad (22)$$

$$K_{Cj}[\mathscr{M}_{Cj} - (\mathscr{M}_{Cj})_r] - [C_j - (C_j)_r] = 0 \qquad (2 \leq j \leq 17) \quad (23)$$

Table 3-1 Equations required to describe the evaporator system—*Continued*

8. Combination of the vapor streams leaving each evaporator

$$V_{E1} + V_{B1} - V_1 = 0 \quad (24)$$

$$V_{Ej} + V_{AFj} + V_{Bj} - V_j = 0 \qquad (2 \leq j \leq 17) \quad (25)$$

$$V_{E1} H_{E1} + V_{B1} H_{B1} - V_1 H_{V1} = 0 \quad (26)$$

$$V_{Ej} H_{Ej} + V_{AFj} H_{AFj} + V_{Bj} H_{Bj} + V_j H_{Vj} = 0 \qquad (2 \leq j \leq 17) \quad (27)$$

9. Material and energy balances on the process liquid associated with the sump of each evaporator

$$L_{E1} - L_1 + \sigma[L_{E1} - L_1]^0 - \frac{(\mathscr{M}_{L1} - \mathscr{M}_{L1}^0)}{\phi\ \Delta t} = 0 \quad (28)$$

$$L_{Ej} + L_{AFj} - L_j - L_{Rj} + \sigma[L_{Ej} + L_{AFj} - L_j - L_{Rj}]^0 - \frac{(\mathscr{M}_{Lj} - \mathscr{M}_{Lj}^0)}{\phi\ \Delta t} = 0 \qquad (2 \leq j \leq 17) \quad (29)$$

$$L_{E1} X_{E1} - L_1 X_{L1} + \sigma[L_{E1} X_{E1} - L_1 X_{L1}]^0 - \frac{(\mathscr{M}_{L1} X_{L1} - \mathscr{M}_{L1}^0 X_{L1}^0)}{\phi\ \Delta t} = 0 \quad (30)$$

$$L_{Ej} X_{Ej} + L_{AFj} X_{AFj} - (L_j + L_{Rj})X_{Lj} + \sigma[L_{Ej} X_{Ej} + L_{AFj} X_{AFj} - (L_j + L_{Rj})X_{Lj}]^0 - \frac{(\mathscr{M}_{Lj} X_{Lj} - \mathscr{M}_{Lj}^0 X_{Lj}^0)}{\phi\ \Delta t} = 0 \qquad (2 \leq j \leq 17) \quad (31)$$

$$L_{E1} h_{E1} - L_1 h_{L1} - Q_{WL1} + \sigma[L_{E1} h_{E1} - L_1 h_{L1}]^0 - \frac{(\mathscr{M}_{L1} h_{L1} - \mathscr{M}_{L1}^0 h_{L1}^0)}{\phi\ \Delta t} = 0 \quad (32)$$

$$L_{Ej} h_{Ej} + L_{AFj} h_{AFj} - (L_j + L_{Rj})h_{Lj} - Q_{WLj} + \sigma[L_{Ej} h_{Ej} + L_{AFj} h_{AFj} - (L_j + L_{Rj})h_{Lj} - Q_{WLj}]^0 - \frac{(\mathscr{M}_{Lj} h_{Lj} - \mathscr{M}_{Lj}^0 h_{Lj}^0)}{\phi\ \Delta t} = 0 \qquad (2 \leq j \leq 17) \quad (33)$$

$$K_{Lj}[\mathscr{M}_{Lj} - (\mathscr{M}_{Lj})_r] - [L_j - (L_j)_r] = 0 \qquad (1 \leq j \leq 17) \quad (34)$$

where

$$Q_{WLj} = (UA)_{WLj}(T_{Lj} - T_{WLj}) \qquad (1 \leq j \leq 17)$$

10. Material and energy holdups on the feed preheaters

$$FX_{F,j+1} - FX_{Fj} + \sigma[FX_{F,j+1} - FX_{Fj}]^0 - \frac{\mathscr{M}_{Fj}(X_{Fj} - X_{Fj}^0)}{\phi\ \Delta t} = 0 \qquad (1 \leq j \leq 16) \quad (35)$$

$$F(h_{Pj} - h_{Fj}) + \sigma[F(h_{Pj} - h_{Fj})]^0 - \left[\frac{\mathscr{M}_{Fj}(h_{Fj} - h_{Fj}^0) - M_{Fj} C_{pMFj}(T_{Fj} - T_{Fj}^0)}{\phi\ \Delta t}\right] = 0 \qquad (1 \leq j \leq 16) \quad (36)$$

(Continued over)

Table 3-1 Equations required to describe the evaporator system—*Continued*

11. Modeling of the acid treater

$$S_F - V_{AF} - F + \sigma[S_F - V_{AF} - F]^0 - \frac{(\mathcal{M}_{F17} - \mathcal{M}^0_{F17})}{\phi\,\Delta t} = 0 \quad (37)$$

$$S_F X_{F18} - F X_{F17} + \sigma[S_F X_{F18} - F X_{F17}]^0 - \frac{(\mathcal{M}_{F17} X_{F17} - \mathcal{M}^0_{F17} X^0_{F17})}{\phi\,\Delta t} = 0 \quad (38)$$

$$S_F h_{P17} - V_{AF} H_{AF} - F h_{F17} + \sigma[S_F h_{P17} - V_{AF} H_{AF} - F h_{F17}]^0 - \left[\frac{M_{F17} C_{pMF17}(T_{F17} - T^0_{F17}) + (\mathcal{M}_{F17} h_{F17} - \mathcal{M}^0_{F17} h^0_{F17})}{\phi\,\Delta t}\right] = 0 \quad (39)$$

$$K_{F17}[\mathcal{M}_{F17} - (\mathcal{M}_{F17})_r] - (F - F_r) = 0 \quad (40)$$

$$S_F(h_{P17} - h_{AF}) - V_A(H_{AF} - h_{AF}) = 0 \quad (41)$$

where the enthalpy h_{AF} of the flashed liquid is computed on the basis of the composition X_{AF}, namely,

$$X_{AF} = \frac{S_F X_{18}}{L_{AF}} = \frac{S_F X_{18}}{S_F - V_{AF}}$$

As indicated in assumption 20, V_{AF} was taken to be fixed at the value it had prior to the upset. V_{AF} was determined at the steady state flow rate S_F by fixing the temperature T_{AF} such that the difference $(T_{P17} - T_{AF})$ was equal to 1°F. Then the above equations were solved for V_{AF}, L_{AF}, and X_{AF}.

12. Material and energy balances for the final condenser

$$(T_{C18} - T_{out})\left[\exp\left(\frac{(UA)_{E18}}{wC_p}\right)\right] - (T_{C18} - T_{in}) = 0 \quad (42)$$

$$V_{17} H_{V17} - V_{BA18} H_{C18} - C_{18} h_{C18} - wC_p(T_{out} - T_{in}) = 0 \quad (43)$$

$$V_{17} - C_{18} - V_{BA18} = 0 \quad (44)$$

13. Material and energy balances on the inlet-feed preheater

$$C_{17} h_{C17} + C_{18} h_{C18} - C_{19} h_{C19} = 0 \quad (45)$$

where

$$C_{19} = C_{18} + C_{17}$$

$$C_{19} C_{pC19}(T_{C19} - T_{C20}) - S_F C_{pF18}(T_{F18} - T_{P18}) = 0 \quad (46)$$

$$(T_{C20} - T_{P18})\left\{\exp\left[(UA)_{F18}\left(\frac{1}{C_{19} C_{pC19}} - \frac{1}{S_F C_{pF18}}\right)\right]\right\} - (T_{C19} - T_{F18}) = 0 \quad (47)$$

14. Plug flow section preceding the inlet-feed preheater

The mathematical model for the plug flow section assumed for the process model in assumption 22, and shown in Fig. 3-16, is a linear model. Inlet values of the physical properties were stored for the end conditions of each time interval. Exit values of the properties were determined by a linear interpolation between the sample values whose times bracketed the run time t_n minus the holdup time.

Table 3-1 Equations required to describe the evaporator system—*Continued*

The equations used to determine the temperature T_{P18} and the feed composition X_{F18} at time t_n are given by

$$T_{P18}\Big|_{t_n} = (1 - \theta)T_{SF}\Big|_{t_{n-k}} + \theta T_{SF}\Big|_{t_{n-k+1}} \quad (48)$$

$$X_{F18}\Big|_{t_n} = (1 - \theta)X_{SF}\Big|_{t_{n-k}} + \theta X_{SF}\Big|_{t_{n-k+1}} \quad (49)$$

where

$$\theta = \frac{t_n - (\mathcal{M}_{F18}/S_F)\Big|_{t_n} - t_{n-k}}{(t_{n-k+1} - t_{n-k})}$$

where k is selected such that

$$t_{n-k} \le t_n - (\mathcal{M}_{F18}/S_F)\Big|_{t_n} < t_{n-k+1}$$

These equations, which are of course independent of the remaining equations for the model, were solved once each time step.

discussed in Sec. 3-1. For any evaporator effect j $(1 \le j \le 17)$ over the time period from t_n to $t_n + \Delta t$, the energy balance for the portion of the wall under consideration is given by

$$\int_{t_n}^{t_n + \Delta t} (Q_{WSj} - Q_{ASj})\,dt = M_{WSj} h_{WSj}\Big|_{t_n + \Delta t} - M_{WSj} h_{WSj}\Big|_{t_n}$$

Use of the implicit method to approximate the integral on the left-hand side of this equation yields the following result upon rearrangement:

$$Q_{WS} - Q_{ASj} + \sigma[Q_{WSj} - Q_{ASj}]^0 - \frac{M_{WSj} C_{pWSj}(T_{WSj} - T^0_{WSj})}{\phi\,\Delta t} = 0 \qquad (1 \le j \le 17) \quad (3\text{-}23)$$

where

$$\sigma = (1 - \phi)/\phi$$

$$Q_{WS1} = (UA)_{WS1}(T_{C0} - T_{WS1})$$

$$Q_{WSj} = (UA)_{WSj}(T_{Cj} - T_{WSj}) \qquad (2 \le j \le 17)$$

$$Q_{ASj} = (UA)_{ASj}(T_{WSj} - T_A) \qquad (1 \le j \le 17)$$

When the metal walls of an evaporator are exposed to process liquid on one side and the surroundings on the other side, the energy balances are based on assumptions 3 and 4 and the models shown in Figs. 3-4 and 3-12. In this

case, the following result is obtained upon reduction of the integral-difference equation to algebraic form:

$$Q_{WLj} - Q_{ALj} + \sigma[Q_{WLj} - Q_{ALj}]^0 - \frac{M_{WLj} C_{pWLj}(T_{WLj} - T^0_{WLj})}{\phi\ \Delta t} = 0 \qquad (1 \le j \le 17) \tag{3-24}$$

where

$$Q_{WLj} = (UA)_{WLj}(T_{Lj} - T_{WLj}) \qquad (1 \le j \le 17)$$
$$Q_{ALj} = (UA)_{ALj}(T_{WLj} - T_A) \qquad (1 \le j \le 17)$$

Material and energy balances on the contents in the evaporator tubes The balances are based on assumptions 1, 5, 6, 7, 8, and 23. Models for this portion of the system are presented in Figs. 3-4, 3-10, and 3-13. The holdup of mass and energy in the evaporator tubes is negligible relative to that in the sumps and is disregarded in the following balances. The component-material balances over the time period from t_n to $t_n + \Delta t$ are given by

$$\int_{t_n}^{t_n+\Delta t} (FX_{F1} - L_{F1} X_{E1})\, dt = 0$$

$$\int_{t_n}^{t_n+\Delta t} (\alpha_{j-1} L_{j-1} X_{L,j-1} + L_{Rj} X_{Lj} - L_{Ej} X_{Ej})\, dt = 0$$

Since the integrals given by these equations are equal to zero for all choices of t_n and $t_n + \Delta t$ in the time domain of interest, it follows that the respective integrands are identically equal to zero for all t lying between t_n and $t_n + \Delta t$. For such cases, the given balance (material or energy) is stated in its instantaneous form corresponding to the end of the time period under consideration as follows:

$$FX_{F1} - L_{E1} X_{E1} = 0 \tag{3-25}$$

$$\alpha_{j-1} L_{j-1} X_{L,j-1} + L_{Rj} X_{Lj} - L_{Ej} X_{Ej} = 0 \qquad (2 \le j \le 17) \tag{3-26}$$

$$F - L_{E1} - V_{E1} + C_{L1} = 0 \tag{3-27}$$

$$\alpha_{j-1} L_{j-1} + L_{Rj} - L_{Ej} - V_{Ej} + C_{Lj} = 0 \qquad (2 \le j \le 17) \tag{3-28}$$

$$Fh_{F1} + Q_{E1} - L_{E1} h_{E1} - V_{E1} H_{E1} + C_{L1} h_{CL1} = 0 \tag{3-29}$$

$$\alpha_{j-1} L_{j-1} h_{L,j-1} + L_{Rj} h_{Lj} + Q_{Ej} - L_{Ej} h_{Ej} - V_{Ej} H_{Ej} + C_{Lj} h_{CLj} = 0 \qquad (2 \le j \le 17) \tag{3-30}$$

where

$$Q_{E1} = (UA)_{E1}(T_{C0} - T_{E1})$$
$$Q_{Ej} = (UA)_{Ej}(T_{Cj} - T_{Ej}) \qquad (2 \le j \le 17)$$

The temperature T_{Ej} of the liquid in the evaporator tubes is computed by using Dühring lines, which may be represented as follows:

$$mT_{C,j+1} + b - T_{Ej} = 0 \qquad (1 \le j \le 17) \tag{3-31}$$

where the slope m depends upon both X_{Ej} and $T_{C,j+1}$, and b depends upon X_{Ej} alone, that is, $m = m(X_{Ej}, T_{C,j+1})$ and $b = b(X_{Ej})$.

Energy and rate equations for the feed preheaters for evaporator effects $2 \le j \le 17$ Models of the seawater preheaters are shown in Figs. 3-4, 3-14, and 3-16. When the mass and energy holdups of a given part of the system are negligible relative to any other part, the integral-difference equations reduce simply to the dynamic form of the algebraic equations required to describe the corresponding steady state process. Thus, on the basis of assumption 13, it follows that the instantaneous rate of heat transfer in the seawater preheaters is given by

$$Q_{Fj} = (UA)_{Fj}\left\{\frac{T_{Pj} - T_{F,j+1}}{\ln\left[(T_{Cj} - T_{F,j+1})/(T_{Cj} - T_{Pj})\right]}\right\} \qquad (2 \le j \le 17) \tag{3-32}$$

On the basis of assumptions 12 and 13, the following expressions are obtained for the energy balances on the seawater preheaters:

$$Q_{Fj} = FC_{pPj}(T_{Pj} - T_{F,j+1}) \qquad (2 \le j \le 16), \tag{3-33}$$

$$Q_{F17} = S_F C_{pP17}(T_{P17} - T_{F18}) \tag{3-34}$$

where Q_{F17} is the rate of heat transfer in the inlet-feed preheater (shown in Fig. 3-16).

Elimination of Q_{Fj} $(2 \le j \le 16)$ from the first two expressions yields

$$(T_{Cj} - T_{Pj})\left\{\exp\left[\frac{(UA)_{Fj}}{FC_{pPj}}\right]\right\} - (T_{Cj} - T_{F,j+1}) = 0 \qquad (2 \le j \le 16) \tag{3-35}$$

Similarly, the elimination of Q_{F17} from the first and third expressions gives

$$(T_{C17} - T_{P17})\left\{\exp\left[\frac{(UA)_{F17}}{S_F C_{pP17}}\right]\right\} - (T_{C17} - T_{F18}) = 0 \tag{3-36}$$

Control of mass holdup in the evaporators The holdups were controlled by either proportional controllers or self-regulated by gravity flow from sump to sump. In either case the following expression was used to relate the holdups and flow rates:

$$K_{Lj}[\mathcal{M}_{Lj} - (\mathcal{M}_{Lj})_r] - [(L_j - (L_j)_r] = 0 \qquad (1 \le j \le 17) \tag{3-37}$$

where the proportionality constant K_{Lj} depends upon the proportional band width or gain of the controller, the type of control valve, and the geometry of the sump. The subscript r denotes the value of the variable when the controlled variable is at its reference point.

The equations for the remaining parts of the system are developed in a manner analogous to that shown above.

Summary of the Mathematical Model

The mathematical model consists of the complete set of 380 independent equations (see Eqs. (1) through (47) of Table 3-1) in 380 unknowns plus the plug flow relationships given by Eqs. (48) and (49) of Table 3-1. The first effect is described by 19 independent equations, one of which is given by each of the following equations numbers: (1), (2), (3), (5), (7), (9), (14) through (18), (22), (24), (27), (30), (32), (34), (35), and (36). Of the variables appearing in these equations, 19 of them are for the first effect. They are as follows: T_{C0}, T_{IC}, T_{C1}, T_{P1}, T_{F1}, T_{E1}, T_{L1}, T_{WS1}, T_{WL1}, T_{V1}, V_{E1}, V_1, C_1, L_{E1}, L_1, X_{F1}, X_{E1}, X_{L1}, and $\mathcal{M}_{L1}$. If the steam temperature T_{C0} is fixed (that is, the steam supply is on pressure control), the supply steam flow rate V_0 becomes the independent variable.

Effects 2 through 17 plus the peripheral equipment are seen to be described above by 361 independent equations. (The independent equations are assigned equation numbers.) In addition to one or more of the variables enumerated for the first effect, these 361 equations contain 361 additional independent variables, which are as follows: T_{Cj}, T_{Pj}, T_{Fj}, T_{Ej}, T_{Lj}, T_{WSj}, T_{WLj}, T_{Vj}, T_{AFj}, V_{Ej}, V_j, V_{AFj}, C_j, L_{Ej}, L_j, L_{AFj}, X_{Fj}, X_{Ej}, X_{Lj}, X_{AFj}, $\mathcal{M}_{Cj}$, and $\mathcal{M}_{Lj}$ (where $2 \leq j \leq 17$ for a total of $22 \times 16 = 352$ variables), plus the following nine variables: T_{F18}, T_{AF}, T_{C18}, T_{out}, T_{C19}, T_{C20}, C_{18}, F, and $\mathcal{M}_{F19}$.

The liquid holdups, such as $\mathcal{M}_{F1}$ and $\mathcal{M}_{C1}$ were fixed by the physical specifications of the equipment. The temperature T_{P18} and the brine concentration X_{F18} were computed once each time step by use of the explicit relationships given by Eqs. (48) and (49). These values were used throughout the course of the solution of the 380 equations for the 380 unknowns.

3-3 ANALYSIS OF THE RESULTS OF FIELD TESTS

To evaluate the ability of the proposed model to predict the dynamic behavior of the desalination plant, several field tests were run on this plant. The predicted behavior of the plant by the model was obtained by solving the equations for the model at the end of each time step and on the basis of a given set of operating conditions and physical parameters for the plant. There follows a brief discussion of the procedures utilized in the testing of the model through the use of field tests.

Calculational Procedures

The 380 equations (Eqs. (7) through (47)) describing the model of the plant were solved simultaneously for the variables at the end of each time step by use of the Newton–Raphson method as demonstrated in Chap. 2. The first step in this

application of the Newton–Raphson method consisted of replacing the zero on the right-hand side of each of the 380 equations by the functional notation f_k ($1 \leq k \leq 380$). In order that any $\Delta t > 0$ might be used at any point in the sequence of calculations without having the inherited error become unbounded, a $\phi = 0.6$ was employed. Also, the generalized scaling procedure (variable scaling and row scaling) described in Chap. 2 was employed. A solution set of variables at the end of the time step under consideration was said to have been obtained when each element of $\Delta\mathbf{Y}$ was equal to or less than 0.000 05 and each element of $\mathbf{F}$ was equal to or less than 0.000 01 (see Eqs. (2-37) through (2-42)).

The program for the unsteady state model could be used to obtain the steady state solution for the given set of operating conditions by setting $\phi = 1$ and by setting $\Delta t = 10^{30}$ hours. This choice of values for ϕ and Δt had the effect of the elimination of the input and output terms at the beginning of the time step as well as the elimination of the accumulation terms, and thereby gave the steady state equations corresponding to the final steady state.

In the application of the Newton–Raphson method, approximations were used for certain of the partial derivatives. In particular, the partial derivatives of the liquid enthalpies with respect to salt content were taken to be equal to zero.

On the average, about four iterations of the Newton–Raphson method were required per time step (Ref. 3). About 15 iterations were required to solve the initial steady state problems. More trials were required for the steady state problem than were required for each time step of the unsteady state problem because the initial guesses for the steady state problem were poorer than those for the unsteady state problem. The initial guesses for the steady state problem were deduced by use of a relatively simple scheme which was similar to those commonly used; see, for example, Perry(20).

The initial guesses for the values of the variables at the end of each time step consisted of taking them equal to the values of these variables which were found at the end of the previous time step. An IBM 360 model 65 computer was used to solve the equations for the model. Approximately one minute was required to obtain a steady state solution, and approximately 20 seconds were required to obtain a solution for each time step of the unsteady state problem.

Determination of Equipment Parameters

Physical dimensions of the holdup volumes, the surface areas, the masses of metal, and the types of materials of the heat sinks were obtained from the construction blueprints of the plant. Since "effective values" were needed in the model, some personal judgment was used in assigning part or all of a mass (or volume) to its counterpart in the process model.

Heat transfer areas for the tubes of the preheaters and evaporators were obtained from the status records of the plant equipment (Ref. 4). Coefficients of heat transfer for the feed preheaters and the evaporators were determined from the results of recent steady state test runs performed and reported by plant personnel (Ref. 4). The coefficients so obtained as well as the heat transfer areas

and masses of metal are presented in Tables 3-2 and 3-3. Although values for the heat transfer coefficients for the evaporators could have been calculated by use of procedures proposed by Huang et al.(17), the experimental values from the steady state tests were used because it was felt that they most closely approximated the values that existed at the time the unsteady state tests were made. Since the coefficients of heat transfer for LTV evaporators vary with operating temperature (Refs. 23, 24), the values used during the numerical evaluation of the mathematical model were adjusted for the effect of temperature (when it differed from those at which the coefficients were evaluated) by use of the relationship reported by Standiford(24). In particular, the derivative of the heat transfer coefficient h_{Ej} with respect to T_{Ej} was taken to be equal to the slope of the line shown in Fig. 3-17.

Other film coefficients employed were computed by use of relationships given by Perry(20) (see Table 3A-1 of App. 3A). Physical properties of the metal walls, tubing, piping, and the insulation were taken from Perry(20) as well as the thermodynamic and physical properties of steam and water (see Table 3A-1).

Enthalpies, specific heats, and boiling point elevations of the brine process liquid were taken from Refs. 2 and 10 (see Table 3A-1).

Table 3-2 Specifications for the evaporators (Ref. 4)

	Heat transfer tubes			
Effect	Area, ft^2	Heat transfer coefficient, $Btu/(h \cdot °F \cdot ft^2)$	Reference temperature, °F	Mass, lb
1	3810	720	266	11 429
2	3420	723	258	10 264
3	3700	561	250	11 110
4	3690	795	242	11 110
5	3700	563	232	11 110
6	3710	702	223	11 146
7	3420	670	214	11 182
8	3420	666	205	10 264
9	3600	412	194	10 900
10	3700	396	185	11 110
11	3710	411	176	11 146
12	4290	259	160	12 864
13	3940	432	148	9 259
14	4000	320	134	6 340
15	3940	345	119	11 828
16	3490	358	104	8 202
17	3730	220	87	8 766
18†	4000	188	80	11 970

Table 3-2—*Continued*

	Effective values for the metal walls					
	Exposed to process liquid			Exposed to steam or condensate		
	Area, ft^2			Area, ft^2		
Effect	Inside	Outside	Mass in 1000's of lb	Inside	Outside	Mass, in 1000's of lb
1	692	657	23.0	308	293	6.56
2	692	657	20.6	774	735	13.3
3	692	657	20.6	782	743	13.4
4	692	657	20.6	628	597	11.4
5	692	657	20.6	657	641	12.0
6	692	657	20.6	796	756	13.0
7	692	657	20.6	627	596	10.9
8	777	738	18.6	737	700	11.3
9	777	738	18.6	700	665	11.7
10	882	838	22.4	734	697	12.2
11	1055	1002	27.4	790	750	13.0
12	1438	1366	34.3	1124	1068	22.4
13	322	205	5.89	929	447	20.9
14	315	121	5.08	1125	431	20.9
15	315	121	5.08	1125	431	20.4
16	315	121	5.08	1125	431	20.4
17	327	137	5.60	1622	963	31.7

† Final condenser.

Test Run 1

During test runs, the plant was operated by the usual plant personnel. Samples from the process lines and data from nonrecording instruments were collected during the test by technical personnel of the plant and by several graduate students from the Department of Chemical Engineering of Texas A&M University.

Test run 1 (assigned the number 8-17-11A by Burdett(3)) consisted of a sequence of upsets in the salt concentration of the seawater feed, see Table 3-4. These upsets were achieved by diluting the incoming seawater with product water from the plant. At the desired time for the initial upset, a valve was partially opened which permitted product water to enter the suction side of the seawater feed pump. The amount of dilution was determined by the change in the refractive index of a sample taken from the discharge side of the pump.

Samples of the process liquid were taken at the outlets of the feed pump, the acid treater, and the evaporator sumps. The sampling was carried out according to a preselected time schedule for each sample point. Flow rates,

Table 3-3 Specifications for the feed preheaters (Ref. 4)

	Heat transfer tubes			Holdup	
				Mass, lb	
Effect	Area, ft^2	Heat transfer coefficient, Btu/(h·°F·ft^2)	Mass, lb	Metal	Liquid
1	520	220	1080	1460	1264
2	3360	348	4000	2949	4935
3	2820	643	5870	2748	4224
4	2290	225	4760	1575	3168
5	3010	250	6270	1374	3747
6	3490	476	7270	2748	5084
7	1790	390	3730	1603	2805
8	1790	400	3730	1775	2224
9	1800	350	3750	1632	2221
10	1770	315	3690	1660	2113
11	1740	310	3620	1660	2083
12	1980	430	4120	2060	2636
13	1460	625	3040	3020	2767
14	1460	400	3040	751	1560
15	1770	405	3690	751	1875
16	2420	345	5050	751	2545
17	2420	435	5050	26950†	11100†
18		155	8310		24800

† Includes volume or mass equivalent for acid treater components.

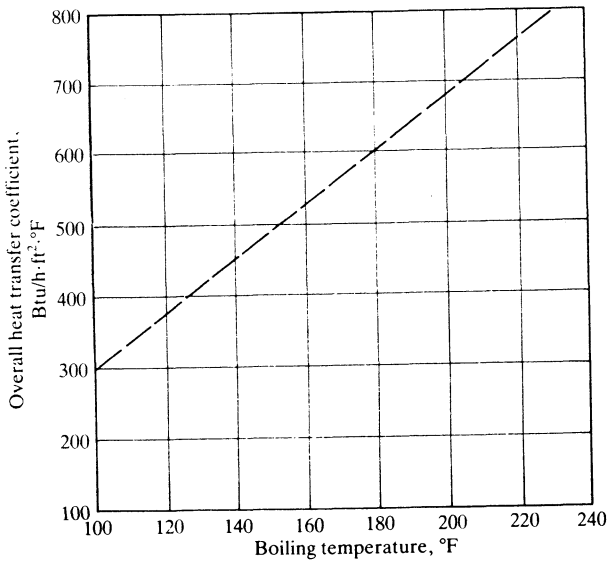

Figure 3-17 Actual coefficients for LTV seawater evaporators of the falling film type. (*F. C. Standiford, "Evaporation," Chem. Eng. vol. 70, p. 157 (1963).*)

Table 3-4 Operating conditions of the evaporator system for test run 1 (Ref. 3)

Parameter	Initial value
Seawater feed rate, thousand pounds per hour	480
Concentration of brine in feed, X_{SF}	0.935
Temperature of feed, °F	82
Temperature of steam to effect 1, °F	300
Dewpoint in first steam chest, °F	270
Steam rate to first steam chest, thousand pounds per hour	26
Cooling water supply rate, thousand pounds per hour	986
Temperature of cooling water, °F	82
Temperature of atmospheric air, °F	80
Control method for steam (= pressure)	

Upset schedule

Time, min	Upset variable	New value	Type of change	Time constant, min	Step size, min
0	X_{SF}	0.692	Linear	1.0	0.5
7	X_{SF}	0.632	Linear	0.5	0.5
10	X_{SF}	0.560	Linear	0.5	0.5
25	X_{SF}	0.576	Linear	0.0	1.0
30	None				2.0
50	None				5.0
80	None				10.0

temperatures, and sump levels were monitored and recorded by the instruments in the control room.

Salt content of each sample was determined by measuring its refractive index. The refractive index was calibrated against the salt content as determined by titration of the calibration samples with silver nitrate. The salt content of the samples was expressed in terms of the concentration factor (C.F.) which represented the ratio of the chlorinity of the sample to the chlorinity of normal seawater (Ref. 9). Chlorinity is the total amount of chlorine (grams) contained in one kilogram of seawater in which all of the bromine and iodine have been replaced by chlorine.

Two sets of variables were used for the comparison of the experimental and calculated results of this test run, namely, the vapor temperatures and the salt concentrations of the brine process liquid. The temperatures of the vapors leaving effects 1 through 12 were monitored during the transient operation by means of thermocouples located in the vapor lines leaving each effect. Salt concentrations were determined for samples which were withdrawn from the discharge side of pumps used to transfer (or recycle) the brine process liquid.

Prior to making run 1, the plant was brought to a steady state with the process variables at typical operating levels, and then the salt concentration of the feed was upset as shown in Table 3-4. Operating specifications for the system of evaporators for run 1 are shown in Table 3-5. Temperatures of the

Table 3-5 Operating specifications within the evaporator system for test run 1 (Ref. 3)

Effect	Vent rates, lb/h: Cascade	Vent rates, lb/h: External	Recycle rates, 1000 lb/h	Feed brine inlet†	Level in sump, % of range‡: Measured	Level in sump, % of range‡: Used	Condensate leakage 1000 lb/h
1	63	0	0	Top	19.5	25	0
2	376	0	0	Top	21.5	11	0
3	138	0	0	Top	19.0	18	0
4	0	360	0	Top	19.5	30	0
5	177	0	0	Top	19.5	24	3
6	146	0	0	Top	19.0	23	0
7	120	0	0	Top	19.5	26	0
8	202	0	0	Top	18.5	18	0
9	148	0	0	Top	19.0	29	0
10	256	0	0	Top	26.0	26	0
11	210	0	130	Sump	27.5	24	0
12	0	300	63	Sump	57	37	0
13	200	0	131	Sump	43	29	2
14	200	0	131	Sump	48	34	0
15	200	0	131	Top	52	27	1
16	200	830	131	Top	64	49	1
17	200	0	131	Top	48	53	3
Final condensate	0	50					

Temperature drop of feed through acid treater, 1°F

† Top of evaporator tubes.
‡ Level controller ranges: 200 inches for Effects 1 through 12, 50 inches for Effects 13 through 17.

exit vapors and the concentrations of the brine process liquid leaving the sumps at the initial steady state are presented in Table 3-6. The average deviation between the measured and the calculated temperatures for the first twelve effects was 1.9°F. If the temperatures indicated by the thermocouples were dewpoint temperatures rather than the actual temperatures of the superheated vapors, then the measured temperatures should be compared to the condensate temperatures of the steam chests of the next effect. When such a comparison was made, an average deviation of 0.9°F was obtained for the first 11 effects, and a deviation of 4.4°F was obtained for the 12th effect. The higher deviation for the 12th effect was attributed to the low value of the heat transfer coefficient used in the calculation (see Table 3-2). Since the agreement between the measured and calculated temperatures was relatively good, no adjustments were made of the heat transfer coefficients or vent rates.

The experimentally determined salt concentrations of the brine process liquid which flowed from the sumps of the evaporators were in good agreement with the values calculated by use of the model (see Table 3-6). At steady state

operation, the good agreement between the calculated and observed salt concentrations implies that the agreement between the actual and the calculated flow rates of the brine process liquid was also good.

Throughout the sequence of upsets in the salt concentrations of the feed, the temperatures and flow rates of the process streams remained relatively constant. The concentration of salt in each of the process liquid streams leaving each of the sumps varied with time as predicted by the model (see Fig. 3-18). Samples of the various process liquid streams were taken at times at which it had been anticipated that the breakpoints of the time-concentration curves would be included. Levels of process liquid in the sumps were measured with differential-pressure transmitters, which were read by use of the display meters located in the control room. The flow of purge water through the pressure taps into the sumps caused significant errors in the determination of some of the liquid levels. Because of this difficulty, estimates of the actual levels were made by use of the breakpoints in the time-concentration curves. These estimated levels were utilized in the calculational procedure. In Table 3-5, both the measured levels recorded during the test and the estimated levels are listed.

The good agreement between the calculated and measured slopes of the time-concentration curves following the breakpoints (see Fig. 3-18) demonstrates that the holdup of the process liquid is adequately described by the use of

Table 3-6 Steady state vapor temperatures and brine concentrations for test run 1 (Ref. 3)

Effect	Temperature of exit vapors, °F: Measured at plant	Temperature of exit vapors, °F: Calculated from model	Concentration of brine from sump, C.F.: Plant sample	Concentration of brine from sump, C.F.: Calculated from model
1	263	262.8	0.97	0.98
2	252	255.3	1.02	1.03
3	246	246.9	1.08	1.08
4	239	240.1	1.13	1.13
5	231	231.6	1.18	1.18
6	223	224.5	1.24	1.25
7	214	216.7	1.30	1.32
8	206	209.1	1.38	1.39
9	197	199.1	1.46	1.47
10	186	188.9	...	1.56
11	176	178.3	1.66	1.67
12	167	165.2	1.78	1.78
13	...	155.5	1.89	1.90
14	...	144.1	2.05	2.05
15	...	133.0	2.22	2.21
16	...	122.0	2.39	2.39
17	...	110.4	2.58	2.54

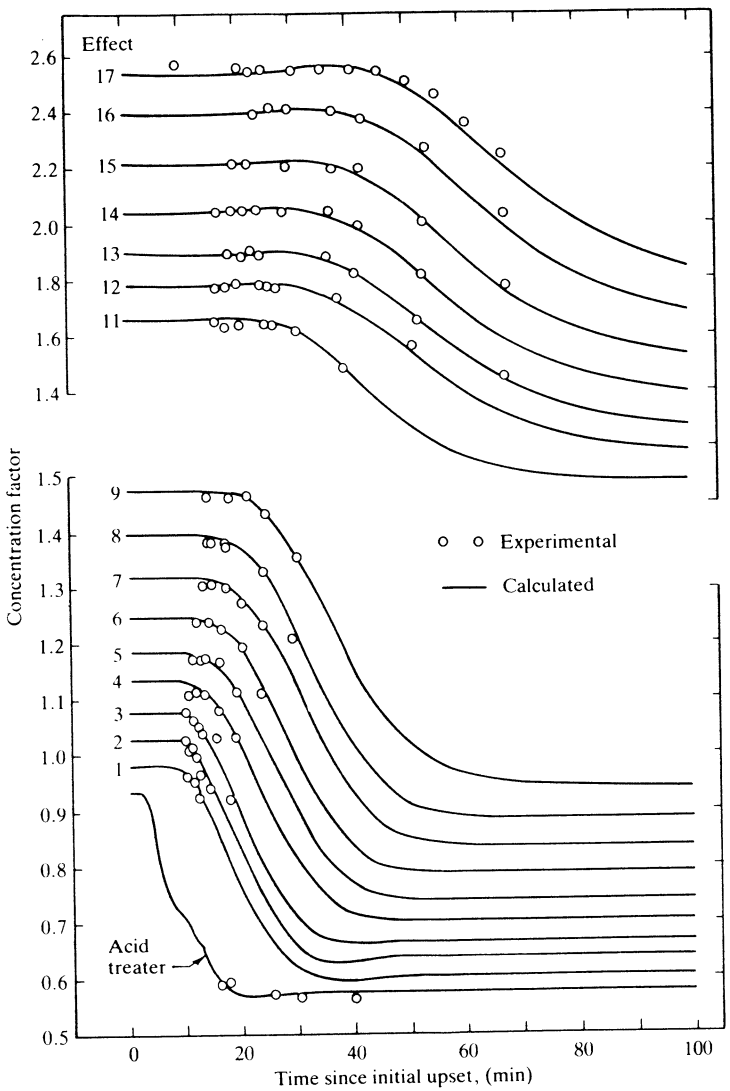

Figure 3-18 Concentrations of brines leaving evaporators sampled during test run 1. (*J. W. Burdett and C. D. Holland: "Dynamics of a Multiple-Effect Evaporator System," AIChE J., vol. 17, p. 1080 (1971). Courtesy of the American Institute of Chemical Engineers.*)

perfect mixers in the process model. Also, it should be pointed out that no corrections or adjustments were made on the experimental results presented herein and elsewhere (Ref. 3).

In a second sequence of upsets of the feed rate (assigned to the number 8-24-11A by Burdett(3)), good agreement between the observed and predicted behavior of the system of evaporators was obtained by Burdett(3).

Actually, some of the observed values of the variables would have had to have been adjusted in order to have placed them in energy and material balance. On the other hand, the model required that the system be in energy-and-material balance at all times. Therefore, no amount of searching for other values of the parameters would have placed the measured and calculated values of the variables in exact agreement.

No attempt was made to use the results of the test runs to obtain values of the parameters except as was stated for the level controllers on the evaporator sumps. Also, an estimate of the condensate leakage was made for run 1 in order to account for inconsistencies in the brine concentrations which were observed at the initial steady state prior to the upset.

Thus, the initial steady state values and the unsteady state values of the variables which were calculated by use of the model represent a fair evaluation of how well the steady state and dynamic response of a system of evaporators could be predicted by use of the proposed model.

It has been demonstrated that a large system may be modeled by modeling each component of the system. For certain systems, the partial differential equations describing the heat transfer may be replaced with good accuracy by a corresponding set of ordinary differential equations through the use of the heat transfer model proposed in Sec. 3-1. Also, it has been demonstrated that certain process equipment in which the holdups are negligible relative to the other parts of the system may be represented by the dynamic form of the steady state equations.

NOTATION

a = constant defined below Eq. (3-13)
A = area perpendicular to the direction of heat transfer, ft^2
C_j = flow rate at which condensate leaves evaporator effect j, lb/h
C_n = constant defined below Eq. (3-13)
C_v, C_p = heat capacities at constant volume and constant pressure, respectively, Btu/(lb °F)
D_i = internal diameter, ft
D_n = constant defined below Eq. (3-13)
E = internal energy above any arbitrary datum, Btu/lb
h = enthalpy of a liquid phase Btu/lb (also, the coefficient of heat transfer is denoted by this symbol and has the units of $Btu/(h \cdot ft^2 \cdot °F)$)

h_e = film coefficient corresponding to an equivalent thermal resistance
C.F. = chlorinity of sample divided by the chlorinity of normal seawater. The chlorinity of seawater is equal to the number of grams of chlorine contained in one kilogram of seawater after all of the bromide and iodide have been replaced by chloride
H = enthalpy of the vapor phase, Btu/lb
H_1, H_2 = constants defined below Eq. (3-13)
k = thermal conductivity, (Btu/h · ft · °F)
K_{Cj}, K_{Lj} = proportionality factors used in the linearized relationships for the flow rates
l = thickness of metal wall, ft
L = flow rate of process liquid, lb/h (also used to denote the length in feet along the axis of a cylinder)
m = slope of Dühring line (see Eq. (3-9)) (also used to denote the mean value of a variable)
$\mathscr{M}$ = mass of liquid holdup, lb
M = mass of metal holdup, lb
P_j = pressure in the vapor space of evaporator effect j, lb/ft^2
Q = rate of heat transfer, Btu/h
T_{co} = temperature of steam to the first effect

Subscripts

av = arithmetic average
A = surroundings or ambient conditions
AF = adiabatic flash of the seawater feed
AF_j = adiabatic flash of the process liquid ($2 \leq j \leq 17$)
BA = bleed to the surroundings
C = condensate
E = evaporate (also refers to the conditions in the tubes of an evaporator)
F = feed
in = inlet conditions of the cooling water to the final condenser
IC = intermediate condition of the condensate leaving the first effect (see Fig. 3-15)
j = effect number (j = 1, 2, 3, ..., 17), and subscripts j = 18, 19, and 20 refer to streams treated by peripheral equipment
L = process liquid at the conditions in the sump
m = mean value
out = temperature of water leaving the final condenser
P = condition of the feed leaving a feed preheater (see Figs. 3-14 through 3-16)
S = steam
V = vapor
WL = variables associated with the transfer of heat from process liquid to a metal wall (also used to denote the mean temperature of the wall (see Fig. 3-12)) (the symbol "AL" refers to the transfer of heat from this wall to the surroundings)
WS = variables associated with the transfer of heat from steam to a metal wall (also used to denote the mean temperature of the wall shown in Fig. 3-11) (the symbol "AS" refers to the transfer of heat from this wall to the surroundings)
r = radius of cylindrical shell (also used to denote the reference point or control point of a controller)
S_F = seawater feed
T = temperature, °F
U = overall coefficient of heat transfer, Btu/(h · ft^2 · °F)
V = flow rate of vapor, lb/h
w = flow rate of coolant to the final condenser, lb/h
x = mass fraction of the solute (also used to denote distance in the boundary problems)
Y_n = a function defined below Eq. (3-13)

Greek letters

α_j = fraction of the liquid L_j entering the tubes of evaporator effect j (see Fig. 3-4) (also used to represent the ratio $(k/\rho C_v)$ in Eq. (3-11))
β_n = the nth positive root of the equation presented below Eq. (3-13)
ρ = density, lb/ft^3
π = 3.1416 radians
σ = $\phi/(1-\phi)$
ϕ = weighting factor for the implicit method

Mathematical symbols

$[f(t)]^0$ = the value of the function $f(t)$ at the beginning of the time period under consideration

REFERENCES

1. C. F. Bonilla: "Design of Multiple-Effect Evaporators for Minimum Area or Minimum Cost," *Trans. AIChE*, **41**: 529 (1945).
2. L. A. Bromley, V. A. Desaussure, J. C. Clipp, and J. S. Wright: "Heat Capacities of Sea Water Solutions at Salinities of 1 to 12% and Temperatures of 2 to 80°C.," *J. Chem. Eng. Data*, **12**: 203 (1967).
3. J. W. Burdett: "Prediction of the Steady State and Unsteady State Response Behavior of a Multiple-Effect Evaporator System," Ph.D. dissertation, Texas A&M University, College Station, Texas, 1970. See also J. W. Burdett and C. D. Holland, "Dynamics of a Multiple Effect Evaporator System," *AIChE J.* **17**: 1080 (1971).
4. K. S. Campbell: Stearns-Roger Corporation, Personal Communication, 1968.
5. H. S. Carslaw and J. C. Jaeger: *Conduction of Heat in Solids*, 2d ed., Oxford University Press, New York, 1959.

6. A. L. Carter and R. R. Kraybill: "Low Pressure Evaporation," *Chem. Eng. Prog.*, **62**:99 (1966).
7. R. V. Churchill: *Operational Mathematics*, 2d ed., McGraw-Hill Book Company, New York, 1958.
8. R. F. Detman: "Combination Process in Large Desalting Plants," *Chem. Eng. Prog.*, **61**:80 (1967).
9. D. I. Dykstra: "Sea Water Desalination by the Falling-Film Process," *Chem. Eng. Prog.*, **61**:80 (1965).
10. "Expanded Partial Enthalpy Tables for Water in Sea Water and NaCl in Aqueous Solution," prepared for U.S. Dept. of the Interior, Office of Saline Water, by Stearns-Roger Corp., Denver, Colorado, 1965.
11. "Fifth Annual Report, Sea Water Desalting Plant and Distillation Development Facility," prepared for U.S. Dept. of the Interior, Office of Saline Water, by Stearns-Roger Corporation, Denver, Colorado, 1966.
12. R. G. E. Franks and W. E. Schiesser: "The Evaluation of Digital Simulation Programs," *Chem. Eng. Prog.*, **63**:68 (1967).
13. "Freeport Plant ME-LTV Operations," *Saline Water Conversion Report for 1966*, Sypt. of Documents, U.S. Government Printing Office, Washington, D.C., pp. 253–257.
14. L. S. Galstaun and E. L. Currier: "The Metropolitan Water District Desalting Project," *Chem. Eng. Prog.*, **63**:65 (1967).
15. "Heat Transfer in Vertical-Tube Evaporation," *Saline Water Conversion Report for 1966*, Supt. of Documents, U.S. Government Printing Office, Washington, D.C., pp. 190–193.
16. C. D. Holland: *Fundamentals and Modeling of Separation Process, Absorption, Distillation, Evaporation, Extraction*, Prentice-Hall, Inc., Englewood Cliffs, N.J., 1975.
17. C. J. Huang, H. M. Lee, and A. E. Dukler: "Mathematical Model and Computer Program for Simulation and Optimum Design of Vertical-Tube Evaporation Plants for Saline Water Conversion," *Desalination*, **6**:25 (1969).
18. S. Itahara and L. I. Stiel: "Optimal Design of Multiple-Effect Evaporators with Vapor Bleed Streams," *I&EC Process Design and Development*, **7**:6 (1968).
19. "Optimum Design of Long-Tube-Vertical Plants," *Saline Water Conversion Report for 1966*, Supt. of Documents, U.S. Government Printing Office, Washington, D.C., pp. 188–190.
20. R. H. Perry, C. H. Chilton, and S. D. Kirkpatrick (eds.): *Chemical Engineers' Handbook*, 4th ed., McGraw-Hill Book Company, New York, 1963.
21. John C. Phillips: "Basic Roles for Analog Computers," *Chem. Eng.*, **70**:97 (April 1963).
22. H. H. Rosenbrock: "Distinctive Problems of Process Control," *Chem. Eng. Prog.*, **58**:43 (1962).
23. *Saline Water Conversion Engineering Data Book*, Supt. of Documents, U.S. Government Printing Office, Washington, D.C., 1965.
24. F. C. Standiford: "Evaporation," *Chem. Eng.*, **70**:157 (December 1963).
25. F. C. Standiford and H. F. Bjofk: "Large Plants for Salt Water Conversion," *Chem. Eng. Prog.*, **63**:70 (1967).

PROBLEMS

3-1 (*a*) Show that Eq. (3-8) may be stated as follows:

$$\begin{pmatrix}\text{Resistance per effective}\\ \text{thermal conductivity film}\end{pmatrix} = \frac{r_{av} - r_1}{k2\pi r_1 L} = \frac{r_2 - r_{av}}{k2\pi r_1 L}$$

(*b*) On the basis of these thermal resistances and the fact that at steady state $Q = Q|_{r_1} = Q|_{r_2}$, show that

$$Q = \frac{T_1 - T_2}{(r_2 - r_1)/k2\pi r_1 L}$$

3-2 When no approximation is made with respect to the relative sizes of r_1 and r_2, one obtains the following expression instead of Eq. (3-3):

$$\ln \frac{r}{r_1} = \left(\frac{\ln r_2/r_1}{T_1 - T_2}\right)(T_1 - T) \tag{A}$$

(*a*) When this relationship is used to evaluate the integral on the left-hand side of Eq. (3-5) on the basis of all the assumptions stated previously except those pertaining to r_1 and r_2, show that the following result is obtained:

$$T_m = T_1 - \left(\frac{T_1 - T_2}{2}\right)\left[\frac{2(r_2/r_1)^2}{(r_2/r_1)^2 - 1} - \frac{1}{\ln r_2/r_1}\right] \tag{B}$$

(*b*) Let r_m denote the value of r at which T takes on the value T_m given by Eq. (B). Show that r_m is given by the following formula:

$$\ln \frac{r_m}{r_1} = \left(\frac{\ln r_2/r_1}{2}\right)\left[\frac{2(r_2/r_1)^2}{(r_2/r_1)^2 - 1} - \frac{1}{\ln r_2/r_1}\right] \tag{C}$$

(*c*) Show that if the equivalent resistances are defined as follows, the model predicts the correct rate of heat transfer as well as the correct heat content.

$$\begin{pmatrix}\text{Equivalent thermal}\\ \text{resistance at } r = r_1\end{pmatrix} = \frac{r_m - r_1}{k2\pi(r_{lm})_1 L} \tag{D}$$

$$\begin{pmatrix}\text{Equivalent thermal}\\ \text{resistance at } r = r_2\end{pmatrix} = \frac{r_2 - r_1}{k2\pi(r_{lm})_2 L} \tag{E}$$

where

$$(r_{lm})_1 = \frac{r_m - r_1}{\ln r_m/r_1}$$

$$(r_{lm})_2 = \frac{r_2 - r_m}{\ln r_2/r_m}$$

(*d*) Show that the formulas for the film coefficients corresponding to the equivalent resistances at r_1 and r_2 as given by Eqs. (D) and (E) are as follows:

$$h_{e,1} = \frac{k/r_1}{\ln r_m/r_1}$$

$$h_{e,2} = \frac{k/r_2}{\ln r_2/r_1 - \ln r_m/r_1}$$

where $\ln r_m/r_1$ is computed by use of Eq. (C).

3-3 (*a*) Make an energy balance on an element of volume from x_j to $x_j + \Delta x$ of Fig. 3-6, over the time period from t_n to $t_n + \Delta t$. Then by use of the mean value theorems followed by a limiting process wherein Δx and Δt are allowed to go to zero, show that Eq. (3-11) follows.

Hint: Begin with

$$\int_{t_n}^{t_n+\Delta t}\left(Q_{cd}\Big|_{x_j,\,t} - Q_{cd}\Big|_{x_j+\Delta x,\,t}\right)dt = \int_{x_j}^{x_j+\Delta x}\left(E\rho S\Big|_{t_n+\Delta t,\,x} - E\rho S\Big|_{t_n,\,x}\right)dx$$

where $Q_{cd} = -kA\,\partial T/\partial x$ = rate of heat transfer (Btu/h) in the positive direction of x (this is Fourier's first law)

A = heat transfer area perpendicular to the direction of heat transfer

S = cross-sectional area of element of volume (note, in this case $A = S$)

(*b*) Show that the boundary conditions given by Eq. (3-12) follow from the energy balances on the films at $x = 0$ and at $x = l$, and as a consequence of the fact that the films do not possess holdup.

3-4 To find the solution that satisfies Eq. (3-11) and the set of boundary conditions given by Eq. (3-12), the following procedure may be employed. The outline of this procedure follows closely the suggestions of Carslaw and Jaeger(5). In this approach one first finds a solution which satisfies Eq. (3-11) and the following set of boundary conditions and initial conditions:

$$\frac{\partial T}{\partial x} - H_1 T = 0 \qquad (x = 0, t > 0) \tag{A}$$

$$\frac{\partial T}{\partial x} + H_2 T = 0 \qquad (x = l, t > 0) \tag{B}$$

$$T = f(x) \qquad (t = 0, 0 \le x \le l) \tag{C}$$

(*a*) Show that a solution of the form

$$T = A\left(\cos \beta x + \frac{H_1}{\beta} \sin \beta x\right) e^{-\alpha \beta^2 t}$$

satisfies Eqs. (3-11), (A), and (B) simultaneously, where β is any one of the positive roots of

$$(\beta^2 - H_1 H_2) \sin \beta l - \beta(H_1 + H_2) \cos \beta l = 0$$

(*b*) Show that if m and n are any two positive and unequal integers

$$\int_0^l X_m X_n \, dx = 0 \qquad (m \neq n)$$

where

$$X_n = \cos \beta_n x + \frac{H_1}{\beta_n} \sin \beta_n x$$

Hint: The following steps are suggested:

1. From the definition of X_n, show that

$$\frac{d^2 X_n}{dx^2} + \beta_n^2 X_n = 0$$

$$\frac{d^2 X_m}{dx^2} + \beta_m^2 X_m = 0$$

2. Next, show that

$$(\beta_m^2 - \beta_n^2) \int_0^l X_m X_n \, dx = \int_0^l \left(X_m \frac{d^2 X_n}{dx^2} - X_n \frac{d^2 X_m}{dx^2} \right) dx$$

Integrate the right-hand side of this expression one time by parts to obtain

$$(\beta_m^2 - \beta_n^2) \int_0^l X_m X_n \, dx = \left(X_m \frac{dX_n}{dx} - X_n \frac{dX_m}{dx} \right) \Bigg|_0^l$$

Use the conditions given by Eqs. (A) and (B) to show that the right-hand side of the above expression is equal to zero.

(*c*) Evaluate

$$\int_0^l X_n^2 \, dx$$

Hint: The following steps are suggested:

1. From the definition of X_n, show that

$$\beta_n^2 \int_0^l X_n^2 \, dx = -\int_0^l X_n \frac{d^2 X_n}{dx^2} \, dx$$

Integrate the right-hand side of this expression one time by parts to obtain

$$\beta_n^2 \int_0^l X_n^2 \, dx = -\left(X_n \frac{dX_n}{dx} \right) \Bigg|_0^l + \int_0^l \left(\frac{dX_n}{dx} \right)^2 dx \tag{D}$$

2. From this definition of X_n, show that for all x $(0 \le x \le l)$

$$\beta_n^2 X_n^2 + \left(\frac{dX_n}{dx} \right)^2 = \beta_n^2 + H_1^2 \tag{E}$$

Integrate this result to obtain

$$\beta_n^2 \int_0^l X_n^2 \, dx = (\beta_n^2 + H_1^2) l - \int_0^l \left(\frac{dX_n}{dx} \right)^2 dx \tag{F}$$

3. Show that Eqs. (D) and (F) may be combined to give

$$2\beta_n^2 \int_0^l X_n^2 \, dx = (\beta_n^2 + H_1^2) l - \left(X_n \frac{dX_n}{dx} \right) \Bigg|_0^l \tag{G}$$

4. Evaluate the last term of Eq. (G) by showing that when $(dX_n/dx)^2$ in Eq. (E) is replaced by its equivalent at $x = 0$ (given by definition of X_n) one obtains

$$X_n^2 = 1 \qquad (x = 0)$$

Similarly, by use of Eqs. (B) and (E), show that

$$X_n^2 = \frac{\beta_n^2 + H_1^2}{\beta_n^2 + H_2^2} \qquad (x = l)$$

Use these results and Eq. (B) to show that

$$\int_0^l X_n^2 \, dx = \frac{l(\beta_n^2 + H_1^2)(\beta_n^2 + H_2^2) + H_2(\beta_n^2 + H_1^2) + H_1(\beta_n^2 + H_2^2)}{2\beta_n^2(\beta_n^2 + H_2^2)}$$

(*d*) Suppose $f(x)$ may be represented by the infinite series

$$f(x) = A_1 X_1 + A_2 X_2 + A_3 X_3 + \cdots$$

Use results obtained above to show that

$$A_n = \frac{\int_0^l X_n f(x) \, dx}{\int_0^l X_n^2 \, dx}$$

where the denominator on the right-hand side has the value obtained in part (*c*).

(*e*) Use the foregoing results to show that

$$T(x, t) = \sum_{n=1}^{\infty} Y_n(x) e^{-\alpha \beta_n^2 t} \int_0^l Y_n(x') f(x') \, dx'$$

where $Y_n(x)$ has the definition given below Eq. (3-13).

3-5 To obtain the solution satisfying Eq. (3-11) and the boundary conditions following it, the following procedure has been suggested by Carslaw and Jaeger(5). Let

$$T = u + w$$

where w is a function of x and t, and u is a function of x alone. More precisely, let u be defined by

$$\frac{d^2u}{dx^2} = 0 \qquad (0 < x < l)$$

$$\frac{du}{dx} - H_1(u - T_A) = 0 \qquad (x = 0)$$

$$\frac{du}{dx} + H_2(u - T_S) = 0 \qquad (x = l)$$

and w by

$$\frac{\partial w}{\partial t} = \alpha \frac{\partial^2 w}{\partial x^2} \qquad (0 < x < l,\ t > 0)$$

$$\frac{\partial w}{\partial x} - H_1 w = 0 \qquad (x = 0,\ t > 0)$$

$$\frac{\partial w}{\partial x} + H_2 w = 0 \qquad (x = l,\ t > 0)$$

$$w = T_A - u \qquad (t = 0,\ 0 \le x \le l)$$

(*a*) Show that Eq. (3-11) and the boundary conditions following it are satisfied by the sum of the two new functions u and w.

(*b*) From the definition of u, show that

$$u = bx + c$$

where

$$b = \frac{T_S - T_A}{1/H_1 + 1/H_2 + l}$$

$$c = \frac{b}{H_1} + T_A$$

(*c*) From the definitions of u, w, and the result given in part (*e*) of Prob. 3-4, obtain the solution given by Eq. (3-13).

3-6 Verify the result given by Eq. (3-15).

3-7 Formulate the boundary conditions given by Eq. (3-18).

3-8 (*a*) If the change of variable

$$U(x, t) = T - T_A$$

is made, show that Eq. (3-11) and the boundary conditions given by Eq. (3-18) become

$$\frac{\partial U}{\partial t} = \alpha \frac{\partial^2 U}{\partial x^2}$$

$$U(x, 0) = 0 \qquad (0 < x < l)$$

$$\frac{\partial U(0, t)}{\partial x} = 0 \qquad (t > 0)$$

$$U(l, t) = T_S - T_A \qquad (t > 0)$$

(*b*) The partial differential equation and the above boundary conditions may be solved by use of Laplace transforms. Given the following Laplace transforms

$$L\left\{\frac{\partial U}{\partial t}\right\} = su(x, s) - U(x, 0) = su(x, s)$$

$$L\left\{\frac{\partial^2 U}{\partial x^2}\right\} = \frac{d^2u}{dx^2}$$

$$L\left\{\frac{\partial U(0, t)}{\partial x}\right\} = \frac{du}{dx}(0, s) = 0$$

$$L\{U(l, t)\} = u(l, s)$$

$$L\{T_S - T_A\} = \frac{T_S - T_A}{s}$$

show that the partial differential equation reduces to the ordinary differential equation

$$\frac{d^2u}{dx^2} - \frac{s}{\alpha} u = 0$$

whose solution which satisfies the initial condition and the boundary conditions is

$$u(x, s) = \left(\frac{T_S - T_A}{s}\right) \frac{\cosh\left(\sqrt{s/\alpha}\right)x}{\cosh\left(\sqrt{s/\alpha}\right)l}$$

(*c*) If the following inverse Laplace transforms are given

$$L^{-1}\{u(x, s)\} = U(x, t)$$

$$L^{-1}\left\{\frac{1}{s}\frac{\cosh\left(\sqrt{s/\alpha}\right)x}{\cosh\left(\sqrt{s/\alpha}\right)l}\right\} = \sum_{n=0}^{\infty} (-1)^n \left\{\operatorname{erfc}\left[\frac{(2n+1)l - x}{2\sqrt{\alpha t}}\right] + \operatorname{erfc}\left[\frac{(2n+1)l + x}{2\sqrt{\alpha t}}\right]\right\}$$

show that the result given by Eq. (3-9) is obtained.

3-9 Use the result given by Eq. (3-19) in the verification of the expression given by Eq. (3-20).

APPENDIX 3A-1

Table 3A-1 Heat transfer coefficients and physical properties used in Chap. 3

1. Heat capacity of brine solution (Ref. 2)†

$$C_p = A_1(S) - A_2(S)T + A_3(S)T^2$$

and

$$A_1(S) = 1.0049 - 0.016\,21S + (3.5261 \times 10^{-4})S^2$$
$$A_2(S) = (3.2506 - 1.4795S + 0.077\,65S^2) \times 10^{-4}$$
$$A_3(S) = (3.8013 - 1.2084S + 0.061\,21S^2)10^{-6}$$

where S = (3.4483)(C.F.), percent salinity
C_p = heat capacity in cal/(gm · °C)
T = temperature in °C
C.F. = concentration factor

† These references are listed at the end of this table.

(*Continued over*)

Table 3A-1 Heat transfer coefficients and physical properties—*Continued*

2. Enthalpy of a brine solution at 60°C relative to water at 32°F (Ref. 3, curve OSW 12.20)

$$h(S)\Big|_{60°C} = \frac{59.938 - 0.408\,33S}{1.8} \quad \text{cal/g}$$

This equation was obtained by curve-fitting the enthalpy data given in Ref. 3.

3. Enthalpy of a brine solution at temperature T and salinity S

$$h(S, T) = A_1(S)(T - T_R) - \frac{A_2(S)(T^2 - T_R^2)}{2} + \frac{A_3(S)(T^3 - T_R^3)}{3} + h(T_R, S) \quad \text{cal/g}$$

where $T_R = 60°C$; $A_1(S)$, $A_2(S)$, $A_3(S)$ are given under section 1 above, and $h(T_R, S)$ is given in section 2 above.

4. Enthalpy of saturated steam (Ref. 2)

$$H = 0.439(T - 100) + 0.5(T^2 - 100^2) \times 10^{-4} - 2\frac{(T^3 - 100^3) \times 10^{-6}}{3} + 1105.2$$

where H is in British thermal units per pound and T is in °F. This equation was obtained by curve fitting the data given in the steam tables of Ref. 2. From this formula, the change in enthalpy of saturated steam with temperature is given by

$$\frac{\partial H}{\partial T} = 0.439 + T \times 10^{-4} - 2T^2 \times 10^{-6}$$

5. Dühring lines for brine solutions (Ref. 3, curve OSW 11.51)

The data in Ref. 3 were used to curve-fit m and b in the Dühring lines

$$T_{Ej} = mT_{C,j+1} + b$$

to give

$$m = m(\text{C.F.}, T_{C,j+1}) = 1.0 + (0.001\,23 + 7.2 \times 10^{-6}T_{C,j+1})\ \text{C.F.}^{1.13}$$

$$b = b(\text{C.F.}) = 0.48\ \text{C.F.}^{1.13}$$

where T_E and $T_{C,j+1}$ are in degrees Fahrenheit.

6. Coefficients of heat transfer U_{WS} (for the transfer of heat from steam to the metal wall)

This coefficient was computed as follows:

$$\frac{1}{U_{WS}} = \frac{1}{h_{fS}} + \frac{1}{h_{eWS}}$$

where h_{eWS} is the effective thermal conductivity film coefficient for the metal wall.

$h_{eWS} = 2k_M A_{WS}\rho_M/M_{WS}$

k_M = thermal conductivity for steel, $k_M = 26$ Btu/(lb ft °F)

ρ_M = density of steel wall, $\rho_M = 490$ lb/ft^3

Table 3A-1 Heat transfer coefficients and physical properties—*Continued*

The heat transfer coefficient for condensing steam h_{fS} was computed as proposed in Perry(2), namely,

$$h_{fS}(T_f, |\Delta T|) = 255.1\left[\frac{\lambda_{\text{water}}(T_f)}{2.42\mu_{\text{water}}(T_f)(1 + |\Delta T|)}\right]^{0.25}$$

where $|\Delta T| = |T_{WS} - T_c|$, °F

$T_f = [T_{WS} + T_c]/2$, °F

T_c = condensation temperature, °F

From a curve fit of the data given in the steam tables by Perry(2), the following equation was obtained for the latent heat of vaporization of water:

$$\lambda_{\text{water}}(T) = 1\,037.2 - 0.593(T - 100)$$

where λ_{water} has the units of British thermal units per pound and T is in degrees Fahrenheit.

The viscosity μ of water was computed by use of the following equation from Perry(2):

$$\frac{100}{\mu} = 2.148[(T - 8.435) + \sqrt{8078.4 + (T - 8.435)^2}] - 120$$

where T is in degrees Celsius and μ is in centipoise.

7. Coefficients of heat transfer U_{WL} (for the transfer of heat from the brine process liquid to the metal wall)

The coefficient was computed as follows:

$$\frac{1}{U_{WL}} = \frac{1}{h_{fL}} + \frac{1}{h_{eWL}}$$

where h_{eWL} is the effective (thermal conductivity) film coefficient for the metal wall

$$h_{eWL} = 2k_M A_{WL}\rho_M/M_{WL}$$

Values of k_M and ρ_M are given in section 6 above. The following relationship (Ref. 2) was used to compute h_{fL}

$$h_{fL} = 50(1 + 0.012T_L)$$

where h_{fL} is in Btu/(h · °F · ft^2) and T_L is the temperature of the brine process liquid in degrees Fahrenheit.

8. Coefficients of heat transfer from the metal walls to the surroundings

These coefficients U_{AL} and U_{AS} in Btu/(h · ft^2 · °F) were computed by use of the following equation given by Perry(2),

$$U_A = 0.27(\Delta T_a)^{0.25}$$

where $\Delta T_a = |T_A - T_a|$, °F

T_a = surface temperature of the insulation, °F

The surface temperature T_a of the insulation was taken to be that T_a which satisfied the relationship

$$(T_A - T)U_A = (T - T_w)h_{\text{ins}}$$

The coefficient of heat transfer across the insulation, h_{ins}, was taken to be equal to unity.

(Continued

Table 3A-1 Heat transfer coefficients and physical properties—*Continued*

9. Density of brine solutions (Ref. 3, curve OSW 11.60)

The density ρ in pounds per cubic foot was computed by use of the following curve-fit of the data given in Ref. 3:

$$\rho = D_0 + D_1 T + D_2 T^2$$

where T is in degress Fahrenheit

$$D_0 = 62.56 + 1.792\,78 \text{ C.F.} + 5.253\,612 \times 10^{-3} \text{ C.F.}^2$$

$$D_1 = 1.658\,722 \times 10^{-4} - 3.259\,245 \times 10^{-3} \text{ C.F.} + 2.046\,45 \times 10^{-4} \text{ C.F.}^2$$

$$D_2 = -5.823\,615 \times 10^{-5} + 7.656\,795 \times 10^{-6} \text{ C.F.} - 4.449\,848 \times 10^{-7} \text{ C.F.}^2$$

1. L. A. Bromley, V. A. Desaussure, J. C. Chipp, and J. W. Wright: "Heat Capacities of Sea Water Solutions at Salinities of 1 to 12% and Temperatures of 2 to 80°C," *J. Chem. Eng. Data*, 12 (1967), 203.
2. R. H. Perry, C. H. Chilton, and S. D. Kirkpatrick, (eds.): *Chemical Engineers' Handbook*, 4th ed., McGraw-Hill Book Company, New York, 1963.
3. *Saline Water Conversion Engineering Data Book*, Supt. of Documents, U.S. Government Printing Office, Washington, D.C., 1965.

CHAPTER

FOUR

SOLUTION OF PROBLEMS INVOLVING CONTINUOUS-DISTILLATION COLUMNS BY USE OF THE TWO-POINT IMPLICIT METHOD

Continuous columns are those columns in which the feed (or feeds) enter the column continuously and products are withdrawn continuously. Batch distillation columns, which do not fall into this class, are treated in Chap. 5.

In Sec. 4-1, the equations used to describe conventional distillation columns at unsteady state are developed. The equations so obtained consist of the component-material balances, the equilibrium relationships, and the energy balances. These equations may be solved by any one of several numerical methods. In this chapter the two-point implicit method is used while the semi-implicit Runge–Kutta method and Gear's method are used in Chaps. 6, 7, and 8.

After the integral difference equations (or the corresponding differential equations) have been reduced to algebraic form by use of the implicit method, the resulting set of implicit equations are solved by use of either one of two procedures, the θ method or the $2N$ Newton–Raphson method.

The $2N$ Newton–Raphson method is applied in a manner analogous to that demonstrated in Chaps. 2 and 3 for systems of evaporators. Application of the θ method is demonstrated in Sec. 4-2 and the $2N$ Newton–Raphson method in Sec. 4-3.

4-1 APPLICATION OF THE IMPLICIT METHOD AND THE THETA METHOD

A *conventional* distillation column is defined as one that has one feed and two product streams, the distillate and bottoms. Any column that differs from a conventional distillation column by having either more than one feed and/or one or more streams withdrawn in addition to the distillate and bottoms is called a *complex column.* A sketch of a conventional column is shown in Fig. 4-1.

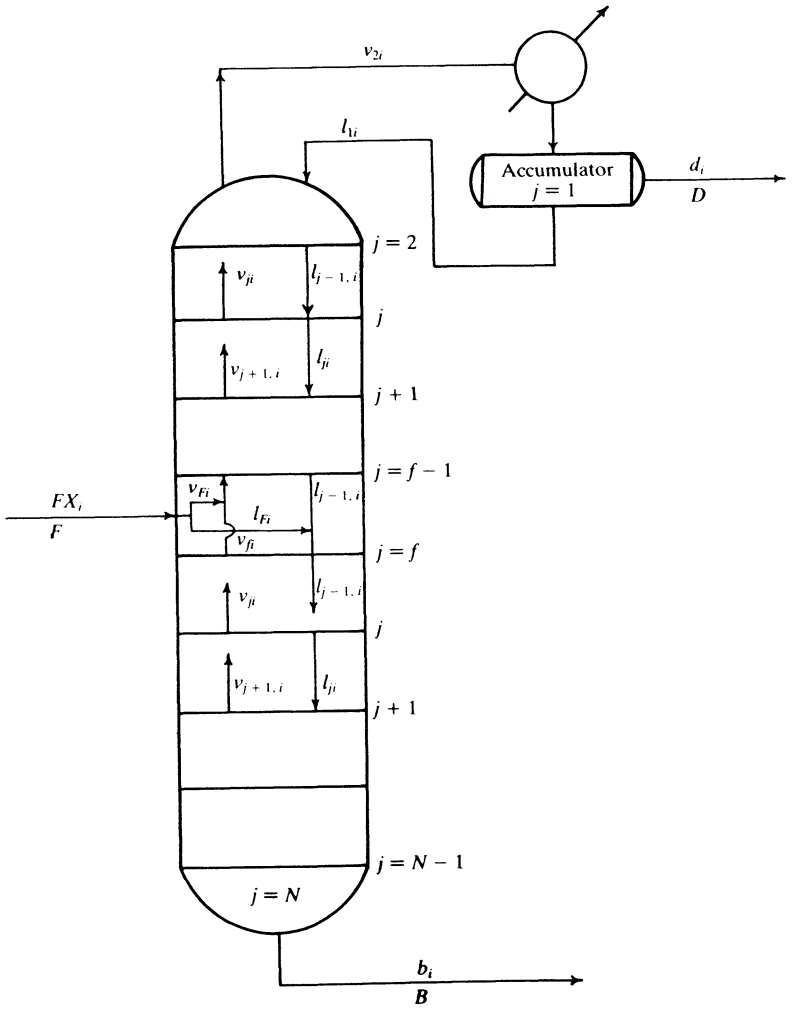

Figure 4-1 Sketch of a conventional distillation column.

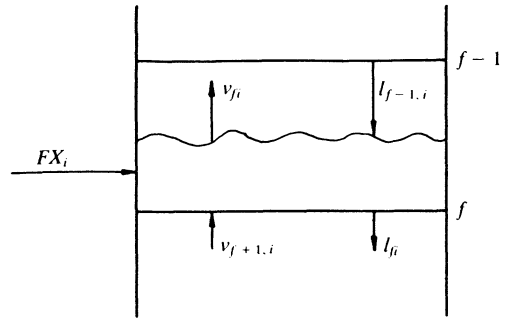

Model 1. Assumed in the McCabe–Thiele method

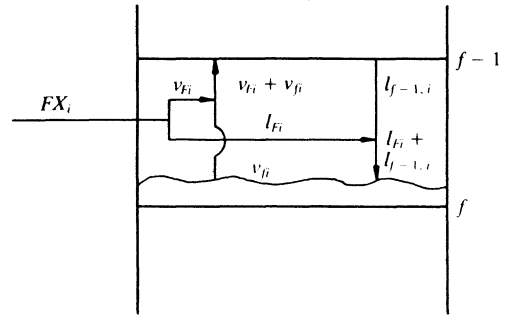

Model 2. Behavior assumed on the feed plate

Figure 4.2 Models for the behavior of the feed plate.

The basic model for the behavior of the gas and liquid phases on the plate of a distillation column that is used in this and the next chapter makes use of the concept of an ideal stage. Although considerable work has been done on liquid mixing, this model does not attempt to include this effect. The liquid holdup is assumed to be perfectly mixed, and the vapor holdup is assumed to be perfectly mixed.

Either one of two models may be used to describe the behavior of the feed plate (see models 1 and 2 in Fig. 4-2). In model 1, it is assumed that the feed is introduced in the liquid on the feed plate and that all of the vapor and all of the liquid leaving the feed plate are in equilibrium. In model 2, it is supposed that the feed flashes upon entering the column and that the liquid formed from the flash mixes perfectly with the liquid on the feed plate and comes to equilibrium with the vapor $\{v_{fi}\}$ leaving the feed plate. The vapor $\{v_{Fi}\}$ formed by the flash is assumed to pass to the plate above without the occurrence of any mass

transfer between this vapor and the liquid on the feed plate. For dewpoint vapor and superheated feeds, $v_{Fi} = FX_i$ and $l_{Fi} = 0$, $V_F = F$, and $L_F = 0$. For bubble-point liquid and subcooled feeds, $l_{Fi} = FX_i$ and $v_{Fi} = 0$, $L_F = F$, and $V_F = 0$. Calculational procedures for making flash calculations are described by Holland(6) (see also Prob. 4-9).

When a feed is introduced above the level of the liquid on the feed plate, model 1 appears to be the best representation of the behavior of the feed plate. When the feed is introduced below the level of liquid on the feed plate, model 2 appears to be the best representation of the feed plate behavior. In the interest of simplicity, the unsteady state equations are developed for only one model in this chapter, model 1.

Certain operating variables, such as the distillate rate D and the holdups, may be regarded as *specified* values. By a specified value is meant that at the beginning of a time increment (time t_n), the value of, say, D is known at times t_n and $t_n + \Delta t$. This implies that at time t_n, the specified values must either be known at time $t_n + \Delta t$ or be calculable from previous sets of transient conditions. In this chapter, it is supposed that at time t_n, the specified values are known at time $t_n + \Delta t$. In a subsequent chapter, however, fluid dynamic relationships are used to compute the holdups at the end of the time period under consideration.

Any interior stage exclusive of the overhead condenser, the feed plate, and the reboiler ($j \neq 1, f, N$) is described by the equations presented below. (The minor variations for stages $j = 1, f, N$ are presented in subsequent sections in which the numerical methods are applied.) In the development of these equations, it is assumed that the vapor and liquid phases are each perfectly mixed. The material and energy balances are made on the contents contained in the space between successive plates over the time period from time t_n to $t_n + \Delta t$. The component-material balance enclosing stage j is as follows for each component i:

$$\int_{t_n}^{t_n+\Delta t} (v_{j+1,i} + l_{j-1,i} - v_{ji} - l_{ji})\, dt = (u_{ji}^V + u_{ji}^L)\Big|_{t_n+\Delta t} - (u_{ji}^V + u_{ji}^L)\Big|_{t_n} \tag{4-1}$$

where v_{ji} is the molar flow rate at which component i leaves stage j in the vapor phase and l_{ji} is the molar flow rate at which component i leaves stage j in the liquid phase. The molar holdups of component i in the vapor and liquid phases on stage j are denoted by u_{ji}^V and u_{ji}^L, respectively.

The total-material balance for any stage j ($j \neq 1, f, N$) is given by

$$\int_{t_n}^{t_n+\Delta t} (V_{j+1} + L_{j-1} - V_j - L_j)\, dt = (U_j^V + U_j^L)\Big|_{t_n+\Delta t} - (U_j^V + U_j^L)\Big|_{t_n} \tag{4-2}$$

Capital letters are used to distinguish the total flow rates and holdups from the corresponding component flow rates and holdups.

The enthalpy balance for any stage j except $j = 1, f, N$ is given by

$$\int_{t_n}^{t_n+\Delta t} \sum_{i=1}^{c} (v_{j+1,i}\hat{H}_{j+1,i} + l_{j-1,i}\hat{h}_{j-1,i} - v_{ji}\hat{H}_{ji} - l_{ji}\hat{h}_{ji})\, dt$$
$$= \sum_{i=1}^{c} (u_{ji}^V \hat{H}_{ji} + u_{ji}^L \hat{h}_{ji})\Big|_{t_n+\Delta t} - \sum_{i=1}^{c} (u_{ji}^V \hat{H}_{ji} + u_{ji}^L \hat{h}_{ji})\Big|_{t_n} \tag{4-3}$$

where $\hat{H}_{ji}$ and $\hat{h}_{ji}$ are the virtual values of the partial molar enthalpies which are defined by

$$\hat{H}_{ji} = H_{ji}^0 + \Omega_j^V(P, T, \{y_{ji}\})$$
$$\hat{h}_{ji} = H_{ji}^0 + \Omega_j^L(P, T, \{x_{ji}\})$$

H_{ji}^0 = enthalpy of one mole of a perfect gas, evaluated at the temperature of the mixture

Ω_j^V, Ω_j^L = departure functions for the vapor and liquid, respectively

Formulas for evaluating the departure functions for various equations of state are given in Ref. 6. As shown in App. 4A-2, the virtual values of the partial molar enthalpies have the property of giving precisely the same enthalpy of a mixture as the partial molar enthalpies, while being significantly less difficult to evaluate.

The component flow rates are related to the total flow rates as follows:

$$0 = \sum_{i=1}^{c} l_{ji} - L_j \qquad (j = 1, 2, \ldots, N) \tag{4-4}$$

$$0 = \sum_{i=1}^{c} v_{ji} - V_j \qquad (j = 1, 2, \ldots, N) \tag{4-5}$$

Similarly, the component and total holdups of the vapor and liquid are related in the following manner:

$$0 = \sum_{i=1}^{c} u_{ji}^L - U_j^L \qquad (j = 1, 2, \ldots, N) \tag{4-6}$$

$$0 = \sum_{i=1}^{c} u_{ji}^V - U_j^V \qquad (j = 1, 2, \ldots, N) \tag{4-7}$$

The equilibrium relationship for each component i on plate j may be expressed as follows:

$$0 = \frac{\gamma_{ji}^L K_{ji} l_{ji}}{\sum_{i=1}^{c} l_{ji}} - \frac{\gamma_{ji}^V v_{ji}}{\sum_{i=1}^{c} v_{ji}} \qquad \begin{matrix} (j = 1, 2, \ldots, N) \\ (i = 1, 2, \ldots, c) \end{matrix} \tag{4-8}$$

where the activity coefficients γ_{ji}^V and γ_{ji}^L, for each component in the vapor and liquid phases, respectively, are defined in Chap. 2.

The fundamental relationships given by Eqs. (4-1) through (4-8) may be solved by a number of numerical methods, several of which are presented in this book. In Sec. 4-2, a combination of the two-point implicit method and the θ method is demonstrated, and in Sec. 4-3, a combination of the two-point implicit method and the $2N$ Newton–Raphson is presented. In Chaps. 6 and 8, the equations are solved by use of the semi-implicit Runge–Kutta method and Gear's method. The latter two methods make use of the material- and energy-balance equations in the form of differential equations rather than integral-difference equations. The differential equations are readily obtained from the integral-difference equations by use of the mean value theorems followed by the limiting process wherein Δt is allowed to go to zero as demonstrated in Chaps. 2 and 3. The resulting differential equations are analogous in form to that which follows for Eq. (4-1):

$$v_{j+1,i} + l_{j-1,i} - v_{ji} - l_{ji} = \frac{d(u_{ji}^V + u_{ji}^L)}{dt} \tag{4-9}$$

Other Forms of the Equilibrium Relationship

In the present development, it is convenient to make use of the mole fractions defined by

$$x_{ji} = \frac{l_{ji}}{\sum_{i=1}^{c} l_{ji}} \qquad y_{ji} = \frac{v_{ji}}{\sum_{i=1}^{c} v_{ji}} \tag{4-10}$$

and consequently

$$\sum_{i=1}^{c} x_{ji} = 1 \qquad \sum_{i=1}^{c} y_{ji} = 1 \tag{4-11}$$

When the equilibrium relationship given by Eq. (4-8) is stated in terms of mole fractions, one obtains

$$y_{ji} = \frac{\gamma_{ji}^L}{\gamma_{ji}^V} K_{ji} x_{ji} \tag{4-12}$$

When the vapor phase forms an ideal solution, $\gamma_{ji}^V = 1$ for all i, and when the liquid phase forms an ideal solution, $\gamma_{ji}^L = 1$ for all i. Thus, when both phases form ideal solutions, Eq. (4-12) reduces to

$$y_{ji} = K_{ji} x_{ji} \tag{4-13}$$

In the subsequent developments in this chapter, this form of the equilibrium relationship is used with the understanding that for the case of nonideal solutions, K_{ji} is to be multiplied by $\gamma_{ji}^L/\gamma_{ji}^V$.

Summation of each side of Eq. (4-13) over all components followed by the restatement of the result so obtained in functional form yields

$$f(T) = \sum_{i=1}^{c} K_{ji} x_{ji} - 1 \tag{4-14}$$

For a specified value of the pressure P and a liquid mixture having the mole fractions $\{x_{ji}\}$, the temperature T required to make $f(T) = 0$ is called the *bubble-point temperature* of the mixture.

When the pressure P and vapor composition are given, the *dewpoint temperature* is that temperature T which makes $F(T) = 0$, where

$$F(T) = \sum_{i=1}^{c} \frac{y_{ji}}{K_{ji}} - 1 \tag{4-15}$$

Equation (4-15) is obtained by first restating Eq. (4-13) in the form $x_{ji} = y_{ji}/K_{ji}$, summing over all components, and then restating the result so obtained in functional form.

In developments which follow, the vapor holdups $\{u_{ji}^V\}$ are neglected because they are small relative to the liquid holdups. The vapor holdups may be included, however, as shown in subsequent chapters.

4-2 SOLUTION OF PROBLEMS INVOLVING CONVENTIONAL DISTILLATION COLUMNS BY USE OF THE IMPLICIT METHOD AND THE THETA METHOD

The calculational procedure based on a combination of the implicit method and the θ method is initiated by consideration of the problem in which the total flow rates remain fixed with respect to time at a set of specified values. In a subsequent section, the enthalpy balances are included in order to account for the variation of the total flow rates.

Application of the Implicit Method to a Combination of the Component-Material Balances and the Equilibrium Relationships

For any stage j ($j \neq 1, f, N$), the integral appearing in Eq. (4-1) may be approximated by use of the two-point implicit method (which was introduced in Chap. 1) as follows:

$$v_{j+1,i} + l_{j-1,i} - v_{ji} - l_{ji} + \sigma(v_{j+1,i}^0 + l_{j-1,i}^0 - v_{ji}^0 - l_{ji}^0) = \frac{u_{ji}}{\phi\,\Delta t} - \frac{u_{ji}^0}{\phi\,\Delta t} \tag{4-16}$$

where $0 \leq \phi \leq 1$ and $\sigma = (1 - \phi)/\phi$.

Observe that the vapor holdup u_{ji}^V has been neglected and u_{ji}^L has been denoted by u_{ji}. Also the values of the variables at the beginning of the time step are identified by a superscript zero, and those at the end of the time period under consideration are identified by the absence of a superscript. The equilibrium relationship given by Eq. (4-13) may be used to eliminate one of the component flow rates by first restating this relationship in terms of the component flow rates as follows. Since $y_{ji} = v_{ji}/V_j$ and $x_{ji} = l_{ji}/L_j$, it follows that Eq. (4-13) may be restated in the form:

$$\frac{v_{ji}}{V_j} = K_{ji}\frac{l_{ji}}{L_j}$$

or

$$l_{ji} = A_{ji} v_{ji} \tag{4-17}$$

where $A_{ji} = L_j/K_{ji}V_j$.

Since the liquid phase is assumed to be perfectly mixed on each stage, the liquid holdups may be stated in terms of the vapor flow rates through the use of Eq. (4-17) in the following manner:

$$u_{ji} = U_j\left(\frac{l_{ji}}{L_j}\right) = \frac{U_j}{L_j} A_{ji} v_{ji} \tag{4-18}$$

Use of this relationship followed by rearrangement permits Eq. (4-16) to be restated in the following form:

$$A_{j-1,i}v_{j-1,i} - \rho_{ji}v_{ji} + v_{j+1,i} = -\sigma(l_{j-1,i}^0 - v_{ji}^0 - l_{ji}^0 + v_{j+1,i}^0) - \frac{u_{ji}^0}{\phi\,\Delta t}$$

$$(j \neq 1, f, N) \tag{4-19}$$

where

$$\rho_{ji} = 1 + A_{ji}(1 + \tau_j)$$

$$\tau_j = (U_j/L_j)/\phi\,\Delta t$$

For any interior stage ($j \neq 1, f, N$) and sets of assumed values for L_j/V_j's, U_j's, and T_j's, Eq. (4-19) is seen to contain three unknown flow rates: $v_{j-1,i}$, v_{ji}, $v_{j+1,i}$.

In a manner similar to that shown for Eq. (4-19), the equations for stages $j = 1, f$, and N are developed. The resulting set of equations follows.

$$-\rho_{1i}v_{1i} + v_{2i} = -f_{1i}$$

$$A_{j-1,i}v_{j-1,i} - \rho_{ji}v_{ji} + v_{j+1,i} = -f_{ji} \qquad (j = 2, 3, \ldots N-1) \tag{4-20}$$

$$A_{N-1,i}v_{N-1,i} - \rho_{Ni}v_{Ni} = -f_{Ni}$$

where

$A_{ji} = L_j/K_{ji}V_j \qquad (2 \leq j \leq N-1)$

$A_{1i} = L_1/K_{1i}D \qquad$ for a partial condenser

$A_{1i} = L_1/D \qquad$ for a total condenser

$A_{Ni} = B/K_{Ni}V_N$

$$f_{ji} = z_{ji} + \sigma(z_{ji}^0 + v_{j+1,i}^0 + l_{j-1,i}^0 - v_{ji}^0 - l_{ji}^0) + \frac{u_{ji}^0}{\phi\,\Delta t}$$

$z_{fi} = FX_i \qquad$ for all other j and i, $z_{ji} = 0$

$v_{1i} = d_i \qquad$ (This symbolism is used in the interest of symmetry, that is, v_{1i} is used to denote d_i regardless of the state in which D is withdrawn, vapor or liquid.)

Equation (4-20) may be restated in matrix form as follows:

$$\mathbf{A}_i\mathbf{v}_i = -\mathbf{f}_i \tag{4-21}$$

where

$$\mathbf{A}_i = \begin{bmatrix} -\rho_{1i} & 1 & 0 & 0 & 0 & \cdots & 0 \\ A_{1i} & -\rho_{2i} & 1 & 0 & 0 & \cdots & 0 \\ 0 & A_{2i} & -\rho_{3i} & 1 & 0 & \cdots & 0 \\ \cdots & \cdots & \cdots & \cdots & \cdots & \cdots & \cdots \\ 0 & \cdots & 0 & A_{N-2,i} & -\rho_{N-1,i} & & 1 \\ 0 & \cdots & 0 & 0 & A_{N-1,i} & & -\rho_{Ni} \end{bmatrix}$$

$$\mathbf{v}_i = [v_{1i} \quad v_{2i} \quad \cdots \quad v_{Ni}]^T$$

$$\mathbf{f}_i = [f_{1i} \quad f_{2i} \quad \cdots \quad f_{Ni}]^T$$

For any given set of values for the temperatures, and L/V's, the equations represented by Eq. (4-21) constitute a linear system of equations in the v_{ji}'s. For equations such as these, which are seen to be of tridiagonal form, the unknown vapor rates may be found by use of the following recurrence formulas, sometimes called the Thomas algorithm (Refs. 5, 9). Consider the system of linear equations in the unknown v_j's ($j = 1, 2, \ldots, N$).

$$\begin{aligned} b_1 v_1 + c_1 v_2 &= d_1 \\ a_2 v_1 + b_2 v_2 + c_2 v_3 &= d_2 \\ a_3 v_2 + b_3 v_3 + c_3 v_4 &= d_3 \\ \cdots\cdots\cdots\cdots\cdots\cdots & \cdots\cdots \\ a_{N-1} v_{N-2} + b_{N-1} v_{N-1} + c_{N-1} v_N &= d_{N-1} \\ a_N v_{N-1} + b_N v_N &= d_N \end{aligned} \tag{4-22}$$

where the a's, b's, and c's are the coefficients of the v_j's which appear in Eq. (4-22). These equations may be solved by use of the following well-known recurrence formulas (Refs. 5, 6, 9) which are applied in the order stated

$$f_1 = c_1/b_1 \qquad g_1 = d_1/b_1$$

$$f_k = \frac{c_k}{b_k - a_k f_{k-1}} \qquad (k = 2, 3, \ldots, N-1) \tag{4-23}$$

$$g_k = \frac{d_k - a_k g_{k-1}}{b_k - a_k f_{k-1}} \qquad (k = 2, 3, \ldots, N)$$

After the f's and g's have been computed, the values of $v_N, v_{N-1}, \ldots, v_2, v_1$, are computed as follows:

$$v_N = g_N$$

$$v_k = g_k - f_k v_{k+1} \qquad (k = N-1, N-2, \ldots, 2, 1) \tag{4-24}$$

The use of this procedure is demonstrated below in Example 4-1.

Instead of evaluating the f_k's and g_k's by use of Eq. (4-23), a modified form of an algorithm originally proposed by Boston and Sullivan(3) for steady state problems may be used. The modified algorithm is shown in Prob. 4-12.

The Theta Method of Convergence

For each time period, successive approximations of the temperatures at the end of the time period are made until a temperature profile is found such that the component-material balances and the enthalpy balances are satisfied as well as the specifications for the column.

The θ method of convergence is an indirect method for choosing a new set of temperatures on the basis of calculated results obtained for the last assumed set of temperatures. This method alters or corrects the mole fractions. On the basis of these mole fractions which reflect the certainties that each component must be in overall material balance and in agreement with specified values for the total distillate rate and the total holdups (the conditions of constraint), a new set of temperatures is found. The θ method of convergence is related in spirit to the concept of the lagrangian multipliers (Ref. 15) in that for each condition of constraint or specification made on the system there exists a multiplier. The θ method of convergence for columns at unsteady state operation is analogous to the θ method for a complex column at steady state operation (Ref. 6). For a complex column at steady state operation, each sidestream withdrawn leads to an additional specification which gives rise to an additional θ multiplier. Similarly, for a column at unsteady state operation, each holdup specified gives rise to an additional θ multiplier:

Specifications: the distillate rate (moles/time) and liquid holdups (moles)

With the exception of U_N, each of the specifications

$$D, U_1, U_2, U_3, \ldots, U_{N-1}, U_N$$

gives rise to a θ multiplier. Other specifications are, of course, made on the column. These specifications consist of the number of plates above and below the feed plate, the complete definition of the feed stream for all t, the column pressure, the type of condenser (total or partial), and the total vapor rate V_2 (or the reflux rate L_1).

A subsequent section presents a development leading to the following consistent set of multipliers:

$$\frac{b_i}{d_i} = \theta_0 \left(\frac{b_i}{d_i}\right)_{ca} \tag{4-25}$$

$$\frac{u_{ji}}{d_i} = \theta_j \left(\frac{u_{ji}}{d_i}\right)_{ca} \qquad (j = 1, 2, \ldots, N-1)$$

Knowledge of the holdup U_N of the reboiler does not give rise to a corresponding θ because u_{Ni}/d_i may be expressed in terms of b_i/d_i as follows:

$$\left(\frac{u_{Ni}}{d_i}\right) = \left(\frac{U_N}{B}\right)\left(\frac{b_i}{d_i}\right) = \theta_0 \left(\frac{U_N}{B}\right)\left(\frac{b_i}{d_i}\right)_{ca} \tag{4-26}$$

The set of θ_j's given by Eq. (4-25) is consistent with the following formula for the calculation of the corrected compositions. The expression for computing the liquid mole fractions follows immediately from the definition of a mole fraction and Eq. (4-25), namely,

$$x_{ji} = \frac{u_{ji}}{\sum_{i=1}^{c} u_{ji}} = \frac{\theta_j \left(\frac{u_{ji}}{d_i}\right)_{ca} d_i}{\sum_{i=1}^{c} \theta_j \left(\frac{u_{ji}}{d_i}\right)_{ca} d_i} = \frac{\left(\frac{l_{ji}}{d_i}\right)_{ca} d_i}{\sum_{i=1}^{c} \left(\frac{l_{ji}}{d_i}\right)_{ca} d_i} \tag{4-27}$$

As shown in Probs. 4-4 and 4-5, a consistent set of mole fractions $\{y_{ji}\}$ for the vapor are given by

$$y_{ji} = \frac{\left(\frac{v_{ji}}{d_i}\right)_{ca} d_i}{\sum_{i=1}^{c} \left(\frac{v_{ji}}{d_i}\right)_{ca} d_i} \tag{4-28}$$

The formula for d_i is based on the requirement that each component be in overall material balance, that is,

$$\int_{t_n}^{t_n+\Delta t} (FX_i - b_i - d_i)\, dt = \sum_{j=1}^{N} u_{ji}\Big|_{t_n+\Delta t} - \sum_{j=1}^{N} u_{ji}\Big|_{t_n} \tag{4-29}$$

After the integral in this expression has been approximated by use of the implicit method, the following formula for d_i is obtained upon replacing the corrected ratios by their equivalents as given by Eq. (4-25):

$$d_i = \frac{FX_i + \sigma[FX_i - d_i - b_i]^0 + \dfrac{1}{\phi\ \Delta t}\displaystyle\sum_{j=1}^{N} u_{ji}^0}{1 + \theta_0\left(\dfrac{b_i}{d_i}\right)_{ca}\left[1 + \left(\dfrac{U_N/B}{\phi\ \Delta t}\right)\right] + \left(\dfrac{1}{\phi\ \Delta t}\right)\displaystyle\sum_{j=1}^{N-1}\theta_j\left(\frac{u_{ji}}{d_i}\right)_{ca}} \tag{4-30}$$

Except for the θ's, the values of all other quantities appearing in Eq. (4-30) are either known or readily determined after the component-material balances have been solved for the v_{ji}'s. By use of Eqs. (4-25) and (4-30), the u_{ji}'s may be stated in terms of the unknown θ_j's. The desired set of θ_j's is that set of positive numbers that makes $g_0 = g_1 = g_2 \cdots = g_{N-1} = 0$, simultaneously, where

$$\begin{aligned} g_0(\theta_0, \theta_1, \theta_2, \ldots, \theta_{N-1}) &= \sum_{i=1}^{c} d_i - D \\ g_j(\theta_0, \theta_1, \theta_2, \ldots, \theta_{N-1}) &= \sum_{i=1}^{c} u_{ji} - U_j \qquad (1 \le j \le N-1) \end{aligned} \tag{4-31}$$

This set of g functions is applicable to a column with a partial condenser (the distillate is removed as a vapor, $v_{1i} = d_i$ (vapor)). When a total condenser is employed, g_1 and θ_1 are excluded from the foregoing set, and u_{1i}/d_i is replaced wherever it appears by its equivalent U_1/D.

The desired set of θ_j's is found by use of the Newton–Raphson method (Refs. 6, 9) in the same manner as that described for complex columns at steady state operation (Ref. 6). The Newton–Raphson method consists of the repeated solution of the linearized Taylor series expansions of the functions $g_0, g_1, \ldots, g_{N-1}$. These equations have the following matrix representation:

$$\mathbf{J}_n \Delta\boldsymbol{\theta}_n = -\mathbf{g}_n \tag{4-32}$$

where

$$\mathbf{J}_n = \begin{bmatrix} \dfrac{\partial g_0}{\partial \theta_0} & \cdots & \dfrac{\partial g_0}{\partial \theta_{N-1}} \\ \vdots & & \vdots \\ \dfrac{\partial g_{N-1}}{\partial \theta_0} & \cdots & \dfrac{\partial g_{N-1}}{\partial \theta_{N-1}} \end{bmatrix}$$

$$\Delta\boldsymbol{\theta}_n = [\Delta\theta_0\ \Delta\theta_1 \quad \cdots \quad \Delta\theta_{N-1}]^T$$

$$\Delta\theta_j = \theta_{j,n+1} - \theta_{jn}$$

$$\mathbf{g}_n = [g_0\, g_1 \quad \cdots \quad g_{N-1}]^T$$

After a given trial calculation through the column has been made (the component-material balances have been solved for the v_{ji}'s), the desired set of θ_j's that makes $g_0 = g_1 = g_2 = \cdots = g_{N-1} = 0$, simultaneously, is found. The desired set of θ_j's is that set of θ_j's ($\theta_j > 0$) that satisfy the Newton–Raphson equations which are represented by Eq. (4-32). On the basis of an assumed set of θ_j's, identified by the subscript n, the g functions and their derivatives that appear in Eq. (4-32) are evaluated. Then the system of equations represented by Eq. (4-32) is solved for the $\Delta\theta_j$'s. The θ_j's to be assumed for the next trial solution of Eq. (4-32) are readily computed ($\theta_{j,n+1} = \theta_{j,n} + \Delta\theta_j$). This process is repeated until a set of θ_j's within the desired degree of accuracy has been found. For the first trial θ_j is taken equal to 1.0 for all j. In the event that one or more of the $\theta_{j,n+1}$'s is negative, all of the corrections $\Delta\theta_j$ are reduced successively by factors of 1/2 until the $\theta_{j,n+1}$'s are all positive. The values of the derivatives may be evaluated by use of the analytical expressions (see Prob. 4-3) or by use of the numerical approximation of the derivative.

Specifications: the molar distillate rate and the liquid holdups in mass or volumetric units

If, instead of molar holdups, the total liquid holdups are specified in mass (or volumetric units), the specified values to be satisfied at time $t_n + \Delta t$ are as follows:

$$D, \mathscr{M}_1, \mathscr{M}_2, \ldots, \mathscr{M}_N$$

In this case the specification $\mathscr{M}_N$ leads to an independent θ namely, θ_N. For, when the $\mathscr{M}_j$'s are specified, the term U_N/B of Eq. (4-26) depends upon the θ_j's. Thus, the expression enclosed by parentheses in Eq. (4-25) should be modified to read ($j = 1, 2, \ldots, N$).

Let the corrected mass (or volumetric) holdup of component i on plate j be denoted by m_{ji}. Then

$$m_{ji} = u_{ji} M_i \tag{4-33}$$

where M_i is the molecular weight (or molar volume) of component i. The formula for m_{ji} in terms of θ_j is readily obtained by replacing u_{ji} by its equivalent as given by Eq. (4-25)

$$m_{ji} = \theta_j\left(\frac{u_{ji}}{d_i}\right)_{ca} d_i M_i \tag{4-34}$$

In a manner analogous to that shown for the development of Eq. (4-30) it is readily shown that

$$d_i = \frac{FX_i + \sigma(F^0X_i^0 - d_i^0 - b_i^0) + \left(\dfrac{1}{\phi\ \Delta t}\right)\displaystyle\sum_{j=1}^{N} u_{ji}^0}{1 + \theta_0\left(\dfrac{b_i}{d_i}\right)_{ca} + \left(\dfrac{1}{\phi\ \Delta t}\right)\displaystyle\sum_{j=1}^{N}\theta_j\left(\frac{u_{ji}}{d_i}\right)_{ca}} \tag{4-35}$$

For the case where the mass (or volumetric) holdups are specified, the g functions to be satisfied are as follows:

$$g_0(\theta_0, \theta_1, \ldots, \theta_N) = \sum_{i=1}^{c} d_i - D$$
$$g_j(\theta_0, \theta_1, \ldots, \theta_N) = \sum_{i=1}^{c} m_{ji} - \mathcal{M}_j \qquad (j = 1, 2, \ldots, N) \tag{4-36}$$

where again the desired set of θ_j's is that set of positive numbers that makes $g_0 = g_1 = \cdots = g_N = 0$, simultaneously. This set of θ_j's may be found by use of the Newton–Raphson method.

When the $\mathcal{M}_j$'s are specified, the corresponding U_j's at time $t_n + \Delta t$ are not known until convergence has been obtained for the given time period under consideration. The U_j's at t_n and at $t_n + \Delta t$ are needed in the component-material balances. The value of U_j at time t_n is, of course, equal to the value obtained at the end of the calculational procedure for the previous time increment. At the end of the first and all subsequent trials for any given time increment, the value of U_j to be used for the next trial may be computed (after the θ_j's have been found) as follows:

$$U_j = \sum_{i=1}^{c} u_{ji} \tag{4-37}$$

Determination of Temperatures

After the θ_j's have been determined, the corresponding values of the corrected mole fractions may be computed by use of Eqs. (4-27) and (4-28). These mole fractions for each plate are used to compute a new set of temperatures. The new set of temperatures is determined by use of the K_b method which eliminates the trial-and-error involved in the use of the conventional bubble-point and dew-point expressions given by Eqs. (4-14) and (4-15). The K value for the base component may be computed by use of either one or two equivalent expressions, Eqs. (4-39) and (4-40). These expressions are developed as follows: Equation (4-13) may be restated in the form

$$y_{ji} = \alpha_{ji} K_{jb} x_{ji} \tag{4-38}$$

where $\alpha_{ji} = K_{ji}/K_{jb}$; the subscript b refers to the base component. When each side of Eq. (4-38) is summed over all components, and the result so obtained solved for K_{jb}, the following formula for calculating K_{jb} at $T_{j,n+1}$ (the new temperature) is obtained:

$$K_{jb}\Big|_{T_{j,n+1}} = \frac{1}{\sum_{i=1}^{c} \alpha_{ji}\Big|_{T_{j,n}} x_{ji}} \tag{4-39}$$

If Eq. (4-38) is rearranged to

$$K_{jb} x_{ji} = \frac{y_{ji}}{\alpha_{ji}}$$

and then summed, an expression different from Eq. (4-39) but equivalent (see Prob. 4-5) is obtained

$$K_{jb}\Big|_{T_{j,n+1}} = \sum_{i=1}^{c} \frac{y_{ji}}{\alpha_{ji}\Big|_{T_{j,n}}} \tag{4-40}$$

The x_{ji}'s and y_{ji}'s that appear in Eqs. (4-39) and (4-40) are computed by use of Eqs. (4-27) and (4-28), respectively.

The desired temperature, $T_{j,n+1}$, may be computed directly by use of a hypothetical base component that has a K value given by

$$\ln K_{jb} = \frac{b}{T_j} + a \tag{4-41}$$

As proposed in Holland(6), the values of a and b are computed on the basis of the upper and lower curve-fit limits of the K for the midboiling or the component just lighter than the midboiling component (a component having K values about midway between those for the lightest and heaviest components of the mixture).

For wide boiling mixtures, the temperatures determined by the bubble-point function (Eq. (4-14)) tended to be alternately too high and too low while the temperatures determined by use of the dewpoint function (Eq. (4-15)) were almost invariant for wide boiling mixtures such as those encountered in absorbers in the natural gas industry.

Reformulation of the Equations of the Theta Method To Avoid Numerical Difficulties

In order to avoid numerical problems arising from the existence of very small to zero values of one or the other of the product rates, Eqs. (4-25), (4-27) through (4-30) may be restated in terms of a new variable p_i which is finite for all values of $(b_i)_{ca}$ and $(d_i)_{ca}$ including zero. The definition of p_i is obtained by finding a common denominator followed by rearrangement of the expression given by Eq. (4-35) for d_i. The resulting equations so obtained are

$$d_i = p_i (d_i)_{ca}$$
$$u_{ji} = p_i (u_{ji})_{ca} \theta_j \tag{4-42}$$

and

$$p_i = \frac{FX_i + \sigma[FX_i - d_i - b_i]^0 + \dfrac{1}{\phi\,\Delta t} \sum_{j=1}^{N} u_{ji}^0}{(d_i)_{ca} + \theta_0 (b_i)_{ca} \left(1 + \dfrac{U_N/B}{\phi\,\Delta t}\right) + \dfrac{1}{\phi\,\Delta t} \sum_{j=1}^{N-1} \theta_j (u_{ji})_{ca}} \tag{4-43}$$

Expressions for the mole fractions given by Eqs. (4-27) and (4-28) are restated in the following form:

$$x_{ji} = \frac{(l_{ji})_{ca}\, p_i}{\sum_{i=1}^{c} (l_{ji})_{ca}\, p_i} \tag{4-44}$$

$$y_{ji} = \frac{(v_{ji})_{ca}\, p_i}{\sum_{i=1}^{c} (v_{ji})_{ca}\, p_i} \tag{4-45}$$

Also, d_i and u_{ji} in the g functions (Eq. (4-36)) are replaced by their equivalents as given by Eq. (4-42).

Before presenting the development of the enthalpy balance equations for the calculation of the total flow rates, the fundamental concepts involved in the procedures presented thus far are illustrated by use of a simple problem for which the α_{ji}'s, L/V's, and U_j's are taken to be fixed for all t at the values shown in Table 4-1. A sketch of this unit is shown in Fig. 4-3. In this problem, it is supposed that initially (time $t = 0$) the column is at steady state operation, and at time $t = 0+$, an upset (a step change) in the composition of the feed shown in Table 4-1 occurs. The steady state solution at the initial conditions is presented in item I of Table 4-1, and the steady state solution at the conditions of the upset is given in item III.

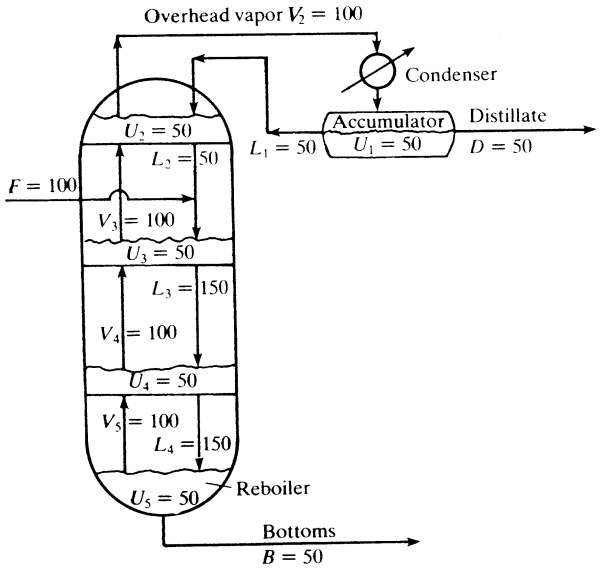

Figure 4-3 Sketch of the column, total flow rates, and holdups specified for Example 4-1.

Table 4-1 Statement and Solution of Example 4-1

Statement Initially ($t = 0$), the column is operating at the steady state conditions that follow in item I. At time $t = 0+$, the upset given in item II occurs. On the basis of $\phi = 0.6$ and $\Delta t = 0.1$ min, find the transient values of the variables at the end of the first time period.

Part A. Initial operating conditions at time $t = 0$

Component	$F^0X_i^0$, lb · mol/min	α_1	Other conditions
1	33.3	1	The column has 3 plates plus a reboiler and a total condenser. The feed enters as a liquid at its bubble-point at the column pressure. The column operates at the following flow rates: $D = B = 50$ lb · mol/min, $L_1 = L_2 = 50$ lb · mol/min, $L_3 = L_4 = 150$ lb · mol/min, and $V_2 = V_3 = V_4 = V_5 = 100$ lb · mol/min.
2	33.3	2	
3	33.4	3	

Initial conditions (at $t = 0$); steady state operation.

I *Steady state solution at the initial conditions*

Component	$d_i^0 = v_{1i}^0$	v_{2i}^0	v_{3i}^0	v_{4i}^0	v_{5i}^0
1	5.5354	11.0708	17.3787	23.1947	35.0356
2	18.0757	36.1514	37.4125	39.6279	38.4225
3	26.3888	52.7777	45.2088	37.1773	26.5417
Component	u_{1i}^0	u_{2i}^0	u_{3i}^0	u_{4i}^0	u_{5i}^0
1	5.5354	11.8432	16.9864	20.9334	27.7645
2	18.0757	19.3368	18.2840	17.8822	15.2242
3	26.3888	18.8199	14.7294	11.1842	7.0111

$K_{1b}^0 = 0.413\,724$, $K_{2b}^0 = 0.467\,391$, $K_{3b}^0 = 0.511\,542$, $K_{4b}^0 = 0.554\,011$, $K_{5b}^0 = 0.630\,942$.

II *Upset in the feed composition at time $t = 0+$*

Component	FX_i	Other conditions
1	16.67	
2	41.67	All other conditions are the same as those given in item I
3	41.66	

III *Steady state solution at the conditions of the upset*

Component	$d_i = v_{1i}$	v_{2i}	v_{3i}	v_{4i}	v_{5i}
1	2.1082	4.2164	7.0931	9.2029	14.9118
2	18.4457	36.8914	40.2528	44.2071	47.5652
3	29.4460	58.8920	52.6540	46.5899	37.5228

(*Continued over*)

Table 4-1 Statement and Solution of Example 4-1—*Continued*

Component	u_{1i}	u_{2i}	u_{3i}	u_{4i}	u_{5i}
1	2.18082	4.9848	7.9215	9.8245	14.5617
2	18.4457	21.8071	22.4771	23.5965	23.2242
3	29.4460	23.2080	19.6013	16.5789	12.2139

$K_{1b} = 0.392\,656$, $K_{2b} = 0.422\,928$, $K_{3b} = 0.447\,708$, $K_{4b} = 0.468\,364$, $K_{5b} = 0.512\,021$.
(Note, the corresponding values of K_{ji} follow from the definition of α_i; namely $K_{ji} = \alpha_i K_{jb}$.)

SOLUTION The component-material balances for any component i for this example may be stated in the form of Eq. (4-22) as follows:

$$b_1 v_1 + c_1 v_2 = d_1$$
$$a_2 v_1 + b_2 v_2 + c_2 v_3 = d_2$$
$$a_3 v_2 + b_3 v_3 + c_3 v_4 = d_3$$
$$a_4 v_3 + b_4 v_4 + c_4 v_5 = d_4$$
$$a_5 v_4 + b_5 v_5 = d_5$$

where

$$b_1 = -\left(1 + \frac{L_1}{D} + \frac{U_1/D}{\phi\,\Delta t}\right) \qquad c_1 = 1$$

$$d_1 = -\sigma(v_{2i}^0 - l_{1i}^0 - v_{1i}^0) - \frac{u_{1i}^0}{\phi\,\Delta t} \qquad a_2 = A_{1i} = \frac{L_1}{D}$$

$$b_2 = -\left[1 + A_{2i}\left(1 + \frac{U_2/L_2}{\phi\,\Delta t}\right)\right] \qquad c_2 = 1$$

$$d_2 = -\sigma(v_{3i}^0 + l_{1i}^0 - v_{2i}^0 - l_{2i}^0) - \frac{u_{2i}^0}{\phi\,\Delta t} \qquad a_3 = A_{2i}$$

$$b_3 = -\left[1 + A_{3i}\left(1 + \frac{U_3/L_3}{\phi\,\Delta t}\right)\right] \qquad c_3 = 1$$

$$d_3 = -FX_i - \sigma(F^0 X_i^0 + v_{4i}^0 + l_{2i}^0 - v_{3i}^0 - l_{3i}^0) - \frac{u_{3i}^0}{\phi\,\Delta t} \qquad a_4 = A_{3i}$$

$$b_4 = -\left[1 + A_{4i}\left(1 + \frac{U_4/L_4}{\phi\,\Delta t}\right)\right] \qquad c_4 = 1$$

Table 4-1 Statement and Solution of Example 4-1—*Continued*

$$d_4 = -\sigma(v_{5i}^0 + l_{3i}^0 - v_{4i}^0 - l_{4i}^0) - \frac{u_{4i}^0}{\phi\,\Delta t} \qquad a_5 = A_{4i}$$

$$b_5 = -\left[1 + A_{5i}\left(1 + \frac{U_5/L_5}{\phi\,\Delta t}\right)\right]$$

$$d_5 = -\sigma(l_{4i}^0 - v_{5i}^0 - b_i^0) - \frac{u_{5i}^0}{\phi\,\Delta t}$$

Note: The values of the variables at the beginning of the first time step may be evaluated at the values at time $t = 0$ or time $t = 0+$. For all variables except FX_i in the expression for d_3, the values at $t = 0$ are equal to those at time $t = 0+$; that is, one may use either of the expressions given above for evaluating d_3 or

$$d_3 = -FX_i - 0 - [FX_i + v_{4i}^0 + l_{2i}^0 - v_{3i}^0 - l_{3i}^0] - \frac{u_{3i}^0}{\phi\,\Delta t}$$

where $FX_i = FX_i^{0+}$.

I *Evaluation of the constants a_j, b_j, c_j, and d_j*

To initiate the first trial for the first Δt, assume that the temperatures at the end of the first time step are the same as those at the beginning of the time period.

Component	b_1	$c_1 = c_2 = c_3 = c_4 = c_5$	d_1	a_2	b_2
1	−18.6666	1.0	−92.2570	1.0	−19.8992
2	−18.6666	1.0	−301.2619	1.0	−10.4496
3	−18.6666	1.0	−439.8143	1.0	−7.2997

Component	d_2	a_3	b_3	d_3	a_4
1	−197.3871	1.0697	−20.2228	−299.7771	2.9322
2	−322.2801	0.5348	−10.6114	−346.4046	1.4661
3	−313.6659	0.3565	−7.4076	−287.1515	0.9774

Component	b_4	d_4	a_5	b_5	d_5
1	−18.7493	−348.8903	2.7075	−15.0002	−462.7429
2	−9.8746	−298.0380	1.3537	−8.0001	−253.7380
3	−6.9164	−186.4048	0.9025	−5.6667	−116.8523

(*Continued over*)

Table 4-1 Statement and Solution of Example 4-1—*Continued*

II *Calculation of the* v_{ji}*'s*

Component	$f_1 = \frac{c_1}{b_1}$	$g_1 = \frac{d_1}{b_1}$	$f_2 = \frac{c_2}{b_2 - a_2 f_1}$	$g_2 = \frac{d_2 - a_2 g_1}{b_2 - a_2 f_1}$
1	−0.053 57	4.9423	−0.503 8	10.1951
2	−0.053 57	16.1390	−0.096 19	32.5527
3	−0.053 57	23.5614	−0.138 0	46.5387

Component	$f_3 = \frac{c_3}{b_3 - a_3 f_2}$	$g_3 = \frac{d_3 - a_3 g_2}{b_3 - a_3 f_2}$	$f_4 = \frac{c_4}{b_3 - a_4 f_3}$	$g_4 = \frac{d_4 - a_4 g_3}{b_4 - a_4 f_4}$
1	−0.049 58	15.4040	−0.053 75	21.1815
2	−0.094 69	34.4524	−0.102 7	35.8007
3	−0.135 8	41.2789	−0.147 4	33.4264

Component	$g_5 = \frac{d_5 - a_5 g_4}{b_5 - a_5 f_4}$ $g_5 = v_{5i}$	$f_4 v_{5i}$	$v_{4i} = g_4 - f_4 v_{5i}$	$f_3 v_{4i}$
1	35.0119	−1.8819	23.0634	−1.1435
2	38.4431	−3.9486	39.7494	−3.7641
3	26.5681	−3.9165	37.3429	−5.0748

Component	$v_{3i} = g_3 - f_3 v_{4i}$	$f_2 v_{3i}$	$v_{2i} = g_2 - f_2 v_{3i}$
1	16.5476	−0.8338	11.0289
2	38.2166	−3.6760	36.2287
3	46.3538	−6.3970	52.9357

Component	$f_1 v_{2i}$	$v_{1i} = (d_i)_{ca} = g_1 - f_1 v_{2i}$	$(b_i)_{ca} = A_{5i} v_{5i}$	$(b_i/d_i)_{ca}$
1	−0.5908	5.5331	27.7458	5.0144
2	−1.9408	18.0798	15.2324	0.8425
3	−2.8358	26.3973	7.0181	0.2659

Component	$\left(\frac{u_{2i}}{d_i}\right)_{ca} = \frac{(U_2/L_2)A_{2i}v_{2i}}{d_i}$	$\left(\frac{u_{3i}}{d_i}\right)_{ca} = \frac{(U_3/L_3)A_{3i}v_{3i}}{d_i}$	$\left(\frac{u_{4i}}{d_i}\right)_{ca} = \frac{(U_4/L_4)A_{4i}v_{4i}}{d_i}$
1	2.1323	2.9231	3.7618
2	1.0718	1.0330	0.9921
3	0.7151	0.5721	0.4255

III *Calculation of* θ_j*'s*

The g functions are as follows:

$$g_0 = \sum_{i=1}^{c} d_i - 50 \qquad g_3 = \sum_{i=1}^{c} u_{3i} - 50$$

$$g_2 = \sum_{i=1}^{c} u_{2i} - 50 \qquad g_4 = \sum_{i=1}^{c} u_{4i} - 50$$

Table 4-1 Statement and Solution of Example 4-1—*Continued*

The θ_j's (found by the Newton–Raphson method) that make $g_0 = g_2 = g_3 = g_4 = 0$, simultaneously, are as follows:

$\theta_0 = 1.000\,382$ $\qquad$ $\theta_3 = 1.001\,186$

$\theta_2 = 0.999\,183$ $\qquad$ $\theta_4 = 1.000\,557$

and

$$d_i = \frac{FX_i + \sigma(F^0X_i^0 - d_i^0 - b_i^0) + (1/\phi\ \Delta t)\sum_{j=1}^{5} u_{ji}^0}{1 + \theta_0\left(\frac{b_i}{d_i}\right)_{ca}\left[1 + \frac{U_5/B}{\phi\ \Delta t}\right] + \frac{U_1/D}{\phi\ \Delta t} + \frac{1}{\phi\ \Delta t}\sum_{j=2}^{4}\theta_j\left(\frac{u_{ji}}{d_i}\right)_{ca}}$$

IV *Calculation of the corrected temperature profile (or* K_{jb}*'s)*

Component	d_i	X_{Di}	$\alpha_i X_{Di}$	u_{2i}	x_{2i}
1	5.5311	0.1106	0.1106	11.7843	0.2357
2	18.0754	0.3615	0.7230	19.3576	0.3871
3	26.3935	0.5279	1.5836	18.8582	0.3772
			2.4172		

$$K_{1b} = \frac{1}{\sum_{i=1}^{c} \alpha_i X_{Di}} = 0.4137$$

Component	$\alpha_i x_{2i}$	u_{3i}	x_{3i}	$\alpha_1 x_{3i}$	u_{4i}
1	0.2357	16.1870	0.3237	0.3237	20.8185
2	0.7743	18.6946	0.3738	0.7478	17.9426
3	1.1315	15.1183	0.3323	0.9071	11.2387
	2.1415			1.9786	

$$K_{2b} = \frac{1}{\sum_{i=1}^{c} \alpha_i x_{2i}} = 0.4670 \qquad K_{3b} = \frac{1}{\sum_{i=1}^{c} \alpha_i x_{3i}} = 0.5054$$

Component	x_{4i}	$\alpha_i x_{3i}$	$b_i = \theta_0(b_i/d_i)_{ca}(d_i)$	$x_{Bi} = x_{5i}$	$\alpha_i x_{5i}$
1	0.4164	0.4164	27.7457	0.5549	0.5549
2	0.3588	0.7177	15.2345	0.3047	0.6094
3	0.2247	0.6743	7.0197	0.1404	0.4212
		1.8084			1.5855

$$K_{4b} = \frac{1}{\sum_{i=1}^{c} \alpha_i x_{4i}} = 0.5530 \qquad K_{5b} = \frac{1}{\sum_{i=1}^{c} \alpha_i x_{5i}} = 0.6307$$

These K_{jb}'s become the assumed values for the next trial for the first Δt, and the assumed value for the K_{ji}'s are given by $K_{ji} = \alpha_i K_{jb}$.

With the total flow rates held fixed, the repeated application of the procedure described above gave the transient values of the variables shown in Figs. 4-4 and 4-5. The effect of the length of the time step on the transient values of b_1/d_1 is shown in Table 4-2. It is to be observed that as the size of the time step becomes very large, say 10^{10}, the steady state solution at the conditions of the upset is obtained at the end of the first time step (see Prob. 4-14).

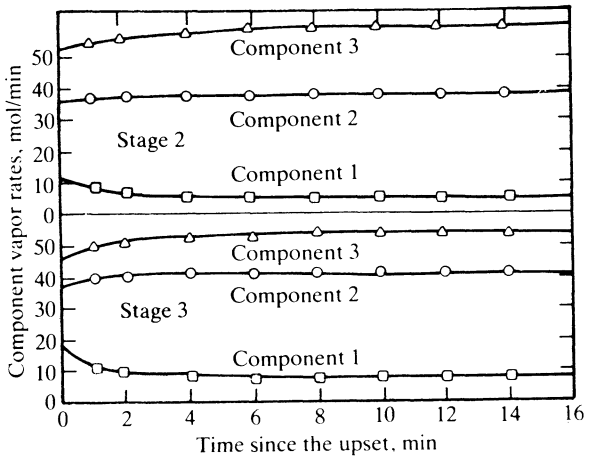

Figure 4-4 Transient values of the component vapor rates for stages 2 and 3, Example 4-1.

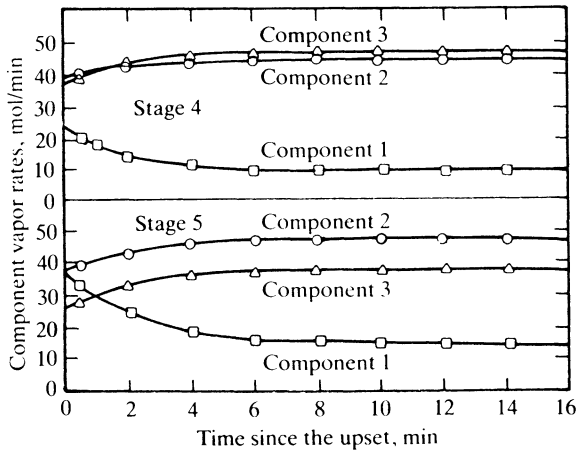

Figure 4-5 Transient values of the component vapor rates for stages 4 and 5, Example 4-1.

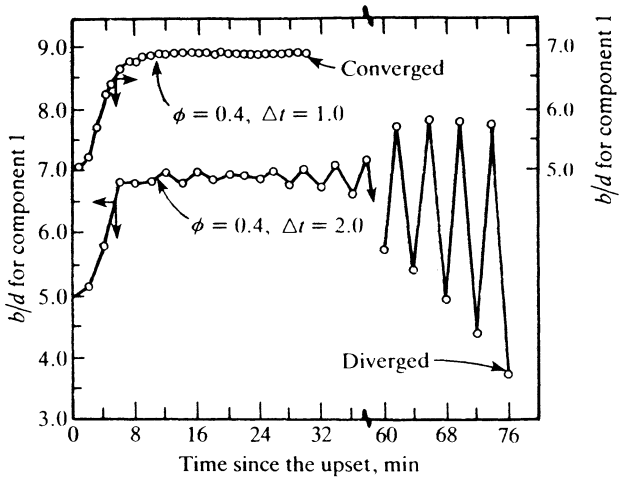

Figure 4-6 Failure of the implicit method for Example 4-1 at $\phi = 0.4$ and $\Delta t = 2.0$.

Table 4-2 Solution of Example 4-1 by the implicit method

$\phi = 0.6$ and time periods range from 1 to 10^{10} min

	b/d for component 1						
Time period	$\Delta t = 1$ min	$\Delta t = 6$ min	$\Delta t = 10$ min	$\Delta t = 20$ min	$\Delta t = 30$ min	$\Delta t = 40$ min	$\Delta t = 10^{10}$ min
1	5.0938	5.7455	6.0143	6.3420	6.4912	6.5079	6.9070
2	5.3493	6.9731	7.2158	7.2242	7.1621	7.1154	
3	5.7572	6.9191	6.8356	6.7840	6.7906	6.8034	
4	6.1413	6.8959	6.9236	6.9632	6.9689	6.9660	
5	6.4126	6.9129	6.9044	6.8830	6.8764	6.8757	
6	6.5952	6.9044	6.9066	6.9175	6.9227	6.9242	
7	6.7133	6.9080	6.9078	6.9025	6.8991	6.8977	
8	6.7870	6.9067	6.9064	6.9089	6.9110	6.9121	
9	6.8329	6.9070	6.9074	6.9063	6.9050	6.9043	
10	6.8613	6.9070	6.9068	6.9073	6.9080	6.9085	
11	6.8787	6.9069	6.9071	6.9069	6.9073	6.9062	
12	6.8895		6.9070			6.9074	
13	6.8961					6.9068	
14	6.9002						
15	6.9028						
20	6.9066						
21	6.9068						
22	6.9068						
23	6.9069						

Constant-Composition Formulation of the Enthalpy Balances

The elimination of one of the total flow rates from each enthalpy balance by use of the corresponding component-material balance yields an expression for computing the total flow rates which was found to be very stable for both steady state and unsteady state problems. This form of the enthalpy balances is called the constant-composition method. There follows an outline of the development of these expressions which are presented in Table 4-3.

On the basis of the corrected x_{ji}'s and the corresponding temperatures found by the K_b method, a new set of total flow rates is found by use of enthalpy and total-material balances. Again, as in the calculation of the temperatures, the most recently calculated values of the variables are used in subsequent equations.

Table 4-3 Constant-composition form of the enthalpy balances

$$Q_C = L_1 \sum_{i=1}^{c}(\hat{H}_{2i} - \hat{h}_{1i})x_{1i} + D\sum_{i=1}^{c}(\hat{H}_{2i} - \hat{H}_{Di})X_{Di}$$

$$+ \sigma\left[L_1^0 \sum_{i=1}^{c}(\hat{H}_{2i} - \hat{h}_{1i}^0)x_{1i}^0 - V_2^0 \sum_{i=1}^{c}(\hat{H}_{2i} - \hat{H}_{2i}^0)y_{2i}^0 + D^0\sum_{i=1}^{c}(\hat{H}_{2i} - \hat{H}_{Di}^0)X_{Di}^0 - Q_C^0\right]$$

$$+ \frac{U_1}{\phi\,\Delta t}\sum_{i=1}^{c}(\hat{H}_{2i} - \hat{h}_{1i})x_{1i} - \frac{U_1^0}{\phi\,\Delta t}\left[\sum_{i=1}^{c}(\hat{H}_{2i} - \hat{h}_{1i}^0)x_{1i}^0\right]$$

$$L_j = \frac{L_{j-1}\sum_{i=1}^{c}(\hat{H}_{j+1,i} - \hat{h}_{j-1,i})x_{j-1,i} - V_j\sum_{i=1}^{c}(\hat{H}_{j+1,i} - \hat{H}_{ji})y_{ji} + \sigma\left[V_{j+1}^0\sum_{i=1}^{c}(\hat{H}_{j+1,i} - \hat{H}_{j+1,i}^0)y_{j+1,i}^0\right]}{\psi_j}$$

$$+ \frac{\sigma\left[L_{j-1}^0\sum_{i=1}^{c}(\hat{H}_{j+1,i} - \hat{h}_{j-1,i}^0)x_{j-1,i}^0 - V_j^0\sum_{i=1}^{c}(\hat{H}_{j+1,i} - \hat{H}_{ji}^0)y_{ji}^0 - L_j^0\sum_{i=1}^{c}(\hat{H}_{j+1,i} - \hat{h}_{ji}^0)x_{ji}^0\right]}{\psi_j}$$

$$\times \frac{-U_j\sum_{i=1}^{c}(\hat{H}_{j+1,i} - \hat{h}_{ji})x_{ji}}{\phi\,\Delta t\,\psi_j} + \frac{U_j^0\sum_{i=1}^{c}(\hat{H}_{j+1,i} - \hat{h}_{ji}^0)x_{ji}^0}{\phi\,\Delta t\,\psi_j} + \frac{\mathscr{H}_j}{\psi_j} \qquad (j = 2, 3, \ldots, N-1)$$

where

$$\psi_j = \sum_{i=1}^{c}(\hat{H}_{j+1,i} - \hat{h}_{ji})x_{ji}$$

$$\mathscr{H}_j = 0 \qquad (j \neq f)$$

$$\mathscr{H}_f = F\sum_{i=1}^{c}(\hat{H}_{f+1,i} - \hat{H}_i)X_i + \sigma F^0\sum_{i=1}^{c}(\hat{H}_{f+1,i} - \hat{H}_i^0)X_i^0$$

$\hat{H}_i$ = virtual value of the enthalpy of component i in the feed, regardless of state

Each enthalpy balance may enclose either only one plate or the top (or bottom) and all plates between the top (or bottom) and each plate j. Each of these methods was investigated and found to be equally reliable.

To illustrate the development of the energy balance equations, the expression for any stage j ($2 \leq j \leq N-1, j \neq f-1, f$) is developed by first applying the implicit method to Eq. (4-3) (with the vapor holdups neglected) to give

$$\sum_{i=1}^{c}(v_{j+1,i}\hat{H}_{j+1,i} + l_{j-1,i}\hat{h}_{j-1,i} - v_{ji}\hat{H}_{ji} - l_{ji}\hat{h}_{ji})$$

$$+ \sigma\left(\sum_{i=1}^{c}(v_{j+1,i}^0\hat{H}_{j+1,i}^0 + l_{j-1,i}^0\hat{h}_{j-1,i}^0 - v_{ji}^0\hat{H}_{ji}^0 - l_{ji}^0\hat{h}_{ji}^0)\right)$$

$$= \frac{\sum_{i=1}^{c}u_{ji}h_{ji}}{\phi\,\Delta t} - \frac{\sum_{i=1}^{c}u_{ji}^0h_{ji}^0}{\phi\,\Delta t} \qquad (j \neq 1, f, N) \quad (4\text{-}46)$$

In the constant-composition method, a component flow rate, say $v_{j+1,i}$, is eliminated from Eq. (4-46) through the use of the component-material balance for stage j (see Eq. (4-16)). The result so obtained may be rearranged to give the formula presented in Table 4-3. For stages $j = 1, f$, and N, the expressions are developed in a similar manner. The first step in the calculational procedure consists of the calculation of the condenser duty Q_C by use of the first expression given in Table 4-3. Next L_2 is computed. After each L_j has been computed by use of an energy balance, the corresponding V_{j+1} may be found by use of the total-material balances. When the total molar holdups are taken to be fixed, then the unsteady state total-material balances reduce to the steady state form namely,

$$V_{j+1} = L_j + D \qquad (j = 1, 2, \ldots, f-1)$$
$$V_{j+1} = L_j - B \qquad (j = f, f+1, \ldots, N-1) \quad (4\text{-}47)$$

Choice of Phi and Step Size

Since the two-point implicit method reduces to the trapezoidal rule which is A stable then, if the equations were linear, one would expect the implicit method to be stable for values of $\phi \geq 1/2$ and to diverge for certain choices of Δt at $\phi < 1/2$. Although the equations were nonlinear, their numerical behavior followed closely that predicted for systems of linear equations. The failure of the implicit method to converge for relatively large Δt's (larger than $\Delta t = 1$) and at values of $\phi < 1/2$ is illustrated in Fig. 4-6. In some examples, oscillations were obtained for $\phi = 1/2$, but not for $\phi > 1/2$ (say $\phi = 0.6$) regardless of the choice of Δt (see Table 4-2).

When relatively small Δt's are used, the truncation error is relatively smaller and more accurate transient solutions are obtained than when relatively large Δt's are employed. It was found that the Δt selected should be larger than 10^{-6} (for the system of units used in the examples) in order to prevent the holdup terms from taking undue dominance in the calculations. As steady state is approached, larger Δt's may be used without loss of accuracy in the transient solutions. The scheme developed and used by Waggoner(16) to solve a wide variety of examples appears to give reliable results. After each upset, the following procedure was used in the selection of the step sizes. The initial Δt was taken to be equal to 1/5 of the holdup time (U_f/L_1), that is,

$$\Delta t = \frac{U_f/L_1}{5}$$

At the end of every 10 time steps, the value of Δt was doubled.

Calculational Procedure

In proceeding from one time increment to the next, the point-slope predictor was used to predict the values of T_j and V_j at the end of the next time period $(t_n + \Delta t)$

$$\begin{aligned} T_j\Big|_{t_n+\Delta t} &= T_j\Big|_{t_n-\Delta t} + 2\,\Delta t \left.\frac{dT_j}{dt}\right|_{t_n} \\ V_j\Big|_{t_n+\Delta t} &= V_j\Big|_{t_n-\Delta t} + 2\,\Delta t \left.\frac{dV_j}{dt}\right|_{t_n} \end{aligned} \tag{4-48}$$

The derivatives of T_j and V_j that appear in Eq. (4-48) were evaluated numerically. After each V_j had been predicted by use of Eq. (4-48), the corresponding value of L_j was computed by use of Eq. (4-47).

In the following discussion, it is supposed that initially the column is at steady state and that at time $t = 0+$ a change in the composition of the feed occurs (note that other initial conditions and upsets may be selected). The calculational procedure for the case where the molar holdups are specified follows:

Step 1 Take $\phi = 0.6$ and choose the first Δt as described in the previous section.

Step 2 Assume values for the temperatures and L/V's at $t_n + \Delta t$. For the first two trials, the values at time t_n are satisfactory. For the second and all subsequent time increments, the values for T_j and V_j are predicted by use of the point-slope predictor (see Eq. (4-48)).

Step 3 Compute d_i, b_i, u_{ji}, and l_{ji} at the end of each increment of time by use of the component-material balances.

Step 4 Find the θ's such that $g_0 = g_1 = g_2 = \cdots = g_{N-1} = 0$ by use of the Newton–Raphson method (see Eq. (4-32)).

Step 5 Compute the temperatures by use of the K_b method (see Eqs. (4-39) and (4-40)). Note that after the corrected u_{ji}'s have been found in step 5, the corrected liquid mole fractions may be computed directly from these. Also, the K_b obtained by use of Eq. (4-39) may be used to compute the y_{ji}'s

$$y_{ji} = K_{jb}\Big|_{T_{j,n+1}} \alpha_{ji}\Big|_{T_{jn}} x_{ji}$$

Step 6 Compute the L/V's for the next trial by use of enthalpy balances.

Step 7 Repeat steps 2 to 6 until $|\theta_j - 1|$ is equal to or less than a preselected number of the order of 10^{-4} or 10^{-5}. Then proceed to the next increment of time by returning to step 1.

For the case where the mass (or volumetric) holdups are specified, the following procedure is employed.

Specification of the Holdups in Mass or Volumetric Units

For the first trial for the first increment of time (where the initial condition is steady state), the variation of the molar holdup is neglected. At the end of the first and all subsequent trials, the molar holdups at time $t_n + \Delta t$ are computed by use of Eqs. (4-33) and (4-34). Also, the g functions given by Eq. (4-36) are employed in the calculational procedure described above.

Examples

A wide variety of problems was solved in the course of the investigation of the properties of the proposed calculational procedure by Waggoner(16). The determination of the θ_j's at the end of each calculation through the column constitutes the only trial-and-error involved in the proposed method. Some of the properties of the θ method are demonstrated by use of Example 4-2 (see Table 4-4). The upset (a change in the feed composition) for this example is about the maximum permitted by the curve-fits. The θ_j's obtained for the first 10 trials of the first time period are shown in Table 4-5. Although the θ's shown in Table 4-5 are to within $\pm 10^{-6}$ of unity, this should not be taken to mean that the corresponding T_j's, v_{ji}'s, and V_j's possess the same absolute accuracy because the values of these variables possess truncation errors that resulted from the approximation of the integrals by the implicit method. The fact that each θ is approximately equal to unity does, however, imply that convergence for the first time period has been obtained, that is, a set of the independent variables, the temperatures, has been found that satisfies the component-material balances (Eq. (4-21)), equilibrium relationships (Eq. (4-39)), and the enthalpy and total-material balances (Table 4-3 and Eqs. (4-46) and (4-47)) to within the accuracy of the computer. Transient values of selected variables of Example 4-2 are presented in Table 4-6. In this example and others that follow, a $\phi = 0.6$ was used unless otherwise noted.

Table 4-4 Statement of Example 4-2

Initial conditions:steady state operation

Specifications				Steady state solution		
Component no.	Component	F^0X^0, mol/min	Other conditions	Plate	Temp., °F	Vapor rate, mol/min
1	C_3H_8	60	$D = 50$, $V_2 = 150$, boiling point liquid feed, total condenser, column press. = 300 lb/in² abs. 4 rectifying stages, 3 stripping stages, including the reboiler. The K data and enthalpy data are given by Holland(6) and reproduced in Tables 4A-1, 4A-2.	1 (condenser)	137.98	50.00
2	n-C_4H_{10}	20		2	142.00	150.00
3	n-C_6H_{14}	20		3	148.43	146.32
				4	158.49	141.10
				5 (feed)	179.33	130.98
				6	199.78	123.73
				7 (reboiler)	248.58	109.10
				Component	d_1	b_1
				C_3H_8	48.3711	11.6289
				n-C_4H_{10}	16.2849×10^{-1}	18.3715
				n-C_6H_{14}	43.6069×10^{-5}	19.9996

Upset for Example 4-2

Component no.	Component	FX, mol/min	Other conditions
1	C_3H_8	10	Same as those stated for the initial steady state solution. In addition, the holdup on each plate, the condenser, and the reboiler is 50 moles.
2	n-C_4H_{10}	40	
3	n-C_6H_{14}	50	

Table 4-5 Convergence of the thetas for Example 4-2

Iterative values of variables for the first time period ($\Delta t = 0.1$ min)

Trial	θ_0	θ_2	θ_3	θ_4	θ_5	θ_6	d_1
1	0.997 970 8	1.000 081 1	1.000 909 4	1.005 401 3	0.994 316 0	0.997 288 6	48.368 97
2	1.000 820 9	0.999 999 8	0.999 919 9	0.999 187 1	1.000 639 7	1.000 380 3	48.371 41
3	1.000 025 3	1.000 006 8	1.000 075 8	1.000 540 2	0.999 272 8	0.999 736 7	48.370 85
4	0.999 984 4	0.999 998 6	0.999 983 6	1.999 841 0	1.000 213 4	1.000 060 0	48.371 04
5	1.000 001 6	1.000 000 7	1.000 006 7	1.000 058 2	0.999 909 6	0.999 979 5	48.370 99
6	0.999 993 2	0.999 999 8	0.999 997 8	0.999 979 7	1.000 033 4	1.000 005 3	48.371 00
7	1.000 002 9	1.000 000 1	1.000 000 7	1.000 007 2	0.999 987 4	0.999 998 9	48.371 00
8	0.999 999 3	1.000 000 0	0.999 999 7	0.999 997 4	1.000 004 7	0.999 999 9	48.371 00
9	1.000 000 6	1.000 000 0	1.000 000 1	1.000 000 9	0.999 998 3	1.000 000 1	48.371 00
10	1.000 000 2	1.000 000 0	0.999 999 9	0.999 999 7	1.000 000 7	0.999 999 9	48.371 00

In order to minimize the computing time required to solve a given problem, the number of trials for each time period was limited. As shown in Table 4-5, good accuracy is obtained after the first few trials for a given Δt. Also, it is seen that for any one Δt, convergence to the desired accuracy may not be obtained if too few trials are employed. The inaccuracies that result from performing too few trials are carried over to the next time period, and it may become impossible to obtain convergence for the next time period regardless of the number of trials performed. These inaccuracies eventually disappear with successive time periods as demonstrated by Waggoner(16).

Table 4-6 Transient conditions for Example 4-2

Events			Transient values of selected variables					
			Component-distillate rates, mol/min			Temperature, °F		
Time period	Length of time period	Cumulative time, min	d_1	d_2	d_3	T_1	T_f	T_N
1	0.1	0.1	48.3710	1.6286	0.0004	137.98	187.37	247.86
2	0.1	0.2	48.3705	1.6291	0.0004	137.98	199.01	246.67
3	0.1	0.3	48.3685	1.6310	0.0004	137.99	207.86	248.97
5	0.1	0.5	48.3543	1.6453	0.0004	138.01	220.35	255.53
10	0.1	1.0	48.1750	1.8246	0.0006	138.27	239.22	283.01
20	0.1	2.0	46.7040	3.2955	0.0026	140.48	264.94	330.21
30	0.2	4.0	35.9441	14.0093	0.0466	148.12	294.39	369.38
40	0.4	8.0	13.8426	35.6452	0.5226	205.06	317.72	393.50
50	0.8	16.0	9.9895	38.1016	1.9100	217.19	335.72	407.41
60	1.6	32.0	9.8698	36.7197	3.4106	220.09	344.82	413.13
70	3.2	64.0	9.8522	36.4856	3.6622	220.58	345.98	413.80
71	6.4	70.4	9.8521	36.4840	3.6639	220.59	345.99	413.81
Final* steady state			9.8520	36.4829	3.6651	220.59	346.00	413.81

* Found by use of a steady state calculational procedure.

On the basis of the results obtained by solving a variety of examples, the following scheme was devised. For each time period, a maximum of 10 trials through the column are made. If before the tenth trial $|\theta_j - 1| \leq 10^{-4}$ for all j, the calculations for the next time period are begun.

Example 4-3, stated in Table 4-7, illustrates this procedure. An upset in the composition of the feed, which included the introduction of a new component into the column, occurred at time $t = 0+$. At the end of 4+ min a second upset occurred, and at the end of 19+ min a third upset occurred such that the final feed did not contain one of the original components. After each upset, the procedure for selecting the size of the time period was reinitiated. The transient solutions of Example 4-3 are illustrated in Figs. 4-7 and 4-8. The average computer time required per time period was 0.19 min (IBM 709).

Table 4-7 Statement of Example 4-3

Initial steady state conditions and solution are the same as Example 4-2, Table 4-4

Upsets for Example 4-3

Component no.	Component	Upset 1 at $t = 0+$ FX	Upset 2 at $t = 4+$ min FX	Upset 3 at $t = 19+$ min FX	Other conditions
1	C_3H_8	50	30	10	All specifications and the molar holdups are the same as those stated in Table 4-4
2	n-C_4H_{10}	10	5	0	
3	i-C_4H_{10}	10	20	40	
4	n-C_6H_{14}	30	45	50	

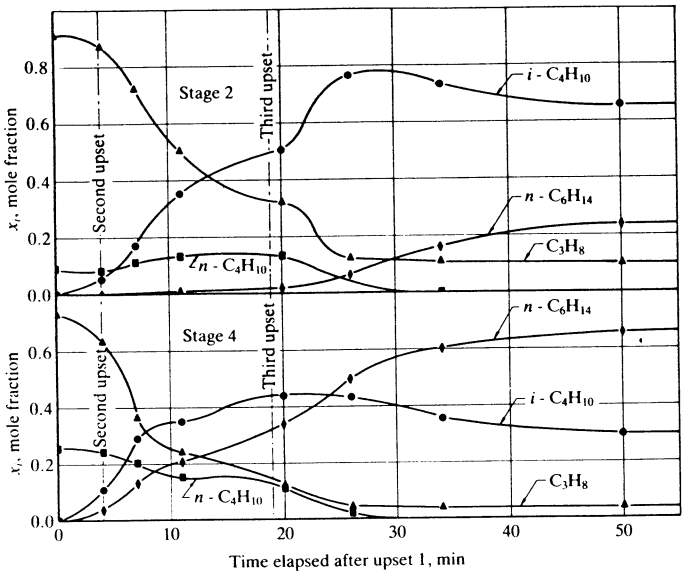

Figure 4-7 Transient values of the mole fractions on plates 2 and 4 after upsets 1, 2, and 3 of Example 4-3. (*R. C. Waggoner and C. D. Holland, "Solution of Problems Involving Conventional and Complex Columns at Unsteady State Operation," AIChE J., vol. 11, p. 112 (1965), Courtesy of the American Institute of Chemical Engineers.*)

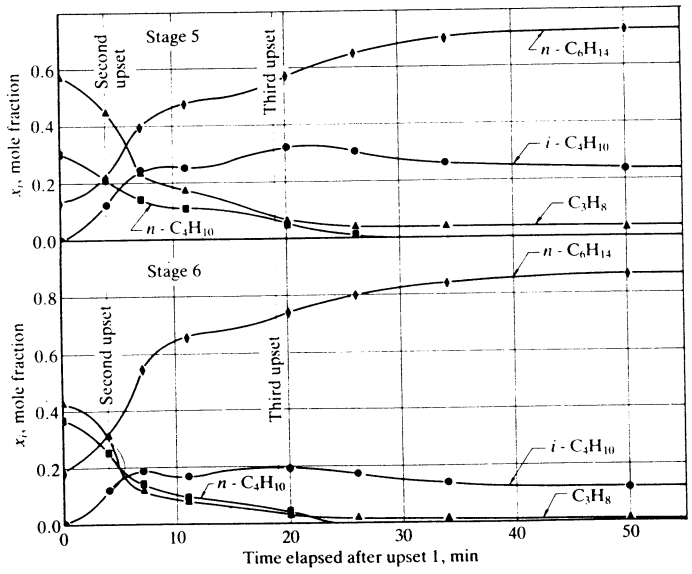

Figure 4-8 Transient values of the mole fractions on plates 4 and 5 after upsets 1, 2, and 3 of Example 4-3. (*R. C. Waggoner and C. D. Holland, "Solution of Problems Involving Conventional and Complex Columns at Unsteady State Operation," AIChE J., vol. 11, p. 112 (1965), Courtesy of the American Institute of Chemical Engineers.*)

Example 4-4, stated in Table 4-8, demonstrates the behavior of the proposed calculational procedure for feeds with wide boiling ranges. Its transient solutions are shown in Table 4-9.

Table 4-8 Statement of Example 4-4

Initial conditions: steady state operation. Upset at time $t = 0+$: a change in feed composition

Specifications				
Component no.	Component	F^0X^0	Upset FX	Other conditions
1	CH_4	6.40	2.0	$D = 31.6$, $V_2 = 94.8$, boiling point liquid feed, partial condenser, column pressure = 300 lb/in^2 abs, 4 rectifying stages, 9 stripping stages including the reboiler. The K data and enthalpy data are given by Holland(6) and by Tables 4A-1 and 4A-2. The conditions stated apply for both the initial steady state solution and the upset at time $t = 0+$. Take the holdups to be fixed at 50 moles per stage ($j = 1, 2, \ldots, 13$).
2	C_2H_6	8.00	10.0	
3	C_3H_6	4.80	6.0	
4	C_3H_8	10.00	12.5	
5	n-C_4H_{10}	12.00	15.0	
6	i-C_4H_{10}	2.80	3.5	
7	n-C_5H_{12}	12.16	15.2	
8	n-C_6H_{14}	9.04	11.3	
9	n-C_7H_{16}	7.20	9.0	
10	n-C_8H_{18}	6.80	8.5	
11	Heavy fraction†	20.80	7.0	

Initial steady state solution				
Stage	Temp., °F	Vapor rates, mol min	Component	d_i^0
1	104.89	31.60	1	6.4000
2	147.29	94.80	2	8.0000
3	166.95	96.79	3	4.7951
4	181.53	95.45	4	9.9727
5	210.17	88.68	5	1.0383
6	237.51	195.88	6	1.3920
7	249.87	229.99	7	1.6958×10^{-1}
8	257.64	244.07	8	9.1141×10^{-6}
9	264.47	249.99	9	6.7911×10^{-8}
10	273.49	249.90	10	5.2789×10^{-10}
11	289.78	242.29	11	2.4488×10^{-12}
12	326.16	219.73		
13	429.36	161.64		

† This component is a 400°F normal boiling fraction.

Table 4-9 Transient Conditions for Example 4-4

Events			Transient values of variables					
			Distillate rates, mol/min					
Time period	Length of time period	Cumulative time min	d_1	d_2	d_3	d_4	d_5	d_6
1	0.1	0.1	6.2477	8.0369	4.8255	10.0366	1.0477	1.4037
2	0.1	0.2	5.5975	8.1930	4.9548	10.3088	1.0884	1.4539
3	0.1	0.3	4.4396	8.4677	5.1853	10.7967	1.1630	1.5454
5	0.1	0.5	2.5707	8.8850	5.5546	11.5910	1.2937	1.7027
10	0.1	1.0	2.0040	9.0033	5.6340	11.8076	1.3676	1.7809
20	0.1	2.0	2.0003	9.4717	5.4798	11.4870	1.3859	1.7723
30	0.2	4.0	1.9995	9.8946	5.4456	11.2244	1.3539	1.6784
40	0.4	8.0	1.9993	9.9386	5.6022	11.3567	1.2212	1.4777
50	0.8	16.0	1.9996	9.9571	5.7493	11.6732	0.9968	1.2202
60	1.6	32.0	1.9998	9.9790	5.8593	11.9944	0.7736	0.9909
70	3.2	64.0	1.9999	9.9930	5.9328	12.2219	0.6184	0.8316
80	6.4	128.0	2.0000	9.9989	5.9658	12.3255	0.5506	0.7572
90	12.8	256.0	2.0000	9.9998	5.9720	12.3453	0.5381	0.7427
94	25.6	358.4	2.0000	9.9999	5.9722	12.3458	0.5378	0.7423

Events			Transient values of variables			
			Distillate rates, mol/min			
Time period	Length of time period	Cumulative time min	d_7	d_8	d_9	d_{10}
1	0.1	0.1	0.001 91	$9.247\,4 \times 10^{-6}$	6.9126×10^{-8}	5.3908×10^{-10}
2	0.1	0.2	0.002 02	$9.831\,5 \times 10^{-5}$	7.4493×10^{-8}	5.8884×10^{-10}
3	0.1	0.3	0.002 20	0.000 011	8.4879×10^{-8}	6.8647×10^{-10}
5	0.1	0.5	0.002 54	0.000 013	1.0522×10^{-7}	8.8382×10^{-10}
10	0.1	1.0	0.002 80	0.000 015	1.2289×10^{-7}	1.0599×10^{-9}
20	0.1	2.0	0.003 14	0.000 018	1.5077×10^{-7}	1.3324×10^{-9}
30	0.2	4.0	0.003 94	0.000 024	2.1082×10^{-7}	1.8854×10^{-9}
40	0.4	8.0	0.004 50	0.000 026	2.1948×10^{-7}	1.8906×10^{-9}
50	0.8	16.0	0.003	0.000 020	1.6021×10^{-7}	1.3011×10^{-9}
60	1.6	32.0	0.002 95	0.000 015	1.0838×10^{-7}	8.2627×10^{-10}
70	3.2	64.0	0.002 33	0.000 011	7.7910×10^{-8}	5.6329×10^{-10}
80	6.4	128.0	0.002 07	$9.705\,0 \times 10^{-6}$	6.5855×10^{-8}	4.6352×10^{-10}
90	12.8	256.0	0.002 02	$9.438\,1 \times 10^{-6}$	6.3702×10^{-8}	4.4599×10^{-10}
94	25.6	358.4	0.002 02	$9.431\,5 \times 10^{-6}$	6.3469×10^{-8}	4.4556×10^{-10}

Table 4-9 Transient Conditions for Example 4-4—*Continued*

Events		Transient values of variables				
		Temp., °F		Vapor rates, mol/min		
Time period	Condenser	Plate 5, feed	Plate 13, reboiler	Plate 5, feed	Plate 6	Plate 13, reboiler
1	105.48	214.49	426.92	101.48	158.61	128.63
2	108.00	217.74	422.31	104.59	144.52	116.09
3	112.40	218.11	417.06	93.03	131.40	106.95
5	119.42	218.21	406.82	84.58	122.12	104.12
10	121.89	218.31	388.93	83.42	120.39	110.99
20	120.95	217.88	368.45	83.82	119.95	120.00
30	119.32	216.93	358.82	83.97	119.38	126.58
40	117.25	215.55	363.73	83.44	118.07	126.44
50	114.15	213.64	366.45	82.46	116.06	125.68
60	111.05	211.11	366.80	81.38	113.75	124.71
70	108.81	208.96	366.68	80.56	111.83	123.85
80	107.73	207.73	366.59	80.19	110.86	123.41
90	107.58	207.48	366.58	80.11	110.67	123.33
94	107.58	207.48	366.57	80.11	110.66	123.33

Comparison of Calculated and Experimental Results

Waggoner(16) used experimental results obtained by Huckaba et al.(7,8) and by Armstrong and Wilkinson(1) for some relatively simple systems at unsteady state operation for comparison with the results obtained by the proposed calculational procedure. Although the systems for which experimental data existed had binary feed mixtures, Waggoner did not take advantage of the mathematical property ($x_2 = 1 - x_1$) of such systems but treated them in the same manner required for multicomponent systems. For all examples considered, the agreement between the calculated and experimental results was good. Of the comparisons made by Waggoner(16), the results are presented for only one experiment, run 1 of Huckaba(7). A description of the experimental conditions employed by Huckaba and the basis of comparison of the calculated and experimental results follows.

Huckaba's work was based on the separation of a binary mixture of methanol and tertiary butanol. These alcohols were chosen because, although their molecular weights are very different, their densities were nearly identical to each other. Constant mass holdup was descriptive of this operation. The equipment used by Huckaba et al.(7,8) consisted of a column with 12 bubble-cap plates. A total condenser and a reboiler were used, and the column was vented to the atmosphere.

A plot of composition versus time was presented for selected trays and for several runs (Refs. 7 and 8). In addition, the feed description and the reflux ratio were given for all runs. Vaporization efficiences were calculated from specified

modified Murphree efficiencies. The numerical values of efficiencies used by Huckaba for the pure components were taken as the modified Murphree efficiencies. These efficiencies led to steady state solutions which were consistent with those presented graphically (Refs. 7 and 8).

Run 1 by Huckaba et al.(7) is simulated by Example 4-5, Table 4-10. A

Table 4-10 Statement of Example 4-5 (Ref. 7)

Initial conditions: steady state operation

Specifications			Steady state solution		
Feed		Other conditions	Plate	Temp., °F	Vapor flow, mol/min
Methanol concentration		$D = 23.91$ mol/min, $L_1 = 56.602$ mol/min, $F = 29.778$ mol/min.†	1	151.19	23.91
			2	155.53	80.51
Weight fraction	Mole fraction	Liquid feed below its bubble-point, total condenser, atmospheric column pressure, 7 rectifying stages (including the condenser), 7 stripping stages (including reboiler). Modified Murphree efficiencies:	3	157.14	79.95
			4	158.95	79.17
			5	160.58	78.42
0.571	0.7548		6	161.97	77.74
			7	164.88	77.15
Temperature = 82.0°F			8	167.62	80.20
			9	170.17	79.21
			10	172.40	78.28
		Methanol *t*-butanol	11	174.29	77.46
		0.389 0.845	12	175.84	76.76
		$2 \le j \le 13$	13	177.08	76.18
		1.0 1.0	14	176.73	75.71
		$j = 1, j = 14$			
		K data and enthalpy data are given in Table 4A-3			

First upset for Example 4-5 at $t = 0+$

Feed		Other conditions	Plate	Methanol concentration: Weight fraction	Methanol concentration: Mole fraction
Methanol concentration		$D = 23.91$ mols/min, $L_1 = 56.602$ mol/min, $F = 27.988$ mol/min			
Weight fraction	Mole fraction	Holdup: Condenser = 32 400 lb			
		Reboiler = 56 400 lb	1	0.821	0.914
0.491	0.6906	Each plate = 1 200 lb	5	0.462	0.665
		All other conditions are	9	0.248	0.433
Temperature = 82.0°F		the same as those specified	13	0.088	0.182
		for the initial steady state solution	14	0.049	0.106

† Note, all rates and holdups are, of course, relative to the feed rate stated.

Table 4-10 Statement of Example 4-5 (Ref. 7)—*Continued*

Second upset for Example 4-5

Feed		Other conditions
Methanol concentration		$D = 23.027$ mol/min, $L_1 = 54.512$ mol/min, $F = 27.988$ mol/min
Weight fraction	Mole fraction	Holdup: Condenser = 32 400 lb
		Reboiler = 56 400 lb
0.491	0.6906	Each plate = 1 200 lb
Temperature = 82°F		All other conditions are the same as those specified for the initial steady state solution.
Time of upset 2		
After 39th Δt	Time after first upset = 38 min	

comparison of the calculated results for this example with the calculated results of Huckaba et al.(7) is presented graphically in Fig. 4-9.

In order to utilize the modified Murphree efficiencies given by Huckaba, a new efficiency, called the vaporization efficiency, E_{ji}, is defined which makes it possible to apply all of the equations for perfect plates by replacing K_{ji} wherever it appears by $E_{ji}K_{ji}$. The modified Murphree efficiency is defined by

$$E_{ji}^{M} = \frac{y_{j+1,i} - y_{ji}}{K_{ji}x_{ji} - y_{ji}} \tag{4-49}$$

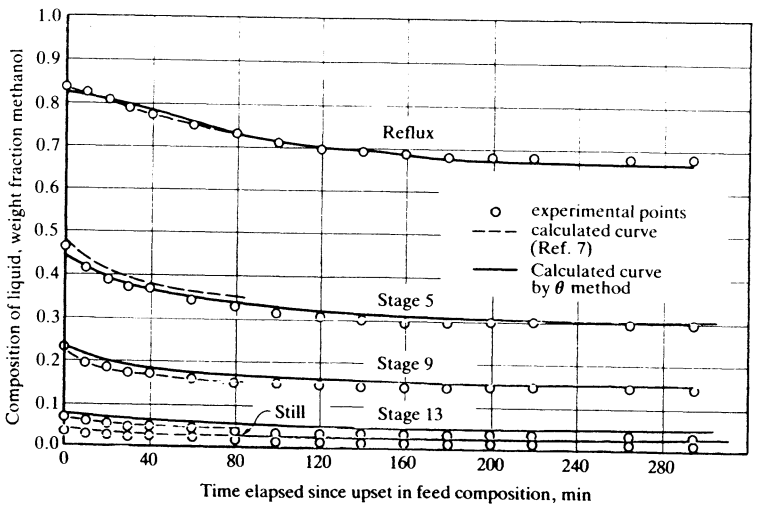

Figure 4-9 Calculated and experimental results for Example 4-5.

where the sum of the $K_{ji}x_{ji}$'s is not necessarily equal to unity. The vaporization efficiency is defined by

$$y_{ji} = E_{ji}K_{ji}x_{ji} \tag{4-50}$$

If values of E_{ji}^M are known as in the case of Example 4-5, the corresponding values of E_{ji} at the end of any trial are found by use of the following formula which is readily obtained by eliminating $K_{ji}x_{ji}$ from Eqs. (4-49) and (4-50) and rearranging to give

$$E_{ji} = E_{ji}^M + (1 - E_{ji}^M)\frac{y_{j+1,i}}{K_{ji}x_{ji}} \tag{4-51}$$

Modified Theta Method of Convergence

In the interest of increasing the speed of performing the calculations for each time period, a method of convergence involving only two θ's for the case of a conventional column was investigated and found to give satisfactory results for all problems considered. In this method, θ_j is set equal to θ_1 for all $j \geq 2$. Thus, for the case where the molar holdups and the rates D and L_1 are specified for a conventional column with a partial condenser, Eq. (4-25) becomes

$$\frac{b_i}{d_i} = \theta_0\left(\frac{b_i}{d_i}\right)_{ca}$$

$$\frac{u_{ji}}{d_i} = \theta_1\left(\frac{u_{ji}}{d_i}\right)_{ca} \qquad (j = 1, 2, \ldots, N-1) \tag{4-52}$$

For a column having a total condenser, θ_1 no longer exists and it is replaced in Eq. (4-52) by some other θ, say $\theta_2 = \theta_j$ $(j = 2, 3, \ldots, N-1)$. The set of θ's greater than zero that satisfies the specifications

$$D, \sum_{j=1}^{N-1} U_j$$

simultaneously is the set that makes $g_0 = g = 0$, where

$$g_0(\theta_0, \theta_1) = \sum_{i=1}^{c} d_i - D$$

$$g(\theta_0, \theta_1) = \sum_{j=1}^{N-1}\sum_{i=1}^{c} u_{ji} - \sum_{j=1}^{N-1} U_j \tag{4-53}$$

(Note that the function g is merely the sum of the g_j's for the holdups given by Eq. (4-31); that is, $g = \sum_{j=1}^{N-1} g_j$.) The formula for d_i as given by Eq. (4-30) reduces to

$$d_i = \frac{FX_i + \sigma[FX_i - d_i - b_i]^0 + \left(\frac{1}{\phi\,\Delta t}\right)\sum_{j=1}^{N} u_{ji}^0}{1 + \theta_0\left(\frac{b_i}{d_i}\right)_{ca}\left(1 + \frac{U_N/B}{\phi\,\Delta t}\right) + \frac{\theta_1}{\phi\,\Delta t}\sum_{j=1}^{N-1}\left(\frac{u_{ji}}{d_i}\right)_{ca}} \tag{4-54}$$

The modified θ method is seen to apply the same correction for each plate. For any one Δt, the number of trials required to obtain convergence by use of the modified θ method was about the same as that required when all of the θ's were employed. The modified θ method was tested with several examples in which very large upsets were involved. The solutions obtained by use of the modified θ method agreed closely with those found by use of the θ method (Refs. 16, 17).

From the solution of problems involving complex columns, it is known that many of these problems will not converge at steady state unless the θ associated with each sidestream is used in the convergence method (Ref. 6). Also, any scheme used to improve the speed of the unsteady state method must reduce to the θ method for steady state operation as the steady state solution is approached. Thus, the following set of θ's should be determined in the modified θ method for complex columns: θ_0, one θ corresponding to each sidestream (vapor or liquid), and one θ corresponding to the sum of the holdups for all those plates without liquid withdrawals. The modified θ method for complex columns at unsteady state operation also gave satisfactory results for all problems considered.

An Exact Solution Given by the Theta Method

Consider a distillation column at unsteady state operation. Suppose that each U_j as well as D and B are fixed at finite and positive values. A total-material balance enclosing the top of the column and any stage j $(j < f)$ over the time period from t_n to $t_n + \Delta t$ is given by

$$\int_{t_n}^{t_n+\Delta t}(V_{j+1} - L_j - D)\,dt = \sum_{k=1}^{j} U_k\Big|_{t_n+\Delta t} - \sum_{k=1}^{j} U_k\Big|_{t_n} \tag{4-55}$$

Application of the mean-value theorems followed by the limiting process wherein Δt is allowed to go to zero yields the following differential equation upon division of each member by V_{j+1}:

$$1 - \frac{L_j}{V_{j+1}} - \frac{D}{V_{j+1}} = \frac{1}{V_{j+1}}\sum_{k=1}^{j}\frac{dU_k}{dt} \tag{4-56}$$

Now suppose that the column is operated in such a manner that dU_j/dt is finite for all j and t. Thus, after the limit of each term of Eq. (4-56), has been taken as V_{j+1} approaches infinity, one obtains

$$\lim_{V_{j+1}\to\infty}\left(\frac{L_j}{V_{j+1}}\right) = 1 \tag{4-57}$$

Since the limit of F/V_{j+1} as V_{j+1} approaches infinity is equal to zero, the restriction that $j < f$ may be removed, and thus Eq. (4-57) holds for all stages, that is,

$$\frac{L_1}{V_2} = \frac{L_2}{V_3} = \cdots = \frac{L_{N-1}}{V_N} = 1 \tag{4-58}$$

Next consider the component-material balance for any stage j ($j < f$)

$$\int_{t_n}^{t_n+\Delta t} (V_{j+1}\, y_{j+1,\,i} - L_j x_{ji} - DX_{Di})\, dt = \sum_{k=1}^{j} U_k x_{ki}\Big|_{t_n+\Delta t} - \sum_{k=1}^{j} U_k x_k\Big|_{t_n} \tag{4-59}$$

Application of the mean-value theorems followed by the limiting process wherein Δt is allowed to go to zero yields the following differential equation upon division of each member by V_{j+1}:

$$y_{j+1,\,i} - \left(\frac{L_j}{V_{j+1}}\right) x_{ji} - \left(\frac{D}{V_{j+1}}\right) X_{Di} = \frac{1}{V_{j+1}} \sum_{k=1}^{j} \frac{du_{ki}}{dt} \tag{4-60}$$

Now suppose that the column is operated in a manner such that du_{ji}/dt is finite for all j and t. Thus, after the limit of each side of Eq. (4-60) has been taken as V_{j+1} approaches infinity, one obtains the result

$$y_{j+1,\,i} = x_{ji} \tag{4-61}$$

since D and each U_j are finite as well as x_{ji} and X_{Di}. Also, the limit of L_j/V_{j+1} as V_{j+1} approaches infinity is equal to unity (Eq. (4-57)). Equation (4-61) also holds for all stages $j \geq f$ since the limit of FX_i/V_{j+1} as V_{j+1} approaches infinity is equal to zero.

A column having the operating conditions characterized by Eqs. (4-57) and (4-61) is said to be at total reflux because it is described by the same set of equations as an actual column in operation at total reflux with $F = D = B = 0$.

The following set of equations is obtained by commencing at the top of the column and solving simultaneously the equilibrium relationships $y_{ji} = K_{ji} x_{ji}$ and the component material balances $y_{j+1,\,i} = x_{ji}$. For a column having a partial condenser, $y_{1i} = X_{Di}$, one obtains

$$\begin{aligned}
x_{1i} &= \frac{y_{1i}}{K_{1i}} = \frac{X_{Di}}{K_{1i}} \\
x_{2i} &= \frac{X_{Di}}{K_1 K_{2i}} \\
&\vdots \quad \vdots \quad \vdots \\
x_{N-1,\,i} &= \frac{X_{Di}}{K_{1i} K_{2i} \cdots K_{N-1,\,i}} \\
x_{Ni} = x_{Bi} &= \frac{X_{Di}}{K_{1i} K_{2i} \cdots K_{N-1,\,i} K_{Ni}}
\end{aligned} \tag{4-62}$$

When each member of Eq. (4-62) is divided by the corresponding member of the equation for the base component b and the resulting equation for each stage j is multiplied by U_j/D, one obtains

$$\begin{aligned}
\frac{u_{1i}}{d_i} &= \frac{1}{\alpha_i}\left(\frac{u_{1b}}{d_b}\right) \\
\frac{u_{2i}}{d_i} &= \frac{1}{\alpha_i^2}\left(\frac{u_{2b}}{d_b}\right) \\
&\vdots \quad \vdots \quad \vdots \\
\frac{u_{N-1,\,i}}{d_i} &= \frac{1}{\alpha_i^{N-1}}\left(\frac{u_{N-1,\,b}}{d_b}\right) \\
\frac{u_{Ni}}{d_i} &= \frac{1}{\alpha_i^{N}}\left(\frac{u_{Nb}}{d_b}\right)
\end{aligned} \tag{4-63}$$

where $\alpha_i = K_{ji}/K_{jb}$ for all i and j.

Since $x_{Ni} = x_{Bi}$, the last expression of Eq. (4-63) may be restated in the following equivalent form:

$$\frac{b_i}{d_i} = \frac{1}{\alpha_i^N}\left(\frac{b_b}{d_b}\right) \tag{4-64}$$

For any two different choices of (u_{jb}/d_b), the expression for stage j of Eq. (4-63) can be stated in the form

$$\left(\frac{u_{ji}}{d_i}\right)_2 = \left[\frac{(u_{jb}/d_b)_2}{(u_{jb}/d_b)_1}\right]\left(\frac{u_{ji}}{d_i}\right)_1 \tag{4-65}$$

Since the ratio for the base component b which is enclosed by brackets depends upon stage j alone, it follows that

$$\left(\frac{u_{ji}}{d_i}\right)_2 = \theta_j \left(\frac{u_{ji}}{d_i}\right)_1 \qquad (j = 1, 2, \ldots, N-1) \tag{4-66}$$

For the Nth stage, a similar analysis of Eq. (4-64) yields

$$\left(\frac{b_i}{d_i}\right)_2 = \frac{(b_b/d_b)_2}{(b_b/d_b)_1}\left(\frac{b_i}{d_i}\right)_1 \tag{4-67}$$

or

$$\left(\frac{b_i}{d_i}\right)_2 = \theta_0 \left(\frac{b_i}{d_i}\right)_1 \tag{4-68}$$

Thus, the θ multipliers defined by Eq. (4-25) are seen to be exact relationships for a column at total reflux.

4-3 APPLICATION OF THE COMBINATION OF THE TWO-POINT IMPLICIT METHOD AND THE 2N NEWTON–RAPHSON METHOD

The solution of the equations for any one time step are carried out in a manner analogous to that demonstrated by Holland(6) for steady state problems. The independent variables are taken to be the N stage temperature $\{T_j\}$ and the N flow ratios $\{L_j/V_j\}$. Corresponding to these $2N$ independent variables, N equilibrium functions and N energy balance functions are formulated.

The N equilibrium functions are formulated by first restating Eqs. (4-4) and (4-5) in the following form:

$$0 = \frac{\sum_{i=1}^{c} l_{ji}}{L_j} - \frac{\sum_{i=1}^{c} v_{ji}}{V_j} \tag{4-69}$$

Elimination of the l_{ji}'s by use of Eq. (4-17) and restatement of the result so obtained in functional form yields the dewpoint form of the function

$$F_j = \frac{1}{V_j} \sum_{i=1}^{c} \left(\frac{1}{K_{ji}} - 1 \right) v_{ji} \qquad (j = 1, 2, \ldots, N) \tag{4-70}$$

For the case where a total condenser is used, the bubble-point form of the function is used, namely,

$$F_1 = \frac{1}{D} \sum_{i=1}^{c} (K_{1i} - 1) d_i \tag{4-71}$$

The enthalpy balance functions (for stages $j = 2, 3, \ldots, f-1, f+1, \ldots, N-1$) are obtained by a rearrangement of Eq. (4-46) followed by restatement in functional form, namely,

$$G_j = \frac{\sum_{i=1}^{c} \left[v_{j+1,i} \hat{H}_{j+1,i} + l_{j-1,i} \hat{h}_{j-1,i} + \sigma(v^0_{j+1,i} \hat{H}^0_{j+1,i} + l^0_{j-1,i} \hat{h}^0_{j-1,i}) + \dfrac{u^0_{ji} \hat{h}^0_{ji}}{\phi \, \Delta t} \right]}{\sum_{i=1}^{c} \left\{ v_{ji} \hat{H}_{ji} + l_{ji} \hat{h}_{ji} + \sigma[v^0_{ji} \hat{H}^0_{ji} + l^0_{ji} \hat{h}^0_{ji}] + \dfrac{u_{ji} \hat{h}_{ji}}{\phi \, \Delta t} \right\}} - 1$$

$$(j = 2, 3, \ldots, f-1, f+1, \ldots, N-1) \tag{4-72}$$

The G functions for stages $j = 1, f$, and N are developed in a manner analogous to that demonstrated above.

The functions F_j and G_j contain the dependent variables $\{v_{ji}\}$, $\{l_{ji}\}$, and $\{V_j\}$. For any choice of values of the independent variables $\{T_j\}$ and $\{L_j/V_j\}$, expressions are needed for computing the values of the dependent variables. The $\{v_{ji}\}$ are found by use of Eq. (4-21) and the corresponding l_{ji}'s are computed by use of the equilibrium relationship, $l_{ji} = A_{ji} v_{ji}$.

Next an equation for computing the $\{V_j\}$ for any set of assumed L_j/V_j's is developed. When the U_j's are assumed to remain constant, the total-material balances are of the following form when only one stage is enclosed by each

balance. For any stage j ($2 \le j \le N-1$, $j \ne f$, N), the total-material balance is given by

$$V_{j+1} + L_{j-1} - V_j - L_j = 0 \tag{4-73}$$

For any given set of L_j/V_j's it is desired to solve the total-material balances for the corresponding set of vapor rates $\{V_j\}$. In the restatement of the total-material balances, it is convenient to define the new variable θ_j as follows:

$$\frac{L_j}{V_j} = \theta_j \left(\frac{L_j}{V_j} \right)_a \qquad (j = 1, 2, \ldots, N) \tag{4-74}$$

where $(L_j/V_j)_a$ is any arbitrary value of L_j/V_j. Taking this assumed ratio equal to the most recently assumed value of L_j/V_j serves to normalize the θ_j's so that at convergence θ_j approaches unity for all j. Let Eq. (4-74) be restated as follows:

$$L_j = r_j V_j \tag{4-75}$$

where

$$r_j = \theta_j \left(\frac{L_j}{V_j} \right)_a$$

Equation (4-75) may be used to restate the total-material balances in terms of either the vapor or liquid rates. When the balances are restated in terms of vapor rates, Eq. (4-73) becomes

$$r_{j-1} V_{j-1} - (1 + r_j) V_j + V_{j+1} = 0 \tag{4-76}$$

The complete set of total-material balances may be represented by the matrix equation

$$\mathbf{RV} = -\mathscr{F} \tag{4-77}$$

$$\mathbf{R} = \begin{bmatrix} -(1+r_1) & 1 & 0 & 0 & \cdots & 0 \\ r_1 & -(1+r_2) & 1 & 0 & \cdots & 0 \\ \cdots & \cdots & \cdots & \cdots & \cdots & \cdots \\ 0 & \cdots & 0 & r_{N-2} & -(1+r_{N-1}) & 1 \\ 0 & \cdots & 0 & 0 & r_{N-1} & -(1+r_N) \end{bmatrix}$$

$$\mathbf{V} = [D \quad V_2 \quad V_3 \quad \cdots \quad V_N]^T$$

$$\mathscr{F} = [0 \quad \cdots \quad 0 \quad F \quad 0 \quad \cdots \quad 0]^T$$

When the $\{\theta_j\}$ and $\{T_j\}$ are taken to be the independent variables rather than the $\{L_j/V_j\}$ and $\{T_j\}$, the A_{ji}'s which appear in the component-material balances become

$$A_{ji} = \frac{\theta_j}{K_{ji}} \left(\frac{L_j}{V_j} \right)_a \tag{4-78}$$

For a conventional distillation column, the following sets of specifications are

commonly made. When Q_C and Q_R are specified, the independent variables are given by

$$\mathbf{x} = [\theta_1 \quad \theta_2 \quad \cdots \quad \theta_N \quad T_1 \quad T_2 \quad \cdots \quad T_N]^T \tag{4-79}$$

If the reflux ratio L_1/D and the boilup ratio V_N/B are specified, then the independent variables are given by

$$\mathbf{x} = [Q_C \quad \theta_2 \quad \theta_3 \quad \cdots \quad \theta_{N-1} \quad Q_R \quad T_1 \quad T_2 \quad \cdots \quad T_N]^T \tag{4-80}$$

Also, one may specify L_1/D and Q_R or Q_C and V_N/B instead of L_1/D and V_N/B. The solution value $\mathbf{x}$ may be found by use of the Newton–Raphson method

$$\mathbf{J}\,\Delta\mathbf{x} = -\mathbf{f} \tag{4-81}$$

where the jacobian matrix $\mathbf{J}$ has the following representation (where $\mathbf{x}$ is given by Eq. (4-79)):

$$\mathbf{J} = \begin{bmatrix} \dfrac{\partial F_1}{\partial \theta_1} & \cdots & \dfrac{\partial F_1}{\partial T_N} \\ \vdots & & \vdots \\ \dfrac{\partial G_N}{\partial \theta_1} & \cdots & \dfrac{\partial G_N}{\partial T_N} \end{bmatrix}$$

$$\Delta\mathbf{x} = [\Delta\theta_1 \quad \Delta\theta_2 \quad \cdots \quad \Delta\theta_N \quad \Delta T_1 \quad \Delta T_2 \quad \cdots \quad \Delta T_N]^T$$

$$\mathbf{f} = [F_1 \quad F_2 \quad \cdots \quad F_N \quad G_1 \quad G_2 \quad \cdots \quad G_N]^T$$

The $2N$ Newton–Raphson equations may be solved by use of any one of the three procedures recently described by Holland(6) for distillation columns at steady state operation. Of the following three procedures only Broyden's method is described briefly.

Procedure 1 Use of analytical expressions for evaluating the partial derivatives of the F_j's and G_j's.

Procedure 2 Broyden's method(4).

Procedure 3 Broyden–Bennett algorithm (Refs. 2, 4).

Broyden's method is applied as outlined in the six steps below Eq. (2-48), except for the fact that for a change in any one of the independent θ_j's the two sets of constraining equations (the component-material balances, Eq. (4-21) and the total-material balances, Eq. (4-73)) must be solved. However, for a change in any of the T_j's it is necessary to solve only the component-material balances because the total-material balances are independent of the temperatures $\{T_j\}$. Also each trial is initiated by taking the assumed values $\{(L_j/V_j)_a\}$ and $\{T_j\}$ equal to the most recently calculated sets of values for these variables, and the assumed θ_j's are taken to be $\theta_1 = \theta_2 = \cdots = \theta_N = 1$. These choices for the $(L_j/V_j)_a$'s and the θ's have the effect of normalizing the θ_j's.

In summary, the equations for the model of a continuous distillation column at unsteady state considered in this chapter consists of the component-

material balances, total-material balances, energy balance and equilibrium relationships. After the integral-difference equations have been reduced to algebraic form by use of the two-point implicit method, they must be solved for the values of the variables at the end of the time step. Two of the possible methods for solving these equations are the θ method and the $2N$ Newton–Raphson method. When the holdups are allowed to vary, as in Chap. 8, the θ method is no longer recommended. Instead, other methods such as Gear's and the semi-implicit Runge–Kutta methods are recommended. These methods are demonstrated in subsequent chapters. Also, a combination of the two-point implicit method and the Newton–Raphson method could be used. It is, however, generally slower than the more powerful multipoint methods mentioned above.

In order to compare the θ method, the modified θ method, and the $2N$ Newton–Raphson method, Examples 4-2 and 4-4 were solved by each of these methods. The results so obtained are presented in Table 4-11. Broyden's method was used in the θ method in the solution of the g functions for the θ's and in the $2N$ Newton–Raphson method. Two procedures were used. In the first

Table 4-11 Comparison of the theta method, the modified theta method, and the $2N$ Newton–Raphson method for Examples 4-2 and 4-4 (Ref. 10)

Example	Method	No. of time steps	Computer time (AMDAHL 470/V6 computer)	Convergence criteria	Compiler
4-2	θ method	94	(1) 4.98‡ (2) 3.50†	Cease if $\lvert 1-\theta_j\rvert \le 10^{-4}$ or $\lvert \Delta T_j\rvert/T_j \le 10^{-5}$ after the 10th trial of a time step	FORTRAN H EXTENDED
4-2	Modified θ method	94	(1) 3.47 (2) 3.04	Same as above	FORTRAN H EXTENDED
4-2	$2N$ Newton–Raphson method	94	(1) 13.03 (2) 3.83	$\phi \le 10^{-4}$ where $\phi = \frac{1}{2N}\left(\sum_{j=1}^{N}(F_j^2 + G_j^2)\right)^{1/2}$	FORTRAN H EXTENDED
4-4	θ method	94	(1) 47.79 (2) 16.09	Same as θ method for Example 4-2	FORTRAN H EXTENDED
4-4	Modified θ method	94	(1) 19.91 (2) 19.12	Same as modified θ method for Example 4-2	FORTRAN H EXTENDED
4-4	$2N$ Newton–Raphson method	94	(1) 107.32 (2) 18.28	Same as $2N$ Newton–Raphson method for Example 4-2	FORTRAN H EXTENDED

† In order to apply the $2N$ Newton–Raphson method as formulated in the text, use the values of Q_C and Q_R, or L_1/D and Q_R found by use of the θ method.

‡ The entry given by (1) represents the time required when the jacobian evaluated once each time step, and the entry given by (2) represents the time required when the jacobian is evaluated only once for each problem provided that Broyden's inequality criterion is satisfied.

(denoted by (1) in Table 4-11), the jacobians were evaluated once per time step; whereas, in the second procedure (denoted by (2) in Table 4-11), the jacobian was evaluated only once per problem provided that the inequality criterion of Broyden's method was satisfied. The values of the elements of the jacobian at the beginning of a given time step were taken to be the values which they had at the end of the previous time step as proposed by Mijares(10).

NOTATION

A_{ji} = absorption factor for component i and plate j
b_i = flow rate of component i in the bottoms, mol/time
B = total flow rate of the bottoms, mol/time
c = total number of components
d_i = flow rate of component i in the distillate, mol/time
D = total flow rate of the distillate, mol/time
$f(T_j)$ = bubble-point function for plate j (T_j is equal to the bubble-point temperature of the liquid leaving plate j, $f(T_j) = 0$)
$\mathbf{f}$ = a column vector of functions
f_k = a quantity that appears in the recursion formulas used to solve the component-material balances
F = total flow rate of the feed
$F(T_j)$ = dewpoint function for plate j (when T_j is equal to the dewpoint temperature of the vapor leaving plate j, $F(T_j) = 0$)
$g_j(\theta_0, \ldots, \theta_{N-1})$ = the jth function of $\theta_0, \theta_1, \ldots, \theta_{N-1}$
g_k = a quantity that appears in the recursion formulas used to solve the component-material balances
$\hat{h}_{ji}, \hat{H}_{ji}$ = enthalpies (Btu/mol) of component i in the liquid and vapor states, respectively, at the temperature of plate j—in the examples solved, ideal solution values were used, that is, $\hat{h}_{ji} = h_{ji}$, $\hat{H}_{ji} = H_{ji}$
$\mathbf{J}$ = jacobian matrix
H = total enthalpy of the feed, regardless of state
H_D = total enthalpy of the distillate, regardless of state
$\hat{H}_{Di}$ = virtual value of the partial molar enthalpy of component i in the distillate (for a partial condenser $\hat{H}_{Di} = \hat{H}_{1i}$ and for a total condenser $\hat{H}_{Di} = \hat{h}_{1i}$)
K_{ji} = equilibrium constant for component i at the temperature and pressure of the liquid leaving plate j (these functions are expressed as polynomials in temperature)

K_{jb} = equilibrium constant for the base component evaluated at the temperature of the liquid leaving plate j (in the K_b method a hypothetical component with a K value given by Eq. (4-41) is selected as the base component)
l_{ji} = flow rate at which component i in the liquid phase leaves plate j, moles per unit time
L_j = total flow rate at which liquid leaves plate j, moles per unit time
m_{ji} = liquid holdup (mass or volume) of component i on plate j.
M_i = molecular weight of component i (also used to denote the volume per mole for component i in the liquid phase on each plate)
$\mathscr{M}_j$ = total liquid holdup on plate j in mass or volumetric units
N = total number of stages including the condenser-accumulator section and the reboiler
Q_C = net energy removed by the condenser per unit time
Q_R = net energy transferred to the system by the reboiler per unit time
t = time in consistent units (t_n is used to denote the time at which the time increment $n + 1$ begins, and $t_n + \Delta t$ the time at which time increment $n + 1$ ends)
u_{ji}^V, u_{ji}^L = vapor and liquid holdups in moles of component i on plate j, respectively
U_j^V, U_j^L = total holdups of vapor and liquid, respectively, on plate j, moles
v_{ji} = flow rate at which component i in the vapor phase leaves plate j, moles/time
V_j = total flow rate at which vapor leaves plate j, moles/time
x_{ji} = mole fraction of component i in the liquid leaving plate j
$\mathbf{x}$ = a column vector of variables
X_i = total mole fraction of component i in the feed (regardless of state)
X_{Di} = total mole fraction of component i in the distillate (regardless of state)
y_{ji} = mole fraction of component i in the vapor phase leaving plate j

Greek letters

α_{ji} = relative volatility of component i at the temperature of plate j ($\alpha_{ji} = K_{ji}/K_{jb}$)

$\gamma_{ji}^{L}, \gamma_{ji}^{V}$ = activity coefficients for component i in the liquid and vapor phases on plate j

θ_0 = a multiplier associated with the distillate and bottoms

θ_j = a multiplier associated with stage j

ϕ = a weight factor used in that evaluation of an integral in terms of the values of a function at times t_n and $t_n + \Delta t$

σ = a constant appearing in the component-material balances and in the enthalpy balances ($\sigma = (1 - \phi)/\phi$)

τ_j = dimensionless time factor for plate j ($\tau_j = (U_j/L_j)/(\phi\ \Delta t)$)

Ω_j = enthalpy departure function (defined below Eq. (4-3); see also App. 4A-2)

Subscripts

ca = calculated value

i = component number ($i = 1$ through $i = c$)

j = plate number; for condenser-accumulator section $j = 1$, for the top plate $j = 2$, for the feed plate $j = f$, for the bottom plate $j = N - 1$, and for the reboiler $j = N$

k = an integer used for counting

n = trial number

Superscripts

0 = value of a variable at the beginning of the time increment under consideration (the absence of a superscript, say v_{ji}, means either the instantaneous value of the variable or the value of the variable at the end of the time period under consideration (time $t_n + \Delta t$)—see context)

L = the liquid phase

V = the vapor phase

Mathematical symbols

$\{x_i\}$ = set of all values of the variables under consideration

REFERENCES

1. W. D. Armstrong and W. L. Wilkinson: "An Investigation of the Transient Response of a Distillation Column, Part II: Experimental Work and Comparison with Theory," *Trans. Inst. Chem. Eng.*, **35**:352 (1957).
2. J. M. Bennett: "Triangular Factors of Modified Matrices," *Numerische Mathematik*, **7**:217 (1965).
3. J. F. Boston and S. L. Sullivan, Jr.: "An Improved Algorithm for Solving Mass Balance Equations in Multistage Separation Processes," *Can. J. Chem. Eng.* **50**:663 (1972).
4. C. G. Broyden: "A Class of Methods for Solving Nonlinear Simultaneous Equations," *Math. Comp.* **19**:557 (1965).
5. E. M. Grabbe, S. Ramo, and D. E. Wooldridge: *Handbook of Automation, Computation, and Control*, vol. 1, chap. 14, p. 34, John Wiley and Sons, New York, 1958.
6. C. D. Holland: *Fundamentals of Multicomponent Distillation*, McGraw-Hill Book Company, New York, 1981.
7. C. E. Huckaba, F. R. Franke, and F. P. May: "An Analysis of Transient Conditions in Continuous Distillation Operations," 55th Annual Meeting AIChE., Chicago, Dec. 20, 1962.
8. C. E. Huckaba: "An Analysis of Transient Conditions in Continuous Distillation Operations," *Chem. Eng. Prog. Symp. Ser.*, **59**(46):38 (1963).
9. Leon Lapidus: *Digital Computation for Chemical Engineers*, McGraw-Hill Book Company, New York, 1962.
10. Mijares, Gerardo: M.S. thesis, Texas A&M University, 1982.
11. W. R. Marshall, Jr., and R. L. Pigford: *The Application of Differential Equations to Chemical Engineering Problems*, p. 146, Newark, Del.: University of Delaware, 1947.
12. R. L. Pigford, J. B. Tepe, and C. J. Garrahan: "Effect of Column Holdup in Batch Distillation," *Ind. Eng. Chem.*, **43**:2592 (1951).
13. A. Rose, C. L. Johnson, and T. J. Williams: "Transient and Equilibrium Time in Continuous Distillation," *Ind. Eng. Chem.*, **48**(7):1173 (1956).
14. H. H. Rosenbrock: "An Investigation of the Transient Response of a Distillation Column, Part I: Solution of the Equations," *Trans. Inst. Chem. Eng.*, **35**:347 (1957).
15. I. S. Sokolnikoff and E. S. Sokolnikoff: *Higher Mathematics for Engineers and Physicists*, p. 163, 2d ed., McGraw-Hill Book Company, 1941.
16. R. C. Waggoner: *Solution of Unsteady State Distillation Problems*, Ph.D. dissertation, Texas A&M University, College Station, Texas, 1964.
17. R. C. Waggoner and C. D. Holland: "Solution of Problems Involving Conventional and Complex Columns at Unsteady State Operation," *AIChE J.*, **11**:112 (1965).
18. D. Yesberg and A. I. Johnson: "Machine Computations for Transient Stagewise Processes," *Can. J. Chem. Eng.*, **38**:48 (1960).

PROBLEMS

4-1 Beginning with the component-material balances in the integral-difference form, show that the corresponding equations obtained by use of the implicit method are those given by Eq. (4-20).

4-2 By use of the implicit method and the relationships given by Eq. (4-25), show that the formula for the corrected distillate rate for any component i is given by Eq. (4-30).

4-3 Find the analytical expressions for the partial derivatives of the function g_0 given by Eq. (4-31) with respect to $\theta_0, \theta_1, \ldots, \theta_{N-1}$.

4-4 Show that Eqs. (4-39) and (4-40) give the same value for K_{jb}. That is, given the expressions for x_{ji} and y_{ji} (Eqs. (4-27) and (4-28)), the relationship $l_{ji} = A_{ji} v_{ji}$, and the expression for K_{jb} (Eq. (4-39)), show that the expression for K_{jb} as given by Eq. (4-40) follows.

4-5 (*a*) Beginning with the following definition of the corrected value of v_{ji}.

$$v_{ji} = \sigma_j \left(\frac{v_{ji}}{d_i}\right)_{ca} d_i$$

show that the expression given by Eq. (4-28) for the corrected value of y_{ji} follows as a consequence.

(*b*) For the case where vapor holdups are specified for a column having a partial condenser, obtain a relationship between the σ_j's and θ_j^V's, where

$$\frac{u_{ji}^V}{d_i} = \theta_j^V \left(\frac{u_{ji}^V}{d_i}\right)_{ca}$$

4-6 Develop the enthalpy balance expressions given in Table 4-2.

4-7 Show that the recursion formulas presented in the text for solving simultaneous equations that are tridiagonal in form may be obtained by use of gaussian elimination.

Hint: Consider first a particular case, say Example 4-1. The component-material balances given in Example 4-1 have the following matrix representation:

$$\begin{bmatrix} b_1 & c_1 & 0 & 0 & 0 \\ a_2 & b_2 & c_2 & 0 & 0 \\ 0 & a_3 & b_3 & c_3 & 0 \\ 0 & 0 & a_4 & b_4 & c_4 \\ 0 & 0 & 0 & a_5 & b_5 \end{bmatrix} \begin{bmatrix} v_1 \\ v_2 \\ v_3 \\ v_4 \\ v_5 \end{bmatrix} = \begin{bmatrix} d_1 \\ d_2 \\ d_3 \\ d_4 \\ d_5 \end{bmatrix}$$

By use of the definitions of f_1, g_1, f_k, g_k, show that after the row operations corresponding to gaussian elimination have been performed, the following result is obtained:

$$\begin{bmatrix} 1 & f_1 & 0 & 0 & 0 \\ 0 & 1 & f_2 & 0 & 0 \\ 0 & 0 & 1 & f_3 & 0 \\ 0 & 0 & 0 & 1 & f_4 \\ 0 & 0 & 0 & 0 & 1 \end{bmatrix} \begin{bmatrix} v_1 \\ v_2 \\ v_3 \\ v_4 \\ v_5 \end{bmatrix} = \begin{bmatrix} g_1 \\ g_2 \\ g_3 \\ g_4 \\ g_5 \end{bmatrix}$$

Commencing with the last row (row 5), apply the multiplication rule.

4-8 Begin with the definition of x_{ji} given by Eq. (4-27) and the definition of a mole fraction $x_{ji} = u_{ji}/U_j$ and show that it is possible to obtain the defining equations for $\{\theta_j\}$, namely, Eqs. (4-25) and (4-31).

4-9 Beginning with the component-material and total-material balances

$$FX_i = v_{Fi} + l_{Fi}$$

$$F = V_F + L_F$$

and the dewpoint expression

$$0 = \sum_{i=1}^{c} \frac{y_{Fi}}{K_{Fi}} - 1$$

(*a*) show that the dewpoint expression can be restated in the form

$$0 = \frac{1}{V_F} \sum_{i=1}^{c} \frac{v_{Fi}}{K_{Fi}} - \sum_{i=1}^{c} \frac{v_{Fi}}{V_F}$$

and in the functional form

$$F(\theta) = \frac{1}{V_F} \sum_{i=1}^{c} \left(\frac{1}{K_{Fi}} - 1\right) v_{Fi}$$

where

$$V_F = \frac{F}{1+\theta} \qquad v_{Fi} = \frac{FX_i}{1 + \theta/K_{Fi}}$$

$$\theta = \frac{L_F}{V_F}$$

(*b*) In an isothermal flash calculation F, $\{X_i\}$, P, and T_F are specified and it is required to find θ, V_F, $\{v_{Fi}\}$, and $\{l_{Fi}\}$. Show how the above equations may be solved by use of Newton's method.

4-10 For the case where model 2 is used for the feed plate (instead of model 1), show how component-material balances, total-material balances, and enthalpy balances presented for model 1 must be modified in order to represent model 2.

4-11 (*a*) Initially a distillation column is at steady state operation at total reflux. From the information given below compute:

$$\{u_{ji}/d_i\},\ \{b_i/d_i\},\ \{u_{ji}\},\ \{d_i\},\ \{b_i\},\ \text{and } \{U_j\}.$$

Given:

Component	X_i	α_i	Other specifications
1	1/3	1	$F = 100$, $N = 3$, partial condenser, $U_3/B = 2$, $u_{1b}/d_b = 1$, $u_{2b}/d_b = 1$,
2	1/3	2	$b_b/d_b = 1$. Note that for a column at steady state operation at total
3	1/3	3	reflux, $u_{ji}/d_i = (u_{jb}/d_b)/\alpha_i^j$ and $b_i/d_i = (b_b/d_b)\alpha_i^{-N}$.
			Also $d_i = FX_i/(1 + b_i/d_i)$.

(*b*) At time $t = 0+$, the feed composition is changed to $X_1 = 1/2$, $X_2 = 1/3$, and $X_3 = 1/6$. If the column remains at total reflux, and if at the end of the first time step ($\Delta t = 0.4$), $u_{1b}/d_b = u_{2b}/d_b = 2$, $b_b/d_b = 4$, and $U_3/B = 2$, compute $\{u_{ji}/d_i\}$, $\{b_j/d_i\}$, $\{u_{ji}\}$, $\{d_i\}$, $\{b_i\}$, and $\{U_j\}$ at the end of the first time step. Take $\phi = 0.6$.

(*c*) Repeat part (*b*) for the case where $(u_{1b}/d_b) = (u_{2b}/d_b) = 4$, $b_b/d_b = 8$, and $U_3/B = 2$ at the end of the first time step.

(*d*) Beginning with the values of the $\{u_{ji}/d_i\}$, $\{b_i/d_i\}$ found at the end of the first time step in part (*b*), the initial conditions of part (*a*), the values of U_1, U_2, and D found in part (*c*), compute the values $(\theta_0, \theta_1, \theta_2)$ necessary to make $g_0 = g_1 = g_2 = 0$ simultaneously, where

$$g_0 = \sum_{i=1}^{c} d_i - D$$

$$g_1 = \sum_{i=1}^{c} u_{1i} - U_1$$

$$g_2 = \sum_{i=1}^{c} u_{2i} - U_2$$

4-12 For the special case of a conventional distillation column at steady state operation, Boston and Sullivan(3) developed an algorithm for computing the f_k's and g_k's at unsteady state operation, the algorithm is given by

$$f_1 = \frac{-1}{m_1} \qquad m_1 = 1 + A_{1i}(1 + \tau_1)$$

$$f_2 = \frac{-m_1}{m_2} \qquad m_2 = s_1 + A_{2i}(1 + \tau_2)m_1$$

$$s_1 = 1 + A_{1i}\tau_1$$

$$f_k = \frac{-m_{k-1}}{m_k} \qquad m_{k+1} = s_k + A_{k+1,i}(1 + \tau_{k+1})m_k$$

$$s_k = s_{k-1} + A_{k,i}\tau_k m_{k-1} \qquad \tau_j = \frac{U_j/L_j}{\phi\ \Delta t} \qquad (k = 2, 3, \ldots, N-1)$$

$$g_1 = \frac{f'_{1i}}{m_1}$$

$$g_2 = (f'_{2i} + A_{1i}g_1)\frac{m_1}{m_2}$$

$$g_k = (f'_{ki} + A_{k-1,i}g_{k-1,i})\frac{m_{k-1}}{m_k} \qquad (k = 2, 3, \ldots, N)$$

For the special case where $b_j = -(1 + A_{ji})$, $c_j = 1$, $a_j = A_{j-1,i}$, $d_j = -f_{ji}$, show that when these quantities are substituted successively into the formulas given by Eq. (4-23) for the f_k's and g_k's, the above expressions are obtained.

4-13 Use the recurrence formulas to obtain the component flow rates of Example 4-1.

4-14 If, prior to an upset, a column is at steady state operation, show that the unsteady state equations for the first time step reduce to the steady state equations at the conditions of the upset when Δt is allowed to increase without bound.

APPENDIX 4A-1 EQUILIBRIUM AND ENTHALPY DATA

Table 4A-1 Equilibrium data†

$P = 300$ lb/in² abs, $(K_i/T)^{1/3} = a_{1i} + a_{2i}T + a_{3i}T^2 + a_{4i}T^3$, ($T$ in °R).

Component	$a_1 \times 10^2$	$a_2 \times 10^5$	$a_3 \times 10^8$	$a_4 \times 10^{12}$
CH_4	32.718 139	−9.695 140 5	6.922 933 4	−47.361 298
C_2H_4	−5.177 995	62.124 576	−37.562 082	8.014 550 1
C_2H_6	−9.840 021 0	67.545 943	−37.459 290	−9.073 245 0
C_3H_6	−25.098 770	102.392 87	−75.221 710	153.847 09
C_3H_8	−14.512 474	53.638 924	−5.305 160 4	−173.583 29
i-C_4H_8	−10.104 481	21.400 418	38.564 266	−353.654 19
i-C_4	−18.967 651	61.239 667	−17.891 649	−90.855 512
n-C_4	−14.181 715	36.866 353	16.521 412	−248.238 43
i-C_5	−7.548 840 0	3.262 363 1	58.507 340	−414.923 23
n-C_5	−7.543 539 0	2.058 423 1	59.138 344	−413.124 09
n-C_6	1.150 691 9	−33.885 839	97.795 401	−542.359 41
n-C_7	5.569 275 8	−50.705 967	112.173 38	−574.893 50
n-C_8	7.171 440 0	−52.608 530	103.720 34	−496.465 51
400	2.527 896 0	−17.311 330	33.502 879	−126.250 39
500	3.312 329 1	−16.652 384	24.310 911	−64.148 982

† S. T. Hadden: "Vapor–Liquid Equilibria in Hydrocarbon Systems," *Chem. Eng. Prog.*, **44**: 37 (1948).

Table 4A-2 Enthalpy data†

$P = 300$ lb/in² abs; $(h_i)^{1/2} = c_{1i} + c_{2i}T + c_{3i}T^2$ (T in °R); $(H_i)^{1/2} = e_{1i} + e_{2i}T + e_{3i}T^2$ (T in °R)

Component	c_1	$c_2 \times 10$	$c_3 \times 10^5$	e_1	$e_2 \times 10^4$	$e_3 \times 10^6$
CH_4	−17.899 210	1.739 570 63	−3.759 611 4	44.445 874	501.045 59	7.320 721 9
C_2H_4	−7.291 500	1.541 196 2	−1.608 8376	56.796 38	615.931 54	2.408 873 0
C_2H_6	−8.485 700	1.628 663 6	−1.949 860 1	61.334 520	588.754 30	11.948 654
C_3H_6	−12.427 900	1.883 465 2	−2.483 9140	71.828 480	658.551 30	11.299 585
C_3H_8	−14.500 060	1.980 222 3	−2.904 883 7	81.795 910	389.819 19	36.470 900
i-C_4H_8	−16.553 450	2.161 865	−3.147 6209	139.174 44	−822.394 88	120.392 98
i-C_4	−16.553 405	2.161 865	−3.147 6209	147.654 14	−1185.294 2	152.877 78
n-C_4	−20.298 110	2.300 574 3	−3.866 341 7	152.667 98	−1153.484 2	146.641 25
i-C_5	−23.356 460	2.501 745 3	−4.391 789 7	130.966 79	−197.986 04	82.549 947
n-C_5	−24.371 540	2.563 620 0	−4.649 969 4	128.901 52	2.050 960 3	64.501 496
n-C_6	−23.870 410	2.676 808 9	−4.419 779 3	85.834 950	1522.391 7	−34.018 595
n-C_7	−25.314 530	2.824 638 9	−4.541 871 8	94.682 620	1479.538 7	−19.105 299
n-C_8	−22.235 050	2.847 842 9	−3.885 081 9	106.328 06	1328.394 9	1.623 073 7
400	−203.321 92	6.393 285 7	−21.611 909	72.328 160	1893.382 2	−59.003 304
500	1.920 530	3.017 923 2	−2.218 3809	138.496 58	1497.817 1	18.641 269

† J. B. Maxwell: *Data Book on Hydrocarbons*, D. Van Nostrand Company, Inc., New York (1955).

Table 4A-3 Equilibrium data† and enthalpy data‡

$$(h_i)^{1/2} = C_{1i} + C_{2i}T + C_{3i}T^2$$
$$(H_i)^{1/2} = e_{1i}$$

$$(K_i/T)^{1/3} = a_{1i} + a_{2i}T + a_{3i}T^2 + a_{4i}T^3 \ (T \text{ in } °\text{R})$$

Component	Pressure lb/in² abs	$a_1 \times 10^2$	$a_2 \times 10^4$	$a_3 \times 10^6$	$a_4 \times 10^{10}$
Benzene	14.7	−14.822 221	2.736 370 9	0.190 786 94	0.525 114 54
t-butanol	14.7	66.229 585	−34.357 736	5.474 829 0	−22.533 968
Carbontetrachloride	14.7	6.326 114 2	−6.778 488 1	1.628 156 8	−6.636 626 2
Methanol	14.7	34.514 954	−20.165 650	3.483 886 7	12.893 764

Component	Pressure lb/in² abs	C_1	$C_2 \times 10$	$C_3 \times 10^5$	e_1
t-Butanol	14.7	−236.641 81	6.429 884 0	−20.758 627	161.021 69
Methanol	14.7	−99.777 949	3.128 517 0	−10.098 542	134.435 70

† T. E. Jordan: *Vapor Pressure of Organic Compounds*, Interscience Publishers, Inc., New York (1954).

‡ C. E. Huckaba, F. R. Franke, and F. P. May: Presented at the 55th Annual Meeting of the American Institute of Chemical Engineers, Chicago, Ill., Dec. 2–6, 1962.

APPENDIX 4A-2 THE VIRTUAL VALUES OF THE PARTIAL MOLAR ENTHALPIES (Refs. 1, 2)

The virtual values of the partial molar enthalpies are defined as follows:

$$\hat{H}_i = \hat{H}_i^0 + \Omega \tag{1}$$

where $\hat{H}_i = \hat{H}_i(P, T, \{n_i\})$ = virtual value of the partial molar enthalpy of component i in a mixture at temperature T and pressure P

H_i^0 = enthalpy of one mole of component i in the perfect gas state at the temperature T and the pressure $P = 1$ atmosphere

$\Omega = H(P, T, \{n_i\}) - H^0(1, T, \{n_i\})$, the enthalpy of one mole of mixture at the temperature T and pressure P minus the enthalpy of one mole of the same mixture in the perfect gas state at T and at $P = 1$ atmosphere (Ω is called the enthalpy departure function)

$H^0 = \sum_{i=1}^{c} (n_i/n)H_i^0$

n_i = moles of component i (n = total number of moles)

Although the virtual values of the partial molar enthalpies are generally unequal to the partial molar enthalpies, they may be used to compute the correct enthalpy of the mixture, that is,

$$nH(P, T, \{n_i\}) = \sum_{i=1}^{c} n_i \bar{H}_i = \sum_{i-1}^{c} n_i \hat{H}_i \tag{2}$$

Much less computational effort is required to compute the enthalpy of a mixture when the virtual values of the partial molar enthalpies are used than is required when the partial molar enthalpies are used.

The equality given by Eq. (2) is readily established by beginning with the fact that the enthalpy of one mole of any mixture may be expressed in terms of H^0 and the departure function Ω as follows

$$H = H^0 + \Omega \tag{3}$$

Then the enthalpy of n moles ($n_1 + n_2 + \cdots + n_c = n$) of a mixture is given by

$$nH = nH^0 + n\Omega \tag{4}$$

Termwise differentiation of Eq. (4) with n_k at constant pressure and temperature, and with all of the n_i's held fixed except for n_k, yields

$$\bar{H}_k = \left(\frac{\partial(nH)}{\partial n_k}\right)_{P,\,T,\,n_{j\neq k}} = \frac{\partial}{\partial n_k}\left(\sum_{i=1}^{c} n_i H_i^0\right) + \left(\frac{\partial n}{\partial n_k}\right)\Omega + n\left(\frac{\partial \Omega}{\partial n_k}\right)_{P,\,T,\,n_{j\neq k}} \tag{5}$$

which reduces to

$$\bar{H}_k = H_k^0 + \Omega + n\left(\frac{\partial \Omega}{\partial n_k}\right)_{P,\,T,\,n_{j\neq k}} \tag{6}$$

Let the subscript k in the above equation be replaced by the subscript i. Multiplication of the resulting expression by n_i followed by the summation over all components yields

$$nH = \sum_{i=1}^{c} n_i \bar{H}_i = \sum_{i=1}^{c} n_i H_i^0 + n\Omega + n\sum_{i=1}^{c} n_i \left(\frac{\partial \Omega}{\partial n_i}\right)_{P,\,T,\,n_{j\neq i}} \tag{7}$$

Since Ω is a homogeneous function of degree zero in the n_i's, it follows from Euler's theorem (App. 1A) that

$$\sum_{i=1}^{c} n_i \left(\frac{\partial \Omega}{\partial n_i}\right)_{P,\,T,\,n\neq i} = 0 \tag{8}$$

Thus, Eq. (7) reduces to

$$nH = \sum_{i=1}^{c} n_i \bar{H}_i = \sum_{i=1}^{c} n_i H_i^0 + n\Omega \tag{9}$$

Multiplication of each term of Eq. (1) by n_i and summation of the resulting expression over all components yields

$$\sum_{i=1}^{c} n_i \hat{H}_i = \sum_{i=1}^{c} n_i \hat{H}_i^0 + n\Omega \tag{10}$$

Comparison of Eqs. (9) and (10) establishes the validity of Eq. (2).

The departure function Ω may be evaluated by use of the formulas given in Ref. 3 below for a number of equations of state.

REFERENCES

1. C. D. Holland, and P. T. Eubank: "Solve More Distillation Problems: Part 2—Partial Molar Enthalpies Calculated: *Hydrocarbon Process*, **53**(11): 176 (1974).
2. C. D. Holland: "Energy Balances for Systems Involving Nonideal Solutions," *Ind. Eng. Chem. Fundam.*, **16**(1): 143 (1977).
3. C. D. Holland: *Fundamentals of Multicomponent Distillation*, McGraw-Hill Book Company, New York, 1981.

CHAPTER

FIVE

SOLUTION OF BATCH-DISTILLATION PROBLEMS

Although batch distillation is one of the oldest of the separation processes, it is still used in a number of industries because it is more economical than the continuous-distillation process. The sketch of a typical batch-distillation column is shown in Fig. 5-1.

The development of calculational procedures for batch distillation, an inherently unsteady state process, has followed a somewhat different path from that of continuous distillation. The calculational procedures proposed in the literature for solving batch-distillation problems follow closely the development of high-speed computing capability. The early efforts are marked by approximate and graphical procedures. With the advent of high-speed computers have come more exact models of the process and the application of numerical methods for solving problems of this type. Beginning with Rayleigh(23), numerous calculational procedures for solving batch-distillation problems have been proposed (Refs. 1, 2, 3, 7, 8, 17, 18, 20, 25, 26, 27).

The description of a typical batch-distillation column is conveniently divided into two parts: (1) the start-up period and (2) the product period. The product period is that part of the distillation process during which a product is withdrawn from the column. The adjustment period that precedes the product period is called the start-up period. Adjustments necessary to bring the column to an operational condition such that a distillate of the desired purity may be withdrawn are made during the start-up period. In order to describe the product period, the operating conditions for the column at the initiation of this period must be known.

Solution of the equations by use of the two-point implicit method and the θ

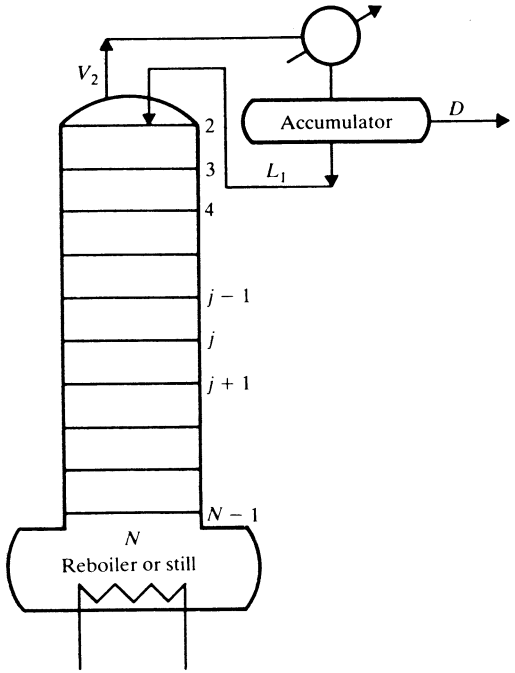

Figure 5-1 Sketch of a batch-distillation column.

method of convergence is presented in Sec. 5-1 for the start-up period. In Sec. 5-2, the use of these same procedures (the two-point implicit method and the θ method of convergence) to solve the equations for the product period is presented, as well as a combination of the two-point implicit method and the $2N$ Newton–Raphson method. Cyclic operation and optimization procedures are treated in Secs. 5-4 and 5-5, respectively.

5-1 THE START-UP PERIOD ($D = 0$, $B = 0$, $F = 0$)

The complete set of specifications for a batch-distillation column for the start-up period are as follows: the number of stages, the reboiler duty, the column pressure, the composition and thermal condition of the feed charge, the holdup on each stage of the column, and the operating condition of total reflux $D = 0$, $B = 0$, and $F = 0$. At this type of operation, a total condenser and a reboiler (total) are, of course, used.

A batch-distillation process may be started up in a variety of ways. The equations, calculational procedure, and convergence method for one such procedure follow. Suppose that at the onset, the plates are filled with the liquid to be distilled. Further, suppose that this liquid is at its bubble-point temperature at the operating pressure. Next suppose that the column is operated at total reflux ($D = 0$, $B = 0$, $F = 0$). The column may be operated at these conditions

until steady state is attained or for any specified amount of time. Then the product period is commenced. Actually, if the product period is to be commenced once the column has attained steady state operating conditions, it is not necessary to follow the process throughout the transient start-up period. Instead, the desired steady state solution at total reflux ($D = 0$, $B = 0$, $F = 0$) may be found as described recently by Holland(14).

The equations for the start-up period consist of the component-material balances, total-material balances, energy balances, and the equilibrium relationships. The basic equations are of the same general form as the corresponding equations of Chap. 4 with allowances being made for the fact that for the start-up period, $D = 0$, $B = 0$, and $F = 0$.

Solution of the Equations for the Start-Up Period by Use of a Combination of the Two-Point Implicit Method and the Theta Method

In the following development, the holdup in the vapor phase is neglected ($u_{ji}^V = 0$ and $U_j^V = 0$). This assumption is a realistic one because the molar vapor holdup is generally small relative to the liquid holdup.

When the integral-difference equations are converted to a set of algebraic equations by use of the two-point implicit method the component-material balances may be stated in the following matrix form:

$$\mathbf{A}_i \mathbf{v}_i = -\mathbf{f}_i \qquad (i = 1, 2, \ldots, c) \tag{5-1}$$

where

$$\mathbf{A}_i = \begin{bmatrix} -\rho_{1i} & 1 & 0 & 0 & 0 & \cdots & 0 \\ 1 & -\rho_{2i} & 1 & 0 & 0 & \cdots & 0 \\ 0 & A_{2i} & -\rho_{3i} & 1 & 0 & \cdots & 0 \\ \cdots & \cdots & \cdots & \cdots & \cdots & \cdots & \cdots \\ 0 & \cdots & 0 & A_{N-2,i} & -\rho_{N-1,i} & & 1 \\ 0 & \cdots & 0 & 0 & A_{N-1,i} & & -\rho_{Ni} \end{bmatrix}$$

$$\mathbf{v}_i = [l_{1i} \quad v_{2i} \quad v_{3i} \quad \cdots \quad v_{Ni}]^T$$

$$\mathbf{f}_i = [f_{1i} \quad f_{2i} \quad \cdots \quad f_{Ni}]^T$$

$$\rho_{ji} = 1 + A_{ji}(1 + \tau_j) \qquad \rho_{Ni} = 1 + \frac{U_N/V_N}{\phi\ \Delta t\ K_{Ni}}$$

$$\rho_{1i} = 1 + \tau_1 \qquad \tau_j = \frac{U_j/L_j}{\phi\ \Delta t} \qquad (j = 1, 2, \ldots, N-1)$$

$$f_{ji} = \sigma[v_{j+1,i}^0 + l_{j-1,i}^0 - v_{ji}^0 - l_{ji}^0] + u_{ji}^0/\phi\ \Delta t \qquad (j = 2, 3, \ldots, N-1)$$

$$f_{1i} = \sigma[v_{2i}^0 - l_{1i}^0] + \frac{u_{1i}^0}{\phi\ \Delta t}$$

$$f_{Ni} = \sigma[l_{N-1,i}^0 - v_{Ni}^0] + \frac{u_{Ni}^0}{\phi\ \Delta t}$$

The Theta Method of Convergence for the Start-Up Period

The formulas for the convergence method may be developed by use of the procedures shown in Chap. 4. In order to increase the speed of the calculational procedure the modified θ method may be used in lieu of the θ method. The formulas are presented first for the θ method and then for the modified θ method of convergence.

Since $b_i = d_i = 0$, it is necessary to define the θ_j's with respect to some quantity other than d_i or b_i, say u_{1i}. Suppose that in addition to the reboiler duty, the composition and boiling point temperature of the initial feed charge, the total holdups $U_1, U_2, \ldots, U_N$ are specified, which in turn fixes U_F. Let the $N-1$ independent θ_j's be defined as follows:

$$\frac{u_{ji}}{u_{1i}} = \theta_j \left(\frac{u_{ji}}{u_{1i}}\right)_{ca} \qquad (j = 2, 3, \ldots, N) \tag{5-2}$$

The θ_j's are to be determined such that the corrected u_{ji}'s are in overall component-material balance and in agreement with the specified values of the U_j's. The formula for u_{1i} is developed as follows. Since the corrected u_{ji}'s are in overall component-material balance, it follows that

$$0 = \sum_{j=1}^{N} u_{ji} - \sum_{j=i}^{N} u_{ji}^0 \tag{5-3}$$

because there are no input or output streams during any time period Δt of the start-up period. Thus, the total moles (or mass) of each component within the column remain fixed throughout the start-up period. To emphasize this, let $U_F X_i$ denote the total moles of component i in the column at time $t = 0$, the beginning of the start-up period. Then Eq. (5-3) may be restated as follows:

$$\sum_{j=1}^{N} u_{ji} = \sum_{j=1}^{N} u_{ji}^0 = U_F X_i \tag{5-4}$$

By use of the relationships given by Eq. (5-2), the following result is readily obtained from Eq. (5-4).

$$u_{1i} = \frac{U_F X_i}{1 + \sum_{j=2}^{N} \theta_j \left(\frac{u_{ji}}{u_{1i}}\right)_{ca}} \tag{5-5}$$

The desired set of θ_j's is that set of positive numbers that makes $g_1 = g_2 = \cdots = g_{N-1} = 0$, simultaneously, where

$$g_j(\theta_2, \theta_3, \ldots, \theta_N) = \sum_{i=1}^{c} u_{ji} - U_j \qquad (1 \le j \le N-1) \tag{5-6}$$

(Instead of the set of functions g_j $(j = 1, 2, \ldots, N-1)$, the set of functions g_j $(j = 2, 3, \ldots, N)$ could have been selected to find the θ_j's $(j = 2, 3, \ldots, N)$.] After the θ_j's have been found by use of the Newton–Raphson method, the corrected

u_{1i}'s are found by using Eq. (5-5). Then the mole fractions are readily computed as follows:

$$x_{ji} = \frac{\left(\frac{u_{ji}}{u_{1i}}\right)_{ca} u_{1i}}{\sum_{i=1}^{c} \left(\frac{u_{ji}}{u_{1i}}\right)_{ca} u_{1i}} \tag{5-7}$$

After the x_{ji}'s have been determined, the temperatures are found in the usual way by the K_b method. These temperatures and compositions are used in the enthalpy balances to determine the flow rates for the next trial for the given time period under consideration.

In the problem solved it was supposed that at time $t = 0$ the feed had already been charged to the column, and at time $t = 0+$ the reboiler duty was changed from zero to some value. The condenser duty Q_C at time $t_n + \Delta t$ is found by use of an enthalpy balance enclosing the entire column. Then the reflux rate L_1 at the end of the time period is found by use of an enthalpy balance enclosing the condenser and the accumulator. Note that at the beginning of the first time period $(t = 0)$, $L_j^0 = V_j^0 = Q_C^0 = Q_R^0 = 0$.

The total flow rates at the end of each time period are found by use of the enthalpy balances which are presented in Table 5-1. This calculational procedure is repeated for each time period until the assumed and calculated temperatures do not change from trial to trial. Then the procedure is repeated for the next time period.

In order to avoid numerical difficulties in the application of the θ method, a new variable p_i should be introduced as demonstrated for columns at steady state operation. For the start-up period the definition of p_i and the corresponding working equations are as follows:

$$p_i = \frac{U_F X_i}{(u_{1i})_{ca} + \sum_{j=2}^{N} \theta_j (u_{ji})_{ca}}$$

$$u_{1i} = p_i (u_{1i})_{ca}$$

$$g_1(\theta_2, \theta_3, \ldots, \theta_N) = \frac{1}{U_1} \sum_{i=1}^{c} p_i (u_{1i})_{ca} - 1 \tag{5-8}$$

$$g_j(\theta_2, \theta_3, \ldots, \theta_N) = \frac{1}{U_j} \sum_{i=1}^{c} \theta_j p_i (u_{ji})_{ca} - 1 \qquad (j = 2, 3, \ldots, N-1)$$

$$x_{ji} = \frac{(u_{ji})_{ca} p_i}{\sum_{i=1}^{c} (u_{ji})_{ca} p_i}$$

Instead of specifying the holdups in molar units, mass or volumetric units may be employed in a manner analogous to that described in Chap. 4. After

Table 5-1 Enthalpy and total material balances expressions for batch distillation columns†

1. Enthalpy and total material balances for the start-up period

$$Q_C = Q_R + \sigma(Q_R^0 - Q_C^0) - \frac{1}{\phi\,\Delta t}\sum_{j=1}^{N}\sum_{i=1}^{c}(u_{ji}h_{ji} - u_{ji}^0 h_{ji}^0)$$

$$V_2 = \frac{Q_C - \sigma\left\{\sum_{i=1}^{c}[v_{2i}^0(H_{2i}^0 - h_{1i}) - l_{1i}^0(h_{1i}^0 - h_{1i})] - Q_C^0\right\} - \frac{1}{\phi\,\Delta t}\sum_{i=1}^{c}u_{1i}^0(h_{1i}^0 - h_{1i})}{\sum_{i=1}^{c}(H_{2i} - h_{1i})y_{2i}}$$

$$L_1 = V_2 + \sigma(V_2^0 - L_1^0)$$

$$V_{j+1} = \frac{V_j\sum_{i=1}^{c}(H_{ji} - h_{ji})y_{ji} - L_{j-1}\sum_{i=1}^{c}(h_{j-1,i} - h_{ji})x_{j-1,i} - \sigma\sum_{i=1}^{c}[v_{j+1,i}^0(H_{j+1,i}^0 - h_{ji}) + l_{j-1,i}^0(h_{j-1,i}^0 - h_{ji})]}{\sum_{i=1}^{c}(H_{j+1,i} - h_{ji})y_{j+1,i}}$$
$$+ \frac{\sigma\sum_{i=1}^{c}[v_{ji}^0(H_{ji}^0 - h_{ji}) + l_{ji}^0(h_{ji}^0 - h_{ji})] - \frac{1}{\phi\,\Delta t}\sum_{i=1}^{c}u_{ji}^0(h_{ji}^0 - h_{ji})}{\sum_{i=1}^{c}(H_{j+1,i} - h_{ji})y_{j+1,i}} \qquad (j = 2, 3, \ldots, N-1)$$

$$L_j = V_{j+1} + L_{j-1} - V_j \qquad (j = 2, 3, \ldots, N-1)$$

2. Enthalpy and total material balances for the product period

$$Q_C = V_2\sum_{i=1}^{c}(H_{2i} - h_{1i})y_{2i} - D\sum_{i=1}^{c}(H_{Di}^* - h_{1i})X_{Di}$$
$$+ \sigma\left[V_2^0\sum_{i=1}^{c}(H_{2i}^0 - h_{1i})y_{2i}^0 - L_1^0\sum_{i=1}^{c}(h_{1i}^0 - h_{1i})x_{1i}^0 - D^0\sum_{i=1}^{c}(H_{Di}^0 - h_{1i})X_{Di} - Q_C^0\right]$$
$$+ \frac{U_1^0}{\phi\,\Delta t}\sum_{i=1}^{c}(h_{1i}^0 - h_{1i})x_{1i}^0$$

$$V_2 = L_1 + D$$

$$V_{j+1} = \frac{-L_{j-1}\sum_{i=1}^{c}(h_{j-1,i} - h_{ji})x_{j-1,i} + V_j\sum_{i=1}^{c}(H_{ji} - h_{ji})x_{ji}}{\sum_{i=1}^{c}(H_{j+1,i} - h_{ji})y_{j+1,i}}$$
$$+ \frac{-\sigma\left[V_{j+1}^0\sum_{i=1}^{c}(H_{j+1,i}^0 - h_{ji}) + L_{j-1}^0\sum_{i=1}^{c}(h_{j-1,i}^0 - h_{ji})x_{j-1}^0\right]}{\sum_{i=1}^{c}(H_{j+1,i} - h_{ji})y_{j+1,i}}$$
$$+ \frac{\sigma\left[V_j^0\sum_{i=1}^{c}(H_{ji}^0 - h_{ji})y_{ji}^0 + L_j^0\sum_{i=1}^{c}(h_{ji}^0 - h_{ji})x_{ji}^0\right] - \frac{U_j^0}{\phi\,\Delta t}\sum_{i=1}^{c}(h_{ji}^0 - h_{ji})x_{ji}^0}{\sum_{i=1}^{c}(H_{j+1,i} - h_{ji})y_{j+1,i}}$$

$(j = 2, 3, \ldots, N-1)$

Table 5-1 Enthalpy and total material balances expressions for batch distillation columns†—*Continued*

$$L_j = V_{j+1} - V_j - L_j \qquad (j = 2, 3, \ldots, N-1)$$

$$Q_R = V_N\sum_{i=1}^{c}(H_{Ni} - h_{N-1,i})y_{Ni}$$
$$- \sigma\left[L_{N-1}^0\sum_{i=1}^{c}(h_{N-1,i}^0 - h_{N-1,i})x_{N-1,i}^0 - V_N^0\sum_{i=1}^{c}(H_{Ni}^0 - h_{N-1,i})y_{Ni}^0 + Q_R^0\right]$$
$$+ \frac{U_N}{\phi\,\Delta t}\sum_{i=1}^{c}(h_{Ni} - h_{N-1,i})x_{Ni} - \frac{U_N^0}{\phi\,\Delta t}\sum_{i=1}^{c}(h_{Ni}^0 - h_{N-1,i})x_{Ni}^0$$

$U_N = U_N^0 - D\,\Delta t$, where D is fixed

*$H_{Di} = h_{1i}$ for a total condenser; $H_{Di} = H_{1i}$ for a partial condenser

3. Enthalpy Balance Functions for the $2N$ Newton–Raphson Method for the Product Point

$$G_1 = \frac{\sum_{i=1}^{c}\left[v_{2i}H_{2i} + \sigma v_{2i}^0 H_{2i}^0 + \frac{u_{1i}^0 h_{1i}^0}{\phi\,\Delta t}\right]}{\sum_{i=1}^{c}\left[l_{1i}h_{1i} + d_i H_{Di} + \sigma(l_{1i}^0 h_{1i}^0 + d_i^0 H_{Di}^0) + \frac{u_{1i}h_{1i}}{\phi\,\Delta t}\right] + Q_C + \sigma Q_C^0} - 1$$

$$G_j = \frac{\sum_{i=1}^{c}\left[v_{j+1,i}H_{j+1,i} + l_{j-1,i}h_{j-1,i} + \sigma(v_{j+1,i}^0 H_{j+1,i}^0 + l_{j-1,i}^0 h_{j-1,i}^0) + \frac{u_{ji}^0 h_{ji}^0}{\phi\,\Delta t}\right]}{\sum_{i=1}^{c}\left[v_{ji}H_{ji} + l_{ji}h_{ji} + \sigma(v_{ji}^0 H_{ji}^0 + l_{ji}^0 h_{ji}^0) + \frac{u_{ji}h_{ji}}{\phi\,\Delta t}\right]} - 1$$

$$G_N = \frac{\sum_{i=1}^{c}\left\{l_{N-1,i}h_{N-1,i} + \sigma[l_{N-1,i}^0 h_{N-1,i}^0] + \frac{u_{Ni}^0 h_{Ni}^0}{\phi\,\Delta t}\right\} + Q_R + \sigma Q_R^0}{\sum_{i=1}^{c}\left[v_{Ni}H_{Ni} + \sigma v_{Ni}^0 H_{Ni}^0 + \frac{u_N h_{Ni}}{\phi\,\Delta t}\right]} - 1$$

† For nonideal solutions, replace h_{ji} and H_{ji} by $\hat{h}_{ji}$ and $\hat{H}_{ji}$.

calculations have been carried out for a large number of time periods, the steady state solution at total reflux ($D = 0$, $B = 0$, $F = 0$) was approached for all problems considered by Barb(1). The steady state solution may be obtained directly by use of one of the procedures recently described by Holland(14).

Modified Theta Method of Convergence for the Start-Up Period

In order to reduce the time required to apply the θ method to the start-up period, the number of θ's and g functions may be reduced in the following manner. Let the θ's corresponding to the holdups be set equal to each other, namely,

$$\theta = \theta_j \qquad (j = 2, 3, \ldots, N) \tag{5-9}$$

The g function is taken to be the sum of the g functions corresponding to the holdups U_j ($j = 1, 2, \ldots, N-1$). Then, in view of Eq. (5-6),

$$g(\theta) = \sum_{j=1}^{N-1} \sum_{i=1}^{c} u_{ji} - \sum_{j=1}^{N-1} U_j \tag{5-10}$$

where

$$\begin{aligned} u_{1i} &= (u_{1i})_{ca}\, p_i \\ u_{ji} &= \theta(u_{ji})_{ca}\, p_i \qquad (j = 2, 3, \ldots, N-1 \\ p_i &= \frac{U_F X_i}{(u_{1i})_{ca} + \theta \sum_{j=2}^{N} (u_{ji})_{ca}} \end{aligned} \tag{5-11}$$

and the mole fractions are given by Eq. (5-8).

Energy Balances

Let the start-up period be commenced at time $t = 0$, or $t_0 = 0$. At time $t = 0+$, suppose the reboiler duty is changed from zero to some value and that it is either held at this value or varied in some prescribed manner for all t for the remainder of the start-up period.

The condenser duty Q_C at time $t_n + \Delta t$ is found by use of an enthalpy balance enclosing the entire column. Then the reflux rate L_1 at the end of the time period is found by use of an enthalpy balance enclosing the condenser and the accumulator. Note that at the beginning of the first time period ($t_0 = 0$), $L_j^0 = V_j^0 = Q_C^0 = Q_R^0 = 0$.

After the liquid rates at the end of the time period have been found by use of the enthalpy balances, the corresponding vapor rates V_j ($2 \le j \le N$) are found by the total-material balance expressions.

The constant-composition form of the enthalpy balances are formulated in a manner analogous to that described in Chap. 4. The resulting expressions are presented in Table 5-1.

After the vapor rates V_j have been found by use of the enthalpy balances of Table 5-1, the corresponding set of liquid rates $\{L_j\}$ may be found by use of the total-material balances as shown in Table 5-1.

In order to determine accurate values of the transient values of the variables, small values of Δt are needed for the first few time periods following an upset. The following scheme which is based on the one proposed by Waggoner(28,29) for continuous columns is recommended. The initial Δt is computed such that $\tau_{av} = 5/\phi$, where

$$\tau_{av} = \frac{(U_j/L_j)_{av}}{\phi\, \Delta t} \tag{5-12}$$

and $(U_j/L_j)_{av}$ is the arithmetic average of this ratio over all stages. At the end of every 10 time periods, the value of τ_{av} is reduced by one-half or Δt is doubled.

Calculational Procedures

In the following discussion, it is supposed that at $t = 0$, each plate contains the liquid feed at its boiling point at the column pressure. At time $t = 0+$, the heating medium to the reboiler is turned on which results in a reboiler duty Q_R. For the time period from t_n to $t_n + \Delta t$, the steps of the calculational procedure are as follows.

Step 1 Take $\phi = 0.6$ and choose Δt as described above.

Step 2 Assume values for the temperatures $\{T_j\}$ and $\{L_j/V_j\}$ at time $t_n + \Delta t$, the end of the time period under consideration. As a first approximation for the first two time steps, the values at time $t_n + \Delta t$ may be taken equal to those at time t_n. A better approximation for the first trial of each time increment is found by use of the point-slope predictor:

$$T_j\Big|_{t_n+\Delta t} = T_j\Big|_{t_n-\Delta t} + 2\,\Delta t \left.\frac{dT_j}{dt}\right|_{t_n}$$

$$V_j\Big|_{t_n+\Delta t} = V_j\Big|_{t_n-\Delta t} + 2\,\Delta t \left.\frac{dV_j}{dt}\right|_{t_n}$$

The derivatives may be evaluated numerically.

Step 3 Compute $\{v_{ji}\}$, $\{l_{ji}\}$, $\{u_{ji}\}$ by use of the component-material balances and equilibrium relationships.

Step 4 Find the θ's such that $g_1 = \cdots = g_{N-1} = 0$ by use of the Newton–Raphson method.

Step 5 Compute a new set of temperatures by use of the K_b method (see Chap. 4) on the basis of the corrected mole fractions.

Step 6 Compute the $\{V_j\}$ and $\{L_j\}$ by use of the energy balances and the total-material balances.

Step 7 Repeat steps 2 through 6 until $|1 - \theta_j|$ is equal to or less than some small preassigned number of the order of 10^{-4} or 10^{-5}. (The solution set of the variables at time $t_n + \Delta t$ become the initial set of values of the variables for the next time period.) Proceed to the next increment of time period by returning to step 1.

5-2 THE PRODUCT PERIOD ($B = 0$, $D > 0$)

During this part of the process, distillate is removed from the column ($D > 0$), and the bottoms rate $B = 0$. In general, a column may be operated in many ways during this part of the process. Consider first the case where two specifications, such as L_1 (or V_2) and D, are made for each time t throughout the product period. These two specifications are used to determine the condenser and reboiler duties. In addition suppose that the liquid holdups U_j ($1 \le j \le N-1$) are specified. In this mode of operation, the holdup U_N of the reboiler (or still) decreases as the product period progresses. It is, of course,

understood that the usual specifications of column pressure, the number of stages, type of condenser (total or partial), and the conditions existing throughout the column at the initiation of the product period have been made.

When the component-material balances are written around each plate and the resulting integral-difference equations converted to algebraic form by use of the implicit method, the system of equations obtained may be represented by matrix Eq. (5-1) by replacing l_{1i} by v_{1i} where $v_{1i} = d_i$ (liquid or vapor) and where l_{ji} and f_{ji} have the following meanings:

$$\rho_{ji} = 1 + A_{ji}(1 + \tau_j) \qquad \rho_{Ni} = 1 + \frac{U_N/V_N}{\phi\ \Delta t\ K_{Ni}}$$

$$\tau_j = \frac{L_j/U_j}{\phi\ \Delta t}$$

$$f_{ji} = \sigma(v^0_{j+1,i} + l^0_{j-1,i} - v^0_{ji} - l^0_{ji}) + \frac{u^0_{ji}}{\phi\ \Delta t} \qquad (j = 2, 3, \ldots, N-1) \tag{5-13}$$

$$f_{1i} = \sigma[v^0_{2i} - l^0_{1i} - d^0_i] + \frac{u^0_{1i}}{\phi\ \Delta t}$$

$$f_{Ni} = \sigma(l^0_{N-1,i} - v^0_{Ni}) + \frac{u^0_{Ni}}{\phi\ \Delta t}$$

For any set of preselected values for ϕ and Δt, together with assumed L/V and temperature profiles, this set of simultaneous equations is readily solved for the v_{ji}'s $(1 \le j \le N)$.

The Theta Method of Convergence for the Product Period

For the case where, in addition to V_2 (or L_1) and D, the molar holdups $U_1, U_2, \ldots, U_{N-1}$ are specified and the column is to be equipped with a partial condenser, the formulas for the θ method of convergence follow. The θ's are defined by

$$\frac{u_{Ni}}{d_i} = \theta_0\left(\frac{u_{Ni}}{d_i}\right)_{ca}$$

$$\frac{u_{ji}}{d_i} = \theta_j\left(\frac{u_{ji}}{d_i}\right)_{ca} \qquad (j = 1, 2, \ldots, N-1) \tag{5-14}$$

The g functions are given by

$$g_0(\theta_0, \theta_1, \theta_2, \ldots, \theta_{N-1}) = \sum_{i=1}^{c} d_i - D$$

$$g_j(\theta_0, \theta_1, \theta_2, \ldots, \theta_{N-1}) = \sum_{i=1}^{c} u_{ji} - U_j \qquad (j = 1, 2, \ldots, N-1) \tag{5-15}$$

Again, the desired set of θ_j's is that set of positive numbers that make $g_0 = g_1 = g_2 = \cdots = g_{N-1} = 0$ simultaneously. These θ_j's may be found by use of the Newton–Raphson method.

The formula for the corrected value of d_i is obtained by using an overall component-material balance.

$$\int_{t_n}^{t_n + \Delta t} (-d_i)\, dt = \sum_{j=1}^{N} (u_{ji} - u^0_{ji})$$

By use of the implicit method, it is readily shown that this expression reduces to

$$d_i = \frac{-\sigma d^0_i + \left(\dfrac{1}{\phi\ \Delta t}\right) \displaystyle\sum_{j=1}^{N} u^0_{ji}}{1 + \dfrac{1}{\phi\ \Delta t}\left[\theta_0\left(\dfrac{u_{Ni}}{d_i}\right)_{ca} + \displaystyle\sum_{j=1}^{N-1} \theta_j\left(\dfrac{u_{ji}}{d_i}\right)_{ca}\right]} \tag{5-16}$$

Also, it is readily shown that compositions consistent with the corrected u_{ji}'s are given by

$$x_{ji} = \frac{\left(\dfrac{u_{ji}}{d_i}\right)_{ca} d_i}{\displaystyle\sum_{i=1}^{c} \left(\frac{u_{ji}}{d_i}\right)_{ca} d_i} \tag{5-17}$$

On the basis of the x_{ji}'s obtained by use of Eq. (5-17), the temperatures for the next trial are found by use of the K_b method. Also, in this application of the implicit method, ϕ was taken equal to 0.6, which gave results free of oscillations. For the case where the column has a total condenser rather than a partial condenser, the multiplier θ_1 is seen to be equal to unity, since $u_{1i}/d_i = U_1/D$. Thus, for a column having a total condenser, the multiplier θ_1 and function g_1 are omitted from the set of θ_j's and g_j's listed above.

Modified Theta Method of Convergence for the Product Period

For the case of a conventional column (with $FX_i = 0$) for which L_1, D, and the U_j's are specified, the multipliers for the modified θ method are obtained by setting $\theta_j = \theta_1$ $(j = 1, 2, \ldots, N-1)$. The g function g_0 is given by the first expression of Eq. (5-15) and

$$g_1(\theta_0, \theta_1) = \sum_{j=1}^{N-1} \sum_{i=1}^{c} u_{ji} - \sum_{j=1}^{N-1} U_j$$

The formula for d_i is obtained from Eq. (5-16) by setting $\theta_j = \theta_1$ $(j = 1, 2, \ldots, N-1)$.

Since the specifications are commonly made on the overhead product, the enthalpy balances should be initiated at the top of the column. When the flow rates V_2 (or L_1) and D are specified, the enthalpy balance enclosing the con-

denser and the accumulator is used to determine the condenser duty. The development of these equations is similar to that demonstrated in Chap. 4, and the final expressions are shown in Table 5-1.

After the vapor rates, the V_j's, have been computed by use of enthalpy balances, the corresponding L_j's are found by use of total-material balances as indicated in Table 5-1.

The calculational procedure and convergence method for the case where the holdups are specified in mass (or volumetric) units are readily developed in the same manner shown in Chap. 4. Furthermore, instead of specifying the distillate rate, other specifications, such as the temperatures of discrete fractions of the distillate, may be made.

Examples

To demonstrate the transient behavior of a column throughout the start-up period, the unsteady state solutions of Examples 5-1 and 5-2 (Tables 5-2 and 5-3) were obtained under the following conditions. Initially, it was supposed that the plates were filled with the liquid to be distilled. The liquid was assumed to be at its bubble-point temperature at the column pressure. The steady state solution was approached to within six significant digits after 4.8 h of column

Table 5-2 Statement of Example 5-1

($D = 0$, $B = 0$, $F = 0$)

Example 5-1

Component	$U_F X_i$	Stage	Holdups, mol
C_3H_8	2.5	1 (condenser)	4
i-C_4H_{10}	7.5	2	1
n-C_4H_{10}	12.5	3	1
i-C_5H_{12}	10.0	4	1
n-C_5H_{12}	17.5	5	1
	50.0	6	1
Other conditions		7	1
Q_R = 350 000 Btu/h;		8	1
column pressure = 300 lb/in^2 abs.		9	1
The column has a		10	1
partial condenser, 12 plates,		11	1
and a reboiler. The K		12	1
data and enthalpy data		13	1
are given in Table 5A-1		14 (reboiler)	34
			50

Initially, all stages are filled with liquid feed at its boiling point at the column pressure.

Table 5-3 Statement and Solution of Example 5-2 (Ref. 21)

1. Statement of Example 5-2

(*a*) All initial conditions are the same as those for Example 5-1. The product period is to be initiated at the end of 2 h of start-up operation as specified in Example 5-1. The product period is to consist of the time required to collect a total of 20 moles of product. The overhead vapor rate for the product period is to be fixed at the value which it had attained at the end of the start-up period. The distillate rate is to be fixed at 0.2 of the value of the overhead vapor rate. A partial condenser is to be used. Find the composition of the total product collected at any time during the product period by use of the θ method, and the modified θ method.

(*b*) Repeat part (*a*) by use of the $2N$ Newton–Raphson method. Use the values of the condenser and reboiler duties, Q_C, Q_R, found in part (*a*) at the end of each time step as the specified values for the $2N$ Newton–Raphson method. Compare the execution times required by each method.

2. Solution of Example

(*a*) The results are displayed in Fig. 5-3.

(*b*) A comparison of the execution times made by Mijares(21) follows.

Comparison of execution times

Method	Computer (AMDAHL 470/V6 Time, s, required for 18 time steps	Convergence criteria	Compiler
θ method	3.27	Cease if $\lvert 1 - \theta_j \rvert \le 10^{-4}$ or $\lvert \Delta T_j \rvert / T_j \le 10^{-5}$, or after the 10th trial for a time step	FORTRAN H EXTENDED
Modified θ method	2.56	Same as θ method	FORTRAN H EXTENDED
$2N$ Newton–Raphson	3.14	$\Phi \le 10^{-4}$ where $\Phi = \frac{1}{2N}\left[\sum_{j=1}^{N}(F_j^2 + G_j^2)\right]^{1/2}$	FORTRAN H EXTENDED

operating time (Refs. 1, 2). A graph of the transient values of the mole fractions for Example 5-1 is presented in Fig. 5-2.

The equations and convergence method for the product period were tested by solving a wide variety of examples. Satisfactory results were obtained for all examples considered. Example 5-2, stated in Table 5-3, was selected for purposes of illustration. The transient compositions of the distillate are displayed in Fig. 5-3.

When the product stream D is collected in a single container, the average mole fraction of each component within the container varies with time as shown in Fig. 5-4. Each curve in Fig. 5-4 is readily obtained from the corresponding curve in Fig. 5-3. Since D is held fixed throughout the product period, the point at time t on a curve in Fig. 5-4 is equal to the integral of the corresponding curve in Fig. 5-3 over the time interval 0 to t divided by the length of the time interval.

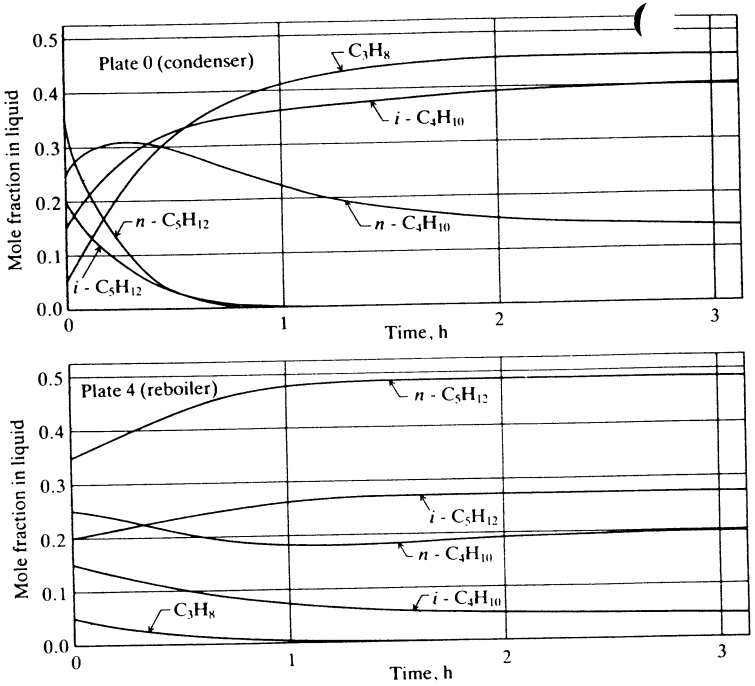

Figure 5-2 Transient compositions for the start-up period, Example 5-1.

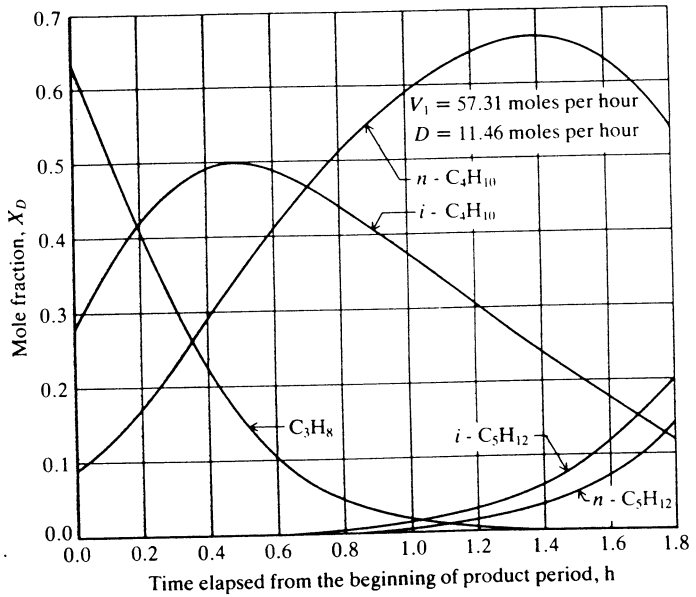

Figure 5-3 Distillate compositions obtained for the product period, Example 5-2.

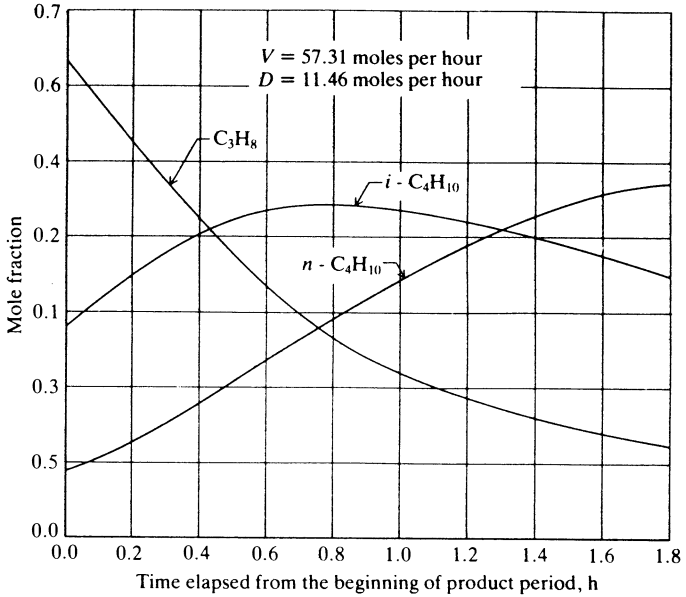

Figure 5-4 Composition of the total product collected at any time during the product period, Example 5-2.

5-3 SOLUTION OF BATCH DISTILLATION PROBLEMS BY USE OF A COMBINATION OF THE TWO-POINT IMPLICIT METHOD AND THE 2N NEWTON–RAPHSON METHOD

For mixtures which form ideal solutions ($K_i = K_i(P, T)$ and $\gamma_i^V = \gamma_i^L = 1$ for all i), the application of the Newton–Raphson method is exact and convergence can be assured provided that the initial estimates are in the region of convergence (Ref. 14).

In order to demonstrate the use of the 2N Newton–Raphson method in conjunction with the two-point implicit method, the equations for use with this combination are formulated for the product period. The equations for other modes of operation are formulated in a similar manner.

Product Period

Again it is supposed that the holdups $\{u_{ji}\}$ throughout the column are known at the initiation of the product period. Also, it is supposed that the liquid holdups U_j $(1 < j < N - 1)$ are specified as well as the usual specifications of column pressure, the number of stages, type of condenser (total or partial), and

the conditions existing throughout the column at the initiation of the product period. The two remaining specifications may be taken to be the reflux ratio L_1/D and the ratio of reboiler holdup-to-vapor rate, U_N/V_N throughout the product period, or one could specify the condenser duty Q_C and the reboiler duty Q_R throughout the product period in lieu of L_1/D and U_N/V_N. Thus, for the case where the condenser duty Q_C and the reboiler duty Q_R are specified, the independent variables are taken to be:

$$\mathbf{x} = [L_1/D,\ L_2/V_2,\ \ldots,\ L_{N-1}/V_{N-1},\ U_N/V_N,\ T_1,\ T_2,\ \ldots,\ T_{N-1},\ T_N]^T \quad (5\text{-}18)$$

The corresponding functions of the $2N$ Newton–Raphson method are the N dewpoint functions and the N enthalpy balance functions

$$\mathbf{f} = [F_1 \quad F_2 \quad \cdots \quad F_N \quad G_1 \quad G_2 \quad \cdots \quad G_N]^T \quad (5\text{-}19)$$

Instead of using the L/V ratios, a new set of independent variables may be defined in a manner similar to that shown in Chap. 4, namely, let

$$\begin{aligned} \frac{L_1}{D} &= \theta_1\left(\frac{L_1}{D}\right)_a \\ \frac{L_j}{V_j} &= \theta_j\left(\frac{L_j}{V_j}\right)_a \qquad (j = 2, 3, \ldots, N-1) \\ \frac{U_N}{V_N\,\Delta t} &= \theta_N\left(\frac{U_N}{V_N}\right)_a\left(\frac{1}{\Delta t}\right) \end{aligned} \quad (5\text{-}20)$$

where Δt is a constant, the value of the time period under consideration. By inclusion of Δt in the last expression, it becomes dimensionless. Again, the subscript a denotes that the ratio may be regarded as an arbitrary constant. By selecting the arbitrary constant to be the most recent value of the ratio in the trial-and-error procedure for the given time step under consideration, the variable θ_j is normalized. Equation (5-18) may be restated in the following form:

$$\mathbf{x} = [\theta_1,\ \theta_2,\ \ldots,\ \theta_N,\ T_1,\ T_2,\ \ldots,\ T_N]^T \quad (5\text{-}21)$$

When a partial condenser is employed, the complete set of N dewpoint functions have the following form:

$$F_j = \frac{1}{V_j}\sum_{i=1}^{c}\left(\frac{1}{K_{ji}} - 1\right)v_{ji} \qquad (j = 1, 2, \ldots, N) \quad (5\text{-}22)$$

where it is of course understood that D is denoted by V_1. When a total condenser is employed, the bubble-point form of the function is used instead of the dewpoint form for the first stage. The bubble-point form of the function is given by

$$F_1 = \frac{1}{D}\sum_{i=1}^{c}(K_{1i} - 1)d_i \quad (5\text{-}23)$$

The enthalpy balance functions are formulated by use of the equations obtained from the integral-difference equations after the two-point implicit method has been applied. They are presented in Table 5-1.

For any choice of the independent variables at the end of the time step under consideration, the values of the dependent variables are found by solving the constraining equations, which consist of the component-material balances and the total-material balances.

The component-material balances are again given by Eq. (5-1) as modified by Eq. (5-13). The total-material balances are developed in the following manner.

Since all of the holdups U_j ($j = 1, 2, \ldots, N-1$) are regarded as fixed while U_N is allowed to vary, the equations for the first $N-1$ stages ($j = 1, 2, \ldots, N-1$) are the same as those for a column at steady state operation. The equations are formulated in a manner analogous to that shown below for stage j, namely,

$$V_{j+1} + L_{j-1} - V_j - L_j = 0 \qquad (j = 2, 3, \ldots, N-1) \quad (5\text{-}24)$$

Then

$$\left(\frac{L_{j-1}}{V_{j-1}}\right)V_{j-1} - \left(1 + \frac{L_j}{V_j}\right)V_j + V_{j+1} = 0 \quad (5\text{-}25)$$

By making use of Eq. (5-20), it is possible to restate Eq. (5-25) as follows:

$$r_j V_{j-1} - (1 + r_j)V_j + V_{j+1} = 0 \qquad (j = 2, 3, \ldots, N-1) \quad (5\text{-}26)$$

where

$$r_j = \theta_j\left(\frac{L_j}{V_j}\right)_a$$

For stage 1, the corresponding total-material balance is given by

$$-(1 + r_1)V_1 + V_2 = 0 \quad (5\text{-}27)$$

where D has been represented for the convenience of symmetry by V_1 and $r_1 = \theta_1(L_1/V_1)_a$. Since the holdup U_N varies with time, the balance enclosing the reboiler is given by

$$\int_{t_n}^{t_n+\Delta t}(L_{N-1} - V_N)\,dt = U_N\Big|_{t_n+\Delta t} - U_N\Big|_{t_n} \quad (5\text{-}28)$$

Application of the two-point implicit method followed by rearrangement yields

$$r_{N-1}V_{N-1} - (1 + r_N)V_N = -\sigma(L^0_{N-1} - V^0_{N-1}) - r^0_N V^0_N \quad (5\text{-}29)$$

where

$$r_N = \frac{U_N/V_N}{\phi\,\Delta t}$$

$$r^0_N = \frac{U^0_N/V^0_N}{\phi\,\Delta t}$$

where the Δt which appears in r_N and r^0_N has the same value, the value at the time period under consideration

Equations (5-26), (5-27), and (5-29) may be stated in the following matrix form.

$$\mathbf{RV} = -\mathscr{F} \tag{5-30}$$

$$\mathbf{R} = \begin{bmatrix} -(1+r_1) & 1 & 0 & 0 & \cdots & 0 \\ r_1 & -(1+r_2) & 1 & 0 & \cdots & 0 \\ \cdots & \cdots & \cdots & \cdots & \cdots & \cdots \\ 0 & \cdots & 0 & r_{N-2} & -(1+r_{N-1}) & 1 \\ 0 & \cdots & \cdots & 0 & r_{N-1} & -(1+r_N) \end{bmatrix}$$

$$\mathbf{V} = [D \quad V_2 \quad V_3 \quad \cdots \quad V_{N-1} \quad V_N]^T$$

$$\mathscr{F} = [0 \quad \cdots \quad 0 \quad \mathscr{F}_N]^T$$

$$\mathscr{F}_N = \sigma(L_{N-1}^0 - V_N^0) + r_N^0 V_N^0$$

The $2N$ Newton–Raphson equations which are solved successively for each time period until the convergence criterion, the quantity

$$\left(\frac{1}{2N}\right)\left[\sum_{j=1}^{N}(F_j^2 + G_j^2)\right]^{1/2}$$

is less than some small preassigned positive number, say 10^{-4} or 10^{-5}. The $2N$ Newton–Raphson equations are given by

$$\mathbf{J}\,\Delta\mathbf{x} = -\mathbf{f} \tag{5-31}$$

where

$$\mathbf{J} = \begin{bmatrix} \frac{\partial F_1}{\partial \theta_1} & \frac{\partial F_1}{\partial \theta_2} & \cdots & \frac{\partial F_1}{\partial \theta_N} & \frac{\partial F_1}{\partial T_1} & \frac{\partial F_1}{\partial T_2} & \cdots & \frac{\partial F_1}{\partial T_N} \\ \vdots & \vdots & & \vdots & \vdots & \vdots & & \vdots \\ \frac{\partial G_N}{\partial \theta_1} & \frac{\partial G_N}{\partial \theta_2} & \cdots & \frac{\partial G_N}{\partial \theta_N} & \frac{\partial G_N}{\partial T_1} & \frac{\partial G_N}{\partial T_2} & \cdots & \frac{\partial G_N}{\partial T_N} \end{bmatrix}$$

$$\Delta\mathbf{x} = [\Delta\theta_1 \quad \Delta\theta_2 \quad \cdots \quad \Delta\theta_N \quad \Delta T_1 \quad \Delta T_2 \quad \cdots \quad \Delta T_N]^T$$

$$\mathbf{f} = [F_1 \quad F_2 \quad \cdots \quad F_N \quad G_1 \quad G_2 \quad \cdots \quad G_N]^T$$

The Newton–Raphson equations may be solved in a number of ways: (1) The use of analytical derivatives and the calculus of matrices, (2) The use of Broyden's method (demonstrated in Chap. 2), and (3) The use of the Broyden–Bennett algorithm. All of these methods are demonstrated by Holland in Ref. 14 for conventional distillation columns at steady state operation.

The basic calculational procedure follows.

Calculational Procedure

1. Assume $\theta_j = 1$ for all j. Take the set $\{(L_j/V_j)_a\}$ equal to the set of values most recently calculated for L_j/V_j at the end of the time step. For the first trial of any time step, the values of L_j/V_j at the end of the time step may be estimated by use of the two-point predictor (presented at the end of Sec. 5-1).

   For any trial of a given time step other than the first one, take the $\{T_j\}$ at the end of the time step to be equal to the most recent set of calculated values. For the first trial of a time step, estimate the $\{T_j\}$ at the end of the time step by use of the two-point predictor (presented at the end of Sec. 5-1).
2. Evaluate the elements of **f** and **J** by use of any one of the three methods listed above.
3. Solve $\mathbf{J}\,\Delta\mathbf{x} = -\mathbf{f}$ for $\Delta\mathbf{x}$, and adjust the corrections until the values of the variables at the end of the time step are within the range of curve-fits and limits by adjusting the parameter β

   $$\mathbf{x}_{k+1} = \mathbf{x}_k + \beta\,\Delta\mathbf{x}_k$$

   When Broyden's method and the Broyden–Bennett algorithms are employed, an additional parameter s, which represents an approximate optimum of the step size, is computed as described in Chap. 2 to give

   $$\mathbf{x}_{k+1} = \mathbf{x}_k + s\beta\,\Delta\mathbf{x}_k$$
4. Test for convergence, and if the criterion for convergence is not within the prescribed limits, update the inverse of the jacobian matrix (Broyden's method) or the **LU** factorization of the jacobian matrix (Broyden–Bennett algorithm) or return to step 2 and reevaluate the elements of the jacobian matrix.

In order to obtain a comparison of the execution times required by the θ method, the modified θ method, and the $2N$ Newton–Raphson method, Example 5-2 (Table 5-3) was solved by each of the methods. Broyden's method was used in the solution of the g functions in the θ methods and in the solution of the jacobian in the $2N$ Newton–Raphson method. In order to achieve maximum speed, the jacobian was evaluated only one time per problem provided that the inequality criterion of Broyden's method was satisfied. When the Broyden method is applied in this manner, the execution times for all three methods are approximately the same.

5-4 CYCLIC OPERATION

Cyclic operation is characterized by two modes of operation, called "transient total reflux" and "stripping." During the total reflux portion of the cycle, liquid reflux is returned to the column, but no product is withdrawn ($L_1 \neq 0$, $D = 0$, $B = 0$, $F = 0$); and during the stripping portion of the cycle, the product is withdrawn, but no reflux is returned to the column ($D \neq 0$, $L_1 = 0$, $F = 0$, $B = 0$). The models and calculational procedures proposed by Barb and Holland(1,2) are presented below.

The extreme difficulty of accurate measurement of small flow rates in laboratory columns strongly favors cyclic operation. This type of operation is commonly achieved through the use of a timer which divides a given total time

period into periods of transient total reflux, ϕ_R, and stripping, ϕ_S. The reflux ratio for this type of operation is taken to be the ratio of ϕ_R to ϕ_S.

Transient Total Reflux Operation ($L_1 \neq 0$, $D = 0$, $B = 0$, $F = 0$)

The component-material balances for any component i are formulated in a manner analogous to that demonstrated in Sec. 5-1. After the component flow rates at the end of the time period have been computed, the values so obtained may be used to compute new sets of compositions from which a new temperature profile may be calculated.

Two convergence methods are presented, the θ method and the modified θ method. The equations are formulated first for the θ method and then for the modified θ method.

Suppose that in addition to the reboiler duty Q_R, the total molar holdups

$$U_1, U_2, U_3, \ldots, U_N$$

are specified. These N holdups give rise to $N - 1$ independent θ's, defined as follows:

$$\frac{u_{ji}}{u_{1i}} = \theta_j \left(\frac{u_{ji}}{u_{1i}}\right)_{ca} \qquad (j = 2, 3, \ldots, N) \tag{5-32}$$

The θ_j's are to be determined such that the corrected u_{ji}'s are in overall component-material balance and in agreement with the specified values of the U_j's. The formula for u_{1i} is developed in the following manner. Since the corrected u_{ji}'s are in overall component-material balance, it follows that

$$0 = \sum_{j=1}^{N} u_{ji} - \sum_{j=1}^{N} u_{ji}^0 \tag{5-33}$$

because there are no input or output streams during any time period Δt of the total reflux portion of a given cycle. Thus, the total moles (or mass) of each component within the column remains fixed throughout the total reflux operation portion of a given cycle. To emphasize this, let $U_F X_i$ denote the total moles of component i in the column at time $t = 0$, the beginning of the given batch distillation, and let $U_p X_{pi}$ denote the moles of component i that have been withdrawn from the column at the beginning of the total reflux portion of the cycle under consideration. Then Eq. (5-33) may be restated as follows:

$$\sum_{j=1}^{N} u_{ji} = \sum_{j=1}^{N} u_{ji}^0 = U_F X_i - U_p X_{pi} \tag{5-34}$$

The following result is readily obtained by use of Eqs. (5-32) and (5-34):

$$u_{1i} = \frac{U_F X_i - U_p X_{pi}}{1 + \sum_{j=2}^{N} \theta_j \left(\frac{u_{ji}}{u_{1i}}\right)_{ca}} \tag{5-35}$$

Thus, the desired set of θ_j's is that set of positive numbers that makes $g_1 = g_2 = \cdots = g_{N-1} = 0$, simultaneously, where

$$g_j(\theta_2, \theta_3, \ldots, \theta_N) = \sum_{i=1}^{c} u_{ji} - U_j \qquad (j = 1, 2, \ldots, N - 1) \tag{5-36}$$

Instead of the set g_j ($j = 1, 2, \ldots, N - 1$), the set g_j ($j = 2, 3, \ldots, N$) may be used to find the θ_j's ($j = 2, 3, \ldots, N$). After the θ_j's have been found by use of the Newton–Raphson method, the corrected u_{1i}'s are found by use of Eq. (5-35). Then the mole fractions are readily computed by use of Eq. (5-7). After the x_{ji}'s have been determined, the temperatures are found in the usual way by use of the K_b method. The temperatures and compositions so obtained are used in the enthalpy balances described in a subsequent section.

Since the calculation of $N - 1$ roots (θ values) is a time-consuming task, the "modified θ method" of convergence is recommended for solving batch distillation problems in the interest of conserving computer time. In the modified θ method, the θ's corresponding to the holdups are set equal to each other, namely

$$\theta = \theta_j \qquad (2 \leq j \leq N) \tag{5-37}$$

The g function is taken to be equal to the sum of the g functions corresponding to the holdups U_j ($j = 1, 2, \ldots, N - 1$). Then from Eq. (5-36), it follows that

$$g(\theta) = \sum_{j=1}^{N-1} \sum_{i=1}^{c} u_{ji} - \sum_{j=1}^{N-1} U_j \tag{5-38}$$

Note that for any one trial by the modified θ method, the individual U_j's may not be satisfied by the respective sums of the component holdups for each plate; however, when a θ is found that makes $g(\theta) = 0$, the component holdups are in agreement with the sum of the U_j's over the entire column.

In the total reflux portion of a given cycle, the reboiler duty is commonly fixed. In theory, the enthalpy balances may be written around each plate or about either end of the column and each plate in the column. In practice, best results were achieved for this type of operation by first determining the condenser duty, Q_C, by use of an enthalpy balance enclosing the entire column. The expression so obtained was reduced to algebraic form by use of the implicit method. The liquid rates L_j were determined by use of enthalpy balances enclosing each plate. These integral-difference equations were reduced to algebraic form by use of the implicit method and solved for the L_j's by use of the constant-composition method. The vapor rates were found by use of total-material balances enclosing each plate. These equations were likewise converted to algebraic form by use of the implicit method.

For the special case where no product has been withdrawn ($U_p = 0$), the equations for transient total reflux operation reduce to those presented for the start-up period of a batch distillation column.

The Stripping Operation

This portion of the cyclic operation is initiated by switching from total reflux (L_1 = finite number, $D = 0$) to total take-off or stripping ($L_1 = 0$, D = finite number, and $Q_C = 0$). The reboiler duty Q_R is either held fixed or its variation throughout the stripping portion of the cycle is specified. In the stripping operation, the U_j's are no longer regarded as fixed, and the liquid rates at the end of each time period are taken equal to zero. That the stripping operation is best represented in this way is evident from the following reasoning. The hottest stream and the one containing the largest fraction of heavy components is the stream V_N leaving the reboiler and entering plate $N-1$. Since the holdup U_{N-1} contains a smaller fraction of heavies than U_N, the vapor V_{N-1} in equilibrium with U_{N-1} will contain a smaller fraction of heavies than V_N. Since the enthalpy per mole of a component generally increases with molecular weight, V_{N-1} is generally greater than V_N. Thus, the holdup U_{N-1} can be expected to decrease throughout the course of the stripping operation. By use of similar reasoning, the results obtained for $j = N-1$ are also shown to follow for all $j < N-1$.

The component-material balances for the stripping portion of any given cycle are developed in a manner analogous to that shown for the total reflux portion of the cycle.

In the stripping operation, the distillate rate D is specified. Thus there exists one θ, which may be defined as follows:

$$\frac{u_{ji}}{d_i} = \theta\left(\frac{u_{ji}}{d_i}\right)_{ca} \qquad (j = 1, 2, \ldots, N) \tag{5-39}$$

The θ that places each component in overall material balance and in agreement with the specification D is that $\theta > 0$ that makes $g_0(\theta) = 0$, where

$$g_0(\theta) = \sum_{i=1}^{c} d_i - D \tag{5-40}$$

The following formula for d_i is found in a manner analogous to that demonstrated for u_{1i}

$$d_i = \frac{-\sigma d_i^0 + \dfrac{1}{\phi\,\Delta t}\displaystyle\sum_{j=1}^{N} u_{ji}^0}{1 + \theta\displaystyle\sum_{j=1}^{N}\left(\frac{u_{ji}}{d_i}\right)_{ca}} \tag{5-41}$$

After the $\{d_i\}$ has been determined, the corrected compositions and temperatures are found by use of Eq. (5-8) and the K_b method (see Chap. 4). These new sets of compositions and temperatures are used in the enthalpy balances.

The expressions for the enthalpy and total-material balances are developed in a manner analogous to that described for total reflux except that the enthalpy balances are solved for the U_j's rather than the V_j's.

Development of Models and Comparison with Experimental Results

The possible combinations of the modes of operation and types of specifications are many. Models for continuous product removal with constant volume, molar, or mass holdups are available (Refs. 25, 26). Further details pertaining to the model for cyclic operation follow.

The model of cyclic operation employed can be described best by use of Fig. 5-5. Point A represents the beginning of one complete cycle. At this point, it is desired to have the reflux rate go to zero and distillate rate go to the specified amount. However, the implicit method weights the final and initial values to give the transition period AB. By making the increment AB more than three orders of magnitude smaller than BC, the overall effect of this transition period on the results obtained for any cycle was very slight. During the time period BC, the stripping operation partially depletes the holdups on the plates of the column.

The transition period CD from stripping to total reflux operation consists of the most physically complex portion of cyclic operation. During period CD, the plates of an actual column are filled sequentially from the top to the bottom resulting in a series of discontinuous operations throughout the column. Since the detailed representation of this action is highly impractical, a simple approximation was made. The time period CD was adjusted so that all of the plates within the column could be filled and reasonable liquid flow rates established. Since period CD represents appreciable real time relative to BC, the weight factor was set to strongly favor the final conditions ($\phi > 1/2$). This scheme gave

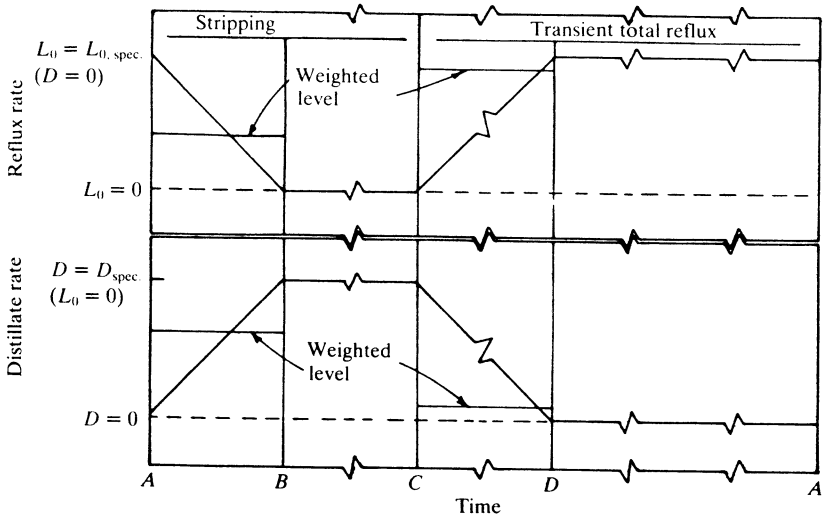

Figure 5-5 Schematic of reflux and distillate flows in cyclic operation.

a good approximation of the step change and tended to minimize the effect of product takeoff during this period.

During the time period DA, the column was operating at transient total reflux. In this cyclic operation, the term "reflux ratio" is taken to mean the ratio of CA to AC.

Comparison of the Models with Experimental Results

The final justification of any model rests on its ability to describe (within the prescribed accuracy) a given physical phenomena. In the following examples, the results of three models are compared with the experimental results and with each other.

The statement of Example 5-3 is given in Table 5-4 and the experimental and calculated results are presented in Fig. 5-6 for Model C. In the area of greatest discrepancy between the calculated and experimental results, it should be noted that the experimental results did not satisfy a total-material balance.

Example 5-4 was selected for the purpose of showing that in the limit, as the total cycle time t_{cycle} of model C approaches zero, the results obtained from model C approach those given by model B. The statement of this example is given in Table 5-4, and some typical results are tabulated in Table 5-5.

Table 5-4 Statement of conditions for Examples 5-3, 5-4, and 5-5

Charge composition				
Compound	Mole fraction	Run information	Examples 5-3 and 5-4	Example 5-5
n-Heptane	0.070	Run no. in Ref. 25	T-10	T-5 and T-13
Methyl cyclohexane	0.217	Reflux ratio	7.5/1	15/1 and 7.5/1
Toluene	0.713	Percent holdup in column and accumulator	9	9 and 18

Properties	Ref.
n-Heptane	
K data	4
Enthalpy and density data	10
Methyl cyclohexane	
K data	4
Enthalpy and density data	9
Toluene	
K data	4
Enthalpy and density data	9

Holdup distribution in column and accumulator: uniform or perfectly mixed

Starting condition: steady state total reflux

Total number of stages: $N = 80$

Pressure: atmospheric

Condenser: partial (vapor distillate)

Model A: Constant molar holdups, continuous operation
Model B: Constant volume holdups, continuous operation
Model C: Constant volume holdups, cyclic operation

Table 5-5 Comparison of model B and model C with different total cycle times, Example 5-4

Mole percent of the initial charge collected as overhead product	Component	Model B	Distillate mole fraction, model C		
			t_{cycle} = 1/2 min	t_{cycle} = 1 min	t_{cycle} = 2 min
1.60	n-Heptane	0.943	0.943	0.940	0.935
4.76	n-Heptane	0.493	0.491	0.497	0.494
4.76	Methyl cyclohexane	0.507	0.509	0.503	0.506
9.03	n-Heptane	0.141	0.133	0.128	0.219
9.03	Methyl cyclohexane	0.859	0.867	0.872	0.871
22.5	n-Heptane	0.080	0.074	0.069	0.065
22.5	Methyl cyclohexane	0.920	0.925	0.929	0.932
26.1	n-Heptane	0.051	0.043	0.038	0.046
26.1	Methyl cyclohexane	0.515	0.520	0.508	0.542
26.1	Toluene	0.434	0.437	0.454	0.412

Example 5-5 was included to demonstrate the validity of the models over a broad range of experimental conditions. A statement of the example appears in Table 5-4 and the results are shown in Fig. 5-7. Although only the results of model B are shown, similar agreement with the experimental results was obtained by use of model C.

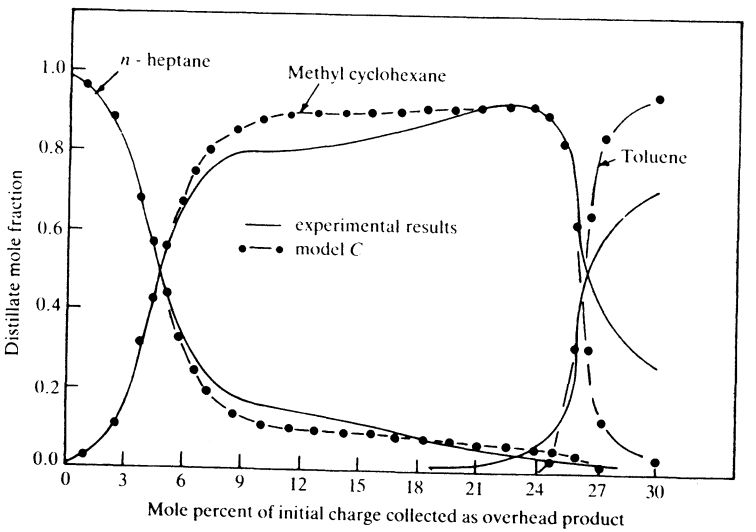

Figure 5-6 Experimental data and results for model C for Example 5-3.

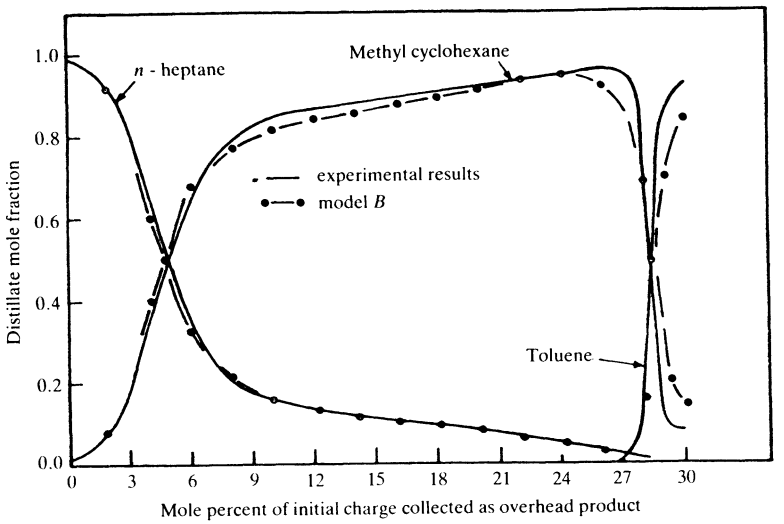

Figure 5-7 Comparison of model *B* and experimental results obtained at a high reflux ratio, Example 5-5.

5-5 OPTIMIZATION OF THE BATCH-DISTILLATION PROCESS

Within the framework of any specific problem under consideration, all of the information needed for "optimization" by various criteria may be generated by obtaining the appropriate transient solutions. The criteria must be determined prior to the solution of the problem so that the necessary information may be noted and preserved. One potentially serious drawback of this approach could be the amount of information which must be stored.

Optimization studies of binary systems with simplifying approximations have been considered previously (Refs. 7, 20). General conclusions reached from these and other studies (Ref. 8) indicate that the distillate policy has a debatable effect on the "yield" (the amount of product of a specified purity).

As an example of the use of the transient solutions in optimization studies, consider the problem of maximizing the "yield." This problem, which represents one of the more realistic sets of possible criteria, may be stated formally as follows:

Maximize:

$$(t_{off} - t_{on})D$$

Subject to:

$$\frac{\text{Moles } i\Big|_{t_{off}} - \text{moles } i\Big|_{t_{on}}}{(t_{off} - t_{on})D} - x_{si} \geq 0$$

where D = specified distillate rate
moles i = moles of component i that have been removed from the column at any time t
t_{off} = time at which the cut is terminated
t_{on} = time at which the cut is initiated
x_{si} = specified purity of component i in the cut under consideration.

A restatement of the objective function in terms of the constraints as suggested by Carroll(3) and further developed by Fiacco and McCormick(12,13) is possible. In particular, since the maximum of the objective function $(t_{off} - t_{on})D$ occurs when the constraint is a pure equality constraint, that is,

$$\frac{\text{Moles } i\Big|_{t_{off}} - \text{moles } i\Big|_{t_{on}}}{(t_{off} - t_{on})D} - x_{si} = 0 \qquad (5\text{-}42)$$

it is possible to restate the constrained optimization problem as an unconstrained optimization problem as follows:

Minimize:

$$-(t_{off} - t_{on})D + R\left[\text{moles } i\Big|_{t_{off}} - \text{moles } i\Big|_{t_{on}} - x_{si}(t_{off} - t_{on})D\right] \qquad (5\text{-}43)$$

where R is a multiplier which is several orders of magnitude greater than the product $(t_{off} - t_{on})D$ but not so great that the product $(t_{off} - t_{on})D$ is insignificant in the number system in use. This problem may be resolved by application of well-known search techniques.

Optimization problems involving the lightest and heaviest components of a mixture constitute special cases in that either the beginning or the termination of the cut is physically fixed. Such problems may be handled as deterministic problems. This fact leads to the observation that if the initial (or final) cut point of any cut is fixed and the purity constraint satisfied as an equality, then the final (or initial) cut point of the cut is fixed. It is shown below that the maximum amount of product of the specified purity will be obtained when the initial and final cut points have the same concentration of the specified component. An alternate procedure for solving the original maximization problem is then a single variable search on the initial point with the final point becoming dependent, that is,

$$t_{off} = f(t_{on}) \qquad \text{so that} \qquad X_{Di}\Big|_{t_{off}} = X_{Di}\Big|_{t_{on}} \qquad (5\text{-}44)$$

with the purity constraint minimized

Minimize:

$$\left|\text{Moles } i\Big|_{t_{off}} - \text{moles } i\Big|_{t_{on}} - x_{si}(t_{off} - t_{on})D\right| \qquad (5\text{-}45)$$

Optimization by use of the functions given by either Eq. (5-43) or (5-44) has proved to be satisfactory and, of course, the two equations give identical results. About the same effort was required to optimize a problem by use of each of these functions.

Proof that X_{Di} (at t_{off}) = X_{Di} (at t_{on}) for Maximum Recovery at a Specified Purity of the Lightest Component of a Mixture

When the purity specification of the cut collected over the time period from t_{on} to t_{off} is taken to be x_{si}, where i is the lightest component of the mixture, then the purity specification may be represented as follows:

$$\frac{\int_{t_{on}}^{t_{off}} d_i\, dt}{(t_{off} - t_{on})D} - x_{si} \geq 0 \tag{5-46}$$

where the distillate rate D is to be held fixed, or

$$\frac{(\int_{t_i}^{t_f} X_{Di}\, dt - \int_{t_i}^{t_{on}} X_{Di}\, dt - \int_{t_{off}}^{t_f} X_{Di}\, dt)}{(t_{off} - t_{on})} - x_{si} \leq 0 \tag{5-47}$$

where t_i and t_f denote the initial and final times for a given distillation. The maximum amount of distillate will be collected in a given cut when $(t_{off} - t_{on})$ is maximized. The values of X_{Di} at which to begin and end the cut, respectively, in order to maximize the amount of distillate collected at the specified purity are found as follows. First the problem is reformulated in the more convenient notation as indicated in Fig. 5-8

$$\frac{\int_0^c f(x)\, dx - \int_0^a f(x)\, dx - \int_b^c f(x)\, dx}{(b - a)} = x_{si} \tag{5-48}$$

where the cut is initiated at time a and terminated at time b, and x_{si} is again the specified purity of the lightest component.

It is desired to maximize $(b - a)$ subject to the condition that the purity specification be satisfied. Then

$$b - a = \frac{1}{x_{si}}\left(\int_0^c f(x)\, dx - \int_0^a f(x)\, dx - \int_b^c f(x)\, dx\right) \tag{5-49}$$

After a has been selected as the independent variable and Leibnitz' rule has been applied for differentiation under the integral sign, one obtains

$$\frac{d(b - a)}{da} = \frac{1}{x_{si}}\left[0 - f(a) + f(b)\frac{db}{da} + 0\right] \tag{5-50}$$

The maximum (or minimum) of $(b - a)$ is found by setting $d(b - a)/da = 0$. Under this condition, Eq. (5-50) reduces to

$$\frac{f(a)}{f(b)} = \frac{db}{da} \tag{5-51}$$

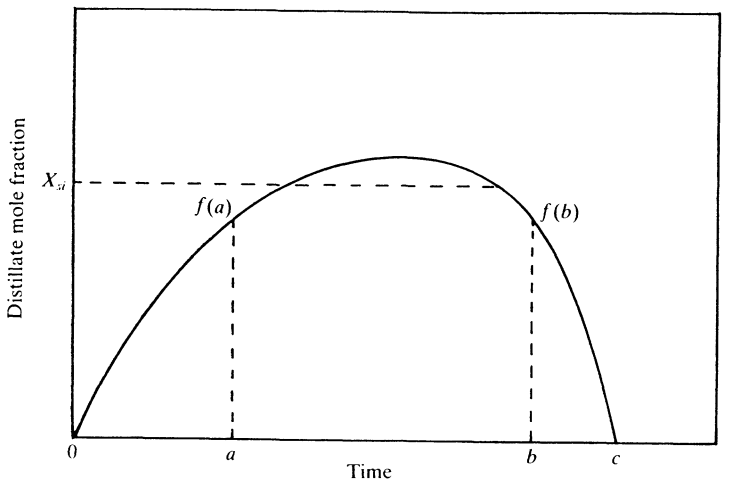

Figure 5-8 Representation of a distillation.

But

$$\frac{d(b - a)}{da} = \frac{db}{da} - 1 = 0 \tag{5-52}$$

or

$$\frac{db}{da} = 1 \tag{5-53}$$

Therefore,

$$\frac{f(a)}{f(b)} = 1 \tag{5-54}$$

or

$$f(a) = f(b) \tag{5-55}$$

Thus, in order to maximize the amount of distillate which can be collected at a specified purity x_{si}, the cut should be initiated and terminated at the same mole fraction $(X_{Di,\,on} = X_{Di,\,off})$. The above development was originally given by Barb(1).

A statement of Example 5-6 appears in Table 5-6, and the results are displayed in Fig. 5-9. The value of the mole fraction of i-C_4H_{10} at the initiation and termination points is 0.452 16. The initial and final points for the cut are shown as functions of dimensionless time; however, sufficient information is generated within the solution of the model to permit the selection to be made on other bases such as overhead temperature.

Table 5-6 Statement of conditions for Example 5-6

Charge composition		
Component	Mole fraction	Constant molar holdup model
C_3H_8	0.05	Reflux ratio: 7.5/1
i-C_4H_{10}	0.15	Holdup distribution in moles: $U_1 = 4$, $U_j = 1 (2 \le j \le 13)$, and $U_{14} = 34$
n-C_4H_{10}	0.25	
i-C_5H_{12}	0.20	Total number of stages: $N = 14$
n-C_5H_{12}	0.35	Pressure: 300 lb/in^2
Properties		Condenser: total (liquid distillate)
The K data and enthalpy data are given in Table 5A-1		For the "i-C_4H_{10} cut," x_s (for i-C_4H_{10}) = 0.47

The use of the exact model proposed has been found to be advantageous in optimization studies. In general, the additional complexity of the model allows simpler, more direct application of optimizing techniques due to the amount of information generated by the more exact models.

As has been demonstrated, the same fundamental relationships used to describe continuous-distillation columns are applicable for describing batch-distillation columns. Although only the θ method and the $2N$ Newton–Raphson method in conjunction with the two-point implicit method have been demonstrated, other methods such as the semi-implicit Runge–Kutta and Gear's

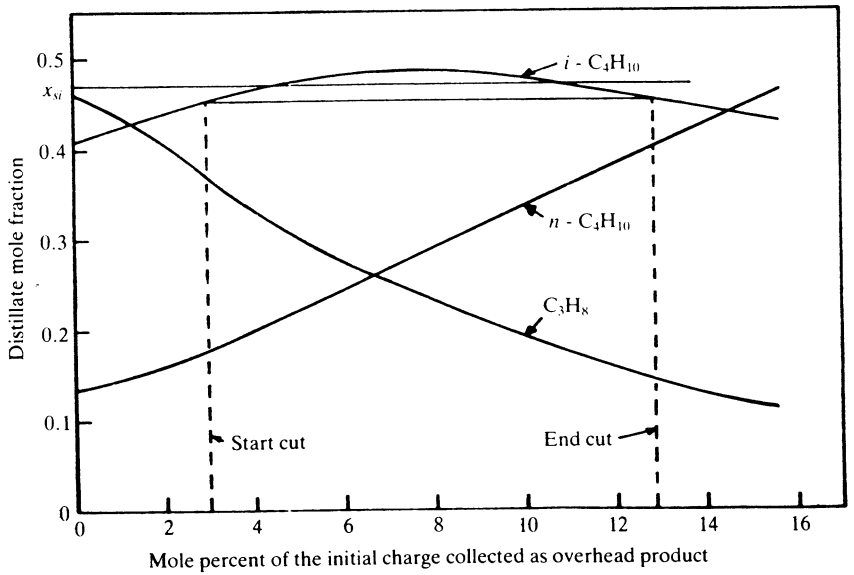

Figure 5-9 Results for Example 5-6: optimization of the yield of i-C_4H_{10} at $x_{si} = 0.47$.

method may be employed. For columns in the process of separating highly nonideal solutions, the latter methods which are presented in Chaps. 6, 7, 8, and 9 are recommended. Alternately, if the two-point implicit method is used, the number of independent variables should be increased to a set comparable with those used in Chaps. 6 through 8. Also, more exact models may be employed wherein hydraulic effects as well as the control system are included in the model as demonstrated in Chap. 8.

NOTATION

(See also Chap. 4.)

f_{ji} = an element of the vector f of Eq. (5-1)
f = a vector appearing in Eq. (5-1)
p_i = a quantity introduced for the purpose of avoiding division by zero (defined for a particular application below Eq. (5-8))
u_{ji} = molar holdup of component i in the liquid state on plate j
U_j = total molar holdup of the liquid on stage j
U_F = total moles of feed introduced to a batch distillation column

Greek letters

ρ_{ji} = a constant appearing on the central diagonal of the jth row of the coefficient matrix of the component-material balances (see, for example, Eq. (5-1))
$\sigma = (1 - \phi)/\phi$
$\tau_{av} = (U_j/L_j)_{av}/(\phi\ \Delta t)$
$\tau_j = (U_j/L_j)/(\phi\ \Delta t)$
ϕ = weight factor used in the implicit method (see Eq. (5-10))

REFERENCES

1. D. K. Barb: "Solution of Problems Involving the Separation of Multi-Component Mixtures by Batch Distillation," Ph.D. dissertation, Texas A&M University, 1967.
2. D. K. Barb and C. D. Holland: "Batch Distillation," *Proceedings of the 7th World Petroleum Congress*, **4**:31 (1967).
3. C. W. Carroll: *Operations Research*, **9**(2):169 (1961).
4. J. C. Chu: *Distillation Equilibrium Data, Reinhold Publishing Corp.*, New York, 1950.
5. M. T. Cichelli, W. D. Westerford, Jr., J. R. Bowman, and James Coull: "Binary Batch Distillation—Relation Between Number of Plates, Reflux Ratio, and Pole Height," *Ind. Eng. Chem.*, **42**:2502 (1940).
6. A. P. Colburn and R. F. Sterns: "The Effect of Column Holdup in Batch Distillation," *Trans. Am. Inst. Chem. Eng.* **37**:291 (1941).
7. A. O. Converse and G. P. Gross: "Optimal Distillation-Rate Policy in Batch Distillation," *I. & E.C. Fundam.*, **2**:217 (1963).
8. A. O. Converse and C. I. Huber: "Effect of Holdup on Batch Distillation Optimization," *I. & E.C. Fundam.*, **4**:475 (1965).
9. R. R. Driesbach: *Physical Properties of Chemical Compounds*, American Chemical Society, Washington, D.C., 1955.

10. R. R. Driesbach: *Physical Properties of Chemical Compounds—II*, American Chemical Society, Washington, D.C., 1959.
11. M. R. Fenske: "Fractionation of Straight-Run Pennsylvania Gasoline," *Ind. Eng. Chem.* **24**:482 (1932).
12. A. V. Fiacco and G. P. McCormick: "The Sequentially Unconstrained Minimization Technique for Nonlinear Programming, A Primal-Dual Method," *Manage. Sci.*, **10**(2):360 (1964).
13. A. V. Fiacco and G. P. McCormick: "Computational Minimization Technique for Nonlinear Programming," *Manage. Sci.*, **10**(4):601 (1964).
14. C. D. Holland: *Fundamentals of Multicomponent Distillation*, McGraw-Hill Book Company, New York (1981).
15. C. D. Holland: *Unsteady State Processes with Applications in Multicomponent Distillation*, Prentice-Hall, Inc., Englewood Cliffs, N.J. 1966.
16. C. D. Holland and N. W. Welch: "Steam Batch Distillation Calculations," *Hydrocarbon Process. Pet. Refiner* **36**:251 (1957).
17. C. E. Huckaba and D. E. Dandly: "Calculation Procedures for Binary Batch Rectification," *AIChE J.*, **6**:335 (1960).
18. E. L. Meadows: "Multicomponent Batch-Distillation Calculations on a Digital Computer," *Chem. Eng. Prog. Symp. Ser. Process Syst. Eng.*, **59**(46):48 (1963).
19. W. L. McCabe and E. W. Thiele: "Graphical Design of Fractionating Columns," *Ind. Eng. Chem.*, **17**:605 (1925).
20. L. G. Mitten and T. Prabhakar: "Optimization of Batch-Reflux Process by Dynamic Programming," *Chem. Eng. Prog. Symp. Ser.*, **60**(50):53 (1964).
21. Mijares, Gerardo, M.S. thesis, Texas A&M University, 1982.
22. J. H. Perry (Editor-in-chief): *Chemical Engineers Handbook*, 2d ed., McGraw-Hill Book Company, New York, 1941, 1938.
23. Lord Rayleigh (J. Strutt): "On the Distillation of Binary Mixtures," *Phil. Mag.* (6) **4**:527 (1902).
24. C. S. Robinson and E. R. Gilliland: *Elements of Fractional Distillation*, 4th ed. McGraw-Hill Book Company, New York, 1950.
25. Arthur Rose: "General Equation for a Batch Distillation Curve," *Ind. Eng. Chem.*, **32**:675 (1940).
26. Arthur Rose and V. S. O'Brien: "Effect of Holdup-Charge Ratio in Laboratory Ternary Batch Distillation," *Ind. Eng. Chem.*, **44**:1480 (1952).
27. E. H. Smoker and Arthur Rose: "Graphic Determination of Batch Distillation Curves for Binary Mixtures," *Trans. Am. Inst. Chem. Eng.*, **36**:285 (1940).
28. R. C. Waggoner: "Solution of Unsteady State Distillation Problems," Ph.D. Dissertation, Texas A&M University, 1964.
29. R. C. Waggoner and C. D. Holland: "Solution of Problems Involving Conventional and Complex Columns at Unsteady State Operation," *AIChE J.*, **11**:112 (1965).

PROBLEMS

5-1 (*a*) For a batch-distillation column operating in the product period ($D > 0$) and for which all of the holdups are negligible except for the still pot, show that the component-material balances and the total-material balances over the time period from t_n to $t_n + \Delta t$ yield the following differential equations.

Hint: Use the mean value theorems and the appropriate limiting process to reduce the integral-difference equations to the following differential equations:

$$-DX_{Di} = \frac{d(U_N x_{Ni})}{dt}$$

$$-D = \frac{dU_N}{dt}$$

(*b*) From the results given in part (*a*), obtain the following equation of Smoker and Rose(27).

$$\ln \frac{U_N}{U_N^0} = \int_{x_{Ni}^0}^{x_{Ni}} \frac{dx_{Ni}}{X_{Di} - x_{Ni}}$$

where the superscript zero denotes the values of the variables at time $t = 0$. Smoker and Rose(27) proposed that the integral appearing on the right-hand side of the above equation be evaluated by use of the graphical method of McCabe and Thiele(19).

5-2 A batch distillation with a single plate, the reboiler, is carried out at constant temperature and pressure by increasing the rate of flow of steam to the column to compensate for the decrease in the concentration of the lower boiling components over the course of the distillation. Also, the unit is to be operated such that the partial pressure of steam in the vapor product is less than the saturation pressure of steam at the temperature of the reboiler. (This problem is based on the development given by Holland and Welch(16)).

(*a*) Beginning with the overall material balance on component i in a batch-distillation column with a single stage and a withdrawal rate D, show that

$$-DX_{Di} = \frac{du_i}{dt}$$

where the plate subscript which would normally be carried by u_i has been dropped, and where

$D = D_v + D_s$
D_v = the molar flow rate of two-phase (or volatile) components in the distillate
D_s = molar flow rate of steam in the distillate at any time t

(*b*) Show

$$-D_v = \frac{dU}{dt}$$

(*c*) By use of the results obtained in part (*a*), show that

$$\alpha_i \left(\frac{u_i}{u_b}\right) = \frac{du_i}{du_b}$$

and that

$$u_i = u_i^0 \left(\frac{u_b}{u_b^0}\right)^{\alpha_i}$$

for all components ($i = 1$ through $i = c$) except steam ($i \neq s$). The superscript zero refers to the values of the variables at $t = 0$. Also in the development of this expression, equilibrium between the vapor (X_{Di}) leaving the column and the liquid (x_i) in the reboiler is assumed, that is,

$$X_{Di} = K_i x_i = K_i \frac{u_i}{U}$$

(*d*) Show that

$$U \frac{du_b}{u_b} = K_b(dU - d\mathscr{D}_s)$$

and that the steam requirement $\mathscr{D}_s$ is given by

$$\sum_{i}^{c} \frac{u_i^0}{} \left[1 - \left(\frac{u_b}{}\right)^{\alpha_i}\right] = K_s(U^0 - U + \mathscr{D}_s)$$

where

$$\frac{d\mathscr{D}_s}{dt} = D_s$$

5-3 (*a*) If the model for the vaporization efficiency (defined by $y_{ji} = E_{ji} K_{ji} x_{ji}$) is taken to be

$$E_{ji} = \beta_j \bar{E}_i$$

as originally suggested by Professor W. H. McAdams (according to Perry(22)), show that α_i in the final result of Prob. 5-2 should be replaced by

$$\frac{\bar{E}_i \alpha_i}{\bar{E}_b}$$

5-4 (*a*) For the case of a batch-distillation column at steady state at total reflux, show that the component-material balances and equilibrium relationships may be restated as follows where $\alpha_{ji} = \alpha_i$ for all j:

$$\frac{u_{2i}}{u_{1i}} = \frac{1}{\alpha_i}\left(\frac{u_{2b}}{u_{1b}}\right)$$

$$\frac{u_{3i}}{u_{1i}} = \frac{1}{\alpha_i^2}\left(\frac{u_{3b}}{u_{1b}}\right)$$

$$\vdots \quad \vdots \quad \vdots$$

$$\frac{u_{Ni}}{u_{1i}} = \frac{1}{\alpha_i^{N-1}}\left(\frac{u_{Nb}}{u_{1b}}\right)$$

(*b*) Suppose that a column is operating at a set of holdups denoted by $(U_1)_1, (U_2)_1, \ldots, (U_N)_1$, and by some scheme, these holdups are changed to the new set denoted by the subscripts $(U_2)_2, (U_2)_2, \ldots, (U_N)_2$. Show that the u_{ji}/u_{1i}'s for the two sets of operations are related by the same multiplier for all components; that is, show that

$$\left(\frac{u_{ji}}{u_{1i}}\right)_2 = \theta_j \left(\frac{u_{ji}}{u_{1i}}\right)_1 \tag{B}$$

where

$$\theta_j = \left(\frac{u_{jb}}{u_{1b}}\right)_2 \Big/ \left(\frac{u_{jb}}{u_{1b}}\right)_1$$

5-5 (*a*) Show that for a batch-distillation column for which $N = 3$, the overall material balance for the start-up period is given by

$$u_{1i} = \frac{U_F X_i}{1 + \dfrac{u_{2i}}{u_{1i}} + \dfrac{u_{3i}}{u_{1i}}} = \frac{U_F X_i}{1 + \dfrac{1}{\alpha_i}\left(\dfrac{u_{2b}}{u_{1b}}\right) + \dfrac{1}{\alpha_i^2}\left(\dfrac{u_{2b}}{u_{1b}}\right)} \tag{C}$$

(*b*) Use Eq. (C) and the results of part (*a*) to determine the holdups U_1, U_2, and U_3 for the two sets of specifications given:

Component	α_i	X_i	Other specifications
1	1	1/3	$N = 3$, $U_F = 100$
2	2	1/3	Set 1: $\dfrac{u_{2b}}{u_{1b}} = 2$, $\dfrac{u_{3b}}{u_{1b}} = 3$
3	3	1/3	Set 2: $\dfrac{u_{2b}}{u_{1b}} = 4$, $\dfrac{u_{3b}}{u_{1b}} = 6$

Ans.: $U_1 = 34.3434$, $U_2 = 34.34343$, $U_3 = 31.31313$.

Ans.: $U_1 = 21.5488$, $U_2 = 41.75084$, $U_3 = 36.7009$.

5-6 Suppose that the column described in part (*a*) of Prob. 5-4 is initially operating at the holdups given for set 1. At this set of holdups, the corresponding values of u_{ji}/u_{1i} are as follows:

Component	$(u_{2i}/u_{1i})_1$	$(u_{3i}/u_{1i})_1$
1	2.000 00	3.000 00
2	1.000 00	0.750 00
3	0.666 66	0.333 33

On the basis of these results, use the θ method of convergence to determine the u_{ji}/u_{1i}'s at the second set of holdups $U_1 = 21.5488$, $U_2 = 41.75084$, $U_3 = 36.7009$. That is, find θ_2 and θ_3 that make $g_1 = g_2 = 0$ simultaneously

$$g_1(\theta_2, \theta_3) = \sum_{i=1}^{c} u_{2i} - U_2$$

$$g_2(\theta_2, \theta_3) = \sum_{i=1}^{c} u_{3i} - U_3$$

Ans.: $\theta_2 = 2$, $\theta_3 = 2$.

5-7 Begin with the integral-difference equations for the energy balance, the component-material balances, and the total-material balances, and obtain the expressions given in item 1 of Table 5-1 for computing the total flow rates $\{V_j\}$ and $\{L_j\}$ at the time period under consideration for the start-up period.

5-8 Develop the expressions given in item 2 of Table 5-1.

5-9 Restate the formulation of the θ method for the product period (Eqs. (5-14), (5-15), (5-16), and (5-17)) in terms of an appropriately defined p_i.

APPENDIX 5A-1

Table 5A-1 *K* values and enthalpies for Examples 5-1, 5-2, and 5-6

1. *K* Values (1) at $P = 300$ lb/in^2 abs

$$(K_i/T)^{1/3} = a_{1i} + a_{2i}T + a_{3i}T^2 + a_{4i}T^3, \ (T \text{ in } ^\circ\text{R})$$

Component	$a_1 \times 10^2$	$a_2 \times 10^5$	$a_3 \times 10^8$	$a_4 \times 10^{12}$
C_3H_8	−14.512 474	53.638 924	−5.305 160 4	−173.583 29
i-C_4H_{10}	−18.967 651	61.239 667	−17.891 649	−90.855 512
n-C_4H_{10}	−14.181 715	36.866 353	16.521 412	−248.238 43
i-C_5H_{12}	−7.548 840	3.262 363 1	58.507 340	−414.923 23
n-C_5H_{12}	−7.543 539	2.058 423 1	59.138 344	−413.124 09

2. Enthalpy data (Ref. 2) at $P = 300$ lb/in^2 abs

$$(h_i)^{1/2} = c_{1i} + c_{2i}T + c_{3i}T^2, \ (H_i)^{1/2} = e_{1i} + e_{2i}T + e_{3i}T^2, \ (T \text{ in } ^\circ\text{R})$$

Component	c_1	$c_2 \times 10$	$c_3 \times 10^5$
C_3H_8	−14.500 060	1.980 222 3	−2.904 883 7
i-C_4H_{10} 16.553 405	2.161 865 0	−3.147 620 9	
n-C_4H_{10}	−20.298 110	2.300 574 3	−3.866 341 7
i-C_5H_{12}	−23.356 460	2.501 745 3	−4.391 789 7
n-C_5H_{12}	−24.371 540	2.563 620 0	−4.649 969 4

Table 5A-1—*Continued*

Component	e_1	$e_2 \times 10^4$	$e_3 \times 10^6$
C_3H_8	81.795 910	389.819 19	36.470 900
i-C_4H_{10}	147.654 14	−1185.294 2	152.877 78
n-C_4H_{10}	152.667 98	−1153.484 2	146.641 25
i-C_5H_{12}	130.966 79	−197.986 04	82.549 947
n-C_5H_{12}	128.901 52	−2.050 960 3	64.501 496

1. S. T. Hadden: "Vapor-Liquid Equilibria in Hydrocarbon Systems," *Chem. Eng. Prog.* **44**: 37 (1948).
2. J. B. Maxwell: *Data Book on Hydrocarbons*, D. Van Nostrand Company, Inc., New York (1956).

APPENDIX 5A-2

Table 5A-2 Data used for Examples 5-3, 5-4, and 5-5

1. K values (Ref. 1)

$$K_{ji} = C_{1i} + C_{2i}\left(\frac{T_j}{1.8} - C_{3i}\right), (T \text{ in } °R)$$

Component	C_1	C_2	C_3
n-heptane	0.94	0.0735	371.0
Methyl cyclohexane	0.85	0.0820	371.0
Toluene	0.60	0.0330	371.0

2. Liquid enthalpies (Refs. 2, 3)

$$h_{ji} = C_{1i}(T_j - 635) + C_{2i} - C_{3i}[(T_j/1.8) - 273]$$

Component	C_1	C_2	C_3
n-heptane	60.12	0.0	0.0
Methyl cyclohexane	58.91	0.0	0.0
Toluene	40.54	0.0	0.0

3. Vapor Enthalpies (Refs. 2, 3)

$$H_{ji} = C_{1i}(T_j - 635) + C_{2i} - C_{3i}[(T_j/1.8) - 273], (T \text{ in } °R)$$

Component	C_1	C_2	C_3
n-heptane	60.12	16 580.2	29.9211
Methyl cyclohexane	58.91	15 882.5	22.1793
Toluene	40.54	16 912.5	22.7534

4. Liquid density (Refs. 2, 3)

$$\rho_L = C_2 + C_3[(T_j/1.8) - 273] - \left(\frac{C_1}{22\,400}\right)\left(\frac{492}{T_j}\right)(P)$$

where ρ_L = density, g/cm^3
P = pressure, 1 atm
T = temperature, °R

Component	C_1	C_3	C_3
n-heptane	100.198	0.700 75	-0.840×10^{-3}
Methyl cyclohexane	98.182	0.786 70	-0.856×10^{-3}
Toluene	92.134	0.885 47	-0.924×10^{-3}

1. J. C. Chu: *Distillation Equilibrium Data*, Reinhold Publishing Corp., New York (1950).
2. R. R. Dreisback: *Physical Properties of Chemical Compounds*, American Chemical Society, Washington, D.C. (1955).
3. R. R. Dreisback: *Physical Properties of Chemical Compounds—II*, American Chemical Society, Washington, D.C. (1959).

PART

TWO

SOLUTION OF STAGED SEPARATION PROBLEMS BY USE OF A SEMI-IMPLICIT RUNGE-KUTTA METHOD AND GEAR'S METHOD

PART

TWO

SOLUTION OF STAGED SEPARATION PROBLEMS BY USE OF A SEMI-IMPLICIT RUNGE-KUTTA METHOD AND GEAR'S METHOD

CHAPTER

SIX

SOLUTION OF UNSTEADY STATE ABSORBER PROBLEMS BY USE OF A SEMI-IMPLICIT RUNGE–KUTTA METHOD AND GEAR'S METHOD

Application of Michelsen's modification (Refs. 8, 9) of the semi-implicit Runge–Kutta method proposed by Caillaud and Padmanabhan(1) as well as Gear's algorithm (Refs. 3, 4) to the equations for an absorber are demonstrated in this chapter. The equations describing the dynamic behavior of an absorber consist of a large set of coupled differential and algebraic equations.

The semi-implicit Runge–Kutta integration formula which was presented and applied in Chap. 1 is modified in Sec. 6-1 such that it may be used to solve a system of coupled differential and algebraic equations. Also, a procedure for changing the step size in a manner which increases the accuracy and efficiency of the semi-implicit Runge–Kutta is presented.

In Sec. 6-2, the application of Gear's method to the solution of simultaneous differential and algebraic equations is demonstrated. The procedure for making a simultaneous change in the order of the method and in the length of the step size is also presented.

In Sec. 6-3, the equations used by McDaniel(10,11) in the modeling of an absorber are formulated and solved by both the Runge–Kutta and Gear methods.

6-1 APPLICATION OF THE SEMI-IMPLICIT RUNGE–KUTTA METHOD TO SYSTEMS OF COUPLED DIFFERENTIAL AND ALGEBRAIC EQUATIONS

Michelsen's modified form of the semi-implicit Runge–Kutta method proposed by Caillaud and Padmanabhan for solving systems of differential equations

$$\frac{d\mathbf{y}}{dt} = \mathbf{f}(\mathbf{y}) \tag{6-1}$$

is modified as shown below such that it can be used to solve coupled differential and algebraic equations. The semi-implicit Runge–Kutta method proposed by Michelsen(8) is given by

$$\begin{aligned}
\mathbf{k}_1 &= h[\mathbf{I} - ha\mathbf{J}_n]^{-1}\mathbf{f}(\mathbf{y}_n) \\
\mathbf{k}_2 &= h[\mathbf{I} - ha\mathbf{J}_n]^{-1}\mathbf{f}(\mathbf{y}_n + b_2\mathbf{k}_1) \\
\mathbf{k}_3 &= [\mathbf{I} - ha\mathbf{J}_n]^{-1}[b_{31}\mathbf{k}_1 + b_{32}\mathbf{k}_2] \\
\mathbf{y}_{n+1} &= \mathbf{y}_n + R_1\mathbf{k}_1 + R_2\mathbf{k}_2 + R_3\mathbf{k}_3
\end{aligned} \tag{6-2}$$

where h = time step
$\mathbf{I}$ = identity matrix
$\mathbf{J}_n$ = jacobian matrix which contains the partial derivatives of $\mathbf{f}$ with respect to the variables $\mathbf{y}$; evaluated at $\mathbf{y}_n$

The constants or parameters in Eq. (6-2) have the following values:

$$\begin{aligned}
&a = 0.435\,867 \\
&b_2 = 3/4 \qquad b_{31} = -0.630\,172 \qquad b_{32} = -0.242\,35 \\
&R_1 = 1.037\,58 \qquad R_2 = 0.834\,94 \qquad R_3 = 1
\end{aligned} \tag{6-3}$$

Michelsen's Algorithm of the Semi-Implicit Runge–Kutta Method for Coupled Differential and Algebraic Equations

Coupled differential and algebraic equations of the form

$$\frac{d\mathbf{y}}{dt} = \mathbf{f}(\mathbf{y}, \mathbf{z}) \tag{6-4}$$

$$\mathbf{0} = \mathbf{g}(\mathbf{y}, \mathbf{z}) \tag{6-5}$$

are encountered in the modeling of separation processes. If the algebraic equations are linear in the z's, then they are easily handled. The z's may be regarded as dependent variables, and for any choice of the y's, the corresponding set of z's is readily obtained by solving the algebraic equations which are of the form of Eq. (6-5). In the interest of simplicity, only one differential equation and one algebraic equation are considered in the following development. The final result

may be generalized for the case of any number of equations as implied by Eqs. (6-4) and (6-5). In the calculation of df/dy, the chain rule may be applied as follows:

$$\frac{df}{dy} = \frac{\partial f}{\partial y} + \frac{\partial f}{\partial z}\frac{\partial z}{\partial y} \tag{6-6}$$

The linear equation in z, $g(y, z) = 0$, may be used to compute the partial derivative $\partial z/\partial y$.

If the equation $g(y, z)$ is nonlinear in z, either one of two procedures may be used, Michelsen's method (Ref. 8) or the generalized algorithm for systems of differential and algebraic equations. The development of Michelsen's method is given below and the generalized algorithm is presented in a subsequent section.

The first step in the development of Michelsen's algorithm is the transformation of the algebraic equations into a set of stiff differential equations as follows:

$$\frac{dy}{dt} = f(y, z) \tag{6-7}$$

$$\frac{dz}{dt} = \frac{1}{\varepsilon}g(y, z) \tag{6-8}$$

where ε is taken to be exceedingly small. The jacobian $\mathbf{J}$ of this set of equations is given by

$$\mathbf{J} = \begin{bmatrix} f_y & f_z \\ \dfrac{1}{\varepsilon}g_y & \dfrac{1}{\varepsilon}g_z \end{bmatrix} \tag{6-9}$$

where the symbols appearing in $\mathbf{J}$ have the usual meanings, namely,

$$f_y = \frac{\partial f}{\partial y} \qquad f_z = \frac{\partial f}{\partial z} \qquad g_y = \frac{\partial g}{\partial y} \qquad g_z = \frac{\partial g}{\partial z}$$

Integration of Eqs. (6-4) and (6-5) by use of Michelsen's semi-implicit Runge–Kutta method yields the following vector for $\mathbf{k}_1$.

$$\begin{bmatrix} k_{1y} \\ k_{1z} \end{bmatrix} = h\begin{bmatrix} (1 - haf_y) & (-haf_z) \\ \left(-\dfrac{1}{\varepsilon}hag_y\right) & \left(1 - \dfrac{hag_z}{\varepsilon}\right) \end{bmatrix}^{-1}\begin{bmatrix} f(y_n, z_n) \\ \dfrac{1}{\varepsilon}g(y_n, z_n) \end{bmatrix} \tag{6-10}$$

or

$$\begin{bmatrix} (1 - haf_y) & (-haf_z) \\ \left(-\dfrac{1}{\varepsilon}hag_y\right) & \left(1 - \dfrac{hag_z}{\varepsilon}\right) \end{bmatrix}\begin{bmatrix} k_{1y} \\ k_{1z} \end{bmatrix} = h\begin{bmatrix} f(y_n, z_n) \\ \dfrac{1}{\varepsilon}g(y_n, z_n) \end{bmatrix} \tag{6-11}$$

After row 2 of Eq. (6-11) has been multiplied by ε and the limit has been taken as ε approaches zero, one obtains the following result upon rearrangement:

$$\begin{bmatrix} F_y & f_z \\ g_y & g_z \end{bmatrix} \begin{bmatrix} k_{1y} \\ k_{1z} \end{bmatrix} = -\frac{1}{a} \begin{bmatrix} f(y_n, z_n) \\ g(y_n, z_n) \end{bmatrix} \tag{6-12}$$

where

$$F_y = f_y - \frac{1}{ha}$$

This formula is easily implemented because of the similarity of the coefficient matrix of Eq. (6-12) and the jacobian matrix.

By following the same procedure shown above for $\mathbf{k}_1$, the following formulas are obtained for $\mathbf{k}_2$ and $\mathbf{k}_3$:

$$\begin{bmatrix} F_y & f_z \\ g_y & g_z \end{bmatrix} \begin{bmatrix} k_{2y} \\ k_{2z} \end{bmatrix} = -\frac{1}{a} \begin{bmatrix} f(y_n + b_2 k_{1y}, z_n + b_2 k_{1z}) \\ g(y_n + b_2 k_{1y}, z_n + b_2 k_{1z}) \end{bmatrix} \tag{6-13}$$

and

$$\begin{bmatrix} F_y & f_z \\ g_y & g_z \end{bmatrix} \begin{bmatrix} k_{3y} \\ k_{3z} \end{bmatrix} = -\frac{1}{ha} \begin{bmatrix} \alpha \\ 0 \end{bmatrix} \tag{6-14}$$

where

$$\alpha = b_{31} k_{1y} + b_{32} k_{2y}$$

The use of the semi-implicit Runge–Kutta method for solving coupled differential and algebraic equations is demonstrated through the use of the following numerical example.

Example 6-1 For the following set of equations

$$\frac{dy}{dt} = z - y$$

$$0 = -\frac{1}{2} y + z - 2$$

find the values of y and z at the end of the first time step by use of the Michelsen's version of the semi-implicit Runge–Kutta method for $h = 1/20$ and for the following set of initial conditions:

$$y(0) = 1/2 \qquad z(0) = 9/4 \qquad y'(0) = 7/4 \qquad z'(0) = 7/8$$

SOLUTION

Let

$$f(y, z) = z - y$$

$$g(y, z) = -\frac{1}{2} y + z - 2$$

Then

$$f(y_0, z_0) = \frac{9}{4} - \frac{1}{2} = \frac{7}{4}$$

$$g(y_0, z_0) = \left(-\frac{1}{2}\right)\left(\frac{1}{2}\right) + \frac{9}{4} - 2 = 0$$

and

$$f_y = \frac{\partial f}{\partial y} = -1 \qquad f_z = \frac{\partial f}{\partial z} = 1$$

$$g_y = \frac{\partial g}{\partial y} = -\frac{1}{2} \qquad g_z = \frac{\partial g}{\partial z} = 1$$

Since $a = 0.4359$ and $h = 0.05$

$$\frac{1}{ha} = \frac{1}{(0.05)(0.4359)} = 45.89$$

and Eq. (6-12) becomes

$$\begin{bmatrix} -46.89 & 1 \\ -0.5 & 1 \end{bmatrix} \begin{bmatrix} k_{1y} \\ k_{1z} \end{bmatrix} = -\frac{1}{0.4359} \begin{bmatrix} 1.75 \\ 0 \end{bmatrix}$$

which is readily solved to give

$$k_{1y} = 0.086\,56$$

$$k_{1z} = 0.043\,28$$

Then

$$y_0 + b_2 k_{1y} = 0.5 + (0.75)(0.086\,56) = 0.564\,92$$

$$z_0 + b_2 k_{1z} = 2.25 + (0.75)(0.043\,28) = 2.282\,46$$

$$f(0.564\,92, 2.282\,46) = 2.282\,46 - 0.564\,92 = 1.717\,54$$

$$g(0.564\,92, 2.282\,46) = \left(-\frac{1}{2}\right)(0.564\,92) + 2.282\,46 - 2 = 0$$

Next k_{2y} and k_{2z} are computed by use of the following form of Eq. (6-13):

$$\begin{bmatrix} -46.89 & 1 \\ -0.5 & 1 \end{bmatrix} \begin{bmatrix} k_{2y} \\ k_{2z} \end{bmatrix} = -\frac{1}{(0.4359)} \begin{bmatrix} 1.717\,54 \\ 0 \end{bmatrix}$$

which leads to

$$k_{2y} = 0.084\,94$$

$$k_{2z} = 0.042\,47$$

Then

$$\alpha = b_{31}k_{1y} + b_{32}k_{2y} = (-0.630\,172)(0.086\,56) + (-0.2435)(0.084\,94)$$
$$= -0.075\,235$$

Next, k_{3y} and k_{3z} are computed by use of Eq. (6-14),

$$\begin{bmatrix} -46.89 & 1 \\ -0.5 & 1 \end{bmatrix}\begin{bmatrix} k_{3y} \\ k_{3z} \end{bmatrix} = \frac{-1}{(0.05)(0.4359)}\begin{bmatrix} -0.075\,235 \\ 0 \end{bmatrix}$$

which lead to

$$k_{3y} = -0.074\,412$$
$$k_{3z} = -0.037\,205$$

Thus, by use of the last expression of Eq. (6-2), one obtains

$$\begin{bmatrix} y_1 \\ z_1 \end{bmatrix} = \begin{bmatrix} 0.5 \\ 2.25 \end{bmatrix} + 1.037\,58\begin{bmatrix} 0.086\,56 \\ 0.043\,28 \end{bmatrix} + 0.834\,94\begin{bmatrix} 0.084\,94 \\ 0.042\,47 \end{bmatrix}$$
$$+ (1)\begin{bmatrix} -0.074\,412 \\ -0.037\,205 \end{bmatrix} = \begin{bmatrix} 0.5863 \\ 2.2932 \end{bmatrix}$$

The behavior of this method for different choices of h as well as the Caillaud and Padmanabhan version of the semi-implicit Runge–Kutta method and Gear's method is presented in Table 6-1.

A Generalized Semi-Implicit Runge–Kutta Algorithm for Systems of Coupled Differential and Algebraic Equations

For many systems of equations, Michelsen's method presented above becomes too time-consuming because of the relatively large number of independent variables and equations. The number of variables normally required in the formulation may be reduced through the use of the generalized semi-implicit Runge–Kutta method for systems. First, this method is developed for a system of differential equations and then it is developed for a system of coupled differential and algebraic equations.

Systems of differential equations Consider the general case where the differential equations are of the form

$$\mathbf{A}_{(n\times n)}\left[\frac{d\mathbf{y}}{dt}\right]_{(n\times 1)} = \mathbf{F}(\mathbf{y})_{(n\times 1)} \tag{6-15}$$

where the dimension of each matrix is carried as a subscript in Eq. (6-15). The subscript n is used hereafter in the semi-implicit Runge–Kutta formulas to denote the number of rows or columns in a matrix, and the number of the time

Table 6-1 Summary of results obtained by different numerical methods for Example 6-1 for step sizes

1. Results obtained at end of one time step

Step size h	Gear's method (2d order)	Cailland and Padmanabhan	Michelsen	Exact solution†
0.5	$y_1 = 1.281\,250$ $z_1 = 2.640\,625$	1.274 438 2.637 218	1.274 434 2.637 099	1.274 20 2.637 10
0.05	$y_1 = 0.586\,424$ $z_1 = 2.293\,212$	0.586 415 2 2.293 208	0.586 415 1 2.293 209	0.586 416 2.293 208
0.005	$y_1 = 0.508\,739$ $z_1 = 2.254\,37$	0.508 739 2.254 369	0.508 738 9 2.254 370	0.508 739 5 2.254 370
0.000 5	$y_1 = 0.500\,874\,9$ $z_1 = 2.250\,438$	0.500 874 8 2.250 438	0.500 874 8 2.250 435	0.500 875 5 2.250 438
0.000 05	$y_1 = 0.500\,087\,5$ $z_1 = 2.250\,044$	0.500 087 4 2.250 044	0.500 087 4 2.250 045	0.050 008 77 2.250 044

2. Results obtained at the end of several time steps

Step size h and number of steps	Gear's Method (2d order)	Caillaud and Padmanabhan	Michelsen	Exact solution†
$h = 0.5$ 10 steps	$y_{10} = 3.729\,600$ $z_{10} = 3.864\,799$	3.712 950 3.856 476	3.712 949 3.856 474	3.712 702 3.856 351
$h = 0.05$ 30 steps	$y_{30} = 2.346\,949$ $z_{30} = 3.173\,464$	2.346 693 3.173 345	2.346 689 3.173 344	2.346 710 3.173 355
$h = 0.005$ 30 steps	$y_{30} = 0.752\,895$ $z_{30} = 2.376\,448$	0.752 895 2 2.376 449	0.752 894 8 2.376 447	0.752 898 2 2.376 450
$h = 0.0005$ 30 steps	$y_{30} = 0.526\,150\,7$ $z_{30} = 2.263\,076$	0.526 149 5 2.263 075	0.526 149 3 2.263 075	0.526 152 6 2.263 077

† $y(t) = 4 - (4 - y(0))e^{-t/2}$
$z(t) = 4 - (4 - z(0))e^{-t/2}$

step is denoted by k. The matrix $\mathbf{A}$ in Eq. (6-15) is independent of y and has the inverse $\mathbf{A}^{-1}$. Since $\mathbf{A}$ is assumed to have an inverse, it may be solved for $d\mathbf{y}/dt$ to give

$$\frac{d\mathbf{y}}{dt} = \mathbf{A}^{-1}\mathbf{F}(\mathbf{y}) = \mathbf{f}(\mathbf{y})$$

where the right-hand side has been denoted by $\mathbf{f}(\mathbf{y})$ to give an equation of the same form as Eq. (6-1). Thus, for the system under consideration, the first expression of Eq. (6-2) may be stated in the form

$$[\mathbf{I} - ha\mathbf{A}^{-1}\mathbf{J}_k][\mathbf{k}_1] = h\mathbf{A}^{-1}\mathbf{F}(\mathbf{y}_k) \tag{6-16}$$

where

$$\mathbf{J} = \text{jacobian of} \left[\frac{\partial \mathbf{F}(\mathbf{y})}{\partial y_l} \qquad (l = 1, 2, \ldots, n) \right]$$

Premultiplication of each member of Eq. (6-16) by $\mathbf{A}$ gives the following expression for computing $\mathbf{k}_1$:

$$[\mathbf{A} - ha\mathbf{J}_k][\mathbf{k}_1] = h\mathbf{F}(\mathbf{y}_k) \tag{6-17}$$

Similarly, the expression for $\mathbf{k}_2$ becomes

$$[\mathbf{A} - ha\mathbf{J}_k][\mathbf{k}_2] = h\mathbf{F}(\mathbf{y}_n + b_2\mathbf{k}_1) \tag{6-18}$$

The expression for computing $\mathbf{k}_3$ is obtained by beginning with the third expression of Eq. (6-2) and carrying out the same set of operations outlined for $\mathbf{k}_1$ to obtain

$$[\mathbf{A} - ha\mathbf{J}_k][\mathbf{k}_3] = \mathbf{A}[b_{31}\mathbf{k}_1 + b_{32}\mathbf{k}_2] \tag{6-19}$$

Systems of differential and algebraic equations Consider the general system of equations

$$\mathbf{B}_{(m\times n)}\left[\frac{d\mathbf{y}}{dt}\right]_{(n\times 1)} = \mathbf{F}(\mathbf{y})_{(m\times 1)} \qquad (m \le n) \tag{6-20}$$

$$\mathbf{0}_{[(n-m)\times 1]} = \mathbf{G}(\mathbf{y})_{[(n-m)\times 1]} \tag{6-21}$$

where $\mathbf{0}$ is the null vector. The rank of the constant matrix $\mathbf{B}$ is m. Next let the square matrix $\mathbf{A}_{(n\times n)}$ be defined by the following partitioned matrix:

$$\mathbf{A}_{(n\times n)} = \begin{bmatrix} \mathbf{A}_{11} & \mathbf{A}_{12} \\ \mathbf{0}_{21} & \mathbf{A}_{22} \end{bmatrix} \tag{6-22}$$

where

$$\mathbf{A}_{11} = \mathbf{A}_{(m\times m)} \qquad \mathbf{A}_{12} = \mathbf{A}_{[m\times(n-m)]}$$

$$\mathbf{0}_{21} = \mathbf{0}_{[(n-m)\times m]} \qquad \mathbf{A}_{22} = \mathbf{A}_{[(n-m)\times(n-m)]} \qquad m \le n \qquad \text{also } [\mathbf{A}_{11} \quad \mathbf{A}_{12}] = \mathbf{B}$$

Let the elements of $\mathbf{A}_{22}$ be picked such that $\mathbf{A}_{(n\times n)}$ has the inverse $\mathbf{A}^{-1}_{(n\times n)}$. Also, let $\varepsilon > 0$ be picked with the understanding that eventually it will be allowed to go to zero. Thus Eqs. (6-20) and (6-21) may be restated in the following form:

$$\mathbf{A}_{(n\times n)}\left[\frac{d\mathbf{y}}{dt}\right]_{(n\times 1)} = \mathscr{F}(\mathbf{y})_{(n\times 1)} \tag{6-23}$$

where

$$\mathscr{F}(\mathbf{y})_{(n\times 1)} = \begin{bmatrix} \mathbf{F}(\mathbf{y}) \\ \dfrac{1}{\varepsilon}\mathbf{G}(\mathbf{y}) \end{bmatrix}_{(n\times 1)}$$

Then

$$\frac{d\mathbf{y}}{dt} = \mathbf{A}^{-1}\mathscr{F}(\mathbf{y}) = \mathbf{f}(\mathbf{y}) \tag{6-24}$$

Let the jacobian $\mathbf{J}$ in Eq. (6-2) be denoted by $\hat{\mathbf{J}}$,

$$\hat{\mathbf{J}} = \left\{\frac{\partial \mathbf{f}}{\partial y}\right\} = \mathbf{A}^{-1}\mathbf{J}$$

$$\mathbf{J} = \begin{bmatrix} \mathbf{J}_{11} & \mathbf{J}_{12} \\ \dfrac{\mathbf{J}_{21}}{\varepsilon} & \dfrac{\mathbf{J}_{22}}{\varepsilon} \end{bmatrix}$$

where

$$\mathbf{J}_{11} = \mathbf{J}_{(m\times m)} \qquad \mathbf{J}_{12} = \mathbf{J}_{[m\times(n-m)]}$$

$$\mathbf{J}_{21} = \mathbf{J}_{[(n-m)\times m]} \qquad \mathbf{J}_{22} = \mathbf{J}_{[(n-m)\times(n-m)]}$$

Thus, the first expression of Eq. (6-2) for $\mathbf{k}_1$ becomes

$$[\mathbf{I} - ha\mathbf{A}^{-1}\mathbf{J}(\mathbf{y}_k)][\mathbf{k}_1] = h\mathbf{A}^{-1}\mathscr{F}(\mathbf{y}_k) \tag{6-25}$$

Premultiplication by $\mathbf{A}$ gives

$$[\mathbf{A} - ha\mathbf{J}(\mathbf{y}_k)][\mathbf{k}_1] = h\mathscr{F}(\mathbf{y}_k) \tag{6-26}$$

The partitioned form of Eq. (6-26) is

$$\begin{bmatrix} \mathbf{A}_{11} & \mathbf{A}_{12} \\ \mathbf{0}_{21} & \mathbf{A}_{22} \end{bmatrix} - ha\begin{bmatrix} \mathbf{J}_{11} & \mathbf{J}_{12} \\ \dfrac{\mathbf{J}_{21}}{\varepsilon} & \dfrac{\mathbf{J}_{22}}{\varepsilon} \end{bmatrix}[\mathbf{k}_1] = h\begin{bmatrix} \mathbf{F}(\mathbf{y}_k) \\ \dfrac{1}{\varepsilon}\mathbf{G}(\mathbf{y}_k) \end{bmatrix} \tag{6-27}$$

and thus

$$\begin{bmatrix} [\mathbf{A}_{11} - ha\mathbf{J}_{11}] & [\mathbf{A}_{12} - ha\mathbf{J}_{12}] \\ \left[-\dfrac{ha}{\varepsilon}\mathbf{J}_{21}\right] & \left[\mathbf{A}_{22} - \dfrac{ha}{\varepsilon}\mathbf{J}_{22}\right] \end{bmatrix}[\mathbf{k}_1] = h\begin{bmatrix} \mathbf{F}(\mathbf{y}_k) \\ \dfrac{\mathbf{G}(\mathbf{y}_k)}{\varepsilon} \end{bmatrix} \tag{6-28}$$

Multiply those rows containing $1/\varepsilon$ by ε (as in gaussian elimination) and then set $\varepsilon = 0$. The resulting partitioned matrix for computing $\mathbf{k}_1$ is given by

$$\begin{bmatrix} [\mathbf{A}_{(m\times m)} - ha\mathbf{J}_{(m\times m)}] & [\mathbf{A}_{[m\times(n-m)]} - ha\mathbf{J}_{[m\times(n-m)]}] \\ [-ha\mathbf{J}_{[(n-m)\times m]}] & [-ha\mathbf{J}_{[(n-m)\times(n-m)]}] \end{bmatrix}[\mathbf{k}_1] = h\begin{bmatrix} \mathbf{F}(\mathbf{y}_k)_{(m\times 1)} \\ \mathbf{G}(\mathbf{y}_k)_{[(n-m)\times 1]} \end{bmatrix} \tag{6-29}$$

Beginning with the second expression of Eq. (6-2) and performing the same set of operations described above for the first expression of Eq. (6-2) gives the

following partitioned matrix for computing $\mathbf{k}_2$:

$$\begin{bmatrix} [\mathbf{A}_{(m\times m)} - ha\mathbf{J}_{(m\times m)}] & [\mathbf{A}_{[m\times(n-m)]} - ha\mathbf{J}_{[m\times(n-m)]}] \\ [-ha\mathbf{J}_{[(n-m)\times m]}] & [-ha\mathbf{J}_{[(n-m)\times(n-m)]}] \end{bmatrix} [\mathbf{k}_2] = h \begin{bmatrix} \mathbf{F}(\mathbf{y}_k + b_2\mathbf{k}_1)_{(m\times 1)} \\ \mathbf{G}(\mathbf{y}_k + b_2\mathbf{k}_2)_{[(n-m)\times 1]} \end{bmatrix} \tag{6-30}$$

The formula for calculating $\mathbf{k}_3$ is developed by commencing with the third expression of Eq. (6-2) and performing the same set of operations described for the first expression of Eq. (6-2). The following result is obtained

$$[\mathbf{A} - ha\mathbf{J}(\mathbf{y}_k)][\mathbf{k}_3] = \mathbf{A}[b_{31}\mathbf{k}_1 + b_{32}\mathbf{k}_3] \tag{6-31}$$

Again, as before

$$\begin{bmatrix} [\mathbf{A}_{11} - ha\mathbf{J}_{11}] & [\mathbf{A}_{12} - ha\mathbf{J}_{12}] \\ \left[\dfrac{-ha}{\varepsilon}\,\mathbf{J}_{21}\right] & \left[\mathbf{A}_{22} - \dfrac{ha}{\varepsilon}\,\mathbf{J}_{22}\right] \end{bmatrix} [\mathbf{k}_3] = \mathbf{A}[b_{31}\mathbf{k}_1 + b_{32}\mathbf{k}_2] \tag{6-32}$$

Multiply each row containing $1/\varepsilon$ by ε and then set $\varepsilon = 0$ to obtain the partitioned matrix formula for $\mathbf{k}_3$.

$$\begin{bmatrix} [\mathbf{A}_{(m\times m)} - ha\mathbf{J}_{(m\times m)}] & [\mathbf{A}_{[m\times(n-m)]} - ha\mathbf{J}_{[m\times(n-m)]}] \\ [-ha\mathbf{J}_{[(n-m)\times m]}] & [-ha\mathbf{J}_{[(n-m)\times(n-m)]}] \end{bmatrix} [\mathbf{k}_3] = \boldsymbol{\alpha}_{(n\times 1)} \tag{6-33}$$

where

$$\boldsymbol{\alpha} = [\alpha_1 \quad \alpha_2 \quad \cdots \quad \alpha_m \quad \alpha_{m+1} \quad \cdots \quad \alpha_n]^T \qquad \alpha_{m+1} = \alpha_{m+2} = \cdots = \alpha_n = 0$$

The nonzero elements $(\alpha_1, \alpha_2, \ldots, \alpha_m)$ are computed as follows:

$$\boldsymbol{\alpha}_{(m\times 1)} = \mathbf{A}_{(m\times n)}[b_{31}\mathbf{k}_1 + b_{32}\mathbf{k}_2] \tag{6-34}$$

Note, $\mathbf{A}_{(m\times n)}$ is actually equal to the matrix $\mathbf{B}_{(m\times n)}$ from the original set of equations, Eq. (6-20).

Selection of Step Size

The step size is to be selected such that the truncation error is maintained within some prescribed upper bound. Unfortunately no simple expressions are known for the precise truncation error in the Runge–Kutta methods (Ref. 6). The local truncation for an mth-order Runge–Kutta method can be approximated by

$$E = Ch^{m+1} \tag{6-35}$$

where C depends upon the higher-order partial derivatives. In order to approximate the truncation error, the following procedure which is based on the so-called Richardson extrapolation technique has been recommended by Michelsen(8).

Suppose that C in Eq. (6-35) remains constant. Then if an algorithm is applied k times in an integration in which the intervals of integration are equally spaced, the total truncation error resulting from the repeated application of the algorithm from $x = a$ to $x = b$ is given by

$$E_T = kCh^{m+1} \tag{6-36}$$

Since $h = (b - a)/k$ or $k = (b - a)/h$, Eq. (6-36) becomes

$$E_T = \frac{(b-a)}{h} Ch^{m+1} \tag{6-37}$$

Next, suppose that y_{k+1} is computed on the basis of two subintervals of sizes h_1 and h_2, where $h_2 = h_1/2$ over the interval from $x = a$ to $x = b$. Then the correct value of y_{k+1}, denoted by y^*_{k+1}, is related to the values $y_{k+1,1}$ and $y_{k+1,2}$ as follows:

$$y^*_{k+1} = y_{k+1,1} + \frac{(b-a)}{h_1} Ch_1^{m+1} \tag{6-38}$$

$$y^*_{k+1} = y_{k+1,2} + \frac{(b-a)}{h_2} Ch_2^{m+1} \tag{6-39}$$

where $y_{k+1,1}$ is computed on the basis of one time increment of size h_1 and $y_{k+1,2}$ is computed on the basis of two time increments of size h_2. Elimination of $(b - a)C$ from these two equations yields the following result upon rearrangement:

$$y^*_{k+1} = \frac{y_{k+1,1} - y_{k+1,2}(h_1/h_2)^m}{1 - (h_1/h_2)^m} \tag{6-40}$$

Since $h_2 = h_1/2$, it follows that

$$y^*_{k+1} = \frac{y_{k+1,1} - 2^m y_{n+1,2}}{1 - 2^m} \tag{6-41}$$

For a third-order Runge–Kutta method, Eq. (6-41) reduces to

$$y^*_{k+1} = \frac{8}{7} y_{k+1,2} - \frac{1}{7} y_{k+1,1} \tag{6-42}$$

The expression for the local truncation error for a single step is obtained by first setting $b - a = h_1$ in Eq. (6-38) to obtain

$$E = Ch_1^{m+1} = y^*_{k+1} - y_{k+1,1} \tag{6-43}$$

Elimination of y^*_{k+1} from Eqs. (6-41) and (6-43) yields

$$E = \frac{2^m(y_{k+1,2} - y_{k+1,1})}{2^m - 1} \tag{6-44}$$

which gives

$$E = \frac{8}{7}(y_{k+1,2} - y_{k+1,1}) \tag{6-45}$$

for a third-order Runge–Kutta. After E has been computed by use of Eq. (6-45), y^*_{k+1} may be computed by use of the following expression which is readily obtained from Eqs. (6-43) and (6-45).

$$y^*_{k+1} = y_{k+1,2} + \frac{E}{8} \tag{6-46}$$

or Eq. (6-43) may be solved directly for y^*_{k+1}. The value y^*_{k+1} is a better value of y_{k+1} than either $y_{k+1,1}$ or $y_{k+1,2}$.

Michelsen(8) proposed the following procedure for changing step size. Let $\boldsymbol{\varepsilon}$ be a prescribed vector of tolerances and let

$$g = \max_i \left| \left(\frac{y_{k+1,2} - y_{k+1,1}}{\varepsilon} \right)_i \right| \tag{6-47}$$

If $g < 1$, the integrated result is accepted and the solution value y^*_{k+1} is found for each member i by use of Eq. (6-46). If $g > 1$ the result is not accepted, and the integration from t_k is repeated with $h_3 = h_1/4$. Then E and y^*_{k+1} are computed by use of Eqs. (6-45) and (6-46) on the basis of $y_{n+1,3}$ and $y_{n+1,2}$, the values corresponding to $h_2 = h_1/2$ and $h_3 = h_1/4$, namely,

$$E = \frac{8}{7}(y_{k+1,3} - y_{k+1,2})$$
$$y^*_{k+1} = y_{k+1,3} + \frac{E}{8} \tag{6-48}$$

Once a step has been accepted, the proposed step length for the new step size h_{k+1} is selected as follows:

$$h_{k+1} = h_k \cdot \min[(4g)^{-0.25}, 3] \tag{6-49}$$

Thus, for $g < 0.25$, Eq. (6-49) gives an increase in h_{k+1} and for $g \leq 3^{-4}/4$, a maximum increase in step size by a factor of 3 is obtained. The factor of 4 in Eq. (6-49) and the empirical restriction on the maximum increase by a factor of 3 were recommended by Michelsen(8) as safety margins to avoid the selection of step sizes which are too large and which would lead to subsequent rejection (would yield values of $g > 1$).

The linear combination of two approximate solutions given by Eq. (6-46) yields a more accurate value of y_{k+1} than either of the two values, $y_{k+1,1}$ and $y_{k+1,2}$, because the dominant error term $0(h^4)$ tends to cancel when the two solutions are combined, and the method in effect becomes fourth order. However, the higher order is achieved at considerable computational expense, the

two extra steps with $h_2 = h_1/2$. Nevertheless, this one-step–two-step approach retains the stability properties of the algorithm, increases its accuracy by one order, and provides a simple means of adjusting the step size (Ref. 8).

6-2 APPLICATION OF GEAR'S METHOD TO SYSTEMS OF COUPLED DIFFERENTIAL AND ALGEBRAIC EQUATIONS

Solution of Differential and Algebraic Equations (Refs. 3, 4, 5)

Examination of the integration formulas (presented below) for Gear's method for systems of algebraic and differential equations such as

$$\frac{d\mathbf{y}}{dt} = \mathbf{f}(\mathbf{y}, \mathbf{z}, t)$$
$$\mathbf{0} = \mathbf{g}(\mathbf{y}, \mathbf{z}, t) \tag{6-50}$$

shows that the integration formulas for algebraic equations are precisely the same as those for differential equations. The fact that one method works for both algebraic and differential equations makes it possible to apply Gear's method to systems of equations in which $\mathbf{y}'$ occurs implicitly of the form

$$\mathbf{F}(\mathbf{y}, \mathbf{y}', \mathbf{z}, \mathbf{z}', t) = \mathbf{0} \tag{6-51}$$

It is not necessary to solve $\mathbf{F}$ for $\mathbf{y}'$ explicitly or to determine which are differential equations. These characteristics of Gear's method permit the formulation of an absorber problem in terms of a smaller set of equations and variables than is required in the formulation by use of the semi-implicit Runge–Kutta method. Equations of the general form

$$\mathbf{0} = \mathbf{f}(\mathbf{y}, \mathbf{z}, \mathbf{y}', \mathbf{z}')$$
$$\mathbf{0} = \mathbf{g}(\mathbf{y}, \mathbf{z}) \tag{6-52}$$

are characteristic of those used to describe the dynamic behavior of absorbers.

For convenience, the equations of Gear's kth-order algorithm for one differential and one algebraic equation are presented.

$$\mathbf{Y}_n = \left[y_n, hy'_n, \frac{h^2}{2!} y^{(2)}_n, \ldots, \frac{h^k}{k!} y^{(k)}_n \right]^T$$
$$\mathbf{Z}_n = \left[z_n, hz'_n, \frac{h^2}{2!} z^{(2)}_n, \ldots, \frac{h^k}{k!} z^{(k)}_n \right]^T \tag{6-53}$$
$$\tilde{\mathbf{Y}}_n = \mathbf{D}\mathbf{Y}_{n-1}$$
$$\tilde{\mathbf{Z}}_n = \mathbf{D}\mathbf{Z}_{n-1}$$

where **D** is the Pascal triangle matrix (see Chap. 1). The Newton–Raphson method is used to find the pair of values b_1 and b_2 which make $F_1(b_1, b_2)$ and $F_2(b_1, b_2)$ equal to zero.

$$\begin{aligned} F_1(b_1, b_2) &= F_1(\tilde{y}_n + \beta_{-1} b_1, h\tilde{y}'_n + b_1, \tilde{z}_n + \beta_{-1} b_2, h\tilde{z}'_n + b_2) \\ F_2(b_1, b_2) &= F_2(\tilde{y}_n + \beta_{-1} b_1, h\tilde{y}'_n + b_1, \tilde{z}_n + \beta_{-1} b_2, h\tilde{z}'_n + b_2) \end{aligned} \tag{6-54}$$

After the solution set $\{b_1, b_2\}$ has been found, the values of $\mathbf{Y}_n$ and $\mathbf{Z}_n$ are computed as follows:

$$\begin{aligned} \mathbf{Y}_n &= \tilde{\mathbf{Y}}_n + b_1 \mathbf{L} \\ \mathbf{Z}_n &= \tilde{\mathbf{Z}}_n + b_2 \mathbf{L} \end{aligned} \tag{6-55}$$

To illustrate the application of Gear's method to equations of the type of Eq. (6-52), Example 6-2 is presented.

Example 6-2 Use Gear's second-order method to compute y and z at the end of the first time step for the following set of equations:

$$0 = z - y + \frac{dz}{dt} - \frac{dy}{dt}$$

$$0 = z + 4y - 2$$

$$y(0) = 1/2 \qquad z(0) = 0$$

$$y'(0) = -0.1 \qquad z'(0) = 0.4$$

$$y^{(2)}(0) = 0.1 \qquad z^{(2)}(0) = -0.4$$

For Gear's second-order method: $\beta_{-1} = 2/3$, $\mathbf{L} = [2/3, 3/3, 1/3]^T$, and take $h = 0.5$.

SOLUTION Let the vectors **Y** and **Z** be defined as follows:

$$\mathbf{Y} = \left[y, hy', \frac{h^2}{2!} y^{(2)} \right]^T$$

$$\mathbf{Z} = \left[z, hz', \frac{h^2}{2!} z^{(2)} \right]^T$$

Then

$$y_0 = 0.5 \qquad hy'_0 = (0.5)(-0.1) = -0.05$$

$$\frac{h^2}{2!} y_0^{(2)} = \left(\frac{1}{4}\right)\left(\frac{1}{2}\right)(0.1) = 0.0125$$

and

$$z_0 = 0, \; hz'_0 = 0.2 \qquad \frac{h^2}{2!} z_0^{(2)} = \left(\frac{1}{4}\right)\left(\frac{1}{2}\right)(-0.4) = -0.05$$

Thus

$$\mathbf{Y}_0 = (0.5, -0.05, 0.0125)^T$$

$$\mathbf{Z}_0 = (0, 0.2, -0.05)^T$$

Then

$$\tilde{\mathbf{Y}}_1 = \mathbf{D}\mathbf{Y}_0 = \begin{bmatrix} 1 & 1 & 1 \\ 0 & 1 & 2 \\ 0 & 0 & 1 \end{bmatrix} \begin{bmatrix} 0.5 \\ -0.05 \\ 0.0125 \end{bmatrix} = \begin{bmatrix} 0.4625 \\ -0.025 \\ 0.0125 \end{bmatrix}$$

and

$$\tilde{\mathbf{Z}}_1 = \mathbf{D}\mathbf{Z}_0 = \begin{bmatrix} 1 & 1 & 1 \\ 0 & 1 & 2 \\ 0 & 0 & 1 \end{bmatrix} \begin{bmatrix} 0 \\ 0.2 \\ -0.05 \end{bmatrix} = \begin{bmatrix} 0.15 \\ 0.10 \\ -0.05 \end{bmatrix}$$

Next find b_1 and b_2 such that $F_1(b_1, b_2) = F_2(b_1, b_2) = 0$, where

$$F_1(b_1, b_2) = (\tilde{z}_1 + \beta_{-1} b_2) - (\tilde{y}_1 + \beta_{-1} b_1) + \frac{1}{h}(h\tilde{z}'_1 + b_2) - \frac{1}{h}(h\tilde{y}'_1 + b_1)$$

$$F_2(b_1, b_2) = (\tilde{z}_1 + \beta_{-1} b_2) + 4(\tilde{y}_1 + \beta_{-1} b_1) - 2$$

The desired values of b_1 and b_2 are

$$b_1 = -0.004\,687\,5$$

$$b_2 = 0.018\,75$$

Thus

$$\mathbf{Y}_1 = \tilde{\mathbf{Y}}_1 + b_1 \mathbf{L} = \begin{bmatrix} 0.4625 \\ -0.025 \\ 0.0125 \end{bmatrix} + (-0.004\,687\,5) \begin{bmatrix} 2/3 \\ 3/3 \\ 1/3 \end{bmatrix} = \begin{bmatrix} 0.459\,375 \\ -0.029\,687\,5 \\ 0.010\,937\,5 \end{bmatrix}$$

and

$$\mathbf{Z}_1 = \tilde{\mathbf{Z}}_1 + b_2 \mathbf{L} = \begin{bmatrix} 0.15 \\ 0.10 \\ -0.05 \end{bmatrix} + (0.018\,75) \begin{bmatrix} 2/3 \\ 3/3 \\ 1/3 \end{bmatrix} = \begin{bmatrix} 0.162\,5 \\ 0.118\,8 \\ -0.043\,75 \end{bmatrix}$$

Change of Step Size

When the past values of y_n (namely, $y_{n-1}, y_{n-2}, \ldots, y_{n-k}$) are carried in terms of the Nordsieck vector (see Chap. 9), a change in step size is easily effected. Let the Nordsieck vector for Gear's integration formula of order k at time t_n and step size h be denoted by

$$\mathbf{Z}_n = \left[y_n, hy'_n, \frac{h^2}{2!} y_n^{(2)}, \frac{h^3}{3!} y_n^{(3)}, \ldots, \frac{h^k}{k!} y_n^{(k)} \right]^T \tag{6-56}$$

For step size $\hat{h} = \alpha h$, the corresponding Nordsieck vector at time t_n is defined by

$$\hat{\mathbf{Z}}_n = \left[\hat{y}_n, \hat{h}\hat{y}'_n, \frac{\hat{h}^2}{2!}\hat{y}_n^{(2)}, \frac{\hat{h}^3}{3!}\hat{y}_n^{(3)}, \ldots, \frac{\hat{h}^k}{k!}\hat{y}_n^{(k)}\right]^T \tag{6-57}$$

Since y_n, $\hat{y}_n$, and all derivatives of y_n and $\hat{y}_n$ are evaluated at the same time $t = t_n$, it follows that

$$\hat{y}_n = y_n,\ \hat{y}'_n = y'_n,\ \hat{y}_n^{(2)} = y_n^{(2)},\ \ldots,\ \hat{y}_n^{(k)} = y_n^{(k)} \tag{6-58}$$

Since $\hat{h} = \alpha h$, it follows that the elements of the vectors $\mathbf{Z}_n$ and $\hat{\mathbf{Z}}_n$ are related as follows:

$$\begin{aligned}
\hat{h}\hat{y}'_n &= \alpha h y'_n \\
\frac{\hat{h}^2}{2!}\hat{y}_n^{(2)} &= \frac{\alpha^2 h^2}{2!} y_n^{(2)} \\
\frac{\hat{h}^3}{3!}\hat{y}_n^{(3)} &= \frac{\alpha^3 h^3}{3!} y_n^{(3)} \\
&\vdots \qquad\qquad \vdots \\
\frac{\hat{h}^k}{k!}\hat{y}_n^{(k)} &= \frac{\alpha^k h^k}{k!} y_n^{(k)}
\end{aligned} \tag{6-59}$$

Thus, the two Nordsieck vectors are related by the diagonal matrix $\Lambda(\alpha)$ as follows:

$$\hat{\mathbf{Z}}_n = \Lambda(\alpha)\mathbf{Z}_n \tag{6-60}$$

where

$$\Lambda(\alpha) = \begin{bmatrix} 1 & 0 & 0 & 0 & \cdots & 0 \\ 0 & \alpha & 0 & 0 & \cdots & 0 \\ 0 & 0 & \alpha^2 & 0 & \cdots & 0 \\ \cdots & \cdots & \cdots & \cdots & \cdots & \cdots \\ 0 & \cdots & 0 & \cdots & \cdots & \alpha^k \end{bmatrix}$$

Simultaneous Change of Step Size and Order

In the development of the formulas for effecting these changes, let it be supposed that a kth-order Gear formula has been used for the last $(k+1)$ time steps. The formulas for effecting changes in step size and order are based on the estimation of the truncation errors for a kth-order, a $(k-1)$-order, and a $(k+1)$-order Gear integration formula. Gear used the following formulas.

$$\left.\begin{aligned}
E &= \frac{h^{k+1}y_n^{(k+1)}}{k+1} && \text{(order } k\text{)} \\
E &= \frac{h^k y_n^{(k)}}{k} && \text{(order } k-1\text{)} \\
E &= \frac{h^{k+2}y_n^{(k+2)}}{k+2} && \text{(order } k+1\text{)}
\end{aligned}\right\} \tag{6-61}$$

where the contributions of the higher-order terms have been neglected in the above statements of the truncation errors.

Let the maximum possible value of E be set equal to $\varepsilon y_{\max}$ where $y_{\max}$ is the largest value which the dependent variable has taken on and ε is a parameter specified for the problem. Let the new step size $\hat{h}$ be denoted by $\hat{h} = \alpha h$. Let h be replaced by $\hat{h}$ and E by $\varepsilon y_{\max}$. When the expressions so obtained are solved for α with weights being imposed to maximize the computational efficiency as proposed by Gear, one obtains

$$\left.\begin{aligned}
\alpha &= \frac{1}{1.2}\left(\frac{(k+1)\varepsilon y_{\max}}{h^{k+1}y_n^{(k+1)}}\right)^{1/(k+1)} && \text{(order } k\text{)} \\
\alpha &= \frac{1}{1.3}\left(\frac{k\varepsilon y_{\max}}{h^k y_n^{(k)}}\right)^{1/k} && \text{(order } k-1\text{)} \\
\alpha &= \frac{1}{1.4}\left(\frac{(k+2)\varepsilon y_{\max}}{h^{k+1}y_n^{(k+2)}}\right)^{1/(k+2)} && \text{(order } k+1\text{)}
\end{aligned}\right\} \tag{6-62}$$

The desired value of α is the maximum value computed by use of Eq. (6-62). The factors 1/1.2, 1/1.3, 1/1.4 were introduced by Gear to provide a bias toward picking a smaller order. Since the change from a lower to a higher order requires more computational effort than does the change from a higher to a lower order, the order should not be increased unless a significant improvement can be achieved by changing order.

In order to evaluate the α's given by Eq. (6-62), procedures are needed for computing the derivatives appearing in these expressions. For the kth-order algorithm, the derivative $y_n^{(k+1)}$ may be approximated by use of the $(k+1)$st elements of $\mathbf{Z}_n$ and $\mathbf{Z}_{n-1}$ as follows:

$$\frac{1}{h}\left(\frac{h^k y_n^{(k)}}{k!} - \frac{h^k y_{n-1}^{(k)}}{k!}\right) \cong \frac{h^k y_n^{(k+1)}}{k!}$$

Then, for order k, the expression

$$h^{k+1}y_n^{(k+1)} = (k!)\left(\frac{h^k y_n^{(k)}}{k!} - \frac{h^k y_{n-1}^{(k)}}{k!}\right) \tag{6-63}$$

may be used to compute $h^{k+1}y_n^{(k+1)}$. Instead of using the above expression for computing the $(k+1)$st derivative, Eq. (6-64) may be used. This expression is developed in the following manner. Let the elements of $\mathbf{Z}_n$ be denoted by $z_{n,1}$, $z_{n,2}$, $\ldots$, $z_{n,k+1}$. Then Eq. (6-63) may be stated in the form

$$h^{k+1}y_n^{(k+1)} = k!(z_{n,k+1} - z_{n-1,k+1}) \tag{6-64}$$

Since $\mathbf{Z}_n = \tilde{\mathbf{Z}}_n + \mathbf{b}_n\mathbf{L}$ (Eq. (1-59)), it follows that the $(k+1)$st elements of $\mathbf{Z}_n$, $\tilde{\mathbf{Z}}_n$, and $\mathbf{L}$ are related in the following way:

$$z_{n,k+1} - \tilde{z}_{n,k+1} = b_n l_{k+1} \tag{6-65}$$

where l_{k+1} is the $(k+1)$st element of $\mathbf{L}$. Since each element on the principal diagonal of the Pascal triangle matrix is equal to unity and since $\tilde{\mathbf{Z}}_n = \mathbf{D}\mathbf{Z}_{n-1}$

(Eq. (1-58)), it follows that the $(k+1)$st element of $\mathbf{Z}_n$ is equal to the $(k+1)$st element of $\mathbf{Z}_{n-1}$, that is,

$$\tilde{z}_{n,k+1} = z_{n-1,k+1} \tag{6-66}$$

Use of Eq. (6-66) to eliminate $\tilde{z}_{n,k+1}$ from Eq. (6-65) followed by the substitution of the result so obtained into Eq. (6-64) yields

$$h^{k+1} y_n^{(k+1)} = k!\, b_n\, l_{k+1} \tag{6-67}$$

For order $k-1$, $h^k y_n^{(k)}$ is observed to be the last element of $\mathbf{Z}_n$.

For a $(k+1)$st-order Gear integration formula, both the $(k+1)$st and $(k+2)$nd derivatives are needed. First the $(k+1)$st derivatives at t_n and t_{n-1} are computed by use of Eq. (6-63). Then

$$\begin{aligned} h^{k+2} y_n^{(k+2)} &= k!\left(\frac{h^{k+1} y_n^{(k+1)}}{k!} - \frac{h^{k+1} y_{n-1}^{(k+1)}}{k!}\right) \\ &= k!\left(\frac{k!\, b_n\, l_{k+1}}{k!} - \frac{k!\, b_{n-1}\, l_{k+1}}{k!}\right) \\ &= k!\, l_{k+1}(b_n - b_{n-1}) \end{aligned} \tag{6-68}$$

Thus, the expressions given by Eq. (6-62) may be stated in the following alternate but perhaps more convenient computational form:

$$\left.\begin{aligned} \alpha &= \frac{1}{1.2}\left(\frac{(k+1)\varepsilon y_{\max}}{k!\, l_{k+1}\, b_n}\right)^{1/(k+1)} && \text{(order } k\text{)} \\ \alpha &= \frac{1}{1.3}\left(\frac{k\varepsilon y_{\max}}{h^k y_n^{(k)}}\right)^{1/k} && \text{(order } k-1\text{)} \\ \alpha &= \frac{1}{1.4}\left[\frac{(k+2)\varepsilon y_{\max}}{k!\, l_{k+1}(b_n - b_{n-1})}\right]^{1/(k+2)} && \text{(order } k+1\text{)} \end{aligned}\right\} \tag{6-69}$$

At the end of each trial n, the truncation error ε_T is computed by use of the following expression:

$$\varepsilon_T = \left[\frac{b_n\, l_{k+1}\, k!}{(k+1) y_{\max}}\right] \leq \varepsilon \tag{6-70}$$

This expression follows immediately from (6-61) and (6-67) after E in the first expression of Eq. (6-61) has been replaced by $\varepsilon_T y_{\max}$. If this criteria is not satisfied, the step size is reduced until it is.

The procedures for control of step size and order provide a method for starting the solution procedure. In the solution of initial value problems, all that is required are the values of the dependent variables at the beginning of the integration interval. The order of the method is set to one and the second components of $\mathbf{Z}_0$ are set equal to zero. The second component of the $\mathbf{Z}_0$ vectors are set to zero because for an arbitrary set of differential and algebraic equations, it is not always possible to obtain values for all of the required derivatives. This in no manner affects the accuracy of the solution, as an examination of the method reveals. The only thing affected is the error control

procedure, which must be suspended until the second step. Thus, the initial value of h chosen should be small, but it will be increased later by the integration routine. Similar considerations also require that tests to increase the order of the method be suspended until the third time step has been completed. Also, Gear and others found that increasing the step size before $(k+1)$ steps had been completed since the last change could result in large accumulated errors, thereby requiring a subsequent reduction of the step size.

Other strategies for change of step size and order can be devised such as using a subset of variables for which initial derivatives are available. To date computational experience indicates that it is best to base truncation error and step size control on the subset of variables that have a derivative in at least one equation of the differential-algebraic system being integrated.

6-3 SOLUTION OF ABSORBER PROBLEMS BY USE OF THE SEMI-IMPLICIT RUNGE–KUTTA METHOD AND GEAR'S METHOD

In this section, the equations for an absorber at unsteady state operation with fixed holdups are formulated first by the semi-implicit Runge–Kutta method and then by Gear's method. A flow diagram for a typical absorber is shown in Fig. 6-1.

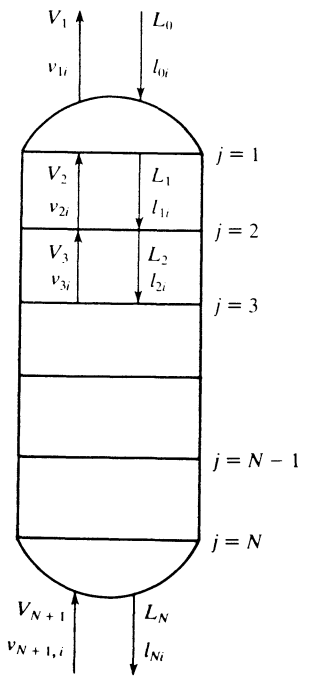

Figure 6-1 Absorber and identifying symbols.

Formulation of the Absorber Equations by the Semi-Implicit Runge–Kutta Method as Proposed by Michelsen

To facilitate the solution of Eqs. (6-71) through (6-77) by use of the semi-implicit Runge–Kutta method, new holdup variables are defined and the component flow rates $\{v_{ji}\}$ and $\{l_{ji}\}$ are restated in terms of the holdups. The new holdup variables are defined because the Runge–Kutta method is applicable for the case where the differential equation contains only one derivative. After these new variables have been defined and the component flow rates have been eliminated, the following expressions are obtained for the component-material balances, the equilibrium relationships, and the energy balances.

The equations needed to describe absorbers at unsteady state operation are a subset of those presented in Chap. 4 for distillation columns except for an additional term in the energy balance corresponding to the heat content of the metal. Except for this one modification, the equations for absorbers are the same as those for any interior plate j ($j \neq 1, f, N-1$) of a conventional distillation column. For convenience, a summary of these equations follows:

$$v_{j+1,i} + l_{j-1,i} - v_{ji} - l_{ji} = \frac{du_{ji}^V}{dt} + \frac{du_{ji}^L}{dt} \qquad \begin{matrix}(j = 1, 2, \ldots, N)\\(i = 1, 2, \ldots, c)\end{matrix} \qquad (6\text{-}71)$$

$$0 = \sum_{i=1}^{c} l_{ji} - L_j \qquad (j = 1, 2, \ldots, N) \qquad (6\text{-}72)$$

$$0 = \sum_{i=1}^{c} v_{ji} - V_j \qquad (j = 1, 2, \ldots, N) \qquad (6\text{-}73)$$

$$0 = \sum_{i=1}^{c} u_{ji}^V - U_j^V \qquad (j = 1, 2, \ldots, N) \qquad (6\text{-}74)$$

$$0 = \sum_{i=1}^{c} u_{ji}^L - U_j^L \qquad (j = 1, 2, \ldots, N) \qquad (6\text{-}75)$$

$$0 = \frac{\gamma_{ji}^L K_{ji} l_{ji}}{\sum_{i=1}^{c} l_{ji}} - \frac{\gamma_{ji}^V v_{ji}}{\sum_{i=1}^{c} v_{ji}} \qquad \begin{matrix}(j = 1, 2, \ldots, N)\\(i = 1, 2, \ldots, c)\end{matrix} \qquad (6\text{-}76)$$

$$\sum_{i=1}^{c} (v_{j+1,i}\hat{H}_{j+1} + l_{j-1,i}\hat{h}_{j-1,i} - v_{ji}\hat{H}_{ji} - l_{ji}\hat{h}_{ji}) = \frac{d\left[\sum_{i=1}^{c} (u_{ji}^V \hat{H}_{ji} + u_{ji}^L \hat{h}_{ji})\right]}{dt} + \mathcal{M}_j \frac{dh_j^S}{dt} \qquad (j = 1, 2, \ldots, N) \qquad (6\text{-}77)$$

where $\mathcal{M}_j$ = mass of metal associated with stage j

C_V^S = heat capacity of the metal $= \dfrac{dh_j^S}{dT_j}$. Note

$$\frac{dh_j^S}{dt} = \frac{dh_j^S}{dT_j}\frac{dT_j}{dt} = C_V^S \frac{dT_j}{dt}.$$

In order to solve these equations by the semi-implicit Runge–Kutta method, it is necessary to restate the component-material balances and energy balances in the form of $y' = f(y)$ by introducing the new variables $\{u_{ji}\}$, E_j^V, E_j^L, and E_j. The resulting set of equations to be solved are then given by

$$\frac{du_{ji}}{dt} = \left(\frac{L_{j-1}}{U_{j-1}^L}\right)u_{j-1,i}^L + \left(\frac{V_{j+1}}{U_{j+1}^V}\right)u_{j+1,i}^V - \left(\frac{L_j}{U_j^L}\right)u_{ji}^L - \left(\frac{V_j}{U_j^V}\right)u_{ji}^V \qquad \begin{matrix}(j = 1, 2, \ldots, N)\\(i = 1, 2, \ldots, c)\end{matrix} \qquad (6\text{-}78)$$

$$0 = u_{ji}^V + u_{ji}^L - u_{ji} \qquad \begin{matrix}(j = 1, 2, \ldots, N)\\(i = 1, 2, \ldots, c)\end{matrix} \qquad (6\text{-}79)$$

$$0 = \sum_{i=1}^{c} u_{ji}^V - U_j^V \qquad (j = 1, 2, \ldots, N) \qquad (6\text{-}80)$$

$$0 = \sum_{i=1}^{c} u_{ji}^L - U_j^L \qquad (j = 1, 2, \ldots, N) \qquad (6\text{-}81)$$

$$0 = \frac{\gamma_{ji}^L K_{ji} u_{ji}^L}{U_j^L} - \frac{\gamma_{ji}^V u_{ji}^V}{U_j^V} \qquad \begin{matrix}(j = 1, 2, \ldots, N)\\(i = 1, 2, \ldots, c)\end{matrix} \qquad (6\text{-}82)$$

$$\frac{dE_j}{dt} = \left(\frac{L_{j-1}}{U_{j-1}^L}\right)E_{j-1}^L + \left(\frac{V_{j+1}}{U_{j+1}^V}\right)E_{j+1}^V - \left(\frac{L_j}{U_j}\right)E_j^L - \left(\frac{V_j}{U_j^V}\right)E_j^V \qquad (6\text{-}83)$$

$$0 = \sum_{i=1}^{c} \hat{h}_{ji} u_{ji}^L - E_j^L \qquad (j = 1, 2, \ldots, N) \qquad (6\text{-}84)$$

$$0 = \sum_{i=1}^{c} \hat{H}_{ji} u_{ji}^V - E_j^V \qquad (j = 1, 2, \ldots, N) \qquad (6\text{-}85)$$

$$0 = \mathcal{M}_j h_j^S - E_j^S \qquad (j = 1, 2, \ldots, N) \qquad (6\text{-}86)$$

$$0 = E_j^S + E_j^V + E_j^L - E_j \qquad (j = 1, 2, \ldots, N) \qquad (6\text{-}87)$$

Equations (6-78) through (6-87) constitute the complete set of $N(3c + 7)$ independent equations. These $N(3c + 7)$ independent equations contain the following $N(3c + 7)$ independent variables $\mathbf{x}$, namely,

$$\mathbf{x} = [(u_{j1} \cdots u_{jc}\ u_{j1}^V \cdots u_{jc}^V\ u_{j1}^L \cdots u_{jc}^L\ V_j\ L_j\ T_j\ E_j\ E_j^V\ E_j^L\ E_j^S)_{j=1,N}]^T \qquad (6\text{-}88)$$

where the notation "$(\ )_{j=1,N}$" means that the elements displayed are to be repeated for $j = 1, 2, 3, \ldots, N-1, N$. In the evaluation of thermodynamic functions, the mole fractions should be replaced, wherever they appear, by the following expressions:

$$x_{ji} = \frac{u_{ji}^L}{\sum_{i=1}^{c} u_{ji}^L} \qquad y_{ji} = \frac{u_{ji}^V}{\sum_{i=1}^{c} u_{ji}^V}$$

In order to demonstrate the characteristics of the semi-implicit Runge–Kutta method, the following example was solved. This example is based on a series of field tests which were made by McDaniel(10,11,12). These tests are described in greater detail in Chap. 7.

The equations and variables of the semi-implicit Runge–Kutta method were ordered in the same manner as described below for Gear's method. Likewise the modified jacobian matrix was solved by use of the same sparse matrix techniques described below for Gear's method.

Example 6-3 A complete statement of this example is presented in Table 6-2. Initially, at time $t = 0$, the absorber is at steady state operation. The steady state solution at the initial conditions is shown in Table 6-3 and at the conditions of the upset in Table 6-4. At time $t = 0+$, a step change in the flow rate of the lean oil is made (see Table 6-2). The semi-implicit Runge–Kutta method was used to obtain the transient solution shown in Table 6-5.

The solutions shown in this chapter were obtained by use of the K data presented in Table 6A-1 and the corrected enthalpies $\{(h_i)_{co}, (H_i)_{co}\}$ which were determined from a series of steady state field tests (Refs. 10, 11), namely,

$$(h_i)_{co} = h_i + \beta C_i^L (T - T_D)$$
$$(H_i)_{co} = H_i + \beta C_i^V (T - T_D)$$

Table 6-2 Statement of Example 6-3

Component	Flow rate, lb·mol/h: Lean oil, L_0	Flow rate, lb·mol/h: Rich Gas, V_{N+1}	Other specifications
CO_2	0.0	14.656 31	*Initial conditions: t = 0, Steady State*
N_2	0.0	4.617 37	The column has 8 stages and operates at a
CH_4	0.0	2233.060	pressure of 722 lb/in² abs. With each stage,
C_2H_6	0.0	158.750 3	there is 612.5 lb of metal having a heat
C_3H_8	0.0	66.127 59	capacity of 0.12 Btu/(lb)(°R). The rich gas
i-C_4H_{10}	0.0	15.829 34	V_{N+1} enters at a temperature $T_{N+1} = 2.0$°F
n-C_4H_{10}	0.0	10.206 40	and the lean oil enters as a liquid at a
i-C_5H_{12}	0.087 32	2.299 97	temperature $T_0 = -1.0$°F. The total holdups
n-C_5H_{12}	0.117 79	1.410 99	in the liquid and vapor phases are as fol-
C_6H_{14}	1.234 24	0.867 19	lows: $U_j^L = 2.50$ lb·mol ($j = 1, 2, \ldots, 8$),
C_7H_{16}	17.853 07	0.266 89	and $U_1^V = 0.085\,656$, $U_j^V = 0.038\,926$ lb·mol
C_8H_{18}	62.569 89	0.024 86	($j = 2, 3, \ldots, N$).
C_9H_{20}	49.946 69	0.000 23	*Upset at time t = 0+*
$C_{10}H_{22}$	24.846 36	0.000 03	$L_0 = 194.713\,72$ lb·mol/h. The composition of
	156.655 36	2508.117 47	L_0 remains the same. The temperature of the lean oil is changed to $T_0 = 2.5$°F.

Table 6-3 Steady state solution of Example 6-3 at the initial set of operating conditions

Plate	T_j, °R	V_j, lb·mol/h	L_j, lb·mol/h
1	484.72	2277.82	236.34
2	490.08	2357.51	253.18
3	490.58	2374.35	259.65
4	489.62	2380.83	266.08
5	487.98	2387.26	273.76
6	485.79	2394.93	284.39
7	482.75	2405.57	302.08
8	477.99	2423.25	386.94

Component	v_{1i}, lb·mol/h	l_{Ni}, lb·mol/h
CO_2	13.030	1.627
N_2	3.746	0.871
CH_4	2132.466	100.591
C_2H_6	113.020	45.731
C_3H_8	13.749	52.378
i-C_4H_{10}	0.323	15.506
n-C_4H_{10}	0.032	10.174
i-C_5H_{12}	0.028	2.360
n-C_5H_{12}	0.027	1.502
C_6H_{14}	0.072	2.029
C_7H_{16}	0.350	17.770
C_8H_{18}	0.694	61.901
C_9H_{20}	0.239	49.708
$C_{10}H_{22}$	0.049	24.798

where $\beta = 0.2561$
T = temperature, °R
$T_D = 0$°R, the datum temperature

Curve-fits of the liquid and vapor enthalpies $\{h_i\}$ and $\{H_i\}$ are presented in Table 6A-2, and the liquid and vapor correction factors $\{C_i^L\}$ and $\{C_i^V\}$ are presented in Table 6A-3.

Formulation of an Absorber by Use of the Generalized Algorithm for the Semi-Implicit Runge–Kutta Method

The system of equations used to describe an absorber are of the form given by Eqs. (6-20) and (6-21). The absorber equations (Eqs. (6-71) through (6-77)) may be solved by use of the generalized Runge–Kutta algorithm for systems of coupled differential and algebraic equations (Eqs. (6-29), (6-30), (6-33), and (6-34)). When the generalized algorithm is used, it is not necessary to define the

Table 6-4 Steady state solution of Example 6-3 at the conditions of the upset

Plate	T_j, °R	V_j, lb·mol/h	L_j, lb·mol/h
1	485.22	2251.98	287.65
2	491.35	2344.93	305.73
3	492.90	2363.01	311.67
4	492.70	2368.95	317.72
5	491.46	2375.00	325.39
6	489.31	2382.67	336.65
7	485.96	2393.93	356.40
8	480.32	2413.69	450.86

Component	v_{1i}, lb·mol/h	l_{Ni}, lb·mol/h
CO_2	12.805	1.851
N_2	3.622	0.996
CH_4	2117.130	115.947
C_2H_6	107.088	51.663
C_3H_8	9.709	56.419
i-C_4H_{10}	0.142	15.688
n-C_4H_{10}	0.012	10.194
i-C_5H_{12}	0.029	2.380
n-C_5H_{12}	0.028	1.530
C_6H_{14}	0.074	2.328
C_7H_{16}	0.356	22.101
C_8H_{18}	0.706	77.090
C_9H_{20}	0.243	61.838
$C_{10}H_{22}$	0.049	30.833

Table 6-5 Transient solutions of Example 6-3 by use of the generalized semi-implicit Runge–Kutta method

	Temperature (°R) at trial no. indicated†			Vapor rates, lb·mol/h at trial no. indicated‡		
Plate	1	10	36	1	10	36
1	484.66	484.48	485.15	2258.54	2253.24	2252.01
2	489.98	489.95	491.24	2352.82	2347.95	2345.00
3	490.56	490.71	492.78	2371.71	2367.76	2363.13
4	489.64	490.03	492.57	2378.28	2374.76	2369.09
5	488.02	488.59	492.35	2384.73	2381.29	2375.15
6	485.83	486.60	489.22	2392.38	2388.77	2382.80
7	482.82	483.79	485.90	2402.90	2398.98	2394.04
8	478.13	479.89	480.29	2420.13	2416.53	2413.74

† A lower bound of 0.1 min for the time step was used.
An upper bound of 5.0 min for the time step was used.
‡ The times corresponding to the trial numbers are as follows:

Trial 1: 0.10 min Trial 10: 1.46 min Trial 36: 15.00 min

The tolerance vector was chosen as one-thousandth of the values at the end of each second half-step.

new variables $\{u_{ji}\}$, E_j^S, and E_j used in the formulation by Michelsen's algorithm. The absorber example may be formulated by use of the generalized Runge–Kutta algorithm in terms of $N(2c + 5)$ equations and $N(2c + 5)$ variables, when the total holdups $\{U_j\}$ and the liquid holdups $\{U_j^L\}$ are known. The $N(2c + 5)$ variables are:

$$\mathbf{x} = [(u_{j1}^V \quad \cdots \quad u_{jc}^V \quad u_{j1}^L \quad \cdots \quad u_{jc}^L \quad V_j \quad L_j \quad T_j \quad E_j^V \quad E_j^L)_{j=1,N}]^T \tag{6-89}$$

and the $N(2c + 5)$ equations follow:

$$0 = \left(\frac{L_{j-1}}{U_{j-1}^L}\right)u_{j-1,i}^L + \left(\frac{V_{j+1}}{U_{j+1}^V}\right)u_{j+1,i}^V - \left(\frac{L_j}{U_j^L}\right)u_{ji}^L - \left(\frac{V_j}{U_j^V}\right)u_{ji}^V - \frac{du_{ji}^V}{dt} - \frac{du_{ji}^L}{dt} \qquad \begin{matrix}(j = 1, 2, \ldots, N)\\(i = 1, 2, \ldots, c)\end{matrix} \tag{6-90}$$

$$0 = \sum_{i=1}^{c} u_{ji}^V - U_j^V \qquad (j = 1, 2, \ldots, N) \tag{6-91}$$

$$0 = \sum_{i=1}^{c} u_{ji}^L - U_j^L \qquad (j = 1, 2, \ldots, N) \tag{6-92}$$

$$0 = \frac{\gamma_{ji}^L K_{ji} u_{ji}^L}{U_j^L} - \frac{\gamma_{ji}^V u_{ji}^V}{U_j^V} \qquad \begin{matrix}(j = 1, 2, \ldots, N)\\(i = 1, 2, \ldots, c)\end{matrix} \tag{6-93}$$

$$0 = \left(\frac{L_{j-1}}{U_{j-1}^L}\right)E_{j-1}^L + \left(\frac{V_{j+1}}{U_{j+1}^V}\right)E_{j+1}^V - \left(\frac{L_j}{U_j^L}\right)E_j^L - \left(\frac{V_j}{U_j^V}\right)E_j^V - \mathscr{M}_j C_V^S \frac{dT}{dt} - \frac{dE_j^L}{dt} - \frac{dE_j^V}{dt} \qquad (j = 1, 2, \ldots, N) \tag{6-94}$$

$$0 = \sum_{i=1}^{c} \hat{h}_{ji} u_{ji}^L - E_j^L \qquad (j = 1, 2, \ldots, N) \tag{6-95}$$

$$0 = \sum_{i=1}^{c} \hat{H}_{ji} u_{ji}^V - E_j^V \qquad (j = 1, 2, \ldots, N) \tag{6-96}$$

Again, the mole fractions appearing in the thermodynamic functions are replaced by their equivalents as shown below Eq. (6-88).

When Example 6-3 was solved by use of the same constraints on the step size for the generalized semi-implicit Runge–Kutta method as was used for Michelsen's method, 83.9 seconds of computer time were required for 15 minutes of process time (see Table 6-6). Thus, for this example, the generalized algorithm for the semi-implicit Runge–Kutta method is approximately twice as fast as Michelsen's method.

Formulation of the Absorber Example by Use of Gear's Method

Since Gear's method may be applied to systems of nonlinear differential equations with variable coefficients, it may be applied to the system of equations consisting of Eq. (6-20) (a system of linear differential equations with constant

Table 6-6 Comparison of the semi-implicit Runge–Kutta methods for Example 6-3

1. Integration parameters for the semi-implicit Runge–Kutta methods

Tolerance vector = $(0.001)y_n^*$
Minimum permitted step size = 0.1 min
Maximum permitted step size = 5.0 min
Initial step size = 0.1 min

2. Performance of Michelsen's algorithm (Eqs. (6-12), (6-13), and (6-14))†

Step	Process Time, min	Cumulative‡ functional evaluations	Cumulative jacobian evaluations
0	0.000	0	0
1	0.100	5	2
2	0.200	10	4
14	1.419	70	28
15	1.519	75	30
46	11.252	220	88
47	13.126	225	90
48	15.000	230	92

3. Performance of the generalized Runge–Kutta algorithm for systems of differential and algebraic equations (Eqs. (6-29), (6-30), (6-31), and (6-32))§

Step	Process time, min	Cumulative functional evaluations	Cumulative jacobian evaluations
0	0.000	0	0
1	0.100	5	2
2	0.200	10	4
10	1.447	50	20
11	1.657	55	22
33	11.185	170	68
34	12.997	175	70
35	15.000	180	72

† Computer time for AMDAHL 470/V8 with FORTRAN H Extended Compiler was 139.12 s.

‡ $(b_{31}k_1 + b_{32}k_2)$ was not counted as functional evaluation.

§ Computer time for AMDAHL 470/V8 with FORTRAN H Extended Compiler was 86.35 s.

coefficients) and Eq. (6-21) (a system of algebraic equations) without any modification of the algorithm given by Eqs. (6-53) through (6-55)).

The equations for an absorber may be formulated in terms of precisely the same $N(2c + 5)$ independent variables shown above for the generalized algorithm of the semi-implicit Runge–Kutta method (see Eq. (6-89)). Likewise the $N(2c + 5)$ equations to be solved are the same as those shown above for the generalized Runge–Kutta algorithm (see Eqs. (6-90) through (6-96)).

Solution of the Newton–Raphson Equations in Gear's Method

Corresponding to each element of $\mathbf{x}$, there is a set of variables $\mathbf{b}$ which may be represented as follows:

$$\mathbf{b} = [(b_{j,1} \quad b_{j,2} \quad \cdots \quad b_{j,c+1} \quad \cdots \quad b_{j,2c+5})_{j=1,N}]^T \tag{6-97}$$

Similarly, let the functions for any stage j be ordered in the same manner as shown by Eqs. (6-90) through (6-96) and identified by the following notation

$$\mathbf{f} = [(f_{j,1} \quad f_{j,2} \quad \cdots \quad f_{j,c} \quad f_{j,c+1} \quad \cdots \quad f_{j,2c+5})_{j=1,N}]^T \tag{6-98}$$

The unknown b's at the end of a given time step may be found by use of the Newton–Raphson method which consists of the repeated solution of

$$\mathbf{J}\,\Delta\mathbf{b} = -\mathbf{f} \tag{6-99}$$

where

$$\Delta\mathbf{b} = \mathbf{b}_{l+1} - \mathbf{b}_l, \text{ where } l \text{ is the trial number.}$$

$$\mathbf{J} = \begin{bmatrix} \dfrac{\partial f_{1,1}}{\partial b_{1,1}} & \cdots & \dfrac{\partial f_{1,1}}{\partial b_{N,2c+5}} \\ \vdots & & \vdots \\ \dfrac{\partial f_{N,2c+5}}{\partial b_{1,1}} & \cdots & \dfrac{\partial f_{N,2c+5}}{\partial b_{N,2c+5}} \end{bmatrix}$$

In order to obtain a jacobian matrix with the sparsity of the one shown in Fig. 6-2, the variables must be appropriately ordered as implied above. By the ordering of the functions is meant the order in which the Newton–Raphson equations are listed. In the proposed ordering, all of the Newton–Raphson equations for the first stage are listed, then those for the second stage, and this process is continued until all of the Newton–Raphson equations for stage N have been listed.

By ordering of the variables is meant the order in which each function is to be differentiated with respect to the variables. In order to achieve the sparsity shown in Fig. 6-2, each function is differentiated first with respect to the variables for the first stage, then those for the second stage, and this process is continued until each function has been differentiated with respect to all of the variables for the Nth stage.

In order to compute the Δb's, the matrix equation may be solved by the well-known method of gaussian elimination. Observe first that arithmetic is to be performed only on the elements in the shaded area. Since the elements outside the shaded area will always be equal to zero, computer time is saved by not performing any arithmetic on these zero elements. By applying gaussian

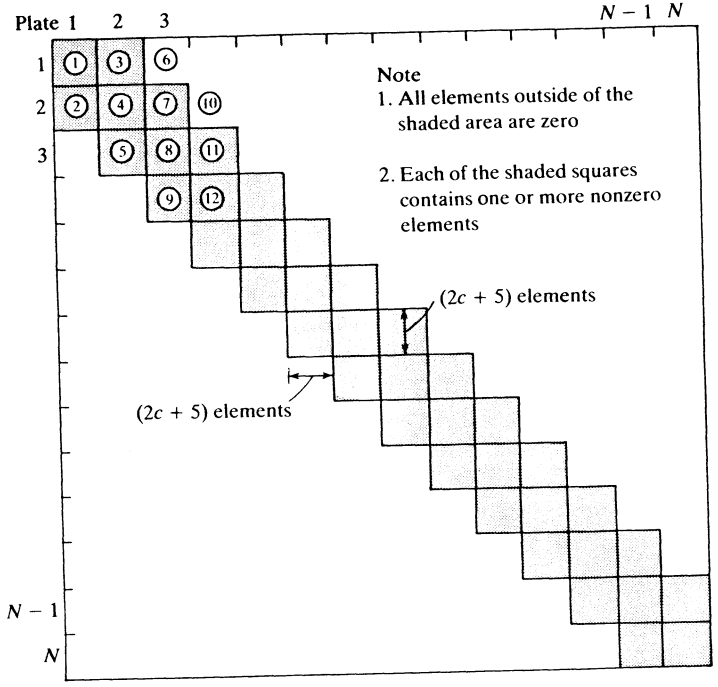

Figure 6-2 Jacobian matrix for Gear's formulation of an absorber.

elimination in a stepwise fashion, it is possible to transform the matrix shown in Fig. 6-2 into the one shown in Fig. 6-3. At any time, only six of the $(2c + 5)$ square submatrices along the diagonal and the corresponding elements of **f** need to be considered instead of the complete $N(2c + 5)$ matrix. In particular, the first step in the transformation of the jacobian matrix of Fig. 6-2 into the upper triangular matrix shown in Fig. 6-3 is to consider the submatrices 1, 2, 3, 4, 6, and 7 of Fig. 6-2. Next, the largest element in column 1 of submatrices 1 and 2 is selected as the pivot element. If the pivot element lies in submatrix 2, then submatrix 6 may be filled in the process of eliminating all elements above the pivot element. After the entire process has been applied to the last column of submatrix 2, the entire process is repeated for the next set of six submatrices, namely, submatrices 4, 5, 7, 8, 10, and 11. If one or more of the pivot elements lie in submatrix 5, then submatrix 10 may be filled or partially filled by the elimination process.

Refinements of the gaussian elimination process which have been described by others (Ref. 13) were employed. For example, the Newton–Raphson equations were scaled as recommended by Tewarson(13) before the gaussian elimination process was initiated. Also the large, sparse jacobian matrix was stored through the use of *linked lists*. This procedure is described and illustrated in Chap. 15 of Ref. 7.

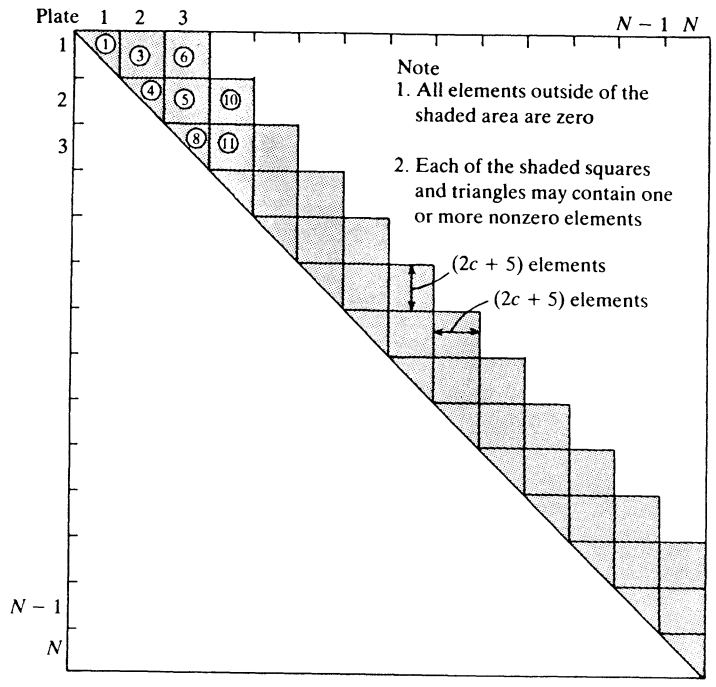

Figure 6-3 Jacobian matrix of Fig. 6-2 after triangularization.

Since all of the variables **x** remain positive and bounded throughout the transient operation, the values of Δb were limited accordingly. For example, suppose that the value of $\Delta b_{ji,\,l+1}$ for the $(l + 1)$st trial gives a negative value of the corresponding variable u^L_{ji}, that is,

$$0 > u^L_{ji} = \tilde{u}^L_{ji} + \beta_{-1}(b_{ji,\,l} + \Delta b_{ji,\,l+1}) \tag{6-100}$$

then each Δb is multiplied successively by factors of 1/2 until $u^L_{ji} > 0$.

Speed is achieved in Gear's method by using the same jacobian for several time steps as indicated in Table 6-7.

Comparison of the Semi-Implicit Runge–Kutta Methods and Gear's Method

For systems of coupled differential and algebraic equations in which the derivatives are linear with constant coefficients, the generalized semi-implicit Runge–Kutta method may be applied directly. The generalized algorithm eliminates the necessity for defining new variables as required to state the differential equations in state-variable form $[y' = f(y)]$ in order to apply Michelsen's semi-implicit method. Thus, in the formulation of the absorber example, $N(3c + 7)$

Table 6-7 Solution of Example 6-3 by use of Gear's Method

1. Gear's method integration parameters

Error control parameter, $\varepsilon = 0.001$
Minimum permitted step size = 0.009 999 9 min
Maximum permitted step size = 5.0 min
Initial step size = 0.01 min
Convergence criterion: $\frac{1}{n}\sum_{i=1}^{n} f_i^2 \leq 9$, where n is the total number of functions f_i.

2. Performance of Gear's method†

Step	Process time, min	Integration order	Cumulative functional evaluations	Cumulative jacobian evaluations
0	0.000	1	0	0
1	0.01	1	3	1
6	0.080	1	22	3
7	0.098	2	24	3
24	1.434	2	77	9
25	1.580	3	79	9
52	11.815	3	165	19
53	11.923	2	167	19
60	16.285	2	187	22

† Computer time for AMDAHL 470/V8 with FORTRAN H Extended Compiler was 28.92 s.

variables were required by Michelsen's method while only $N(2c + 5)$ were required by the semi-implicit Runge–Kutta method and Gear's method.

In order to solve systems of differential equations with variable coefficients and one or more derivatives of nonlinear form by use of the generalized semi-implicit Runge–Kutta method, it is necessary to define an appropriate set of new variables which produces a new set of equations in which all derivatives appear in linear form with constant coefficients. To solve the same problem by use of Michelsen's method would require the definition of an appropriate set of new variables which would reduce the original set of equations to state-variable form. On the other hand, Gear's method may be applied directly to systems of nonlinear differential equations with variable coefficients. New variables may be introduced, of course, as desired to simplify the computations.

A significant advantage of Gear's method over the semi-implicit Runge–Kutta methods is the fact that the derivatives may be approximated in the Newton–Raphson determination of the set of $\{b_j\}$ of Gear's method which are required to satisfy all of the equations. Approximation of the derivatives appearing in the Newton–Raphson method does not reduce the order of Gear's method because it is independent of the method used to find the $\{b_j\}$. However, in the case of the Runge–Kutta methods, the derivatives appear in the algorithm itself and the approximation of these derivatives reduces the order of the algorithm to the order of the approximation. Because of the complex thermodynamic functions which are used in the description of nonideal mixtures, the development of the analytical expressions for the derivatives required by the semi-implicit Runge–Kutta methods can become an enormous task.

To compare the performance of the three formulations described above, Example 6-3 was solved by each method. The performance of Michelsen's method is given in item 2 of Table 6-6. As shown there 139.12 seconds of computer time was required to follow the process for the first 15 minutes following the upset while the generalized semi-implicit Runge–Kutta method required 86.35 seconds for the first 15 minutes of process time as shown in item 3 of Table 6-6. Thus, the generalized semi-implicit Runge–Kutta method is seen to be 1.61 times faster than Michelsen's method for the absorber example.

The performance of Gear's method in the solution of Example 6-3 is presented in Table 6-7. Since it required 28.92 seconds of computer time for the first 15 minutes of process time, Gear's method is seen to be 2.98 times faster than the generalized Runge–Kutta method and 4.81 times faster than Michelsen's semi-implicit Runge–Kutta method. Although the comparison of the two Runge–Kutta methods is exact, the comparisons of the Runge–Kutta methods with Gear's method is not exact because the procedures used to change the size of the time steps differed.

NOTATION

(See also Chaps. 4 and 5.)

E_j^L = energy holdup in the liquid phase on stage j
E_j^V = energy holdup in the vapor phase on stage j
E_j^S = energy holdup in the metal associated with stage j
E_j = total energy holdup in the liquid and vapor phases and metal associated with stage j
$\hat{h}_{ji}$ = virtual value of the partial molar enthalpy of component i in liquid (see App. 4A-2)
$\hat{H}_{ji}$ = virtual value of the partial molar enthalpy of component i in the vapor (see App. 4A-2)
h_j^S = enthalpy of the metal at the temperature of stage j
u_{ji}^L = molar holdup of component i in the liquid on plate j
u_{ji}^V = molar holdup of component i in the vapor on plate j
u_{ji} = total molar holdup of component i on plate j
U_j^L = total molar holdup of liquid on plate j
U_j^V = total molar holdup of vapor on plate j

Greek letters

γ_{ji}^L = activity coefficient of component i in the liquid phase on stage j [$\gamma_{ji}^L = \gamma_{ji}^L(P, T, \{x_{ji}\})$]
γ_{ji}^V = activity coefficient of component i in the vapor phase of stage j [$\gamma_{ji}^V = \gamma_{ji}^V(P, T, \{y_{ji}\})$]

REFERENCES

1. J. B. Caillaud and L. Padmanabhan: "An Improved Semi-Implicit Runge–Kutta Method for Stiff Systems," *Chem. Eng. J.* (English), **2**:227 (1971).
2. An Feng, S. E. Gallun, and C. D. Holland: "Development and Comparison of a Generalized Semi-Implicit Runge–Kutta Method and Gear's Method to Coupled Differential and Algebraic Equations Appearing in Distillation Models," Submitted to *Comput. Chem. Eng.* 1982.
3. C. W. Gear: *Numerical Initial Value Problems in Ordinary Differential Equations*, Prentice-Hall, Inc., Englewood Cliffs, N.J., 1971.
4. C. W. Gear: "The Automatic Integration of Ordinary Differential Equations," *Communs. ACM*, **14**(3): 1976 (1971*a*).
5. S. E. Gallun and C. D. Holland: "Gear's Procedure for the Simultaneous Solution of Differential and Algebraic Equations with Application in Unsteady State Distillation," *Computers and Chemical Engineering*, **6**(3): 231 (1982).
6. F. B. Hildbrand: *Introduction to Numerical Analysis*, McGraw-Hill Book Company, New York, 2d ed., 1974.
7. C. D. Holland: *Fundamentals of Multicomponent Distillation*, McGraw-Hill Book Company, New York, 1981.
8. M. L. Michelsen: "An Efficient General Purpose Method of Integration of Stiff–Ordinary Differential Equations," *AIChE J.* **22**(3):594 (1976).
9. M. L. Michelsen: "Semi-Implicit Runge–Kutta Methods for Stiff Systems, Program Description, and Application Examples," Institutlet for Kemiteknik Danmarks tekniske Hojskoli Bygning 229DK-2800, Lyngby, Denmark.
10. R. McDaniel, A. A. Bassyoni, and C. D. Holland: "Use of the Results of Field Tests in the Modeling of Packed Distillation Columns and Packed Absorbers—III," *Chem. Eng. Sci.*, **25**:633 (1970).
11. R. McDaniel: "Packed Absorbers at Steady State and Unsteady State Operation," Ph.D. dissertation, Texas A&M University, College Station, Texas, 1969.
12. R. McDaniel and C. D. Holland: "Modeling of Packed Absorbers at Unsteady State Operation—IV," *Chem. Eng. Sci.*, **25**:1283 (1970).
13. R. P. Tewarson: *Sparse Matrices*, Academic Press, New York, (1973).

PROBLEM

6-1 Formulate the equations required to solve the model given in Sec. 2-4 for a triple-effect evaporator with boiling point elevation by use of each of the following algorithms:

(*a*) Michelsen's version of the semi-implicit Runge–Kutta method.
(*b*) The generalized semi-implicit Runge–Kutta method.
(*c*) Gear's method.

APPENDIX 6A EQUILIBRIUM AND ENTHALPY DATA

Table 6A-1 Curve-fit parameters† for K values‡

Component	a_{1i}	a_{2i}	a_{3i}	a_{4i}
Carbon dioxide	$-0.628\,222\,23 \times 10^{-1}$	$0.306\,888\,02 \times 10^{-3}$	$0.399\,964\,68 \times 10^{-6}$	$-0.578\,998\,63 \times 10^{-9}$
Nitrogen	$0.505\,968\,21 \times 10^{0}$	$-0.434\,883\,64 \times 10^{-3}$	$-0.150\,099\,91 \times 10^{-5}$	$0.344\,941\,54 \times 10^{-8}$
Methane	$0.155\,849\,34 \times 10^{0}$	$-0.152\,057\,75 \times 10^{-3}$	$0.503\,492\,12 \times 10^{-6}$	$-0.177\,135\,46 \times 10^{-9}$
Ethane	$0.914\,860\,37 \times 10^{-1}$	$-0.163\,559\,44 \times 10^{-3}$	$0.337\,419\,24 \times 10^{-6}$	$0.147\,971\,50 \times 10^{-9}$
Propane	$0.377\,695\,08 \times 10^{-1}$	$-0.644\,917\,02 \times 10^{-4}$	$0.292\,336\,27 \times 10^{-6}$	$-0.485\,976\,80 \times 10^{-11}$
i-Butane	$0.367\,083\,55 \times 10^{-1}$	$-0.943\,109\,63 \times 10^{-4}$	$0.280\,266\,48 \times 10^{-6}$	$0.104\,627\,97 \times 10^{-10}$
n-Butane	$0.372\,312\,78 \times 10^{-1}$	$-0.136\,350\,85 \times 10^{-3}$	$0.375\,846\,53 \times 10^{-6}$	$-0.692\,377\,41 \times 10^{-10}$
i-Pentane	$0.197\,470\,34 \times 10^{-1}$	$-0.402\,849\,84 \times 10^{-4}$	$0.144\,391\,95 \times 10^{-6}$	$0.566\,567\,90 \times 10^{-10}$
n-Pentane	$0.154\,145\,96 \times 10^{-1}$	$-0.347\,361\,06 \times 10^{-4}$	$0.125\,910\,28 \times 10^{-6}$	$0.731\,571\,33 \times 10^{-10}$
Hexane	$0.887\,657\,52 \times 10^{-3}$	$0.370\,826\,46 \times 10^{-4}$	$-0.407\,469\,51 \times 10^{-7}$	$0.151\,872\,03 \times 10^{-9}$
Heptane	$0.636\,773\,56 \times 10^{-2}$	$-0.644\,097\,60 \times 10^{-5}$	$0.317\,939\,74 \times 10^{-7}$	$0.782\,843\,79 \times 10^{-10}$
Octane	$0.996\,747\,99 \times 10^{-2}$	$-0.346\,735\,91 \times 10^{-4}$	$0.823\,052\,91 \times 10^{-7}$	$0.210\,223\,92 \times 10^{-10}$
Nonane	$0.787\,933\,92 \times 10^{-2}$	$-0.238\,861\,25 \times 10^{-4}$	$0.524\,359\,51 \times 10^{-7}$	$0.257\,934\,78 \times 10^{-10}$
Decane	$0.641\,465\,56 \times 10^{-2}$	$-0.161\,311\,04 \times 10^{-4}$	$0.300\,052\,50 \times 10^{-7}$	$0.302\,660\,26 \times 10^{-10}$

† $\sqrt[3]{K_i/T} = a_{1i} + a_{2i}\,T + a_{3i}\,T^2 + a_{4i}\,T^3$ (T in °R).
‡ Based on data provided by Exxon Company, U.S.A. These values were determined for a pressure of 800 lb/in^2 abs and a temperature range of -25 to $+40$°F.

Table 6A-2 Enthalpy data†

1. Curve-fit parameters‡ for the liquid enthalpies

Component	g_{1i}	g_{2i}	g_{3i}	g_{4i}
Carbon dioxide	$0.225\,240\,75 \times 10^{4}$	$0.544\,626\,43 \times 10^{1}$	$0.279\,100\,80 \times 10^{-1}$	$-0.187\,653\,35 \times 10^{-4}$
Nitrogen	$0.158\,371\,12 \times 10^{4}$	$0.373\,151\,21 \times 10^{1}$	$0.176\,558\,57 \times 10^{-1}$	$-0.146\,620\,71 \times 10^{-4}$
Methane	$0.816\,351\,81 \times 10^{3}$	$0.720\,646\,00 \times 10^{1}$	$0.153\,540\,34 \times 10^{-1}$	$-0.844\,064\,56 \times 10^{-5}$
Ethane	$0.974\,047\,12 \times 10^{3}$	$0.114\,542\,94 \times 10^{2}$	$0.793\,995\,34 \times 10^{-2}$	$-0.421\,831\,83 \times 10^{-6}$
Propane	$0.212\,375\,10 \times 10^{4}$	$0.463\,835\,24 \times 10^{1}$	$0.317\,268\,30 \times 10^{-1}$	$-0.125\,803\,01 \times 10^{-4}$
i-Butane	$0.175\,436\,28 \times 10^{4}$	$0.924\,568\,56 \times 10^{1}$	$0.302\,060\,13 \times 10^{-1}$	$-0.895\,846\,64 \times 10^{-5}$
n-Butane	$0.323\,091\,92 \times 10^{4}$	$0.661\,755\,47 \times 10^{1}$	$0.382\,623\,86 \times 10^{-1}$	$-0.161\,109\,35 \times 10^{-4}$
i-Pentane	$0.336\,116\,63 \times 10^{4}$	$0.395\,526\,70 \times 10^{1}$	$0.549\,256\,47 \times 10^{-1}$	$-0.258\,696\,82 \times 10^{-4}$
n-Pentane	$0.434\,543\,75 \times 10^{4}$	$0.105\,963\,39 \times 10^{2}$	$0.437\,315\,11 \times 10^{-1}$	$-0.196\,374\,75 \times 10^{-4}$
Hexane	$-0.441\,504\,69 \times 10^{4}$	$0.703\,545\,99 \times 10^{2}$	$-0.674\,700\,74 \times 10^{-1}$	$0.602\,456\,57 \times 10^{-4}$
Heptane	$0.667\,070\,16 \times 10^{2}$	$0.181\,590\,73 \times 10^{2}$	$0.381\,648\,84 \times 10^{-1}$	$-0.428\,370\,73 \times 10^{-5}$
Octane	$-0.106\,325\,78 \times 10^{2}$	$0.192\,299\,50 \times 10^{2}$	$0.401\,864\,13 \times 10^{-1}$	$-0.705\,218\,89 \times 10^{-6}$
Nonane	$-0.791\,419\,92 \times 10^{4}$	$0.816\,151\,43 \times 10^{2}$	$-0.795\,019\,27 \times 10^{-1}$	$0.839\,435\,09 \times 10^{-4}$
Decane	$-0.678\,103\,52 \times 10^{4}$	$0.741\,085\,51 \times 10^{2}$	$-0.583\,157\,06 \times 10^{-1}$	$0.750\,871\,55 \times 10^{-4}$

2. Curve-fit parameters§ for the vapor enthalpies

Component	d_{1i}	d_{2i}	d_{3i}	d_{4i}
Carbon dioxide	$0.139\,789\,77 \times 10^{5}$	$-0.963\,594\,63 \times 10^{1}$	$0.382\,284\,22 \times 10^{-1}$	$-0.268\,701\,70 \times 10^{-4}$
Nitrogen	$0.486\,386\,72 \times 10^{4}$	$-0.212\,273\,79 \times 10^{1}$	$0.175\,656\,68 \times 10^{-1}$	$-0.113\,670\,06 \times 10^{-4}$
Methane	$0.632\,554\,30 \times 10^{4}$	$-0.207\,477\,57 \times 10^{1}$	$0.185\,326\,34 \times 10^{-1}$	$-0.106\,304\,16 \times 10^{-4}$
Ethane	$0.106\,289\,34 \times 10^{5}$	$-0.287\,188\,34 \times 10^{1}$	$0.248\,770\,94 \times 10^{-1}$	$-0.132\,332\,22 \times 10^{-4}$
Propane	$0.139\,543\,83 \times 10^{5}$	$-0.419\,302\,56 \times 10^{1}$	$0.326\,141\,45 \times 10^{-1}$	$-0.154\,833\,40 \times 10^{-4}$
i-Butane	$0.940\,889\,84 \times 10^{4}$	$0.392\,626\,80 \times 10^{2}$	$-0.555\,965\,94 \times 10^{-1}$	$0.515\,073\,92 \times 10^{-4}$
n-Butane	$0.573\,023\,44 \times 10^{4}$	$0.751\,177\,37 \times 10^{2}$	$-0.131\,208\,84 \times 10^{0}$	$0.105\,179\,08 \times 10^{-3}$
i-Pentane	$0.830\,819\,53 \times 10^{4}$	$0.752\,677\,92 \times 10^{2}$	$-0.129\,458\,43 \times 10^{0}$	$0.108\,456\,97 \times 10^{-3}$
n-Pentane	$0.128\,042\,11 \times 10^{5}$	$0.616\,540\,07 \times 10^{2}$	$-0.973\,652\,01 \times 10^{-1}$	$0.843\,987\,22 \times 10^{-4}$
Hexane	$0.230\,016\,84 \times 10^{5}$	$0.277\,449\,19 \times 10^{2}$	$-0.315\,454\,94 \times 10^{-1}$	$0.499\,812\,89 \times 10^{-4}$
Heptane	$0.148\,768\,16 \times 10^{5}$	$0.593\,424\,38 \times 10^{2}$	$-0.818\,532\,71 \times 10^{-1}$	$0.814\,298\,55 \times 10^{-4}$
Octane	$0.327\,932\,15 \times 10^{5}$	$-0.350\,402\,83 \times 10^{2}$	$0.111\,629\,55 \times 10^{0}$	$-0.426\,474\,29 \times 10^{-4}$
Nonane	$0.470\,246\,46 \times 10^{5}$	$-0.953\,950\,35 \times 10^{2}$	$0.245\,475\,29 \times 10^{0}$	$-0.132\,096\,38 \times 10^{-3}$
Decane	$0.552\,382\,11 \times 10^{5}$	$-0.131\,956\,18 \times 10^{3}$	$0.325\,183\,69 \times 10^{0}$	$-0.181\,883\,84 \times 10^{-3}$

† Based on data provided by Exxon Company, U.S.A. These values were determined for a pressure of 800 lb/in² abs and a temperature range of −25 to +40°F.

‡ $h_i = g_{1i} + g_{2i}T + g_{3i}T^2 + g_{4i}T^3$ (T in °R)

§ $H_i = d_{1i} + d_{2i}T + d_{3i}T^2 + d_{4i}T^3$ (T in °R)

Table 6A-3 Enthalpy correction factors†

1. Mean heat capacities (Btu/lb · mol)

Component	C_i^V	C_i^L
Carbon dioxide	8.461	19.219
Nitrogen	6.836	10.611
Methane	8.272	16.019
Ethane	11.698	18.601
Propane	16.133	26.041
i-Butane	21.106	31.605
n-Butane	21.511	31.813
i-Pentane	25.451	38.321
n-Pentane	26.044	38.589
Hexane	31.074	46.835
Heptane	36.287	51.030
Octane	41.326	56.341
Nonane	47.374	62.409
Decane	52.643	68.895

† Calculated using the same enthalpy data as used in Table 6A-2 on a basis of $T_D = 0°R$.

CHAPTER

SEVEN

MODELING OF PACKED ABSORBERS AT UNSTEADY OPERATION

The use of field tests in the modeling of a packed absorber at unsteady state operation is demonstrated in this chapter. Both steady state and unsteady state field tests were used in the formulation of the unsteady state model for the absorber at the Zoller Gas Plant (see Figs. 7-1 and 7-2).

After the fundamental relationships and the proposed model for the packed absorber have been presented in Sec. 7-1, they are utilized in Sec. 7-2 in conjunction with the results of the field tests to determine the parameters of the model.

7-1 FUNDAMENTAL RELATIONSHIPS

The concepts of mass and heat transfer sections make it possible to represent a continuous mass transfer process by an equivalent stepwise process, that is, by an equivalent column with plates. In the proposed model, the column is divided into elements of height Δz_j, as shown in Fig. 7-3, and the mass and heat transfer that occurs within each element is described by the mass and heat transfer relationships.

Definitions of the Mass and Heat Transfer Sections

The mass and heat transfer sections for unsteady state operation are defined such that each element of packing Δz_j of the packed column becomes a per-

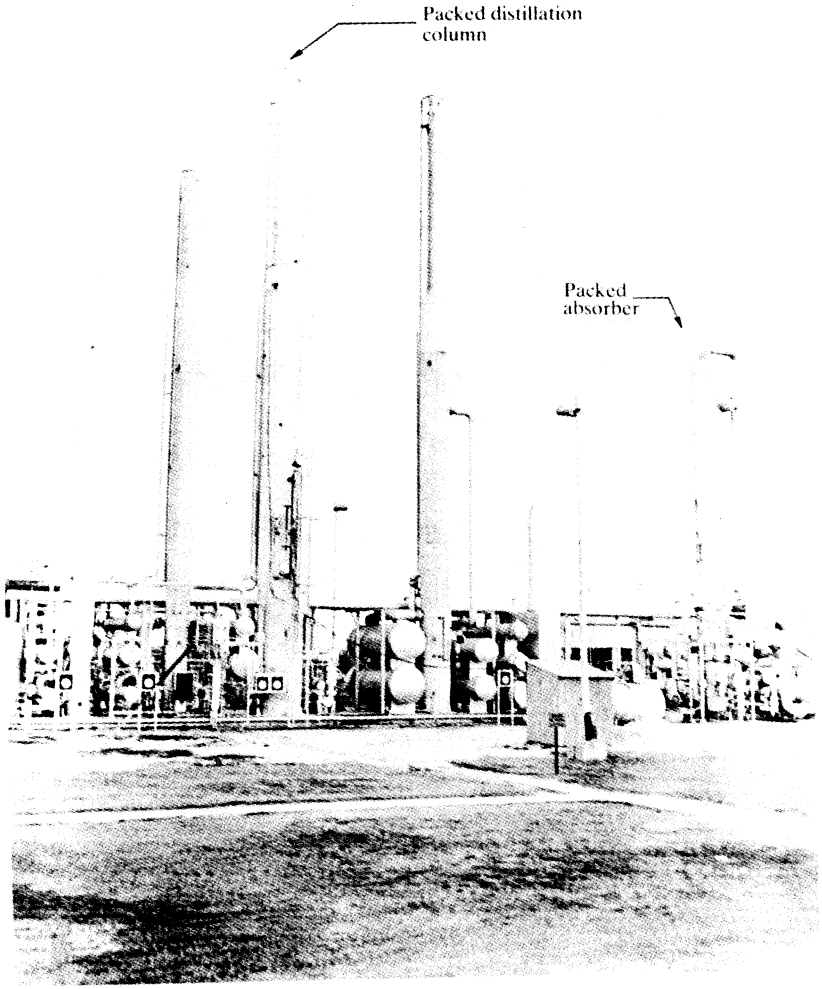

Figure 7-1 The Zoller Gas Plant. (*R. McDaniel, A. A. Bassyoni, and C. D. Holland, "Use of the Results of Field Tests in the Modeling of Packed Distillation Columns and Packed Absorbers—III," Chem. Eng. Sci., vol. 25, p. 634 (1970). Courtesy Chemical Engineering Science.*)

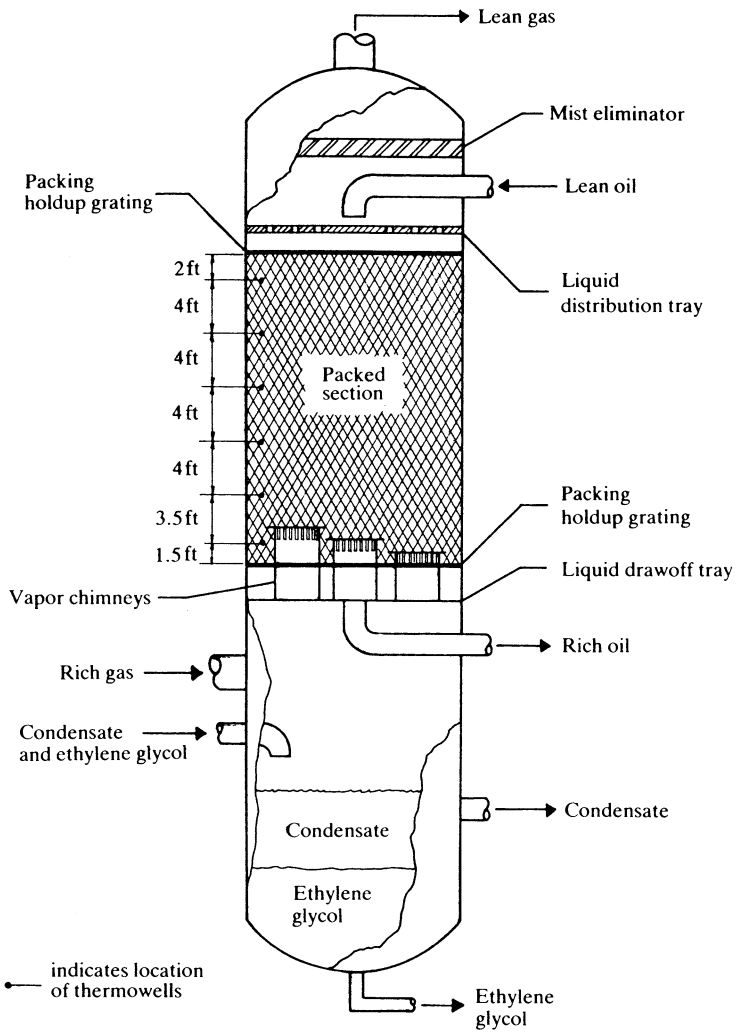

Figure 7-2 The absorber of the Zoller Gas Plant. (*R. McDaniel, A. A. Bassyoni, and C. D. Holland, "Use of the Results of Field Tests in the Modeling of Packed Distillation Columns and Packed Absorbers—III," Chem. Eng. Sci., vol. 25, p. 636 (1970). Courtesy Chemical Engineering Science.*)

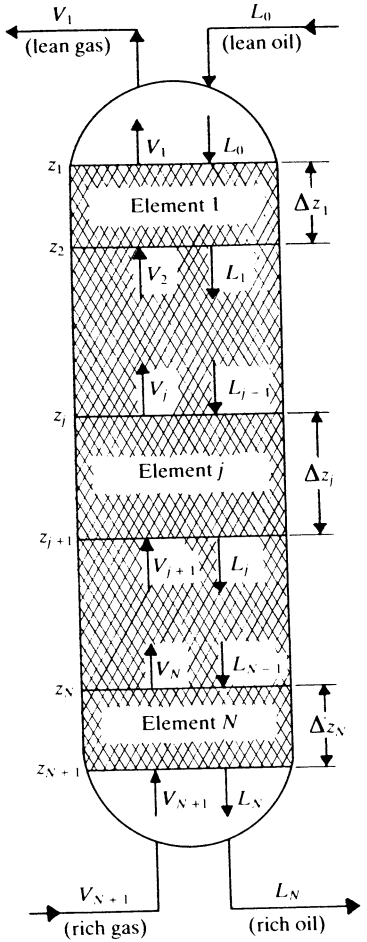

Figure 7-3 Sketch of a typical packed absorber. (*R. E. Rubac, R. McDaniel, and C. D. Holland, "Packed Distillation Columns and Absorbers at Steady State Operation," AIChE J., vol. 11, p. 569 (1969). Courtesy American Institute of Chemical Engineers.*)

fectly mixed section, that is,

$$\begin{aligned} y_{ji} &= E_{ji} K_{ji} x_{ji} \\ x_i &= x_{ji} \qquad (z_j < z \le z_{j+1}) \\ y_i &= y_{ji} \qquad (z_j \le z < z_{j+1}) \end{aligned} \tag{7-1}$$

where x_{ji} and y_{ji} are the mole fractions of component i in the vapor and liquid streams leaving the jth element of packing. For the case where the liquid phase forms a nonideal solution, the quantity K_{ji} is preceded by the ratio of activity coefficients, $\gamma_{ji}^L/\gamma_{ji}^V$.

The heat transfer section having an efficiency e_j is defined by

$$\begin{aligned} T_j^V &= e_j T_j^L \qquad T_j^L = T_j^S \\ T^V &= T_j^V \qquad (z_j \le z < z_{j+1}) \\ T^L &= T_j^L \qquad (z_j < z \le z_{j+1}) \end{aligned} \tag{7-2}$$

This definition supposes that the temperatures of the vapor and liquid phase are uniform but different over each element of packing. Also, the temperature of the packing is taken to be equal to that of the liquid in each element. Throughout the remainder of the development, perfect heat transfer sections ($e_j = 1$) are assumed, that is,

$$T_j^V = T_j^L = T_j^S = T_j \tag{7-3}$$

As a consequence of the definitions of the heat and mass transfer sections and the assumption of perfect heat transfer sections, the equations required to describe the model are the same as those introduced in Chap. 6. The expression for the heat content of the packing is developed as follows:

Let the total mass of packing contained in the element Δz_j be denoted by $\mathcal{M}_j$. Since the bulk density of the packing is constant, it follows that

$$\mathcal{M}_j = \int_{z_j}^{z_{j+1}} \rho_b S \, dz = \rho_b S \, \Delta z_j \tag{7-4}$$

where ρ_b = mass of packing per unit volume of bed
S = internal cross-sectional area of the column

Since the temperature of the packing is taken to be constant and equal to T_j over element Δz_j, it follows that the heat content of the packing contained in the jth element at any time t is given by

$$\mathcal{M}_j h_j^S$$

where h_j^S is the heat content of the packing in British thermal units per unit mass of packing. Although more general models which take into account mixing effects (Ref. 6) may be proposed, the relatively simple model described above gave an adequate representation of the experimental results.

Thus the differential equation representing the energy balance is given by

$$\sum_{i=1}^{c}(v_{j+1,i}\hat{H}_{j+1,i} + l_{j-1,i}\hat{h}_{j-1,i} - v_{ji}\hat{H}_{ji} - l_{ji}\hat{h}_{ji}) = \frac{d\left(\sum_{i=1}^{c} u_{ji}^{V}\hat{H}_{ji}\right)}{dt} + \frac{d\left(\sum_{i=1}^{c} u_{ui}^{L}\hat{h}_{ji}\right)}{dt} + \mathscr{M}_j C_V^S \frac{dT_j}{dt} \quad (7\text{-}5)$$

where

$$C_V^S = \frac{dh_j^S}{dT_j}$$

7-2 ANALYSIS OF THE RESULTS OF THE FIELD TESTS

The field tests consisted of two tests made at steady state operation and one at unsteady state operation of the packed absorber at the Zoller Gas Plant. The results of these tests were used in the development of a model for the unsteady state operation of this absorber as described in a subsequent section. There follows an abbreviated description of the experimental procedures used and the results obtained by McDaniel(4).

Description of the Field Tests

Initially, at time $t = 0$, the absorber was at steady state operation, and at time $t = 0+$, the lean oil rate was changed abruptly from its initial steady state value of 156.655 lb·mol/h to 194.714 lb·mol/h. The temperatures recorded are given in Table 7-1. The times given in this table are only approximate because it took about two minutes to record all of the temperatures. The times do correspond, however, to the precise times at which the temperatures of the lean oil, lean gas, rich oil, and rich gas were observed. At the instant of the upset, the temperature of the lean oil increased immediately from −1.0 to +2.5°F.

Several samples of the inlet gas were taken before and after the field tests. Since the upset had no effect on the composition of this stream, the analyses were averaged to obtain the results given in Table 7-2. The flow rate and compositions of the rich gas were determined by making a simple flash calculation on the inlet gas at the temperature in the space below the rich oil drawoff tray and at the column pressure. Several samples of the lean oil were also taken during the upset. No significant differences in the compositions could be detected, hence, the analyses were averaged to obtain the results given in Table 7-2.

Two samples were taken from both the lean gas and rich oil streams prior to the upset. Two more samples were taken from these streams two hours after the upset. For the first 30 minutes after the upset, samples were taken every five

Table 7-1 Observed temperatures for the unsteady state field test (Refs. 3, 4)

	Temperatures (°F) at the cumulative time (min) indicated					
Depth of packing, ft	0 (initial steady state)	5	10	20	30	120
0 (lean oil)	−1.0	2.5	2.5	2.5	2.5	2.5
0 (lean gas)	26.0	26.0	27.0	27.0	27.0	27.0
2	22.0	24.0	25.0	25.0	25.0	25.0
6	31.5	33.0	34.0	34.0	34.0	34.0
10	28.0	32.0	32.0	33.0	33.4	34.0
14	23.5	25.4	27.2	28.4	29.0	29.4
18	19.4	20.0	21.0	22.0	22.0	22.5
21.5	13.0	13.0	13.5	13.5	14.0	14.0
21.5†	13.0	13.0	14.0	14.0	14.0	14.0
23	−2.5	−2.5	−2.5	−2.5	−2.5	−2.5
23 (rich oil)	20.0	20.0	21.0	21.0	21.0	21.0
23 (rich gas)‡	2.0	2.0	2.0	2.0	2.0	2.0

† This thermowell was contained in a V-shaped trough.

‡ This thermowell was located in the vapor space below the liquid drawoff tray.

Table 7-2 Feed analyses for the unsteady state field test (Refs. 3, 4)

Component	Lean oil (mol %)	Rich gas (mol %)
CO_2	0.0	0.606
N_2	0.0	0.176
CH_4	0.0	86.407
C_2H_6	0.0	6.643
C_3H_8	0.0	3.329
i-C_4H_{10}	0.0	1.027
n-C_4H_{10}	0.0	0.788
i-C_5H_{12}	0.056	0.271
n-C_5H_{12}	0.075	0.213
C_6H_{14}	0.0788	0.289
C_7H_{16}	11.396	0.208
C_8H_{18}	39.941	0.043
C_9H_{20}	31.883	0.001
$C_{10}H_{22}$	15.861	0.0002

Table 7-3 Lean gas analyses (in mol %) for the unsteady state field test (Refs. 3, 4)

	Cumulative time, min							
Component	0	5	10	15	20	25	30	120
CO_2	0.572	0.569	0.569	0.569	0.569	0.569	0.569	0.569
N_2	0.165	0.161	0.161	0.161	0.161	0.161	0.161	0.161
CH_4	93.652	94.044	94.063	94.059	94.056	94.059	94.057	94.059
C_2H_6	4.936	4.723	4.719	4.723	4.727	4.723	4.725	4.724
C_3H_8	0.595	0.432	0.419	0.419	0.418	0.419	0.417	0.418
i-C_4H_{10}	0.015	0.008	0.006	0.006	0.006	0.006	0.006	0.006
n-C_4H_{10}	0.002	0.001	0.001	0.001	0.001	0.001	0.001	0.001
i-C_5H_{12}	0.001	0.001	0.001	0.001	0.001	0.001	0.001	0.001
n-C_5H_{12}	0.001	0.001	0.001	0.001	0.001	0.001	0.001	0.001
C_6H_{14}	0.003	0.003	0.003	0.003	0.003	0.003	0.003	0.003
C_7H_{16}	0.015	0.015	0.015	0.015	0.015	0.015	0.015	0.015
C_8H_{18}	0.030	0.030	0.030	0.030	0.030	0.030	0.031	0.030
C_9H_{20}	0.010	0.010	0.010	0.010	0.010	0.010	0.011	0.010
$C_{10}H_{22}$	0.002	0.002	0.002	0.002	0.002	0.002	0.002	0.002

minutes from the two streams. For the next hour, samples were taken every 10 minutes. A five-minute interval was about the shortest time in which samples could be taken manually. The analyses of the lean gas are presented in Table 7-3. The complete sets of flow rates and product distributions at the initial and final steady states were obtained by material balance. In the analysis of the field test at unsteady state operation which follows, the transient values of the component flow rates (or compositions) of only one stream were needed. The compositions of the lean gas were used in the modeling of the absorber.

Use of the Results of Field Tests in the Modeling of the Packed Absorber at Unsteady State Operation

Although only two steady state field tests (see Tables 7-4 and 7-5) and one unsteady state field test are presented herein, the results of a series of steady state field tests on this same absorber were used to determine the number of mass transfer sections (Refs. 2, 3) by the following procedure.

The first step in the proposed modeling procedure for packed absorbers consists of a logical extension of the concept of the "height equivalent to a theoretical plate" (called HETP) proposed by Peters(5), to columns in the process of separating multicomponent mixtures. For such a column, a number N of perfect transfer sections does not necessarily exist such that all calculated and observed product distributions may be placed in a one-to-one correspondence.

For any given N, the objective function O_1 was used for any one run and the objective function $\bar{O}_1$ was used over all runs R to give a measure of the

Table 7-4 Initial steady state of the unsteady state field test (Refs. 3, 4)

	Flow rates, lb · mol/h				
Component	Lean oil, L_0	Rich gas, V_{N+1}	Lean gas, V_1	Rich oil, L_N	Product distribution, l_{Ni}/v_{1i}
CO_2	0.0	14.656 31	13.036	1.620	0.124 3
N_2	0.0	4.617 37	3.755	0.863	0.229 8
CH_4	0.0	2233.060	2133.470	99.624	0.046 69
C_2H_6	0.0	158.750 3	112.445	46.307	0.411 8
C_3H_8	0.0	66.127 59	13.560	52.568	3.877
i-C_4H_{10}	0.0	15.829 34	0.347	15.483	$0.446\,8 \times 10^2$
n-C_4H_{10}	0.0	10.206 40	0.035	10.172	$0.291\,8 \times 10^3$
i-C_5H_{12}	0.087 32	2.299 97	0.027	2.360	$0.863\,3 \times 10^2$
n-C_5H_{12}	0.117 79	1.410 99	0.027	1.502	$0.553\,9 \times 10^2$
C_6H_{14}	1.234 24	0.867 19	0.071	2.031	$0.287\,6 \times 10^2$
C_7H_{16}	17.868 07	0.266 89	0.342	17.777	$0.518\,5 \times 10^2$
C_8H_{18}	62.569 89	0.024 86	0.682	61.913	$0.907\,7 \times 10^2$
C_9H_{20}	49.946 69	0.000 23	0.235	49.712	$0.211\,5 \times 10^3$
$C_{10}H_{22}$	24.846 36	0.000 03	0.047	24.799	$0.523\,4 \times 10^3$
Total	156.655 3	2508.113	2278.059	386.709	

$T_0 = -1.0°F$, $T_{N+1} = 2.0°F$, and column pressure = 722 lb/in^2 abs; $\mathcal{M}_{total} = 4900$ lb, and $\mathcal{M}_j = 612.5$ lb.

Table 7-5 Final steady state of the unsteady state field test (Refs. 3,4)

	Flow rates, lb · mol/h				
Component	Lean oil, L_0	Rich gas, V_{N+1}	Lean gas, V_1	Rich oil, L_N	Product distribution, l_{Ni}/v_{1i}
CO_2	0.0	14.656 43	12.810	1.846	0.144 1
N_2	0.0	4.617 41	3.630	0.987	0.271 9
CH_4	0.0	2233.079	2118.147	114.948	0.054 27
C_2H_6	0.0	158.751 6	106.372	52.231	0.492 4
C_3H_8	0.0	66.128 17		56.721	6.029
i-C_4H_{10}	0.0	15.829 48	0.146	15.684	$0.107\,5 \times 10^3$
n-C_4H_{10}	0.0	10.206 49	0.012	10.194	$0.823\,1 \times 10^3$
i-C_5H_{12}	0.108 53	2.299 99	0.027	2.381	$0.866\,7 \times 10^2$
n-C_5H_{12}	0.146 41	1.411 00	0.027	1.531	$0.571\,2 \times 10^2$
C_6H_{14}	1.534 09	0.867 19	0.070	2.332	$0.335\,1 \times 10^2$
C_7H_{16}	22.190 35	0.266 89	0.337	22.120	$0.655\,7 \times 10^2$
C_8H_{18}	77.770 81	0.024 86	0.671	77.124	$0.114\,9 \times 10^3$
C_9H_{20}	62.080 90	0.000 23	0.231	61.850	$0.267\,4 \times 10^3$
$C_{10}H_{22}$	30.882 63	0.000 03		50.836	$0.661\,5 \times 10^3$
Total	194.713 70	2508.135	2251.919	450.929	

$T_0 = 2.5°F$, $T_{N+1} = 2.0°F$, column pressure = 722 lb/in^2 abs, and the specific heat of the packing was taken to be 0.12 Btu/lb or for all T.

deviations of the calculated values from the experimental product distributions for all components:

$$O_1 = \frac{1}{c}\sum_{i=1}^{c} |\ln \theta_i| \tag{7-6}$$

$$\bar{O}_1 = \frac{1}{Rc}\sum_{r=1}^{R}\sum_{i=1}^{c} |\ln \theta_{ir}| \tag{7-7}$$

where $\theta_i = (b_i/d_i)_{exp}/(b_i/d_i)_{ca}$, and θ_{ir} is the value of θ_i for run number r.

Although $\bar{O}_1$ is a function of not only the number of mass transfer sections N but also of the sets of vaporization efficiencies E_{ji} over all stages j, components i, and runs R, the number of variables over which $\bar{O}_1$ was to be searched was reduced by taking N to be equal to the number of perfect mass transfer sections required to minimize $\bar{O}_1$. By perfect mass transfer sections is meant that

$$E_{ji} = 1 \qquad \text{for all } j \text{ and } i \tag{7-8}$$

and over all runs R. Thus, the calculated values of b_i/d_i used in Eq. (7-6) were obtained by use of the customary equations for perfect plates. From the plot of $\bar{O}_1$ in Fig. 7-4, for the steady state runs of McDaniel et al.(3) it is seen that $\bar{O}_1$

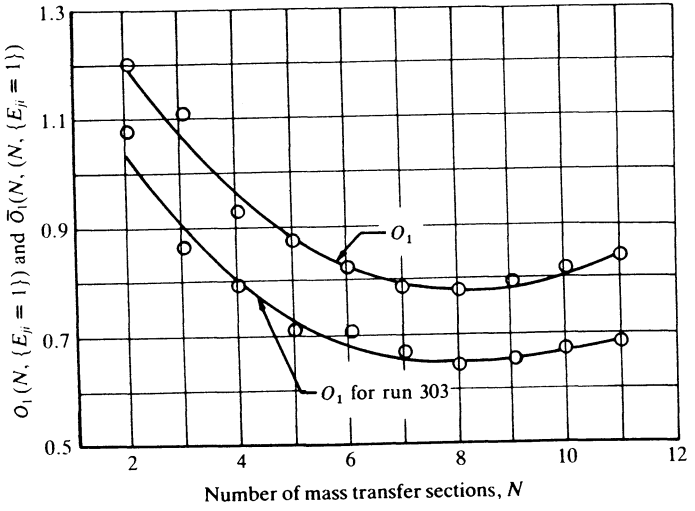

Figure 7.4 Variation of the functions O_1 and $\bar{O}_1$ with the number of perfect mass transfer sections in the absorber. (*R. McDaniel, A. A. Bassyoni, and C. D. Holland, "Use of the Results of Field Tests in the Modeling of Packed Distillation Columns and Packed Absorbers—III," Chem. Eng. Sci., vol. 25, p. 636 (1970). Courtesy Chemical Engineering Science.*)

Table 7-6 Vaporization efficiencies for the initial and final steady states of the unsteady state field test (Refs. 3, 4)

Component	$\bar{E}_i$, initial steady state	$\bar{E}_i$, final steady state	$\bar{E}_{im}$, geometric mean
CO_2	2.1945	2.2998	2.2465
N_2	0.0491	0.0501	0.0496
CH_4	1.3768	1.4032	1.3899
C_2H_4	0.9093	0.9823	0.9451
C_3H_8	0.7842	0.8293	0.8064
i-C_4H_{10}	0.9128	0.9263	0.9196
n-C_4H_{10}	0.9511	0.9665	0.9588
i-C_5H_{12}	0.9315	0.9734	0.9522
n-C_5H_{12}	0.9375	0.9504	0.9439
C_6H_{14}	0.5988	0.6310	0.6147
C_7H_{16}	0.4984	0.5244	0.5112
C_8H_{18}	0.6479	0.6753	0.6615
C_9H_{20}	0.5985	0.6228	0.6105
$C_{10}H_{22}$	0.4984	0.5257	0.5119
β_1	1.0791	1.0948	1.0869
β_N	0.0267	0.9134	0.9200

passes through a minimum at or near the integral value

$$N = 8 \tag{7-9}$$

This value, $N = 8$, was used in the modeling of the unsteady state data. To further reduce the objective function $\bar{O}_1$, a set of vaporization efficiencies were determined by use of the simple product model

$$\begin{aligned} E_{1i} &= \beta_1 \bar{E}_i \\ E_{ji} &= \bar{E}_i \qquad (j = 2, 3, \ldots, N-1) \\ E_{Ni} &= \beta_N \bar{E}_i \end{aligned} \tag{7-10}$$

In this model, a complete set of $\bar{E}_i$'s ($i = 1, 2, \ldots, c$) and two β's, β_1 and β_N, were found. The set of component efficiencies $\bar{E}_i$ was determined such that the values of l_{Ni}/v_{1i} computed by use of the model were in agreement with the experimental values. The two values of β_j (β_1 and β_N) were selected such that the two terminal temperatures T_1 and T_N computed by use of the model were equal to the experimentally observed temperatures. The temperatures measured within the packing were not very reliable and they are generally unavailable and were consequently not used in the modeling of the column.

A stepwise procedure for determining the component efficiency $\bar{E}_i$ for each component i and plate factors $\{\beta_1, \beta_N\}$ for any steady state run (or for any time step of an unsteady state run) is described elsewhere (see for example Refs. 2 and 4). This procedure was used to determine the two sets of $\bar{E}_i$'s and the two sets of β_1's and β_N's (see Table 7-6) for the two steady state field tests shown in

Tables 7-4 and 7-5. These two field tests represent the initial and final steady states of the unsteady state field test. Also the K data of Table 6A-1 were used. The enthalpies employed consisted of those given in Table 6A-2 and corrected by use of the correction factors given in Table 6A-3. These correction factors for the enthalpies were determined as described previously (Refs. 2, 3) such that all of the steady state absorber runs were placed in the best possible balance.

To average the component efficiencies for a given component i over a series of runs, the geometric mean suggested previously was employed, namely,

$$\bar{E}_{i,m} = [\bar{E}_{i,1} \cdot \bar{E}_{i,2} \quad \cdots \quad \bar{E}_{i,R}]^{1/R} \tag{7-11}$$

Likewise, the average values of β_1 and β_N over all runs were taken equal to their corresponding geometric mean values $\{\beta_{1,m}, \beta_{N,m}\}$. These geometric mean values $\{\bar{E}_{i,m}\}$ and $\{\beta_{1,m}, \beta_{N,m}\}$ are presented in Table 7-6 for the two field tests shown in this table. These efficiencies are in good agreement with those obtained for a series of steady state tests which were made by McDaniel et al.(3,4) about one year earlier.

The mean values of the efficiencies presented in Table 7-6 were used in the model for the unsteady state operation of the column. The liquid and vapor holdups in the column were estimated by using a free space of 156 cubic feet. (This space was 98 percent of the total volume occupied by the packing.) The molar volume of the liquid was taken to be 1.9035 $ft^3/lb \cdot mol$, and the molar volume of the vapor was taken to be 378.7 $ft^3/lb \cdot mol$. These molar volumes were computed on the basis of the lean gas and the rich oil streams at the conditions at which they left the absorber. Since the total volume of the vapor and liquid must be equal to the total free space, it follows that the total molar holdups U_P^V and U^L must satisfy the following relationship

$$378.7\ U_P^V + 1.9035\ U^L = 156 \tag{7-12}$$

where U_P^V is the molar holdup of the vapor within the void space of the packing.

In addition to the free space in the packing there was approximately 17.7 cubic feet of space above the packing. Since this space contained only vapor, it follows that the total molar holdup U^V of the vapor is given by

$$U^V = U_P^V + 17.7/378.7 \tag{7-13}$$

Equation (7-12) would permit a maximum liquid holdup of 81.95 $lb \cdot mol$, and Eqs. (7-12) and (7-13) permit a maximum vapor holdup U^V of 0.459 $lb \cdot mol$. The parameter U^L was determined from the results of the unsteady state run by use of a procedure based upon the following considerations.

If the initial steady state, the conditions of the upset, and the holdups are specified for an existing column, then the transient values of the variables may be calculated. For the case where the vapor holdup and the change in the heat

content of the packing in each section are negligible, then Eq. (6-71) of Chap. 6 and Eq. (7-5) may be reduced to the following differential equations:

$$v_{j+1,i} + l_{j-1,i} - v_{ji} - l_{ji} = \frac{du_{ji}^L}{dt} \tag{7-14}$$

$$V_{j+1} H_{j+1} + L_{j-1} h_{j-1} - V_j H_j - L_j h_j = \frac{d(U_j^L h_j)}{dt} \tag{7-15}$$

respectively. If U_j^L is constant, and if

$$U_j^L = U^L/N \tag{7-16}$$

then

$$\frac{du_{ji}^L}{dt} = \frac{U^L}{N}\frac{dx_{ji}}{dt} = \frac{1}{N}\frac{dx_{ji}}{(t/U^L)} \tag{7-17}$$

and since U^L is equal to the sum of the U_j^L's which is independent of time, it follows that

$$\frac{d(U_j^L h_j)}{dt} = \frac{U^L}{N}\frac{dh_j}{dt} = \frac{1}{N}\frac{dh_j}{d(t/U^L)} \tag{7-18}$$

These equations imply that if the transient value of any variable were plotted versus t/U^L, then the resulting plot would constitute a generalized relationship which would hold for every choice of U^L. (For the absorber used in the field tests, the plot would constitute an approximation because the vapor holdups and the change in the heat content of the packing were not negligible.) Thus, the fractional response of any component may be regarded as a function of t/U^L. In particular, let the fractional response of the mole fraction of propane in the lean gas be defined by

$$\text{Fractional response} = \frac{y_1 - y_1^I}{y_1^F - y_1^I} \tag{7-19}$$

where y_1^I is the initial value of the mole fraction, y_1^F is the final mole fraction, and y_1 is the mole fraction of propane in the lean gas at any time t. The mole fraction of propane was selected for consideration because it exhibited a significant variation with respect to time as shown in Table 7-3.

To obtain a set of values for the fractional response versus t/U^L, a liquid holdup $U^L = 20$ $lb \cdot mol$ was arbitrarily selected. The corresponding vapor holdup U_P^V was 0.311 $lb \cdot mol$. The corresponding holdups for each of the mass transfer sections follows:

$$U_j^L = 2.5; \qquad (1 \le j \le 8)$$

$$U_1^V = 0.0856 \qquad U_j^V = 0.0389 \qquad (2 \le j \le 8)$$

In the solution of the corresponding unsteady state problems by use of the semi-implicit Runge–Kutta method, a $\Delta t = 0.1$ min was used in the routine as

the lower bound of the time step (see Eq. (6-49)). The K data presented in Table 6A-1 with vaporization efficiencies given in Table 7-6 and the enthalpies presented in Table 6A-2 with the corrections given in Table 6A-3 were used.

From the transient solution so obtained, the fractional response of propane versus t/U^L (shown in Fig. 7-5) was obtained. From the experimental results presented in Tables 7-3, 7-4, and 7-5, the experimental value of the fractional response at $t = 5$ min is seen to be equal to 0.9209. From Fig. 7-5, the value of t/U^L corresponding to a fractional response of 0.9209 is 0.1958. Thus, the next predicted value of U^L is given by

$$U^L = \frac{5.0}{0.1958} = 25.536 \text{ lb} \cdot \text{mol}$$

The corresponding value of U_P^V as given by Eq. (7-12) is 0.283 58 lb · mol. On the basis of these values of the holdups U^L and U_P^V, the following distribution of holdups is obtained:

$$U_j^L = 3.192 \qquad (1 \le j \le 8)$$

$$U_1^V = 0.082\,186 \qquad U_j^V = 0.035\,447 \qquad (2 \le j \le 8)$$

By use of these holdups, the unsteady state problem was again solved. At the end of $t = 5$ min, a fractional response of 0.9147 was obtained for propane. This value was considered to be close enough to the observed value. The results of this transient solution for propane are presented in Fig. 7-6. An examination of this figure shows good agreement between the predicted and the observed

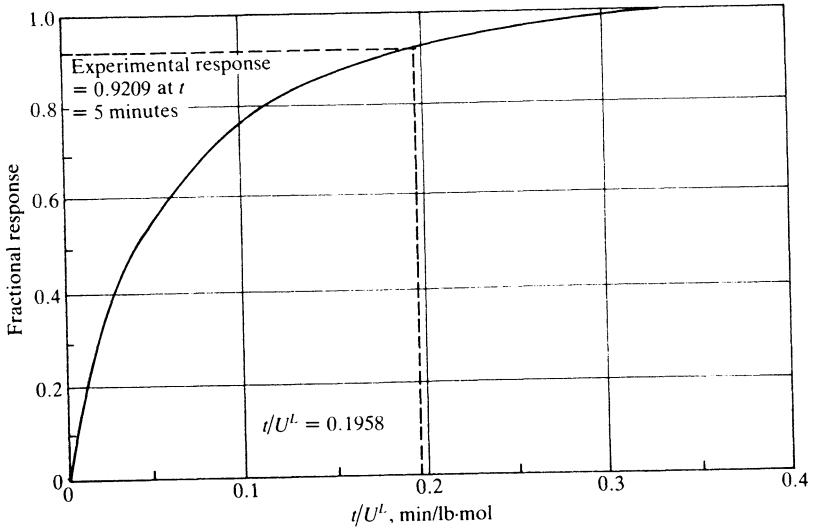

Figure 7-5 Fractional response of the mole fraction of propane in the lean gas; predicted on the basis of $U^L = 20$ lb · mol

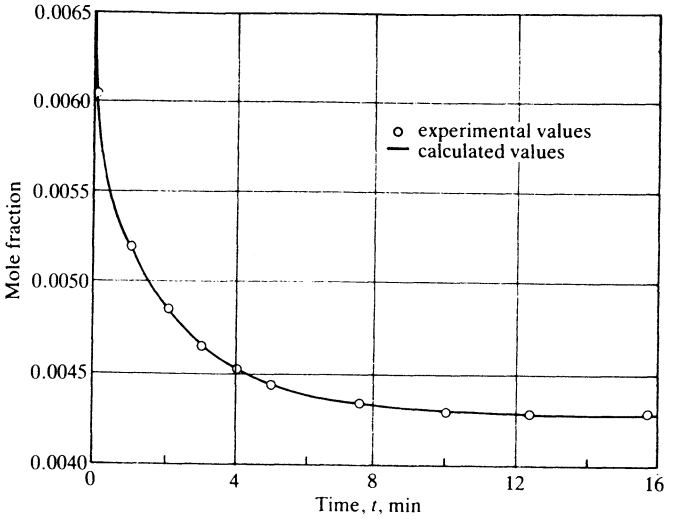

Figure 7-6 Transient values of the mole fraction of propane in the lean gas, predicted on the basis of $U^L = 25.536$ lb · mol

mole fractions for propane. Transient values of the temperatures and lean gas rates are shown in Table 7-7. These results were obtained by Feng(1).

Again it has been demonstrated that the models based primarily on information available to the design engineer may be used to predict the dynamic

Table 7-7 Selected transient values of the variables (Ref. 1)

	Temperature (°R) at end of time step indicated†			Vapor rate V_1 (lb · mol/h) at end of time step indicated†		
Plate	1	20	60	1	20	60
1	484.66	484.47	485.15	2259.00	2253.18	2252.01
2	489.99	489.86	491.23	2353.04	2347.88	2345.01
3	490.56	490.75	492.77	2371.82	2367.66	2363.16
4	489.64	490.10	492.56	2378.41	2374.64	2369.11
5	488.01	488.70	491.33	2384.85	2381.16	2375.17
6	485.83	486.72	489.21	2392.54	2388.64	2382.83
7	482.81	483.89	485.89	2403.10	2398.84	2394.06
8	478.11	479.18	480.29	2420.39	2416.41	2413.75

† A lower bound of 0.1 min on the size of the time step was used. The cumulative process time corresponding to the time steps listed follows:

Time step	*Time*
1	0.10 min
20	2.01 min
60	17.97 min

Also the tolerance vector was chosen as one-thousandth of the initial steady state values.

behavior of a process. Except for the liquid holdup, the values of all other parameters appearing in the model were estimated from design information and steady state field tests. In order to make the model independent of the field tests at unsteady state, a reliable method for the prediction of the liquid holdup in a packed column is obviously needed.

NOTATION

(See also Chaps. 1–5.)

H_{ji}, h_{ji} = enthalpy of component i in the vapor and liquid phases, respectively, in the element of packing Δz_j, Btu/lb · mol
h_j^s = enthalpy of the packing, Btu/unit mass
t = time in consistent units (t_n denotes the beginning and t_{n+1} the end of any given time period under consideration; $\Delta t = t_{n+1} - t_n$,
u_{ji}^L, u_{ji}^V = holdup of component i in the jth element of packing in the liquid and vapor phases, respectively, mol
u_{ji} = $u_{ji}^L + u_{ji}^V$, total molar holdup of component i in the jth element of packing
U_j^L, U_j^V = total holdup of liquid and vapor, respectively, in the jth element of packing, mol
U_j = total holdup of component i in element j
$\mathcal{M}_j$ = total mass of packing contained in the jth element of packing

Subscripts

L = liquid
V = vapor
S = packing

REFERENCES

1. An Feng: Ph.D. dissertation, Texas A&M University, 1983.
2. C. D. Holland: *Fundamentals and Modeling of Separation Process; Absorption, Distillation, Evaporation, and Extraction*, Prentice-Hall, Inc., Englewood Cliffs, N.J., 1975.
3. Ronald McDaniel, A. A. Bassyoni, and C. D. Holland: "Use of the Results of Field Tests in the Modeling of Packed Distillation Columns and Packed Absorbers—III," *Chem. Eng. Sci.*, **25:** 633 (1970).
4. Ronald McDaniel: "Packed Absorbers at Steady State and Unsteady State Operation," Ph.D. dissertation, Texas A&M University, College Station, Texas, 1969. See also: Ronald McDaniel and C. D. Holland: "Modeling of Packed Absorbers at Unsteady State Operation—IV," *Chem. Eng. Sci.*, **25:** 1283 (1970).
5. W. A. Peters, Jr.: "The Efficiency and Capacity of Fractionating Columns," *Ind. Eng. Chem.*, **14:** 476 (1922).
6. N. J. Tetlow, D. M. Groves, and C. D. Holland: "A Generalized Model for the Dynamic Behavior of a Distillation Column," *AIChE J.*, **13:** 476 (1967).

CHAPTER

EIGHT

MODELING OF A DISTILLATION COLUMN AND ITS CONTROL SYSTEM

Application of Gear's method and the semi-implicit Runge–Kutta method to the equations for the equilibrium relationships, component-material balances, and energy balances of a distillation column is carried out in the same manner as shown in Chap. 6 for absorbers. In this chapter a more exact model for the column is used which includes the prediction of the liquid holdup on each plate. Thus, in Sec. 8-1 (the formulation of the model for the distillation column) major consideration is given to the development of the equations for the dynamic behavior of the liquid holdup on each plate, and to the development of the equations for the control system.

The equations developed in Sec. 8-1 are solved for a distillation column to determine its transient behavior for a specified upset. These results are presented in Sec. 8-2.

8-1 FORMULATION OF THE MODEL FOR A DISTILLATION COLUMN BY USE OF GEAR'S METHOD

A fluid dynamic analysis of the liquid and vapor on each plate is used to develop expressions for the holdup of liquid on each plate and in the downcomer. Then the equations for the column are formulated by use of Gear's algorithm.

Dynamic Analysis of a Sieve Tray

In the analysis of a sieve tray, the change of the holdup with time on both the tray and in the downcomer is taken to be negligible over any discrete increment of time. Thus, the steady state equations may be regarded as dynamic relationships which represent the behavior of the column at any instant.

In the application of Bernouli's theorem to the liquid as it flows from point (1) of plate j to point (2) of plate $j+1$ (see Fig. 8-1), let the datum for measuring all heads be taken as point (2). Then

$$\frac{P_j}{\rho_j^L} + \frac{g}{g_c} Z_{L,j+1} + \frac{g}{g_c} (S_{j+1} - Z_{L,j+1}) \frac{\rho_{j+1}^V}{\rho_{j+1}^L} = \frac{P_{j+1}}{\rho_{j+1}^L} + \sum_i F_i \tag{8-1}$$

where $\Sigma_i F_i$ = frictional losses
g = acceleration of gravity
g_c = Newton's law conversion factor
P = pressure
S = tray spacing
Z_L = distance shown in Fig. 8-1, in inches of vapor-free liquid
$Z_s = h_w + h_{ow}$, in inches of vapor-free liquid
ρ^L = mass density of the vapor-free liquid
ρ^V = mass density of the vapor

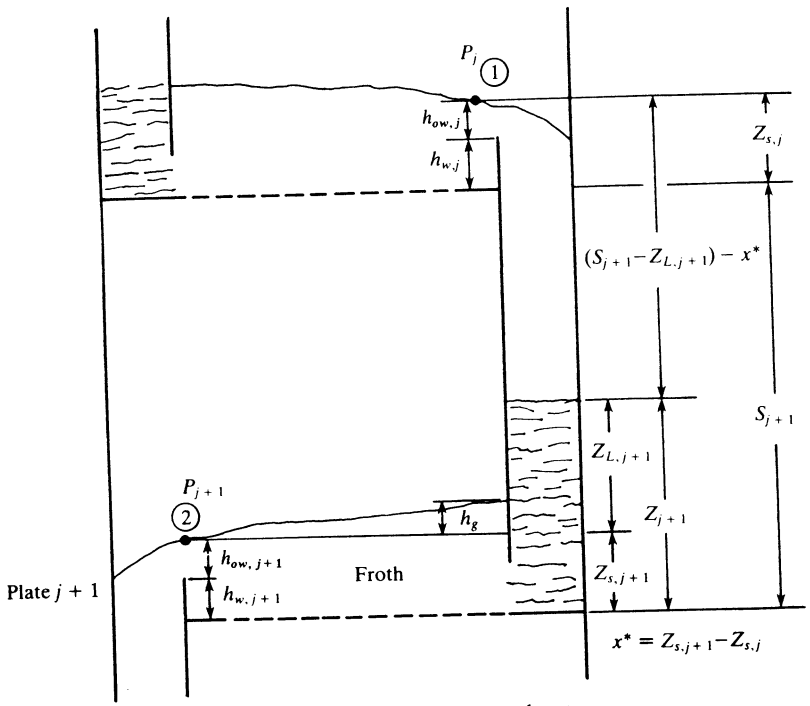

Figure 8-1 Modeling of a distillation column and its control system

In the formulation of Eq. (8-1), the change $(Z_{s,j+1} - Z_{sj})$ in the height of liquid on stages j and $j+1$ was neglected. Also, the kinetic energy effects were taken to be negligible. The frictional losses, $\Sigma_i F_i$, consist of the head lost by the liquid in flowing down the downcomer (which is taken to be negligible), the head lost by flowing under the downcomer weir, and the head lost in flowing across the plate. Thus,

$$\sum_i F_i = \frac{g}{g_c} h_{dc} + \frac{g}{g_c} h_g \tag{8-2}$$

where h_{dc} = head loss by the liquid in flowing under the downcomer in inches of vapor-free liquid
h_g = hydraulic gradient, the head loss by the liquid in flowing across the plate in inches of vapor-free liquid

Equation (8-1) may be solved for $Z_{L,j+1}$ to give

$$Z_{L,j+1} = \frac{\left(\frac{P_{j+1}}{\rho_{j+1}^L} - \frac{P_j}{\rho_j^L}\right)\frac{g_c}{g} + h_{dc,j+1} + h_{g,j+1} - S_{j+1}\frac{\rho_{j+1}^V}{\rho_{j+1}^L}}{(1 - \rho_{j+1}^V/\rho_{j+1}^L)} \tag{8-3}$$

The height of liquid Z_{j+1} in the downcomer is found by adding $Z_{s,j+1}$ to both sides of Eq. (8-3) and rearranging to obtain

$$Z_{j+1} = \frac{\left(\frac{P_{j+1}}{\rho_{j+1}^L} - \frac{P_j}{\rho_j^L}\right)\frac{g_c}{g} + h_{dc,j+1} + h_{g,j+1} + Z_{s,j+1} - (S_{j+1} + Z_{s,j+1})\frac{\rho_{j+1}^V}{\rho_{j+1}^L}}{(1 - \rho_{j+1}^V/\rho_{j+1}^L)} \tag{8-4}$$

Since $\rho_{j+1}^V/\rho_{j+1}^L$ is generally negligible, Eq. (8-4) reduces to

$$Z_{j+1} = \left(\frac{P_{j+1}}{\rho_{j+1}^L} - \frac{P_j}{\rho_j^L}\right)\frac{g_c}{g} + h_{dc,j+1} + h_{g,j+1} + Z_{s,j+1} \tag{8-5}$$

Application of Bernouli's theorem to the vapor as it goes from point (2) to point (1) gives

$$\left(\frac{P_{j+1}}{\rho_{j+1}^V} - \frac{P_j}{\rho_j^V}\right)\frac{g_c}{g} = \frac{\rho_j^L}{\rho_j^V}(h_{0,j} + h_{L,j}) + (S_{j+1} - Z_{s,j+1}) \tag{8-6}$$

where the pressure drop across stage j is equal to the dry hole pressure drop, $h_{0,j}$, plus the pressure drop of the liquid $h_{L,j}$ as it passes up through the liquid on stage j. (Both of these head losses are in inches of vapor-free liquid.) If it is assumed that $\rho_j^V = \rho_{j+1}^V$ and $\rho_j^L = \rho_{j+1}^L$ for stages j and $j+1$, then Eq. (8-6) may be restated in the form

$$\left(\frac{P_{j+1} - P_j}{\rho_j^L}\right)\frac{g_c}{g} = h_{0,j} + h_{L,j} + (S_{j+1} - Z_{s,j+1})\frac{\rho_j^V}{\rho_j^L} \tag{8-7}$$

When ρ_j^V/ρ_j^L is regarded as negligible, Eq. (8-7) reduces to

$$\left(\frac{P_{j+1} - P_j}{\rho_j^L}\right)\frac{g_c}{g} = h_{0,j} + h_{L,j} \tag{8-8}$$

The following formulas may be used for the calculation of the head losses h_{dc}, h_0, h_{ow}, h_L, and h_g. The head loss h_{dc}, corresponding to the pressure drop resulting from the flow of liquid under the downcomer, may be calculated by use of the conventional formula for submerged weirs

$$h_{dc} = 0.057\left(\frac{Q}{A_{dc}}\right)^2 \tag{8-9}$$

where h_{dc} = head loss in inches of vapor-free liquid
Q = flow rate of the liquid under the downcomer weir in gallons per minute
A_{dc} = clearance area between the downcomer and the floor of the tray in square inches

If the tray is equipped with an inlet weir, Leibson et al.(12) recommend that Eq. (8-9) be modified as follows:

$$h_{dc} = 0.068\left(\frac{Q}{A_{dc}}\right)^2 \tag{8-10}$$

The head equivalent to the dry hole pressure drop, h_0, may be calculated by use of the following equation for thick plate orifices

$$h_0 = 0.186\left(\frac{u_0}{C_0}\right)^2\frac{\rho^V}{\rho^L} \tag{8-11}$$

where h_0 = dry hole pressure drop of vapor across the perforations in inches of vapor-free liquid
u_0 = linear velocity of the vapor through the perforation in feet per second

Values of the discharge coefficient C_0 are given by the chart presented in Fig. 8-2 which was prepared by Leibson et al.(12). The linear velocity of the vapor through the orifice on plate j may be computed by use of the following formula:

$$u_{0,j} = \frac{\sum_{i=1}^{c} v_{j+1,i}}{60A_0\,\bar{\rho}_{j+1}^V} \tag{8-12}$$

where A_0 = total area of holes (or perforations)
$\bar{\rho}_{j+1}^V$ = molar density of the liquid
$v_{j+1,i}$ = molar flow rate of component i in the vapor entering stage j from the stage below, $j + 1$

The equivalent height of vapor-free liquid over the weir may be calculated [illegible] modified version of the Francis weir formula

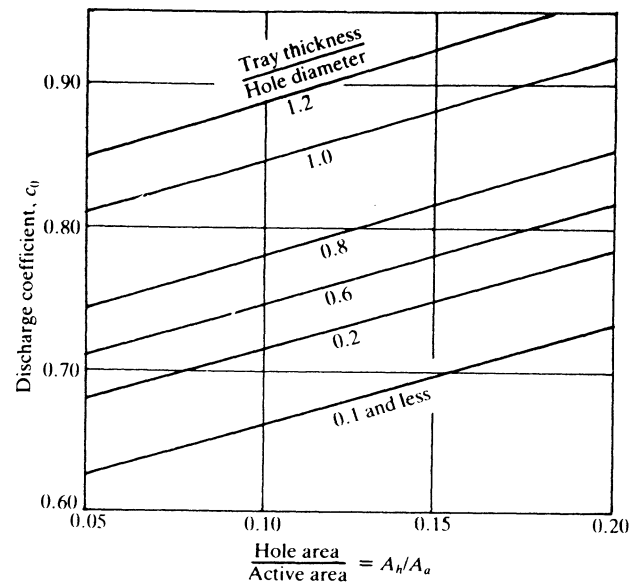

Figure 8-2 Discharge coefficients for the flow of vapor through sieve trays. (*I. Leibson, R. W. Kelly, and L. A. Bullington, Pet. Refiner, vol. 36(2), p. 127 (1957), by courtesy Hydrocarbon Processing.*)

which was proposed by Bolles(1). For a straight segmental weir

$$h_{ow} = 0.48F_w\left[\frac{Q}{l_w}\right]^{2/3} \tag{8-13}$$

where F_w = weir constriction correction factor (see Fig. 8-3)
h_{ow} = equivalent height of vapor-free liquid, in
l_w = length of weir, in
Q = liquid flow rate, gallons per minute

The pressure drop through the aerated liquid h_L has been correlated as a function of $(h_w + h_{ow})$ and $(h_w + h_{ow} + \frac{1}{2}h_g)$. Fair (2) proposes the following correlation

$$h_L = \beta(h_w + h_{ow} + \tfrac{1}{2}h_g) \tag{8-14}$$

where h_L = head loss in inches of vapor-free liquid
β = aeration factor, dimensionless

A graph for estimating β is given in Fig. 8-4. Also given in Fig. 8-4 is a curve for estimating the relative froth density ϕ which is defined as follows:

$$\phi = \frac{h_L}{h_f} \tag{8-15}$$

where h_f = actual height of the froth, in inches.

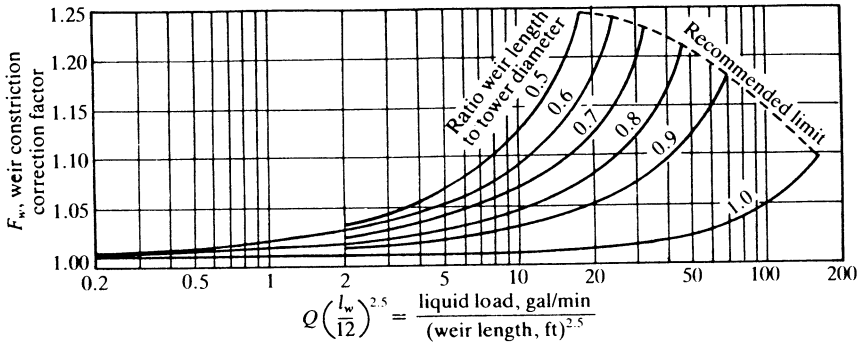

Figure 8-3 The correction factor for effective weir length. (*W. L. Bolles, Pet. Refiner, vol. 25, p. 613 (1946), by courtesy Hydrogen Processing.*)

The following theoretical relationship between ϕ and β was developed by Hutchinson et al.(10):

$$\beta = \frac{\phi + 1}{2} \tag{8-16}$$

Van Winkle(16) gives the following formula for computing h_L:

$$h_L = F_f(h_w + h_{ow}) \tag{8-17}$$

The foam factor F_f is computed by use of the following formula:

$$F_f = 1.0 - 0.372\,19\omega_j(\rho_j^V)^{1/2} \tag{8-18}$$

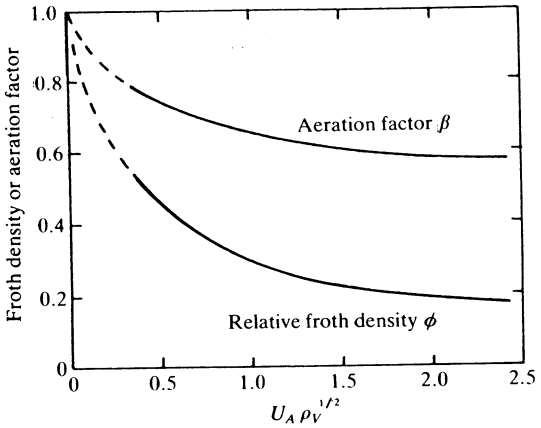

Figure 8-4 Aeration factor and froth density for bubble-cap, sieve, and valve plates, u_A = linear vapor velocity through the active area, ft/s; ρ_v = vapor density, lb/ft^3. (*B. D. Smith, Design of Equilibrium Stage Processes, McGraw-Hill Book Company, New York, 1963, by courtesy McGraw-Hill Book Company.*)

and the linear velocity ω_j is computed by use of

$$\omega_j = \frac{\sum_{i=1}^{c} v_{ji}}{60A_a\bar{\rho}_j^V} \tag{8-19}$$

where A_a = active area of a sieve tray (area between the outlet weir and the downcomer, in square feet).

Hugmark and O'Connell(9) presented the following correlation for calculation of the hydraulic gradient for a sieve plate

$$h_g = \frac{f\omega_f^2 l_f}{12g_c r_h} \tag{8-20}$$

where h_g = hydraulic gradient in inches of vapor-free liquid
f = friction factor (see Fig. 8-5)
g_c = Newton's law conversion factor, 32.17
l_f = length of flow path across plate, ft
r_h = hydraulic radius of the aerated mass, ft (defined below)
ω_f = velocity of the aerated mass in feet per second

A graph of the friction factor f as a function of Reynolds number is shown in Fig. 8-5. The Reynolds number used in this correlation is defined as follows:

$$N_{\text{Re}} = \frac{r_h\omega_f\rho^L}{\mu_L} \tag{8-21}$$

where ρ^L = mass density of the vapor-free liquid, lb/ft^3
μ_L = viscosity of the vapor-free liquid, lb/(ft · s)

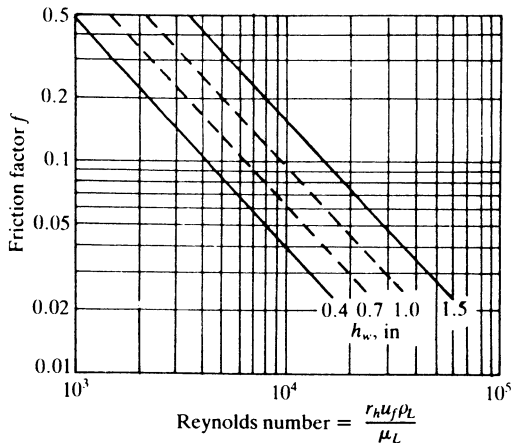

Figure 8-5 Friction factor used in the calculation of the hydraulic gradient, h_g, for sieve trays with crossflow. (*B. D. Smith, Design of Equilibrium Stage Processes, McGraw-Hill Book Company, New York, 1963, by courtesy McGraw-Hill Book Company.*)

The hydraulic r_h of the aerated mass is defined as follows:

$$r_h = \frac{\text{cross section}}{\text{wetted perimeter}} = \frac{h_f D_f}{2h_f + 12D_f} \tag{8-22}$$

where D_f = arithmetic average of the tower diameter and the weir length, ft
h_f = froth height in inches (estimated by the use of Eq. (8-15) and Fig. 8-4)

The velocity ω_f of the aerated mass in feet per second is taken to be the same as that of the vapor-free liquid, and it is calculated as follows:

$$\omega_f = \frac{1}{5}\left(\frac{q}{h_L D_f}\right) \tag{8-23}$$

where q is the liquid flow rate in cubic feet per minute.

Formulation of the Model for the Distillation Column by Use of Gear's Algorithm

For a distillation column with a total condenser, the model for the column exclusive of the controllers is formulated as shown below. The equations consist of the component-material balances, the energy balances, the equilibrium relationships, the pressure drop relationships, and the heights of liquid in the downcomers. They are stated for each stage j ($j = 1, 2, \ldots, N$) in the order enumerated. Following a statement of the equations is a discussion of those equations introduced for the first time.

$$0 = -\frac{(L_1 + D)u_{1i}}{\sum_{i=1}^{c} u_{1i}} + v_{2i} - \frac{du_{1i}}{dt} \qquad (i = 1, 2, \ldots, c) \tag{8-24}$$

$$0 = F_j X_{ji} + \frac{L_{j-1}u_{j-1,i}}{\sum_{i=1}^{c} u_{j-1,i}} - \frac{L_j u_{ji}}{\sum_{i=1}^{c} u_{ji}} - v_{ji} + v_{j+1,i} - \frac{du_{ji}}{dt}$$

$$(i = 1, 2, \ldots, c) \quad (j = 2, 3, \ldots, N-1) \tag{8-25}$$

(Note $F_j X_{ji} = 0$ for all j except $j = f$, the feed plate.)

$$0 = \frac{L_{N-1}u_{N-1,i}}{\sum_{i=1}^{c} u_{N-1,i}} - \frac{L_N u_{Ni}}{\sum_{i=1}^{c} u_{Ni}} - v_{Ni} - \frac{du_{Ni}}{dt} \qquad (i = 1, 2, \ldots, c) \tag{8-26}$$

$$0 = \sum_{i=1}^{c} u_{ji} - \bar{\rho}_j^L \bar{U}_j \qquad (j = 1, 2, \ldots, N) \tag{8-27}$$

$$0 = \sum_{i=1}^{c} v_{2i}\hat{H}_{2i} - \frac{(L_1 + D)E_1}{\sum_{i=1}^{c} u_{1i}} - Q_C - \frac{dE_1}{dt} \tag{8-28}$$

$$0 = \frac{L_{j-1}E_{j-1}}{\sum_{i=1}^{c} u_{j-1,i}} - \frac{L_j E_j}{\sum_{i=1}^{c} u_{ji}} + \sum_{i=1}^{c}\left[v_{j+1,i}\hat{H}_{j+1,i} - v_{ji}\hat{H}_{ji}\right] - \frac{dE_j}{dt}$$

$$(j = 2, 3, \ldots, N-1) \tag{8-29}$$

$$0 = \frac{L_{N-1}E_{N-1}}{\sum_{i=1}^{c} u_{N-1,i}} - \frac{L_N E_N}{\sum_{i=1}^{c} u_{Ni}} - \sum_{i=1}^{c} v_{Ni}\hat{H}_{Ni} + Q_R - \frac{dE_N}{dt} \tag{8-30}$$

$$0 = \sum_{i=1}^{c} u_{ji}\hat{h}_{ji} - E_j \qquad (j = 1, 2, \ldots, N) \tag{8-31}$$

$$0 = \gamma_{1i}^V\left(\frac{Y_{1i}}{\sum_{i=1}^{c} Y_{1i}}\right) - \gamma_{1i}^L K_{1i}\left(\frac{u_{1i}}{\sum_{i=1}^{c} u_{1i}}\right) \qquad (i = 1, 2, \ldots, c) \tag{8-32}$$

$$0 = \sum_{i=1}^{c} Y_{1i} - 1 \tag{8-33}$$

$$\left(\text{Note: } y_{1i} = Y_{1i} \Big/ \sum_{i=1}^{c} Y_{1i}\right)$$

$$0 = \gamma_{ji}^V\left(\frac{v_{ji}}{\sum_{i=1}^{c} v_{ji}}\right) - \gamma_{ji}^L K_{ji}\left(\frac{u_{ji}}{\sum_{i=1}^{c} u_{ji}}\right) \qquad \begin{matrix}(i = 1, 2, \ldots, c)\\ (j = 2, 3, \ldots, N)\end{matrix} \tag{8-34}$$

$$0 = P_2 - P_1 - \left(\sum_{i=1}^{c} v_{2i}\right)^2 \bar{\rho}_2^V \left[\frac{P_2 - P_1}{\left(\sum_{i=1}^{c} u_{2i}\right)^2 \bar{\rho}_2^V}\right]_{\text{ref}} \tag{8-35}$$

$$0 = \left(\frac{P_{j+1} - P_j}{\rho_j^L}\right) - \frac{g}{g_c}h_{0j} - \frac{g}{g_c}h_{Lj} \qquad (j = 2, 3, \ldots, N-1) \tag{8-36}$$

$$0 = Z_{j+1} - \left(\frac{P_{j+1} - P_j}{\rho_j^L}\right)\frac{g_c}{g} - h_{dc,j+1} - h_{w,j+1} - h_{ow,j+1}$$

$$(j = 1, 2, \ldots, N-1) \tag{8-37}$$

Equations (8-24) through (8-37) consist of $[N(2c + 5) - 1]$ independent equations in $[N(2c + 5) + 4]$ independent variables, namely,

$$\mathbf{x} = [Q_C\ D\ L_1\ E_1\ P_1\ T_1\ Z_1\ Y_{1,1} \cdots Y_{1,c}\ u_{1,1} \cdots u_{1,c}\ (L_j\ E_j\ P_j\ T_j\ Z_j\ u_{j,1} \cdots u_{j,c}\ v_{j,1} \cdots v_{j,c})_{j=2,N}\ Q_R\ Z_{N+1}]^T \quad (8\text{-}38)$$

where $(\ )_{j=2,N}$ means that the arguments are to be repeated for $j = 2, 3, \ldots N$. The variables Z_1 and Z_{N+1} are the heights of vapor-free liquid in the accumulator and the base of the column. These variables appear in the expressions (given below) for the holdups of the accumulator $\bar{U}_1$, and the base of the column $\bar{U}_N$. Thus, in order to solve the above equations, five variables must be fixed.

Equation (8-27) expresses the constraint that the sum of the molar holdups $\{u_{ji}\}$ on each stage must be equal to the total molar holdup. For stage 1, the volumetric holdup consists of the liquid in the reflux accumulator and is computed by use of the formula

$$\bar{U}_1 = l_R\left\{\left[\frac{\pi}{2} + \sin^{-1}\left(\frac{2Z_1}{D_R} - 1\right)\right]\left(\frac{D_R}{2}\right)^2 + \left(Z_1 - \frac{D_R}{2}\right)(Z_1 D_R - Z_1^2)^{0.5}\right\} \quad (8\text{-}39)$$

where D_R = diameter of the accumulator, ft
l_R = length of the accumulator, ft
$\bar{U}_1$ = volumetric holdup in the reflux accumulator, ft^3
Z_1 = height of vapor-free liquid in the accumulator, ft

For stages $j = 2, 3, \ldots, N - 1$, the volumetric holdup Z_j is computed by use of

$$\bar{U}_j = \bar{\rho}_j^L\left[\left(\frac{h_{Lj}}{12}\right)A_a + \left(\frac{Z_j}{12}\right)A_d\right] \quad (8\text{-}40)$$

The holdup of liquid in the bottom of the tower, in the reboiler and in the associated lines was approximated as follows:

$$\bar{U}_N = 100 + \frac{\pi Z_{N+1} D_T^2}{4} \quad (8\text{-}41)$$

where the volume of the reboiler and associated lines is taken to be equal to 100 cubic feet and where

Z_{N+1} = height of liquid in the bottom of the column, ft (see Fig. 8-6)
D_T = inside diameter of the column, ft

Also, note that in Eq. (8-32), the mole fraction y_{1i} has been replaced by its equivalent

$$Y_{1i} \Big/ \sum_{i=1}^{c} Y_{1i}$$

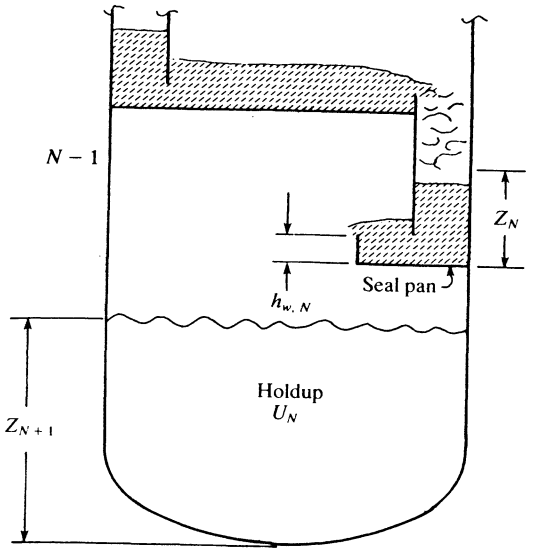

Figure 8-6 Seal pan and bottom of the column

and furthermore this replacement should be made wherever y_{1i} appears implicitly in any equation.

Equation (8-35) relates the pressure P_1 in the reflux accumulator to the pressure P_2 on the top plate, and thereby accounts for the pressure drop of the vapor in flowing from the top plate through the condenser tubes. This equation is a modification of the expression given by Lord et al.(13) for the pressure drop of the condensing vapors on the tube side of a shell and tube exchanger. In the use of this equation, it was assumed that for deviations from a reference state, the pressure drop varied directly with the vapor density and the square of the vapor flow rate. The hydraulic gradient (see Eq. (8-5)) is usually small and was neglected in Eq. (8-37) in the modeling of the column.

Modeling of Controllers and Control Valves

A typical control system for a distillation column is shown in Fig. 8-7 in which the variables to be controlled are P_1, Z_1, L_1, T_k, and Z_{N+1} where T_k is the temperature of a preselected plate k which is to be used to regulate the steam rate to the reboiler.

First the fundamental equations for typical controllers and control valves are presented and then these are used to model the controllers and control valves used for the column shown in Fig. 8-7.

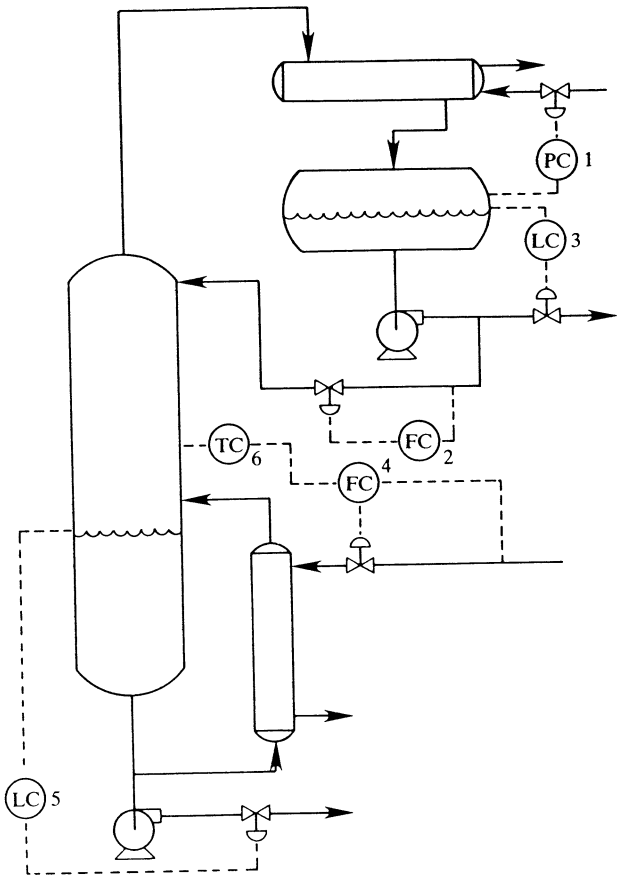

Figure 8-7 Control system used in modeling the distillation column

Equations for Controllers

A proportional controller is defined as one in which the difference between the output and the input of the controller is proportional to the deviation of the control variable from the control point, namely,

$$p = K_c e + p_0 \tag{8-42}$$

where c = input value of the control variable
$e = r - c$
K_c = proportional gain constant
p = output of the controller
p_0 = reference output of the controller
r = reference value of variable, the set point

Observe that if at a given set of operating conditions, the system is at steady state at the control point $c = r$, then $p = p_0$. Now if, say, a step change in the load occurs, the control variable c will depart from the control point r, giving rise to an output p which is unequal to p_0. Then at the new steady state $r \neq c$ and $p \neq p_0$.

When integral or reset action is added to the controller, the controller has the capacity to reset the reference output as required to eventually bring the control variable back to the control point. Such a controller is called a *proportional-integral* controller, and its action is described by

$$p = K_c\left(e + \frac{1}{\tau_I}\int_{0+}^{t} e\,dt\right) + p_0 \tag{8-43}$$

where τ_I = integral time constant.

A third mode of control produces a controller output proportional to the rate of change of the measured variable. When this mode of control is combined with a proportional-integral controller, the combination is called a *proportional-integral-rate* controller which is described by

$$p = K_c\left(e + \frac{1}{\tau_I}\int_{0+}^{t} e\,dt + \tau_D\frac{de}{dt}\right) + p_0 \tag{8-44}$$

where τ_D = time constant for the rate mode. This rate mode of control is sometimes called *derivative action.*

Gallun(3) used proportional-integral controllers in the simulation of a distillation column. In the formulation of the controllers by Gear's method the following equations were used. Let the function I be defined as follows:

$$I = \int_{0+}^{t} e\,dt + \frac{\tau_I}{K_c}p_0 \tag{8-45}$$

Then

$$0 = K_c\left(e + \frac{I}{\tau_I}\right) - p \tag{8-46}$$

and

$$0 = e - \frac{dI}{dt} \tag{8-47}$$

For each controller, a pair of equations of the form of Eqs. (8-46) and (8-47) are used in Gear's algorithm.

Equations (8-46) and (8-47) constitute two additional equations in three variables c, p, and I, which are to be solved for each proportional-integral controller added to the system.

Equations for Control Valves

The output of a controller may be used as the input to another controller or to operate a control valve. If the signal is used to drive an air-operated control valve there will be dynamics associated with the response of the valve to changes in the controller output. Suppose that the valve position responds to a controller output in a first-order manner as follows:

$$\tau_v \frac{d\delta}{dt} + \delta = 0.0625p - 0.25 \tag{8-48}$$

where p is in milliamperes, t is in seconds, and δ is the valve position which ranges from $\delta = 0$ to $\delta = 1$. At steady state

$$\frac{d\delta}{dt} = 0 \tag{8-49}$$

Thus, for an input p of 4 mA, at steady state

$$\delta = 0$$

and for an input of 20 mA (the maximum output of the controller),

$$\delta = 1$$

Thus, as the input p ranges from 4 to 20 mA, the control valve goes through its complete range from 0 to 1.

Modeling of the Controllers and Control Valves for a Distillation Column

The control system shown in Fig. 8-7 has as its objective the control of the five variables (P_1, Z_1, L_1, T_k, and Z_{N+1}) enumerated previously. Each controller is described by two equations of the form of Eqs. (8-46) and (8-47) and each control valve is described by an equation of the form of Eq. (8-48). In addition to these three equations, an additional relationship is needed for the device used to measure the variable to be controlled.

Consider first the modeling of the control system used to control the pressure P_1. The four new equations associated with the controller of the pressure P_1 are as follows. For control system 1:

$$0 = c_1 + 12.0 - 0.032P_1 \tag{8-50}$$

$$0 = p_1 - K_{c1}\left[(c_1 - r_1) + \frac{I_1}{\tau_{I,1}}\right] \tag{8-51}$$

$$0 = c_1 - r_1 - \frac{dI_1}{dt} \tag{8-52}$$

$$0 = -0.25 + 0.0625p_1 - \delta_1 - \tau_{v,1}\frac{d\delta_1}{dt} \tag{8-53}$$

Equation (8-50) describes the sensing device of the accumulator pressure P_1 which produces an output signal of 4 to 20 mA as the pressure P_1 varies from 500 to 1000 mm of mercury absolute. Equations (8-51) and (8-52) are a restatement of Eqs. (8-46) and (8-47) for the pressure controller. The definition of the error used in these equations has been changed, however, to reflect the fact that the control valve for the cooling water should open when the column pressure exceeds the set point. Equation (8-53) is a restatement of the valve position equation (Eq. (8-48)).

For control of the reflux rate L_1 (or the corresponding volumetric rate q_1), the equations are analogous in form for control system 2 as those shown for the pressure controller, namely,

$$0 = c_2 - 4.0 - \left(\frac{q_1}{200}\right)^2 \tag{8-54}$$

$$0 = p_2 - K_{c2}\left[(r_2 - c_2) + \frac{I_2}{\tau_{I,2}}\right] \tag{8-55}$$

$$0 = r_2 - c_2 - \frac{dI_2}{dt} \tag{8-56}$$

$$0 = -0.25 + 0.0625p_2 - \delta_2 - \tau_{v,2}\frac{d\delta_2}{dt} \tag{8-57}$$

where q_1 is equal to the volumetric flow rate in gallons per minute. Equation (8-54) describes the behavior of the primary measuring element and it produces an output signal r_2 ranging from 4 to 20 mA as the flow rate of the reflux varies from 0 to 800 gal/min. Equations (8-55) and (8-56) describe the controller action and Eq. (8-57) describes the control valve behavior.

Similarly, the equations for the liquid level control system for the accumulator (control system 3) are as follows:

$$0 = c_3 - 4.0 - 1.6Z_1 \tag{8-58}$$

$$0 = p_3 - K_{c3}\left[(c_3 - r_3) + \frac{I_3}{\tau_{I,3}}\right] \tag{8-59}$$

$$0 = c_3 - r_3 - \frac{dI_3}{dt} \tag{8-60}$$

$$0 = -0.25 + 0.0625p_3 - \delta_3 - \tau_{v,3}\frac{d\delta_3}{dt} \tag{8-61}$$

Equation (8-58) represents the behavior of the sensing device which gives an output signal of 4 to 20 mA as the accumulator level varies from 0 to 10 ft. Equations (8-59) and (8-60) describe a proportional-integral controller which causes the product (distillate) valve to open as the accumulator level rises above the set point. Equation (8-61) relates the overhead product-valve position to the controller output.

The liquid-level control system for the base of the column (control system 5) is described by the following set of equations:

$$0 = c_5 - 20 - 4Z_{N+1} \tag{8-62}$$

$$0 = p_5 - K_{c5}\left[(c_5 - r_5) + \frac{I_5}{\tau_{I,5}}\right] \tag{8-63}$$

$$0 = c_5 - r_5 - \frac{dI_5}{dt} \tag{8-64}$$

$$0 = -0.25 + 0.0625p_5 - \delta_5 - \tau_{v,5}\frac{d\delta_5}{dt} \tag{8-65}$$

Equation (8-62) describes the sensing element which produces an output signal of 4 to 20 mA as the liquid level Z_{N+1} in the base of the tower is varied from 6 to 10 ft. Equations (8-63) and (8-54) describe the controller and Eq. (8-65) describes the behavior of the control valve.

The steam flow rate to the reboiler is regulated by a cascade control system as indicated in Fig. 8-7. The set point of the steam-flow control system (control system 4) is provided by the temperature-control system (control system 6). The complete set of equations for the steam-flow control system and the temperature control system follow:

$$0 = c_4 - 4 - 16\left(\frac{w_s}{3000}\right)^2 \tag{8-66}$$

$$0 = p_4 - K_{c4}\left[(p_6 - c_4) + \frac{I_4}{\tau_{I,4}}\right] \tag{8-67}$$

$$0 = p_6 - c_4 - \frac{dI_4}{dt} \tag{8-68}$$

$$0 = -0.25 + 0.0625p_4 - \delta_4 - \tau_{v,4}\frac{d\delta_4}{dt} \tag{8-69}$$

$$0 = T_k - T_M - \tau_M\frac{dT_M}{dt} \tag{8-70}$$

$$0 = c_6 + 236 - 0.4T_M \tag{8-71}$$

$$0 = p_6 - K_{c6}\left[(r_6 - c_6) + \frac{I_6}{\tau_{I,6}}\right] \tag{8-72}$$

$$0 = r_6 - c_6 - \frac{dI_6}{dt} \tag{8-73}$$

Equations (8-66) through (8-69) describe the steam-flow control system. Equation (8-66) represents the measuring device for the steam-flow rate and it produces a signal c_4 of 4 to 20 mA as the steam-flow rate varies from 0 to 3000 pounds of steam per minute. Equations (8-67) and (8-68) describe the proportional controller which controls the steam rate. Note that the set point p_6 of the proportional controller is an output of the proportional-temperature controller (Eqs. (8-72) and (8-73)). Equation (8-69) relates the stem position of the steam-flow control valve to the output of the steam-flow controller. Equations (8-70) and (8-71) describe a temperature measuring device with first-order dynamics and a transducer which produces an output signal of 4 to 20 mA as the measured temperature T_M varies from 600 to 640°R. Equations (8-72) and (8-73) describe an ideal proportional-integral controller operating on the measured temperature T_M of plate k. The temperature T_k is the actual temperature T_j for the particular plate $j = k$. The output p_6 is fed back to the steam-flow controller as its set point.

Equations (8-50) through (8-73) consist of 24 independent equations in 24 additional independent variables, namely,

$$I_1, I_2, \ldots, I_6, p_1, p_2, \ldots, p_6, c_1c_2, \ldots, c_6, T_M, \delta_1, \delta_2, \ldots, \delta_5$$

which now gives a total of $[N(2c + 5) + 23]$ independent equations and $[N(2c + 5) + 28]$ independent variables.

Equations for the description of the heat transfer and fluid flow for the condenser, accumulator, the base of the tower, and the reboiler are formulated in a manner similar to that shown for evaporators. Gallun(3) used an additional 21 independent equations and 21 independent variables to describe the heat transfer and fluid flow for the condenser-accumulator and the reboiler which resulted in a total of $[N(2c + 5) + 44]$ independent variables, a listing of which follows:

$$\begin{aligned}\mathbf{x} = [&c_1\ p_1\ I_1\ c_2\ p_2\ I_2\ c_3\ p_3\ I_3\ \delta_1\ \delta_2\ \delta_3\ q_w\ T_{wo}\ T_{mc}\ q_1\ q_2\ P_{d1}\ P_{S1}\\ &Q_C\ D\ Y_{1,1} \cdots Y_{1,c}\ T_1\ P_1\ u_{1,1} \cdots u_{1,c}\ L_1\ E_1\ Z_1\\ &(v_{j,1} \cdots v_{j,c}\ u_{j,1} \cdots u_{j,c}\ T_j\ P_j\ L_j\ E_j\ Z_j)_{j=2,N}\ Q_R\ q_N\\ &w_c\ w_s\ T_s\ E_s\ T_{mr}\ \rho_s\ P_{S2}\ P_{d2}\ \delta_4\ \delta_5\ T_M\ c_4\ p_4\ I_4\ c_5\ p_5\ I_5\ c_6\ p_6\ I_6]^T\end{aligned} \tag{8-74}$$

The variables q_w, T_{wo}, T_{mc}, q_1, q_2, P_{d1}, P_{S1}, $q_N w_c$, w_s, T_s, E_s, T_{mr}, ρ_s, P_{S2}, P_{d2} are associated with the heat transfer and fluid flow of the condenser, accumulator, the base of the column, and the reboiler. These symbols are defined in the Notation, and the corresponding independent equations involving these variables are given by Gallun(3).

When the equations and variables are ordered in this fashion, they give rise to a jacobian matrix which has the characteristic of being almost band.

8-2 SOLUTION OF EXAMPLE 8-1 BY USE OF GEAR'S METHOD

This example is one of those used by Gallun(3) to demonstrate the formulation of the equations for a distillation column by use of Gear's method(4,5,6). This example consists of an extractive distillation of acetone from methanol and ethanol with water as the extractive agent. The response of the closed-loop control system

to a change in the set point temperature on stage 35 from $T_{35,c} = 626.2261°R$ at the initial steady state (time $t = 0$) to $T_{35,c} = 631.226°R$ at time $t = 0+$.

The column contained 48 plates plus a reboiler plus a total condenser for a total of 50 stages. A statement of the compositions of the feeds appears in Table 8-1. The enthalpy of the liquid phase was approximated by use of the assumption of ideal solution behavior. Virtual values of the partial molar enthalpies (see App. 4A-2) were used for the vapor phase. The departure function Ω for the vapor phase was evaluated by use of the first two terms of the virial equation of state. The second virial coefficient was approximated as described by Prausnitz et al.(14). The parameters needed in the above calculations were taken from page 213 of Ref. (14). The resulting equations are presented by Gallun(3). The activity coefficients were calculated by use of the Wilson equation using the constants given in Table 8A-1. The fugacity coefficients for the vapor phase were computed by use of Eqs. (3-10) through (3-12) of Chap. 3 and pages 143 to 144 of App. A of Prausnitz et al.(14). The results are given in Table 8A-1.

The five variables fixed are the pressure P_1, the liquid level in the accumulator Z_1, the flow rate of the reflux L_1 (or q_1), and the temperature T_{35} of stage 35. These values are listed in Table 8-2.

A listing of the hydraulic parameters and certain initial values are given in Table 8-3, and the time constants in Table 8-4. Values of selected variables at the initial steady state are shown in Tables 8-5 and 8-6. The response as reflected by selected variables is shown in Table 8-7, and a comparison of the initial and final temperature profiles appears in Table 8-8. The initial and final flow rates of each component in the distillate and bottom products are shown in Table 8-9.

Table 8-1 Compositions and enthalpies of the feeds at the initial steady state (Ref. 3)

	Component flow rates of feed, lb · mol/min				
Feed stage	Methanol	Acetone	Ethanol	Water	Enthalpy Btu/min
3	0.0	0.0	0.0	5.0	6 118.898
5	25.0	0.5	5.0	197.5	513 543.30
21	65.0	25.0	5.0	5.0	146 509.60

Table 8-2 Controller set points at the initial steady state (Ref. 3)

Controller	Set point in physical units	Set point r_k, mA
1	760 mmHg abs	12.32
2	490.135 gal/min	10.005 8
3	3 ft	8.8
5	8 ft	12.0
6	626.2261°R	14.490 44

Table 8-3 Hydraulic parameters and initial steady state values of selected variables (Ref. 3)

1. Hydraulic parameters

Variable		Value
A_{aj}	$(j = 2, 3, \ldots, 49)$	141.372 ft²
A_{dj}	$(j = 2, 3, \ldots, 49)$	17.6715 ft²
A_{0j}	$(j = 2, 3)$	18 ft²
	$(j = 4, 5, \ldots, 49)$	13 ft²
A_{Tj}		176.714 ft²
A_{dc}	$(j = 2, 3, \ldots, 49)$	0.908 375 ft²
C_{0j}	$(j = 2, 3)$	0.75 ft/s
	$(j = 4, 5, \ldots, 49)$	0.72 ft/s
D_0		0.1875 in
D_R		10 ft
D_T		15 ft
h_{wj}	$(j = 2, 3, \ldots, 49)$	1.0 in
$h_{w,50}$		1.25 in
l_{wj}	$(j = 2, 3, \ldots, 49)$	130.806 in
$l_{w,50}$		149.0 in
l_R		16.0 ft
m_t		0.093 75 in

2. Initial steady state values of selected variables

Variable	Value	Variable	Value
D	23.248	q_{50}	923.47
E_s	10 433.20	T_M	626.22
P_{d1}	135.33	T_{sc}	726.17
P_{d2}	132.31	T_{mc}	579.44
P_{S1}	44.89	T_{w0}	570.22
P_{S2}	71.21	w_s	1349.84
Q_C	1 122 967	$(\rho_2^V)_{ref}$	0.002 549 852
Q_R	1 360 293		
q_1	490.14		
q_2	196.01		

Table 8-4 Time constants (Ref. 3)

Controller number, k	Controller gain, $K_{c,k}$	Controller, $\tau_{I,k}$ min	Value time constant, $\tau_{v,k}$ min
1	1.50	3.00	0.15
2	0.25	0.10	0.15
3	1.10	0.75	0.15
4	0.15	0.25	0.20
5	0.50	1.00	0.15
6	0.50	0.60	

$\tau_M = 0.20$ min

Table 8-5 Values of selected variables at the initial steady state (Ref. 3)

Stage	T_j, °R	P_j, mmHg abs	L_j, lb · mol/min	$\sum_{i=1}^{c} v_{ji}$, lb · mol/min	$\sum_{i=1}^{c} u_{ji}$, lb · mol	Z_j, ft	E_j, Btu × 10^{-3}
1	594.37	760.0	58.12	.....	281.29	3.00	831.28
2	598.32	787.09	56.09	81.37	19.71	0.33	58.54
5	626.84	797.59	257.50	72.91	71.39	0.52	186.83
10	633.06	820.52	258.01	72.91	72.27	0.52	196.78
15	635.60	842.98	258.36	73.29	72.77	0.51	200.32
20	633.23	865.01	260.70	74.18	73.80	0.58	198.39
25	623.00	891.57	367.15	82.01	84.37	1.08	222.18
30	624.63	918.93	367.82	82.68	84.48	1.08	225.42
35	626.22	946.16	368.46	83.33	84.59	1.08	228.58
40	627.80	973.28	369.08	83.96	84.69	1.09	231.67
45	629.90	1000.21	369.38	84.41	84.77	1.07	234.90
50	645.24	1025.55	285.00	82.18	3494.91	8.00	10 236.91

Table 8-6 Initial values of the control system variables (Ref. 3)

		Controller variables			
Controller	Controller	c_k, mA	P_k, mA	I_k, mA	δ_k, mA
1	Accumulator pressure	12.320	11.589	23.179	0.474 33
2	Reflux flow rate	10.006	13.834	5.534	0.614 63
3	Liquid level in accumulator	8.800	10.191	6.948	0.386 92
4	Steam flow rate	7.239	15.076	25.127	0.692 28
5	Liquid level in base of column	12.000	9.428	18.857	0.339 28
6	Temperature, $T_{35,c}$	14.491	7.239	8.687	

Table 8-7 Transient response of selected variables of Example 1 (Ref. 3)

Step	t, min	T_{35}, °R	P_{35}, mmHg	L_{50}, lb · mol/min	w_s, lb/min
	0^-	626.23	946.16	285.00	1349.84
0	0^+	626.23	946.16	285.00	1349.84
9	1.0292	626.88	958.00	285.72	1621.64
14	2.4230	628.81	993.46	281.91	1905.14
17	3.7269	630.55	1026.37	264.39	2035.32
20	5.0307	631.47	1045.26	236.69	2054.81
23	6.3346	631.52	1049.32	211.24	2037.56
26	7.6384	631.03	1044.91	197.89	2031.34
29	8.9423	630.48	1039.79	200.75	2056.92
31	10.0130	630.25	1037.77	210.84	2097.40
33	11.1695	630.32	1039.75	223.33	2146.41
35	12.4116	630.70	1044.59	233.24	2188.09
37	13.6538	631.15	1049.00	236.67	2206.60
39	14.8960	631.52	1050.57	234.89	2202.03
41	16.1382	631.76	1048.60	231.23	2180.47

Table 8-7 Transient response of selected variables of Example 1 (Ref. 3)—*Continued*

Step	t, min	T_{35}, °R	P_{35}, mmHg	L_{50}, lb · mol/min	w_s, lb/min
43	17.3803	631.92	1043.63	229.02	2147.94
45	18.6225	632.08	1036.59	230.23	2106.67
47	19.8646	632.29	1028.08	235.09	2054.49
49	21.6967	632.65	1012.66	246.80	1951.39
50	22.9076	632.75	1000.17	255.86	1869.52
51	24.1186	632.63	985.55	264.88	1783.38
55	25.3295	632.23	969.34	273.11	1703.28
57	26.7564	631.63	954.20	281.63	1638.48
62	27.9617	631.23	948.56	287.67	1616.08
65	29.6570	631.02	950.38	293.84	1620.04
67	31.0803	631.12	956.50	295.83	1632.08
69	32.5037	631.29	962.60	294.24	1636.12
71	33.9270	631.35	966.37	289.48	1630.42
73	35.5265	631.22	967.90	282.55	1623.94
75	37.3024	630.96	968.98	276.67	1633.68
77	39.0782	630.80	972.09	274.62	1665.03
79	40.8541	630.85	977.43	274.64	1704.44
81	42.6299	631.06	982.87	273.76	1733.51
83	44.4058	631.28	986.00	271.02	1742.73
85	46.5336	631.40	985.64	267.39	1732.71
86	47.7734	631.40	983.97	266.34	1722.39
87	49.0133	631.37	981.90	266.45	1712.15
88	50.4353	631.32	979.67	267.86	1702.51
89	51.8573	631.29	977.94	270.08	1695.45
92	52.9238	631.28	977.05	272.02	1691.71
93	54.1901	631.27	976.39	273.89	1687.90
94	55.4564	631.28	975.99	275.08	1684.30
95	56.7227	631.27	975.72	275.57	1680.92
96	58.4598	631.25	975.47	275.40	1677.66
97	60.1969	631.21	975.45	274.74	1677.02
98	61.9340	631.18	975.77	274.03	1679.40
99	63.6711	631.16	976.42	273.47	1684.02
100	65.4083	631.17	977.23	273.05	1689.37
101	67.1454	631.19	978.08	272.67	1693.92
102	68.8825	631.21	978.68	272.29	1696.79
103	70.6195	631.23	978.97	271.93	1697.85
104	72.8104	631.24	978.95	271.62	1697.41
105	75.0012	631.24	978.67	271.56	1696.00
106	77.1919	631.24	978.32	271.75	1694.33
107	79.6910	631.24	977.98	272.08	1692.57

(*Continued over*)

Table 8-7 Transient response of selected, variables of Example 1 (Ref. 3)—*Continued*

Step	t, min	T_{35}, °R	P_{35}, mmHg	L_{50}, lb · mol/min	w_s, lb/min
108	82.1901	631.23	977.74	272.39	1691.14
112	83.5321	631.23	977.66	272.50	1690.59
114	85.0297	631.23	977.62	272.54	1690.23
116	88.2703	631.22	977.64	272.49	1690.50
117	90.8869	631.22	977.78	272.40	1691.09
118	93.5034	631.22	977.88	272.32	1691.66
119	97.7311	631.22	977.97	272.22	1692.15
120	101.9587	631.23	977.99	272.18	1692.30
121	106.9586	631.23	977.99	272.17	1692.26
122	111.9586	631.23	977.97	272.18	1692.17
123	116.9586	631.23	977.96	272.18	1692.11
124	121.9586	631.23	977.96	272.18	1692.10

Table 8-8 Selected values of the initial and final temperature profiles (Ref. 3)

Stage	Initial temp., °R	Final temp., °R
1	594.37	596.20
2	598.32	603.64
5	626.84	635.87
10	633.06	638.28
15	635.60	640.38
20	633.23	634.07
25	623.00	624.30
30	624.63	626.49
35	626.22	631.23
40	627.80	641.28
45	629.90	645.98
50	645.24	653.45

Table 8-9 Component flow rates in the distillate and bottoms for Example 8-1 (Ref. 3)

	$d_i = \frac{Du_{1i}}{\sum_{i=1}^{c} u_{1,i}}$		$b_i = \frac{L_{50}u_{50,i}}{\sum_{i=1}^{c} u_{50,i}}$	
Component	Initial value	Final value, t = 121.96 min	Initial value	Final value, t = 121.96 min
Methanol	0.0728	1.1319	65.1772	64.1118
Acetone	19.1484	25.4802	6.3518	0.0181
Ethanol	1.6953	5.0002	8.3047	4.9906
Water	2.3287	4.4632	205.1712	203.0592

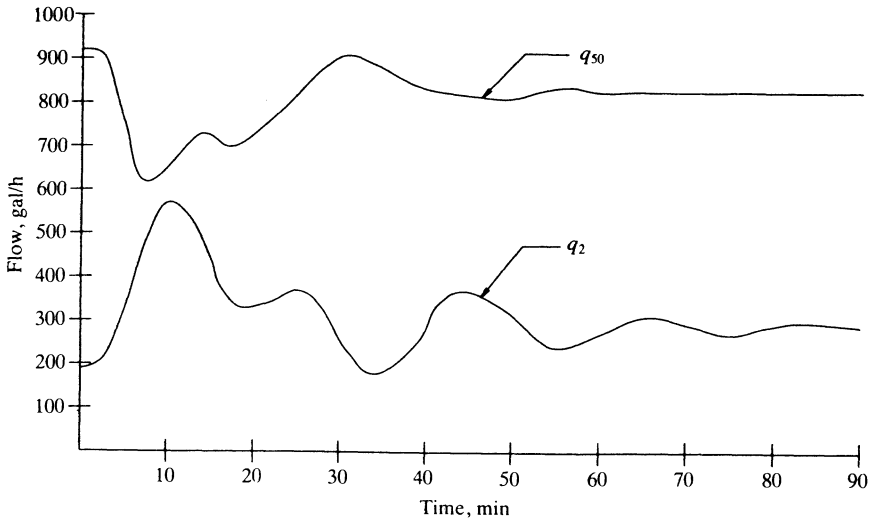

Figure 8-8 Response of bottom and distillate total flow rates. q_{50} = flow rate of bottoms and q_1 = flow rate of distillate in gallons per minute

The response of the total flow rates of the distillate and bottoms is displayed in Fig. 8-8. The pressure responses in the accumulator and the base of the column are given in Fig. 8-9.

The integration parameters employed in the application of Gear's method are listed in Table 8-10. To obtain the transient response over a period of about two hours, the execution time required to integrate the 693 equations was about 170 seconds of execution time. Solutions were obtained on the AMDAHL 470 V/6 computer using extended FORTRAN H. The performance of the step size and order control procedure during the solution of Example 8-1 is shown in Table 8-11.

Calculational Procedure Used in the Solution of Example 8-1

When the equations and variables are ordered as shown by Eqs. (8-73) and (8-74), a jacobian matrix similar to the one shown in Fig. 6-2 is obtained which has the characteristic of being almost band. Because of this structure of the jacobian matrix, the Newton–Raphson formulation of the steady state equations for a distillation column were referred to by Holland(7) as the Almost Band Algorithm. In the case of the dynamic model presented above, the temperature controller leads to off-diagonal elements (elements which lie outside of the shaded area shown in Fig. 6-2) in the jacobian because $T_j = T_k = T_{35}$ appears in the equations for stages $j = k$, $k - 1$, $k + 1$ (Eqs. (8-9), (8-36), (8-37), and the cascade controllers of the temperature and the steam rate, see Eqs. (8-66) through (8-73)). Such off-diagonal elements may be efficiently handled by use of the Kubiček algorithm which is described below.

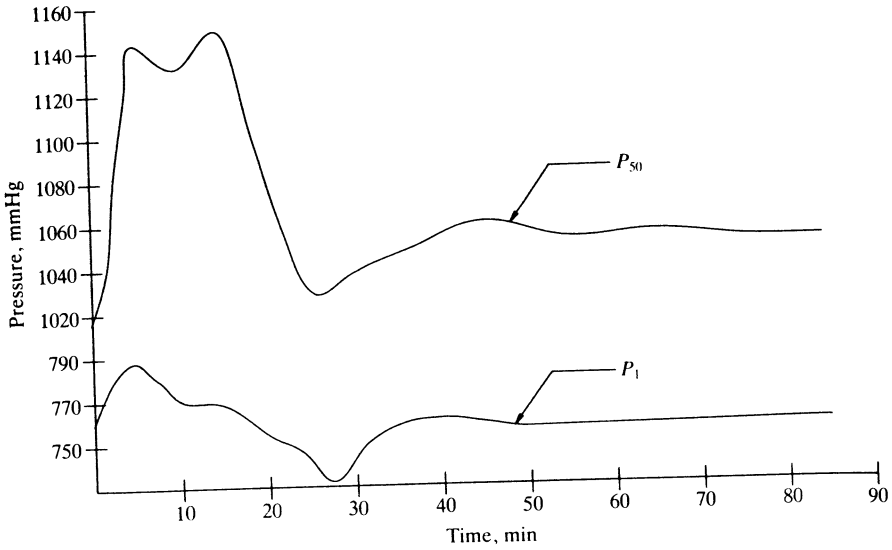

Figure 8-9 Responses of the receiver pressure (P_1) and the base pressure (P_{50})

Table 8-10 Integration parameters for Gear's method for Example 8-1 (Ref. 3)

Parameter	Value
Error control parameter	0.01
Minimum permitted step size	0.005 min
Maximum permitted step size	5.00 min
Initial step size	0.03 min

Table 8-11 Performance of Gear's algorithm for Example 8-1 (Ref. 3)

Step	Time, min	Order of Gear's method	Cumulative function evaluations	Cumulative jacobian evaluations
0	0.000	1	0	0
9	1.024	1	33	5
10	1.242	2	36	5
31	10.013	2	121	16
32	10.548	3	124	16
60	27.292	3	232	30
61	27.962	2	234	30
110	82.502	2	438	57
111	82.659	1	440	57
124	121.959	1	487	63

Kubiček Algorithm

Kubiček(11) proposed an efficient algorithm for solving matrices which contain a relatively small number of elements lying outside the banded region, such as the derivatives with respect to the temperature T_{35} (the controlled temperature) of Example 8-1. The submatrices clustered along the principal diagonal are treated by gaussian elimination while the nonzero elements lying above and below the submatrices are treated by the Kubiček algorithm. Since the nonzero elements lying above the submatrices in the upper triangular portion of the matrix offer no difficulty, their treatment by the Kubiček algorithm is optional.

Kubiček's algorithm is based on Householder's identity (Ref. 8)

$$(\mathbf{A} + \mathbf{WCZ}^T)^{-1} = \mathbf{A}^{-1} - \mathbf{A}^{-1}\mathbf{W}(\mathbf{C}^{-1} + \mathbf{Z}^T\mathbf{A}^{-1}\mathbf{W})^{-1}\mathbf{Z}^T\mathbf{A}^{-1} \tag{8-75}$$

where $\mathbf{A}$ is an n-by-n matrix, $\mathbf{W}$ and $\mathbf{Z}$ are n-by-m matrices, and $\mathbf{c}$ is an m-by-m matrix. Suppose that a solution to the set of equations

$$\mathbf{Bx} = \mathbf{b} \tag{8-76}$$

is desired where $\mathbf{B}$ is an n-by-n matrix and $\mathbf{x}$ and $\mathbf{b}$ are conformable column vectors. Then let

$$\mathbf{B} = \mathbf{A} + \mathbf{R} = \mathbf{A} + \mathbf{R}_1\mathbf{I}_m\mathbf{R}_2^T \tag{8-77}$$

where $\mathbf{R}_1$ and $\mathbf{R}_2$ are of order $n \times m$ and $\mathbf{I}_m$ is an identity matrix of order $m \times m$. Thus

$$(\mathbf{A} + \mathbf{R}_1\mathbf{I}_m\mathbf{R}_2^T)\mathbf{x} = \mathbf{b} \tag{8-78}$$

Then

$$\mathbf{x} = [\mathbf{A} + \mathbf{R}_1\mathbf{I}_m\mathbf{R}_2^T]^{-1}\mathbf{b} \tag{8-79}$$

Application of Householder's identity (Eq. (8-79)) gives

$$\begin{aligned}\mathbf{x} &= [\mathbf{A}^{-1} - \mathbf{A}^{-1}\mathbf{R}_1(\mathbf{I}_m^{-1} + \mathbf{R}_2^T\mathbf{A}^{-1}\mathbf{R}_1)^{-1}\mathbf{R}_2^T\mathbf{A}^{-1}]\mathbf{b} \\ &= \mathbf{A}^{-1}\mathbf{b} - \mathbf{A}^{-1}\mathbf{R}_1(\mathbf{I}_m^{-1} + \mathbf{R}_2^T\mathbf{A}^{-1}\mathbf{R}_1)^{-1}\mathbf{R}_2^T + \mathbf{A}^{-1}\mathbf{b}\end{aligned} \tag{8-80}$$

Let the vector $\mathbf{y}$ and the matrix $\mathbf{V}$ be defined as follows:

$$\mathbf{Ay} = \mathbf{b} \tag{8-81}$$

$$\mathbf{AV} = \mathbf{R}_1 \tag{8-82}$$

Then Eq. (8-80) becomes

$$\mathbf{x} = \mathbf{y} - \mathbf{V}[\mathbf{I}_m^{-1} + \mathbf{R}_2\mathbf{V}]^{-1}\mathbf{R}_2^T\mathbf{y} \tag{8-83}$$

Let

$$\mathbf{z} = (\mathbf{I}_m + \mathbf{R}_2^T\mathbf{V})^{-1}\mathbf{R}_2^T\mathbf{y} \tag{8-84}$$

Since $\mathbf{I}_m^{-1} = \mathbf{I}_m$, it is evident that Eq. (8-83) may be written as follows:

$$\boldsymbol{x} = \mathbf{y} - \mathbf{Vz} \tag{8-85}$$

The order of calculations is as follows where it is supposed that the **LU** factorization of the matrix **A** has been obtained, and it is desired to solve the matrix equation $\mathbf{Bx} = \mathbf{b}$.

Step 1 Find **R** by use of the defining equation $\mathbf{R} = \mathbf{B} - \mathbf{A}$. Form the matrix $\mathbf{R}_1$ from the columns of **R** containing nonzero elements and choose $\mathbf{R}_2$ such that $\mathbf{R} = \mathbf{R}_1\mathbf{I}_m\mathbf{R}_2^T$. (Alternatively, form the matrix $\mathbf{R}_2$ from the rows of **R** containing nonzero elements and choose $\mathbf{R}_1$ such that $\mathbf{R} = \mathbf{R}_1\mathbf{I}_m\mathbf{R}_2^T$.)

Step 2 Solve Eq. (8-81) for **y**.

Step 3 Solve Eq. (8-82) for **V**.

Step 4 Compute $\mathbf{R}_2^T\mathbf{V}$ and $\mathbf{R}_2^T\mathbf{y}$.

Step 5 Solve Eq. (8-84) for **z**.

Step 6 Solve Eq. (8-85) for **x**.

NOTATION

A_a = active area of a sieve-tray area between the outlet weir and the downcomer, ft^2

A_d = cross-sectional area of the downcomer, ft^2

A_0 = total area of holes, ft^2

A_T = total cross-sectional area of the column, ft^2

A_{dc} = clearance area between the downcomer and the floor of the tray, in^2

c_k = set point of controller k in milliamps

D = total distillate rate, lb · mol/min

D_0 = diameter of holes, in

D_R = diameter of reflux accumulator, ft

D_T = diameter of column, ft

e = control error, departure of the control variable c from its reference value r, $e = r - c$

E_j = energy of the liquid holdup of stage j, Btu

E_s = holdup of energy in the steam chest of reboiler

$h_{0,j}$ = dry hole pressure drop, inches of vapor-free liquid

$h_{L,j}$ = pressure drop of the vapor as it passes through the liquid on plate j, inches of vapor-free liquid

$h_{dc,j}$ = pressure drop experienced by the liquid in flowing down the downcomer, inches of vapor-free liquid

$h_{w,j}$ = height of weir, in

$h_{ow,j}$ = height of liquid over the weir, inches of vapor-free liquid

$\hat{h}_{ji}$ = virtual value of the partial molar enthalpy of component i in the liquid on plate j, Btu/lb · mol

$\hat{H}_{ji}$ = virtual value of the partial molar enthalpy of component i in the vapor on plate j, Btu/lb · mol

I_k = function used in the description of proportional-integral controller

K_{ji} = ideal solution K value for component i on plate j

K_{ck} = proportional gain constant for controller k

l_R = length of the reflux accumulator, ft

l_W = length of weir, in

L_j = total molar flow rate of the liquid leaving stage j, lb · mol/h

m_t = thickness of metal of sieve tray, in

p_k = output of the kth controller, mA

P_j = pressure on stage j, lb/ft^2 abs

P_{d1}, P_{d2} = discharge pressure of pumps 1 and 2, respectively

P_{S1}, P_{S2} = suction pressure of pumps 1 and 2, respectively

q_1 = volumetric flow rate of reflux, ft^3/min

q_2 = volumetric flow rate of the distillate, ft^3/min

q_N = volumetric flow rate of the bottoms, ft^3/min

q_w = volumetric flow rate of the cooling water, ft^3/min

Q_C = condenser duty, Btu/min

Q_R = reboiler duty, Btu/min

T_j = temperature of stage j, °R

T_k = temperature of the particular stage $j = k$ in °R

T_{mc} = temperature of condenser tubes

T_{mr} = temperature of reboiler tubes

T_M = measured value of the specified temperature

T_s = temperature of saturated steam in the reboiler

T_{sc} = temperature of saturated steam to the reboiler

T_{w0} = outlet temperature of the cooling water from the condenser

u_{ji} = molar holdup of component i on stage j

$\mathcal{U}_f$ = linear velocity

U_j = total molar holdup on stage j

γ_{ji}^L = activity coefficient for component i and stage j, $\gamma_{ji}^L = \gamma_{ji}^L (P_j, T_j, \{x_{ji}\})$

γ_{ji}^V = activity coefficient for component i and stage j, $\gamma_{ji}^V = \gamma_{ji}^V (P_j, T_j, \{y_{ji}\})$.

$\bar{U}_j$ = total volumetric holdup of stage j

v_{ji} = molar flow rate of component i leaving stage j

w_c = mass flow rate of the condensate leaving the reboiler

w_s = mass flow rate of steam to the reboiler

Z_j = height of liquid in downcomer, inches vapor-free liquid

Z_1 = height of liquid in the accumulator, ft

Z_{N+1} = height of liquid in the base of column, ft

$Y_{1,i}$ = mole fraction variable for component i in the vapor above the liquid in the accumulator

Greek letters

δ_k = valve position of control valve for the kth controller
ρ^V, ρ^L = mass density of the vapor and the vapor-free liquid, respectively
$\bar{\rho}^V$, $\bar{\rho}^L$ = molar density of the vapor and the vapor-free liquid, respectively
ρ_s = mass density of the saturated steam in the reboiler
$\tau_{I,k}$ = time constant for the kth proportional-integral controller
$\tau_{v,k}$ = time constant for the kth control valve

REFERENCES

1. W. L. Bolles: "Rapid Graphical Method of Estimating Tower Diameter and Tray Spacing of Bubble-Plate Fractionators," *Pet. Refiner*, **25**(12): 103 (1946).
2. J. R. Fair: Chap. 15 of *Design of Equilibrium Stage Processes*, by B. D. Smith, McGraw-Hill Book Company, New York, 1963.
3. S. E. Gallun: Dissertation, Texas A&M University, 1979.
4. C. W. Gear: "The Automatic Integration of Ordinary Differential Equations," *Commun. ACM*, **14**(3): 176 (1971).
5. C. W. Gear: *Numerical Initial Value Problems in Ordinary Differential Equations*, Prentice-Hall, Inc., Englewood Cliffs, N.J. (1971).
6. C. W. Gear: "Simultaneous Solution of Differential-Algebraic Equations," *IEEE Trans. Circuit Theory*, **18**(1): 89 (1971).
7. C. D. Holland: *Fundamentals of Multicomponent Distillation*, McGraw-Hill Book Company, New York, 1981.
8. A. S. Householder: *Principles of Numerical Analysis*, McGraw-Hill Book Company, New York, 1953.
9. G. A. Hughmark and H. E. O'Connell: "Design of Perforated Plate Fractionating Towers," *Chem. Eng. Prog.* **53**: 127 (1957).
10. M. H. Hutchinson, A. G. Buron, and B. P. Miller: "Aerated Flow Principles Applied to Sieve Plates," Paper presented at Los Angeles AIChE Meeting, May 1949.
11. M. Kubiček, V. Hlaváček, and F. Procháska: "Global Modular Newton–Raphson Technique for Simulation of an Interconnected Plant Applied to Complex Rectifying Columns," *Chem. Eng. Sci.*, **31**: 277 (1976).
12. I. Leibson, R. E. Kelley, L. A. Bullington: "How to Design Perforated Trays," *Pet. Refiner*, **36**(2): 127 (1957).
13. R. C. Lord, P. E. Minton, and R. P. Slusser: "Design of Heat Exchangers," *Chem. Eng.*, **62**(2): 96 (1970).
14. J. M. Prausnitz, C. A. Eckert, R. V. Orye, and J. P. O'Connell: *Computer Calculations for Multicomponent Vapor-Liquid Equilibria*, Prentice-Hall, Inc., Englewood Cliffs, N.J. (1967).
15. B. D. Smith: *Design of Equilibrium Stage Processes*, McGraw-Hill Book Company, New York, 1963.
16. Mathew, Van Winkle: *Distillation*, McGraw-Hill Book Company, New York, 1973.

PROBLEMS

8-1 Use the Kubiček algorithm to solve the equation $\mathbf{Bx} = \mathbf{b}$, where

$$\begin{bmatrix} 1 & 0 & 0 & 0 \\ 0 & 2 & 0 & 0 \\ 3 & 0 & 3 & 0 \\ 0 & 0 & 2 & 4 \end{bmatrix} \begin{bmatrix} x_1 \\ x_2 \\ x_3 \\ x_4 \end{bmatrix} = \begin{bmatrix} 1 \\ 4 \\ 6 \\ 4 \end{bmatrix}$$

and the **LU** factorization of the matrix **A** is known

$$\mathbf{A} = \begin{bmatrix} 1 & 0 & 0 & 0 \\ 0 & 2 & 0 & 0 \\ 0 & 0 & 3 & 0 \\ 0 & 0 & 0 & 4 \end{bmatrix} = \begin{bmatrix} 1 & 0 & 0 & 0 \\ 0 & 1 & 0 & 0 \\ 0 & 0 & 1 & 0 \\ 0 & 0 & 0 & 1 \end{bmatrix} \begin{bmatrix} 1 & 0 & 0 & 0 \\ 0 & 2 & 0 & 0 \\ 0 & 0 & 3 & 0 \\ 0 & 0 & 0 & 4 \end{bmatrix}$$

APPENDIX 8A

Table 8A-1 Equilibrium and enthalpy data, and relationships used in the solution of Example 8-1

1. Liquid enthalpies†

$$h_i = a_i b_i T + c_i T^2 \ (T \text{ in } ^\circ\text{R}), \text{ Btu/lb mol}$$

Component	a_i	b_i	c_i
Methanol	$-0.311\,943\,6 \times 10^4$	$-0.414\,519\,8 \times 10$	$0.213\,110\,6 \times 10^{-1}$
Acetone	$-0.115\,334 \times 10^5$	$0.177\,034\,8 \times 10^2$	$0.116\,643\,5 \times 10^{-1}$
Ethanol	$0.404\,634\,8 \times 10^3$	$-0.241\,028\,6 \times 10^2$	$0.472\,823\,0 \times 10^{-1}$
Water	$-0.878\,380\,59 \times 10^4$	$0.175\,845\,0 \times 10^2$	$0.365\,136\,9 \times 10^{-3}$

2. Ideal gas and pure component vapor enthalpies‡

$$H_i = a_i + b_i T + c_i T^2 + d_i T^3 + e_i T^4 (T \text{ in } ^\circ\text{R}), \text{ Btu/lb mol}$$

Component	a_i	b_i	c_i
Methanol	$0.117\,411\,9 \times 10^5$	$0.712\,149\,5 \times 10$	$0.557\,944\,2 \times 10^{-2}$
Acetone	$0.867\,332 \times 10^4$	$0.473\,579\,9 \times 10$	$0.145\,286\,0 \times 10^{-1}$
Ethanol	$0.106\,486 \times 10^5$	$0.751\,599\,7 \times 10$	$0.115\,136\,0 \times 10^{-1}$
Water	$0.154\,587\,1 \times 10^5$	$0.802\,252\,6 \times 10$	$-0.474\,572\,2 \times 10^{-3}$

Component	d_i	e_i
Methanol	$-0.450\,617\,0 \times 10^{-6}$	$-0.209\,190\,4 \times 10^{-10}$
Acetone	$-0.112\,139\,7 \times 10^{-5}$	$-0.201\,817\,3 \times 10^{-9}$
Ethanol	$-0.168\,209\,6 \times 10^{-5}$	$0.903\,633\,3 \times 10^{-10}$
Water	$0.687\,804\,7 \times 10^{-6}$	$-0.143\,975\,2 \times 10^{-9}$

3. Antoine constants§

$$\log P_i = A_i - \left(\frac{B_i}{C_i + T}\right) \qquad (P_i \text{ in mmHg}, T \text{ in } ^\circ\text{C})$$

Component	A_i	$B_i \times 10^{-3}$	$C_i \times 10^{-2}$
Methanol	7.878 63	1.473 11	2.300 00
Acetone	7.024 47	1.160 00	2.240 00
Ethanol	8.044 94	1.554 30	2.226 50
Water	7.966 81	1.668 21	2.280 00

(*Continued over*)

Table 8A-1 Equilibrium and enthalpy data, and relationships used in the solution of Example 8-1—*Continued*

4. Molar volume constants§

$\alpha_i = a_i + b_i T + c_i T^2$ (α_i in cm³/g·mol, T in°R)

Component	a_i	b_i	c_i
Methyl alcohol	$0.645\,109\,4 \times 10^2$	$-0.109\,535\,9$	$0.119\,552\,6 \times 10^{-3}$
Acetone	$0.568\,652\,3 \times 10^2$	$0.468\,039 \times 10^{-2}$	$0.509\,497\,8 \times 10^{-4}$
Ethanol	$0.537\,002\,7 \times 10^2$	$-0.172\,817\,6 \times 10^{-1}$	$0.493\,820\,0 \times 10^{-4}$
Water	$0.228\,867\,6 \times 10^2$	$-0.202\,312\,1 \times 10^{-1}$	$0.211\,589\,9 \times 10^{-4}$

5. Wilson parameters§

$\lambda_{ij} - \lambda_{ii}$, cal/g mol

Component	1 (methanol)	2 (acetone)	3 (ethanol)	4 (water)
1 (methanol)	0.0	$0.664\,08 \times 10^3$	$0.598\,44 \times 10^3$	$0.205\,30 \times 10^3$
2 (acetone)	$-0.214\,95 \times 10^3$	0.0	$0.381\,70 \times 10^2$	$0.439\,64 \times 10^3$
3 (ethanol)	$0.511\,39 \times 10^3$	$0.418\,96 \times 10^3$	0.0	$0.382\,30 \times 10^3$
4 (water)	$0.482\,16 \times 10^3$	$0.140\,549 \times 10^3$	$0.955\,49 \times 10^3$	0.0

6. Physical constants¶

Component	T_c K	P_c, atm	v_c, cm³/g-mol	ω	ω_H	μ Debye	η
Methanol	513.2	78.5	118.0	0.557	0.105	1.66	1.21
Acetone	508.7	46.6	213.5	0.309	0.187	2.88	0.00
Ethanol	516.0	63.0	161.3	0.637	0.152	1.69	1.10
Water	647.4	218.3	55.2	0.344	0.010	1.83	0.00

T_c = critical temperature
P_c = critical pressure
v_c = critical volume
ω = acentric factor
ω_H = accentric factor of the homograph of the component
μ = dipole moment
η = self-interaction parameter

7. Equilibrium and enthalpy relationships used in the solution of Example 8-1††

1. *Equilibrium relationship*

The form of the equilibrium relationship used herein

$$\gamma_i^V f_i^V y_i = \gamma_i^L f_i^L x_i \tag{1}$$

may be restated in the form of Eq. (4) on p. 5 of Prausnitz, et al.†

$$\phi_i y_i P = y_i x_i f_i^{OL} \tag{2}$$

Table 8A-1 Equilibrium and enthalpy data, and relationships used in the solution of Example 8-1—*Continued*

which may be restated in the following form for plate j

$$y_{ji}\phi_{ji}P_j = \gamma_{ji}P_{ji}^S\phi_{ji}^{OL} \tag{3}$$

where $\phi_{ji}^{OL} = f_{ji}^{OL}/P_{ji}^S$
P_{ji}^S = saturation pressure of component i at the temperature of the mixture
$x_{ji} = l_{ji}/\sum_{i=1}^{c} l_{ji}$
$y_{ji} = v_{ji}/\sum_{i=1}^{c} v_{ji}$

When these definitions are substituted into Prausnitz' equation of Chap. 4, Eq. (4) is obtained for the calculation of γ_{ji}, namely,

$$\gamma_{ji} = \left\{\exp\left[1 - \sum_{k=1}^{c}\left(\frac{l_{jk}\Lambda_{ki}}{\sum_{m=1}^{c} l_{jk}\Lambda_{km}}\right)\right]\right\}\frac{\sum_{m=1}^{c} l_{jm}}{\sum_{m=1}^{c} l_{jm}\Lambda_{im}} \tag{4}$$

where

$$\Lambda_{ki} = \frac{v_{ji}^L}{v_{jk}^L}\exp\left[-\frac{(\lambda_{ki} - \lambda_{kk})}{RT_j}\right]$$

The Antoine equation is used to calculate P_{ji}^S, and ϕ_{ji}^{OL} was computed by use of the equations given below which were taken from RSTATE of Prausnitz, et al. Although ϕ_{ji}^{OL} should be differentiated with respect to temperature in the Newton–Raphson procedure, it was found that this step could be eliminated with the saving of considerable computational effort.

The following equations were used to compute ϕ_{ji}^{OL}

$$\begin{aligned}
\phi_{ji}^S &= \exp\,[f_1 + \omega_i f_2]\\
f_1 &= -3.502\,135\,8 + T_r\{5.608\,559\,5 + T_r[-3.076\,574 + T_r(0.573\,350\,15)]\}\\
f_2 &= -3.769\,041\,8 + T_r(4.353\,872\,9 + T_r(0.316\,613\,7 + T_r(0.126\,661\,84 + T_r(-1.166\,228\,3\\
&\quad + T_r(-0.106\,657\,30 + T_r(0.121\,474\,36 + T_r(0.189\,270\,37 + T_r(0.149\,369\,06 + T_r(0.024\,364\,816\\
&\quad + T_r(-0.068\,603\,516 + T_r(-0.015\,172\,164 + T_r(0.012\,089\,114)))))))))))
\end{aligned} \tag{6}$$

$T_r = T_j/T_{ci}$
ω_i = acentric factor; see item 6 above
$\phi_{ji}^{OL} = \phi_{ji}^S \exp\,[-v_{ji}^L P_{ji}^S/(RT_j)]$

where $R = 1.987$ cal/gm·mol·K.

The vapor phase fugacity coefficient ϕ_{ji} was calculated exactly as described in Chap. 3, in Prausnitz et al., and Eqs. (10) through (23) were used directly.

2. *Enthalpy deviations*

The enthalpy H_i of pure component i is related to its fugacity f_i by the well-known thermodynamic relationship given in Eq. (7). The fugacity can be related to an equation of state through Eq. (8). The equation of state used in the Prausnitz monograph is given by Eq. (9) where Z has the usual meaning as defined by Eq. (10).

$$H_i - H_i^0 = -RT^2\left(\frac{\partial \ln f_i}{\partial T}\right)_P \tag{7}$$

$$\ln\left(\frac{f_i}{P}\right) = \int_0^P \left(\frac{Z-1}{P}\right)dP \tag{8}$$

(Continued over)

Table 8A-1 Equilibrium and enthalpy data, and relationships used in the solution of Example 8-1—*Continued*

$$Z = 1 + B/v \tag{9}$$

$$Z = Pv/RT \tag{10}$$

Equations (9) and (10) can be used to integrate Eq. (8) and the result substituted into Eq. (7) gives Eq. (11). Equation (12) is the result of eliminating v between Eqs. (9) and (10).

$$H_i - H_i^0 = -RT^2\left(2 - \frac{1}{Z}\right)\left(\frac{\partial Z}{\partial T}\right)_P \tag{11}$$

$$Z = \frac{1 + \sqrt{1 + 4BP/RT}}{2} \tag{12}$$

In the calculation of ϕ_{ji}^V, a mixture virial B is calculated using mixing rules described in Chap. 3 of the monograph. If B is substituted into Eqs. (11) and (12), the result is the virtual value of the partial molar enthalpy, Ω. Rigorous application of the Almost Band Algorithm requires that the derivative of Ω be calculated with respect to temperature for use in the convergence procedure. This was not done in the solution of Example 8-1.

† Taken from an M.S. thesis by S. E. Gallun, Texas A&M University, 1975.

‡ Based on the correlation of Rihani and Doraiswany on pp. 182 through 186 of *The Properties of Gases and Liquids*, by R. C. Reid and T. K. Sherwood, 2d ed., McGraw-Hill Company, New York, 1966.

§ Taken from M. J. Holmes and J. Van Winkle, "Predictions of Ternary Vapor-Liquid Equilibria in Miscible Systems from Binary Data," *Ind. Eng. Chem.*, **62**(1):21 (1970).

¶ Taken from J. M. Prausnitz, C. A. Eckert, R. V. Orye, and J. P. O'Connell, *Computer Calculations for Multicomponent Vapor-Liquid Equilibria*, Prentice-Hall, Englewood Cliffs, N.J. (1967).

†† J. M. Prausnitz, C. A. Eckert, R. V. Orye, and J. P. O'Connell, *Computer Calculations for Multicomponent Vapor-Liquid Equilibria*, Prentice-Hall, Englewood Cliffs, N.J. (1967).

CHAPTER

NINE

DEVELOPMENT OF RUNGE–KUTTA METHODS AND MULTISTEP INTEGRATION ALGORITHMS

Selected integration algorithms introduced throughout this book are developed from first principles in this chapter. In Sec. 9-1, the techniques used to develop the well-known fourth-order Runge–Kutta algorithms are demonstrated by the development of the second-order Runge–Kutta method. A detailed development of the semi-implicit Runge–Kutta method is also presented. In Sec. 9-2, a general development of the multistep integration formulas is presented. Emphasis is placed on the development of Gear's algorithms for differential and algebraic equations.

9-1 RUNGE–KUTTA METHODS

Although algorithms may be developed directly by use of the Taylor series expansion of a function, such algorithms are unacceptable from a practical point of view because of the difficulty of computing the partial derivatives. Methods giving accuracies equivalent to the Taylor expansions wherein the last term retained is the term in h^2, h^3, and h^4 are known as the Runge–Kutta methods. Fortunately, these methods require only the evaluation of the function at two, three, or four values of the variable in each interval $x_n \leq x \leq x_{n+1}$.

The explicit Runge–Kutta methods are algorithms of the form

$$y_{n+1} = y_n + \phi(x_n, y_n, h) \tag{9-1}$$

where ϕ has been termed the increment function by Henrici(8).

The Explicit Runge–Kutta Method of Order 2

In the second-order algorithm, the increment function is

$$\phi = ak_1 + bk_2 \tag{9-2}$$

and a formula is to be found for

$$y_{n+1} = y_n + ak_1 + bk_2 \tag{9-3}$$

where

$$k_1 = hf(x_n, y_n)$$
$$k_2 = hf(x_n + \alpha h, y_n + \beta k_1)$$

and a, b, α, β, are constants to be determined so that Eq. (9-2) will agree with the Taylor series expansion of the same order.

Expansion of $y(x_{n+1})$ in a Taylor series through terms of order h^3 gives

$$y(x_{n+1}) = y(x_n) + hy'(x_n) + \frac{h^2}{2!}y^{(2)}(x_n) + \frac{h^3}{3!}y^{(3)}(x) + O(h^4) \tag{9-4}$$

For the general case of a differential equation of the form $y' = f(x, y)$, it follows that

$$y^{(2)}(x) = \frac{d^2y}{dx^2} = \frac{df(x, y)}{dx} = \frac{\partial f}{\partial x}\frac{dx}{dx} + \frac{\partial f}{\partial y}\frac{dy}{dx} = f_x + f_y f \tag{9-5}$$

and

$$\begin{aligned} y^{(3)}(x) &= \frac{d^2f(x, y)}{dx^2} = \frac{d(f_x + f_y f)}{dx} \\ &= \frac{\partial(f_x + f_y f)}{\partial x}\frac{dx}{dx} + \frac{\partial(f_x + f_y f)}{\partial y}\frac{dy}{dx} \\ &= f_{xx} + f_y f_x + f_{xy} f + f_{xy} f + f_y f_y f + f_{yy} ff \end{aligned} \tag{9-6}$$

Therefore

$$y(x_{n+1}) = y(x_n) + hf(x_n, y_n) + \frac{h^2}{2}(f_x + f_y f)_n + \frac{h^3}{3!}(f_{xx} + 2ff_{xy} + f_{yy} f^2 + f_x f_y + f_y^2 f)_n + O(h^4) \tag{9-7}$$

where the subscript n denotes that all the functions and their derivatives are to be evaluated at (x_n, y_n).

The Taylor series expansion† of the multivariable function k_2 about (x_n, y_n) gives

$$\frac{k_2}{h} = f(x_n + \alpha h, y_n + \beta k_1)$$
$$= f(x_n, y_n) + \alpha h f_x + \beta k_1 f_y + \frac{\alpha^2 h^2}{2} f_{xx} + \alpha h \beta k_1 f_{xy} + \frac{\beta^2 k_1^2}{2} f_{yy} + \cdots \tag{9-8}$$

Substitution of this expression into Eq. (9-3) and replacement of k_1 by its definition, followed by rearrangement in powers of h gives

$$y_{n+1} = y_n + (a + b)hf + bh^2(\alpha f_x + \beta f f_y) + bh^3\left(\frac{\alpha^2}{2} f_{xx} + \alpha\beta f f_{xy} + \frac{\beta^2}{2} f^2 f_{yy}\right) + \cdots \tag{9-9}$$

where all derivatives are to be evaluated at (x_n, y_n). Upon comparison of Eqs. (9-7) and (9-9), it is seen that in order for the corresponding powers of h and h^2 to agree it is necessary that

$$\begin{aligned} a + b &= 1 \\ b\alpha = b\beta &= \frac{1}{2} \end{aligned} \tag{9-10}$$

There are many solutions to Eq. (9-10), one of the simplest being

$$a = b = \frac{1}{2} \qquad \alpha = \beta = 1 \tag{9-11}$$

which gives the formula

$$y_{n+1} = y_n + \frac{1}{2}(k_1 + k_2) \tag{9-12}$$

where

$$k_1 = hf(x_n, y_n)$$
$$k_2 = hf(x_n + h, y_n + k_1)$$

† The first few terms of the two variable Taylor series are:

$$f(x + r, y + s) = f(x, y) + rf_x(x, y) + sf_y(x, y) + \frac{r^2}{2} f_{xx}(x, y) + rsf_{xy}(x, y) + \frac{s^2}{2} f_{yy}(x, y) + O[(|r| + |s|)^3]$$

The formula for the truncation error of Eq. (9-12) is found by use of Eqs. (9-7), (9-9), and (9-11).

$$y(x_{n+1}) - y_{n+1} = \frac{h^3}{12}(-f_{xx} - 2ff_{xy} - f_{yy}f^2 + 2f_x f_y + 2f_y^2 f) + O(h^4) \quad (9\text{-}13)$$

The complexity of the coefficient in this error term is characteristic of all Runge–Kutta methods, and this is one of the least desirable features of the Runge–Kutta methods. Equation (9-13) does show, however, that the truncation error for the second-order Runge–Kutta method is proportional to h^3.

The development of the higher-order Runge–Kutta methods is carried out in a manner analogous to that demonstrated for the second-order method. Two of the most popular forms are the fourth-order methods. The fourth-order method attributed to Runge is given by Eq. (1-45). One of the most widely used fourth-order Runge–Kutta methods is the one attributed to Gill(7) which is given by Eq. (1-46).

Unfortunately the explicit Runge–Kutta methods are unstable for systems of stiff differential equations, systems having widely different time constants.

The Semi-Implicit Runge–Kutta Methods

Systems of linear, ordinary differential equations having widely different time constants are characterized by widely different eigenvalues which lead to problems of both stability and accuracy as discussed in the section on Stability of Numerical Methods in Chap. 1.

A number of modifications of the Runge–Kutta method and other methods have been proposed for the solution of stiff systems. There follows a development of a third-order semi-implicit Runge–Kutta method as originally proposed by Caillaud and Padmanabhan(2). The formula for this method is as follows:

$$\mathbf{y}_{n+1} = \mathbf{y}_n + R_1\mathbf{k}_1 + R_2\mathbf{k}_2 + R_3\mathbf{k}_3 \quad (9\text{-}14)$$

The formulas for $\mathbf{k}_1$, $\mathbf{k}_2$, and $\mathbf{k}_3$ are:

$$\mathbf{k}_1 = h[\mathbf{I} - ha_1\mathbf{J}(\mathbf{y}_n)]^{-1}\mathbf{f}(\mathbf{y}_n) \quad (9\text{-}15)$$

$$\mathbf{k}_2 = h[\mathbf{I} - ha_1\mathbf{J}(\mathbf{y}_n)]^{-1}\mathbf{f}(\mathbf{y}_n + b_2\mathbf{k}_1) \quad (9\text{-}16)$$

$$\mathbf{k}_3 = h[\mathbf{I} - ha_1\mathbf{J}(\mathbf{y}_n)]^{-1}[\mathbf{J}(\mathbf{y}_n)](b_{31}\mathbf{k}_1 + b_{32}\mathbf{k}_2) \quad (9\text{-}17)$$

In the analysis which follows, a single differential equation is to be integrated, namely,

$$\frac{dy}{dt} = f(y) \quad (9\text{-}18)$$

and

$\mathbf{J}(\mathbf{y}_n)$ = jacobian, which contains the partial derivatives of the functions $\mathbf{f}$ with respect to each of the variables $\mathbf{y}$.

For a single differential equation, the matrices in Eqs. (9-14) through (9-17) reduce to scalars, which is implied in the following development by the omission of boldface type. The coefficients a_1, b_2, b_{31}, b_{32}, R_1, R_2, and R_3 are determined by matching Eq. (9-14) with the Taylor series expansion of $y(x_{n+1})$ and by the suitable selection of parameters to give a root to the difference equation which has the desired characteristics. In the determination of the values of the arbitrary constants, the scalar form of Eqs. (9-14) through (9-17) is used.

The first step in the development is the expansion of $[1 - a_1 hA]^{-1}$ in a power series, where A denotes the single term $[A = f_y(y_n)]$ contained by the jacobian matrix.

$$(1 - a_1 hA)^{-1} = 1 + \sum_{i=1}^{\infty}(a_1 hA)^i \quad (9\text{-}19)$$

and $|a_1 hA| < 1$. The expression for k_1 becomes

$$k_1 = hf + a_1 h^2 Af + a_1^2 h^3 A^2 f + a_1^3 h^4 A^3 f + \cdots \quad (9\text{-}20)$$

The Taylor series expansion of $f(y_n + b_2 k_1)$ is given by

$$f(y_n + b_2 k_1) = f(y_n) + b_2 k_1 f_y(y_n) + \frac{(b_2 k_1)^2}{2!} f_{yy}(y_n) + \cdots \quad (9\text{-}21)$$

For convenience, let the second and third partial derivatives of $f(y)$ with respect to y and evaluated at y_n be denoted by B and C, respectively. Then Eq. (9-21) becomes

$$f(y_n + b_2 k_1) = f + b_2 k_1 A + \frac{b_2^2 k_1^2 B}{2!} + \frac{b_2^3 k_1^3 C}{3!} + \cdots \quad (9\text{-}22)$$

Use of Eqs. (9-19), (9-20), and (9-22) permits Eq. (9-16) to be restated in the following form:

$$k_2 = hf + (a_1 + b_2)h^2 Af + (a_1^2 + 2a_1 b_2)h^3 A^2 f + \frac{b_2^2}{2} h^3 Bf^2 + \cdots \quad (9\text{-}23)$$

Similarly, use of Eqs. (9-19), (9-20), and (9-23) to reduce the expression given by Eq. (9-17) for k_3 yields

$$k_3 = b_3 h^2 Af + h^3 A^2 f(2a_1 b_3 + b_2 b_{32}) + \cdots \quad (9\text{-}24)$$

where

$$b_3 = b_{31} + b_{32}$$

Substitution of the expressions for k_1, k_2, and k_3 into Eq. (9-14) yields the following expression upon rearrangement:

$$\begin{aligned} y_{n+1} = y_n &+ (R_1 + R_2)(hf) + [R_1 a_1 + R_2(a_1 + b_2) + R_3 b_3](h^2 Af) \\ &+ [R_1 a_1^2 + R_2(a_1^2 + 2a_1 b_2) + R_3(2a_1 b_3 + b_2 b_{32})] \\ &\times (h^3 A^2 f) + \frac{R_2 b_2^2}{2}(h^3 Bf^2) \end{aligned} \quad (9\text{-}25)$$

The Taylor series expansion of $y(t_n + h)$ is given by

$$y(t_n + h) = y(t_n) + h\frac{dy}{dt} + \frac{h^2}{2!}\frac{d^2y}{dt^2} + \frac{h^3}{3!}\frac{d^3y}{dt^3} + O(h^4) \tag{9-26}$$

Since $dy/dt = f$, it follows that

$$\frac{d^2y}{dt^2} = \frac{\partial f}{\partial y}\frac{dy}{dt} = f_y f = Af$$

and

$$\frac{d^3y}{dt^3} = \frac{\partial(f_y f)}{\partial y}\frac{dy}{dt} = f_{yy} f^2 + f_y^2 f = Bf^2 + A^2 f$$

Thus,

$$y(t_n + h) = y_n + hf + \frac{h^2}{2}Af + \frac{h^3}{6}A^2 f + \frac{h^3}{6}Bf^2 + O(h^4) \tag{9-27}$$

Comparison of the coefficients of (hf), (h^2Af), (h^3A^2f), and (h^3Bf^2) of Eqs. (9-25) and (9-27) gives the following equations:

$$R_1 + R_2 = 1 \tag{9-28}$$

$$R_1 a_1 + R_2(a_1 + b_2) + R_3 b_3 = \tfrac{1}{2} \tag{9-29}$$

$$R_1 a_1^2 + R_2(a_1^2 + 2a_1 b_2) + R_3(2a_1 b_3 + b_2 b_{32}) = \tfrac{1}{6} \tag{9-30}$$

$$\tfrac{1}{2}R_2 b_2^2 = \tfrac{1}{6} \tag{9-31}$$

To study the characteristic root of Eq. (9-14), the expressions for k_1, k_2, and k_3 are evaluated for the linear equation $y' = \lambda y$ or $f(y_n) = \lambda y_n$. Observe that after f has been replaced by λy_n and A by λ, the definition of k_1 (Eq. (9-15)) reduces to

$$k_1 = \frac{h\lambda y_n}{1 - a_1 h\lambda} \tag{9-32}$$

For $f(y_n) = \lambda y_n$, the function $f(y_n + b_2 k_1)$ in Eq. (9-16) becomes

$$f(\lambda y_n + \lambda b_2 k_1) = \lambda y_n + \lambda b_2 k_1 .$$

Thus, the definition of k_2 (Eq. (9-16)) reduces to

$$k_2 = \frac{h\lambda y_n}{1 - a_1 h\lambda} + \frac{b_2(h\lambda)^2 y_n}{(1 - a_1 h\lambda)^2} \tag{9-33}$$

Similarly

$$k_3 = \frac{b_3(h\lambda)^2 y_n}{(1 - a_1 h\lambda)^2} + \frac{b_{32} b_2(h\lambda)^3 y_n}{(1 - a_1 h\lambda)^3} \tag{9-34}$$

After these expressions have been substituted in Eq. (9-14), the result so obtained may be rearranged to the following form:

$$y_{n+1} = \mu(h\lambda) y_n \tag{9-35}$$

where

$$\mu(h\lambda) = \frac{1 + Z_1 h\lambda + Z_2 h^2\lambda^2 + Z_3 h^3\lambda^3}{(1 - a_1 h\lambda)^3} \tag{9-36}$$

$$Z_1 = 1 - 3a_1$$

$$Z_2 = 3a_1^2 - 2a_1 + R_2 b_2 + R_3 b_3$$

$$Z_3 = -a_1^3 + a_1^2 - a_1(R_2 b_2 + R_3 b_3) + R_3 b_2 b_{32}$$

Let

$$x = R_2 b_2 + R_3 b_3 \tag{9-37}$$

$$y = R_3 b_2 b_{32} \tag{9-38}$$

Then Eqs. (9-32), (9-24), and (9-23) may be used to obtain

$$x = \tfrac{1}{2} - a_1 \tag{9-39}$$

$$y = \tfrac{1}{6} - a_1 + a_1^2 \tag{9-40}$$

and thus

$$Z_1 = 1 - 3a_1$$

$$Z_2 = 3a_1^2 - 3a_1 + \tfrac{1}{2} \tag{9-41}$$

$$Z_3 = -a_1^3 + 3a_1^2 - \frac{3a_1}{2} + \frac{1}{6}$$

Upon setting

$$R_2 b_2^3 = \tfrac{1}{4} \qquad R_3 = 1 \tag{9-42}$$

the following solution is obtained

$$a_1 = 0.435\,866\,6$$

$$b_2 = \frac{3}{4}$$

$$b_{32} = \frac{4}{3}\left(\frac{1}{6} - a_1 + a_1^2\right) = -0.105\,627$$

$$b_{31} = \frac{1}{18} - a_1 - b_{32} = -0.274\,684$$

$$R_1 = \frac{11}{27}$$

$$R_2 = \frac{16}{27}$$

$$R_3 = 1$$

(Note, it can be shown that the values of k_1, k_2, and k_3 are independent of the choice of R_3.)

In order to make the method A-stable, the constant a_1 was picked such that $Z_3 = 0$. Thus, the numerator of $\mu(h\lambda)$ becomes of order 2 while the denominator is of order 3 in $h\lambda$. Thus, the procedure becomes strongly A-stable, and it requires one jacobian evaluation and two functional evaluations per step. This version of the semi-implicit Runge–Kutta method represents a significant improvement over the original version proposed by Rosenbrock(11).

Michelsen's Method

Michelsen(9,10) proposed a slightly different version of the Caillaud–Padmanabhan algorithm in which the following expression was used for $\mathbf{k}_3$:

$$\mathbf{k}_3 = [\mathbf{I} - ha_1 \mathbf{J}(\mathbf{y}_n)]^{-1}[b_{31}\mathbf{k}_1 + b_{32}\mathbf{k}_2] \tag{9-43}$$

By following the same procedure used by Cailland and Padmanabhan(2), Michelsen obtained the following set of parameters when the expression given by Eq. (9-43) is used instead of Eq. (9-17) for $\mathbf{k}_3$.

$$\begin{aligned} a^3 - 3a^2 + \frac{3a}{2} - \frac{1}{6} &= 0 \\ a_1 &= 0.435\,867 \\ R_1 = \frac{11}{27} - b_{31} &= 1.037\,58 \\ R_2 = \frac{16}{27} - b_{32} &= 0.834\,94 \\ R_3 &= 1 \\ b_2 &= \frac{3}{4} \\ b_{32} = \frac{2}{9a_1}(6a_1^2 - 6a_1 + 1) &= -0.242\,35 \\ b_{31} = -\frac{1}{6a_1}(8a_1^2 - 2a_1 + 1) &= -0.630\,172 \end{aligned} \tag{9-44}$$

Michelsen's method has been found to be one of the most efficient methods for small, medium, and even large dimensional systems of ordinary differential equations. It is more efficient than both Rosenbrock's and Caillaud and Padmanabhan's methods.

9-2 MULTISTEP NUMERICAL-INTEGRATION ALGORITHMS

A general procedure is presented for the development of the multistep algorithms such as the Adams–Bashford, Adams–Moulton, and Gear algorithms for solving systems of stiff differential and algebraic equations. This development is

based on several sources (Refs. 3, 4, 5, 6). Because of the length of the development, one should not conclude that the final result is difficult to apply. Quite the contrary. Use of the Nordsieck vector simplifies the method and reduces the effort required to make simultaneous changes in step size and order.

Consider the ordinary differential equation

$$\frac{dx}{dt} = f(x, t) \tag{9-45}$$

The value of the variable x computed by use of the algorithm at time t_n is denoted by x_n, and the exact value of x at time t_n is denoted by $x(t_n)$.

In general any algorithm which gives the exact value of x for an initial-value problem having an exact solution given by a kth-degree polynomial is called a numerical integration formula of order k. The term "order" as used here is not to be confused with the order of the Taylor or Runge–Kutta algorithms.

The multistep numerical-integration algorithms may be stated in the following general form:

$$\begin{aligned} x_{n+1} = \alpha_0 x_n + \alpha_1 x_{n-1} + \cdots + \alpha_p x_{n-p} + h[\beta_{-1} f(x_{n+1}, t_{n+1}) \\ + \beta_0 f(x_n, t_n) + \beta_1 f(x_{n-1}, t_{n-1}) + \cdots + \beta_p f(x_{n-p}, t_{n-p})] \end{aligned} \tag{9-46}$$

or, more compactly,

$$x_{n+1} = \sum_{i=0}^{p} \alpha_i x_{n-i} + h \sum_{i=-1}^{p} \beta_i f(x_{n-i}, t_{n-i}) \tag{9-47}$$

Observe that Eq. (9-47) contains $2p + 3$ parameters, namely, $\alpha_0, \alpha_1, \ldots, a_p, \beta_{-1}, \beta_0, \beta_1, \ldots, \beta_p$. These $2p + 3$ parameters are to be selected such that if the solution $x(t)$ of an initial-value problem is given by a polynomial of degree k, then Eq. (9-47) gives the exact solution

$$x_{n+1} = x(t_{n+1})$$

From the theory of equations, one recalls that the number of parameters required to uniquely determine a kth-degree polynomial is equal to $k + 1$. For example, a straight line (a polynomial of degree 1) is determined by two parameters, and a parabola (a polynomial of degree 2) is determined by three parameters. Thus, the number of parameters $2p + 3$ must be equal to or greater than $k + 1$.

The $2p + 3$ parameters are picked such that the corrector is exact for all polynomial solutions which are equal to or less than degree k in the following manner.

Constraints for the Corrector Parameters

Let the polynomial solution of the initial-value problem be denoted by

$$x(t) = a_0 + a_1 t + a_2 t^2 + \cdots + a_k t^k \tag{9-48}$$

The expression for the constraints are found by beginning with a polynomial solution of degree zero.

Case 1 $k = 0 \quad x(t) = a_0 \quad x'(t) = 0$

Thus

$$x_{n+1} = a_0$$

and since $x'(t) = 0$

$$f(x_{n-i}, t_{n-i}) = 0$$

Also since $x(t) = a_0$, it follows that

$$x_{n-i} = a_0,$$

Substitution of these values in Eq. (9-47) gives

$$a_0 = \sum_{i=0}^{p} \alpha_i a_0 + h \sum_{i=-1}^{p} (\beta_i)(0)$$

which reduces to

$$1 = \sum_{i=0}^{p} \alpha_i \tag{9-49}$$

Case 2 $k = 1 \quad x(t) = a_0 + a_1 t \quad x'(t) = a_1$

Let $t_n = 0$, $t_{n+1} = h$, $t_{n-1} = -h$, $t_{n-2} = -2h$, $t_{n-i} = -ih$.

Then

$$x_{n+1} = a_0 + a_1 h \qquad x_n = a_0 \qquad x_{n-1} = a_0 - a_1 h$$
$$x_{n-i} = a_0 - a_1(ih) \qquad f(x_{n-i}, t_{n-i}) = a_1$$

Substitution of these results into Eq. (9-47) gives

$$a_0 + a_1 h = \sum_{i=0}^{p} \alpha_i (a_0 - a_1(ih)) + h \sum_{i=-1}^{p} \beta_i a_1$$

and

$$a_0 + a_1 h = a_0 \sum_{i=0}^{p} \alpha_i + a_1 h \left[\sum_{i=0}^{p} \alpha_i (-i) + \sum_{i=-1}^{p} \beta_i \right]$$

Comparison of the coefficients of a_0 and $a_1 h$ yields the relationship giving Eq. (9-49) and

$$\sum_{i=1}^{p} \alpha_i (-i) + \sum_{i=-1}^{p} \beta_i = 1 \tag{9-50}$$

Case 3 $k = 2 \quad x(t) = a_0 + a_1 t + a_2 t^2$

$$x'(t) = f(x, t) = a_1 + 2a_2 t$$
$$x_{n+1} = a_0 + a_1 h + a_2 h^2$$
$$x_{n-i} = a_0 + a_1(-ih) + a_2(-ih)^2$$
$$f(x_{n-i}, t_{n-i}) = a_1 + 2a_2(-ih)$$

Substitution of these results into Eq. (9-47) yields

$$a_0 + a_1 h + a_2 h^2 = \sum_{i=0}^{p} \alpha_i [a_0 + a_1(-ih) + a_2(-ih)^2]$$
$$+ h \sum_{i=-1}^{p} \beta_i [a_1 + 2a_2(-ih)]$$
$$= a_0 \left[\sum_{i=0}^{p} \alpha_i \right] + a_1 h \left[\sum_{i=0}^{p} \alpha_i (-i) + \sum_{i=-1}^{p} \beta_i \right]$$
$$+ a_2 h^2 \left[\sum_{i=-1}^{p} \alpha_i (-i)^2 + 2 \sum_{i=1}^{c} (-i)\beta_i \right]$$

Comparison of the coefficients of a_0, $a_1 h$, and $a_2 h^2$ yields the relationships given by Eqs. (9-49), (9-50), and

$$\sum_{i=1}^{p} (-i)^2 \alpha_i + 2 \sum_{i=-1}^{p} (-i)\beta_i = 1 \tag{9-51}$$

For $k = 3$, the relationships given by Eqs. (9-49), (9-50), (9-51), and

$$\sum_{i=1}^{p} (-i)^3 \alpha_i + 3 \sum_{i=-1}^{p} (-i)^2 \beta_i = 1 \tag{9-52}$$

are obtained. Continuation of this process shows that the constraints on the parameters which are necessary for the corrector (Eq. (9-47)) to give the exact value of x when the solution to the initial-value problem is given by a polynomial of degree k are as follows:

$$\sum_{i=0}^{p} \alpha_i = 1$$
$$\sum_{i=1}^{p} (-i)^j \alpha_i + j \sum_{i=-1}^{p} (-i)^{j-1} \beta_i = 1 \qquad (j = 1, 2, \ldots, k) \tag{9-53}$$

A number of multistep algorithms may be obtained by making suitable choices of the parameters $\{\alpha_i\}$ and $\{\beta_i\}$. For example, the kth-order Adams–Bashforth algorithm is an explicit multistep algorithm obtained by setting

$$p = k - 1 \qquad \alpha_1 = \alpha_2 = \cdots = \alpha_{k-1} = 0 \qquad \beta_{-1} = 0$$

in Eq. (9-47). Similarly, the kth-order Adams–Moulton algorithm is an implicit algorithm obtained by setting

$$p = k - 2 \qquad \alpha_1 = \alpha_2 = \alpha_3 = \cdots = \alpha_{k-2} = 0$$

The remaining parameters are then determined by use of Eq. (9-53) in the same manner as demonstrated below for Gear's third-order algorithm.

Gear's Corrector Algorithm (Refs. 5, 6)

Gear's kth-order corrector algorithm is an implicit algorithm which is obtained by setting

$$p = k - 1 \qquad \beta_0 = \beta_1 = \beta_2 = \cdots = \beta_{k-1} = 0$$

Thus, Gear's corrector is given by

$$x_{n+1} = \alpha_0(k)x_n + \alpha_1(k)x_{n-1} + \alpha_2(k)x_{n-2} + \cdots + \alpha_{k-1}(k)x_{n-k+1} + h[\beta_{-1}(k)f(x_{n+1}, t_{n+1})] \tag{9-54}$$

where the notation $\alpha_i(k)$ and $\beta_{-1}(k)$ is used to emphasize the fact that the values of the α_i's and β_{-1} depend upon the order k of the method. The $k+1$ parameters $\alpha_0, \alpha_1, \alpha_2, \ldots, \alpha_{k-1}, \beta_{-1}$ are to be determined such that Eq. (9-52) gives an exact solution for all initial-value problems which have exact solutions given by polynomials of degree k.

For the case of Gear's kth-order algorithm, Eq. (9-53) consists of $k+1$ independent equations which may be represented as follows:

$$\sum_{i=0}^{k-1} \alpha_i = 1$$
$$\sum_{i=1}^{k-1} (-i)^j \alpha_i + j\beta_{-1} = 1 \qquad (j = 1, 2, \ldots, k) \tag{9-55}$$

Thus, for

$$\begin{aligned}
j = 0: &\quad \alpha_0 + \alpha_1 + \cdots + \alpha_{k-1} = 1 \\
j = 1: &\quad -\alpha_1 - 2\alpha_2 - 3\alpha_3 + \cdots + [-(k-1)]\alpha_{k-1} + \beta_{-1} = 1 \\
j = 2: &\quad \alpha_1 + 4\alpha_2 + 9\alpha_3 + \cdots + [-(k-1)]^2\alpha_{k-1} + 2\beta_{-1} = 1 \\
j = 3: &\quad -\alpha_1 - 8\alpha_2 - 27\alpha_3 + \cdots + [-(k-1)]^3\alpha_{k-1} + 3\beta_{-1} = 1 \\
&\quad \vdots \\
j = k: &\quad (-1)^k\alpha_1 + (-2)^k\alpha_2 + (-3)^k\alpha_3 + \cdots + [-(k-1)]^k\alpha_{k-1} + k\beta_{-1} = 1
\end{aligned} \tag{9-56}$$

In matrix notation, these equations have the following representation:

$$\begin{bmatrix} 1 & 1 & 1 & 1 & \cdots & 1 & 0 \\ 0 & -1 & -2 & -3 & \cdots & [-(k-1)] & 1 \\ 0 & 1 & 4 & 9 & \cdots & [-(k-1]^2 & 2 \\ 0 & -1 & -8 & -27 & \cdots & [-(k-1)]^3 & 3 \\ \vdots & \vdots & \vdots & \vdots & \vdots & \vdots & \\ 0 & (-1)^k & (-2)^k & (-3)^k & \cdots & [-(k-1)]^k & k \end{bmatrix} \begin{bmatrix} \alpha_0(k) \\ \alpha_1(k) \\ \alpha_2(k) \\ \alpha_3(k) \\ \vdots \\ \beta_{-1}(k) \end{bmatrix} = \begin{bmatrix} 1 \\ 1 \\ 1 \\ 1 \\ \vdots \\ 1 \end{bmatrix} \tag{9-57}$$

Gear's Third-Order Corrector Algorithm, $k = 3$

In this case Eq. (9-57) becomes

$$\begin{bmatrix} 1 & 1 & 1 & 0 \\ 0 & -1 & -2 & 1 \\ 0 & 1 & 4 & 2 \\ 0 & -1 & -8 & 3 \end{bmatrix} \begin{bmatrix} \alpha_0 \\ \alpha_1 \\ \alpha_2 \\ \beta_{-1} \end{bmatrix} = \begin{bmatrix} 1 \\ 1 \\ 1 \\ 1 \end{bmatrix}$$

The solution is

$$\alpha_0 = \frac{18}{11} \qquad \alpha_1 = \frac{-9}{11} \qquad \alpha_2 = \frac{2}{11} \qquad \beta_{-1} = \frac{6}{11}$$

Thus, the Gear third-order implicit corrector is given by

$$x_{n+1} = \frac{18}{11}x_n - \frac{9}{11}x_{n-1} + \frac{2}{11}x_{n-2} + h\left[\frac{6}{11}f(x_{n+1}, t_{n+1})\right] \tag{9-58}$$

The parameters for the Gear correctors for orders $k = 1$ through $k = 6$ are given in Table 9-1.

Table 9-1 Parameters for Gear's Corrector

Order (k)	α_0	α_1	α_2	α_3	α_4	α_5	β_{-1}
1	1	.....	...	.....	...	.....	1
2	$\frac{4}{3}$	$-\frac{1}{3}$	...	.....	...	.....	$\frac{2}{3}$
3	$\frac{18}{11}$	$-\frac{9}{11}$	$\frac{2}{11}$	.....	...	.....	$\frac{6}{11}$
4	$\frac{48}{25}$	$-\frac{36}{25}$	$\frac{16}{25}$	$-\frac{3}{25}$	...	.....	$\frac{12}{25}$
5	$\frac{300}{137}$	$-\frac{300}{237}$	$\frac{200}{137}$	$-\frac{75}{137}$	$\frac{12}{137}$	.....	$\frac{60}{137}$
6	$\frac{360}{147}$	$-\frac{450}{147}$	$\frac{400}{147}$	$-\frac{225}{147}$	$\frac{72}{147}$	$-\frac{10}{147}$	$\frac{60}{147}$

Gear's Predictors

Gear's kth-order predictor is an explicit algorithm which is obtained by setting

$$p = k - 1 \qquad \beta_{-1} = \beta_1 = \beta_2 = \cdots = \beta_{k-1} = 0 \tag{9-59}$$

Thus

$$x_{n+1} = \bar{\alpha}_0(k)x_n + \bar{\alpha}_1(k)x_{n-1} + \bar{\alpha}_2(k)x_{n-2} + \cdots + \bar{\alpha}_{k-1}(k)x_{n-k+1} + h\bar{\beta}_0(k)f(x_n, t_n) \tag{9-60}$$

In this case the constraints are given by

$$\begin{gathered} \sum_{i=0}^{k-1} \bar{\alpha}_i = 1 \\ \sum_{i=1}^{k-1} (-i)\bar{\alpha}_i + \bar{\beta}_0 = 1 \qquad (j = 2, 3, \ldots, k-1) \\ \sum_{i=1}^{k-1} (-i)^j \bar{\alpha}_i = 1 \end{gathered} \tag{9-61}$$

where the overbars on the parameters are used to distinguish them from those of Gear's kth-order corrector. Thus, for

$$\begin{array}{lccccccc} j=0: & \bar{\alpha}_0 + \bar{\alpha}_1 + & & & \cdots + & \bar{\alpha}_{k-1} & = 1 \\ j=1: & -\bar{\alpha}_1 - & 2\bar{\alpha}_2 - & 3\bar{\alpha}_3 + \cdots + [-(k-1)]\,\bar{\alpha}_{k-1} + \bar{\beta}_0 & = 1 \\ j=2: & \bar{\alpha}_1 + & 4\bar{\alpha}_2 + & 9\bar{\alpha}_3 + \cdots + [-(k-1)]^2\bar{\alpha}_{k-1} & = 1 \\ j=3: & -\bar{\alpha}_1 - & 8\bar{\alpha}_2 - & 27\bar{\alpha}_3 + \cdots + [-(k-1)]^3\bar{\alpha}_{k-1} & = 1 \\ \vdots & \vdots & \vdots & \vdots \quad \vdots & \vdots & \vdots \\ j=k: & (-1)^k\bar{\alpha}_1 + (-1)^k\bar{\alpha}_2 + (-1)^k\bar{\alpha}_3 + \cdots + [-(k-1)]^k\bar{\alpha}_{k-1} & = 1 \end{array} \tag{9-62}$$

and restatement of these equations in matrix notation gives

$$\begin{bmatrix} 1 & 1 & 1 & 1 & \cdots & 1 & 0 \\ 0 & -1 & -2 & -3 & \cdots & [-(k-1)] & 1 \\ 0 & 1 & 4 & 9 & \cdots & [-(k-1)]^2 & 0 \\ 0 & -1 & -8 & -27 & \cdots & [-(k-1)]^3 & 0 \\ \vdots & \vdots & \vdots & \vdots & \vdots & \vdots & \vdots \\ 0 & (-1)^k & (-2)^k & (-3)^k & \cdots & [-(k-1)]^k & 0 \end{bmatrix} \begin{bmatrix} \bar{\alpha}_0(k) \\ \bar{\alpha}_1(k) \\ \bar{\alpha}_2(k) \\ \bar{\alpha}_3(k) \\ \vdots \\ \bar{\beta}_0(k) \end{bmatrix} = \begin{bmatrix} 1 \\ 1 \\ 1 \\ 1 \\ \vdots \\ 1 \end{bmatrix} \tag{9-63}$$

Gear's Third-Order Predictor

For this case, Eq. (9-63) reduces to

$$\begin{bmatrix} 1 & 1 & 1 & 0 \\ 0 & -1 & -2 & 1 \\ 0 & 1 & 4 & 0 \\ 0 & -1 & -8 & 0 \end{bmatrix} \begin{bmatrix} \bar{\alpha}_0 \\ \bar{\alpha}_1 \\ \bar{\alpha}_2 \\ \bar{\beta}_0 \end{bmatrix} = \begin{bmatrix} 1 \\ 1 \\ 1 \\ 1 \end{bmatrix} \tag{9-64}$$

The solution is found to be

$$\bar{\alpha}_0 = -\frac{3}{2} \qquad \bar{\alpha}_1 = 3 \qquad \bar{\alpha}_2 = -\frac{1}{2} \qquad \bar{\beta}_0 = 3 \tag{9-65}$$

and thus Gear's 3rd-order explicit predictor is

$$x_{n+1} = -\frac{3}{2}x_n + 3x_{n-1} - \frac{1}{2}x_{n-2} + 3hf(x_n, t_n) \tag{9-66}$$

The parameters for the Gear predictors for orders $k = 1$ through $k = 6$ are given in Table 9-2.

Gear's Method

Gear has proposed that the predictors and correctors be combined as demonstrated below. The symbol $\tilde{x}_{n+1}$ is used to distinguish the values of x computed at time t_{n+1} by the predictor from those computed by the corrector, that is,

$$x_{n+1} = \alpha_0 x_n + \alpha_1 x_{n-1} + \cdots + \alpha_{k-1}x_{n-k+1} + h\beta_{-1}x'_{n+1} \tag{9-67}$$

$$\tilde{x}_{n+1} = \bar{\alpha}_0 x_n + \bar{\alpha}_1 x_{n-1} + \cdots + \bar{\alpha}_{k-1}x_{n-k+1} + h\bar{\beta}_0 x'_n \tag{9-68}$$

When the second expression is subtracted from the first, the result so obtained may be rearranged to the form

$$x_{n+1} = \tilde{x}_{n+1} + \beta_{-1}[hx'_{n+1} - (\gamma_0 x_n + \cdots + \gamma_{k-1}x_{n-k+1} + \delta_0 hx'_n)] \tag{9-69}$$

$$\gamma_i = (\bar{\alpha}_i - \alpha_i)/\beta_{-1} \tag{9-70}$$

$$\delta_0 = \bar{\beta}_0/\beta_{-1} \tag{9-71}$$

Let the quantity $\tilde{x}'_{n+1}$ be defined as follows:

$$h\tilde{x}'_{n+1} = \gamma_0 x_n + \gamma_1 x_{n-1} + \cdots + \gamma_{k-1}x_{n-k+1} + \delta_0 hx'_n \tag{9-72}$$

Table 9-2 Parameters for Gear's Predictor

Order (k)	$\bar{\alpha}_0$	$\bar{\alpha}_1$	$\bar{\alpha}_2$	$\bar{\alpha}_3$	$\bar{\alpha}_4$	$\bar{\alpha}_5$	$\bar{\beta}_0$
1	1	...	.....	...	....	...	1
2	0	1	.....	...	....	...	2
3	$-\frac{3}{2}$	$\frac{6}{2}$	$-\frac{1}{2}$	...	....	...	$\frac{6}{2}$
4	$-\frac{10}{3}$	$\frac{18}{3}$	$-\frac{6}{3}$	$\frac{1}{3}$	....	...	$\frac{12}{3}$
5	$-\frac{65}{12}$	$\frac{120}{12}$	$-\frac{60}{12}$	$\frac{20}{12}$	$-\frac{3}{12}$	...	$\frac{60}{12}$
6	$-\frac{77}{10}$	$\frac{150}{10}$	$-\frac{100}{10}$	$\frac{50}{10}$	$-\frac{15}{10}$	$\frac{2}{10}$	$\frac{60}{10}$

Then Eq. (9-69) may be rewritten in the form

$$x_{n+1} = \tilde{x}_{n+1} + \beta_{-1}(hx'_{n+1} - h\tilde{x}'_{n+1}) \tag{9-73}$$

Let the quantity b be defined such that

$$x_{n+1} = \tilde{x}_{n+1} + \beta_{-1}b \tag{9-74}$$

$$hx'_{n+1} = h\tilde{x}'_{n+1} + b \tag{9-75}$$

That is, the quantity b is to be determined such that $G(b) = 0$, where

$$G(b) = hf(\tilde{x}_{n+1} + \beta_{-1}b, t_{n+1}) - (h\tilde{x}'_{n+1} + b) \tag{9-76}$$

Statement of the Corrector and Predictor in Matrix Form

In the control of step size and order of the predictor-corrector pair, it is convenient to state the corrector and predictor in matrix form. To do this, let the following vectors and matrices be defined.

$$\mathbf{X}_{n+1} = [x_{n+1} \quad hx'_{n+1} \quad x_n \quad x_{n-1} \quad \cdots \quad x_{n-k}]^T \tag{9-77}$$

$$\tilde{\mathbf{X}}_{n+1} = [\tilde{x}_{n+1} \quad h\tilde{x}'_{n+1} \quad x_n \quad x_{n-1} \quad \cdots \quad x_{n-k}]^T \tag{9-78}$$

$$\mathbf{B} = \begin{bmatrix} \bar{\alpha}_0 & \bar{\beta}_0 & \bar{\alpha}_1 & \bar{\alpha}_2 & \cdots & \bar{\alpha}_{k-2} & \bar{\alpha}_{k-1} \\ \gamma_0 & \delta_0 & \gamma_1 & \gamma_2 & \cdots & \gamma_{k-2} & \gamma_{k-1} \\ 1 & 0 & 0 & 0 & \cdots & 0 & 0 \\ 0 & 0 & 1 & 0 & \cdots & 0 & 0 \\ \vdots & \vdots & \vdots & \vdots & \vdots & \vdots & \vdots \\ 0 & \cdots & \cdots & \cdots & 0 & 1 & 0 \end{bmatrix} \tag{9-79}$$

$$\mathbf{C} = [\beta_{-1} \quad 1 \quad 0 \quad \cdots \quad 0]^T \tag{9-80}$$

On the basis of the above definitions of the predictor $\tilde{\mathbf{X}}_{n+1}$, the corrector $\mathbf{X}_{n+1}$, the matrix $\mathbf{B}$ and vector $\mathbf{C}$, it is easily verified as shown below that the predictor and the corrector may be stated as follows:

$$\tilde{\mathbf{X}}_{n+1} = \mathbf{B}\mathbf{X}_n \tag{9-81}$$

$$\mathbf{X}_{n+1} = \tilde{\mathbf{X}}_{n+1} + b\mathbf{C} \tag{9-82}$$

That the predictor and corrector may be recovered by carrying out the matrix operations implied by Eqs. (9-81) and (9-82) is demonstrated for the special case of the third-order equations:

$$\mathbf{B}\mathbf{X}_n = \begin{bmatrix} \bar{\alpha}_0 & \bar{\beta}_0 & \bar{\alpha}_1 & \bar{\alpha}_2 \\ \gamma_0 & \delta_0 & \gamma_1 & \gamma_2 \\ 1 & 0 & 0 & 0 \\ 0 & 0 & 1 & 0 \end{bmatrix} \begin{bmatrix} x_n \\ hx'_n \\ x_{n-1} \\ x_{n-2} \end{bmatrix} = \begin{bmatrix} (\bar{\alpha}_0 x_n + \bar{\beta}_0 hx'_n + \bar{\alpha}_1 x_{n-1} + \bar{\alpha}_2 x_{n-2}) \\ (\gamma_0 x_n + \delta_0 hx'_n + \gamma_1 x_{n-1} + \gamma_2 x_{n-2}) \\ x_n \\ x_{n-1} \end{bmatrix}$$

From Eqs. (9-68) and (9-72), the first two elements are seen to be $\tilde{x}_{n+1}$ and $h\tilde{x}'_{n+1}$. Thus

$$\mathbf{B}\mathbf{X}_n = [\tilde{x}_{n+1} \quad h\tilde{x}'_{n+1} \quad x_n \quad x_{n-1}]^T = \tilde{\mathbf{X}}_{n+1}$$

Then

$$\tilde{\mathbf{X}}_{n+1} + b\mathbf{C} = \begin{bmatrix} \tilde{x}_{n+1} \\ h\tilde{x}'_{n+1} \\ x_n \\ x_{n-1} \end{bmatrix} + \begin{bmatrix} \beta_{-1}b \\ b \\ 0 \\ 0 \end{bmatrix} = \begin{bmatrix} \tilde{x}_{n+1} + \beta_{-1}b \\ h\tilde{x}'_{n+1} + b \\ x_n \\ x_{n-1} \end{bmatrix}$$

Thus, it follows from Eqs. (9-74) and (9-75) that

$$\tilde{\mathbf{X}}_{n+1} + b\mathbf{C} = \begin{bmatrix} x_{n+1} \\ hx'_{n+1} \\ x_n \\ x_{n-1} \end{bmatrix} = \mathbf{X}_{n+1}$$

The Nordsieck Vector

The simultaneous change of the size of the time step and the order is easily effected through the use of the Nordsieck vector $\mathbf{Z}$. For an algorithm of order k

$$\mathbf{Z}_n = \left[x_n, hx'_n, \frac{h^2}{2!}x_n^{(2)}, \frac{h^3}{3!}x_n^{(3)}, \ldots, \frac{h^k}{k!}x_n^{(k)} \right]^T \tag{9-83}$$

The matrix $\mathbf{T}$ required to transform $\mathbf{X}_n$ into $\mathbf{Z}_n$,

$$\mathbf{Z}_n = \mathbf{T}\mathbf{X}_n \qquad \text{or} \qquad \mathbf{X}_n = \mathbf{T}^{-1}\mathbf{Z}_n \tag{9-84}$$

is found as demonstrated below for the case where $k = 3$. For the third-order algorithm, the two vectors are

$$\mathbf{X}_n = [x_n, hx'_n, x_{n-1}, x_{n-2}]^T$$

$$\mathbf{Z}_n = \left[x_n, hx'_n, \frac{h^2}{2!}x_n^{(2)}, \frac{h^3}{3!}x_n^{(3)} \right]^T$$

For a differential equation whose solution is a third-order polynomial, the following set of equations apply:

$$x(t) = a_0 + a_1 t + a_2 t^2 + a_3 t^3$$

$$x'(t) = a_1 + 2a_2 t + 3a_3 t^2$$

$$x^{(2)}(t) = 2a_2 + 6a_3 t$$

$$x^{(3)}(t) = 6a_3$$

For $t_n = 0$, $t_{n-1} = -h$, $t_{n-2} = -2h$

$$x_n = a_0$$
$$x'_n = a_1$$
$$x_n^{(2)} = 2a_2$$
$$x_n^{(3)} = 6a_3$$

Also

$$x_{n-1} = x(-h) = a_0 - ha_1 + a_2 h^2 - a_3 h^3$$

Thus

$$x_{n-1} = x_n - (hx'_n) + \left(\frac{h^2}{2} x_n^{(2)}\right) - \left(\frac{h^3}{6} x_n^{(3)}\right) \tag{9-85}$$

Similarly

$$x_{n-2} = x(-2h) = a_0 - 2a_1 h + 4a_2 h^2 - 8a_3 h^3$$

Thus

$$x_{n-2} = x_n - 2(hx'_n) + 4\left(\frac{h^2}{2} x_n^{(2)}\right) - 8\left(\frac{h^3}{6} x_n^{(3)}\right) \tag{9-86}$$

Since x_n and hx'_n appear in both vectors $\mathbf{X}_n$ and $\mathbf{Z}_n$, the following two additional equations are needed, namely,

$$x_n = x_n \tag{9-87}$$
$$hx'_n = hx'_n \tag{9-88}$$

When Eqs. (9-85) through (9-88) are stated in matrix form, one obtains

$$\begin{bmatrix} 1 & 0 & 0 & 0 \\ 0 & 1 & 0 & 0 \\ 1 & -1 & 1 & -1 \\ 1 & -2 & 4 & -8 \end{bmatrix} \begin{bmatrix} x_n \\ hx'_n \\ \frac{h^2}{2} x_n^{(2)} \\ \frac{h^3}{6} x_n^{(3)} \end{bmatrix} = \begin{bmatrix} x_n \\ hx'_n \\ x_{n-1} \\ x_{n-2} \end{bmatrix} \tag{9-89}$$

which is recognized as $\mathbf{T}^{-1}\mathbf{Z}_n = \mathbf{X}_n$ for $k = 3$. Since $\mathbf{TX}_n = \mathbf{Z}_n$, the matrix $\mathbf{T}$ is found by obtaining the inverse of the coefficient matrix of Eq. (9-89). The result, $\mathbf{TX}_n = \mathbf{Z}_n$, is

$$\begin{bmatrix} 1 & 0 & 0 & 0 \\ 0 & 1 & 0 & 0 \\ -\frac{7}{4} & \frac{6}{4} & \frac{8}{4} & -\frac{1}{4} \\ -\frac{3}{4} & \frac{2}{4} & \frac{4}{4} & -\frac{1}{4} \end{bmatrix} \begin{bmatrix} x_n \\ hx'_n \\ x_{n-1} \\ x_{n-2} \end{bmatrix} = \begin{bmatrix} x_n \\ hx'_n \\ \frac{h^2}{2} x_n^{(2)} \\ \frac{h^3}{6} x_n^{(3)} \end{bmatrix} \tag{9-90}$$

Thus, the predicted value $\tilde{\mathbf{Z}}_n$ of $\mathbf{Z}_n$ is related to the predicted value of $\tilde{\mathbf{X}}_n$ of $\mathbf{X}_n$ as follows:

$$\tilde{\mathbf{Z}}_n = \mathbf{T}\tilde{\mathbf{X}}_n = \mathbf{TBX}_{n-1} = \mathbf{TBT}^{-1}\mathbf{Z}_{n-1} \tag{9-91}$$

Thus

$$\tilde{\mathbf{Z}}_n = \mathbf{DZ}_{n-1} \tag{9-92}$$

where

$$\mathbf{D} = \mathbf{TBT}^{-1} \tag{9-93}$$

Since

$$\mathbf{Z}_n = \mathbf{TX}_n = \mathbf{T}[\tilde{\mathbf{X}}_n + b\mathbf{C}] \tag{9-94}$$

it follows that

$$\mathbf{Z}_n = \tilde{\mathbf{Z}}_n + b\mathbf{L} \tag{9-95}$$

where

$$\mathbf{L} = \mathbf{TC}$$

The matrix $\mathbf{D}$ is the Pascal triangle, that is, for $k = 3$

$$\mathbf{D} = \mathbf{TBT}^{-1} = \begin{bmatrix} 1 & 1 & 1 & 1 \\ 0 & 1 & 2 & 3 \\ 0 & 0 & 1 & 3 \\ 0 & 0 & 0 & 1 \end{bmatrix} \tag{9-96}$$

The nonzero element $d_{i+1,j+1}$ in the $j+1$st column and the $i+1$st row of the Pascal triangle matrix is given by

$$d_{i+1,j+1} = \frac{j!}{(j-i)!\,i!} \qquad (k+1) > j \geq i \geq 0$$

Also, for $k = 3$,

$$\mathbf{L} = \left[\frac{16}{11}, \frac{11}{11}, \frac{6}{11}, \frac{1}{11}\right]^T \tag{9-97}$$

The vector $\mathbf{L}$ for $k = 1$ through $k = 6$ is presented in Table 9-3.

Calculational Procedure for a Fixed Step Size and Order

1. Use the original differential equation

$$x' = f(x, t)$$

and the initial conditions to estimate the elements of $\mathbf{Z}_0$ for order k and step size h

$$\mathbf{Z}_0 = \left[x_0, hx'_0, \frac{h^2}{2!} x''_0, \ldots, \frac{h^k}{k!} x_0^{(k)}\right]^T$$

2. Use the Pascal triangle matrix $\mathbf{D}$ and $\mathbf{Z}_0$ to compute $\tilde{\mathbf{Z}}_1$ as follows:

$$\tilde{\mathbf{Z}}_1 = \mathbf{DZ}_0$$

Table 9-3 Elements of the vector L and values of β_{-1} for Gear's algorithm of order k†

Elements of L	Order: $k = 1, 2, \ldots, 6$					
	1	2	3	4	5	6
l_0	1	$\frac{2}{3}$	$\frac{6}{11}$	$\frac{24}{50}$	$\frac{120}{274}$	$\frac{720}{1764}$
l_1	1	$\frac{3}{3}$	$\frac{11}{11}$	$\frac{50}{50}$	$\frac{274}{274}$	$\frac{1764}{1764}$
l_2		$\frac{1}{3}$	$\frac{6}{11}$	$\frac{35}{50}$	$\frac{225}{274}$	$\frac{1624}{1764}$
l_3			$\frac{1}{11}$	$\frac{10}{50}$	$\frac{85}{274}$	$\frac{735}{1764}$
l_4				$\frac{1}{50}$	$\frac{15}{274}$	$\frac{175}{1764}$
l_5					$\frac{1}{274}$	$\frac{21}{1764}$
l_6						$\frac{1}{1764}$

† Note, β_{-1} corresponds to l_0.

For the nth time step the relationship is

$$\tilde{\mathbf{Z}}_n = \mathbf{D}\mathbf{Z}_{n-1}$$

3. Use those elements of $\tilde{\mathbf{Z}}_n$ which are needed in the determination of the b that makes $G(x_n, t_n) = 0$, where

$$G(\tilde{x}_n + \beta_{-1}b, t_n) = hf(\tilde{x}_n + \beta_{-1}b, t_n) - h(\tilde{x}'_n + b)$$

where

$$x_n = \tilde{x}_n + \beta_{-1}b$$

$$hx'_n = h\tilde{x}'_n + b$$

4. Compute the value of $\mathbf{Z}_n$ at time t_n as follows:

$$\mathbf{Z}_n = \tilde{\mathbf{Z}}_n + b\mathbf{L}$$

where the vector $\mathbf{L}$ for order $k = 1$ through $k = 6$ is given in Table 9-3, and return to step 2.

A considerable saving in computational effort on large problems may be achieved by carrying out the matrix multiplication implied in step 2 by successive additions as suggested by Gear(6).

Simultaneous Differential and Algebraic Equations

Consider the case where a set of algebraic equations are to be solved simultaneously with a set of differential equations. The corrector

$$x_{n+1} = \alpha_0 x_n + \alpha_1 x_{n-1} + \cdots + \alpha_k x_{n-k} + \alpha_{k+1} x_{n-(k+1)} + h\beta_{-1} f(x_{n+1}, u_{n+1}, t_{n+1}) \tag{9-98}$$

may be used to solve the algebraic equation

$$0 = g(x_{n+1}, u_{n+1}, t_{n+1}) \tag{9-99}$$

First the constraints which the parameters of the algorithm must satisfy when the exact solution to Eq. (9-99) is a polynomial of the kth degree, say,

$$u(t) = a_0 + a_1 t + a_2 t^2 + \cdots + a_k t^k \tag{9-100}$$

are determined.

Let the approximation of $u(t)$ obtained by passing a curve through a number of points of previous time steps be denoted by $u_{n+1} = u(t_{n+1})$. Then

$$u_{n+1} = \eta_0 u_n + \eta_1 u_{n-1} + \eta_2 u_{n-2} + \cdots + \eta_p u_{n-p} \tag{9-101}$$

or

$$u_{n+1} = \sum_{i=0}^{p} \eta_i u_{n-i} \tag{9-102}$$

The constraints on the parameters $\{\eta_i\}$ are found in the same manner shown for Gear's correctors and predictors.

Case 1 $k = 0$ $u(t) = a_0$ $u_{n+1} = a_0$ $u_{n-i} = a_0$

Substitution in Eq. (9-101) gives

$$a_0 = \sum_{i=0}^{p} \eta_i a_0$$

and thus

$$\sum_{i=0}^{p} \eta_i = 1 \tag{9-103}$$

Case 2 $k = 1$ $u(t) = a_0 + a_1 t$

Let

$$t_n = 0, \quad t_{n+1} = h, \quad t_{n-1} = -h, \quad t_{n-2} = -2h, \quad t_{n-i} = -ih$$

Then

$$u_n = a_0 \qquad u_{n+1} = a_0 + a_1 h \qquad u_{n-i} = a_0 - i a_1 h$$

Thus, Eq. (9-101) becomes

$$a_0 + a_1 h = \sum_{i=0}^{p} a_0 \eta_i + \sum_{i=0}^{p} \eta_i (-i) a_1 h$$

$$= a_0 \left(\sum_{i=0}^{p} \eta_i \right) + a_1 h \left[\sum_{i=1}^{p} (-i) \eta_i \right]$$

Comparison of the coefficients a_0 and $a_1 h$ yields the relationship given by Eq. (9-103) and

$$\sum_{i=1}^{p} (-i) \eta_i = 1 \tag{9-104}$$

For $k = 2$, one obtains the relationships given by Eqs. (9-103), (9-104), and

$$\sum_{i=1}^{p} \eta_i (-i)^2 = 1 \tag{9-105}$$

The power to which $(-i)$ is raised in the last expression of each set is seen to be equal to the degree of the polynomial. Then for a kth-degree polynomial, the last expression of the set is given by

$$\sum_{i=1}^{p} \eta_i (-i)^k = 1$$

In order for Eq. (9-102) to be exact when the solution to $g(x_{n+1}, u_{n+1}, t_{n+1}) = 0$ is given by a kth-degree polynomial, it is necessary that

$$p \geq k \tag{9-106}$$

in Eq. (9-102). For $p = k$ there are $k + 1$ parameters $(\eta_0, \eta_1, \eta_2, \ldots, \eta_k)$, and the above analysis gives $k + 1$ equations of constraint which the parameters must satisfy, namely,

$$\sum_{i=0}^{k} \eta_i = 1$$

$$\sum_{i=1}^{k} (-i)^j \eta_i = 1, \qquad (j = 1, 2, 3, \ldots, k) \tag{9-107}$$

and the elements of the matrix for determining the $\eta_i(k)$ are shown in the matrix equation below:

$$\begin{bmatrix} 1 & 1 & 1 & 1 & \cdots & 1 \\ 0 & -1 & -2 & -3 & \cdots & -k \\ 0 & 1 & 4 & 9 & \cdots & (-k)^2 \\ 0 & -1 & -8 & -27 & \cdots & (-k)^3 \\ \vdots & \vdots & \vdots & \vdots & & \vdots \\ 0 & (-1)^k & (-2)^k & (-3)^k & \cdots & (-k)^k \end{bmatrix} \begin{bmatrix} \eta_0(k) \\ \eta_1(k) \\ \eta_2(k) \\ \eta_3(k) \\ \vdots \\ \eta_k(k) \end{bmatrix} = \begin{bmatrix} 1 \\ 1 \\ 1 \\ 1 \\ \vdots \\ 1 \end{bmatrix} \tag{9-108}$$

For the case where $k = 3$, the following results are obtained by solving Eq. (9-108) for $k = 3$

$$\eta_0 = 4 \qquad \eta_1 = -6 \qquad \eta_2 = 4 \qquad \eta_3 = -1 \tag{9-109}$$

Let the vectors $\tilde{\mathbf{W}}_{n+1}$ and $\mathbf{W}_{n+1}$ be defined as follows:

$$\mathbf{W}_{n+1} = [u_{n+1}, u_n, u_{n-1}, \ldots, u_{n-k+1}]^T \tag{9-110}$$

$$\tilde{\mathbf{W}}_{n+1} = [\tilde{u}_{n+1}, u_n, u_{n-1}, \ldots, u_{n-k+1}]^T \tag{9-111}$$

Then $\tilde{\mathbf{W}}_{n+1}$ and $\mathbf{W}_n$ are related by the following transformation:

$$\tilde{\mathbf{W}}_{n+1} = \mathbf{E}\mathbf{W}_n \tag{9-112}$$

where

$$\mathbf{E} = \begin{bmatrix} \eta_0 & \eta_1 & \eta_2 & \cdots & \eta_{k-1} & \eta_k \\ 1 & 0 & 0 & \cdots & 0 & 0 \\ 0 & 1 & 0 & \cdots & 0 & 0 \\ \cdots & \cdots & \cdots & \cdots & \cdots & \cdots \\ 0 & 0 & 0 & \cdots & 1 & 0 \end{bmatrix} \tag{9-113}$$

That Eq. (9-112) is correct is readily demonstrated by carrying out the matrix multiplication for $k = 3$

$$\mathbf{E}\mathbf{W}_n = \begin{bmatrix} \eta_0 & \eta_1 & \eta_2 & \eta_3 \\ 1 & 0 & 0 & 0 \\ 0 & 1 & 0 & 0 \\ 0 & 0 & 1 & 0 \end{bmatrix} \begin{bmatrix} u_n \\ u_{n-1} \\ u_{n-2} \\ u_{n-3} \end{bmatrix} = \begin{bmatrix} (\eta_0 u_n + \cdots + \eta_3 u_{n-3} \\ u_n \\ u_{n-1} \\ u_{n-2} \end{bmatrix}$$

$$= [\tilde{u}_{n+1}, u_n, u_{n-1}, u_{n-2}]^T = \tilde{\mathbf{W}}_{n+1} \tag{9-114}$$

Let d be selected such that

$$g(u_n, t_n) = 0 \tag{9-115}$$

$$u_n = \tilde{u}_n + \beta_{-1} d \tag{9-116}$$

Next observe that

$$\mathbf{W}_n = \tilde{\mathbf{W}}_n + d\mathbf{F} \tag{9-117}$$

where

$$\mathbf{F} = [\beta_{-1} \quad 0 \quad 0 \quad \cdots \quad 0]^T \tag{9-118}$$

Verification of Eq. (9-117) follows:

$$\tilde{\mathbf{W}}_n + b\mathbf{F} = \begin{bmatrix} \tilde{u}_n \\ u_{n-1} \\ u_{n-2} \\ \vdots \\ u_{n-k} \end{bmatrix} + d \begin{bmatrix} \beta_{-1} \\ 0 \\ \vdots \\ 0 \end{bmatrix} = \begin{bmatrix} \tilde{u}_n + \beta_{-1} d \\ u_{n-1} \\ u_{n-2} \\ \vdots \\ u_{n-k} \end{bmatrix} = \begin{bmatrix} u_n \\ u_{n-1} \\ u_{n-2} \\ \vdots \\ u_{n-k} \end{bmatrix} = \mathbf{W}_n$$

Statement of the Vector $\mathbf{W}_n$ in Terms of the Nordsieck Vector $\mathbf{Y}_n$

For the case where $k = 3$, the transformation $\mathbf{Q}$ required to transform $\mathbf{W}_n$ into $\mathbf{Y}_n$

$$\mathbf{Y}_n = \mathbf{Q}\mathbf{W}_n \tag{9-119}$$

is found as follows. Let

$$u(t) = a_0 + a_1 t + a_2 t^2 + a_3 t^3 \tag{9-120}$$

Then

$$u'(t) = a_1 + 2a_2 t + 3a_3 t^2$$
$$u^{(2)}(t) = 2a_2 + 6a_3 t$$
$$u^{(3)}(t) = 6a_3$$

At $t = t_n = 0$, $t_{n-1} = -h$, $t_{n-2} = -2h$, $t_{n-3} = -3h$, the following results are obtained in the same manner as demonstrated previously

$$u_n = a_0$$
$$u'_n = a_1$$
$$u_n^{(2)} = 2a_2$$
$$u_n^{(3)} = 6a_3$$
$$u_{n-1} = u(-h) = u_n - (hu'_n) + \left(\frac{h^2}{2} u_n^{(2)}\right) - \left(\frac{h^3}{3!} u_n^{(3)}\right)$$
$$u_{n-2} = u_n - 2(hu'_n) + 4\left(\frac{h^2}{2} u_n^{(2)}\right) - 8\left(\frac{h^3}{3!} u_n^{(3)}\right)$$

and

$$u_{n-3} = u(-3h) = a_0 - 3a_1 h + 9a_2 h^2 - 27a_3 h^3$$
$$= u_n - 3(hu_n) + 9\left(\frac{h^2}{2} u_n^{(2)}\right) - 27\left(\frac{h^3}{3!} u_n^{(3)}\right)$$

Thus, the matrix equation $\mathbf{Q}^{-1}\mathbf{Y}_n = \mathbf{W}_n$ has the following representation:

$$\begin{bmatrix} 1 & 0 & 0 & 0 \\ 1 & -1 & 1 & -1 \\ 0 & -2 & 4 & -8 \\ 1 & -3 & 9 & -27 \end{bmatrix} \begin{bmatrix} u_n \\ hu'_n \\ \frac{h^2}{2} u_n^{(2)} \\ \frac{h^3}{3!} u_n^{(3)} \end{bmatrix} = \begin{bmatrix} u_n \\ u_{n-1} \\ u_{n-2} \\ u_{n-3} \end{bmatrix} \tag{9-121}$$

where the matrix $\mathbf{Q}$ required to transform $\mathbf{W}_n$ into $\mathbf{Y}_n$ is the inverse of the matrix appearing in Eq. (9-121), that is,

$$\mathbf{Q} = \begin{bmatrix} 1 & 0 & 0 & 0 \\ \frac{11}{6} & -3 & \frac{3}{2} & -\frac{1}{3} \\ 1 & -\frac{5}{2} & 2 & -\frac{1}{2} \\ \frac{1}{6} & -\frac{1}{2} & \frac{1}{2} & -\frac{1}{6} \end{bmatrix} \tag{9-122}$$

Also,

$$\tilde{\mathbf{Y}}_n = \mathbf{Q}\tilde{\mathbf{W}}_n = \mathbf{Q}\mathbf{E}\mathbf{W}_{n-1} = \mathbf{Q}\mathbf{E}\mathbf{Q}^{-1}\mathbf{Y}_{n-1} \tag{9-123}$$

and thus

$$\tilde{\mathbf{Y}}_n = \mathbf{D}\mathbf{Y}_{n-1} \tag{9-124}$$

where $\mathbf{D}$ is the Pascal triangle

$$\mathbf{D} = \mathbf{Q}\mathbf{E}\mathbf{Q}^{-1} \tag{9-125}$$

and

$$\mathbf{Q}^{-1} = \begin{bmatrix} 1 & 0 & 0 & 0 \\ 1 & -1 & 1 & -1 \\ 1 & -2 & 4 & -8 \\ 1 & -3 & 9 & -27 \end{bmatrix}$$

In order to reduce the number of matrices to be stored, advantage may be taken of the fact that

$$\mathbf{Q}\mathbf{F} = \mathbf{T}\mathbf{C} \tag{9-126}$$

For example for the third-order Gear method $\beta_{-1} = 6/11$ and

$$\mathbf{Q}\mathbf{F} = \left[\frac{6}{11}, 1, \frac{6}{11}, \frac{1}{11}\right]^T \tag{9-127}$$

Also,

$$\mathbf{L} = \mathbf{T}\mathbf{C} = \left[\frac{6}{11}, 1, \frac{6}{11}, \frac{1}{11}\right]^T \tag{9-128}$$

The relationships given by Eqs. (9-126) through (9-128) permit $\mathbf{Y}_n$ to be stated in terms of $\mathbf{Y}_n$, $\mathbf{L}$, and the scalar d. For

$$\mathbf{Y}_n = \mathbf{Q}\mathbf{W}_n = \mathbf{Q}[\tilde{\mathbf{W}}_n + d\mathbf{F}] = \mathbf{Q}\tilde{\mathbf{W}}_n + d\mathbf{Q}\mathbf{F}$$

or

$$\mathbf{Y}_n = \tilde{\mathbf{Y}}_n + d\mathbf{L} \tag{9-129}$$

The order in which the equations are applied is as follows:

$$\tilde{\mathbf{Y}}_n = \mathbf{D}\mathbf{Y}_{n-1} \tag{9-130}$$

$$\mathbf{Y}_n = \tilde{\mathbf{Y}}_n + d\mathbf{L} \tag{9-131}$$

where d is selected such that

$$g(\tilde{u}_n + d\beta_1, t_n) = 0$$

Thus, the algorithms for algebraic equations are seen to be of the same form as those for differential equations.

Calculational Procedure for the Simultaneous Solution of a Differential and an Algebraic Equation for a Fixed Step Size and Order

1. Use the original differential equation

$$x' = f(x, x', u, u', t)$$

and the algebraic equation

$$g(x, u, t) = 0$$

and the initial conditions to estimate the elements of $\mathbf{Z}_0$ and $\mathbf{Y}_0$ for order k and step size h.

$$\mathbf{Z}_0 = \left[x_0, hx'_0, \frac{h^2}{2!} x_0^{(2)}, \ldots, \frac{h^k}{k!} x_0^{(k)} \right]^T$$

$$\mathbf{Y}_0 = \left[u_0, hu'_0, \frac{h^2}{2!} u_0^{(2)}, \ldots, \frac{h^k}{k!} u_0^{(k)} \right]^T$$

2. Use the Pascal triangle matrix $\mathbf{D}$, $\mathbf{Z}_0$, and $\mathbf{Y}_0$ to compute $\tilde{\mathbf{Z}}_1$ and $\tilde{\mathbf{Y}}_1$. For the nth trial

$$\tilde{\mathbf{Z}}_1 = \mathbf{D}\mathbf{Z}_0$$

$$\tilde{\mathbf{Y}}_1 = \mathbf{D}\mathbf{Y}_0$$

3. Use those elements of $\tilde{\mathbf{Z}}_n$ and $\tilde{\mathbf{Y}}_n$ which are needed in the determination of b and d which satisfies the following functions simultaneously:

$$G(\tilde{x}_n, x'_n, u_n, t_n) = hf(\tilde{x}_n + \beta_{-1} b, hx'_n + b, \tilde{u}_n + \beta_{-1} d, t_n) - (h\tilde{x}'_n + b)$$

$$g(\tilde{x}_n, u_n, t_n) = g(\tilde{x}_n + \beta_{-1} b, \tilde{u}_n + \beta_{-1} d, t_n)$$

4. After the set (b, d) has been found that makes $G = g = 0$, compute $\mathbf{Z}_n$ and $\mathbf{Y}_n$ at time t_n as follows:

$$\mathbf{Z}_n = \tilde{\mathbf{Z}}_n + b\mathbf{L}$$

and

$$\mathbf{Y}_n = \tilde{\mathbf{Y}}_n + d\mathbf{L}$$

REFERENCES

1. B. Carnahan, H. A. Luther, and J. O. Wilkes: *Applied Numerical Methods*, John Wiley & Sons, New York, 1969.
2. J. B. Caillaud and L. Padmanabhan: "An Improved Semi-Implicit Runge–Kutta Method for Stiff Systems," *Chem. Eng. J.* **2**:227 (1971).
3. L. O. Chua and Pen-Min Lin: *Computer-Aided Analysis of Electronic Circuits*, Prentice-Hall, Inc., Englewood Cliffs, N.J., 1975.
4. C. W. Gear: "Simultaneous Numerical Solution of Differential-Algebraic Equations," *IEEE Trans. Circuit Theory*, **18**(1):89 (1971).
5. C. W. Gear: *Numerical Initial Value Problems in Ordinary Differential Equations*, Prentice-Hall, Inc., Englewood Cliffs, N.J. (1971).
6. C. W. Gear: "The Automatic Integration of Ordinary Differential Equations," *Commun. ACM*, **14**(3):176 (1971).
7. S. Gill: "A Process for the Step-by-Step Integration of Differential Equations in an Automatic Computing Machine," *Proc. Cambridge Phil. Soc.*, **47**:96–108 (1951).
8. P. Henrici: *Discrete Variable Methods in Ordinary Differential Equations*, John Wiley & Sons, New York, 1962.
9. M. L. Michelsen: "An Efficient General Purpose Method of Integration of Stiff Ordinary Differential Equations," *AIChE J.*, **22**(3):544 (1976).
10. M. L. Michelsen: "Application of the Semi-Implicit Runge–Kutta Methods for Integration of Ordinary and Partial Differential Equations," *Chem. Eng. J.*, **14**:107 (1977).
11. H. H. Rosenbrock: "Some General Implicit Processes for Numerical Solution of Differential Equations," *Computer J.*, **5**:320 (1953).

PROBLEMS

9-1 Develop the formulas given by Eq. (9-61) for the constraints on the $\{\bar{\alpha}_i\}$ and $\{\bar{\beta}_i\}$.

9-2 If $\mathbf{T}^{-1}$ is given by the coefficient matrix of Eq. (9-89), show that $\mathbf{T}$ is given by the coefficient matrix of Eq. (9-90).

9-3 Obtain the numerical values of the elements of $\mathbf{B}$ for a third-order Gear method; see the expression for $\mathbf{B}$ which is given below Eq. (9-82).

9-4 Use the numerical values of the elements of $\mathbf{T}$, $\mathbf{T}^{-1}$, and $\mathbf{B}$ from Probs. 9-2 and 9-3 to show that

$$\mathbf{T}\mathbf{B}\mathbf{T}^{-1} = \mathbf{D}$$

9-5 Obtain the values given for η_0, η_1, η_2, and η_3 by Eq. (9-109).

9-6 Use the values of η's found in Prob. 9-5 and the values of $\mathbf{Q}$, $\mathbf{Q}^{-1}$, and $\mathbf{E}$ given by Eqs. (9-122) through (9-125) to show that

$$\mathbf{Q}\mathbf{E}\mathbf{Q}^{-1} = \mathbf{D}$$

PART

THREE

SOLUTION OF PROBLEMS INVOLVING CONTINUOUS-SEPARATION PROCESSES

CHAPTER

TEN

DEVELOPMENT OF NUMERICAL METHODS APPLICABLE TO DIFFERENTIAL AND PARTIAL DIFFERENTIAL EQUATIONS

In this chapter abbreviated developments are presented for some of the numerical techniques used to solve differential and partial differential equations encountered in Chaps. 11, 12, and 13. The method of orthogonal collocation is developed in Sec. 10-1, finite difference methods in Sec. 10-2, and the method of characteristics in Sec. 10.3.

10-1 THE ORTHOGONAL COLLOCATION METHOD

The application of the method of orthogonal collocation to the solution of differential equations involves the use of the following concepts: (1) orthogonal polynomials, (2) evaluation of definite integrals by use of gaussian quadratures, and (3) the Method of Weighted Residuals and Orthogonal Collocation. The use of orthogonal collocation in the solution of partial differential equations is demonstrated in Chap. 12.

Since each of these three concepts is involved in the orthogonal collocation method for the solution of differential equations, a brief treatment of each of these topics is given before attempting to show how the combination of these concepts is used to solve differential equations.

Orthogonal Polynomials

Two functions $g_n(x)$ and $g_m(x)$ selected from a family of functions $\{g_k(x)\}$ are said to be orthogonal with respect to a positive weighting function $W(x)$ over the closed interval $[a, b]$ if

$$\int_a^b W(x)g_n(x)g_m(x)\,dx = 0 \qquad (n \neq m)$$

and (10-1)

$$\int_a^b W(x)[g_n(x)]^2\,dx > 0 \qquad (n = m)$$

If the above relationships hold for all n, then the functions $\{g_k(x)\}$ constitute a set of orthogonal functions.

Examples of sets of orthogonal polynomials are the Legendre, Laguerre, Chebyshev, and Hermite polynomials.

Legendre Polynomials

The Legendre polynomials $L_k(x)$ are orthogonal on the closed interval $[-1, 1]$ with respect to the weighting function $W(x) = 1$, that is,

$$\int_{-1}^{1} L_n(x)L_m(x)\,dx = 0 \qquad (n \neq m)$$

$$\int_{-1}^{1} [L_n(x)]^2\,dx > 0 \qquad (n = m) \tag{10-2}$$

The first three polynomials are

$$L_0(x) = 1$$

$$L_1(x) = x \tag{10-3}$$

$$L_2(x) = \tfrac{1}{2}(3x^2 - 1)$$

and the general recursion relation is

$$L_n(x) = \left(\frac{2n-1}{n}\right)xL_{n-1}(x) - \left(\frac{n-1}{n}\right)L_{n-2}(x) \qquad (n \geq 2) \tag{10-4}$$

Laguerre Polynomials

The Laguerre polynomials $\mathscr{L}_k(x)$ are orthogonal on the closed interval $[0, \infty]$ with respect to the weighting function $W(x) = e^{-x}$, that is,

$$\int_0^\infty e^{-x}\mathscr{L}_n(x)\mathscr{L}_m(x)\,dx = 0 \qquad (n \neq m)$$

$$\int_0^\infty e^{-x}[\mathscr{L}_n(x)]^2\,dx > 0 \qquad (n = m) \tag{10-5}$$

The first three Laguerre polynomials are as follows:

$$\mathscr{L}_0(x) = 1$$

$$\mathscr{L}_1(x) = -x + 1 \tag{10-6}$$

$$\mathscr{L}_2(x) = x^2 - 4x + 2$$

and the general recursion formula is given by

$$\mathscr{L}_n(x) = (2n - x - 1)\mathscr{L}_{n-1}(x) - (n-1)^2\mathscr{L}_{n-2}(x) \qquad (n \geq 2) \tag{10-7}$$

Chebyshev Polynomials

The Chebyshev polynomials $T_k(x)$ are orthogonal on the closed interval $[-1, 1]$ with respect to the weighting function

$$W(x) = \frac{1}{\sqrt{1-x^2}}$$

that is

$$\int_{-1}^{1} \frac{1}{\sqrt{1-x^2}} T_n(x)T_m(x)\,dx = 0 \qquad (n \neq m)$$

$$\int_{-1}^{1} \frac{1}{\sqrt{1-x^2}} [T_n(x)]^2\,dx > 0 \qquad (n = m) \tag{10-8}$$

The first three polynomials are

$$T_0(x) = 1$$

$$T_1(x) = x \tag{10-9}$$

$$T_2(x) = 2x^2 - 1$$

and

$$T_n(x) = 2xT_{n-1}(x) - T_{n-2}(x) \qquad (n \geq 2) \tag{10-10}$$

Hermite Polynomials

The Hermite polynomials are orthogonal on the closed interval $[-\infty, \infty]$ with respect to the weighting function $W(x) = e^{-x^2}$, that is,

$$\int_{-\infty}^{\infty} e^{-x^2}H_n(x)H_m(x)\,dx = 0 \qquad (n \neq m)$$

$$\int_{-\infty}^{\infty} e^{-x^2}[H_n(x)]^2\,dx > 0 \qquad (n = m) \tag{10-11}$$

The first three functions are

$$H_0(x) = 1$$

$$H_1(x) = 2x$$

$$H_2(x) = 4x^2 - 2$$

and the general recursion formula is

$$H_n(x) = 2xH_{n-1}(x) - 2(n-1)H_{n-2}(x) \qquad (n \geq 2) \qquad (10\text{-}12)$$

Jacobi Polynomials

The Jacobi orthogonal polynomials $P_n^{(\alpha,\beta)}(x)$ employed herein are defined on the closed interval [0, 1] with respect to the weighting function $W(x) = x^\beta(1-x)^\alpha$ where $\alpha > -1$ and $\beta > -1$, that is,

$$\int_0^1 (1-x)^\alpha x^\beta P_n^{(\alpha,\beta)}(x) P_m^{(\alpha,\beta)}(x)\, dx = 0 \qquad (n \neq m) \qquad (10\text{-}13)$$

and

$$\int_0^1 (1-x)^\alpha x^\beta [P_n^{(\alpha,\beta)}(x)]^2\, dx > 0 \qquad (n = m)$$

For each choice of the pair of parameters (α, β) of the weighting function, a corresponding set of orthogonal polynomials denoted by $P_n^{(\alpha,\beta)}(x)$ is obtained. Expressions for the polynomials are readily obtained by use of Rodriques' formula (Ref. 8)

$$(1-x)^\alpha x^\beta P_n^{(\alpha,\beta)}(x) = \frac{(-1)^n \Gamma(\beta+1)}{\Gamma(n+\beta+1)} \frac{d^n[(1-x)^{n+\alpha} x^{n+\beta}]}{dx^n} \qquad (10\text{-}14)$$

where $\Gamma(n)$ is the gamma function and for integers $\Gamma(n+1) = n\ \Gamma(n) = n!$ For example, the first four polynomials corresponding to $\alpha = \beta = 0$ (the weighting function $W(x) = (1-x)^0 x^0 = 1$) are found by use of Eq. (10-14) as follows:

$$P_0^{(0,0)}(x) = \frac{(-1)^0 \Gamma(1)}{\Gamma(1)} = 1$$

$$P_1^{(0,0)}(x) = \frac{(-1)\Gamma(1)}{\Gamma(2)} \frac{d[(1-x)x]}{dx} = 2x - 1$$

and

$$P_2^{(0,0)}(x) = \frac{(-1)^2 \Gamma(1)}{\Gamma(3)} \frac{d^2}{dx^2}[(1-x)^2 x^2] = 1 - 6x + 6x^2$$

$$P_3^{(0,0)}(x) = \frac{(-1)^3 \Gamma(1)}{\Gamma(4)} \frac{d^3[(1-x)^3 x^3]}{dx^3} = 1 - 12x + 30x^2 - 20x^3$$

The set of polynomials defined by Eq. (10-13) are commonly referred to in the literature as "shifted" Jacobi polynomials and the polynomials defined with respect to the weighting function $(1-x)^\alpha x^\beta$ on the closed interval $[-1, 1]$ are called the Jacobi polynomials. In this treatment, the "shifted" Jacobi polynomials are referred to herein as simply Jacobi polynomials.

As pointed out by Stroud and Secrest(16), the sequence of polynomials $\{L_n(x)\}$, $\{\mathscr{L}_n(x)\}$, $\{T_n(x)\}$, $\{P_n(x)\}$ which satisfy the respective orthogonal relationships given by Eqs. (10-2), (10-5), (10-8), (10-11), and (10-13) are unique. Each nth-degree polynomial has real coefficients and n distinct real roots interior to the respective interval of integration (Ref. 16). These and other properties as well as the zeros of these polynomials are given by Stroud and Secrest(16).

One of the most important characteristics of orthogonal polynomials is the fact that any arbitrary nth-degree polynomial with real coefficients

$$f_n(x) = \sum_{i=0}^{n} a_i x^i \qquad (10\text{-}15)$$

may be represented by a linear combination of any one of the above families of orthogonal polynomials as follows:

$$f_n(x) = \sum_{i=0}^{n} b_i F_i(x) \qquad (10\text{-}16)$$

where $F_i(x)$ is the ith-degree polynomials of any one of the above families.

Example 10-1 Expand the polynomial

$$f_3(x) = 20x^3 + 32x^2 - 18x + 1$$

in terms of the Jacobi polynomials $P_0^{(0,0)}(x)$, $P_1^{(0,0)}(x)$, $P_2^{(0,0)}(x)$, $P_3^{(0,0)}(x)$.

SOLUTION The first three Jacobi functions are listed below Eq. (10-14). Substitution of the Jacobi polynomials into Eq. (10-16) gives

$$\begin{aligned} f_3(x) &= b_0(1) + b_1(2x-1) + b_2(1-6x+6x^2) \\ &\quad + b_3(1-12x+30x^2-20x^3) \\ &= (b_0 - b_1 + b_2 + b_3) + x(2b_1 - 6b_2 - 12b_3) \\ &\quad + x^2(6b_2 + 30b_3) + x^3(-20b_3) \end{aligned}$$

Comparison of coefficients of these two polynomials gives:

Coefficients of x^3:

$$-20b_3 = 20 \qquad b_3 = -1$$

Coefficients of x^2:

$$6b_2 + 30b_3 = 32 \qquad b_2 = \frac{31}{3}$$

Coefficients of x:

$$2b_1 - 6b_2 - 12b_3 = -18 \qquad b_1 = 16$$

and

$$b_0 - b_1 + b_2 + b_3 = 1 \qquad b_0 = \frac{23}{3}$$

Thus the series expansion in terms of the Jacobi polynomials is

$$f_3(x) = \frac{23}{3} P_0^{(0,0)}(x) + 16P_1^{(0,0)}(x) + \frac{31}{3} P_2^{(0,0)}(x) - P_3^{(0,0)}(x)$$

Gaussian Quadrature

The numerical approximation of a definite integral may be represented by the following expression which is commonly known as a quadrature

$$\int_a^b f(x)\,dx \cong \sum_{i=0}^{n} w_i f(x_i) \tag{10-17}$$

where the w_i's are the $n+1$ positive weights given to the $n+1$ functional values $f(x_i)$. If x_i and w_i are not fixed, it follows that there are $2n+2$ parameters which could be used to define a polynomial of degree $2n+1$. (Note: the number of parameters required to define a polynomial is equal to one plus the degree of the polynomial, for example, $f(x) = mx + b$ is of degree one and is defined by fixing m and b.) It is shown below that if $f(x)$ is a polynomial of degree $2n+1$, then the relation given by Eq. (10-17) becomes exact when the $n+1$ points $\{x_i\}$ at which the function $f(x)$ and the weights are to be evaluated (hereafter called the collocation points) are taken to be the roots of an associated orthogonal polynomial of degree $n+1$. It should also be noted that all the roots of any polynomial of a set of orthogonal polynomials are single and real.

A more general form of Eq. (10-17) includes the weighting function $W(x)$

$$\int_a^b W(x)f(x)\,dx \cong \sum_{i=0}^{n} w_i f(x_i) \tag{10-18}$$

For each choice of the weighting function $W(x)$, a different set of weights $\{w_i\}$ in the quadrature is obtained. When the weighting function $W(x)$ takes on the values appearing in the above defining equations, the corresponding expressions obtained for computing the weights $\{w_i\}$ of the quadrature are called the Gauss–Legendre, Gauss–Laguerre, Gauss–Chebyshev, Gauss–Hermite, and Gauss–Jacobi quadratures.

Since all of these quadratures may be developed in the same general manner, only the development for the Gauss–Jacobi quadrature is given. The development presented follows closely the one presented by Carnahan et al.(2) for the Gauss–Legendre quadrature.

In the development of this procedure, one may begin with the lagrangian form of the interpolating polynomial for the function $f(x)$, namely,

$$f(x) = \phi_n(x) + \mathscr{R}_n(x) \tag{10-19}$$

where $\phi_n(x)$ is an interpolating polynomial of degree n and $\mathscr{R}_n(x)$ is the remainder. These functions are defined as follows:

$$\phi_n(x) = \sum_{i=0}^{n} l_i(x) f(x_i) \tag{10-20}$$

$$l_i(x) = \prod_{\substack{j=0 \\ j \neq i}}^{n} \frac{(x - x_j)}{(x_i - x_j)} \tag{10-21}$$

$$\mathscr{R}_n(x) = \left[\prod_{i=0}^{n} (x - x_i)\right] \frac{f^{(n+1)}(\xi)}{(n+1)!} \qquad (a < \xi < b) \tag{10-22}$$

where $\{x_j\}$ (or $\{x_i\}$) is an arbitrarily selected set of base points, which are also sometimes called nodes. For convenience, let

$$p_{n+1}(x) = \prod_{j=0}^{n} (x - x_j) \tag{10-23}$$

and

$$q_n(x) = \frac{f^{(n+1)}(\xi)}{(n+1)!} \tag{10-24}$$

Then the remainder may be restated as follows:

$$\mathscr{R}_n(x) = p_{n+1}(x) q_n(x) \tag{10-25}$$

Developments of the lagrangian polynomials $p_{n+1}(x)$ are given in standard texts on numerical methods. (See, for example, Refs. 2, 4, 10.)

Gauss–Jacobi Quadrature

The development of the Gauss–Jacobi quadrature is initiated by multiplying each member of Eq. (10-19) by the weighting function $W(x)$ and integrating over the closed interval $[a, b]$ to give

$$\int_a^b W(x)f(x)\,dx = \int_a^b W(x)\phi_n(x)\,dx + \int_a^b W(x)\mathscr{R}_n(x)\,dx \tag{10-26}$$

The objective of the following development is to find the formula for w_i and the set of $\{x_i\}$ which gives the following equality:

$$\int_a^b W(x)f(x)\,dx = \sum_{i=0}^{n} w_i f(x_i) \tag{10-27}$$

when $f(x)$ is a polynomial of degree $2n+1$ and

$$W(x) = (1 - x)^{\alpha} x^{\beta} \qquad (\alpha > -1, \beta > -1) \tag{10-28}$$

In the following development, the values of a and b are taken to be $a = 0$, and $b = 1$. Then after having observed that the x_i's, and therefore the $f(x_i)$'s, are

fixed values, Eq. (10-26) may be restated as follows:

$$\int_0^1 W(x)f(x)\,dx = \sum_{i=0}^{n}\left[f(x_i)\int_0^1 W(x)l_i(x)\,dx\right] + \int_0^1 W(x)p_{n+1}(x)q_n(x)\,dx \tag{10-29}$$

Thus

$$\int_0^1 W(x)f(x)\,dx = \sum_{i=0}^{n} w_i f(x_i) + \int_0^1 W(x)p_{n+1}(x)q_n(x)\,dx \tag{10-30}$$

where w_i is defined by

$$w_i = \int_0^1 W(x)l_i(x)\,dx \tag{10-31}$$

The object of the following development is to show that if $f(x)$ is a polynomial of degree $2n + 1$, then the remainder term

$$\int_0^1 W(x)p_{n+1}(x)q_n(x)\,dx = 0 \tag{10-32}$$

when the set of $n + 1$ base points, the $\{x_i\}$, are the roots of the Jacobi polynomial of degree $n + 1$.

Since $f(x)$ has been assumed to be a polynomial of degree $2n + 1$, it follows that $q_n(x)$ must be a polynomial of degree n, since $p_{n+1}(x)$ is of degree $n + 1$ (see Eq. (10-23)) and $l_i(x)$ is of degree n (see Eq. (10-21)). Expansion of the polynomial $q_n(x)$ in terms of a set of Jacobi polynomials (see Eq. (10-16) and Example 10-1) yields

$$q_n(x) = b_0 P_0(x) + b_1 P_1(x) + \cdots + b_n P_n(x) \tag{10-33}$$

where the superscripts (α, β) have been omitted in the interest of simplicity. Then the remainder term becomes

$$\int_0^1 W(x)p_{n+1}(x)q_n(x)\,dx$$

$$= \int_0^1 (1-x)^\alpha x^\beta [b_0 p_{n+1}(x)P_0(x) + b_1 p_{n+1}(x)P_1(x) + \cdots + b_n p_{n+1}(x)P_n(x)]\,dx \tag{10-34}$$

Examination of Eq. (10-34) shows that if $p_{n+1}(x)$ is equal to a constant times $P_{n+1}(x)$ (the Jacobi polynomial of degree $n + 1$), then the right-hand side of Eq. (10-34) is identically equal to zero by the orthogonality property. Now it will be shown that $p_{n+1}(x)$ can be made equal to a constant times the jacobian polynomial $P_{n+1}(x)$. Let the Jacobi polynomial $P_{n+1}(x)$ be stated in the product form:

$$P_{n+1}(x) = a_{n+1}\prod_{i=0}^{n}(x - x_i) \tag{10-35}$$

where a_{n+1} is the coefficient of x^{n+1} and the $\{x_i\}$ are the roots of $P_{n+1}(x)$. Comparison of Eqs. (10-23) and (10-35) shows that if the base points appearing in the expression for $p_{n+1}(x)$ are taken to be the roots of the Jacobi polynomial $P_{n+1}(x)$, then

$$p_{n+1}(x) = \frac{1}{a_{n+1}} P_{n+1}(x) \tag{10-36}$$

and consequently when $p_{n+1}(x)$ is replaced in Eq. (10-34) by its equivalent as given by Eq. (10-36), the remainder will be equal to zero.

Thus, when the $\{x_i\}$ are the roots of $P_{n+1}(x)$ and $f(x)$ is of degree $2n + 1$ or less, then Eq. (10-30) reduces to exact relationship

$$\int_0^1 W(x)f(x)\,dx = \sum_{i=0}^{n} w_i f(x_i) \tag{10-37}$$

where the w_i's are computed by use of Eq. (10-31). It should be noted that the converse of this statement is also true, that is, if Eq. (10-37) holds for all polynomials $f(x)$ of degree $2n + 1$, then the set $\{x_i\}$ of $n + 1$ collocation points are the zeros of the orthogonal polynomial P_{n+1}. Furthermore, the weights are all positive.

If the degree of $f(x)$ is greater than $2n + 1$, and only $n + 1$ collocation points are used, then the Gauss–Jacobi quadrature given by Eq. (10-37) is no longer exact. However, the quadrature becomes exact for all continuous functions in the closed interval [0, 1] as the number of collocation points is increased indefinitely, that is,

$$\lim_{n\to\infty}\sum_{i=1}^{n} w_i f(x_i) = \int_0^1 W(x)f(x)\,dx$$

Example 10-2 Evaluate the following function by use of a two-point Gauss–Jacobi quadrature:

$$\int_0^1 (1-x)x^3\,dx$$

SOLUTION Let $f(x) = x^3$. Since $W(x) = (1-x)^\alpha x^\beta$, take $\alpha = 1$, $\beta = 0$ to give $W(x) = 1 - x$. Thus, $W(x)f(x) = (1-x)x^3$. The Rodriques' formula (Eq. (10-14)) for $\alpha = 1$, $\beta = 0$, and $n = 2$ gives

$$(1-x)P_2^{(1,0)}(x) = \frac{(-1)^2\Gamma(1)}{\Gamma(2+1)}\frac{d^2[(1-x)^3x^2]}{dx^2}$$

which yields the result

$$P_2^{(1,0)}(x) = 1 - 8x + 10x^2$$

and the roots are

$$x = \frac{4 \pm \sqrt{6}}{10} \qquad x_0 = 0.644\,948\,97 \qquad x_1 = 0.155\,051\,03$$

To compute the weights, use is made of Eq. (10-31)

$$w_0 = \int_0^1 W(x) l_0(x)\, dx = \int_0^1 \frac{(1-x)(x-x_1)}{(x_0-x_1)}\, dx = \frac{1}{(x_0-x_1)}\left(\frac{1}{6} - \frac{x_1}{2}\right)$$

$$w_0 = 0.181\,958\,61$$

$$w_1 = \int_0^1 W(x) l_1(x)\, dx = \int_0^1 \frac{(1-x)(x-x_0)}{(x_1-x_0)}\, dx$$

$$= \frac{1}{(x_1-x_0)}\left(\frac{1}{6} - \frac{x_0}{2}\right)$$

$$w_1 = 0.318\,041\,22$$

$$f(x_0) = x_0^3 = 0.268\,270\,7$$

$$f(x_1) = x_1^3 = 0.003\,727\,55$$

Then

$$\int_0^1 (1-x)x^3\, dx = \sum_{i=0}^{1} w_i f(x_i) = (0.181\,958\,6)(0.268\,270\,7) + (0.318\,041\,22)(0.003\,727\,55) = 0.05$$

This two-point Gauss–Jacobi quadrature is exact because $f(x)$ is a polynomial of $2n + 1 = 3$ and $n + 1 = 2$ points are used in the quadrature. Note that

$$\int_0^1 (1-x)x^3\, dx = \left(\frac{x^4}{4} - \frac{x^5}{5}\right)\Bigg|_0^1 = \frac{1}{20} = 0.05$$

Instead of finding the roots of the polynomials and the values of the weights $\{w_i\}$ as shown in this example, the values may be taken directly from tables (Ref. 11).

Method of Weighted Residuals and Orthogonal Collocation

There follows first a qualitative presentation of the general concepts of the Method of Weighted Residuals and Orthogonal Collocation. These concepts are then quantified by a more precise treatment.

In the Method of Weighted Residuals, the function $f(x)$ in Eq. (10-37), becomes the residual $R(\mathbf{a}, x)$. The residual is that which remains after an assumed trial solution has been substituted into the differential equation. The parameters $\mathbf{a}$ appear in the trial solution. An exact solution would require that the parameters or coefficients $\mathbf{a}$ be picked such that the remainder is zero at

every x over the interval of integration and such that the boundary conditions are satisfied. In an effort either to satisfy these conditions or to come as close as possible to satisfying them, the following approach is taken. First, the trial solution is selected at the outset such that it satisfies the boundary conditions. Secondly the parameters $\mathbf{a}$ are picked such that the integral of the weighted residual over the interval of integration is equal to zero, that is,

$$\int_0^1 W(x)R(\mathbf{a}, x)\, dx \cong \sum_{i=0}^{n} w_i R(\mathbf{a}, x_i) = 0 \tag{10-38}$$

and this condition is satisfied by picking the parameters $\mathbf{a}$ such that each $R(\mathbf{a}, x_i) = 0$, that is,

$$\begin{aligned} R(\mathbf{a}, x_0) &= 0 \\ R(\mathbf{a}, x_1) &= 0 \\ &\vdots \\ R(\mathbf{a}, x_n) &= 0 \end{aligned} \tag{10-39}$$

Thus, by choosing the $n + 1$ parameters $\mathbf{a}$ such that both Eqs. (10-38) and (10-39) are satisfied, one achieves the following results: (1) the residual is equal to zero at least $n + 1$ times in the interval of integration along the x axis, and (2) the integral of the weighted residuals $W(x)R(\mathbf{a}, x)$ is approximately equal to zero over the interval of integration. Although both of these conditions taken together do not necessarily achieve the condition of the exact solution (that the residual is zero at each x over the interval of integration), they do "come close" to doing so. The purpose of the weight function $W(x)$ is to suppress the values taken on by the absolute value of the function $R(\mathbf{a}, x)$ for values of x between its zeros. Finlayson(6) states that the weighting function $W(x) = 1 - x$ gives faster convergence for lower-order approximations (smaller values of n) and $W(x) = 1$ gives faster convergence for many chemical engineering problems.

Use of the collocation points as the roots of orthogonal polynomials was first advanced by Lanczos(12) and was developed further by Clenshaw and Norton(3), Norton(13), and Wright(21) for the solution of ordinary differential equations. In these applications, which consisted primarily of initial-value problems, Chebyshev polynomials were employed. Horvay and Spiess(9) used polynomials which were orthogonal on the boundary. Villadsen and Stewart(18) developed an orthogonal collocation method for boundary-value problems.

Application of the Method of Orthogonal Collocation to Linear Differential Equations

The procedure represented by Eq. (10-39) is called *optimal collocation* by Villadsen and Michelsen(19) and *orthogonal collocation* by Finlayson(6). When the relationship given by Eq. (10-38) is exact and the $\{a_i\}$ are selected by Eq. (10-39), it follows that the integral of Eq. (10-38) is identically equal to zero, or

the $\{a_i\}$ is picked such that the residual is orthogonal to the weighting function—thus the name "orthogonal collocation."

To illustrate the application of orthogonal collocation, consider the following linear differential equation with variable coefficients:

$$u\frac{d^2y}{du^2} + \frac{dy}{du} - py = 0 \tag{10-40}$$

with the boundary conditions that $y = 1$ at $u = 1$ and all derivatives are finite and p is constant. This example, which was used by Villadsen and Michelsen(19), represents a model for diffusion accompanied by a first-order irreversible, isothermal reaction in the radial direction of a cylindrical catalyst pellet. The above equation is obtained from the following equation

$$\frac{d^2y}{dx^2} + \frac{1}{x}\frac{dy}{dx} - 4py = 0 \tag{10-41}$$

with the boundary conditions: $y = 1$ at $x = 1$, $dy/dx = 0$ at $x = 0$ by making the change of variable $u = x^2$.

The first step in the solution of this equation is to select a power series which satisfies the boundary condition. The following nth-degree polynomial is seen to satisfy the boundary condition

$$y_n(u) = 1 + (1 - u)\sum_{j=1}^{n} a_j u^{j-1} \tag{10-42}$$

The rest of the procedure is best illustrated by use of the following example.

Example 10-3 Find the solution of Eq. (10-40) by use of two collocation points for the case where $p = 9/4$. Take the trial solution to be the expression given by Eq. (10-42) for $n = 2$, namely,

$$y(u) = 1 + (1 - u)(a_1 + a_2 u) \tag{10-43}$$

SOLUTION The expression for the residual is found by first differentiating $y(u)$ with respect to u

$$\frac{dy}{du} = -a_1 + a_2(1 - 2u)$$

and thus

$$\frac{d^2y}{du^2} = -2a_2$$

Substitution of these expressions into Eq. (10-40) followed by the collection of terms yields

$$R(\mathbf{a}, u) = \tfrac{1}{4}[a_1(9u - 13) + a_2(9u^2 - 25u + 4) - 9]$$

Thus, for the weight function $W(u) = 1 - u$ (note: $\alpha = 1$, $\beta = 0$ in Eq. (10-13)), one obtains

$$\int_0^1 (1 - u)R(\mathbf{a}, u)\, du = \sum_{i=0}^{1} w_i R(\mathbf{a}, u_i)$$

where u_i $(i = 0, 1)$ are the roots of the Jacobi orthogonal polynomial $P_2^{(1,0)}(u)$, the polynomial produced in Example 10-2. Also observe that the integral in this case is exactly equal to the sum from $i = 0$ to $i = 1$ of $w_i R(\mathbf{a}, u_i)$. Now let the $\{u_i\}$ be selected such that $R(\mathbf{a}, u)$ is orthogonal to $(1 - u)$ or such that each $R(\mathbf{a}, u_i)$ is equal to zero. Since $u_0 = 0.644\,948\,97$ and $u_1 = 0.155\,051\,03$, the values a_1, and a_2 are to be found such that

$$R(\mathbf{a}, u_0) = 0 = (-7.195\,46)a_1 + (-8.380\,092)a_2 - 9$$
$$R(\mathbf{a}, u_1) = 0 = (-11.604\,541)a_1 + (0.340\,091\,6)a_2 - 9$$

Solution of these simultaneous equations for a_1 and a_2 yields

$$a_1 = -0.787\,223\,56$$
$$a_2 = -0.398\,034\,34$$

Thus

$$y(u) = 1 + (1 - u)(-0.787\,223\,56 - 0.398\,034\,34u)$$

The exact solution of Example 10-3 as given by Villadsen and Michelsen(19) is

$$y(u) = \frac{I_0(2\sqrt{pu})}{I_0(2\sqrt{p})} = \frac{1 + pu + \frac{1}{4}(pu)^2 + \frac{1}{36}(pu)^3 + \frac{1}{576}(pu)^4 + \cdots}{1 + p + \frac{1}{4}p^2 + \frac{1}{36}p^3 + \frac{1}{576}p^4 + \cdots} \tag{10-44}$$

$$I_0(z) = \sum_{i=0}^{\infty} \frac{\left(\frac{1}{4}z^2\right)^i}{(i!)^2} \qquad \text{(modified Bessel function of order zero)}$$

To make one comparison of the results given by the approximate solution for $y(u)$ found in Example 10-3 with the exact solution given by Eq. (10-44), let $p = 9/4 = 2.25$ and $u = 0.4$. The solution found in Example 10-3 by use of a two-point orthogonal collocation gives

$$y(0.4) = 0.432$$

and Eq. (10-44) gives

$$y(0.4) = 0.433$$

Application of the Method of Orthogonal Collocation to Nonlinear Differential Equations

First the method of orthogonal collocation will be applied to a nonlinear differentiation equation by use of the same procedure demonstrated above for linear differential equations. Then in order to avoid the difficulties encountered, a procedure attributed by Finlayson(6) to Vichnevetsky(17) is used.

For the case of a nonlinear differential equation, difficulties may be encountered in picking an appropriate set $\{a_i\}$ which satisfy Eq. (10-40) and which give realistic values for y over the interval [0, 1]. For example, consider the case where y in the last term of Eq. (10-41) is replaced by y^2 to give

$$u\frac{d^2y}{du^2} + \frac{dy}{du} - py^2 = 0 \tag{10-45}$$

where $y \geq 0$ for all u. Furthermore, suppose that it is desired to approximate the solution of Eq. (10-45) by use of one quadrature point and that for a trial function the linear function given by setting $n = 1$ in Eq. (10-42) is to be used, namely,

$$y(u) = 1 + (1 - u)a_1 \tag{10-46}$$

with the weighting function $W(u) = 1 - u$ (where $\alpha = 1$, $\beta = 0$). The corresponding Jacobi polynomial is $P_1^{(1,0)}(u) = 3u - 1$. The root of $P_1^{(1,0)}(u)$ is $u_0 = 1/3$. Thus, a_1 is to be selected such that

$$\int_0^1 (1 - u)R_0(a_1, u)\,du = w_0\,R_0(a_1, u_0) = 0 \tag{10-47}$$

or such that $R_0(a_1, u_0) = 0$, that is,

$$R_0(a_1, u_0) = -a_1 - p[1 + (1 - u_0)a_1]^2 = 0$$

For the constant $p = 9/4$, the two values of a_1 which satisfy this equation are

$$a_1\begin{Bmatrix} -0.6771 \\ -3.32 \end{Bmatrix} \tag{10-48}$$

Since $y(u) \geq 0$ for all u, the root (-3.32) must be discarded since it gives negative values of y over a portion of the interval.

Obviously, as the order of the trial solution is increased, it becomes more difficult to pick a suitable set of a_i's which give realistic values for $y(u)$ throughout the interval of integration.

If it is known that over the interval [0, 1] of interest for the independent variable u, the dependent variable y is always positive, then it becomes advantageous to restate the residual in terms of the $\{y(u_k)\}$ where the $\{u_k\}$ are the roots of the corresponding Jacobi polynomial. The following procedure has been recommended by Finlayson(6) and by Villadsen and Michelsen(19).

Suppose that the trial solution of Eq. (10-45) is assumed to be the nth-degree polynomial given by Eq. (10-42). Let

$$Y(u) = y(u) - 1 \tag{10-49}$$

Then for each root u_i $(i = 1, 2, \ldots, n)$ of the associated Jacobi polynomial, the corresponding value of $Y(u_i)$ is given by

$$Y(u_i) = \sum_{j=1}^{n} a_j(u_i^{j-1} - u_i^j) \qquad (i = 1, 2, \ldots, n) \tag{10-50}$$

and then

$$\left.\frac{dy(u)}{du}\right|_{u_i} = \left.\frac{dY(u)}{du}\right|_{u_i} = \sum_{j=1}^{n} a_j[(j-1)u_i^{j-2} - ju_i^{j-1}] \qquad (j = 1, 2, \ldots, n) \tag{10-51}$$

and

$$\left.\frac{d^2y(u)}{du^2}\right|_{u_i} = \left.\frac{d^2Y(u)}{du^2}\right|_{u_i} = \sum_{j=1}^{n} a_j[(j-1)(j-2)u_i^{j-3} - j(j-1)u_i^{j-2}]$$

$$(j = 1, 2, \ldots, n) \tag{10-52}$$

The set of equations represented by Eq. (10-50) may be stated in matrix form

$$\mathbf{Y} = \mathbf{Qa} \tag{10-53}$$

where

$$\mathbf{Y} = [Y(u_1) \quad Y(u_2) \quad \cdots \quad Y(u_n)]^T$$

$$\mathbf{a} = [a_1 \quad a_2 \quad \cdots \quad a_n]^T$$

$$\mathbf{Q} = \begin{bmatrix} Q_{11} & Q_{12} & \cdots & Q_{1n} \\ \vdots & & & \\ Q_{n1} & Q_{n2} & \cdots & Q_{nn} \end{bmatrix} \qquad Q_{ij} = u_i^{j-1} - u_i^j$$

Similarly, for the sets of equations given by Eqs. (10-51) and (10-52)

$$\frac{d\mathbf{y}}{du} = \mathbf{Ca} \tag{10-54}$$

$$\frac{d^2\mathbf{y}}{du^2} = \mathbf{Da} \tag{10-55}$$

where $\mathbf{C}$ and $\mathbf{D}$ have the same general form shown for $\mathbf{Q}$, and

$$C_{ij} = (j-1)u_i^{j-2} - ju_i^{j-1}$$

$$D_{ij} = (j-1)(j-2)u_i^{j-3} - j(j-1)u_i^{j-2} \tag{10-56}$$

After Eq. (10-53) has been solved for $\mathbf{a}$,

$$\mathbf{a} = \mathbf{Q}^{-1}\mathbf{Y} \tag{10-57}$$

this result may be used to eliminate $\mathbf{a}$ from Eqs. (10-54) and (10-55)

$$\frac{d\mathbf{y}}{du} = \mathbf{CQ}^{-1}\mathbf{Y} = \mathbf{AY} \tag{10-58}$$

and

$$\frac{d^2\mathbf{y}}{du^2} = \mathbf{D}\mathbf{Q}^{-1}\mathbf{Y} = \mathbf{B}\mathbf{Y} \tag{10-59}$$

where the elements of **A** and **B** are numbered in the same manner shown for **Q**.

In order to evaluate the residual at each root u_i, expressions are needed for

$$\left.\frac{dy(u)}{du}\right|_{u_i} \quad \text{and} \quad \left.\frac{d^2y(u)}{du^2}\right|_{u_i}$$

These expressions may be obtained by application of the multiplication rule to row i of Eqs. (10-58) and (10-59) to obtain

$$\left.\frac{dy(u)}{du}\right|_{u_i} = A_{i1}\,Y(u_1) + A_{i2}\,Y(u_2) + \cdots + A_{in}\,Y(u_n)$$

$$= \sum_{j=1}^{n} A_{ji}\,Y(u_j) \tag{10-60}$$

Similarly

$$\left.\frac{d^2y(u)}{du^2}\right|_{u_i} = \sum_{j=1}^{n} B_{ij}\,Y(u_j) \tag{10-61}$$

Substitution of these expressions into Eq. (10-45) yields the following expression for the residual

$$R_i(u_i, \mathbf{Y}) = u_i \sum_{j=1}^{n} B_{ij}\,Y(u_j) + \sum_{j=1}^{n} A_{ij}\,Y(u_j) - py^2(u_i) \qquad (i = 1, 2, \ldots, n) \tag{10-62}$$

which is readily rearranged to give

$$R_i(u_i, \mathbf{y}) = \sum_{j=1}^{n} (u_i B_{ij} + A_{ij})y(u_j) - \sum_{j=1}^{n} (u_i B_{ij} + A_{ij}) - py^2(u_i)$$

$$(i = 1, 2, \ldots, n) \tag{10-63}$$

The sets of constants $\{A_{ij}\}$ and $\{B_{ij}\}$ may be calculated by use of the definitions given by Eqs. (10-58) and (10-59), respectively. The unknowns in Eq. (10-63) are: $y(u_1)$, $y(u_2)$, ..., $y(u_n)$. The desired set of y's is that set of positive numbers which makes

$$\begin{aligned} R_1(u_1, \mathbf{y}) &= 0 \\ R_2(u_2, \mathbf{y}) &= 0 \\ &\vdots \quad \vdots \\ R_n(u_n, \mathbf{y}) &= 0 \end{aligned} \tag{10-64}$$

where

$$\mathbf{y} = [y(u_1)y(u_2) \cdots y(u_n)]^T$$

The desired set **y** may be found by use of the Newton–Raphson method.

To demonstrate the application of the procedure described above, it is used to solve a linear differential equation instead of a nonlinear equation. A linear differential equation is used in order to reduce the effort required to solve the set of equations represented by Eq. (10-63). For example, if the procedure is used to solve Eq. (10-40), the final result is given by Eq. (10-63) with $y^2(u_i)$ replaced by $y(u_i)$.

Example 10-4 Use the above procedure to solve the linear differential equation given by Eq. (10-40). Take $n = 2$ and $p = 9/4$.

(*a*) Find $y(u_1)$ and $y(u_2)$.

(*b*) Use the values of $y(u_1)$ and $y(u_2)$ found in (*a*) to compute a_1 and a_2.

SOLUTION (*a*) From the definition of **Q** (see Eq. (10-50)), it follows that

$$\mathbf{Q} = \begin{bmatrix} (1 - u_1) & (u_1 - u_1^2) \\ (1 - u_2) & (u_2 - u_2^2) \end{bmatrix}$$

Since $u_1 = 0.644\,948\,97$ and $u_2 = 0.155\,051\,03$ (see Example 10-2), it follows that

$$\mathbf{Q} = \begin{bmatrix} 0.355\,051\,1 & 0.228\,989\,8 \\ 0.844\,949\,0 & 0.131\,010\,2 \end{bmatrix}$$

and its inverse is readily found to be

$$\mathbf{Q}^{-1} = \begin{bmatrix} -0.891\,411\,5 & 1.558\,078\,3 \\ 5.749\,149\,7 & -2.415\,816\,9 \end{bmatrix}$$

Since

$$\mathbf{C} = \begin{bmatrix} -1 & (1 - 2u_1) \\ -1 & (1 - 2u_2) \end{bmatrix} \qquad \mathbf{D} = \begin{bmatrix} 0 & -2 \\ 0 & -2 \end{bmatrix}$$

Then

$$\mathbf{A} = \mathbf{C}\mathbf{Q}^{-1} = \begin{bmatrix} -0.775\,254\,9 & -0.857\,738\,1 \\ 4.857\,738\,3 & -3.224\,745 \end{bmatrix} = \begin{bmatrix} A_{11} & A_{12} \\ A_{21} & A_{22} \end{bmatrix}$$

and

$$\mathbf{B} = \mathbf{D}\mathbf{Q}^{-1} = \begin{bmatrix} -11.498\,298 & 4.831\,633\,8 \\ -11.498\,298 & 4.831\,633\,8 \end{bmatrix} = \begin{bmatrix} B_{11} & B_{12} \\ B_{21} & B_{22} \end{bmatrix}$$

For $n = 2$, Eq. (10-63) becomes

$$R_1(u_1, \mathbf{y}) = (u_1 B_{11} + A_{11})y(u_1) + (u_1 B_{12} + A_{12})y(u_2)$$

$$- [(u_1 B_{11} + A_{11}) + (u_1 B_{12} + A_{12})] - \tfrac{9}{4}y(u_1) = 0$$

$$R_2(u_2, \mathbf{y}) = (u_2 B_{21} + A_{21})y(u_1) + (u_2 B_{22} + A_{22})y(u_2)$$

$$- [(u_2 B_{21} + A_{21}) + (u_2 B_{22} + A_{22})] - \tfrac{9}{4}y(u_2) = 0$$

After the values given above for the A's, B's, and u's have been substituted into the expressions for $R_1(u_1, \mathbf{y})$ and $R_2(u_2, \mathbf{y})$, these linear equations may be solved for $y(u_1)$ and $y(u_2)$ to give

$$y(u_1) = 0.629\,349\,5$$

$$y(u_2) = 0.282\,689\,5$$

Thus, in summary when the differential equations are nonlinear, the set of positive y's which make the R's equal to zero may be found by use of the Newton–Raphson method. The usefulness of this formulation obviously depends upon one's knowing in advance from physical considerations that the y's are positive throughout the interval of integration.

(*b*) The coefficients a_1 and a_2 may be found by use of the above results and Eq. (10-57) as follows:

$$\mathbf{a} = \mathbf{A}^{-1}\mathbf{Y} = \begin{bmatrix} -0.891\,411\,5 & 1.558\,078\,3 \\ 5.749\,149\,7 & -2.415\,816\,9 \end{bmatrix} \begin{bmatrix} -0.370\,650\,5 \\ -0.717\,310\,5 \end{bmatrix}$$

where $Y(u_1) = y(u_1) - 1$ and $Y(u_2) = y(u_2) - 1$. After the implied matrix multiplication has been performed one obtains

$$\begin{bmatrix} a_1 \\ a_2 \end{bmatrix} = \begin{bmatrix} -0.787\,223\,8 \\ -0.398\,034\,4 \end{bmatrix}$$

As should be expected, these values of a_1 and a_2 are in agreement with those found in Example 10-3.

Other Applications of Orthogonal Collocation

The application of the method of orthogonal collocation to other types of problems is discussed in Chap. 12 as it is applied to some specific problems.

Some areas of interest and possible development which do not appear to have been discussed to any appreciable extent by proponents of the method are the choice of weighting functions and the choice of orthogonal polynomials whose roots are used as the collocation points. Jacobi polynomials appear to have been used almost exclusively.

10-2 SOLUTION OF PARTIAL DIFFERENTIAL EQUATIONS BY FINITE DIFFERENCE METHODS

The application of the methods of finite differences is initiated from first principles by the solution of a simple parabolic differential equation by use of an explicit method. Next implicit methods are introduced with particular emphasis being given to the implicit method of Crank–Nicolson(5). The Crank–Nicolson

method is not only more accurate than the explicit methods, but is stable for all ratios of $\Delta t/\Delta x^2$, whereas $\Delta t/\Delta x^2$ must be less than the upper bound deduced below for the explicit method to be stable.

Finite Difference Approximations of Partial Derivatives

Let $u(x, t)$ be a continuous function of time and distance with continuous partial derivatives over time and distance. The x-t space is divided into equally spaced grid points as shown in Fig. 10-1. The quantities Δx and Δt are defined such that they are always positive, that is,

$$\Delta x = x_{j+1} - x_j > 0$$

and

$$\Delta t = t_{n+1} - t_n > 0$$

The grid notation (j, n) represents the point (x_j, t_n), and at this point the value of the function $u(x, t)$ is denoted by $u(j\,\Delta x, n\,\Delta t)$. The value of u at the grid point $(j\,\Delta x, n\,\Delta t)$ is denoted by $u_{j,n}$.

The first few terms of a Taylor series expansion of the function $u(x, t)$ about the point (x_j, t_n) and in the forward direction to the point (x_{j+1}, t_n) is given by

$$u_{j+1,n} \cong u_{j,n} + \Delta x u_x + \frac{(\Delta x)^2}{2!} u_{xx} + \frac{(\Delta x)^3}{3!} u_{xxx} + \frac{(\Delta x)^4}{4!} u_{xxxx} \qquad (10\text{-}65)$$

where the derivatives

$$u_x, u_{xx}, \ldots, u_{xxxx} = \frac{\partial u}{\partial x}, \frac{\partial^2 u}{\partial x^2}, \ldots, \frac{\partial^4 u}{\partial x^4}$$

are to be evaluated at the point (x_j, t_n). Similarly, the first five terms of the Taylor series expansion of the function $u(x, t)$ about the point (x_j, t_n) to the

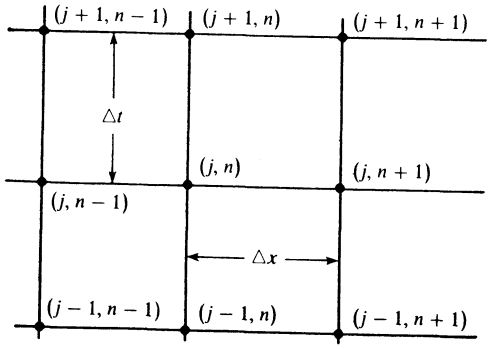

Figure 10-1 Notation used to identify grid points

point (x_j, t_{n+1}) is given by

$$u_{j,n+1} \cong u_{j,n} + \Delta t u_t + \frac{(\Delta t)^2}{2!} u_{tt} + \frac{(\Delta t)^3}{3!} u_{ttt} + \frac{(\Delta t)^4}{4!} u_{tttt} \tag{10-66}$$

where

$$u_t, u_{tt}, \ldots, u_{tttt} = \frac{\partial u}{\partial t}, \frac{\partial^2 u}{\partial t^2}, \ldots, \frac{\partial^4 u}{\partial t^4}$$

When $u(x, t)$ is expanded in the backward direction with respect to x from (x_j, t_n) to (x_{j-1}, t_n) one obtains

$$u_{j-1,n} \cong u_{j,n} - \Delta x u_x + \frac{(\Delta x)^2}{2!} u_{xx} - \frac{(\Delta x)^3}{3!} u_{xxx} + \frac{(\Delta x)^4}{4!} u_{xxxx} \tag{10-67}$$

where

$$\Delta x = x_j - x_{j-1}$$

The *forward difference* formula with respect to x at a fixed t is obtained by solving Eq. (10-65) for u_x and rearranging to obtain

$$\left.\frac{\partial u}{\partial x}\right|_{x_j, t_n} = \frac{u_{j+1,n} - u_{j,n}}{\Delta x} + O(\Delta x) \tag{10-68}$$

The *backward difference* formula with respect to x at a fixed t is obtained by solving Eq. (10-67) for u_x and rearranging to obtain

$$\left.\frac{\partial u}{\partial x}\right|_{x_j, t_n} = \frac{u_{j,n} - u_{j-1,n}}{\Delta x} + O(\Delta x) \tag{10-69}$$

In the definition of the differences, the point of reference is taken to be the point (x_j, t_n) in Fig. 10-1.

A formula for the expression of u_x in terms of the *central difference* is obtained by subtracting each member of Eq. (10-67) from the corresponding members of Eq. (10-65) to give

$$\left.\frac{\partial u}{\partial x}\right|_{x_j, t_n} = \frac{u_{j+1,n} - u_{j-1,n}}{2\,\Delta x} + O[(\Delta x)^2] \tag{10-70}$$

An expression for u_{xx} may be obtained by addition of the corresponding members of Eqs. (10-65) and (10-67) followed by rearrangement to obtain

$$\left.\frac{\partial^2 u}{\partial x^2}\right|_{x_j, t_n} = \frac{u_{j+1,n} - 2u_{j,n} + u_{j-1,n}}{(\Delta x)^2} + O[(\Delta x^2)] \tag{10-71}$$

Equation (10-71) is classified as a second *central difference formula* because the points of evaluation with respect to x are symmetrically located about the point (j, n), and it is commonly denoted by $\delta^2 u_{j,n}$, that is,

$$\delta^2 u_{j,n} = \frac{u_{j+1,n} - 2u_{j,n} + u_{j-1,n}}{(\Delta x)^2} + O[(\Delta x)^2] \tag{10-72}$$

The *first central difference* $\delta u_{j,n}$ corresponds to the first partial derivative of u with respect to x and it is defined by

$$\delta u_{j,n} = \frac{u_{j+(1/2),n} - u_{j-(1/2),n}}{\Delta x} + O[(\Delta x)^2] \tag{10-73}$$

Explicit Finite Difference Methods

The explicit method is applied to the simple parabolic differential equation

$$\frac{\partial u}{\partial t} = \sigma \frac{\partial^2 u}{\partial x^2} \qquad (0 < x < 1 \qquad t > 0) \tag{10-74}$$

When the left-hand side of this equation is approximated by use of Eq. (10-66) and the right-hand side by Eq. (10-71), one obtains

$$\frac{u_{j,n+1} - u_{j,n}}{\Delta t} = \sigma \frac{u_{j-1,n} - 2u_{jn} + u_{j+1,n}}{(\Delta x)^2} \tag{10-75}$$

with a truncation error of order $O[\Delta t + (\Delta x)^2]$. Equation (10-75) may be rearranged to the form

$$u_{j,n+1} = \lambda u_{j-1,n} + (1 - 2\lambda) u_{j,n} + \lambda u_{j+1,n} \tag{10-76}$$

where

$$\lambda = \frac{\sigma\,\Delta t}{(\Delta x)^2}$$

The application of the explicit finite-difference method is illustrated by use of the following numerical example.

Example 10-5 Solve the parabolic differential equation given by Eq. (10-74) subject to the initial condition

$$u(x, 0) = 0 \qquad (0 < x < 1)$$

and the boundary conditions

$$u(0, t) = 300$$

$$u(1, t) = 300$$

Take $\sigma = 1$, $\Delta t = 0.01$, $\Delta x = (0.1)\sqrt{3}$, and use five time steps and five space steps.

SOLUTION

$$\lambda = \frac{1(0.01)}{[(0.1)\sqrt{3}]^2} = \frac{1}{3}$$

For $\lambda = 1/3$, Eq. (10-76) becomes

$$u_{j,n+1} = \frac{u_{j-1,n} + u_{j,n} + u_{j+1,n}}{3}$$

As shown in the table below, $u_{0,0} = 300$, $u_{1,0} = 0$, $u_{2,0} = 0$, $u_{3,0} = 0$, $u_{4,0} = 0$, and $u_{5,0} = 300$. The values of u at the end of the first time step are computed as follows:

$$u_{1,1} = \frac{u_{0,0} + u_{1,0} + u_{2,0}}{3} = \frac{300 + 0 + 0}{3} = 100$$

$$u_{2,1} = \frac{u_{1,0} + u_{2,0} + u_{3,0}}{3} = \frac{0 + 0 + 0}{3} = 0$$

$$u_{3,1} = \frac{u_{2,0} + u_{3,0} + u_{4,0}}{3} = \frac{0 + 0 + 0}{3} = 0$$

$$u_{4,1} = \frac{u_{3,0} + u_{4,0} + u_{5,0}}{3} = \frac{0 + 0 + 300}{3} = 100$$

For the second time step

$$u_{1,2} = \frac{u_{0,1} + u_{1,1} + u_{2,1}}{3} = \frac{300 + 100 + 0}{3} = 133.33$$

$$u_{2,2} = \frac{u_{1,1} + u_{2,1} + u_{3,1}}{3} = \frac{100 + 0 + 0}{3} = 33.3$$

$$u_{3,2} = \frac{u_{2,1} + u_{3,1} + u_{4,1}}{3} = \frac{0 + 0 + 100}{3} = 33.3$$

$$u_{4,2} = \frac{u_{3,1} + u_{4,1} + u_{5,1}}{3} = \frac{0 + 100 + 300}{3} = 133.33$$

Continuation of this calculational procedure gives the results shown in the table below.

Time subscript	Value of variable $u_{j,n}$					
n	$u_{0,n}$	$u_{1,n}$	$u_{2,n}$	$u_{3,n}$	$u_{4,n}$	$u_{5,n}$
0	300	0	0	0	0	300
1	300	100	0	0	100	300
2	300	133.33	33.33	33.33	133.33	300
3	300	155.55	66.66	66.66	155.55	300
4	300	174.07	96.29	96.29	174.07	300
5	300	190.12	122.22	122.22	190.12	300

Although the explicit method is seen to be easy to apply, it becomes unstable unless the values of Δt and Δx are selected such that $0 < \lambda < 1/2$. To demonstrate instability of the method for values of $\lambda > 1/2$, Example 10-6 is presented.

Example 10-6 This example is the same as Example 10-5 except Δt and Δx are selected such that $\lambda = 1$.

SOLUTION For $\lambda = 1$, Eq. (10-16) becomes

$$u_{j,n+1} = u_{j-1,n} - u_{j,n} + u_{j+1,n}$$

When the calculations are carried out in the same manner demonstrated for Example 10-5, the results shown in the following table are obtained.

Time subscript	Value of variable $u_{j,n}$					
n	$u_{0,n}$	$u_{1,n}$	$u_{2,n}$	$u_{3,n}$	$u_{4,n}$	$u_{5,n}$
0	300	0	0	0	0	300
1	300	300	0	0	300	300
2	300	0	300	300	0	300
3	300	600	0	0	600	300
4	300	−300	600	600	−300	300
5	300	1200	−300	−300	1200	300

An examination of these results shows that each variable $u_{j,n}$ oscillates with an amplitude that increases with time, which is characteristic of unstable behavior.

Stability

There follows an analysis which predicts the unstable behavior exhibited by Example 10-6. This analysis makes use of the amplitude factor of the Fourier series solution of the difference equation. This approach is attributed by Richtmyer(14) to J. von Neumann. In this method one assumes a trial solution to the difference equation of the form

$$u_{j,n} = A\beta^n e^{imj\Delta x} \tag{10-77}$$

where $i = \sqrt{-1}$, and A, β, m are constants with m being an integer. Substitution of the trial solution into the difference equation (Eq. (10-75)) gives the following expression upon rearrangement:

$$A\beta^n e^{imj\Delta x}(\beta - 1) = \left[\frac{-2\sigma\,\Delta t}{(\Delta x)^2}\right] A\beta^n e^{imj\Delta x}\left[1 - \frac{(e^{im\Delta x} + e^{-im\Delta x}}{2}\right]$$

or

$$\beta - 1 = (-2\lambda)(1 - \cos m\,\Delta x)$$

Thus, the trial solution satisfies Eq. (10-75), provided that

$$\beta = \beta(m) = 1 - 2\lambda(1 - \cos m\,\Delta x) \tag{10-78}$$

Since the sum of any number of solutions is also a solution, the general solution is the sum of all possible solutions

$$u_{j,n} = \sum_{-\infty}^{\infty} A_m e^{imj\,\Delta x}[\beta(m)]^n \tag{10-79}$$

over all values of m. The constants A_m are selected such that the boundary and initial conditions are satisfied. The development of the formula for the calculation of the coefficients A_m is omitted, however, because the formula is not needed in the stability analysis. The stability analysis makes use of only the expression for the amplitude factor $\beta(m)$.

In order to achieve stability, it is evident from Eqs. (10-78) and (10-79) that the stability condition is

$$|\beta(m)| \leq 1 \tag{10-80}$$

or the most negative value of $\beta(m)$ must not be less than -1. Thus

$$\beta(m) = 1 - 2\lambda(1 - \cos m\,\Delta x) \geq -1$$

The most negative value of $\beta(m)$ is seen to occur at $\cos m\,\Delta x = -1$. Then

$$1 - 4\lambda \geq -1 \qquad \text{or} \qquad -4\lambda \geq -2$$

and

$$2\lambda \leq 1$$

or

$$\frac{2\sigma\,\Delta t}{(\Delta x)^2} \leq 1$$

Thus, in order for the explicit method to remain stable, it is necessary that $\Delta t/(\Delta x)^2$ be selected such that

$$\frac{\Delta t}{(\Delta x)^2} \leq \frac{1}{2\sigma} \tag{10-81}$$

or

$$\lambda \leq 1/2$$

Implicit Methods

The stability condition given by Eq. (10-81) has the unfortunate consequence that if a relatively small Δx is chosen in the interest of accuracy, the allowed Δt may be so small that the computer time required becomes unacceptable.

This difficulty is not encountered when implicit methods are used. If the right-hand side of Eq. (10-74) is approximated at the time t_{n+1}, instead of t_n, then the following implicit form is obtained instead of Eq. (10-75):

$$\frac{u_{j,n+1} - u_{j,n}}{\Delta t} = \sigma\,\frac{u_{j-1,n+1} - 2u_{j,n+1} + u_{j+1,n+1}}{(\Delta x)^2} \tag{10-82}$$

As will be shown, Eq. (10-82) is stable under all conditions. This equation is a special case of the general class of implicit methods which is obtained by using for the right-hand side of the difference equation a weighted average of the right-hand members of Eqs. (10-75) and (10-82) to give

$$\frac{u_{j,n+1} - u_{j,n}}{\Delta t} = \sigma[\theta\delta^2 u_{j,n+1} + (1 - \theta)\delta^2 u_{jn}] \tag{10-83}$$

where the operator δ^2 is defined by Eq. (10-72), and θ is a real constant, generally thought of as lying in the interval $0 \leq \theta \leq 1$. When $\theta = 0$, as in the preceding section, the system is called *explicit*. If $\theta \neq 0$, the system is called implicit. The method is called implicit because $u_{j,n+1}$ appears on both sides of the equation and one must solve the complete set of simultaneous linear difference equations for the system in order to obtain the set of $\{u_{jn}\}$ for each time step.

To illustrate, suppose that $\theta = 1$. Then Eq. (10-83) reduces to

$$\lambda u_{j-1,n+1} - (1 + 2\lambda)u_{j,n+1} + \lambda u_{j+1,n+1} = -u_{j,n} \tag{10-84}$$

The values of the variables at the end of the first time step (when five increments are used as in Example 10-5) are found by solving the following set of equations simultaneously.

$$\begin{aligned}
-(1 + 2\lambda)u_{1,1} + \lambda u_{2,1} &= -u_{1,0} - \lambda u_{0,1} \\
\lambda u_{1,1} - (1 + 2\lambda)u_{2,1} + \lambda u_{3,1} &= -u_{2,0} \\
\lambda u_{2,1} - (1 + 2\lambda)u_{3,1} + \lambda u_{4,1} &= -u_{3,0} \\
\lambda u_{3,1} - (1 + 2\lambda)u_{4,1} &= -u_{4,0} - \lambda u_{5,1}
\end{aligned} \tag{10-85}$$

These equations are represented by tridiagonal matrices. The solutions may be found by use of recurrence formulas presented in Part 1. The results found for the first time step are used in the equations for the second time step. The equations for the second time step are obtained by increasing by one the second subscript in Eq. (10-85).

Stability of the Implicit Methods

This analysis is analogous to that shown for the explicit equations. A trial solution of the form of Eq. (10-77) is again assumed and substituted into Eq. (10-83). The trial solution satisfies Eq. (10-83) provided that the growth

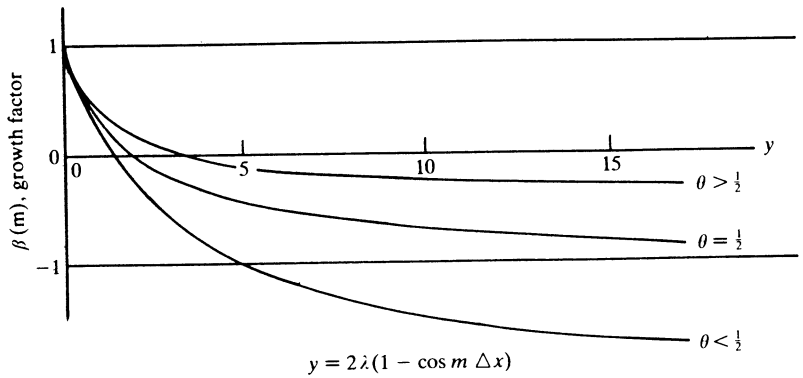

Figure 10-2 Variation of the growth factor $\beta(m)$ with y. (*R. D. Richtmyer: Difference Methods for Initial-Value Problems, Interscience Publishers, Inc., New York (1962), Courtesy Interscience Publishers.*)

factor β is given by

$$\beta = \beta(m) = \frac{1 - 2(1-\theta)\lambda(1 - \cos m\,\Delta x)}{1 + 2\theta\lambda(1 - \cos m\,\Delta x)} \tag{10-86}$$

A graph of $\beta(m)$ versus $y = 2\lambda(1 - \cos m\,\Delta x)$ which was taken from Richtmyer(14) is shown in Fig. 10-2. The growth factor $\beta(m)$ is real for all real m, and never exceeds $+1$. As y increases through positive values, the value of $\beta(m)$ decreases monotonically from 1 to $-(1-\theta)/\theta$. If $1/2 \le \theta \le 1$, the asymptote is not less than -1; hence, the difference equations are always stable. If on the other hand $0 \le \theta < 1/2$, y must be restricted, for stability, by the value at which the curve intersects the line $\beta(m) = -1$. Thus, the stability condition is

$$\begin{aligned} \frac{2\sigma\,\Delta t}{(\Delta x)^2} &\le \frac{1}{1-2\theta} \qquad \text{if } 0 \le \theta \le 1/2 \\ \text{No restriction} &\qquad \text{if } 1/2 \le \theta \le 1 \end{aligned} \tag{10-87}$$

The most common choices of θ are 0, 1/2, 1. The first ($\theta = 0$) gives the explicit method, Eq. (10-75), and the second ($\theta = 1/2$) corresponds to the well-known Crank–Nicholson (Ref. 5) method. The third ($\theta = 1$) gives the implicit method, Eq. (10-82).

10-3 THE METHOD OF CHARACTERISTICS

The method of characteristics was first brought to the attention of chemical engineers by Acrivos(1) after it had already been used successfully in the field of compressible flow (Ref. 15) and heat and mass transfer problems (Ref. 7). The method is applied herein to systems of hyperbolic partial differential equations.

Development of the Method

This method makes it possible to replace a hyperbolic partial differential equation by an equivalent ordinary differential equation which is to be integrated along a specified curve. To illustrate the application as well as the development of the method, relatively simple examples are used. First suppose it is desired to find a numerical solution to the following set of partial differential equations subject to the initial conditions and boundary conditions enumerated below:

$$\frac{\partial\phi}{\partial t} + \frac{\partial\phi}{\partial z} = -k_1(\phi - b\Psi) \tag{10-88}$$

$$\frac{\partial\Psi}{\partial t} = k_2(\phi - b\Psi) \tag{10-89}$$

$$\phi = \phi_0 \quad \text{at} \quad z = 0 \qquad \text{for all } t > 0 \tag{10-90}$$

$$\Psi = 0 \quad \text{at} \quad t = 0 \qquad \text{for all } z \ge 0 \tag{10-91}$$

In order to transform Eq. (10-88) into an equivalent ordinary differential equation, first observe that $\phi(t, z)$ may be expanded by the chain rule as follows:

$$\frac{d\phi}{dz} = \frac{\partial\phi}{\partial z}\frac{dz}{dz} + \frac{\partial\phi}{\partial t}\frac{dt}{dz} \tag{10-92}$$

which gives $d\phi/dz$ for all possible sets $\{z, t\}$. However, observe that if one sets $dt/dz = 1$, then Eq. (10-92) reduces to

$$\left(\frac{d\phi}{dz}\right)_{\text{I}} = \frac{\partial\phi}{\partial t} + \frac{\partial\phi}{\partial z} \qquad \left(\text{at} \quad \frac{dt}{dz} = 1\right) \tag{10-93}$$

which is seen to be identically equal to the left-hand side of Eq. (10-88). Thus, Eq. (10-88) may be reduced to the ordinary differential equation, namely,

$$\left(\frac{d\phi}{dz}\right)_{\text{I}} = -k_1(\phi - b\Psi) \qquad \left(\text{at} \quad \frac{dt}{dz} = 1\right) \tag{10-94}$$

The subscript I denotes the fact that $d\phi/dz$ is to be evaluated along any straight line having slope $dt/dz = 1$. In this method, the requirement that $dt/dz = 1$ for Eq. (10-93) is called characteristic I.

Upon expansion of Ψ by the chain rule, one obtains

$$\frac{d\Psi}{dt} = \frac{\partial\Psi}{\partial t}\frac{dt}{dt} + \frac{\partial\Psi}{\partial z}\frac{dz}{dt} \tag{10-95}$$

If $d\Psi/dt$ is evaluated along the line $z =$ constant (characteristic II), then Eq. (10-95) reduces to

$$\left(\frac{d\Psi}{dt}\right)_{\text{II}} = \frac{\partial\Psi}{\partial t} \qquad (\text{at} \quad z = \text{const}) \tag{10-96}$$

and Eq. (10-89) has been reduced to the ordinary differential equation

$$\left(\frac{d\Psi}{dt}\right)_{II} = k_2(\phi - b\Psi) \qquad (\text{at} \quad z = \text{const}) \tag{10-97}$$

The space of interest, the z-t space, is shown in Fig. 10-3. Thus, the original set of two partial differential equations has been reduced to two ordinary differential equations which are to be integrated along their respective characteristic lines. These two ordinary differential equations may be solved by any of the numerical methods used to integrate ordinary differential equations provided that the equations are integrated along their respective characteristics. For convenience, equal increments of $\Delta z = 1$ and $\Delta t = 1$ are used in the construction of the graph in Fig. 10-3. The 45° lines represent characteristic I, $dz/dt = 1$, and the vertical lines represent characteristic II, $z = \text{const}$. Note, the points $z = 0, z = 1, z = 2, \ldots$ along the z axis are located by

$$z = m\,\Delta x \tag{10-98}$$

where m is some positive integer. Similarly, the points $t = 0, 1, 2, \ldots$ along the t axis are given by

$$t = n\,\Delta t \tag{10-99}$$

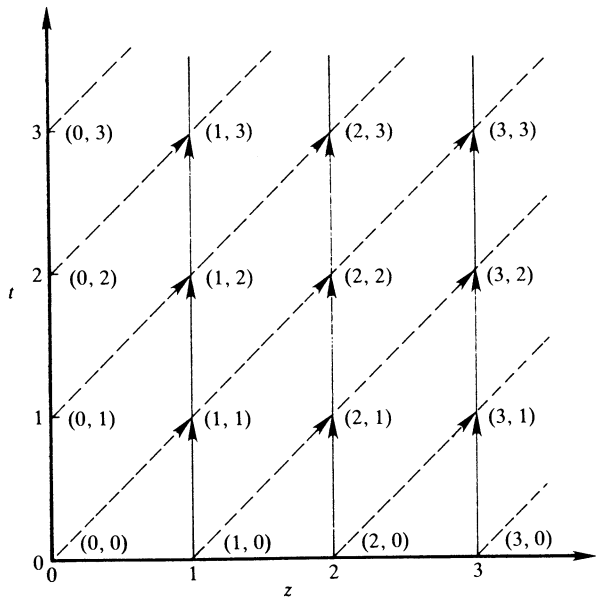

Figure 10-3 Sketch of the z-t place. (Note for Example 10-5, $\phi_0 = \phi(0, 0) = \phi(1, 0) = \cdots = \phi(n, 0)$ along the t axis. Along the z axis, $\Psi(0.\ 0) = \Psi(0, 1) = \cdots = \Psi(0, m) = 0$.)

where n is some positive integer. Thus, any point (z, t) may be represented by

$$(z, t) = (m\,\Delta z, n\,\Delta t) = (m, n) \tag{10-100}$$

The direction of integration for ϕ is along the line $dt/dz = 1$, and for Ψ the direction of integration is along the line $z = \text{const}$ as shown by the arrows in Fig. 10-3. Thus, in order to perform these integrations numerically, values of ϕ and Ψ along both axes, $t = 0$ and $z = 0$, are needed. The initial condition gives directly

$$\phi(0, 0) = \phi(0, 1) = \phi(0, 2) = \cdots = \phi(0, n) = \phi_0 \tag{10-101}$$

and the boundary condition gives directly

$$\Psi(0, 0) = \Psi(1, 0) = \Psi(2, 0) = \cdots = \Psi(m, 0) = 0 \tag{10-102}$$

To obtain values for $\phi(m, 0)$ and $\Psi(0, n)$, it is necessary to impose the initial condition and the boundary condition on Eqs. (10-94) and (10-97), respectively.

At the initial condition $\Psi = 0$ at $t = 0$, for all z, Eq. (10-94) reduces to

$$\left(\frac{d\phi}{dz}\right)_{I} = -k_1\phi \qquad (t = 0, z \geq 0) \tag{10-103}$$

which is readily integrated to give

$$\phi(z, 0) = \phi_0 e^{-k_1 z} \tag{10-104}$$

When the boundary condition $\phi = \phi_0$ at $z = 0$ for all $t > 0$ is imposed on Eq. (10-97), one obtains

$$\left(\frac{d\Psi}{dt}\right)_{II} = k_2(\phi_0 - b\Psi) \qquad (z = 0, t > 0) \tag{10-105}$$

Integration with respect to t yields

$$\Psi(0, t) = \frac{\phi_0}{b}(1 - e^{-k_2 b t}) \tag{10-106}$$

To illustrate the solution of Eqs. (10-88) and (10-89) by the method of characteristics, one complete set of calculations for the first increment in time and space is carried out in the following example.

Example 10-7 For the partial differential equations and initial and boundary conditions given by Eqs. (10-88) through (10-91), find the values of ϕ and Ψ at the end of the first increment in time and space. Take $\Delta t = 1$, $\Delta z = 1$, $k_1 = 0.09$, $k_2 = 0.1$, $b = 2$, and $\phi_0 = 2$. In this example use the integral form of the trapezoidal rule, namely,

$$\int_a^b f(x)\,dx = \left[\frac{f(a) + f(b)}{2}\right](b - a)$$

SOLUTION Integration of Eq. (10-94) from (0, 0) to (1, 1) (see Fig. 10-3) along $dt/dz = 1$ gives

$$\int_{(0,0)}^{(1,1)} \left(\frac{d\phi}{dz}\right)_I dz = -k_1 \int_{(0,0)}^{(1,1)} (\phi - b\Psi)\, dz \tag{1}$$

After the integral on the right-hand side of Eq. (1) has been approximated by use of the trapezoidal rule, the resulting expression obtained after integration is readily rearranged to give

$$\phi(1,1) = \phi(0,0) - \frac{k_1}{2}\{[\phi(1,1) - b\Psi(1,1)] + [\phi(0,0) - b\Psi(0,0)]\}$$

Since $\phi(0,0) = \phi_0 = 2$ and $\Psi(0,0) = 0$

$$\phi(1,1) = 2 - \frac{0.09}{2}[\phi(1,1) - 2\Psi(1,1) + 2] \tag{2}$$

Integration of Eq. (10-95) from point (1, 0) to (1, 1) along the path $z = \text{const}$ yields

$$\int_{(1,0)}^{(1,1)} \left(\frac{d\Psi}{dt}\right)_{II} dt = k_2 \int_{(1,0)}^{(1,1)} (\phi - b\Psi)\, dt \tag{3}$$

In a manner analogous to that described for the integration of Eq. (1), the following result is obtained for Eq. (3):

$$\Psi(1,1) = \Psi(1,0) + \frac{k_2}{2}\{[\phi(1,1) - b\Psi(1,1)] + [\phi(1,0) - b\Psi(1,0)]\}$$

Since $\Psi(1,0) = 0$ and since $\phi(1,0)$ is given by Eq. (10-104)

$$\phi(1,0) = \phi_0 e^{-k_1 \Delta z} = 2e^{-(0.09)(1)} = 1.827\,862$$

The above expression involving $\Psi(1,1)$ and $\phi(1,1)$ reduces to

$$\Psi(1,1) = 0.0 + \frac{0.1}{2}[\phi(1,1) - 2\Psi(1,1) + 1.827\,862] \tag{4}$$

Since Eqs. (2) and (4) are linear in $\phi(1,1)$ and $\Psi(1,1)$, they may be solved simultaneously to give

$$\phi(1,1) = 1.842\,118$$

$$\Psi(1,1) = 0.166\,817\,3$$

(In the event that the equations corresponding to Eqs. (2) and (4) are nonlinear in $\phi(1,1)$ and $\Psi(1,1)$ they may be solved by use of the Newton–Raphson method.) Values of ϕ and Ψ at other points on the grid are found in a manner analogous to that demonstrated for the point (1, 1).

REFERENCES

1. A. Acrivos: "Method of Characteristics Technique," *Ind. Eng. Chem.*, **48**(4):703 (1956).
2. B. Carnahan, H. A. Luther, and J. O. Wilkes: *Applied Numerical Methods*, John Wiley & Sons, New York, 1969.
3. C. W. Clenshaw and H. T. Norton: "The Solution of Non-Linear Ordinary Differential Equations in Chebyshev Series," *Comput. J.* **6**:88 (1963).
4. S. D. Conte and Carl de Boor: *Elementary Numerical Analysis*, 2d ed. McGraw-Hill Book Company, 1972.
5. J. Crank and P. Nicolson: "A Practical Method for Numerical Evaluation of Partial Differential Equations of the Heat Conduction Type," *Proc. Comb. Phil. Soc.*, **43**:50–67 (1947).
6. B. A. Finlayson: *The Method of Weighted Residuals and Variational Principles*, Academic Press, New York, 1972.
7. J. Friedley: *Dynamic Behavior of Processes*, Prentice-Hall, Inc., Englewood Cliffs, N.J., 1972.
8. F. B. Hildebrand: *Introduction to Numerical Analysis*, 2d ed., McGraw-Hill Book Company, 1974.
9. G. Horvay and F. N. Spiess: "Orthogonal Edge Polynomials in the Solution of Boundary Value Problems," *Q. Appl. Math.*, **12**:57 (1954).
10. R. W. Hamming: *Numerical Methods for Scientists and Engineers*, 2d ed., McGraw-Hill Book Company, 1973.
11. V. I. Krylov, V. V. Lugin, and L. A. Yanovich: *Tables for Numerical Integration of Functions with Power Singularities* $\int_0^1 x(1-x)f(x)\,dx$, Minsk: Izdat. Akad. Nauk BSSR, 1963 (Russian), 1979.
12. C. Lanczos: *Applied Analysis*, Prentice-Hall, Inc., Englewood Cliffs, N.J., 1956.
13. H. T. Norton: "The Iterative Solution of Nonlinear Ordinary Differential Equations in Chebyshev Series," *Comp. J.*, **7**:76 (1964).
14. R. D. Richtmyer: *Difference Methods for Initial-Value Problems*, Interscience Publishers, Inc., New York, 1962.
15. A. H. Shapiro: *Dynamics and Thermodynamics of Compressible Fluid Flow*, Ronald Press, New York, 1953.
16. A. H. Stroud and Don Secrest: *Gaussian Quadrature Formulas*, Prentice-Hall, Inc., N.J., 1966.
17. R. Vichnevetsky: "Generalized Finite-Difference Approximations for the Parallel Solution of Initial Value Problems," *Simulation*, **12**:223 (1969).
18. J. Villadsen and W. E. Stewart: "Solution of Boundary-Value Problems by Orthogonal Collocation," *Chem. Eng. Sci.*, **22**:1483 (1967).
19. J. Villadsen and M. L. Michelsen: *Solution of Differential Equations Models by Polynomial Approximation*, Prentice-Hall, Inc., N.J., 1978.
20. J. Villadsen: *Selected Approximation Methods for Chemical Engineering Problems*, Printed in offset by Reproset, Copenhagen, 1970.
21. K. Wright: "Chebyshev Collocation Methods for Ordinary Differential Equations," *Comput. J.*, **6**:358 (1964).

CHAPTER

ELEVEN

FUNDAMENTALS OF ADSORPTION PROCESSES

The adsorption process belongs to a more general class of unit operation which is sometimes called *percolation.* A percolation process is defined as any process in which a fluid is passed through a bed of material which has the capacity to alter the concentration of the fluid. This definition includes some classic unit operations such as ion exchange, adsorption, chromotography, drying, and washing. These operations are performed in order to obtain (*a*) purification of the diluents, (*b*) separation of products, and (*c*) recovery of solutes.

Most of the percolation processes are similar to adsorption which is the only percolation process considered in detail in this chapter. Most adsorbents are very porous and most of their surface area is in the interior of the adsorbent. Thus, the adsorption process consists of the sequence of mass transfer operations whereby the solute is transported into the interior of the adsorbent where it is adsorbed.

When a fluid containing solute components which are candidates for adsorption is passed through a bed, the mass transfer steps may be categorized as follows.

1. Within the flowing fluid stream, the solute is transported by diffusion in both the axial direction (the direction of bulk flow) and the radial direction (the direction perpendicular to the direction of bulk flow.)
2. The solute is transferred from the bulk conditions of the fluid phase to film on the surface of the adsorbent. (The two-film theory for mass transfer is assumed.)

3. The solute is transferred from the film to the fluid phase in a pore of an adsorbent.
4. The solute is transported through the pore by diffusion.
5. At any point along the pore, the solute is subject to adsorption on the surface.
6. After adsorption the solute may be transported along the surface or through the solid phase by diffusion.

Models which have been proposed for the description of the adsorption process generally make use of one or more of the above steps of the mass transfer mechanism. The remaining omitted steps of the mechanism are assumed to be either very "fast" if in series or very "slow" if in parallel. The terms "fast" and "slow" are used to mean that the rate constants for these steps are very large or very small, respectively, relative to those for the other steps.

In this chapter, the subject of adsorption is introduced by consideration of the adsorption step and the two mass transport processes, convective mass transfer and diffusion. The adsorption of both pure solutes and mixtures is considered in Sec. 11-1, and the adsorption of a single solute is considered in Secs. 11-2 and 11-3. Section 11-2 is devoted to convective mass transfer, the mass transfer process which is analogous to the convective heat transfer process. To demonstrate the behavior of convective mass transfer processes, an analytical solution is presented for a relatively simple problem. In Sec. 11-3, the roles of pore and surface diffusion in the adsorption process are illustrated by the use of the analytical solutions for some relatively simple problems.

11-1 PHYSICAL ADSORPTION OF PURE GASES AND MIXTURES BY SOLID ADSORBENTS

The fact that many gases exist in an adsorbed state on adsorbents such as charcoal at temperatures far above their criticals suggests the use of adsorbents in separation processes. Models for the adsorption of both pure components and mixtures are developed in this chapter.

When a gas is brought into contact with an evacuated solid (such as charcoal) and part of it is taken up by the solid, any one of several processes may have occurred. When the gas molecules are either attached to the surface or occupy the void spaces within the solid (such as pores, cracks, or capillaries), the process is known as *adsorption.* If the interactions between the gas and the solid are weak, similar to those involved in condensation, the process is called *physical adsorption,* and if the interaction between the adsorbed molecules and the surface is strong, similar to chemical bonding, the process is called *chemical adsorption.* Physical adsorption is also called *van der Waals adsorption,* which implies that van der Waals forces are also involved in physical adsorption. Adsorption processes are exothermic, a result which has been verified experi-

mentally, time and again. The heats of adsorption are of the same order of magnitude as the heats of vaporization.

The amount of a gas absorbed by physical adsorption at a given pressure increases as the saturation temperature is approached. At a given temperature and pressure, the amount of a gas adsorbed increases with the normal boiling point of the gas or with the critical temperature, and the amount adsorbed normally decreases as the temperature is increased. Chemical adsorption, on the other hand, does not generally occur at relatively low temperatures. Also, the initial amounts adsorbed increase as the temperature is increased. The rate of chemical adsorption is relatively fast at first and then very slow. On the other hand, physical adsorption occurs almost instantaneously. The lag in the adsorption process was first attributed to the diffusion of gas molecules into the interior of the adsorbent by McBain(25). Physical adsorption is readily reversible with respect to temperature and pressure, whereas chemically adsorbed gases are difficult to remove even by evacuation and heating.

Types of Physical Adsorption

The behavior of adsorbents, exhibited by their equilibrium adsorptions of a variety of gases, has led to a classification of the types of physical adsorptions. Since the initial observations of C. K. Scheele in 1773 of the adsorption of gases by solids, a wide variety of both adsorbents and adsorbates have been investigated. Among the practical adsorbents are the silica gels, activated aluminas, silica aluminas, molecular sieves, and activated charcoals. The results of adsorption experiments are most commonly presented in the form of *adsorption isotherms*, volume-adsorbed as a function of pressure at constant temperature. A variety of shapes of curves have been observed by the various investigators who have studied the adsorption of many different gases by many different types of adsorbents. Brunauer et al.(3) suggested the classification of these results according to the five types of isotherms shown in Fig. 11-1. Adsorption isotherms of type I are generally attributed to unimolecular adsorption. These curves are also referred to as Langmuir isotherms because they are described by the model proposed by Langmuir(17,18,19). The S-shaped or sigmoid isotherms, type II, are generally regarded as being descriptive of multimolecular adsorption. Brunauer(4) suggested that type III isotherms represent the formation of multimolecular layers before a unimolecular layer has been adsorbed, and that types IV and V reflect the occurrence of capillary condensation.

Models for the Physical Adsorption of Pure Components

In an attempt to explain the wide variety of experimental results characterized by Fig. 11-1, many theories and models have been proposed. One of the best known of these is *Henry's law* which may be used to describe many adsorptions at relatively low pressures.

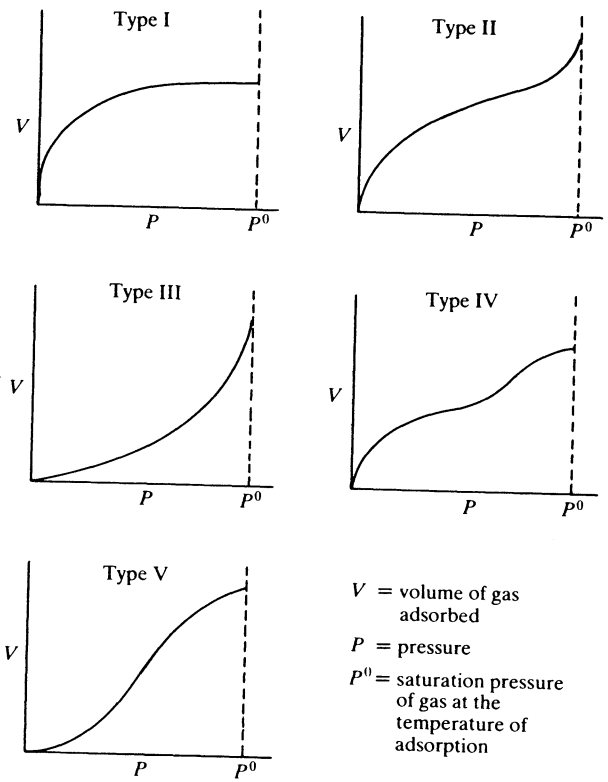

Figure 11-1 The five types of physical adsorption. (*S. Brunauer, L. S. Deming, W. E. Deming and E. Teller, "On a Theory of Van der Waals Adsorption of Gases," J. Am. Chem. Soc. vol. 62, p. 1723 (1940). Courtesy American Chemical Society.*)

Henry's law This law may be stated in the form

$$v = k_0 P \tag{11-1}$$

where k_0 is the Henry law constant, P is the adsorption equilibrium pressure, and v is the volume adsorbed (at °C and 1 atm) per unit mass of adsorbent.

For intermediate pressures, the Freundlich equation is commonly used.

Freundlich equation This empirical equation is of the form

$$v = k_1 P^{1/N} \tag{11-2}$$

where k_1 is a constant depending on the gas and the adsorbent and $N > 1$.

Langmuir equation The Langmuir equation is regarded by many as perhaps the single most important equation in the field of adsorption (Ref. 4). Three derivations of this equation have been presented; the original kinetic derivation of Langmuir(17,18,19), the thermodynamic derivation of Volmer(27), and statistical derivations by Fowler(8) and others. Of these, only the kinetic derivation is presented.

When a molecule strikes the surface of an adsorbent, it may be either elastically reflected from the surface without any energy exchange taking place or it may be inelastically adsorbed with the release of energy. Langmuir(17,18,19) attributed the phenomenon of adsorption to the average time that a molecule resides on the surface of an adsorbent. In summary, the postulates of Langmuir are as follows:

1. Of the molecules striking the surface, only those that strike the bare surface are candidates for adsorption. That is, molecules that strike an adsorbed molecule are elastically reflected.
2. The probability of evaporation of a molecule from the surface is the same whether or not the neighboring positions on the surface are empty or filled by other molecules. This amounts to assuming that the interaction between adsorbed molecules is negligible.

Let μ be equal to the number of molecules striking a unit of surface area per unit time. Let θ be equal to the fraction of the surface covered by adsorbed molecules. Then, the candidates for adsorption by postulate 1 are given by $(1 - \theta)\mu$. If the condensation coefficient on the bare surface is α, then the rate of adsorption is equal to $\alpha(1 - \theta)\mu$. Let v denote the rate of evaporation from a completely covered surface. Then by postulate 2, the rate of desorption is equal to $v\theta$. Then at equilibrium

$$\alpha(1 - \theta)\mu = v\theta \tag{11-3}$$

or

$$\theta = \frac{(\alpha/v)\mu}{1 + (\alpha/v)\mu} \tag{11-4}$$

The following expression for μ (the number of molecules striking one square centimeter of surface per second) is given by the kinetic theory of gases (Ref. 21)

$$\mu = \frac{P}{(2\pi mkT)^{1/2}} \tag{11-5}$$

where m is the mass of the molecule, k is the Boltzmann constant, and T is the temperature of the gas in degrees Kelvin. An expression for v may be deduced from the concepts of the kinetic theory. Let q denote the heat given off when a molecule is adsorbed. Then to be desorbed, a molecule must possess an energy equal to or greater than q. If it is supposed that the adsorbed molecules possess a maxwellian energy distribution in two degrees of freedom, then it can be shown that the fraction of molecules having an energy equal to or greater than q is given by $e^{-q/kT}$. Thus, Eq. (11-4) may be restated as follows:

$$\theta = \frac{bP}{1 + bP} \tag{11-6}$$

where the dependence of b upon temperature is given by

$$b = \frac{\alpha e^{q/kT}}{(2\pi mkT)^{1/2}} \tag{11-7}$$

Equation (11-6) is commonly stated in the following alternate but equivalent form

$$\frac{v}{v_m} = \frac{bP}{1 + bP} \tag{11-8}$$

where v_m is equal to the volume of gas adsorbed at (0°C and 1 atm) per unit mass of adsorbent when the adsorbent is covered with a complete unimolecular layer. It is generally possible to obtain a satisfactory fit with Eq. (11-8), the Langmuir equation.

The BET equation The multimolecular adsorption theory proposed by Braunauer, Emmett, and Teller(5) was the first attempt to present a unified theory of physical adsorption of pure gases. The equations resulting from this theory may be used to correlate the five types of adsorption shown in Fig. 11-1. The multimolecular theory of adsorption constitutes a generalization of Langmuir's

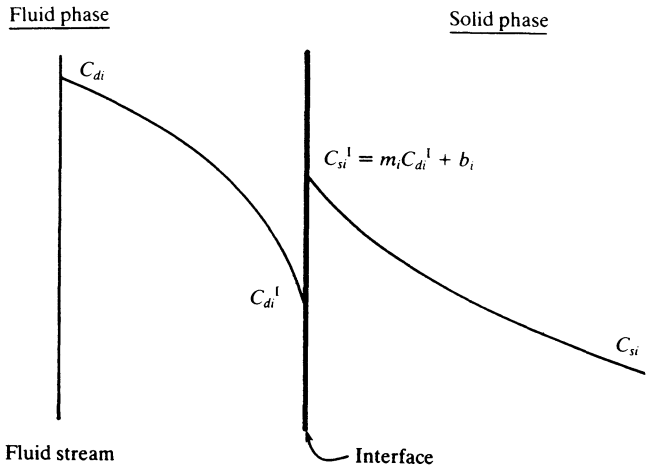

Figure 11-2 Concentration profile for mass transfer from the fluid stream to the adsorbed phase.

theory in that the restriction of unimolecular adsorption is removed. In addition the following postulates are made:

1. Let $s_0, s_1, s_2, \ldots, s_n$ represent the surface area covered by 0, 1, 2, ..., n layers of adsorbed molecules. Postulate that the rate of condensation on s_j is equal to the rate of evaporation from surface s_{j+1} ($j = 0, 1, 2, \ldots, n$).
2. Postulate that the evaporation-condensation properties of the molecules in the second and higher adsorbed layers are the same as those of the lower layers.

By postulate 1, the rate of adsorption on the bare surface is equal to the rate of evaporation from the first layer

$$a_1 P s_0 = b_1 s_1 e^{-E_1/RT} \tag{11-9}$$

where E_1 is the heat of adsorption for the first layer, and a_1 and b_1 are constants. Since

$$\text{Rate of adsorption on bare surface} = a_1 P s_0 \propto \alpha(1-\theta)\mu$$

$$\text{Rate of desorption from surface covered by one layer} = b_1 s_1 e^{-E_1/RT} \propto \theta v$$

Equation (11-9) consists of an alternate statement of Langmuir's equation for unimolecular adsorption and involves the assumption that a_1, b_1, and E_1 are independent of adsorbed molecules already present in the first layer. Similarly, the rate of condensation on the first layer is equal to the rate of evaporation from the second layer. Then, in general, the rate of condensation of the jth layer is equal to the rate of evaporation from the $(j+1)$st layer

$$a_{j+1} P s_j = b_{j+1} s_{j+1} e^{-E_j/RT} \qquad (j = 0, 1, 2, \ldots, n) \tag{11-10}$$

It is of interest to note that in spite of the fact that Langmuir's name is commonly associated with unimolecular adsorption, he also formulated a set of equations in 1918 (see Ref. 19) for the case where the adsorption spaces may hold more than one adsorbed molecule. These equations were of the same form as those given by Eq. (11-10), but their summation was handled in a different manner than that proposed by Brunauer, Emmett, and Teller(5).

To effect the summation of the expressions given by Eq. (11-10), Brunauer, Emmett, and Teller assumed that all adsorbed layers after the first one could be characterized in the same way by requiring that

$$\frac{a_2}{b_2} = \frac{a_3}{b_3} = \cdots = \frac{a_n}{b_n} = \frac{a}{b}$$
$$E_2 = E_3 = \cdots = E_n = E_L \tag{11-11}$$

where E_L is the heat of liquefaction. The result so obtained is given by

$$\frac{v}{v_m} = \frac{cP}{(P^0 - P)[1 + (c-1)P/P^0]} \tag{11-12}$$

where v is equal to the total volume of gas adsorbed and v_m is equal to the volume of gas required to cover the surface of the adsorbent with a unimolecular layer. The total pressure of the adsorption is denoted by P and the vapor pressure (or saturation pressure) of the gas at the temperature of the adsorption experiment is denoted by P^0. The constant c is given by

$$c = \left(\frac{a_1/b_1}{a/b}\right) \exp\left[\frac{E_1 - E_L}{RT}\right] \tag{11-13}$$

Equation (11-12) is commonly referred to as the BET equation (after Brunauer–Emmett–Teller(5)).

Development of a Kinetic Model for the Adsorption of Mixtures of Gases in Multimolecular Layers

The development of the model for the adsorption of a mixture of gases is a rather obvious extension of Langmuir's model for the adsorption of pure components. The model for the adsorption of mixtures in unimolecular layers was first proposed by Markham and Benton(22). The model for unimolecular adsorption is obtained as a special case of the more general model for adsorption in multimolecular layers.

Hill(13) proposed an extension of the BET equations for the adsorption of multicomponent mixtures of gases in infinitely many adsorbed layers. Arnold(1) presented a variation of Hill's extension of the BET equations. Hill's equations were applied by Mason and Cooke(24), who found that their experimental results could be represented on the basis of two or three adsorbed layers.

The postulates upon which the models for adsorption of multicomponent mixtures as proposed by Gonzalez and Holland(11,12) follow.

1. Molecules striking either the bare surface or the covered surface are candidates for adsorption.
2. The probability of the evaporation of a molecule from an adsorbed layer is independent of whether or not the neighboring positions in a given layer are empty or filled. (This assumption could be highly inaccurate for the adsorption of highly polar compounds).
3. The total number of sites available for adsorption is independent of pressure but dependent upon temperature.
4. The total number of sites available for adsorption is the same for all components. (This assumption has the same weakness as the second postulate).
5. The adsorption of a given molecule in a given layer is independent of the identity of the molecule adsorbed beneath it in the previous layer.
6. The ratios of adsorption equilibrium constants for the $(j+1)$st and the jth layers are equal to the same constants for all components.
7. The adsorption process is assumed to be at equilibrium.

These assumptions follow closely those originally proposed by Langmuir(17,18,19).

Let S_0 denote the moles of vacant adsorption sites on the bare surface, and let S_1 denote the moles of sites on the surface S_0 which are covered by an adsorbed molecule. Let S_2 denote the moles of sites which contain two layers of adsorbed molecule. Let A_1, A_2 ..., A_c denote the molecules involved in the adsorption process. The number of sites covered by any type of molecule is assumed to be a function only of its equilibrium constant. The mechanism consists of the following system of reactions at a state of dynamic equilibrium:

$$\begin{aligned} A_i(g) + S_0 &\underset{k_1'}{\overset{k_1}{\rightleftharpoons}} A_i S_0 \\ A_i(g) + S_1 &\underset{k_2'}{\overset{k_2}{\rightleftharpoons}} A_i S_1 \\ &\vdots \\ A_i(g) + S_{j-1} &\underset{k_j'}{\overset{k_j}{\rightleftharpoons}} A_i S_{j-1} \end{aligned} \tag{11-14}$$

Consider first the adsorption on the bare surface. Since each reaction is assumed to be in equilibrium, the expression for this equilibrium is given by

$$\frac{k_{1i}}{k'_{1i}} = K_{1i} = \frac{C_{1i}}{p_i C_{s,0}} \qquad (i = 1, 2, \ldots, c) \tag{11-15}$$

and thus

$$C_{1i} = K_{1i} p_i C_{s,0} \tag{11-16}$$

Let C_T denote the total number of moles of adsorption sites on the bare surface. Then

$$C_{s,0} = C_T - \sum_{i=1}^{c} C_{1i} = C_T - C_{s,0} \sum_{i=1}^{c} K_{1i} p_i$$

which is readily solved for $C_{s,0}$ to give

$$C_{s,0} = \frac{C_T}{1 + \sum_{i=1}^{c} K_{1i} p_i} \tag{11-17}$$

After this expression for $C_{s,0}$ has been substituted into Eq. (11-16), one obtains

$$C_{1i} = \frac{C_T K_{1i} p_i}{1 + \sum_{i=1}^{c} K_{1i} p_i} \tag{11-18}$$

For the case of the adsorption of a pure component, Eq. (11-18) reduces to Langmuir's isotherm, Eq. (11-8). An expression for the adsorption of mixtures

which was of the same general form as Eq. (11-18) was proposed by Markham and Benton(22). Actually the model proposed by Markham and Benton was more general than the one given by Eq. (11-18) in that the total number of sites available for adsorption was assumed to depend upon the identity of each component, that is, the model of Markham and Benton is given by replacing C_T in Eq. (11-18) by C_{Ti}.

The model for multilayer adsorption is developed in the following manner. Since the reaction representing adsorption on the jth adsorbed layer is assumed to be at equilibrium, one obtains

$$C_{ji} = K_{ji} p_i C_{s,j-1} \qquad (j = 1, 2, \ldots, n) \tag{11-19}$$

and

$$C_{sj} = \sum_{i=1}^{c} C_{ji} - \sum_{i=1}^{c} C_{j+1,i} \tag{11-20}$$

Let

$$\phi_j = \sum_{i=1}^{c} K_{ji} p_i \tag{11-21}$$

Elimination of C_{ji} and $C_{j+1,i}$ from Eq. (11-20) through the use of Eqs. (11-19) and (11-21) yields

$$C_{sj} = C_{s,j-1} \phi_j - C_{s,j} \phi_{j+1} \tag{11-22}$$

Thus

$$C_{sj} = \frac{\phi_j C_{s,j-1}}{1 + \phi_{j+1}} \qquad (j = 1, 2, \ldots, n) \tag{11-23}$$

The expression for C_{sn} is obtained by the substitutional process whereby one begins with the expression for $C_{s,0}$ (Eq. (11-17)) and substitutes it into the expression for C_{s1} (Eq. (11-23) with $j = 1$). Continuation of this process whereby the expression for $C_{s,j-1}$ is substituted into the one for $C_{s,j}$ yields

$$C_{s,n-1} = \frac{C_T \phi_1 \phi_2 \cdots \phi_{n-1}}{(1 + \phi_1)(1 + \phi_2) \cdots (1 + \phi_n)} \tag{11-24}$$

When this result is substituted into Eq. (11-23), one obtains the expression for the concentration of component i in the nth adsorbed layer, namely,

$$C_{ni} = K_{ni} p_i \left[\frac{C_T \phi_1 \phi_2 \cdots \phi_{n-1}}{(1 + \phi_1)(1 + \phi_2) \cdots (1 + \phi_n)} \right] \tag{11-25}$$

The total concentration of component i in all adsorbed layers is given by

$$C_i = \sum_{j=1}^{n} C_{ji} = p_i C_T \sum_{j=1}^{n} \frac{K_{ji} \phi_1 \phi_2 \cdots \phi_{j-1}}{(1 + \phi_1)(1 + \phi_2) \cdots (1 + \phi_j)} \tag{11-26}$$

Since this expression for C_i contains a large number of parameters, C_T, $\{K_{ji}\}$, $\{\phi_j\}$, Gonzalez and Holland(11,12) proposed the following postulate for the purpose of reducing the number of parameters to be determined experimentally, namely,

$$\frac{K_{2i}}{K_{1i}} = \frac{K_{3i}}{K_{2i}} = \cdots = \frac{K_{n+1,i}}{K_{ni}} = v \tag{11-27}$$

where v is the same constant for all i. On the basis of this postulate it can be shown that Eq. (11-26) reduces to

$$C_i = p_i C_T \sum_{j=1}^{n} \frac{K_{1i} v^{j(j-1)/2} \phi_1^{j-1}}{(1+\phi_1)(1+v\phi_1)(1+v^2\phi_j)\cdots(1+v^{j-1}\phi_1)} \tag{11-28}$$

Gonzalez and Holland(11,12) showed that the adsorptions of many systems could be adequately described by two-layer adsorption ($j = 2$).

The Fritz–Schluender isotherm In order to obtain a satisfactory fit of the adsorption data for organic liquids in aqueous mixtures, Fritz and Schluender(10) used the following relationship

$$C_i = \frac{a_{i0} C_{pi}^{b_{i0}}}{c_i + \sum_{j=1}^{n} a_{ij} C_{pj}^{b_{ij}}} \tag{11-29}$$

where C_{pi} is the concentration of component i in the fluid phase in the pore, and C_i is the concentration of i in the adsorbed phase. Parameters to be determined by use of experimental data are c_i, $a_{i,j}$, and $b_{i,j}$.

11-2 MASS TRANSFER BY THE CONVECTIVE TRANSPORT MECHANISM

The name "convective transport mechanism" is given herein to mass transfer processes in which the rate of mass transfer can be expressed as a linear function of a fugacity difference, a partial pressure difference, or a concentration difference. This name is used because this mass transfer process is analogous to the convective heat transfer process in which the rate of heat transfer is a linear function of the temperature difference, and because of the need to distinguish between the transfer of mass by this process and the transfer of mass by diffusion.

There follows first a development of the rate expressions for the convective mass transport mechanism, and then the model for a fixed-bed adsorption column in which the rate controlling step for mass transfer is the convective mass transport mechanism.

The Convective Mass Transport Mechanism

The convective mass transport mechanism is based on the two-film theory of mass transfer. The rate expressions based on this theory may be formulated by consideration of the case where a fluid phase is passed through a fixed adsorbent bed. Suppose that the concentration is constant in the radial direction (the direction perpendicular to the direction of flow).

A sketch of the concentration profile is shown in Fig. 11-2. The rate of mass transfer of component i from the bulk conditions of the fluid phase to the interface is given by

$$r_{di} = k_{di} a_d (C_{di} - C_{di}^{\mathrm{I}}) \tag{11-30}$$

where r_{di} = moles transferred per unit time per unit volume of empty bed
a_d = interfacial area between the fluid phase and the solid phase per unit volume of empty column
C_{di} = concentration of component i at the bulk conditions of the fluid stream, moles per unit of void volume (the free volume between the pellets), C_{di}^{I} is the concentration on the fluid side of the interface
k_{di} = mass transfer coefficient (volume of empty column per unit of time per unit of interfacial area)

The rate of transfer across the interface is assumed to be very fast relative to the other steps, which amounts to the assumption that a dynamic equilibrium exists at the interface, that is,

$$C_{si}^{\mathrm{I}} = m_i C_{di}^{\mathrm{I}} + b_i \tag{11-31}$$

The rate of transfer from the interface to the adsorbed phase is given by

$$r_{si} = k_{si} a_s (C_{si}^{\mathrm{I}} - C_{si}) \tag{11-32}$$

where r_{si} = moles transferred per unit time per unit volume of pellet
a_s = interfacial area between the fluid phase and the solid phase per unit volume of pellet
C_{si} = moles of component i in the adsorbed phase per unit volume of pellet
k_{si} = mass transfer coefficient (pellet volume per unit of time per unit of interfacial area)

Two expressions may be obtained for the overall mass transfer coefficient, one to be used with the solid phase concentrations and the other to be used with the fluid phase concentrations. First the expression for the rate of mass transfer in terms of the solid phase compositions is developed. Observe that

$$r_{di}\left(\frac{1}{1-\varepsilon}\right) = r_{si} \tag{11-33}$$

$$\frac{a_d}{1-\varepsilon} = a_s \tag{11-34}$$

where ε = (volume of voids between the pellets)/(volume of bed)
$1 - \varepsilon$ = (volume of pellets)/(volume of bed)

Thus,

$$r_{si} = \left(\frac{1}{1-\varepsilon}\right) k_{di} a_d (C_{di} - C_{di}^{\mathrm{I}}) = k_{si} a_s (C_{si}^{\mathrm{I}} - C_{si}) \tag{11-35}$$

Linear equilibrium relationships between the fluid phase and the adsorbed phase are assumed, namely, Eq. (11-31) and

$$C_{si}^{*} = m_i C_{di} + b_i \tag{11-36}$$

where m_i and b_i depend on each component i but are independent of composition and where C_{si}^{*} is the concentration which the adsorbed phase would have if it were in equilibrium with a fluid phase having the concentration C_{di}. The above relationships may be used to restate the rate of mass transfer in terms of the concentration difference $(C_{si}^{*} - C_{si})$ and the corresponding overall mass transfer coefficient

$$r_{si} = K_{si} a_s (C_{si}^{*} - C_{si}) \tag{11-37}$$

where

$$\frac{1}{K_{si}} = \frac{m_i}{k_{di}} + \frac{1}{k_{si}}$$

In a similar manner, the following rate expression in terms of the concentration difference $(C_{di} - C_{di}^{*})$ and the overall mass transfer coefficient K_{di} is obtained:

$$r_{di} = K_{di} a_d (C_{di} - C_{di}^{*}) \tag{11-38}$$

where

$$\frac{1}{K_{di}} = \frac{1}{k_{di}} + \frac{1}{m_i k_{si}} \tag{11-39}$$

and

$$C_{si} = m_i C_{di}^{*} + b_i \tag{11-40}$$

where C_{di}^{*} is the concentration which the fluid phase would have if it were in equilibrium with an adsorbed phase having a concentration C_{si}.

Component-Material Balance on Component i in the Solid Phase over the Time Period from t_n to $t_n + \Delta t$

First observe that $r_{si}(1 - \varepsilon)$ denotes the moles of component i transferred from the fluid phase to the solid phase per unit time per unit volume of empty column.

The material balance is made on a fixed-bed adsorption column of cross-sectional area S through which a fluid phase is flowing. Assume that the concentration is constant in the radial direction (the direction perpendicular to fluid flow). The balance on component i in the adsorbed (or solid) phase contained in

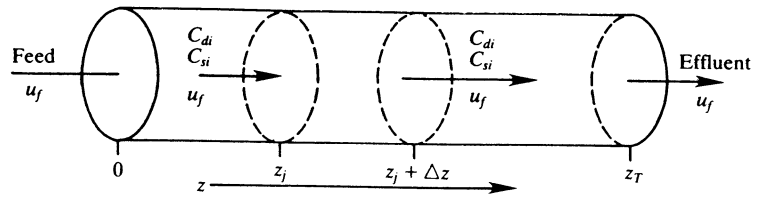

Figure 11-3 Sketch of a fixed-bed adsorber.

the element of volume $S\,\Delta z$ (see Fig. 11-3) over the time period from time t_n to $t_n + \Delta t$ is given by

$$\int_{t_n}^{t_n+\Delta t} \left[\int_{z_j}^{z_j+\Delta z} r_{si}(1-\varepsilon) S\, dz \right] dt$$

$$= \int_{z_j}^{z_j+\Delta z} \left[(1-\varepsilon) S C_{si}\Big|_{t_n+\Delta t,\, z} - (1-\varepsilon) S C_{si}\Big|_{t_n,\, z} \right] dz \tag{11-41}$$

Application of the mean value theorems followed by the limiting process whereby Δz and Δt are allowed to go to zero yields

$$r_{si} = \frac{\partial C_{si}}{\partial t} \qquad (0 < z < z_T) \tag{11-42}$$

where z_T is the total length of the adsorbent bed and the expression for r_{si} is given by Eq. (11-37).

Mass Balance on Component i in the Fluid Phase over the Time Period Δt in a Fixed-Bed Adsorption Column

In this model, which is sometimes referred to as the Glueckauf model, it is assumed that the fluid phase is perfectly mixed in the radial direction (the direction perpendicular to the direction of flow) and that the rate of mass transfer by diffusion in the fluid phase is negligible in all directions. Also, it is supposed that u_f, the linear velocity of the fluid phase, is independent of time and position. The material balance on component i is made on the volume $\varepsilon S \Delta z$ over the time period from t_n to $t_n + \Delta t$

$$\int_{t_n}^{t_n+\Delta t} \left[u_f \varepsilon S C_{di}\Big|_{z_j,\, t} - u_f \varepsilon S C_{di}\Big|_{z_j+\Delta z,\, t} - \int_{z_j}^{z_j+\Delta z} r_{si}(1-\varepsilon) S\, dz \right] dt$$

$$= \int_{z_j}^{z_j+\Delta z} \left[\varepsilon S C_{di}\Big|_{t_n+\Delta t,\, z} - \varepsilon S C_{di}\Big|_{t_n,\, z} \right] dz \tag{11-43}$$

Application of the mean value theorems followed by the limiting process wherein Δz and Δt are allowed to go to zero yields the following result:

$$-\frac{\partial(u_f \varepsilon S C_{di})}{\partial z} - r_{si}(1-\varepsilon)S = \frac{\partial(\varepsilon S C_{di})}{\partial t} \qquad (0 < z < z_T) \tag{11-44}$$

Since u_f, ε, and S are assumed to be independent of time and position

$$-u_f \frac{\partial C_{di}}{\partial z} - \left(\frac{1-\varepsilon}{\varepsilon}\right) r_{si} = \frac{\partial C_{di}}{\partial t} \qquad (0 < z < z_T) \tag{11-45}$$

Use of Eqs. (11-33) and (11-38) permits the above equation to be restated in the following form, which is used in subsequent developments:

$$-u_f \frac{\partial C_{di}}{\partial z} - \frac{K_{di} a_d}{\varepsilon}(C_{di} - C_{di}^*) = \frac{\partial C_{di}}{\partial t} \tag{10-46}$$

Similarly, Eq. (11-42) may be stated in the following forms by use of Eqs. (11-33), (11-37), and (11-38):

$$\frac{\partial C_{si}}{\partial t} = \left(\frac{K_{di} a_d}{1-\varepsilon}\right)(C_{di} - C_{di}^*) \tag{11-47}$$

or

$$\frac{\partial C_{si}}{\partial t} = K_{si} a_s (C_{si}^* - C_{si})$$

Solution of the Glueckauf Model for the Special Case of the Adsorption of a Single Solute Component in a Fixed-Bed Adsorber

Although analytical solutions have been obtained for Eqs. (11-46) and (11-47) for a number of different sets of boundary and initial conditions, the analytical solution for only one set of conditions is presented. In particular consider the fixed-bed adsorber shown in Fig. 11-3. It is desired to find the outlet concentration $C_d(z_T, t)$ at any time t after the initiation of the adsorption process at time $t = 0$. Initially, at $t = 0$, the amount of solute on the adsorbent is uniform for all z and its concentration is denoted by $C_s(z, 0)$. For all $t > 0$, the adsorbent is contacted with a gas which has a solute concentration C_d^0 at $z = 0$. More precisely

$$\text{at } t = 0, \qquad C_s(z, 0) = C_s^0 \qquad \text{for all } z \tag{11-48}$$

$$\text{at } z = 0, \qquad C_d(0, t) = C_d^0 \qquad \text{for all } t \tag{11-49}$$

In the development which follows, it is supposed that the carrier fluid is dilute in the solute (the component which is to be adsorbed). Consequently, it can be assumed with good accuracy that the molar density is independent of

time and position. Thus

$$C_d = \rho_d y \qquad C_d^* = \rho_d w \tag{11-50}$$

where y is the mole fraction of the solute in the fluid phase and w is the mole fraction which the solute would have if it were in equilibrium with the adsorbed (or solid) phase. Thus, Eq. (11-46) may be restated in the following form:

$$-\left(\frac{u_f \varepsilon}{K_d a_d}\right)\frac{\partial y}{\partial z} - \left(\frac{\varepsilon}{K_d a_d}\right)\frac{\partial y}{\partial t} = y - w \tag{11-51}$$

Use of Eq. (11-40) and the above definitions of the mole fractions permits Eq. (11-47) to be restated in the form

$$\left[\frac{m(1-\varepsilon)}{K_d a_d}\right]\frac{\partial w}{\partial t} = y - w \tag{11-52}$$

As demonstrated by others (Refs. 23, 26), the partial differential equations given by Eqs. (11-51) and (11-52) may be reduced to simpler form by making the following changes of variables. Let

$$\eta = \frac{K_d a_d}{u_f \varepsilon} z \qquad \tau = \frac{K_d a_d}{m(1-\varepsilon)}\left(t - \frac{z}{u_f}\right) \tag{11-53}$$

The partial derivatives appearing in Eqs. (11-51) and (11-52) are computed in terms of the new variables by use of the chain rule as follows:

$$\begin{aligned}
\frac{\partial y}{\partial z} &= \frac{\partial y}{\partial \tau}\frac{\partial \tau}{\partial z} + \frac{\partial y}{\partial \eta}\frac{\partial \eta}{\partial z} = \left[\frac{-K_d a_d}{m(1-\varepsilon)u_f}\right]\frac{\partial y}{\partial \tau} + \left(\frac{K_d a_d}{u_f \varepsilon}\right)\frac{\partial y}{\partial \eta} \\
\frac{\partial y}{\partial t} &= \frac{\partial y}{\partial \tau}\frac{\partial \tau}{\partial t} + \frac{\partial y}{\partial \eta}\frac{\partial \eta}{\partial t} = \frac{\partial y}{\partial \tau}\frac{\partial \tau}{\partial t} = \left[\frac{K_d a_d}{m(1-\varepsilon)}\right]\frac{\partial y}{\partial \tau} \\
\frac{\partial w}{\partial t} &= \frac{\partial w}{\partial \tau}\frac{\partial \tau}{\partial t} + \frac{\partial w}{\partial \eta}\frac{\partial \eta}{\partial t} = \frac{\partial w}{\partial \tau}\frac{\partial \tau}{\partial t} = \left[\frac{K_d a_d}{m(1-\varepsilon)}\right]\frac{\partial w}{\partial \tau}
\end{aligned} \tag{11-54}$$

Substitution of the results given by Eq. (11-54) into Eqs. (11-51) and (11-52) yields

$$-\frac{\partial y}{\partial \eta} = y - w \tag{11-55}$$

$$\frac{\partial w}{\partial \tau} = y - w \tag{11-56}$$

The initial condition and boundary condition corresponding to Eqs. (11-48) and (11-49) are

$$w(\eta, 0) = w^0 \qquad \text{at } \tau = 0 \text{ for all } \eta \tag{11-57}$$

$$y(0, \tau) = y^0 \qquad \text{at } \eta = 0 \text{ for all } \tau \tag{11-58}$$

Equations (11-55) through (11-58) were first solved by Anzelius(2) for an analogous problem in heat transfer. Furnas(9) extended the work of Anzelius and presented solutions in the form of charts. Hougen and Marshall(14) formulated and solved the adsorption problem stated. The problem may be solved by use of Laplace transforms in a manner analogous to that demonstrated by Mickley et al.(26); see Prob. 11-7. The results are as follows:

$$\frac{w(\eta, \tau) - w^0}{y^0 - w^0} = e^{-\eta} \int_0^\tau e^{-\lambda} J_0(2i\sqrt{\eta\lambda})\, d\lambda \tag{11-59}$$

and

$$\frac{y^0 - y(\eta, \tau)}{y^0 - w^0} = e^{-\tau} \int_0^\eta e^{-\xi} J_0(2i\sqrt{\tau\xi})\, d\xi \tag{11-60}$$

A graph of the behavior predicted by Eq. (11-60) is presented in Fig. 11-4 for an adsorber of length $z_T = 50$ cm. Other parameters for the adsorber are $K_d a_d = 0.10\ s^{-1}$, $u_f = 0.14$ cm/s, $m = 1.1$, and $\varepsilon = 0.50$. For this set of parameters, the corresponding value of $\eta = 71.43$. Observe that there is no appreciable amount of solute in the effluent from $\tau = 0$ up to τ equal to approximately 25. For $\tau > 25$, the breakthrough of the solute occurs. At $\tau \cong 110$, the adsorbent is saturated with the solute and $z(\eta, \tau) \cong y^0$.

Leland and Holmes(20) pointed out that the designer wishes to know not the instantaneous concentrations of the gas leaving the bed at any time but, rather, the cumulative fraction recovered out of the total quantity of a given

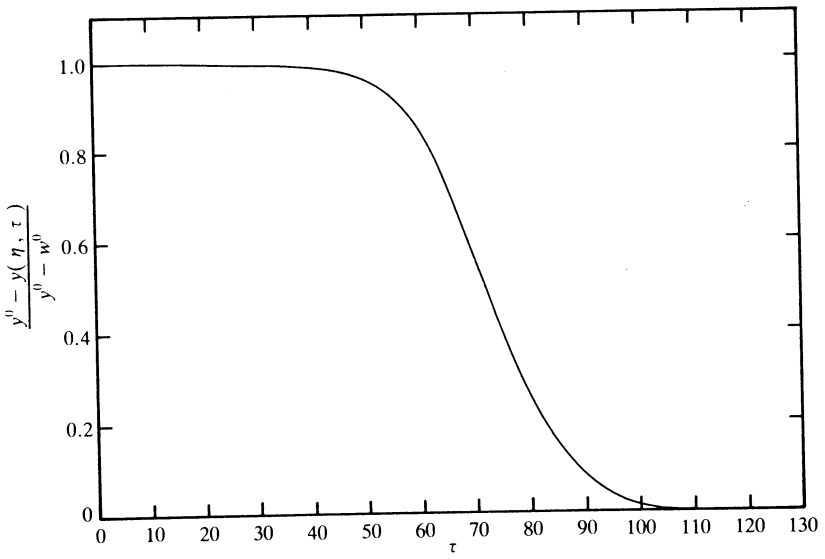

Figure 11-4 Breakthrough curve predicted by Eq. (11-60). ($z_T = 50$ cm, $K_d a_d = 0.1\ s^{-1}$, $u_f = 0.14$ cm/s, $\varepsilon = 0.50$, $m = 1.1$, $\eta = 71.43$.)

component entering the bed during the adsorption cycle. The cumulative fraction recovered is defined by

$$\phi(t) = \frac{\int_0^t u_f S\rho_d [y^0 - y(\eta, \tau)]\, dt}{\int_0^t u_f S\rho_d y^0\, dt} \tag{11-61}$$

Equation (11-60) may be used to reduce Eq. (11-61) to

$$\phi(t) = \frac{y^0 - w^0}{ty^0} \int_0^t e^{-\tau} \int_0^\eta e^{-\xi} J_0(2i\sqrt{\xi\tau})\, d\xi\, dt \tag{11-62}$$

For the case where $w^0 = 0$ and the holdup in the vapor phase is negligible ($\tau = [K_d a_d/m(1 - \varepsilon)]t$), Leland and Holmes(20) present a graph of $\phi(t)$.

11-3 THE ROLE OF PORE AND SURFACE DIFFUSION IN THE ADSORPTION PROCESS

As outlined at the outset, transport by diffusion may occur in the fluid stream exterior to the adsorbent as well as within the pore and on the surface of the adsorbent. In the following development, two special cases are considered. In the first of these, pore diffusion is assumed to be the rate-controlling step and in the second special case, pore diffusion plus surface diffusion are assumed to be the rate-controlling steps. All other steps in series with these are assumed to be "fast" (they have very large rate constants relative to the two diffusion steps under consideration). The adsorption step is also assumed to be fast.

Pore Diffusion

In 1909, McBain(25) initiated the study of adsorption rate processes. Any lag in the adsorption process was attributed by McBain to the inaccessibility of the adsorbent surface to the molecules being adsorbed. McBain assumed that the measurable process could be attributed to the transport of the adsorbed molecules through the solid solution on the surface. However since the transport along the surface was assumed to proceed by Fick's law, the general form of the solution is the same as for diffusion through the pore.

In the present treatment, the adsorbent is assumed to be cylindrical and the pores are taken to be in the direction of the principal axis as shown in Fig. 11-3. Let S denote the cross-sectional area of the pellet and ε_p the fraction of voids (volume of pores/volume of the pellet). Suppose that initially each pore is filled with an inert gas. At time $t \geq 0$, the pure solute is introduced at each end of the pore at $z = 0$ and $z = L$. The transport of the solute to the interior of the pellet and the inert gas to the exterior is assumed to occur by Fick's law

$$J_{pi} = -D_{pi} \frac{\partial C_{pi}}{\partial z} \tag{11-63}$$

where J_{pi} = moles of solute i diffusing into the pore in the positive direction of z per unit time per unit of pore area perpendicular to the direction z
C_{pi} = concentration of solute i, moles per unit of pore volume
D_{pi} = diffusion coefficient for component i in the pore

In the following material balance on the solute component, the subscript i is dropped as a matter of convenience. The material balance on the solute in the element of pore volume from z_j to $z_j + \Delta z$ and over the time period from t_n to $t_n + \Delta t$ is given by

$$\int_{t_n}^{t_n+\Delta t} \left(\varepsilon_p S J_p \Big|_{z_j,\, t} - \varepsilon_p S J_p \Big|_{z_j+\Delta z,\, t} \right) dt = \int_{z_j}^{z_j+\Delta z} C_p \varepsilon_p S \, dz \Big|_{t_n+\Delta t} - \int_{z_j}^{z_j+\Delta z} C_p \varepsilon_p S \, dz \Big|_{t_n} \tag{11-64}$$

Application of the mean-value theorems followed by the limiting process wherein Δz and Δt are allowed to go to zero yields

$$\frac{-\partial(\varepsilon_p S J_p)}{\partial z} = \frac{\partial(\varepsilon_p S C_p)}{\partial t} \qquad (0 < z < L,\ t > 0) \tag{11-65}$$

If ε_p, D_p, and S are taken to be independent of time and position, then Eq. (11-65) reduces to

$$D_p \frac{\partial^2 C_p}{\partial z^2} = \frac{\partial C_p}{\partial t} \qquad (0 < z < L,\ t > 0) \tag{11-66}$$

The initial and boundary conditions stated above many be quantified as follows:

$$\begin{aligned} C_p(0, t) &= C_p^0 \qquad (z = 0,\ t > 0) \\ C_p(L, t) &= C_p^0 \qquad (z = L,\ t > 0) \\ C_p(z, 0) &= 0 \qquad (0 < z < L,\ t \le 0) \end{aligned} \tag{11-67}$$

The solution which satisfies the partial differential equation, the initial condition, and the boundary conditions is

$$C_p(z, t) = C_p^0 \left\{ 1 - \frac{4}{\pi} \sum_{m=1}^{\infty} \frac{\left[\sin (2m-1) \frac{\pi z}{L} \right] e^{-(2m-1)\,\delta t}}{2m-1} \right\} \tag{11-68}$$

where $\delta = D_p \pi^2 / L^2$. This solution may be obtained by the product method as outlined in Prob. 11-9. The behavior predicted by Eq. (11-68) is shown in Fig. 11-5 for a system described by the following parameters: $C_p^0 = 0.001$ gm/cm^3, $L = 0.1$ cm, and $D_p = 8.0 \times 10^{-6}$ cm^2/s. For each of several times, the concentration profile of the solute as a function of pore length is shown. Since the

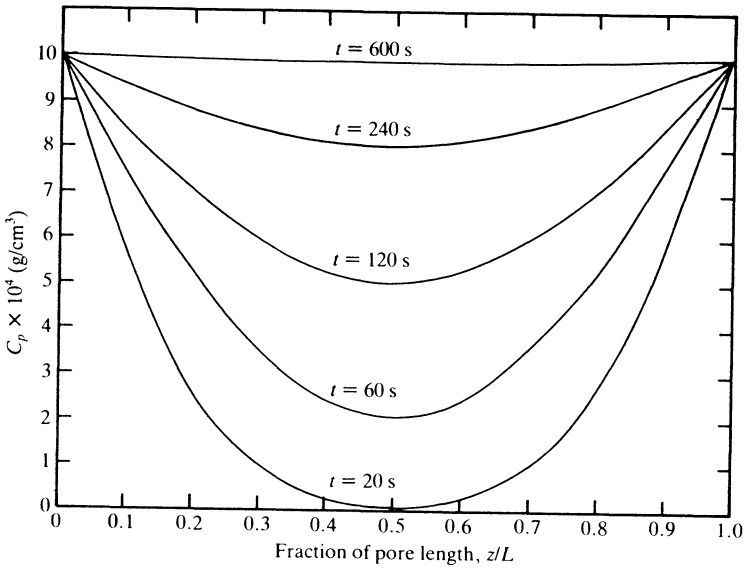

Figure 11-5 Concentration profiles in the pores as predicted by Eq. (11-68). ($C_p^0 = 0.001$ gm/cm^3, $L = 0.1$ cm, and $D_p = 8.0 \times 10^{-6}$ cm^2/s.)

pore was assumed to be open at both ends (see Eq. (11-67)), the minimum of each profile occurs at $z/L = 0.5$. Initially, when little of the solute has been adsorbed, the profiles are seen to be relatively steep. As the amount of solute adsorbed increases (with time), the profiles become flatter.

Now let the accumulation of solute within the pore over the time period from $t = 0$ to any time t be denoted by Q. Since J_p is the rate of diffusion of the solute in the positive direction of z, it follows by the law of conservation of mass that the material balance for the solute over the time period from $t = 0$ to any time t is given by

$$\underbrace{\int_0^t \varepsilon_p S J_p \Big|_{z=0} dt}_{\substack{\text{input of solute} \\ \text{at } z = 0}} - \underbrace{\int_0^t \varepsilon_p S J_p \Big|_{z=L} dt}_{\substack{\text{output of solute} \\ \text{at } z = L}} = Q \begin{pmatrix} \text{accumulation of solute} \\ \text{from } t = 0 \text{ to any } t \end{pmatrix} \tag{11-69}$$

Use of Eqs. (11-63) and (11-68) yields the following result upon carrying out the integration indicated by Eq. (11-69):

$$Q = \frac{8 \varepsilon_p S L}{\pi^2} C_p^0 \left[\frac{\pi^2}{8} - \sum_{m=1}^{\infty} \frac{e^{-(2m-1)^2\,\delta t}}{(2m-1)^2} \right] \tag{11-70}$$

Simultaneous Pore Diffusion and Surface Diffusion

The model in which the slowest step is the simultaneous diffusion through the pores and the solid appears to have been proposed first by Damköhler(7). The further assumption that a state of equilibrium exists between the gas phase and the adsorbed phase at each z throughout each pore is made, that is,

$$C_s = mC_p + b \tag{11-71}$$

where the subscript i has been dropped because only one component, the solute, is assumed to be a candidate for adsorption. Initially the pore is filled with an inert component which is not adsorbed. At time $t \geq 0$, pure solute is available at the entrance ($z = 0$) to the pore, and the pore is assumed to be closed at the other end ($z = L$).

Let the rate of diffusion of the solute i along the surface of the pore be denoted by

$$J_{si} = -D_{si}\frac{\partial C_{si}}{\partial z} \tag{11-72}$$

where J_{si} = moles of solute i diffusing in the positive direction of z per unit time per unit of pellet surface perpendicular to z
C_{si} = moles of solute adsorbed per unit volume of pellet

A material balance on the solute over the time period from t_n to $t_n + \Delta t$ and the element of volume of a pellet from z_j to $z_j + \Delta z$ is given by

$$\int_{t_n}^{t_n+\Delta t}\left[(\varepsilon_p SJ_p + SJ_s)\Big|_{z_j,t} - (\varepsilon_p SJ_p + SJ_s)\Big|_{z_j+\Delta z,\,t}\right]dt$$

$$= \int_{z_j}^{z_j+\Delta z}\left[(\varepsilon_p SC_p + SC_s)\Big|_{t_n+\Delta t,\,z} - (\varepsilon_p SC_p + SC_s)\Big|_{t_n,\,z}\right]dz \tag{11-73}$$

Application of the mean-value theorems followed by the limiting process wherein Δz and Δt are allowed to go to zero yields

$$-\frac{\partial(\varepsilon_p SJ_p + SJ_s)}{\partial z} = \frac{\partial(\varepsilon_p SC_p + SC_s)}{\partial t} \qquad (0 < z < L,\ t > 0) \tag{11-74}$$

where ε_p = volume of pores per unit volume of pellet
S = cross-sectional area of the cylindrical pellet

If it is now assumed that ε_p, S, D_p, and D_s are independent of time and position, Eqs. (11-63) and (11-72) may be used to eliminate J_p and J_s from Eq. (11-74) to give

$$\varepsilon_p D_p\frac{\partial^2 C_p}{\partial z^2} + D_s\frac{\partial^2 C_s}{\partial z^2} = \varepsilon_p\frac{\partial C_p}{\partial t} + \frac{\partial C_s}{\partial t} \tag{11-75}$$

Use of Eq. (11-71) to express C_s in terms of C_p yields

$$D\frac{\partial^2 C_p}{\partial z^2} = \frac{\partial C_p}{\partial t} \qquad (0 < z < L,\ t > 0) \tag{11-76}$$

where

$$D = \frac{\varepsilon_p D_p + mD_s}{1 + m}$$

The following initial conditions and boundary conditions were used by Damköhler:

$$\begin{aligned} C_p(0, t) &= C_p^0 && (z = 0,\ t > 0)\\ \frac{\partial C_p(L, t)}{\partial z} &= 0 && (z = L,\ t > 0)\\ C_p(z, 0) &= 0 && (0 \leq z \leq L,\ t = 0) \end{aligned} \tag{11-77}$$

The solution which satisfies the partial differential equation (Eq. (11-76)) and the conditions given by Eq. (11-77) is

$$C_p(z, t) = C_p^0\left\{1 - \frac{4}{\pi}\sum_{n=0}^{\infty}\frac{\left\{\exp\left[-\left(\frac{2n+1}{2L}\right)^2\pi^2\,Dt\right]\right\}\left[\sin\left(\frac{2n+1}{2L}\right)\pi z\right]}{(2n+1)}\right\} \tag{11-78}$$

Profiles of the solute concentration in the pores at different times as predicted by Eq. (11-78) are shown in Fig. 11-6. The values of the parameters used

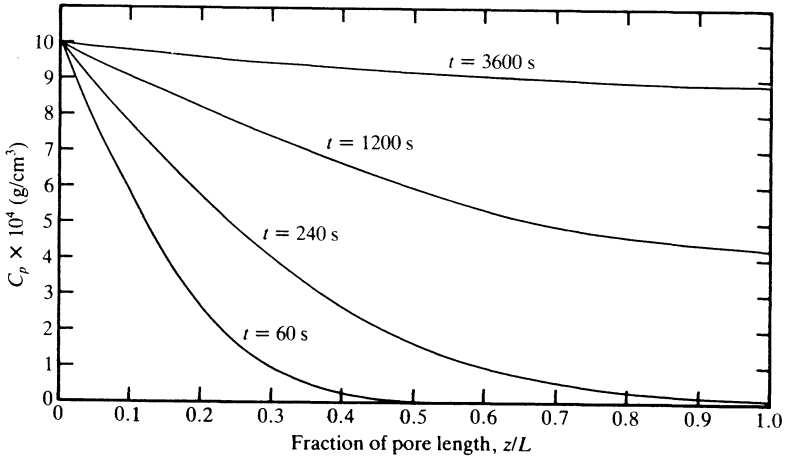

Figure 11-6 Concentration profiles in the pores as predicted by Eq. (11-78). ($C_p^0 = 0.001$ gm/cm^3, $L = 0.1$ cm, $D_p = 8.0 \times 10^{-6}$ cm^2/s.)

to obtain these profiles are as follows: $C_p^0 = 0.001$ g/cm^3, $L = 0.1$ cm, $D_p = 8.0 \times 10^{-6}$ cm^2/s, $D_s = 1.5 \times 10^{-7}$ cm^2/s, $\varepsilon_p = 0.7$, $m = 1.1$, and $D = 2.745 \times 10^{-6}$ cm^2/s. Again, it is to be observed that at low adsorptions or small times, the concentration profiles are steep and become flatter as the amount adsorbed increases. Also, observe that the concentration gradient is zero at $z/L = 1.0$ as required by the second condition of Eq. (11-77).

Damkhöler obtained the following expression for the fractional approach to equilibrium

$$E = 1 - \frac{8}{\pi^2} \sum_{n=0}^{\infty} \frac{e^{-(2n+1/2L)^2 \pi^2 \, Dt}}{(2n+1)^2} \tag{11-79}$$

where

$$E = \frac{\int_0^L C_p(z, t)\, dz}{LC_p^0}$$

In addition to the solutions of McBain and Damköhler, other authors have obtained solutions to the partial differential for other sets of initial and boundary conditions. (See, for example, Wicke(28).)

NOTATION

a_d = interfacial area between the fluid phase and the solid phase per unit volume of empty column
a_j = parameter appearing in the development of the BET equation
a_s = interfacial area between the fluid phase and the solid phase per unit volume of pellet
b = a constant in Langmuir's isotherm, defined by Eqs. (11-6) and (11-7)
b_i = intercept in the linear equilibrium relationship (see Eqs. (11-31), (11-35), (11-36), and (11-40))
b_j = parameter appearing in the development of the BET equation
c = number of components in the mixture
C_{di} = concentration of component i at the bulk conditions of the fluid stream, moles per unit of void volume, the free volume between the pellets (C_{di}^{I} is the concentration of component i at the fluid–solid interface; C_{di}^{*} is the concentration which component i would have in the fluid phase if it were in equilibrium with component i in the solid phase with the concentration C_{si})
C_{ji} = concentration of adsorbed component i in the jth layer, moles per unit mass of adsorbent
C_i = total concentration of adsorbed component i, moles per unit mass of adsorbent

C_{pi} = concentration of component i in the pore of an adsorbent, moles of component i per unit pore volume
C_{Sj} = concentration of vacant sites in the jth layer, moles per unit mass of adsorbent
C_{si} = concentration of component i in the adsorbed phase, moles per unit volume of pellet
D_{pi} = diffusion coefficient for the diffusion of component i in the pore of an adsorbent, dimensions of (length)^2 per unit time
D_{si} = diffusion coefficient for the diffusion of component i through the solid phase of an adsorbent, dimensions of (length)^2 per unit time
D = diffusion coefficient defined beneath Eq. (11-76)
E = fractional approach to equilibrium (defined beneath Eq. (11-80))
E_L = heat of liquefaction
E_j = heat of adsorption of the jth layer
J_{pi} = moles of component i diffusing into a pore in the positive direction of z per unit time per unit of void area perpendicular to z (see Eq. (11-63))
J_{si} = moles of component i diffusing in the positive direction z per unit time per unit of pellet surface perpendicular to z
k_{ji} = rate constant for the adsorption of component i in layer j
k'_{ji} = rate constant for the desorption of component i from layer j
K_{ji} = adsorption equilibrium constant for component i adsorbed in layer j ($K_{ji} = k_{ji}/k'_{ji'}$)
k_{di} = mass transfer coefficient for component i (volume of empty column per unit time per unit of interfacial area (see Eq. (11-30)))
k_{si} = mass transfer coefficient for component i (pellet volume per unit time per unit of interfacial area (see Eq. (11-32))
K_{di} = overall mass transfer coefficient, same units as k_{di} (defined by Eq. (11-39))
K_{si} = overall mass transfer coefficient, same units as k_{si} (defined below Eq. (11-37))
L = length of pore
m_i = slope of equilibrium relationship (see, for example, Eq. (11-31) and (11-36))
P = total pressure
p_i = partial pressure of component i
q = energy per molecule (see Eq. (11-7))
Q = accumulation of adsorbed solute (defined by Eq. (11-69))
r_{di} = moles of component i transferred per unit time per unit volume of empty bed
r_{si} = moles of component i transferred per unit time per unit volume of pellet
s_j = surface area covered by j layers (appears in the development of the BET equation)

S = cross-sectional area
S_j = moles of sites on surface S_{j-1} which are covered by adsorbed molecules
t = time
T = temperature
u_f = linear velocity
v = volume of gas adsorbed (at 0°C and 1 atm) per unit mass of adsorbent
v_m = volume of gas adsorbed (at 0°C and 1 atm) per unit mass of adsorbent when the adsorbent is covered with a complete unimolecular layer
w = mole fraction which the solute would have in the fluid phase if it were in equilibrium with the adsorbed phase
y = mole fraction of solute in the fluid phase
z = positive direction for mass transfer

Greek Letters

α = fraction of the molecules striking the surface which stick
δ = constant appearing in Eq. (11-68)
ε = volume of voids between the pellets per unit volume of bed
ε_p = volume of pores per unit volume of pellet
ν = rate of evaporation from a completely covered surface (also used to denote the ratio defined by Eq. (11-28))
μ = number of molecules striking a unit surface per unit time
ϕ_j = a parameter defined by Eq. (11-21)
ξ = dummy variable of integration
θ = fraction of the adsorption surface covered by a unimolecular layer of adsorbed molecules
ρ_d = density of the fluid phase

REFERENCES

1. James R. Arnold: "Adsorption of Gas Mixtures. Nitrogen–Oxygen on Anatase," *J. Am. Chem. Soc.*, **71**: 104 (1949).
2. A. Anzelius: "Uber Erwarming vermittels durchstromender Medien," *Z. Angew. Math. Mech.*, **6**: 291 (1926).
3. S. Brunauer, L. S. Deming, W. E. Deming, and E. Teller: "On a Theory of Van der Waals Adsorption of Gases," *J. Am. Chem. Soc.* **62**: 1723 (1940).
4. S. Brunauer: *The Adsorption of Gases and Vapors*, Princeton University Press, Princeton, 1945.
5. S. Brunuaer, P. H. Emmett, and E. Teller: "Adsorption of Gases in Multicomponent Layers," *J. Am. Chem. Soc.*, **60**: 309 (1939).
6. R. V. Churchill: *Operational Mathematics*, 2d ed., McGraw-Hill Book Company, New York, 1958.
7. G. Damköhler: Uber Die Adsorption geschwindigkert Von Gasen an Porosen Adsorbentien, *Z. Phys. Chem.*, **174**: 222 (1935).
8. R. H. Fowler: "A Statistical Derivation of Langmuir's Adsorption Isotherm," *Proc. Cambridge Philos. Soc.*, **31**: 260 (1935).

9. C. C. Furnas: "Heat Transfer from a Gas Stream to a Bed of Broken Solids," *Trans. Am. Inst. Chem. Eng.*, **24**: 142 (1930).
10. W. Fritz and E. V. Schulender: "Simultaneous Adsorption Equilibria of Organic Solutes in Dilute Aqueous Solutions on Activated Carbon," *Chem. Eng. Sci.*, **29**: 1279 (1974).
11. A. J. Gonzalez and C. D. Holland. "Adsorption Equilibria of Multicomponent Mixtures by Solid Adsorbents," *AIChE J.*, **16**: 718 (1970).
12. A. J. Gonzalez and C. D. Holland: "Adsorption Equilibria of Light Hydrocarbon Gases on Activated Carbon and Silica Gel," *AIChE J.*, **17**: 1080 (1971).
13. T. L. Hill: "Theory of Multimolecular Adsorption from a Mixture of Gases," *J. Chem. Phys.*, **14**: 265 (1946).
14. O. A. Hougen and W. R. Marshall, Jr.: "Adsorption from a Fluid Stream Flowing through a Stationary Granular Bed," *Chem. Eng. Prog.*, **43**: 197 (1947).
15. E. Glueckauf: "Theory of Chromatography, Part 10: Formulae for Diffusion into Spheres and their Application to Chromatography," *Trans. Faraday Soc.*, **51**: 1540 (1955).
16. O. A. Hougen and K. M. Watson: *Chemical Process Principles*, Part III, John Wiley & Sons, New York, 1948.
17. I. Langmuir: "Chemical Reactions at Very Low Pressures," *J. Am. Chem. Soc.*, **35**: 105 (1913).
18. I. Langmuir: "Chemical Reactions at Low Pressures," *J. Am. Chem. Soc.*, **37**: 1139 (1915).
19. I. Langmuir: "The Adsorption of Gases on Plane Surface of Glass, Mica, and Platinum," *J. Am. Chem. Soc.*, **40**: 1361 (1918).
20. T. W. Leland, Jr., and R. E. Holmes: "The Design of Hydrocarbon Recovery Units Using Solid Adsorbents," *J. Pet. Tech.*, **179** (February 1962).
21. L. B. Loeb: *Kinetic Theory of Gases*, McGraw-Hill Book Company, New York, 1927.
22. E. C. Markham and A. Benton: "The Adsorption of Gas Mixtures by Silica," *J. Am. Chem. Soc.*, **53**: 497 (1931).
23. W. R. Marshall, Jr., and R. L. Pigford: *The Application of Differential Equations to Chemical Engineering Problems*, University of Delaware, 1947.
24. J. Mason and C. E. Cooke, Jr.: "Adsorption of Hydrocarbon Mixtures at High Pressure," *AIChE J.*, **12**: 1097 (1966).
25. J. W. McBain: "Der Mechanisms der Adsorption ("Sorption") von Wasserstoff durch Kohlenstoff," *Z. Phys. Chem.*, **68**: 471 (1908).
26. H. S. Mickley, T. K. Sherwood, and C. E. Reed: *Applied Mathematics in Chemical Engineering*, 2d ed., McGraw-Hill Book Company, New York, 1957.
27. M. Volmer: "Thermodynamische der Zustangleichung fur Adsorbierte Stoffe," *Z. Phys. Chem.*, **115**: 253 (1925).
28. Von E. Wicke: "Empirische and Theoretische Utersuchungen der Sorptiongeschwindig kert von Gasen an porosen Stoffen I," *Kolloid Z.*, **86**: 167 (1939).

PROBLEMS

11-1 On the basis of the postulate given by Eq. (11-27), show that

(*a*) $K_{2i} = \nu K_{1i}$; $K_{3i} = \nu^2 K_{2i}$; ...; $K_{ni} = \nu^{n-1} K_{1i}$

(*b*) $\phi_2 = \nu\phi_1$; $\phi_3 = \nu^2\phi_1$; ...; $\phi_n = \nu^{n-1}\phi_1$

11-2 On the basis of the relationship given by Eqs. (11-19) and (11-27), show that the ratio of the concentration of component i to that of any arbitrary component k in the jth layer is equal to this same ratio in the $j+1$st layer, that is, show that

$$\frac{C_{1i}/C_{1k}}{C_{2i}/C_{2k}} = \frac{C_{2i}/C_{2k}}{C_{3i}/C_{3k}} = \cdots = \frac{C_{n-1,i}/C_{n-1,k}}{C_{ni}/C_{nk}} = 1$$

11-3 On the basis of the relationship given by Eq. (11-27), show that the relationship given by Eq. (11-28) follows as a consequence from Eq. (11-26).

11-4 (*a*) When the rate expressions for the transfer of mass to and from the interface of the adsorbent are given by Eq. (11-35) and the relationship between concentrations in the adsorbed phase and the fluid phase are given by Eq. (11-36), obtain the expression given by Eq. (11-37) for r_{si} and the formula given below it for the overall mass transfer coefficient K_{si}.

(*b*) Obtain the expression given by Eq. (11-38) for r_{di} and Eq. (11-39) for K_{di}.

11-5 Use the mean-value theorems and the appropriate limiting process needed to obtain Eq. (11-42) from Eq. (11-41).

11-6 In the same manner as described in Prob. 11-5, obtain Eq. (11-44) from Eq. (11-43).

11-7 Use Laplace transforms to solve Eqs. (11-55) and (11-56) subject to the initial condition and boundary condition given by Eqs. (11-57) and (11-58).

11-8 Apply the mean-value theorems and the limiting process required to reduce Eq. (11-64) to Eq. (11-65).

11-9 (*a*) Obtain the solution which satisfies the partial differential equation given by Eq. (11-66) and the conditions given by Eq. (11-67). To solve by the product method for the separation of variables, the following suggestion is made for obtaining the solution given by Eq. (11-68).

Hint: Define a new function $V(z, t)$ and $\phi(z)$ as follows:

$$C_p(z, t) = V(z, t) + \phi(z)$$

where $\phi(z)$ is further defined by

$$\phi(0) = C_p^0 \qquad (t > 0)$$

$$\phi(L) = C_p^0 \qquad (t > 0)$$

$$\frac{\partial^2 \phi}{\partial z^2} = 0 \qquad (0 < z < L, t > 0)$$

(*b*) Obtain the expression given by Eq. (11-69) for the accumulation Q.

11-10 (*a*) Obtain the solution given by Eq. (11-78) which satisfies the partial differential equation (Eq. (11-76)) and the conditions given by Eq. (11-77).

Hint: Define the new functions $V(z, t)$ and $\phi(z)$ as follows:

$$C_p(z, t) = V(z, t) + \phi(z)$$

$$\phi(0) = C_p^0$$

$$\frac{\partial^2 \phi(z)}{\partial z^2} = 0$$

$$\frac{\partial \phi(L)}{\partial z} = 0$$

(*b*) Obtain the result given by Eq. (11-79).

11-11 Show that Eqs. (11-46) and (11-47) may be restated in the forms given by Eqs. (11-51) and (11-52), respectively.

11-12 Use the change in variables given by Eq. (11-53) to transform Eqs. (11-51) and (11-52) to the form given by Eqs. (11-55) and (11-56).

CHAPTER

TWELVE

SEPARATION OF MULTICOMPONENT MIXTURES BY USE OF ADSORPTION COLUMNS

In Sec. 12-1 the Glueckauf model which was developed in Chap. 11 is used to model the separation of a multicomponent mixture in a fixed-bed adsorption column. The equations are solved by use of a combination of the method of characteristics and the trapezoidal rule. The results predicted by the model for a typical column are compared with the observed experimental results (see Example 12-1).

In Sec. 12-2 a model based on pore and axial diffusion is developed. The method of solution consists of a combination of orthogonal collocation and the semi-implicit Runge–Kutta method. In Example 12-2, the results predicted by the model are compared with those observed experimentally.

In Sec. 12-3 a model for an adiabatically operated fixed-bed adsorption column is developed. The equations describing the model are solved by use of a combination of the method of characteristics, the trapezoidal rule, and the Newton–Raphson method.

In Sec. 12-4, a brief description of the periodic operation of a commercial adsorption column is presented.

12-1 THE GLUECKAUF MODEL

The equations for this model were developed in Chap. 11. Isothermal operation and perfect mixing in the radial direction of the column were assumed as well as a negligible change in the flow rate of the gas stream through the bed. The

rate of mass transfer is given by

$$r_{si} = \frac{\partial C_{si}}{\partial t} = K_{si} a_s (C_{si}^* - C_{si}) \tag{12-1}$$

A mass balance on any component i is given by

$$-u_f \frac{\partial C_{di}}{\partial z} - \left(\frac{1-\varepsilon}{\varepsilon}\right) \frac{\partial C_{si}}{\partial t} = \frac{\partial C_{di}}{\partial t} \tag{12-2}$$

The initial conditions and the boundary conditions are as follows:

$$C_{si}(z, 0) = C_{si}^0 \qquad (0 \le z \le z_T, t \le 0) \tag{12-3}$$

$$C_{di}(z, 0) = 0 \qquad (0 \le z \le z_T, t \le 0) \tag{12-4}$$

$$C_{di}(0, t) = C_{di}^0 \qquad (z = 0, t > 0) \tag{12-5}$$

Elimination of the time derivative of C_{si} from Eq. (12-2) by use of Eq. (12-1) gives

$$u_f \frac{\partial C_{di}}{\partial z} + \frac{\partial C_{di}}{\partial t} = \left(\frac{\varepsilon - 1}{\varepsilon}\right) K_{si} a_s (C_{si}^* - C_{si}) \tag{12-6}$$

Let the following dimensionless variables be defined

$$\tau = \frac{u_f t}{z_T} \qquad Z = \frac{z}{z_T} \qquad \bar{C}_{si} = C_{si}/C_{si}^{*0}$$

$$\bar{C}_{si}^* = C_{si}^*/C_{si}^{*0} \qquad C_{si}^{*0} = C_{si}^*(C_{di}^0) = g_i(C_{di}^0) \tag{12-7}$$

$$\bar{C}_{di} = C_{di}/C_{di}^0$$

where the g_i's are the functional forms of the equilibrium relationships which are shown below. After the change in variables has been made, Eq. (12-6) reduces to

$$\frac{\partial \bar{C}_{di}}{\partial Z} + \frac{\partial \bar{C}_{di}}{\partial \tau} = \left(\frac{z_T}{u_f C_{di}^0}\right)\left(\frac{\varepsilon - 1}{\varepsilon}\right) K_{si} a_s C_{si}^{*0} (\bar{C}_{si}^* - \bar{C}_{si}) \tag{12-8}$$

Similarly, with the change in variables given by Eq. (12-7), Eq. (12-1) becomes

$$\frac{\partial \bar{C}_{si}}{\partial \tau} = \left(\frac{K_{si} a_s z_T}{u_f}\right)(\bar{C}_{si}^* - \bar{C}_{si}) \tag{12-9}$$

and the initial and boundary conditions in terms of the new variables are

$$\bar{C}_{si}(Z, 0) = C_{si}^0/C_{si}^{*0} \qquad (0 \le Z \le 1, \tau \le 0) \tag{12-10}$$

$$\bar{C}_{di}(Z, 0) = 0 \qquad (0 \le Z \le 1, \tau \le 0) \tag{12-11}$$

$$\bar{C}_{di}(0, \tau) = 1 \qquad (Z = 0, \tau > 0) \tag{12-12}$$

Equations (12-8) and (12-9) may be solved by the Method of Characteristics as described in Chap. 10. The choice of the characteristics is made as outlined

below. Expansion of $\bar{C}_{di}$ by the chain rule gives

$$\frac{d\bar{C}_{di}}{dZ} = \frac{\partial \bar{C}_{di}}{\partial Z}\frac{dZ}{dZ} + \frac{\partial \bar{C}_{di}}{\partial \tau}\frac{d\tau}{dZ} \tag{12-13}$$

Let $d\tau/dZ = 1$ for characteristic I. Thus, Eq. (12-13) becomes

$$\left(\frac{d\bar{C}_{di}}{dZ}\right)_{\text{I}} = \frac{\partial \bar{C}_{di}}{\partial Z} + \frac{\partial \bar{C}_{di}}{\partial \tau} \qquad (\text{along } d\tau/dZ = 1) \tag{12-14}$$

and Eq. (12-8) is reduced from a partial to an ordinary differential equation, namely,

$$\left(\frac{d\bar{C}_{di}}{dZ}\right)_{\text{I}} = \left(\frac{z_T}{u_f C_{di}^0}\right)\left(\frac{\varepsilon - 1}{\varepsilon}\right) K_{si} a_s C_{si}^{*0} (\bar{C}_{si}^* - \bar{C}_{si}) \qquad (\text{along } d\tau/dZ = 1) \tag{12-15}$$

Consider now the reduction of Eq. (12-9) from a partial to an ordinary differential equation by the Method of Characteristics. Expansion of $\bar{C}_{si}$ by the chain rule gives

$$\frac{d\bar{C}_{si}}{d\tau} = \frac{\partial \bar{C}_{si}}{\partial \tau}\frac{d\tau}{d\tau} + \frac{\partial \bar{C}_{si}}{\partial Z}\frac{dZ}{d\tau} \tag{12-16}$$

Let $dZ/d\tau = 0$, or $Z =$ constant for characteristic II. Thus, Eq. (12-16) reduces to

$$\left(\frac{d\bar{C}_{si}}{d\tau}\right)_{\text{II}} = \frac{\partial \bar{C}_{si}}{\partial \tau} \qquad (\text{along } Z = \text{const}) \tag{12-17}$$

and consequently Eq. (12-9) becomes

$$\left(\frac{d\bar{C}_{si}}{d\tau}\right)_{\text{II}} = \left(\frac{K_{si} a_s z_T}{u_f}\right)(\bar{C}_{si}^* - \bar{C}_{si}) \qquad (\text{along } Z = \text{const}) \tag{12-18}$$

Next, for convenience, let the quantities χ and θ be defined as follows:

$$\chi = \left(\frac{z_T}{u_f C_{di}^0}\right)\left(\frac{\varepsilon - 1}{\varepsilon}\right)(K_{si} a_s C_{si}^{*0}) \tag{12-19}$$

$$\theta = \frac{K_{si} a_s z_T}{u_f} \tag{12-20}$$

Then the two ordinary differential equations which are to be solved simultaneously are

$$\left(\frac{d\bar{C}_{di}}{dZ}\right)_{\text{I}} = \chi(\bar{C}_{si}^* - \bar{C}_{si}) \qquad (\text{along } d\tau/dZ = 1) \tag{12-21}$$

$$\left(\frac{d\bar{C}_{si}}{d\tau}\right)_{\text{II}} = \theta(\bar{C}_{si}^* - \bar{C}_{si}) \qquad (\text{along } Z = \text{const}) \tag{12-22}$$

Values of the mass transfer coefficient $K_{si}a_s$ for each component were estimated separately by Balzi et al.(1) by matching the model predictions to the single-component breakthrough curves from a column 41 cm long.

Example 12-1 A liquid mixture of butanol-2, *t*-amylalcohol, and phenol is passed over a fixed-bed adsorption column which contains activated carbon as the adsorbent. On the basis of the Glueckauf model developed above, determine the concentration profiles for $C_{d1}(z, t)$, $C_{d2}(z, t)$ and $C_{d3}(z, t)$ for columns having lengths $z_T = 0.41$ m, and $z_T = 0.82$ m. Butanol-2 is denoted as component 1, *t*-amylalcohol as component 2, and phenol as component 3.

The equilibrium relationships for this ternary system are given by

$$C_{s1}^* = \frac{1.05C_{d1}^{1.134}}{C_{d1}^{0.73} + 1.44C_{d2}^{0.793} + 0.53C_{d3}^{0.467}} = g_1(C_{di}) \qquad (12\text{-}23)$$

$$C_{s2}^* = \frac{1.09C_{d2}^{1.182}}{C_{d2}^{0.831} + 0.52C_{d1}^{0.884} + 0.30C_{d3}^{0.536}} = g_2(C_{di}) \qquad (12\text{-}24)$$

$$C_{s3}^* = \frac{0.79C_{d3}^{0.224}}{C_{d3}^{0.002} + 1.07C_{d1}^{0.286} + 0.79C_{d2}^{0.235}} = g_3(C_{di}) \qquad (12\text{-}25)$$

The values of the system parameters are: $u_f = 0.002\,72$ m/s, $\varepsilon = 0.5$, $K_{s1}a_s = 6912\ s^{-1}$, $K_{s2}a_s = 6336\ s^{-1}$, $K_{s3}a_s = 4248\ s^{-1}$, $C_{s1}^0 = C_{s2}^0 = C_{s3}^0 = 0$, $C_{d1}^0 = 0.915$ kg/m^3, $C_{d2}^0 = 0.912$ kg/m^3, and $C_{d3}^0 = 0.997$ kg/m^3. The adsorbent material was Filtrasorb 400, and the above values were taken from Ref. 1.

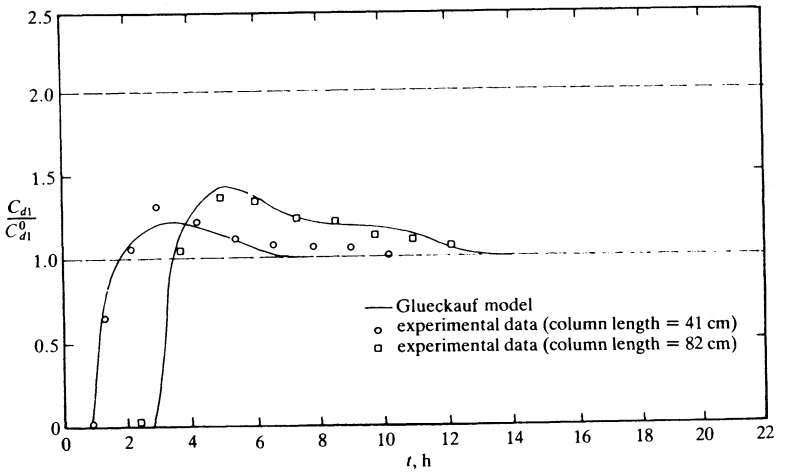

Figure 12-1 Breakthrough curve of butanol-2 in simultaneous three-component adsorption

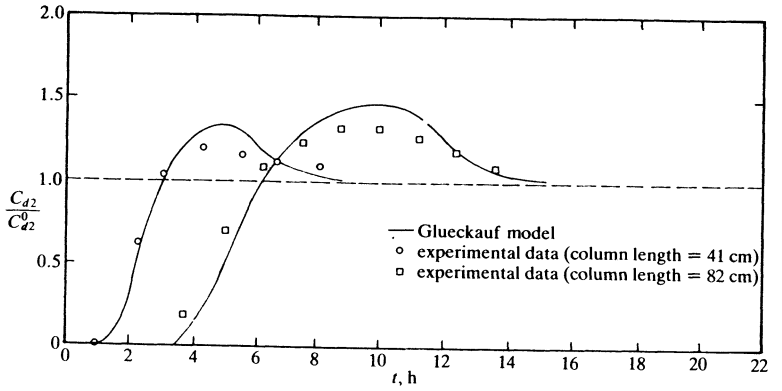

Figure 12-2 Breakthrough curve of *t*-amylalcohol in simultaneous three-component adsorption

Equations (12-21) and (12-22) were solved simultaneously for this system through the use of the trapezoidal rule in a manner similar to that described for Example 12-3 except for the fact that the semi-implicit Runge–Kutta method was used in Example 12-3 in lieu of the trapezoidal rule. The results obtained by the solution of the Glueckauf model for this example are presented in Figs. 12-1 through 12-3.

Although the Glueckauf model predicts the appropriate trends, it does not fit the experimental data very well. In the case of phenol, the breakthrough times predicted are much later than those observed experimentally. This discrepancy between theory and experiment is attributed primarily to the fact that in the Glueckauf model, the resistance to intraparticle diffusion was neglected. Also axial diffusion of mass in the flowing stream was neglected in this model. In the next section a more comprehensive mass diffusional model is presented.

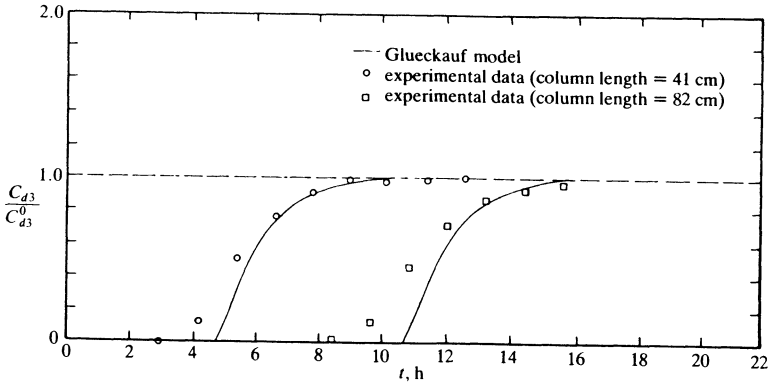

Figure 12-3 Breakthrough curve of phenol in simultaneous three-component adsorption

12-2 THE FILM RESISTANCE AND DIFFUSION MODEL

The adsorption of solute components from a fluid stream as it passes through a fixed-bed adsorption column may be represented by a model which is based on three transport mechanisms. These mechanisms are as follows: (1) axial diffusion in the direction of flow of the fluid, (2) transfer of the solute from the bulk conditions of the fluid stream to the opening of the pore, and (3) transport of the solute through the pore by diffusion. The development of the equations required to describe this model follow.

Material Balance on Component i in the Fluid Stream

Consider a cyclindrical adsorption column which is filled with cyclindrical pellets through which the fluid stream containing the solutes is flowing. Let the cross-sectional area of the column be denoted by S and the linear velocity of the stream by u_f.

In the development of the first equation given below it is supposed that the adsorbent pellets are cyclindrical. Mass transfer from the fluid stream to the ends of the pellets is taken to be negligible in order to avoid the difficulty of treating two-dimensional diffusion within the pellets. Pore diffusion is assumed to occur in the radial direction in the pellets and from the exterior of the pellet at $r = r_0$ to the principal axis of the pellet at $r = 0$.

The rate of mass transfer of a solute in the axial direction (the direction of flow of the fluid stream) by diffusion is denoted by J_{Li} (moles of solute i diffusing in the positive direction of z per unit time per unit of void area perpendicular to the direction z) and

$$J_{Li} = -D_{Li}\frac{\partial C_{di}}{\partial z} \tag{12-26}$$

The rate of mass transfer from the bulk conditions of the fluid stream to the external pellet surface (the opening of the pores) is given by

$$r_{Li} = K_{Li}a(C_{di} - C_{pi})\Big|_{r_0} \tag{12-27}$$

where r_{Li} = moles of solute i transferred per unit time per unit of pellet volume
a = surface area of the cyclindrical pellet per unit of volume of the pellet $= (2\pi r_0 L)/(\pi r_0^2 L) = 2/r_0$

The material balance on solute i over the time period from t_n to $t_n + \Delta t$ over the element of volume of the adsorption bed from z to $z + \Delta z$ is given by

$$\int_{t_n}^{t_n+\Delta t}\left[u_f S\varepsilon C_{di}\Big|_{z_j,\,t} - u_f S\varepsilon C_{di}\Big|_{z_j+\Delta z,\,t} + \varepsilon S J_{Li}\Big|_{z_j,\,t} - \varepsilon S J_{Li}\Big|_{z_j+\Delta z,\,t} - \int_{z_j}^{z_j+\Delta z} r_{Li}(1-\varepsilon)S\,dz\right]dt = \int_{z_j}^{z_j+\Delta z}\left(\varepsilon S C_{di}\Big|_{t_n+\Delta t,\,z} - \varepsilon S C_{di}\Big|_{t_n,\,z}\right)dz \tag{12-28}$$

Application of the mean-value theorems followed by the limiting process wherein Δz and Δt are allowed to go to zero gives the following result upon observing that z_j and t_n were arbitrarily selected

$$-u_f\frac{\partial C_{di}}{\partial z} - \frac{\partial J_{Li}}{\partial z} - \left(\frac{1-\varepsilon}{\varepsilon}\right)r_{Li} = \frac{\partial C_{di}}{\partial t} \tag{12-29}$$

Substitution of the expressions for J_{Li} and r_{Li} into Eq. (12-29) yields

$$-u_f\frac{\partial C_{di}}{\partial z} + D_{Li}\frac{\partial^2 C_{di}}{\partial z^2} - \left(\frac{1-\varepsilon}{\varepsilon}\right)\left(\frac{2}{r_0}\right)K_{Li}(C_{di} - C_{pi})\Big|_{r_0} = \frac{\partial C_{di}}{\partial t} \tag{12-30}$$

For the case where the column is filled with spherical pellets, the material balance corresponding to Eq. (12-30) is obtained by replacing $2/r_0$ in Eq. (12-30) by $3/r_0$.

Pore Diffusion

After the solute molecules have been transported from the bulk conditions of the fluid phase to the exterior of the pellets, they are transported to the interior of the pellets by the mechanism of pore diffusion. For diffusion in the positive direction of r instead of z, the variable z is replaced by the variable r in Eq. (12-26) to obtain the following defining equations for the pore and solid phase diffusion rates J_{pi} and J_{si}, respectively:

$$J_{pi} = -D_{pi}\frac{\partial C_{pi}}{\partial r} \tag{12-31}$$

$$J_{si} = -D_{si}\frac{\partial C_{si}}{\partial r} \tag{12-32}$$

Again, as in the case of cylindrical pellets, mass transfer through the ends of the pellet is neglected in order to avoid the necessity for treating two-dimensional diffusion within the pellet.

Material balance A material balance on solute i in the element of volume from z_j to $z_j + \Delta z$ (the direction of fluid flow of the fluid stream) and r_j to $r_j + \Delta r$ over the time period from t_n to $t_n + \Delta t$ is given by

$$\int_{t_n}^{t_n+\Delta t}\int_{z_j}^{z_j+\Delta z}\left[2\pi r(\varepsilon_p J_{pi} + J_{si})\Big|_{r_j,\,t,\,z} - 2\pi r(\varepsilon_p J_{pi} + J_{si})\Big|_{r_j+\Delta r,\,t,\,z}\right]dz\,dt = \int_{r_n}^{r_n+\Delta r}\int_{z_j}^{z_j+\Delta z}2\pi r\left[(\varepsilon_p C_{pi} + C_{si})\Big|_{t_n+\Delta t,\,z,\,r} - (\varepsilon_p C_{pi} + C_{si})\Big|_{t_n,\,z,\,r}\right]dz\,dr \tag{12-33}$$

where ε_p = volume of pores in the pellet per unit of volume of pellet

Application of the mean-value theorems to Eq. (12-33) followed by the limiting process wherein Δz, Δr, and Δt are allowed to go to zero, and observing that z_j,

r_j, and t_n were all arbitrarily selected yields

$$\frac{1}{r}\frac{\partial}{\partial r}\left[r\left(\varepsilon_p D_{pi}\frac{\partial C_{pi}}{\partial r}+D_{si}\frac{\partial C_{si}}{\partial r}\right)\right]=\varepsilon_p\frac{\partial C_{pi}}{\partial t}+\frac{\partial C_{si}}{\partial t} \tag{12-34}$$

For the case where the column is filled with spherical pellets and r denotes the radius of the sphere, Eq. (12-33) becomes

$$\int_{t_n}^{t_n+\Delta t}\left[4\pi r^2(\varepsilon_p J_{pi}+J_{si})\Big|_{r_j,\,t}-4\pi r^2(\varepsilon_p J_{pi}+J_{si})\Big|_{r_j+\Delta r,\,t}\right]dt$$

$$=\int_{r_j}^{r_j+\Delta\pi}4\pi r^2\left[(\varepsilon_p C_{pi}+C_{si})\Big|_{t_n+\Delta t,\,r}-(\varepsilon_p C_{pi}+C_{si})\Big|_{t_n,\,r}\right]dr \tag{12-35}$$

and the corresponding partial differential equation is given by

$$\frac{1}{r^2}\frac{\partial\left[r^2\left(\varepsilon_p D_{pi}\frac{\partial C_{pi}}{\partial r}+D_{si}\frac{\partial C_{si}}{\partial r}\right)\right]}{\partial r}=\varepsilon_p\frac{\partial C_{pi}}{\partial t}+\frac{\partial C_{si}}{\partial t} \tag{12-36}$$

The cross-diffusion coefficients D_{pij} for components i and j were taken equal to zero for $i\neq j$ ($D_{pij}=0$, $i\neq j$) in this development. Liapis and Litchfield(2) showed that the cross coefficients are one or two orders of magnitude smaller than the D_{pii}'s and may be neglected with good accuracy.

It has been the practice in the application of the film resistance and diffusion model to consider the pore diffusion to be fast relative to the parallel mechanism of solid diffusion, that is $J_{pi}\gg J_{si}$. Also, since, physical adsorption is assumed to be exceedingly fast, a state of equilibrium between the pore phase concentration C_{pi} and the adsorbed phase concentration C_{si} is assumed, that is, the following form of the chain rule may be used to evaluate $\partial C_{si}/\partial t$:

$$\frac{\partial C_{si}}{\partial t}=\sum_{j=1}^{c}\left(\frac{\partial C_{si}^*}{\partial C_{pj}}\right)\frac{\partial C_{pj}}{\partial t} \tag{12-37}$$

In view of the assumption that $J_{pi}\gg J_{si}$ and Eq. (12-37), the material balances given by Eqs. (12-34) and (12-36) reduce to

$$\frac{1}{r^\alpha}\frac{\partial\left(r^\alpha\varepsilon_p D_{pi}\frac{\partial C_{pi}}{\partial r}\right)}{\partial r}=\varepsilon_p\frac{\partial C_{pi}}{\partial t}+\sum_{j=1}^{c}\frac{\partial C_{si}^*}{\partial C_{pj}}\frac{\partial C_{pj}}{\partial t} \tag{12-38}$$

where $\alpha=1$ for cylindrical pellets, and $\alpha=2$ for spherical pellets.

Initial and boundary conditions for the film resistance and diffusion model Initially it is supposed that the concentrations of the solutes are equal to zero throughout the adsorption bed, that is,

$$C_{di}=0 \qquad (0\leq z\leq z_T,\ t\leq 0) \tag{12-39}$$

The boundary condition at the inlet $z=0$ of the adsorption bed is given by making a material balance at $z=0$

$$u_f C_{0i}(t)-u_f C_{di}\Big|_{z=0}-J_{Li}\Big|_{z=0}=0 \qquad (z=0,\ t>0)$$

or

$$u_f C_{0i}(t)-u_f C_{di}\Big|_{z=0}+D_{Li}\frac{\partial C_{di}}{\partial z}\Big|_{z=0}=0 \tag{12-40}$$

At the outlet of the adsorber ($z=z_T$), mass transfer by diffusion ceases or $J_{Li}=0$, and thus

$$\frac{\partial C_{di}}{\partial z}\Big|_{z=z_T}=0 \qquad (z=z_T,\ t>0) \tag{12-41}$$

(This boundary condition is analogous to the one in heat transfer in which the end of a bar is perfectly insulated.)

The rate of convective mass transport r_{Li} from the fluid phase to the surface ($r=r_0$) of a cyclindrical pellet plus the rates of pore and solid diffusion in the positive direction of r at r_0 must be equal to zero since there can be no accumulation at the surface $r=r_0$. Thus, at any time t

$$\int_{z_j}^{z_j+\Delta z}\left[(\varepsilon_p 2\pi r_0 J_{pi}+2\pi r_0 J_{si})\Big|_{r_0}+\pi r_0^2 r_{Li}\right]dz=0 \tag{12-42}$$

where it is supposed that the pellets are placed end to end in the direction z. Since the above holds for all z ($0<z<z_T$), it follows that

$$\varepsilon_p 2\pi r_0 J_{pi}\Big|_{r_0}+2\pi r_0 J_{si}\Big|_{r_0}+(\pi r_0^2)\left[K_{Li}\left(\frac{2}{r_0}\right)(C_{di}-C_{pi})\right]\Big|_{r_0}=0$$

or

$$\varepsilon_p D_{pi}\frac{\partial C_{pi}}{\partial r}\Big|_{r_0}+D_{si}\frac{\partial C_{si}}{\partial r}\Big|_{r_0}-K_{Li}(C_{di}-C_{pi})\Big|_{r_0}=0 \tag{12-43}$$

For a spherical pellet, the material balance corresponding to Eq. (12-43) at any $t>0$ is given by

$$\varepsilon_p 4\pi r_0^2 J_{pi}+4\pi r_0^2 J_{si}+\frac{4}{3}\pi r_0^3 K_{Li}\left(\frac{3}{r_0}\right)(C_{di}-C_{pi})\Big|_{r_0}=0 \qquad (0\leq z\leq z_T,\ t>0) \tag{12-44}$$

which is seen to reduce to Eq. (12-43). Since the assumption has been made that pore diffusion is fast relative to solid diffusion ($J_{si}\ll J_{pi}$), the above equations may be simplified by setting $J_{si}=0$ to give, for either a cyclindrical or a spherical pellet,

$$\varepsilon_p D_{pi}\frac{\partial C_{pi}}{\partial r}\Big|_{r_0}-K_{Li}(C_{di}-C_{pi})\Big|_{r_0}=0 \qquad (0\leq z\leq z_T,\ t>0) \tag{12-45}$$

Along the axis ($r = 0$) of each cyclindrical pellet, symmetry requires

$$\left.\frac{\partial C_{pi}}{\partial r}\right|_{r=0} = \left.\frac{\partial C_{si}}{\partial r}\right|_{r=0} = 0 \qquad (0 \le z \le z_T,\ t > 0) \tag{12-46}$$

Similarly, at the center of each spherical pellet, symmetry requires the condition given by Eq. (12-46).

It is supposed that initially a state of equilibrium exists between each component in the fluid phase within the pore and the adsorbed solute on the surface. The distribution of component concentrations at $t \le 0$ is assumed to be independent of z. Thus

$$\begin{aligned} C_{pi}(0, r) &= C_{pi}^0(r) \qquad (0 < z < z_T,\ t \le 0) \\ C_{si}(0, r) &= C_{si}^0(r) \qquad (0 < z < z_T,\ t \le 0) \end{aligned} \tag{12-47}$$

The values $C_{si}^0(r)$ may be computed by use of the appropriate isotherm and the specified values of $C_{pi}^0(r)$.

Example 12-2 A mixture of butanol-2 and t-amylalcohol is passed through a fixed-bed adsorption column. On the basis of the mass transfer model developed above and the assumption that solid diffusion makes an insignificant contribution to the transport of mass, the values of $C_{di}(t, z)$ are to be predicted at $z = z_T$. Butanol-2 is taken as component 1 and t-amylalcohol as component 2. The equilibrium isotherms for the binary system over the adsorbent Filtrasorb 400 are

$$C_{s1}^* = \frac{1.06C_{p1}^{1.217}}{C_{p1}^{0.812} + 0.626C_{p2}^{0.764}}$$

$$C_{s2}^* = \frac{1.07C_{p2}^{1.254}}{C_{p2}^{0.906} + 0.045C_{p1}^{0.634}}$$

Perform the calculations for two different column lengths, $z_T = 0.41$ m and $z_T = 0.82$ m. The values of the parameters of the system are shown in Table 12-1. The values of these parameters were taken from Ref. 3.

Solve the example by use of a combination of the method of orthogonal collocation and the third-order semi-implicit Runge–Kutta method of Michelsen (see Chaps. 1, 9, and 10).

SOLUTION The method of orthogonal collocation is applied by first choosing a new set of variables which have values lying between 0 and 1. Consider first Eq. (12-30) as modified for a spherical pellet and let

$$\begin{aligned} &\xi = z/z_T \qquad \tau = tD_{p1}/A_0 \qquad \rho = r^2/r_0^2 \qquad A_0 = \pi r_0^2 \\ &\bar{C}_{di} = C_{di}/C_{0i} \qquad \bar{C}_{pi} = C_{pi}/C_{0i} \qquad \bar{C}_{si}^* = C_{si}^*/C_{s0i}^* \end{aligned} \tag{1}$$

$\mathrm{Pe}_i = z_T u_f / D_{Li}$ = Peclet number $\qquad \mathrm{Sh}_i = 2r_0 K_{Li}/\varepsilon_p D_{pi}$ = Sherwood number

Table 12-1 Values of the parameters for Example 12-2, the adsorption of the binary mixture of butanol-2 and t-amylalcohol on Filtrasorb 400 adsorbent (Ref. 3)

Parameter	Units	Numerical value
C_{01}	g/cm³	0.001
C_{02}	g/cm³	0.001
$C_{d1}(0, z)$	g/cm³	0.0
$C_{d2}(0, z)$	g/cm³	0.0
$C_{p1}(0, r)$	g/cm³	0.0
$C_{p2}(0, r)$	g/cm³	0.0
D_{L1}	cm²/s	0.04
D_{L2}	cm²/s	0.04
D_{p1}	cm²/s	7.40×10^{-6}
D_{p2}	cm²/s	13.03×10^{-6}
K_{L1}	cm/s	2.12×10^{-3}
K_{L2}	cm/s	1.68×10^{-3}
r_0	cm	0.05
u_f	cm/s	0.28
ε	.....	0.5
ε_p	.....	0.94

Also C_{s0i}^* is used to denote the concentration of adsorbed solute i at equilibrium when the fluid phase concentration is C_{0i} at $z < 0$. When the change in variables listed by Eq. (1) is made, Eq. (12-30) for spherical pellets reduces to

$$\frac{\partial \bar{C}_{d1}}{\partial \tau} = -\alpha_1 \frac{\partial \bar{C}_{d1}}{\partial \xi} + \alpha_2 \frac{\partial^2 \bar{C}_{d1}}{\partial \xi^2} - \alpha_3(\bar{C}_{d1} - \bar{C}_{p1})\Big|_{\rho=1} \tag{2}$$

$$\frac{\partial \bar{C}_{d2}}{\partial \tau} = -\alpha_4 \frac{\partial \bar{C}_{d2}}{\partial \xi} + \alpha_5 \frac{\partial^2 \bar{C}_{d2}}{\partial \xi^2} - \alpha_6(\bar{C}_{d2} - \bar{C}_{p2})\Big|_{\rho=1} \tag{3}$$

where

$$\alpha_1 = \alpha_4 = \frac{u_f A_0}{z_T D_{p1}} \qquad \alpha_2 = \frac{u_f A_0}{z_T \,\mathrm{Pe}_1 D_{p1}}$$

$$\alpha_3 = \left(\frac{1-\varepsilon}{\varepsilon}\right)\left(\frac{3}{r_0}\right)\left(\frac{K_{L1} A_0}{D_{p1}}\right) \qquad \alpha_5 = \frac{u_f A_0}{z_T \,\mathrm{Pe}_2 D_{p1}}$$

$$\alpha_6 = \left(\frac{1-\varepsilon}{\varepsilon}\right)\left(\frac{3}{r_0}\right)\left(\frac{K_{L2} A_0}{D_{p1}}\right)$$

For spherical pellets, Eq. (12-38) for pore diffusion reduces to the following expressions for components 1 and 2:

$$\psi_1 \frac{\partial \bar{C}_{p1}}{\partial \tau} + \psi_2 \frac{\partial \bar{C}_{p2}}{\partial \tau} = \frac{\varepsilon_p A_0}{r_0^2}\left(4\rho \frac{\partial^2 \bar{C}_{p1}}{\partial \rho^2} + 6\frac{\partial \bar{C}_{p1}}{\partial \rho}\right) \tag{4}$$

$$\psi_3 \frac{\partial \bar{C}_{p1}}{\partial \tau} + \psi_4 \frac{\partial \bar{C}_{p2}}{\partial \tau} = \frac{2}{\mathrm{Sh}_2}\left(4\rho \frac{\partial^2 \bar{C}_{p2}}{\partial \rho^2} + 6\frac{\partial \bar{C}_{p2}}{\partial \rho}\right) \tag{5}$$

where

$$\psi_1 = \varepsilon_p + \frac{C^*_{s01}}{C_{01}}\frac{\partial \bar{C}^*_{s1}}{\partial \bar{C}_{p1}} \qquad \psi_2 = \frac{C^*_{s01}}{C_{01}}\frac{\partial \bar{C}^*_{s1}}{\partial \bar{C}_{p2}}$$

$$\psi_3 = \left(\frac{2C^*_{s02} r_0^2 K_{L1}}{A_0 \varepsilon_p \mathrm{Sh}_1 C_{02} K_{L2}}\right)\frac{\partial \bar{C}^*_{s2}}{\partial \bar{C}_{p1}}$$

$$\psi_4 = \left(\frac{2r_0^2 K_{L1}}{A_0 \mathrm{Sh}_1 \varepsilon_p K_{L2} C_{02}}\right)\left(\varepsilon_p C_{02} + C^*_{s02}\frac{\partial \bar{C}^*_{s2}}{\partial \bar{C}_{p2}}\right)$$

Restatement of the initial and boundary conditions (Eqs. (12-39) through (12-41), (12-45), (12-46), and (12-47)) in terms of the new variables yields

$$\bar{C}_{di} = 0 \qquad (0 \le \xi \le 1, \tau \le 0) \tag{6}$$

$$\bar{C}_{di}(0, \tau) = 1 + \frac{1}{\mathrm{Pe}_i}\left(\frac{\partial \bar{C}_{di}}{\partial \xi}\right)\bigg|_{\xi=0} \qquad (\tau > 0) \tag{7}$$

$$\left(\frac{\partial \bar{C}_{di}}{\partial \xi}\right)\bigg|_{\xi=1} = 0 \qquad (\xi = 1, \tau > 0) \tag{8}$$

$$\bar{C}_{pi} = 0 \qquad (0 \le \rho \le 1, \tau \le 0) \tag{9}$$

$$\frac{4}{\mathrm{Sh}_i}\left(\frac{\partial \bar{C}_{pi}}{\partial \rho}\right)\bigg|_{\rho=1} = (\bar{C}_{di} - \bar{C}_{pi})\bigg|_{\rho=1} \qquad (0 \le \xi \le 1, \tau > 0) \tag{10}$$

$$\left(\frac{\partial \bar{C}_{pi}}{\partial \rho}\right)\bigg|_{\rho=0} = 0 \qquad (0 \le \xi \le 1, \tau > 0) \tag{11}$$

When the method of orthogonal collocation is applied to the space variables ξ and ρ, Eqs. (2) through (5) and (6) through (11) become

$$\frac{d\bar{C}_{d1,j}}{d\tau} = -\alpha_1 \sum_{l=1}^{N+2} A_{j,l}\bar{C}_{d1,l} + \alpha_2 \sum_{l=1}^{N+2} B_{j,l}\bar{C}_{d1,l} - \alpha_3(\bar{C}_{d1,j} - \bar{C}_{p1,N+1})$$

$$(j = 2, 3, \ldots, N+1) \tag{12}$$

$$\frac{d\bar{C}_{d2,j}}{d\tau} = -\alpha_4\left(\sum_{l=1}^{N+2} A_{j,l}\bar{C}_{d2,l}\right) + \alpha_5\left(\sum_{l=1}^{N+2} B_{j,l}\bar{C}_{d2,l}\right) - \alpha_6(\bar{C}_{d2,j} - \bar{C}_{p2,N+1})$$

$$(j = 2, 3, \ldots, N+1) \tag{13}$$

where $\alpha_1, \alpha_2, \ldots, \alpha_6$ are defined beneath Eq. (3) and N is equal to the number of interior collocation points. Equations (4) and (5) become

$$\psi_1 \frac{d\bar{C}_{p1,j}}{d\tau} + \psi_2 \frac{d\bar{C}_{p2,j}}{d\tau} = \frac{\varepsilon_p A_0}{r_0^2}\left(4\rho_j \sum_{l=1}^{N+1} B_{j,l}\bar{C}_{p1,l} + 6\sum_{l=1}^{N+1} A_{j,l}\bar{C}_{p1,l}\right)$$

$$(j = 1, 2, \ldots, N) \tag{14}$$

$$\psi_3 \frac{d\bar{C}_{p1,j}}{d\tau} + \psi_4 \frac{d\bar{C}_{p2,j}}{d\tau} = \frac{2}{\mathrm{Sh}_2}\left(4\rho_j \sum_{l=1}^{N+1} B_{j,l}\bar{C}_{p2,l} + 6\sum_{l=1}^{N+1} A_{j,l}\bar{C}_{p2,l}\right)$$

$$(j = 1, 2, \ldots, N) \tag{15}$$

The initial and boundary conditions given by Eqs. (6) through (11) become

$$\bar{C}_{d1,j} = \bar{C}_{d2,j} = 0 \qquad (j = 1, 2, \ldots, N+2, \tau \le 0) \tag{16}$$

$$\bar{C}_{d1,1} = 1 + \frac{1}{\mathrm{Pe}_1}\sum_{l=1}^{N+2} A_{1,l}\bar{C}_{d1,l} \qquad (\xi = 0, \tau > 0) \tag{17}$$

$$\bar{C}_{d2,1} = 1 + \frac{1}{\mathrm{Pe}_2}\sum_{l=1}^{N+2} A_{1,l}\bar{C}_{d2,l} \qquad (\xi = 0, \tau > 0) \tag{18}$$

$$\sum_{l=1}^{N+2} A_{N+2,l}\bar{C}_{d1,l} = 0 \qquad (\xi = 1, \tau > 0) \tag{19}$$

$$\sum_{l=1}^{N+2} A_{N+2,l}\bar{C}_{d2,l} = 0 \qquad (\xi = 1, \tau > 0) \tag{20}$$

$$\bar{C}_{p1,j} = \bar{C}_{p2,j} = 0 \qquad (j = 1, 2, \ldots, N+1, \tau \le 0) \tag{21}$$

$$\frac{4}{\mathrm{Sh}_1}\left(\sum_{l=1}^{N+1} A_{N+1,l}\bar{C}_{p1,l}\right) = \bar{C}_{d1,j} - \bar{C}_{p1,N+1} \qquad (j = 2, 3, \ldots, N+1) \tag{22}$$

$$\frac{4}{\mathrm{Sh}_2}\left(\sum_{l=1}^{N+1} A_{N+1,l}\bar{C}_{p2,l}\right) = \bar{C}_{d2,j} - \bar{C}_{p2,N+1} \qquad (j = 2, 3, \ldots, N+1) \tag{23}$$

It should be noted that the boundary points $\xi = 0$ and $\xi = 1$ are taken as external collocation points in Eqs. (2) and (3), whereas only the boundary point $\rho = 1$ was taken as an external collocation point.

Equations (17) through (20) may be used to reduce the number of terms in the summations in Eqs. (12) and (13) to $l = 2$ to $l = N + 1$ by use of the

following procedure. First, Eqs. (17) through (20) are solved for $\bar{C}_{d1,1}$, $\bar{C}_{d2,1}$, $\bar{C}_{d1,N+2}$, and $\bar{C}_{d2,N+2}$ to give the following expressions:

$$\bar{C}_{di,1} = \frac{\dfrac{\mathrm{Pe}_i}{A_{1,N+1}} + \displaystyle\sum_{l=2}^{N+1}\left(\frac{A_{1,l}}{A_{1,N+1}} + \frac{A_{N+2,l}}{A_{N+2,N+2}}\right)\bar{C}_{di,l}}{\dfrac{\mathrm{Pe}_i}{A_{1,N+2}} - \dfrac{A_{1,1}}{A_{1,N+2}} - \dfrac{A_{N+2,1}}{A_{N+2,N+2}}} \qquad (i = 1, 2) \quad (24)$$

$$\bar{C}_{di,N+2} = \frac{\dfrac{\mathrm{Pe}_i}{A_{1,1} - \mathrm{Pe}_i} + \displaystyle\sum_{l=2}^{N+1}\left(\frac{A_{1,l}}{A_{1,1} - \mathrm{Pe}_i} - \frac{A_{N+2,l}}{A_{N+2,1}}\right)\bar{C}_{di,l}}{\dfrac{A_{N+2,N+2}}{A_{N+2,1}} - \dfrac{A_{1,N+2}}{A_{1,1} - \mathrm{Pe}_i}} \qquad (i = 1, 2) \quad (25)$$

Use of the four expressions (Eqs. (24) and (25) with $i = 1, 2$) to eliminate the concentrations at $\xi = 0$ and $\xi = 1$ ($\bar{C}_{d1,1}$, $\bar{C}_{d2,1}$, $\bar{C}_{d1,N+2}$, $\bar{C}_{d2,N+2}$) from Eqs. (12) and (13) results in a reduction of the number of terms in the summations. After the above substitutions have been made, the summations in Eqs. (12) and (13) run from $l = 2$ to $l = N + 1$. For convenience, let these resulting forms of Eqs. (12) and (13) be denoted by Eqs. (12′) and (13′). Although Eqs. (12′) and (13′) are readily obtained by direct substitution, they are not presented because of their complexity. The $\{A_{j,l}\}$ and $\{B_{j,l}\}$ were evaluated on the basis of power series in the concentrations as outlined in Probs. 12-1 through 12-3. The orthogonal polynomials were taken to be the Jacobi polynomials $P_N^{(0,0)}(\xi)$ of order $N = 8$. The roots of these polynomials were taken as the interior collocation points. Liapis and Rippin(3) showed that the results obtained with $N = 8$ differed from those for $N > 8$ in the fourth digit, thereby justifying the use of only 8 collocation points.

Equations (22) and (23) may be used to reduce the sums in Eqs. (14) and (15) such that they are taken from $l = 1$ to $l = N$ as shown below. Solution of Eq. (22) for $\bar{C}_{p1,N+1}$ yields

$$\bar{C}_{p1,N+1} = \frac{\bar{C}_{d1,j} - \dfrac{4}{\mathrm{Sh}_1}\displaystyle\sum_{l=1}^{N} A_{N+1,l}\bar{C}_{p1,l}}{1 + \dfrac{4}{\mathrm{Sh}_1}A_{N+1,N+1}} \qquad (26)$$

and Eq. (23) yields

$$\bar{C}_{p2,N+1} = \frac{\bar{C}_{d2,j} - \dfrac{4}{\mathrm{Sh}_2}\displaystyle\sum_{l=1}^{N} A_{N+1,l}\bar{C}_{p2,l}}{1 + \dfrac{4}{\mathrm{Sh}_2}A_{N+1,N+1}} \qquad (27)$$

Use of these expressions to eliminate $\bar{C}_{p1,N+1}$ and $\bar{C}_{p2,N+1}$ from Eqs. (14) and (15), respectively, yields two expressions having summations ranging from $l = 1$ to $l = N$, and these are denoted for convenience by Eqs. (14′)

and (15′). In these equations, the concentrations corresponding to $\rho = 1$ have been eliminated. The collocation was performed by use of the roots of the orthogonal polynomials $P_N^{(0,0)}(\rho)$ of order $N = 8$, and the number of the interior points of the collocation process was taken to be 8. It should be noted that the polynomials for $\bar{C}_{p1}$ and $\bar{C}_{p2}$ were constructed such that the boundary conditions at $\rho = 0$ were satisfied (see Eq. (11) and Prob. 12-2).

Thus, the problem has now been reduced to solving simultaneously the equations denoted by Eqs. (12′), (13′), (14′), (15′) and the initial conditions given by Eqs. (6) and (9). Equations (12′) through (15′) constitute $4N$ equations; in $4N$ unknown concentrations (exclusive of the initial concentrations which are given by Eqs. (6) and (9)). This set of equations was solved by the semi-implicit Runge–Kutta method as modifed by Michelsen. This method is applied to the above set of differential equations in the same manner demonstrated in Chaps. 1, 6, and 9. The time step $\Delta\tau$ which corresponds to h in the semi-implicit Runge–Kutta algorithm was varied between 0.001 at the beginning of the simulation when the equations were very stiff to 0.1 as the stiffness of the ordinary differential equations became less pronounced.

The results of the simulation are shown in Figs. 12-4 and 12-5. It is seen that good agreement between the predicted results and the experimental results is obtained. An interesting phenomenon to be observed is the fact

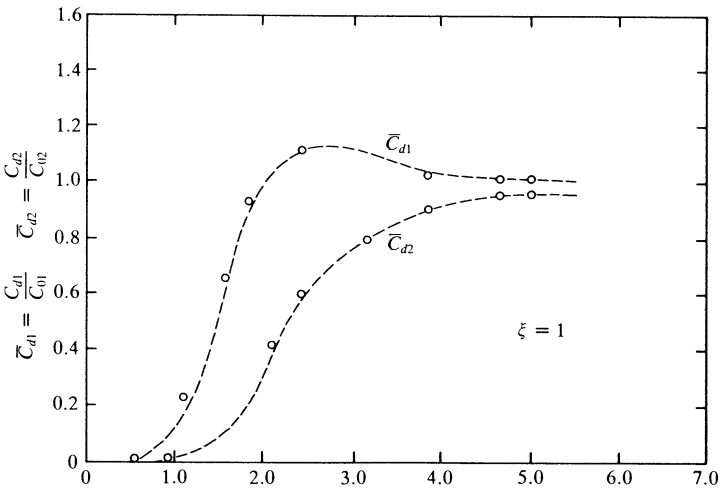

Figure 12-4 Outlet concentrations ($\xi = 1$) predicted by the film resistance and diffusion model, Example 12-2. (O: experimental data, ---: predicted results, $z_T = 0.41$ m.) (*A. I. Liapis and D. W. T. Rippin: "The Simulation of Binary Adsorption in Activated Carbon Columns Using Estimates of Diffusional Resistance within the Carbon Particles Derived from Batch Experiments," Chem. Eng. Sci., vol. 33, p. 593 (1978), Courtesy Pergamon Press.*)

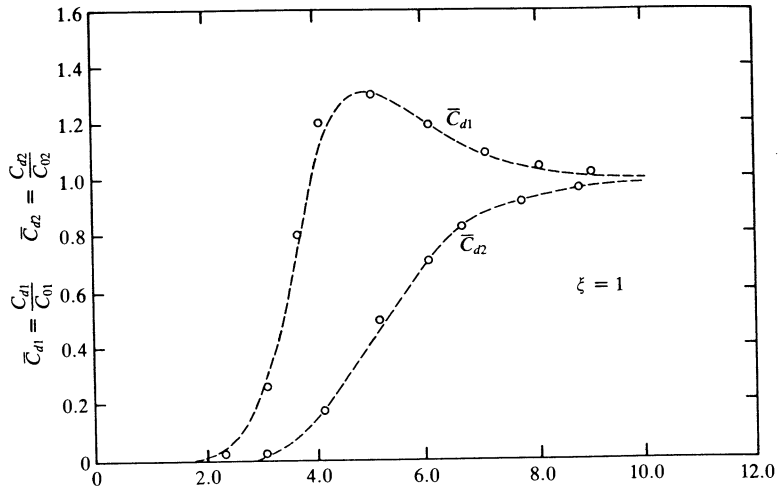

Figure 12-5 Outlet concentrations ($\xi = 1$) predicted by use of the film resistance and diffusion model, Example 12-2. (O: experimental data, ---: predicted results, $z_T = 0.82$ m.) (*A. I. Liapis and D. W. T. Rippin: "The Simulation of Binary Adsorption in Activated Carbon Columns Using Estimates of Diffusional Resistance within the Carbon Particles Derived from Batch Experiments," Chem. Eng. Sci., vol. 33, p. 593 (1978), Courtesy of Pergamon Press.*)

that the outlet concentration of the less preferentially adsorbed component, butanol-2, exceeds its inlet concentration to the adsorption column for a certain period of time, which is indicative of the behavior of competitive multicomponent adsorption.

12-3 ADIABATIC OPERATION OF A FIXED-BED ADSORPTION COLUMN

In the following model for a fixed-bed adsorption column, the operation is adiabatic in the sense that the column is perfectly insulated (no heat losses). The mass transfer model is analogous to the one described in Sec. 11-1 in that the rate-controlling step is the transfer of mass from the bulk conditions of the fluid phase to the adsorbent surface.

Component-Material Balances

The component-material balances for component i in the fluid and solid phases are given by Eqs. (11-45) and (11-42), respectively. For convenience of use in the following developments, these equations are repeated and renumbered as follows:

$$-u_f \frac{\partial C_{di}}{\partial z} - \left(\frac{1-\varepsilon}{\varepsilon}\right) r_{si} = \frac{\partial C_{di}}{\partial t} \qquad (0 < z < z_T,\ t > 0) \qquad (12\text{-}48)$$

and

$$r_{si} = \frac{\partial C_{si}}{\partial t} \qquad (0 < z < z_T,\ t > 0) \qquad (12\text{-}49)$$

Energy Balance on the Fluid Phase

Two independent energy balances exist, one for each phase. In the following development, the enthalpies of the pure components in the fluid phase (denoted by H_i) and in the solid phase (denoted by h_i) are assumed to be functions of temperature alone. Again u_f, ε, and S are assumed to be independent of z and t. Thus, an energy balance on the fluid phase contained in the element of volume from z_j to $z_j + \Delta z$ over the time period from t_n to $t_n + \Delta t$ is given by

$$\int_{t_n}^{t_n+\Delta t} \left[\left(u_f \varepsilon S \sum_{i=1}^{c} C_{di} H_i \right)\Big|_{z_j,\,t} - \left(u_f \varepsilon S \sum_{i=1}^{c} C_{di} H_i \right)\Big|_{z_j+\Delta z,\,t} + \int_{z_j}^{z_j+\Delta z} (1-\varepsilon) S \left(q - \sum_{i=1}^{c} r_{si} H_i \right) dz \right] dt$$

$$= \int_{z_j}^{z_j+\Delta z} \left[\left(\varepsilon S \sum_{i=1}^{c} C_{di} H_i \right)\Big|_{t_n+\Delta t,\,z} - \left(\varepsilon S \sum_{i=1}^{c} C_{di} H_i \right)\Big|_{t_n,\,z} \right] dz \qquad (12\text{-}50)$$

Application of the mean-value theorems followed by the limiting process wherein Δz and Δt are allowed to go to zero with the observation that z_j and t_n were arbitrarily selected yields the following result:

$$-u_f \frac{\partial \sum_{i=1}^{c} C_{di} H_i}{\partial z} - \left(\frac{1-\varepsilon}{\varepsilon}\right) \sum_{i=1}^{c} r_{si} H_i + \left(\frac{1-\varepsilon}{\varepsilon}\right) q = \frac{\partial \sum_{i=1}^{c} C_{di} H_i}{\partial t}$$

$$(0 < z < z_T,\ t > 0) \qquad (12\text{-}51)$$

where $q = h_s a_h (T_s - T_d)$ = rate of heat transfer from the solid phase to the fluid phase, energy per unit time per unit volume of pellet

a_h = interfacial area for heat transfer, interfacial area per unit volume of pellet

In order to reduce Eq. (12-51) to a more convenient form, the following symbols are introduced

$$\begin{aligned} c_{pdi} &= \partial H_i / \partial T_d & c_{psi} &= \partial h_i / \partial T_s \\ c_{pd} &= \sum_{i=1}^{c} y_i c_{pdi} & c_{ps} &= \sum_{i=1}^{c} x_i c_{psi} \\ C_{di} &= \rho_d y_i & C_{si} &= \rho_s x_i \end{aligned} \qquad (12\text{-}52)$$

where y_i is the mole fraction of component i in the fluid phase and x_i is the mole fraction of component i in the solid phase. Since

$$\frac{\partial \sum_{i=1}^{c} C_{di} H_i}{\partial z} = \sum_{i=1}^{c} C_{di} \frac{\partial H_i}{\partial T_d} \frac{\partial T_d}{\partial z} + \sum_{i=1}^{c} H_i \frac{\partial C_{di}}{\partial z}$$

$$= \rho_d c_{pd} \frac{\partial T_d}{\partial z} + \sum_{i=1}^{c} H_i \frac{\partial C_{di}}{\partial z} \tag{12-53}$$

and

$$\frac{\partial \sum_{i=1}^{c} C_{di} H_i}{\partial t} = \rho_d c_{pd} \frac{\partial T_d}{\partial t} + \sum_{i=1}^{c} H_i \frac{\partial C_{di}}{\partial t} \tag{12-54}$$

it is evident that Eq. (12-51) may be restated in the following form:

$$-u_f \rho_d c_{pd} \frac{\partial T_d}{\partial z} - u_f \sum_{i=1}^{c} H_i \frac{\partial C_{di}}{\partial z} - \left(\frac{1-\varepsilon}{\varepsilon}\right) \sum_{i=1}^{c} r_{si} H_i + \left(\frac{1-\varepsilon}{\varepsilon}\right) q$$

$$= \rho_d c_{pd} \frac{\partial T_d}{\partial t} + \sum_{i=1}^{c} H_i \frac{\partial C_{di}}{\partial t} \tag{12-55}$$

Further simplification is possible by use of the following expression which may be obtained by first multiplying Eq. (12-48) by H_i and then summing over all components i to obtain

$$-u_f \sum_{i=1}^{c} H_i \frac{\partial C_{di}}{\partial z} - \left(\frac{1-\varepsilon}{\varepsilon}\right) \sum_{i=1}^{c} r_{si} H_i = \sum_{i=1}^{c} H_i \frac{\partial C_{di}}{\partial t} \tag{12-56}$$

Subtraction of Eq. (12-56) from Eq. (12-55) yields

$$-u_f \rho_d c_{pd} \frac{\partial T_d}{\partial z} + \left(\frac{1-\varepsilon}{\varepsilon}\right) q = \rho_d c_{pd} \frac{\partial T_d}{\partial t} \tag{12-57}$$

or

$$u_f \rho_d c_{pd} \frac{\partial T_d}{\partial z} + \rho_d c_{pd} \frac{\partial T_d}{\partial t} = \left(\frac{1-\varepsilon}{\varepsilon}\right) h_s a_h (T_s - T_d) \tag{12-58}$$

Energy Balance on the Solid Phase

The energy balance enclosing the solid phase over the time period from t_n to $t_n + \Delta t$ and the volume of bed from z_j to $z_j + \Delta z$ is given by

$$\int_{t_n}^{t_n+\Delta t} \left(\int_{z}^{z_j+\Delta z} \left(\sum_{i=1}^{c} r_{si} H_i - q \right) (1-\varepsilon) S \, dz \, dt \right.$$

$$= \int_{z_j}^{z_j+\Delta z} \left(\sum_{i=1}^{c} C_{si} h_i \Big|_{t_n+\Delta t,\, z} - \sum_{i=1}^{c} C_{si} h_i \Big|_{t_n,\, z} \right) (1-\varepsilon) S \, dz \tag{12-59}$$

Application of the mean-value theorems to Eq. (12-59) followed by the limiting process whereby Δt and Δz are allowed to go to zero, and with the understanding that Δt and Δz were arbitrarily selected, yields the following result:

$$\sum_{i=1}^{c} r_{si} H_i - q = \sum_{i=1}^{c} C_{si} \frac{\partial h_i}{\partial T_s} \frac{\partial T_s}{\partial t} + \sum_{i=1}^{c} h_i \frac{\partial C_{si}}{\partial t} \tag{12-60}$$

From Eq. (12-60) subtract the expression obtained by first multiplying each member of Eq. (12-49) by h_i and then summing over all components to obtain the following result upon replacing q by its definition given below Eq. (12-51):

$$-\sum_{i=1}^{c} \Delta H_i \frac{\partial C_{si}}{\partial t} + h_s a_h (T_d - T_s) = \rho_s c_{ps} \frac{\partial T_s}{\partial t} \qquad (0 < z < z_T,\ t > 0) \tag{12-61}$$

where

$$\Delta H_i = h_i - H_i$$

For convenience, the expression given by Eq. (12-49) for the rate of mass transfer is combined with Eq. (12-1) and restated for convenience as follows:

$$\frac{\partial C_{si}}{\partial t} = K_{si} a_s (C_{si}^* - C_{si}) \qquad (i = 1, 2, \ldots, c) \tag{12-62}$$

Use of Eq. (12-62) permits Eqs. (12-48) and (12-61) to be restated in the following form:

$$u_f \frac{\partial C_{di}}{\partial z} + \frac{\partial C_{di}}{\partial t} = -\left(\frac{1-\varepsilon}{\varepsilon}\right) K_{si} a_s (C_{si}^* - C_{si}) \qquad (i = 1, 2, \ldots, c) \tag{12-63}$$

$$\rho_s c_{ps} \frac{\partial T_s}{\partial t} = h_s a_h (T_d - T_s) - \sum_{i=1}^{c} \Delta H_i K_{si} a_s (C_{si}^* - C_{si}) \tag{12-64}$$

Equations (12-58) and (12-62) through (12-64) constitute $2c + 2$ equations which are to be solved subject to the following initial conditions

$$\begin{aligned} C_{si}(z, 0) &= C_{si}^0(z) \qquad (0 < z < z_T,\ t \le 0) \\ C_{di}(z, 0) &= C_{di}^0(z) \qquad (0 < z < z_T,\ t \le 0) \\ T_s(z, 0) &= T_s^0(z) \qquad (0 < z < z_T,\ t \le 0) \\ T_d(z, 0) &= T_d^0(z) \qquad (0 < z < z_T,\ t \le 0) \end{aligned} \tag{12-65}$$

and boundary conditions

$$\begin{aligned} C_d(0, t) &= C_{di,\,\text{in}} \qquad (z = 0,\ t > 0) \\ T_d(0, t) &= T_{d,\,\text{in}} \qquad (z = 0,\ t > 0) \end{aligned} \tag{12-66}$$

Harwell et al.(4) used the following form of the Markham and Benton equilibrium relationship:

$$C_{si}^* = \frac{C_{Ti} K_i C_{di}}{1 + \sum_{i=1}^{c} K_i C_{di}} \tag{12-67}$$

where C_{Ti} is constant for each component i. On the basis of the expression given by Eq. (12-67), the following expression was developed by Harwell et al.(4) for expressing the dependency of K_i on temperature and pressure, namely,

$$K_i = K_{0i}\, T_s^{-1/2}\, \mathrm{Pe}^{-\Delta H_i/RT_s} \qquad (i = 1, 2, \ldots, c) \tag{12-68}$$

where K_{0i} is a constant for each component i.

Equations (12-58), (12-62), (12-63), and (12-64) may be stated in the following dimensionless form:

$$\frac{\partial \bar{C}_{di}}{\partial \tau} + \frac{\partial \bar{C}_{di}}{\partial z} = -\eta_i(\bar{C}^*_{si} - \bar{C}_{si}) \qquad (i = 1, 2, \ldots, c) \tag{12-69}$$

$$\frac{\partial \bar{T}_d}{\partial \tau} + \frac{\partial \bar{T}_d}{\partial Z} = \theta(\bar{T}_s - \bar{T}_d) \tag{12-70}$$

$$\frac{\partial \bar{C}_{si}}{\partial \tau} = \xi_i(\bar{C}^*_{si} - \bar{C}_{si}) \qquad (i = 1, 2, \ldots, c) \tag{12-71}$$

$$\frac{\partial \bar{T}_s}{\partial \tau} = \beta(\bar{T}_d - \bar{T}_s) - \lambda \sum_{i=1}^{c} \delta_i(\bar{C}^*_{si} - \bar{C}_{si}) \qquad (i = 1, 2, \ldots, c) \tag{12-72}$$

The dimensionless independent and dependent variables are defined as follows:

$$\begin{aligned} &\tau = u_f t/z_T \qquad && Z = z/z_T \qquad && \bar{C}^*_{si} = C^*_{si}/C^*_{si,\,\mathrm{in}}(0) \\ &\bar{C}_{di} = C_{di}/C_{di,\,\mathrm{in}}(0) \qquad && \bar{T}_s = T_s/T_{d,\,\mathrm{in}}(0) \\ &\bar{T}_d = T_d/T_{d,\,\mathrm{in}}(0) \qquad && \bar{C}_{si} = C_{si}/C^*_{si,\,\mathrm{in}}(0) \end{aligned} \tag{12-73}$$

The dimensionless parameters appearing in Eqs. (12-69) through (12-72) have the following definitions:

$$\begin{aligned} &\eta_i = \left(\frac{1-\varepsilon}{\varepsilon}\right)\frac{K_{si}\, a_s\, z_T\, C^*_{si,\,\mathrm{in}}(0)}{u_f\, C_{di,\,\mathrm{in}}(0)} \qquad && \theta = \left(\frac{1-\varepsilon}{\varepsilon}\right)\frac{h_s\, a_h\, z_T}{u_f\, \rho_d\, c_{pd}} \\ &\xi_i = \frac{z_T\, K_{si}\, a_s}{u_f} \qquad && \beta = \frac{z_T\, h_s\, a_h}{u_f\, \rho_s\, c_{ps}} \qquad && \lambda = \frac{z_T}{u_f\, \rho_s\, c_{ps}\, T_{d,\,\mathrm{in}}(0)} \\ &\delta_i = \Delta H_i\, K_{si}\, a_s\, C^*_{si,\,\mathrm{in}}(0) \end{aligned} \tag{12-74}$$

This model for the adiabatic adsorption of multicomponent mixtures has been used by Liapis and Crosser(5) to simulate the adsorption of ethane–carbon dioxide mixtures by beds of 5*A* molecular sieves. The model predictions agree fairly well with the experimental data, and one may use this model to design, with good accuracy, fixed adsorption beds which are adiabatically operated.

Solution of Eqs. (12-69) through (12-72) by the Method of Characteristics

The solution of Eqs. (12-69) through (12-72) may be effected by the Method of Characteristics as described in Chap. 10. The choice of the characteristics is made as outlined below. Consider first Eq. (12-69). Expansion of $\bar{C}_{di}$ by the chain rule gives

$$\frac{d\bar{C}_{di}}{dZ} = \frac{\partial \bar{C}_{di}}{\partial Z}\frac{dZ}{dZ} + \frac{\partial \bar{C}_{di}}{\partial \tau}\frac{d\tau}{dZ} \tag{12-75}$$

Let $d\tau/dZ = 1$. Then along characteristic I, Eq. (12-75) becomes

$$\left(\frac{d\bar{C}_{di}}{dZ}\right)_{\mathrm{I}} = \frac{\partial \bar{C}_{di}}{\partial Z} + \frac{\partial \bar{C}_{di}}{\partial \tau} \qquad (\text{along } d\tau/dZ = 1) \tag{12-76}$$

Thus, Eq. (12-69) reduces to

$$\left(\frac{d\bar{C}_{di}}{dZ}\right)_{\mathrm{I}} = -\eta_i(\bar{C}^*_{si} - \bar{C}_{si}) \qquad (i = 1, 2, \ldots, c) \qquad (\text{along } d\tau/dZ = 1) \tag{12-77}$$

Similarly, characteristic I reduces Eq. (12-70) to

$$\left(\frac{d\bar{T}_d}{dZ}\right)_{\mathrm{I}} = \theta(\bar{T}_s - \bar{T}_d) \qquad (\text{along } d\tau/dZ = 1) \tag{12-78}$$

Next consider Eq. (12-71). Expansion of $\bar{C}_{si}$ by the chain rule gives

$$\frac{d\bar{C}_{si}}{d\tau} = \frac{\partial \bar{C}_{si}}{\partial \tau}\frac{d\tau}{d\tau} + \frac{\partial \bar{C}_{si}}{\partial Z}\frac{dZ}{d\tau} \tag{12-79}$$

Take $dZ/d\tau = 0$, or $Z = \text{const}$ as characteristic II. Then Eq. (12-79) reduces to

$$\left(\frac{d\bar{C}_{si}}{d\tau}\right)_{\mathrm{II}} = \frac{\partial \bar{C}_{si}}{\partial \tau} \qquad (\text{along } Z = \text{const}) \tag{12-80}$$

Thus, along characteristic II, Eqs. (12-71) and (12-72) reduce to

$$\left(\frac{d\bar{C}_{si}}{d\tau}\right)_{\mathrm{II}} = \xi_i(\bar{C}^*_{si} - \bar{C}_{si}) \qquad \begin{matrix}(i = 1, 2, \ldots, c) \\ (\text{along } Z = \text{const})\end{matrix} \tag{12-81}$$

$$\left(\frac{d\bar{T}_s}{d\tau}\right)_{\mathrm{II}} = \beta(\bar{T}_d - \bar{T}_s) - \lambda \sum_{i=1}^{c} \delta_i(\bar{C}^*_{si} - \bar{C}_{si}) \qquad \begin{matrix}(i = 1, 2, \ldots, c), \\ (\text{along } Z = \text{const})\end{matrix} \tag{12-82}$$

The application of these equations is demonstrated by use of the following numerical example.

Example 12-3 A mixture of benzene and cyclohexane is passed through a fixed-bed adsorption column which is assumed to be perfectly insulated. On the basis of the simultaneous mass and heat transfer model developed above, the values of $\bar{C}_{di}(Z, \tau)$, $\bar{C}_{si}(Z, \tau)$, $\bar{T}_d(Z, \tau)$, and $\bar{T}_s(Z, \tau)$ are to be predicted at each of the mesh points (i, j) shown in Fig. 12-6. The data to be used for this example are presented in Table 12-2.

The example is to be solved by use of a combination of the Method of Characteristics, the trapezoidal rule, and the Newton–Raphson method. (*a*) Formulate the equations required to determine the values of $\bar{C}_{si}(0, \tau)$ and $\bar{T}_s(0, \tau)$. (*b*) Formulate the equations needed to find the values of all variables at the point (1, 1).

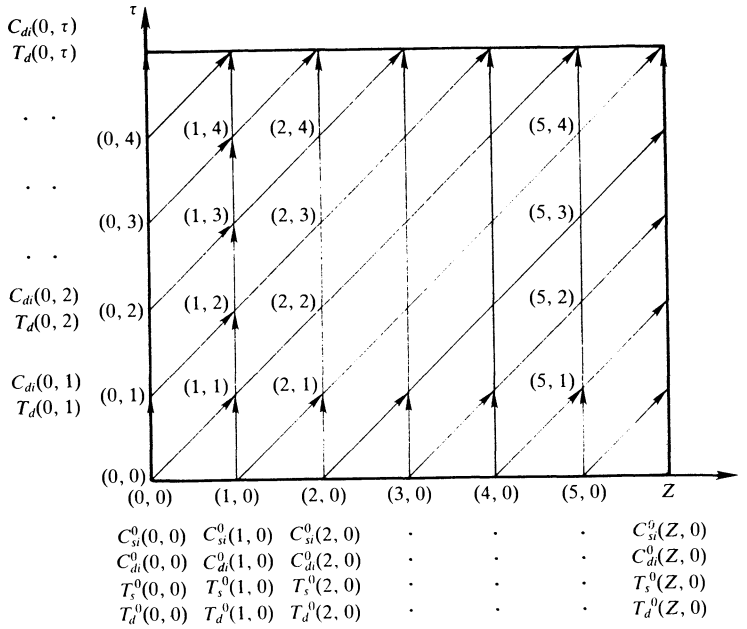

Figure 12-6 Sketch of the characteristics with initial values and boundary values of the variables for Example 12-3.

SOLUTION In Fig. 12-6, a plot of characteristics I and II is shown. Also, along each axis, the known values of the variables at $(0, \tau)$ and $(Z, 0)$ are listed. Since the values of $\bar{C}_{s1}(0, \tau)$, $\bar{C}_{s2}(0, \tau)$, and $\bar{T}_3(0, \tau)$ are unknown, their values must be determined before the values of the variables at the points (1, 2), (1, 3), ... can be determined.

First the equations needed to compute $\bar{C}_{si}(0, 1)$ and $\bar{T}_s(0, 1)$ are formulated. Application of the trapezoidal rule gives

$$\bar{C}_{si}(0, 1) = \bar{C}_{si}(0, 0) + \frac{h}{2}\left[\frac{d\bar{C}_{si}(0, 0)}{d\tau} + \frac{d\bar{C}_{si}(0, 1)}{d\tau}\right] \qquad (i = 1, 2) \qquad (1)$$

$$\bar{T}_s(0, 1) = \bar{T}_s(0, 0) + \frac{h}{2}\left[\frac{d\bar{T}_s(0, 0)}{d\tau} + \frac{d\bar{T}_s(0, 1)}{d\tau}\right] \qquad (2)$$

When the derivatives appearing in Eqs. (1) and (2) are evaluated by use of Eqs. (12-80) and (12-82) and the resulting expressions restated in functional notation, one obtains

$$f_i = -\bar{C}_{si}(0, 1) + \bar{C}_{si}(0, 0) + \frac{h}{2}\{\xi_i[\bar{C}^*_{si}(0, 0) - \bar{C}_{si}(0, 0)] + \xi_i[\bar{C}^*_{si}(0, 1) - \bar{C}_{si}(0, 1)\} \qquad (i = 1, 2) \quad (3)$$

$$f_3 = -\bar{T}_s(0, 1) + \bar{T}_s(0, 0) + \frac{h}{2}\left\{\beta[\bar{T}_d(0, 0) - \bar{T}_s(0, 0)] - \lambda\sum_{i=1}^{2}\delta_i[\bar{C}^*_{si}(0, 0) - \bar{C}_{si}(0, 0)] + \beta[\bar{T}_d(0, 1) - \bar{T}_s(0, 1)] - \lambda\sum_{i=1}^{2}\delta_i[\bar{C}^*_{si}(0, 1) - \bar{C}_{si}(0, 1)]\right\} \qquad (4)$$

Table 12-2 Values of the parameters for Example 12-3, the adsorption of the binary mixture of benzene and cyclohexane (Ref. 4)

Parameter	Units	Numerical value
z_T	m	0.5
u_f	m/s	0.0015
$C_{d2,\,in}$	mol benzene / mol gas	0.030, $t > 0$
$C_{d1,\,in}$	mol cyclohexane / mol gas	0.020, $t > 0$
$a_s = a_h$	m^2/m^3	6000
ε	.....	0.360
$\rho_{d,\,m}$	mol/m^3	1.41×10^3
C_{pd}	J/(mol K)	37.7
C_{ps}	J/(g K)	1.05
ρ_s	g/m^2	1.3×10^6
h	$J/(m^2s)$	41.9
K_{s1}	$g/(m^2s)$	1.0
K_{s2}	$g/(m^2s)$	0.80
ΔH_1	J/mol	-3.27×10^4
ΔH_2	J/mol	-4.35×10^4
$T_{d,\,in}$	K	293, $t > 0$
$T^0_d(z) = T^0_s(z)$	K	293, $0 \le z \le z_T$, $t > 0$
$C^0_{s1}(z) = C^0_{s2}(z)$	mol i / g solid	1×10^{-15}, $0 \le z \le z_T$, $t \le 0$
$C^0_{d,\,1}(z) = C^0_{d,\,2}(z)$	mol i / mol gas	1×10^{-15}, $0 \le z \le z_T$, $t \le 0$
P	atm	34
$C_{T,\,1}$	mol of sites, component 1 / g solid	2.90×10^{-3}
$C_{T,\,2}$	mol of sites, component 2 / g solid	3.67×10^{-3}
$K_{0,\,1}$	$(K)^{1/2}$ / atm	1.26×10^{-2}
$K_{0,\,2}$	$(K)^{1/2}$ / atm	4.37×10^{-4}

The quantities $\bar{C}^*_{si}(0, 0)$ and $\bar{C}^*_{si}(0, 1)$ are given by the equilibrium relationship, namely,

$$C^*_{si}(0, 0) = \frac{C_{Ti} K_i[T_s(0, 0)]C_{di}(0, 0)}{1 + \sum_{i=1}^{2} K_i[T_s(0, 0)]C_{di}(0, 0)} \qquad (i = 1, 2) \tag{5}$$

$$C^*_{si}(0, 1) = \frac{C_{Ti} K_i[T_s(0, 1)]C_{di}(0, 1)}{1 + \sum_{i=1}^{2} K_i[T_s(0, 1)]C_{di}(0, 1)} \qquad (i = 1, 2) \tag{6}$$

Examination of the above equations shows that the functions f_1, f_2, and f_3 contain three unknowns $\bar{C}_{s1}(0, 1)$, $\bar{C}_{s2}(0, 1)$, and $\bar{T}_s(0, 1)$. The values of these three variables, which are required to make $f_1 = f_2 = f_3 = 0$, may be found by use of the Newton–Raphson method. The values so obtained are used to compute the next set of values $\bar{C}_{si}(0, 2)$, $\bar{C}_{s2}(0, 2)$, and $\bar{T}_s(0, 2)$. This stepwise process is repeated until all of the desired values of the variables along the τ axis (at $\tau = 0$) have been determined.

(*b*) The values of the variables at the point (1, 1) of Fig. 12-6 are evaluated by integration of Eqs. (12-77) and (12-78) from (0, 0) to (0, 1) along the line defined by characteristic I, $d\tau/dZ = 1$ and by integration of Eqs. (12-81) and (12-82) from (0, 1) to (1, 1) along the line defined by characteristic II, Z = const. In particular

$$\bar{C}_{si}(1, 1) = \bar{C}_{si}(0, 0) + \frac{h}{2}\left[\frac{d\bar{C}_{si}(0, 0)}{d\tau} + \frac{d\bar{C}_{si}(1, 1)}{d\tau}\right] \qquad (i = 1, 2) \tag{7}$$

$$\bar{T}_s(1, 1) = \bar{T}_s(0, 0) + \frac{h}{2}\left[\frac{d\bar{T}_s(0, 0)}{d\tau} + \frac{d\bar{T}_s(1, 1)}{d\tau}\right] \tag{8}$$

$$\bar{C}_{di}(1, 1) = \bar{C}_{di}(1, 0) + \frac{\Delta Z}{2}\left[\frac{d\bar{C}_{di}(1, 0)}{dZ} + \frac{d\bar{C}_{di}(1, 1)}{dZ}\right] \qquad (i = 1, 2) \tag{9}$$

$$\bar{T}_d(1, 1) = \bar{T}_d(1, 0) + \frac{\Delta Z}{2}\left[\frac{d\bar{T}_d(1, 0)}{dZ} + \frac{d\bar{T}_d(1, 1)}{dZ}\right] \tag{10}$$

The derivatives appearing in Eqs. (7) through (10) are given by Eqs. (12-77), (12-78), (12-81), and (12-82). For example,

$$\frac{d\bar{C}_{di}(1, 1)}{dZ} = -\eta_i[\bar{C}^*_{si}(1, 1) - \bar{C}_{si}(1, 1)] \qquad (i = 1, 2) \tag{11}$$

$$\frac{d\bar{T}_d}{dZ} = \theta[\bar{T}_s(1, 1) - \bar{T}_d(1, 1)] \tag{12}$$

where $\bar{C}^*_{si}(1, 1)$ is given in terms of $\bar{T}_s(1, 1)$ and $\bar{C}_{ji}(1, 1)$ by Eq. (12-67).

After the derivatives appearing in Eqs. (7) through (10) have been replaced by their equivalents as given by Eqs. (12-77), (12-78), (12-81), and (12-82) and the resulting expressions are stated in functional notation, the Newton–Raphson method may be applied successively to determine the values of the variables, $\bar{C}_{di}(1, 1)$, $\bar{C}_{d2}(1, 1)$, $\bar{C}_{si}(1, 1)$, $\bar{C}_{s2}(1, 1)$, $\bar{T}_d(1, 1)$, and $\bar{T}_s(1, 1)$.

Interpretation of the Numerical Results for Example 12-3

Selected values of the variables obtained over the time period $\tau = 140$ by use of the numerical methods described above are presented in Fig. 12-7. Profiles of the variables at $\tau = 10$ over the total length of the bed are shown in Fig. 12-8. A computation time of 20 minutes was typical for the AMDAHL 470V/6 computer for time and space steps ranging from 0.01 to 0.03.

First, observe in Fig. 12-7 that component 1 (cyclohexane) which is not as strongly adsorbed as component 2 (benzene) exhibits a breakthrough 35 dimensionless time units before component 2. Because of this significant difference in breakthrough times, it is evident that the performance of a binary adsorption column cannot be approximated by a single pseudocomponent.

For the equilibrium isotherm employed (Eq. (12-67)), there exists an inversion of the relative adsorptivity for the benzene–cyclohexane system. The following expression for the relative adsorptivity γ is obtained by use of Eqs. (12-67) and (12-68):

$$\gamma = \frac{C^*_{s,1}/C_{d,1}}{C^*_{s,2}/C_{d,2}} = \frac{C_{T1} K_{01}}{C_{T2} K_{02}} \exp\left[-(\Delta H_1 - \Delta H_2)/RT_s\right] \tag{12-83}$$

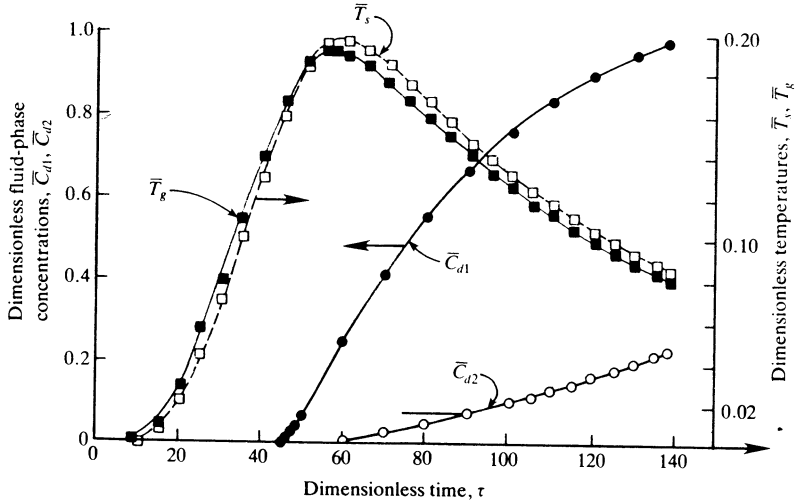

Figure 12-7 Outlet concentrations and temperatures predicted by the adiabatic model for a fixed-bed adsorption column, Example 12-3. (*J. H. Harwell, A. I. Liapis, R. J. Litchfield and D. T. Hanson: "A Non-Equilibrium Model for Fixed-Bed Multicomponent Adiabatic Adsorption," Chem. Eng. Sci., vol. 35, p. 2287 (1980), Courtesy Pergamon Press.*)

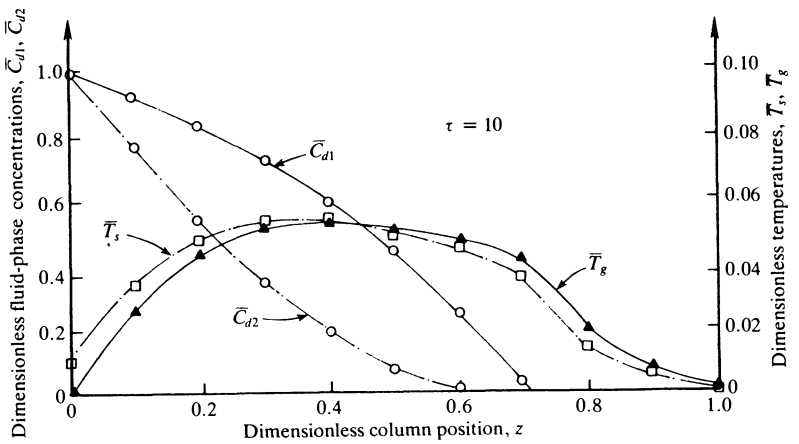

Figure 12-8 Concentrations and temperatures profiles predicted by the adiabatic model for a fixed-bed adsorption column, Example 12-3. (*J. H. Harwell, A. I. Liapis, R. J. Litchfield, and D. T. Hanson: "A Non-Equilibrium Model for Fixed-Bed Multicomponent Adiabatic Adsorption," Chem. Eng. Sci., vol. 35, p. 2287 (1980), Courtesy Pergamon Press.*)

The inversion in adsorptivity occurs at $\gamma = 1$. The T_s required to make $\gamma = 1$ is denoted by $T_{s,\text{inv}}$. For the benzene–cyclohexane system, $T_{s,\text{inv}} = 449.9$ K.

A comment regarding the relative magnitudes of $\bar{C}_{s,1}$, $\bar{C}_{s,2}$, $\bar{C}^*_{s,1}$, and $\bar{C}^*_{s,2}$ is in order. When the solid temperature T_s is less than the inversion temperature, the value of $\bar{C}_{s,1}$ is larger than that of $\bar{C}_{s,2}$ even though there is actually more of component 2 adsorbed than component 1. The relative magnitudes of $\bar{C}_{s,1}$ and $\bar{C}_{s,2}$ result from the difference in the normalizing factors $C^*_{s,1}$ and $C^*_{s,2}$.

The two fluid-phase mass waves in Fig. 12-7 have distinctively different shapes and different velocities. The mass wave of the more strongly adsorbed component, $\bar{C}_{d,2}$, is concave away from the origin and moves at a slower velocity than does the mass wave for component 1.

The thermal waves or temperature profiles (both in the fluid phase $\bar{T}_d$ and in the solid phase $\bar{T}_s$) move at a greater velocity than do the mass waves. Further interpretations have been presented by Harwell et al.(4).

12-4 PERIODIC OPERATION

In order to utilize adsorption columns in continuous processes, it is necessary to devise a process whereby one adsorption bed is cleaned while another one is being used. For example, suppose that a set of three columns is available. At any one time, two columns connected in series may be operated in the adsorption cycle while the third column is placed in the cleaning cycle. After the first

column has become loaded with one or more of the components to be separated, it is removed from the system and placed in the cleaning cycle. The clean column is then placed after and in series with the second column. The second column then becomes the next column to be removed from the adsorption cycle and placed in the cleaning cycle. Obviously, a large number of columns could be used in the process whereby one (or more) columns is always in the cleaning process. In the limit as the number of columns and the frequency of changing cycles for one of the columns is increased indefinitely, the condition of steady-state countercurrent operation is reached. The same limit is obtained if the analysis is made in terms of pulsed columns (Ref. 6).

The mathematical model that describes periodic operation is the same as that for a fixed bed. The solution procedure for a single column is easily adopted to a multicolumn system. After a column switch, the initial conditions must be adjusted for the start of the new adsorption cycle. That part of the profile is deleted which corresponds to the saturated column that has been removed. The profile of the remaining column is shifted toward the feed inlet and the profile for the newly regenerated column is added at the outlet end of the series of columns.

The criterion for the removal of a loaded column at the inlet end of the system and the introduction of a regenerated column at the outlet end of the system of columns is selected in a manner which tends to maximize the use of the adsorbent.

Comparison of Fixed-Bed Operation and Periodic Operation

The adsorption model developed in Sec. 12-2 (based on film resistance and diffusion) was used to compare fixed-bed operation with periodic operation. The adsorption system used was the same as the one used for fixed-bed operation, 2-butanol and *t*-amylalcohol. Six different column lengths of 30, 41, 82, 123, 150, and 200 cm were used and the system parameters used in the film resistance and diffusion model of Sec. 12-2.

The criterion used for column switching was arbitrarily taken to be that time at which the concentration of either component in the effluent reached 1 percent of its value in the feed. Figure 12-9 shows the relationship between carbon utilization and column length for different numbers of subdivisions for a given total length. The different numbers of subdivisions correspond to the numbers of columns in a given adsorption system composed of multiple columns. A carbon utilization of 100 percent corresponds to the case where the amount of solute adsorbed is equal to that predicted by the equilibrium isotherm. As the number of columns is allowed to increase without bound ($N \rightarrow \infty$), countercurrent operation at steady state is approached (Ref. 7). It is seen in Fig. 12-9 that the greatest improvement in carbon utilization occurs when the single column is divided into two columns, while for more subdivisions the corresponding improvement is smaller. For small columns even a small number of subdivisions gives almost the same efficiency as the

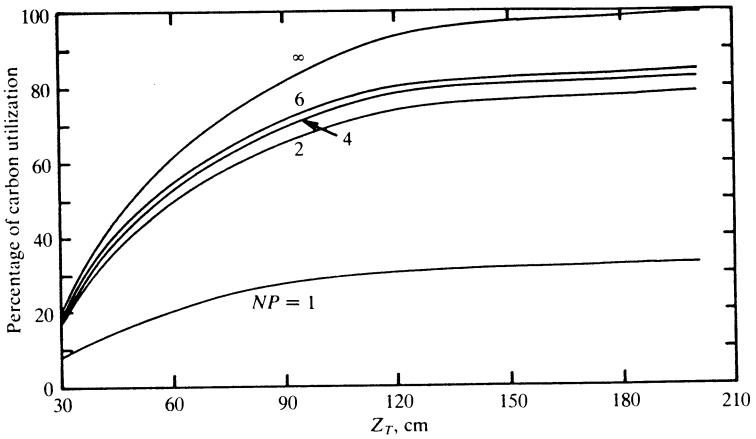

Figure 12-9 Percentage of carbon utilization versus column length with number of columns as a parameter (*NP*) for the butanol-2 and *t*-amylalcohol system. (*A. I. Liapis and D. W. T. Rippin: "The Simulation of Binary Adsorption in Continuous Countercurrent Operation and a Comparison with Other Operating Modes. AIChE J., vol. 25, no. 3, p. 455 (1979). Courtesy American Institute of Chemical Engineers.*)

continuous-countercurrent operation. For large columns many more subdivisions would be required.

The results shown lead to the conclusion that subdividing a column into two or more columns and operating them periodically in a countercurrent mode gives an increase in the utilization of the adsorbent which is proportional to the number of columns employed.

NOTATION

a = interfacial area for mass transfer from the fluid phase to the pore openings, interfacial area per unit volume of pellet

a_h = interfacial area for heat transfer, interfacial area per unit volume of pellet

a_s = interfacial area for mass transfer from the fluid to the solid phase, interfacial area per unit volume of pellet

A_{jl} = constants generated in the orthogonal collocation method (see Example 12-2)

B_{jl} = constants generated in the orthogonal collocation method (see Example 12-2 and Chap. 10)

c_{pdi} = heat capacity for component i in the fluid phase, energy per unit mass (or mole) per degree temperature

c_{pd} = heat capacity for a unit mass (or mole) of the fluid phase, energy per unit mass (or mole) per degree temperature

c_{psi} = heat capacity for component i in the solid phase, energy per unit mass (or mole) per degree temperature

c_{ps} = heat capacity for a unit mass (or mole) of the solid phase, energy per unit mass (or mole) per degree temperature

C_{di} = concentration of component i at the bulk conditions of the fluid phase (moles of component i per unit of void volume (the free volume between the pellets))

$\bar{C}_{di}$ = a normalized value of C_{di} (dimensionless)

C_{si} = concentration of component i in the solid (or adsorbed) phase (moles per unit volume of pellet)

$\bar{C}_{si}$ = a normalized value of C_{si} (dimensionless)

D_{Li} = diffusivity for component i in the fluid phase (dimensions of (length)^2/time)

D_{pi} = diffusivity for component i in the fluid phase within the pore of an absorbent (dimensions of (length)^2/time)

D_{si} = diffusivity for component i in the solid (or adsorbed) phase (dimensions of (length)^2/time)

h_i = enthalpy of component i in the solid phase, energy per mole (or per unit mass) of component i

h_s = heat transfer coefficient, energy per unit time per unit of interfacial area per degree (°C, °F, K, °R)

H_i = enthalpy of component i in the fluid phase, energy per mole (or per unit mass)

J_{Li} = moles of component i diffusing in the positive direction of z (or r) in the fluid phase per unit of void area perpendicular to the direction z

J_{pi} = moles of component i diffusing in the positive direction of z (or r) in the fluid phase per unit time per unit of void area perpendicular to z

J_{si} = moles of component i diffusing in the positive direction of z (or r) in the solid phase per unit time per unit of pellet surface perpendicular to z

K_i = a constant depending on component i which appears an expression for an equilibrium adsorption isotherm (see Eqs. (12-67) and (12-68))

K_{0i} = a constant appearing in Eq. (12-68)

K_{si} = overall mass transfer coefficient (dimensions of pellet volume per unit time per unit of interfacial area)

L = length of a pore

Pe = Peclet number (used and defined in Example 12-2)

r = radius of the adsorbent pellet as measured from center of pellet

r_0 = external radius of the adsorbent
r_{Li} = moles of solute i transferred per unit time per unit of pellet volume (see Eq. (12-27))
Sh = Sherwood number (used and defined in Example 12-2)
t = time
u_f = linear velocity in the positive direction of z
z = distance
z_T = total length of the adsorption bed
Z = normalized distance ($Z = z/z_T$)

Greek letters

α = 0, 1, 2 for a slab, cylinder, or sphere
$\alpha_1, \alpha_2, \ldots, \alpha_6$ = parameters appearing in Eqs. (2) and (3) of Example 12-2
β = parameter defined by Eq. (12-74)
δ_i = parameter defined by Eq. (12-74)
ε = volume of voids per unit volume of bed
ε_p = volume of pores per unit volume of pellet
η_i = parameter defined by Eq. (12-74)
θ = parameter defined by Eq. (12-74)
λ = parameter defined by Eq. (12-74)
ξ_i = parameter defined by Eq. (12-74)
ξ = parameter defined by Eq. (1) of Example 12-2
ρ = parameter defined by Eq. (1) of Example 12-2
τ = parameter defined by Eq. (1) of Example 12-2
$\psi_1, \ldots, \psi_4$ = parameters defined beneath Eqs. (4) and (5) of Example 12-2

REFERENCES

1. M. W. Balzi, A. I. Liapis, and D. W. T. Rippin: "Applications of Mathematical Modelling to Simulation of Multi-Component Adsorption in Activated Carbon Columns," *Trans. I. Chem. E.*, **56:**145 (1978).
2. A. I. Liapis and R. J. Litchfield: "A Note on the Off-Diagonal Terms of the Effective Pore Diffusivity Matrix," *Trans. I. Chem. E.*, **59:**122 (1981).
3. A. I. Liapis and D. W. T. Rippin: "The Simulation of Binary Adsorption in Activated Carbon Columns Using Estimates of Diffusional Resistance within the Carbon Particles Derived from Batch Experiments," *Chem. Eng. Sci.*, **33:**593 (1978).
4. J. H. Harwell, A. I. Liapis, R. J. Litchfield, and D. T. Hanson: "A Non-Equilibrium Model for Fixed-Bed Multicomponent Adiabatic Adsorption," *Chem. Eng. Sci.*, **35:**2287 (1980).
5. A. I. Liapis and O. K. Crosser: "Comparison of Model Predictions with Non-Isothermal Sorption Data for Ethane–Carbon Dioxide Mixtures in Beds of 5A Molecular Sieves," *Chem. Eng. Sci.*, **37:**958 (1982).
6. A. I. Liapis: Ph.D. thesis, E.T.H. Zürich, Switzerland, 1977.
7. A. I. Liapis and D. W. T. Rippin: "The Simulation of Binary Adsorption in Continuous Countercurrent Operation and Comparison with Other Operating Modes," *AIChE J.*, **25:**455 (1979).

PROBLEMS

12-1 Develop the expressions for the approximate solutions for C_{d1} and C_{d2} of Example 12-2, when the Jacobi polynomials $P_N^{(0,0)}(\xi)$ of order $N = 8$ are used. Include the points $\xi = 0$ and $\xi = 1$ as external collocation points and show that these expressions satisfy Eq. (8) of Example 12-2.

12-2 Develop the expressions for the approximate solutions for C_{p1} and C_{p2} of Example 12-2, when the Jacobi polynomials $P_N^{(0,0)}(\rho)$ of order $N = 8$ are used. Include the point $\rho = 1$ as an external collocation point and show that these expressions satisfy Eq. (11) of Example 12-2.

12-3 Using the procedure outlined in Chap. 10 for the orthogonal collocation method, evaluate the discretization matrices $\{A_{j,i}\}$ and $\{B_{j,i}\}$, and the locations of the internal collocation points for the approximate solutions developed in Probs. 12-1 and 12-2.

12-4 Show that when the changes of variables listed in Eq. (1) of Example 12-2 in the text are made, Eq. (12-30) for binary adsorption on spherical pellets reduces to the expressions given by Eqs. (2) and (3) of Example 12-2 in the text.

CHAPTER

THIRTEEN

MODELING AND SOLUTION OF THE EQUATIONS FOR THE FREEZE-DRYING PROCESS

The process called freeze-drying is an example of a separation process in which water is removed from a material by sublimation. Water is removed directly as a vapor from the frozen substance (the ice phase) without its ever having passed through the liquid phase. Consequently, it is necessary that the temperature of the sublimation zone of a material being freeze-dried be held below the triple-point temperature of the water or the aqueous solution in the material being dried (Ref. 8).

Freeze-drying plays an important role in the manufacture of many substances which would otherwise suffer bacterial degradation in the presence of a small amount of moisture. Some common applications of the freeze-drying process are the manufacture of blood plasma, vaccines, antibiotics, hormones, alkaloids, vegetables, coffee, soup, and milk.

The freeze-drying process usually operates at low temperatures and pressures, and the principal advantage lies in the high quality of the product. The freeze-drying process is, however, slow and energy-intensive, and the product, although of high quality, is generally expensive.

Section 13-1 is devoted to the formulation of the model of the freeze-drying process, and Sec. 13-2 to the solution of the corresponding equations describing the model.

13-1 MODELING OF THE FREEZE-DRYING PROCESS

Although only one model is considered, the one proposed by Litchfield and Liapis(11,12), several others have been published with the earliest being due to King(8). King postulated the uniform retreating ice front (URIF) model. This model has considerable appeal because of its simplicity. It attempts to account for the removal of the first 75 to 90 percent of the moisture. The remaining moisture is present in the form of physically or chemically adsorbed water or water of crystallization. In addition, some moisture may be physically trapped within pockets in the material, from which it can leave only through small channels which offer a high resistance to mass transfer. Although the "bound" water constitutes a small proportion of the total, its effect is significant as it frequently takes as long to remove it as it does the free water.

However, the URIF model has been shown by Sheng and Peck(19) to be quite inaccurate for predicting drying times even for the removal of free water. Sheng and Peck(19) proposed a model which takes bound water into account and which gives good agreement over the entire drying period. This model is limited, however, by the assumptions of (1) constant surface and interface temperatures, (2) a heat transfer controlled process, and (3) that bound water leaves only after all of the ice has sublimated.

The model of Litchfield and Liapis(12), which is presented herein, does not suffer from the above restrictions. Sublimation and desorption of water are allowed to take place simultaneously. This is in agreement with experimental results of Moffert(15), who determined the moisture content in layers of suede 3.6 cm thick while it was undergoing the freeze-drying process. Concentrations varied from 3 g water per 100 g solids at the dried surface to about 33 g water per 100 g solids near the interface. Moffert's results agree with those of Gentzler and Schmidt(4) who postulated an empirical relationship for moisture content in terms of the temperature difference between a given place in the dried layer and the ice interface.

In the freeze-drying process, the frozen material is placed in the drying chamber, which is then evacuated. A heat source radiates energy to the surface of the substance, where it is transferred through the dried layer to the frozen interface by conduction. As sublimation proceeds, the frozen interface recedes. Water vapor travels in a counter direction to that of the heat flow, since it is formed at the interface and collected as ice on the condenser surface at the top of the vacuum chamber.

The one-dimensional system shown in Fig. 13-1 consists of a heat source which is positioned above a slab of material of thickness z_T which is to be dried. At any time during the drying process, the slab is considered as two parts, the dried layer and the undried or frozen layer. The two layers are separated by an interface. In particular, the model is based on the following assumptions:

1. Only one-dimensional heat and mass flows, normal to the surface, and interface, are considered.

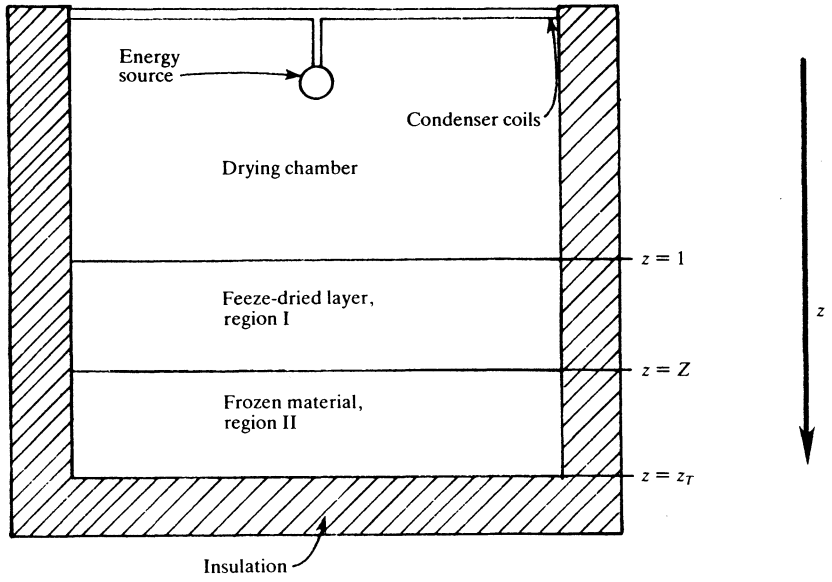

Figure 13-1 Sketch of the freeze-drying process

2. Sublimation occurs at the interface at a distance Z from the surface of the sample.
3. The thickness of the interface is taken to be infinitesimal. This assumption has been validated for most applications by Harper(7).
4. A binary mixture of water vapor and inert gas flows through the dried layer.
5. At the ice interface, the concentration of water vapor is in equilibrium with the ice.
6. As the interface recedes, it leaves behind a partially dried layer which consists of the material to be dried and adsorbed water (the solid phase). The vapor phase consists of water vapor and an inert gas which are assumed to be in thermal equilibrium with the solid phase.
7. The frozen region is considered to be homogeneous, of uniform thermal conductivity, density, and specific heat, and to contain an insignificant proportion of dissolved gases.
8. The sides and bottom of the slab are assumed to be perfectly insulated against the transfer of mass and heat.
9. The total pressure P of the drying chamber is maintained by the control of the amounts of inerts (noncondensable gases) in the vapor phase through the use of an appropriately sized condenser and vacuum pump and the necessary controls. (Most of the inert gases in the system are assumed to enter through leaks.)

Heat Transfer by Conduction through the Frozen Phase (Region II) ($Z < z < z_T$)

The interface between the dried phase and the frozen phase represents a moving boundary whose position is denoted by $Z(t)$ or simply Z. Let q_{cd} denote the rate of heat transfer per unit area by conduction in the positive direction of z (see Fig. 13-1). This rate of heat transfer as given by Fourier's first law in the frozen phase (region II) is

$$q_{cd} = -k_{II} \frac{\partial T_{II}}{\partial z} \tag{13-1}$$

where k_{II} is the thermal conductivity of region II and $T_{II}(z, t)$ is the temperature at any z and t. An energy balance on the element of volume from z_j to $z_j + \Delta z$ over the time period from t_n to $t_n + \Delta t$ is given by

$$\int_{t_n}^{t_n+\Delta z} \left[(q_{cd}\, S)\Big|_{z_j, t} - (q_{cd}\, S)\Big|_{z_j+\Delta z,\, t} \right] dt = \int_{z_j}^{z_j+\Delta z} \left[(h_{II}\, \rho_{II}\, S)\Big|_{t_n+\Delta t,\, z} - (h_{II}\, \rho_{II}\, S)\Big|_{t_n,\, z} \right] dz \tag{13-2}$$

Application of the mean-values theorems followed by the limiting process wherein Δz and Δt are allowed to go to zero and with the recognition that z_j, Δz, t_n, and Δt were arbitrarily selected within the space and time domains of interest yields

$$-\frac{\partial q_{cd}}{\partial z} = \frac{\partial (h_{II}\, \rho_{II}\, S)}{\partial t} \qquad (Z < z < z_T,\ t > 0) \tag{13-3}$$

where the interface between regions I and II is located at $z = Z$. Thus, if k_{II} and ρ_{II} are independent of temperature, and h_{II} is a function of the temperature T_{II} alone, then Eq. (13-3) becomes

$$k_{II} \frac{\partial^2 T_{II}}{\partial z^2} = \rho_{II} \frac{\partial h_{II}}{\partial T_{II}} \frac{\partial T_{II}}{\partial t} = \rho_{II}\, c_{pII} \frac{\partial T_{II}}{\partial t}$$

or

$$\frac{\partial T_{II}}{\partial t} = \alpha_{II} \frac{\partial^2 T_{II}}{\partial z^2} \qquad (Z < z < z_T,\ t > 0) \tag{13-4}$$

where

$$\alpha_{II} = \frac{k_{II}}{\rho_{II}\, c_{pII}}$$

Component Material Balances for Region I ($0 < z < Z$)

The gas or vapor phase consists of water vapor and inert gases, and the solid phase consists of the dried material with physically adsorbed water. The equations are formulated for the general case of any number of components in the vapor and solid phases.

Let N_i denote the total molar flow rate of component i in the positive direction of z per unit time per unit of cross-sectional area. Then the component-material balance for any component i in the element of volume from z_j to $z_j + \Delta z$ of region I over the time period from t_n to $t_n + \Delta t$ is given by

$$\int_{t_n}^{t_n+\Delta t} \left(SN_i\Big|_{z_j,\,t} - SN_i\Big|_{z_j+\Delta z,\,t} \right) dt = \int_{z_j}^{z_j+\Delta z} \left[(\varepsilon C_{gi} S + C_{si} S)\Big|_{t_n+\Delta t,\,z} - (\varepsilon C_{gi} S + C_{si} S)\Big|_{t_n,\,z} \right] dz \quad (13\text{-}5)$$

where S is the cross-sectional area of the slab (perpendicular to the direction z). In the same manner as described beneath Eq. (13-2), the above equation is readily reduced to the following differential equation:

$$-\frac{\partial N_i}{\partial z} = \varepsilon \frac{\partial C_{gi}}{\partial t} + \frac{\partial C_{si}}{\partial t} \qquad (0 < z < Z,\ t > 0) \quad (13\text{-}6)$$

For the inert gas component (i = in), $C_{si} = 0$, and Eq. (13-6) reduces to

$$-\frac{\partial N_{\text{in}}}{\partial z} = \varepsilon \frac{\partial C_{g\text{in}}}{\partial t} \qquad (0 < z < Z,\ t > 0) \quad (13\text{-}7)$$

At low pressures, the concentrations of water vapor and the inert gas are given by the perfect gas law

$$p_i = C_{gi} RT \quad (13\text{-}8)$$

Thus, for water ($i = w$) and the inert (i = in), Eq. (13-6) and (13-7) become

$$-\frac{\partial N_w}{\partial z} = \frac{\varepsilon}{RT}\frac{\partial p_w}{\partial t} + \frac{\partial C_{sw}}{\partial t} \qquad (0 < z < Z,\ t > 0) \quad (13\text{-}9)$$

and

$$-\frac{\partial N_{\text{in}}}{\partial z} = \frac{\varepsilon}{RT}\frac{\partial p_{\text{in}}}{\partial t} \qquad (0 < z < Z,\ t > 0) \quad (13\text{-}10)$$

where the derivatives involving the temperatures have been omitted because Gunn(2) showed that they were negligible.

Energy Balance on Region I, the Dried Layer ($0 < z < Z$)

For convenience and generalization, each phase is assumed to consist of a multicomponent mixture. All components in both phases are assumed to be in

thermal equilibrium at the temperature $T_I(z, t)$. Let the enthalpy of a component in the vapor phase be denoted by H_i and in the solid phase by h_i. Then the energy balance over the element of volume from z_j to $z_j + \Delta z$ over the time period from t_n to $t_n + \Delta t$ is given by

$$\int_{t_n}^{t_n+\Delta t} \left(q_{cd} S\Big|_{z_j,\,t} - q_{cd} S\Big|_{z_j+\Delta z,\,t} + \Sigma_i N_i H_i\Big|_{z_j,\,t} - \Sigma_i N_i H_i\Big|_{z_j+\Delta z,\,t} \right) dt = \int_{z_j}^{z_j+\Delta z} \left[(\Sigma_i \varepsilon C_{gi} H_i + \Sigma_i C_{si} h_i)\Big|_{t_n+\Delta t,\,z} - (\Sigma_i \varepsilon C_{gi} H_i + \Sigma_i C_{si} h_i)\Big|_{t_n,\,z} \right] S\, dz \quad (13\text{-}11)$$

In the same manner as described beneath Eq. (13-2), the above equation is readily reduced to

$$-\frac{\partial q_{cd}}{\partial z} - \frac{\partial \Sigma_i N_i H_i}{\partial z} = \frac{\partial \Sigma_i \varepsilon C_{gi} H_i}{\partial t} + \frac{\partial \Sigma_i C_{si} h_i}{\partial t} \qquad (0 < z < Z,\ t > 0) \quad (13\text{-}12)$$

where Σ_i denotes the sum over all components i present.

Equation (13-12) may be restated in terms of the heat of evaporation by use of the following procedure. Multiply each term of Eq. (13-6) by H_i and sum over all components i to obtain

$$-\Sigma_i \left(\frac{\partial N_i}{\partial z} \right) H_i = \Sigma_i \left(\varepsilon \frac{\partial C_{gi}}{\partial t} \right) H_i + \Sigma_i \frac{\partial C_{si}}{\partial t} H_i \quad (13\text{-}13)$$

After having carried out the partial differentiation implied in Eq. (13-12), subtract Eq. (13-13) from the result so obtained to give

$$-\frac{\partial q_{cd}}{\partial z} - \Sigma_i N_i \frac{\partial H_i}{\partial z} = \Sigma_i \varepsilon C_{gi} \frac{\partial H_i}{\partial t} + \Sigma_i C_{si} \frac{\partial h_i}{\partial t} + \Sigma_i (h_i - H_i) \frac{\partial C_{si}}{\partial t} \quad (13\text{-}14)$$

Since H_i and h_i have been assumed to be functions of T_I alone, it follows that

$$\frac{\partial H_i}{\partial z} = \frac{\partial H_i}{\partial T_I}\frac{\partial T_I}{\partial z} = c_{pgi}\frac{\partial T_I}{\partial z}$$
$$\frac{\partial h_i}{\partial t} = \frac{\partial h_i}{\partial T_I}\frac{\partial T_I}{\partial t} = c_{psi}\frac{\partial T_I}{\partial t} \quad (13\text{-}15)$$

Let

$$N_T c_{pg} = N_T \Sigma_i y_i c_{pgi} = \Sigma_i N_i c_{pgi} \qquad N_T = \Sigma_i N_i$$
$$C_{Tg} c_{pg} = C_{Tg} \Sigma_i y_i c_{pgi} = \Sigma_i C_{gi} c_{pgi} \qquad C_{Tg} = \Sigma_i C_{gi}$$
$$C_{Ts} c_{ps} = C_{Ts} \Sigma_i x_i c_{psi} = \Sigma_i C_{si} c_{psi} \qquad C_{Ts} = \Sigma_i C_{si} \quad (13\text{-}16)$$

Use of the above definitions and relationships permits Eq. (13-10) to be restated in the following form for the case of a single adsorbed component:

$$k_{1e}\frac{\partial^2 T_I}{\partial z^2} - N_T c_{pg}\frac{\partial T_I}{\partial z} = \rho_{1e} c_{ple}\frac{\partial T_I}{\partial t} - \Delta H_v \frac{\partial C_{sw}}{\partial t} \qquad (13\text{-}17)$$

where $\Delta H_i = H_w - h_w$ = heat of vaporization of absorbed water
$\rho_{1e} c_{ple} = C_{Tg} c_{pg} + C_{Ts} c_{ps} \cong$ equivalent density and heat capacity of the combined vapor and solid phase of region I

Note that either mass or molar units may be used in the above equations, since

$$N_T c_{pg} = \bar{N}_T \bar{c}_{pg} \qquad C_{Tg} c_{pg} = \bar{C}_{Tg} \bar{c}_{pg} \qquad (13\text{-}18)$$

where the quantities without overbars are in molar units and those with overbars are in mass units.

Material Balance on the Adsorbed Water ($0 < z < Z$)

Let r_w denote the rate of mass transfer of water from the bulk conditions of the vapor phase to the adsorbed phase in moles per unit time per unit volume of bed. Then a material balance on the adsorbed phase is given by

$$\int_{t_n}^{t_n+\Delta t}\left(\int_{z_j}^{z_j+\Delta z} r_w S\, dz\right) dt = \int_{z_j}^{z_j+\Delta z}\left(C_{sw}S\Big|_{t_n+\Delta t,\, z} - C_{sw}S\Big|_{t_n,\, z}\right) dz \qquad (13\text{-}19)$$

As described previously, this expression may be reduced to the following partial differential equation:

$$r_w = \frac{\partial C_w}{\partial t} \qquad (13\text{-}20)$$

The rate of mass transfer from the vapor phase to the adsorbed phase is given by

$$r_w = K_{sw} a_s (C^*_{sw} - C_{sw}) \qquad (13\text{-}21)$$

where a_s is the interfacial area per unit volume of dried bed, K_{sw} is the overall mass transfer coefficient for water vapor, and C^*_{sw} is the concentration which water would have in the dried phase if it were in equilibrium with the vapor phase. Elimination of r_w from Eqs. (13-20) and (13-21) gives

$$\frac{\partial C_{sw}}{\partial t} = K_{sw} a_s (C^*_{sw} - C_{sw}) \qquad (13\text{-}22)$$

A relationship for C^*_{sw} was fitted by application of a flexible pattern search to the data of King et al.(9) for freeze-dried turkey. It was found impossible, however, to fit an isotherm to the data both below and above 0°C, and separate

isotherm expressions were developed. Expressions obtained for the weight fraction X^*_w (where $C^*_{sw} = \rho_s X^*_w$, where ρ_s is the mass density) are as follows:

$$X^*_w = \frac{2.32 \times 10^{-4} p_w^{0.1594} \exp(962.779/T)}{1 - 0.0101 p_w^{0.1594} \exp(962.779/T)} \qquad (T > 0°C) \qquad (13\text{-}23)$$

and

$$X^*_w = \frac{1.766 \times 10^{-4} \exp(1035.786/T) p_w^{0.267}}{1 - 3.69 \times 10^{-3} \exp(1035.786/T) p_w^{0.267}} \qquad (T < 0°C) \qquad (13\text{-}24)$$

The expressions given by Eqs. (13-23) and (13-24) are seen to be based on the Sips type II adsorption isotherms. The standard deviation in the values of X^*_w as reported by Litchfield and Liapis(13) was 0.009 for Eq. (13-23) and 0.012 for Eq. (13-24).

Mass Transport Rate Expressions for the Dried Phase ($0 < z < Z$)

The following equations for the rate of transport of the binary mixture through the dried region are based on the diffusion equations of Evans et al.(1) and the D'Arcy equation for viscous flow:

$$N_w = -\frac{1}{RT}\left(k_1 \frac{\partial p_w}{\partial z} + k_2 p_w \frac{\partial P}{\partial z}\right) \qquad (13\text{-}25)$$

$$N_{in} = -\frac{1}{RT}\left(k_3 \frac{\partial p_{in}}{\partial z} + k_4 p_{in} \frac{\partial P}{\partial z}\right) \qquad (13\text{-}26)$$

where $P = p_w + p_{in}$ = the total pressure

These equations are based on the supposition that the water vapor can escape through the dried layer by bulk molecular diffusion, and through the inert gas by Knudsen diffusion and by viscous flow in response to a gradient in total pressure. Surface and thermal modes of diffusion were not considered because they have been found to be unimportant contributors (Ref. 2). Gunn and King(3) have shown that the contribution of viscous flow to N_w and N_{in} is small. At low chamber pressures or in the absence of an inert gas, the Knudsen diffusion term is the most significant term, and at higher pressures when an inert gas is present, the bulk diffusion term becomes rate-controlling. Thus, Eqs. (13-25) and (13-26) may be reduced to

$$N_w = -\frac{k_1}{RT}\frac{\partial p_w}{\partial z} \qquad (13\text{-}27)$$

$$N_{in} = -\frac{k_3}{RT}\frac{\partial p_{in}}{\partial z} \qquad (13\text{-}28)$$

A further simplification is possible. Since Gunn(2) has shown that the partial pressure of the inert gas varies by only a small fraction, the variation of the

partial pressure of the inert gas may be neglected in the evaluation of k_1. Thus, Eq. (13-27) can be solved without recourse to Eq. (13-28) which becomes redundant. The condition at the interface ($z = 0$) follows Fourier's law; that is, $q_I = -k_{Ie}\,(\partial T_I/\partial z)|_{z=0}$.

Conditions at the interface ($z = Z$) The boundary condition for the moving interface Z between the dried layer (region I) and frozen layer (region II) is effected by use of material and energy balances as follows. Let u denote the velocity at which the interface moves in the positive direction of z. Then over the time period from t_n to $t_n + \Delta t$, the interface moves a distance $u\,\Delta t$. Thus, the energy in the element of volume $Su\,\Delta t$ at time t_n is $uS\,\Delta t\,\Sigma_i C_{IIi} h_{IIi}$ and the energy in the element of volume $Su\,\Delta t$ at time $t_n + \Delta t$ is $uS\,\Delta t\,(\Sigma_i \varepsilon C_{gi} H_i + \Sigma_i C_{si} h_i)$. The net rate of transfer of energy from the boundary Z in the positive direction of z over the time period from t_n to $t_n + \Delta t$ is $S\,\Delta t\,\Sigma_i N_i H_i$. The net rate of heat transfer to and away from the boundary Z during the time period Δt is $S\,\Delta t(q_I - q_{II})$.

Thus

$$q_I - q_{II} + \Sigma_i N_i H_i = u\Sigma_i \varepsilon C_{gi} H_i + u\Sigma_i C_{si} h_i - u\Sigma_i C_{IIi} h_{IIi} \qquad (13\text{-}29)$$

The corresponding component-material balance is given by

$$N_i = \varepsilon u C_{gi} + u C_{si} - u C_{IIi} \qquad (13\text{-}30)$$

Multiplication of each member of Eq. (13-30) by h_{IIi} and summing over all components i gives

$$\Sigma_i N_i h_{IIi} = u\Sigma_i \varepsilon C_{gi} h_{IIi} + u\Sigma_i C_{si} h_{IIi} - u\Sigma_i C_{IIi} h_{IIi} \qquad (13\text{-}31)$$

Subtraction of Eq. (13-31) from (13-29) followed by rearrangement yields

$$q_I - q_{II} + \Sigma_i N_i(H_i - h_{IIi}) = u\Sigma_i \varepsilon C_{gi}(H_i - h_{IIi}) + u\Sigma_i C_{si}(h_{si} - h_{IIi}) \qquad (13\text{-}32)$$

Thus

$$-k_{Ie}\frac{\partial T_I}{\partial z} + k_{II}\frac{\partial T_{II}}{\partial z} + (N_T - \varepsilon u C_{Tg})\,\Delta H_s = uC_{Ts}(c_{ps} T_I - c_{pII} T_{II}) \qquad (z = Z,\ t > 0) \qquad (13\text{-}33)$$

where the datum temperature for the enthalpies is taken to be absolute zero and

$$\Delta H_s = \Sigma_i y_i(H_i - h_{IIi}) \cong y_w(H_w - h_{II,\,w}) = \text{heat of sublimation of water}$$

The total-material balance at the interface is obtained by summing each member of Eq. (13-30) over all components i to give the following result upon solving for u, the rate of advance of the interface, dZ/dt, that is,

$$u = \frac{dZ}{dt} = \frac{N_T}{\varepsilon C_{Tg} + C_{Ts} - C_{TII}} \qquad (13\text{-}34)$$

At the interface at $z = Z$, the partial pressure of water in equilibrium with the frozen solid is given by the thermodynamic equilibrium relationship

$$p_w = 133.32 \exp\,[(23.9936 - 2.19\,\Delta H_s)/T] \qquad \text{at } z = Z \qquad (13\text{-}35)$$

Also since most of the inert gas present enters through leaks in the chamber and not from the ice phase, the partial pressure gradient of the inert must be equal to zero at the interface, that is,

$$\left.\frac{\partial p_{in}}{\partial z}\right|_{z=Z} = 0 \qquad (z = Z,\ 0 < t < t_{z=z_T}) \qquad (13\text{-}36)$$

Also, it is assumed that thermal equilibrium exists at the interface Z, which is expressed by

$$T_I = T_Z = T_{II} \qquad (z = Z,\ t > 0) \qquad (13\text{-}37)$$

Conditions at the boundary $z = z_T$ Since the bottom as well as the sides are assumed to be perfectly insulated, it follows that $q_{II} = 0$ at $z = z_T$, or

$$\frac{\partial T_I}{\partial z} = 0 \qquad (t > t_{Z=z_T}) \qquad (13\text{-}38)$$

$$\frac{\partial T_{II}}{\partial z} = 0 \qquad (z = z_T,\ t \geq 0) \qquad (13\text{-}39)$$

Initial conditions Initially when the slab is placed in the drying chamber, the temperature of the slab is at most a function of z, that is,

$$T_I = T_{II} = T_Z = T^0(z) \qquad (0 \leq z \leq z_T,\ t \leq 0) \qquad (13\text{-}40)$$

If, initially, the interface Z is not at the surface ($z = 0$), then the concentration of adsorbed water is uniform throughout the dried layer, that is,

$$C_{sw} = C_{sw}^0 \qquad (0 < z < Z,\ t \leq 0) \qquad (13\text{-}41)$$

Other initial conditions are as follows:

$$p_w = p_{w0} \qquad (z = 0,\ t > 0) \qquad (13\text{-}42)$$

$$p_w = p_w^0 \qquad (0 < z \leq Z,\ t \leq 0) \qquad (13\text{-}43)$$

$$p_{in} = p_{in}^0 \qquad (0 < z \leq Z,\ t \leq 0) \qquad (13\text{-}44)$$

$$T_I = T_s \qquad (z = 0,\ t > 0) \qquad (13\text{-}45)$$

13-2 SOLUTION OF THE MOVING-BOUNDARY PROBLEM

The moving boundary of the system was transformed into a fixed-boundary problem by use of the method proposed by Liapis and Litchfield(12) which involves the introduction of two dimensionless variables. First, however, an

additional simplification which involves Eq. (13-4) is possible. The time constant associated with this equation has been estimated from the experimental data of Meo(14), Gunn(2), and Sandall et al.(18) and found to be an order of magnitude smaller than for Eq. (13-17). Thus, the time derivative of Eq. (13-4) may be set equal to zero which gives

$$\frac{\partial T_{II}}{\partial t} = 0 \qquad (Z \le z < z_T) \tag{13-46}$$

$$\frac{\partial^2 T_{II}}{\partial z^2} = 0 \qquad (Z \le z < z_T) \tag{13-47}$$

The solution which satisfies these conditions and the condition $\partial T_{II}/\partial z = 0$ at z_T is

$$T_{II} = \text{const} = T_Z \qquad (Z \le z < z_T) \tag{13-48}$$

Thus

$$\frac{\partial T_{II}}{\partial z} = 0 \qquad (Z \le z < z_T) \tag{13-49}$$

In order to immobilize the boundary at $z = Z$, Litchfield and Liapis(13) suggest making the following changes in variables. Let

$$\xi = \frac{z}{Z(t)} \qquad (0 \le z \le Z) \tag{13-50}$$

$$\phi = \frac{z - Z(t)}{z_T - Z(t)} \qquad (Z \le z < z_T) \tag{13-51}$$

Thus

$$\left(\frac{\partial T_I}{\partial z}\right)_t = \frac{1}{Z}\left(\frac{\partial T_I}{\partial \xi}\right)_t \tag{13-52}$$

$$\left(\frac{\partial^2 T_I}{\partial z^2}\right)_t = \frac{1}{Z^2}\left(\frac{\partial^2 T_I}{\partial \xi^2}\right)_t \tag{13-53}$$

$$\left(\frac{\partial T_I}{\partial t}\right)_z = \left(\frac{\partial T_I}{\partial t}\right)_\xi - \frac{\xi}{Z}\frac{dZ}{dt}\left(\frac{\partial T_I}{\partial \xi}\right)_t \tag{13-54}$$

$$\left(\frac{\partial^2 T_{II}}{\partial z^2}\right)_t = \frac{1}{(z_T - Z)^2}\left(\frac{\partial^2 T_{II}}{\partial \phi^2}\right)_t \tag{13-55}$$

$$\left(\frac{\partial T_{II}}{\partial t}\right)_z = \left(\frac{\partial T_{II}}{\partial t}\right)_\phi + \left(\frac{\partial T_{II}}{\partial \phi}\right)_t \frac{dZ}{dt}\left(\frac{\phi - 1}{z_T - Z}\right) \tag{13-56}$$

In view of Eqs. (13-46) through (13-49), it follows that

$$\left(\frac{\partial T_{II}}{\partial \phi}\right)_t = 0 \qquad \left(\frac{\partial T_{II}}{\partial t}\right)_\phi = 0 \qquad \left(\frac{\partial^2 T_{II}}{\partial \phi^2}\right)_t = 0 \tag{13-57}$$

The above transformations and relationships may be used to reduce Eqs. (13-17) and (13-22) to

$$\left(\frac{\partial T_I}{\partial t}\right)_\xi = \frac{\alpha_{Ie}}{Z^2}\left(\frac{\partial^2 T_I}{\partial \xi^2}\right)_t - \frac{N_T c_{pg}}{Z\rho_{Ie} c_{pIe}}\left(\frac{\partial T_I}{\partial \xi}\right)_t + \frac{\xi}{Z}\left(\frac{dZ}{dt}\right)\left(\frac{\partial T_I}{\partial \xi}\right)_t + \frac{\Delta H_v}{\rho_{Ie} c_{pIe}}\left(\frac{\partial C_{sw}}{\partial t}\right)_z \qquad (0 \le \xi \le 1) \tag{13-58}$$

$$\left(\frac{\partial C_{sw}}{\partial t}\right)_\xi = K_{sw} a_s (C^*_{sw} - C_{sw}) + \frac{\xi}{Z}\frac{dZ}{dt}\left(\frac{\partial C_{sw}}{\partial \xi}\right)_t \qquad (0 \le \xi < 1) \tag{13-59}$$

The above relationships and Eq. (13-49) may be used to reduce Eq. (13-33) to

$$\frac{-k_{Ie}}{Z}\left(\frac{\partial T_I}{\partial \xi}\right)_t + (N_T - \varepsilon u C_{Tg})\,\Delta H_s = u C_{Ts}(c_{ps} T_I - c_{pII} T_{II}) \qquad (\xi = 1,\ 0 < t < t_{Z=z_T}) \tag{13-60}$$

Equations (13-9) and (13-10) become

$$\left(\frac{\partial p_w}{\partial t}\right)_\xi = -\frac{RT_I}{\varepsilon Z}\left(\frac{\partial N_w}{\partial \xi}\right)_t + \frac{\xi}{Z}\frac{dZ}{dt}\left(\frac{\partial p_w}{\partial \xi}\right)_t - \frac{RT_I}{\varepsilon}\left(\frac{\partial C_{sw}}{\partial t}\right)_z \tag{13-61}$$

$$\left(\frac{\partial p_{in}}{\partial t}\right)_\xi = -\frac{RT_I}{\varepsilon Z}\left(\frac{\partial N_{in}}{\partial \xi}\right)_t + \frac{\xi}{Z}\frac{dZ}{dt}\left(\frac{\partial p_{in}}{\partial \xi}\right)_t \tag{13-62}$$

Equation (13-27) becomes

$$N_w = -\frac{k_1}{ZRT_I}\left(\frac{\partial p_w}{\partial \xi}\right)_t \tag{13-63}$$

and the corresponding expression for N_{in} is not restated since it is redundant as discussed above. Use of Eq. (13-63) permits the elimination of $(\partial N_w/\partial \xi)_t$ from Eq. (13-61) to give

$$\left(\frac{\partial p_w}{\partial t}\right)_\xi = \frac{k_1}{\varepsilon Z^2}\left(\frac{\partial^2 p_w}{\partial \xi^2}\right)_t + \frac{\xi}{Z}\frac{dZ}{dt}\left(\frac{\partial p_w}{\partial \xi}\right)_t - \frac{RT_I}{\varepsilon}\left(\frac{\partial C_{sw}}{\partial t}\right)_z \tag{13-64}$$

Method of solution Equations (13-58), (13-59), and (13-64) together with the set of boundary and initial conditions (Eqs. (13-34), (13-35), and (13-40) through (13-45) and (13-60)) comprise a set of nonlinear partial differential equations which must be solved numerically. Greenfield(6) determined the characteristics of several finite difference techniques on problems of this type and found that the method of Crank–Nicholson was superior from standpoint of stability and execution time. This procedure was used by Litchfield and Liapis(13) in the solution of problems described below. Execution times were of the order of 2 to 5 h on a DEC PDP11. The authors state, however, that the time could have been further reduced by streamlining the program.

The only numerical problem encountered was the stability of the method for small values of Z, which occurred at the beginning of a run. For instance, the initial step size was constrained by the stability of the response to about 1/20 sec. As Z increased, step sizes of several seconds were possible. The accuracy of the method was investigated with 4, 6, and 8 space points, and 6 space points were found to be satisfactory.

In order to demonstrate the method of solution, the Crank–Nicholson method is applied to the principal working equations. First of all, the total derivative dZ/dt was replaced wherever it appeared by the finite difference approximation, namely,

$$\frac{dZ}{dt} \cong \frac{Z_{n+1} - Z_n}{\Delta t} \tag{13-65}$$

Application of the Crank–Nicholson method to (13-58) gives

$$\frac{T_{1j,\,n+1} - T_{1j,\,n}}{\Delta t} = \frac{\alpha_{1e}}{\bar{Z}_n^2}\left(\tfrac{1}{2}\delta^2 T_{1j,\,n+1} + \tfrac{1}{2}\delta^2 T_{1j,n}\right) - \frac{\bar{N}_{wj,\,n} c_{pg}}{\bar{Z}_n \rho_{1e} c_{ple}}\left(\tfrac{1}{2}\delta T_{1j,\,n+1} + \tfrac{1}{2}\delta T_{1j,\,n}\right)$$
$$+ \frac{\Delta H_v}{\rho_{1e} c_{ple}}\left(\frac{C_{swj,\,n+1} - C_{swj,\,n}}{\Delta t}\right) + \frac{\bar{\xi}_j}{\bar{Z}_n}\left(\frac{Z_{n+1} - Z_n}{\Delta t}\right)\left(\tfrac{1}{2}\delta T_{1j,\,n+1} + \tfrac{1}{2}\delta T_{1j,\,n}\right)$$
$$(j = 1, 2, \ldots, 6) \tag{13-66}$$

Equation (13-59) becomes

$$\frac{C_{swj,\,n+1} - C_{swj,\,n}}{\Delta t} = K_{sw} a_s (C^*_{swj,\,n+1} - C_{swj,\,n+1}) + \frac{\bar{\xi}_j}{\bar{Z}_n}\left(\tfrac{1}{2}\delta C_{swj,\,n+1} + \tfrac{1}{2}\delta C_{swj,\,n}\right)\left(\frac{Z_{n+1} - Z_n}{\Delta t}\right)$$
$$(j = 1, 2, \ldots, 6) \tag{13-67}$$

and Eq. (13-61) becomes

$$\frac{p_{wj,\,n+1} - p_{wj,\,n}}{\Delta t} = \frac{k_1}{\varepsilon \bar{Z}_n^2}\left(\tfrac{1}{2}\delta^2 p_{w,\,j+1} + \tfrac{1}{2}\delta^2 p_{wj,\,n}\right) + \frac{\bar{\xi}_j}{\bar{Z}_n}\left(\tfrac{1}{2}\delta p_{wj,\,n+1} + \tfrac{1}{2}\delta p_{wj,\,n}\right)\left(\frac{Z_{n+1} - Z_n}{\Delta t}\right)$$
$$- \frac{R\bar{T}_{1j,\,n}}{\varepsilon}\left(\frac{C_{swj,\,n+1} - C_{swj,\,n}}{\Delta t}\right) \qquad (j = 1, 2, \ldots, 6) \tag{13-68}$$

where the second central difference is defined by Eq. (10-72), and the first central difference of an arbitrary variable u with respect to ξ is defined by

$$\delta u_{j,\,n+1} = \frac{u_{j+1,\,n+1} - u_{j-1,\,n+1}}{2\,\Delta\xi} \tag{13-69}$$

and

$$\bar{\xi}_j = \frac{\xi_{j+1} + \xi_j}{2}$$

$$\bar{Z}_n = \frac{Z_{n+1} + Z_n}{2}$$

$$\bar{T}_{1,\,j,\,n} = \frac{T_{1,\,j+1,\,n+1} + T_{1,\,j,\,n}}{2}$$

Equation (13-63) becomes

$$\bar{N}_{wj,\,n} = \frac{-k_1}{R\bar{T}_{1j,\,n}\bar{Z}_n}\left(\tfrac{1}{2}\delta p_{wj,\,n+1} + \tfrac{1}{2}\delta p_{wj,\,n}\right) \qquad (j = 1, 2, \ldots, 6) \tag{13-70}$$

Since Eq. (13-34) applies at the interface, it is to be applied once each time step while the above equations are applied six times for each time step. Thus, Eq. (13-34) becomes

$$\frac{Z_{n+1} - Z_n}{\Delta t} = \frac{\bar{N}_{w6,\,n}}{\varepsilon C_{Tg} + C_{Ts} - C_{TII}} \tag{13-71}$$

For any one time step (say from t_n to t_{n+1}), Eqs. (13-66), (13-67), (13-68), (13-70), and (13-71) consist of 25 equations in 25 unknown values at the end of the time step, namely the values of $\mathbf{x}$ at t_{n+1}, where

$$\mathbf{x} = [(C_{swj} N_{wj} p_{wj} T_{1j})_{j=1,\,6}\, Z_{n+1}]^T \tag{13-72}$$

This general approach was used by Litchfield and Liapis(13) to obtain the results presented herein.

The model was used to simulate the freeze-drying of turkey meat at the experimental conditions used by Sandall(17), and the results of two experiments are presented below. The physical data needed for the model was either available in Ref. 17 or could be calculated. The overall mass transfer coefficient $K_{sw} a_s$ was estimated by use of a method proposed by Lam(10). In particular, an analytical series solution was obtained to a simplified diffusion problem in which the accumulation was neglected, and linearized water vapor pressure, temperature, and concentration profiles were used for the adsorption regime. The mass transfer coefficient was then characterized in terms of known system parameters and an experimentally determined half-life measurement for adsorption. Although an independent measurement was not available, the half-life could be estimated from the desorption-only part of the experimental drying curves. By use of this method, $K_{sw} a_s$ was estimated to be $13.5 \times 10^{-4}\ s^{-1}$ for Sandall's run 23 and $7.8 \times 10^{-4}\ s^{-1}$ for run 38.

The estimation of C^0_{sw} presented a more difficult problem, since C^0_{sw} is a characteristic property of a material, and experimental measurements of the

quantity were not available. However, Sandall's(17) experimental results indicate that for run 23, sublimation terminates (or at least, the ice front has disappeared) when about 15 percent of the initial water remains. Unfortunately, the adsorbed moisture profile in the dried layer at this time depends upon the drying history of sublimation, and also when desorption is assumed. This gives a value of C^0_{sw} immediately adjacent to the sublimation interface corresponding to about 31 percent of moisture by weight. The corresponding value of $C^0_{sw} = 0.103$ g/cm^3 was used in the computer simulations. Clearly, it would be desirable to determine the value of C^0_{sw} experimentally.

Table 13-1 gives the values of the parameters used in the determination of the curves shown in Figs. 13-2 and 13-3. In order to achieve the relatively good agreement shown, minor adjustments in the values of $K_{sw}a_s$ were made.

An obvious deficiency in the model is the use of a linear equation for mass transfer, characterized by the one parameter $K_{sw}a_s$ which lumps together several mechanisms of desorption and diffusion. In spite of this limitation, its effect on the simulation results does not appear to be too significant.

A comprehensive adsorption–sublimation model for free-drying has been presented. This model permits sorption and sublimation to take place simultaneously, and predicts the concentration of adsorbed water as a function of time and position throughout the dried region. The model may also be used to predict the overall drying time with good accuracy.

Table 13-1 Values used for the parameters in the solution of the problems shown in Figs. 13-2 and 13-3

Parameter	Value used in Fig. 13-2	Value used in Fig. 13-3
p_{in}	0.0 N/m^2	0.0 N/m^2
p_{w0}	266.4 N/m^2	119.9 N/m^2
z_T	0.00584 m	0.00602 m
c_{pl}	2.931 kJ/kg K	2.931 kJ/kg K
p_{PII}	1.968 kJ/kg K	1.968 kJ/kg K
c_{pg}	1.6747 kJ/kg K	1.6747 kJ/kg K
p_{ple}	2.931 kJ/kg K	2.931 kJ/kg K
ρ_I	333.0 kg/m^3	333.0 kg/m^3
ρ_{II}	1133.0 kg/m^3	1133.0 kg/m^3
K_w	4×10^{-3} m^2/s	4×10^{-3} m^2/s
$C_2 D^0_w$	4.1813 N/s	4.1813 N/s
T_s	30°C	60°C
ΔH	2791.2 kJ/kg	2791.2 kJ/kg
k_{le}	69.92×10^{-6} kW/m K	79.98×10^{-6} kW/m K
$K_{sw}a_s$	17.49×10^{-5} s^{-1}	5×10^{-4} s^{-1}
ρ_s	310 kg/m^3	310 kg/m^3
C^0_{sw}	0.103 g/cm^3	0.103 g/cm^3
ε	0.74	0.74

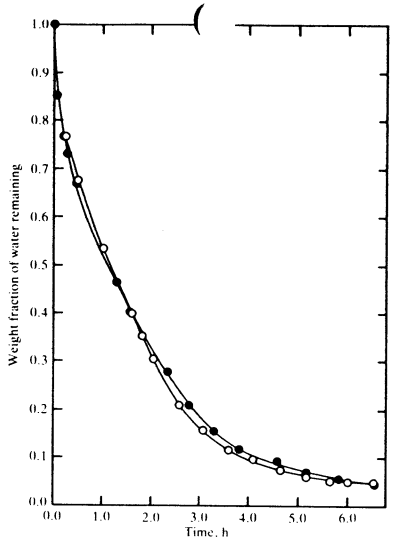

Figure 13-2 Freeze-drying of turkey meat (Surface temperature $T_s = 30$°C, pressure = 266.4 N/m^2, no inerts. Sandall's experimental results (17), run on 23, on absolute moisture basis. O: adsorption-sublimation model.) (*R. J. Litchfield and A. I. Liapis: "An Adsorption-Sublimation Model for Freeze-Drying," vol. 34 (no. 9), p. 1085 (1979). Courtesy Chemical Engineering Science.*)

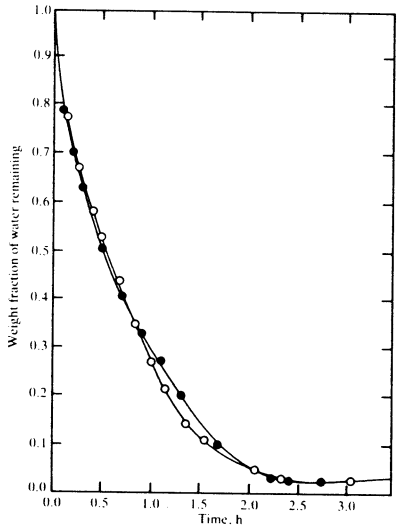

Figure 13-3 Freeze-drying of turkey meat (Surface temperature $T_s = 60$°C, pressure = 119.9 N/m^2, no inerts. Sandall's experimental results (17), run no. 38, on absolute moisture basis. O: Adsorption-Sublimation model.) (*A. I. Liapis "An Adsorption-Sublimation Model for Freeze-Drying," vol. 34 (no. 9), p. 1085 (1979). Courtesy Chemical Engineering Science.*)

NOTATION

a_s = interfacial area between the gas and the adsorbed phases, area per unit of bulk volume of the dried layer

c_{pi} = heat capacity of component i, energy per unit mass per K (or energy per mole per K)

C_1 = constant which depends only upon the structure of the porous medium and gives the relative Knudsen flow permeability

C_2 = constant which depends only upon the structure of the porous medium and is the ratio of the bulk diffusivity within the porous medium to the free gas bulk diffusivity, dimensionless

C_{01} = constant which depends only upon the structure of the porous medium and gives the relative D'Arcy flow permeability

C_{gi} = concentration of component i in the gas phase, moles (or mass) per unit of void volume of the dried phase

C_{sw} = concentration of water in the adsorbed (or solid phase), moles (or mass) per unit of bulk volume of the dried phase

C_{sw}^0 = initial concentration of bound water

D_w = free gas mutual diffusivity in a binary mixture of water vapor and inert gas

h_i = enthalpy of component i in the solid phase, energy per mole (or per unit mass)

H_i = enthalpy of component i in the vapor phase, energy per mole (or per unit mass)

$\Delta H_V = H_w - h_w$ = heat of vaporization of adsorbed water

$\Delta H_s = H_w - h_{\text{II},w}$ = heat of sublimation of water from the ice phase to the vapor phase

k = thermal conductivity, energy per K per unit of length

k_1 = bulk diffusivity constant $= (C_2 D_w K_w)/(C_2 D_w + K_{mx})$

k_2, k_4 = self-diffusivity constant $= k_w k_{\text{in}}(C_2 D_w P + K_{mx} P) + C_{01}/\mu_{mx}$

k_3 = bulk diffusivity constant $= C_2 D_w K_{\text{in}}/(C_2 D_w + K_{mx})$

K_{sw} = overall mass transfer coefficient for desorption, length/unit time

K_w = Knudsen diffusivity, $K_w = C_1\sqrt{RT/M_w}$ where M_w is the molecular weight of water

K_{in} = Knudsen diffusivity, $K_{\text{in}} = C_1\sqrt{RT/M_{\text{in}}}$ where M_{in} is the molecular weight of the inerts

K_{mx} = mean Knudsen diffusivity for the binary gas mixture, $K_{mx} = y_w K_{\text{in}} + y_{\text{in}} K_w$

N_i = flux for component i, moles (or mass) of component transferred per unit time per unit area

N_{in} = flux for the inert gas

N_w = flux for water vapor

N_T = total flux, $N_T = N_{\text{in}} + N_w$

p_{in} = partial pressure of the inert gas

p_w = partial pressure of the water vapor

P = total pressure

q_{cd} = rate of heat by conduction, energy per unit time per unit area

r_w = rate of adsorption of water vapor, moles (or mass) transferred per unit time per unit of bulk volume of the dried region

t = time

T = temperature

u = velocity at which the ice interface advances

R = gas constant

S = cross-sectional area

x_i = mole fraction of species i in the solid phase

X_w = mass fraction of water vapor in the adsorbed phase

y_i = mole fraction of species i in the vapor phase

z = distance

Z = gas-ice interface location

z_T = total thickness of the slab (see Fig. 13-1)

Greek Letters

α = thermal diffusivity

ε = volume of voids per unit volume of material

μ = viscosity

ξ = dimensionless variable (defined by Eq. (13-50))

ρ = density

Σ_i = sum over all components i present

ϕ = dimensionless variable, defined by Eq. (13-51)

Subscripts

i = component

in = inert gas

Ie = equivalent for region I

I = region I

II = region II

mx = mixture of water vapor and inerts

s = surface

w = water

Z = interface

REFERENCES

1. R. B. Evans, G. M. Watson, and E. A. Mason: "Gaseous Diffusion in Porous Media II; Effect of Pressure Gradients," *J. Chem. Phys.*, **36:** 1894 (1962).
2. R. D. Gunn: Ph.D. dissertation, University of California, 1967.
3. R. D. Gunn and C. J. King: "Mass Transport Characteristics of Freeze-Dried Foods," *Chem. Eng. Prog., Symp., Ser.*, **67**(108): 94 (1971).
4. G. L. Gentzler and F. W. Schmidt: "Thermodynamic Properties of Various Water Phases Relative to Freeze-Drying," *Trans. ASAE* **16:** 179 (1973).
5. E. Glueckauf and P. Coates: "Transport Mechanisms in Chromotography," *Trans. Faraday Soc.*, **51:** 1540 (1955).
6. P. F. Greenfield: "Cyclic-Pressures Freeze-Drying," *Chem. Eng. Sci.*, **29:** 2115 (1974).
7. J. C. Harper: "Transport Properties of Gases in Porous Media at Reduced Pressures with Reference to Freeze-Drying," *AIChE J.*, **8:** 298 (1962).
8. C. J. King: *Freeze-Drying of Foods*, CRC Press, 1971.
9. C. J. King, W. K. Lam, and O. C. Sandall: "Physical Properties Important for Freeze-Drying Poultry Meat," *Food Tech.*, **22:** 1302 (1968).
10. W. K. Lam: M.Sc. thesis, University of California, 1967.
11. A. I. Liapis and R. J. Litchfield: "Optimal Control of a Freeze-Dryer—I; Theoretical Development and Quasi-Steady State Analysis," *Chem. Eng. Sci.*, **34:** 975 (1979).
12. A. I. Liapis and R. J. Litchfield: "Numerical Solution of Moving Boundary Transport Problems in Finite Media by Orthogonal Collocation," *Comput. Chem. Eng.*, **3:** 615 (1979).
13. R. J. Litchfield and A. I. Liapis: "An Adsorption-Sublimation Model for a Freeze-Dryer," *Chem. Eng. Sci.*, **34**(9): 1085 (1979).
14. D. Meo: M.S. thesis, University of Rochester, New York, 1972.
15. H. T. Moffert: *IBVT* (now Springer Inst.), *Annu. Rep.*, Wageningen, Netherlands, 1965.
16. R. Perry and C. Chilton: (eds.): *Chemical Engineers Handbook*, 5th ed., McGraw-Hill Book Company, New York, 1973.
17. O. C. Sandall: Ph.D. dissertation, University of California, 1966.
18. O. C. Sandall, C. J. King, and C. R. Wilke: "The Relationship Between Transport Properties and Rates of Freeze-Drying of Poultry Meat," *AIChE J.*, **13:** 428 (1967).
19. T. R. Sheng and R. E. Peck: "Rates for Freeze-Drying," *AIChE Symp. Ser.*, **73**(163): 124 (1975).

PROBLEMS

13-1 For the change in variables given by Eqs. (13-50) and (13-51), produce the relationships given by Eqs. (13-52) through (13-56).

13-2 Use the relationships developed in Prob. 13-1 to show that Eqs. (13-17) and (13-22) may be restated in the form given by Eqs. (13-58) and (13-59).

13-3 Use the relationship developed in Prob. 13-1 and Eq. (13-49) to show that Eq. (13-33) may be reduced to the form given by Eq. (13-60).

13-4 Show that by use of the relationships developed in Prob. 13-1 the expressions given by Eqs. (13-9), (13-10), and (13-27) may be reduced to those given by Eqs. (13-61) through (13-63), respectively.

13-5 Use Eq. (13-27) to show that Eq. (13-64) may be obtained from Eq. (13-61).

CHAPTER

FOURTEEN

THERMODYNAMICS OF THE PHYSICAL ADSORPTION OF PURE GASES AND MULTICOMPONENT GAS MIXTURES BY SOLID ADSORBENTS

In 1878, Gibbs developed adsorption equations on the basis of purely thermodynamic considerations. Later Volmer(15) applied Gibbs' equation and an equation of state for the adsorbed layer to derive Langmuir's adsorption isotherm for unimolecular adsorption.

Adsorption processes may be regarded as consisting of three phases: the gas phase, the adsorbed phase, and the adsorbent phase (Refs. 7, 8, 9, 13). This approach to the analysis of adsorption systems is preferred over the alternate approach of Gibbs, who regarded the system as being composed of two phases separated by an interface surface which possessed no volume (Ref. 1).

The forces involved in adsorption are the surface forces, a measure of which is given by the surface tension exhibited by a substance. The molecules in the surface of a solid or liquid phase are attracted to the center of the solid or liquid phase by the interior molecules of this phase. To achieve a balance of forces, the surface molecules tend to attract foreign molecules of, say, a gas phase to the surface of the solid or liquid phase. These surface forces are also responsible for the lateral migration of surface molecules. This phenomenon is readily observed by performing numerous simple experiments. The well-known phenomena of "spreading" and "wetting" are caused by the surface forces. For example when a drop of oil is placed on the surface of a second liquid with which it is immiscible, say water, the oil quickly spreads over the water. This spreading is caused by the movement of water molecules along the interface in

an effort to adjust to the unbalance in forces caused by the presence of the oil molecules. The spreading of a liquid over a solid surface is known as the "wetting" of the solid by the liquid.

The tendency of, say, an oil drop to spread on a water surface and to exhibit two-dimensional behavior analogous to the three-dimensional behavior of a gas was an early observation. By placing a strip of wood on the surface of water in a rectangular container, de Boer(1) states that Miss Packels demonstrated in 1890 that the film of a second liquid, say oil, could be compressed by doing work on the strip of wood. Because of this behavior, surface films are commonly referred to as two-dimensional gases. Langmuir(12) followed by others developed balances which could be used to measure directly the spreading pressure exerted by films on liquid surfaces.

The spreading pressure of a film may be determined indirectly through the measurement of the surface tension of the surface of a pure liquid both before and after contamination with a second immiscible liquid (Ref. 1). Consider, for example, the case of a water surface separated into two parts by a barrier of length l centimeters (see Fig. 14-1). On one side of the barrier, the liquid (say water) surface is contaminated by a two-dimensional gas which exerts a pressure of π (dyn/cm), and on the other side of the barrier, a pure water surface exists. Furthermore, the spreading pressure is supposedly balanced by applying an external force (equal in magnitude to π) to the barrier as indicated in Fig. 14-1.

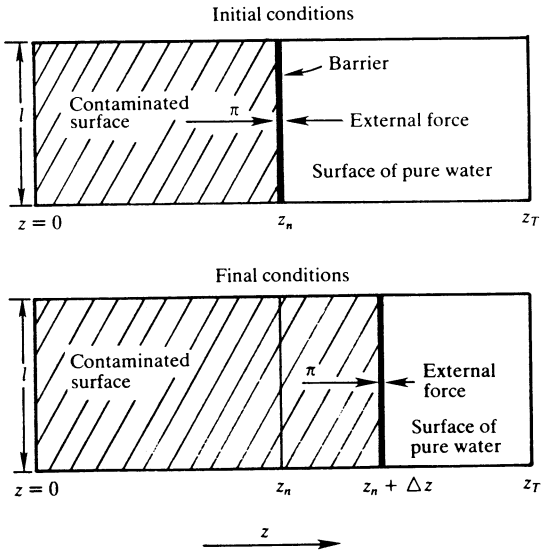

Figure 14-1 Initial and final conditions of a liquid surface.

Now suppose the barrier is allowed to move against an external force in a continuous manner to the position $z_n + \Delta z$ (see Fig. 14-1). The relationship between the spreading pressure π, the surface tension of the pure water surface γ_0, and the surface tension γ of the contaminated surface is obtained by making an energy balance. Let the total surface in Fig. 14-1 from $z = 0$ to $z = z_T$ be regarded as the system and everything else within the universe as the surroundings. Then, the energy of the system initially, $U_{\text{sys, 1}}$, is given by

$$U_{\text{sys, 1}} = \underbrace{\int_0^{z_n} \gamma l \, dz}_{\substack{\text{energy of the} \\ \text{contaminated} \\ \text{surface}}} + \underbrace{\int_{z_n}^{z_T} \gamma_0 l \, dz}_{\substack{\text{energy of the} \\ \text{pure water} \\ \text{surface}}} \tag{14-1}$$

Let the initial energy of the surroundings be denoted by $U_{\text{surr, 1}}$, and the energy of the universe by $\mathscr{U}$. Then at the initial conditions

$$\int_0^{z_n} \gamma l \, dz + \int_{z_n}^{z_T} \gamma_0 l \, dz + U_{\text{surr, 1}} = \mathscr{U} \tag{14-2}$$

At the final conditions, the energy of the system is given by

$$U_{\text{sys, 2}} = \int_0^{z_n + \Delta z} \gamma l \, dz + \int_{z_n + \Delta z}^{z_T} \gamma_0 l \, dz \tag{14-3}$$

In going from the initial to the final conditions, the work that is done by the system on the surroundings is equal to the integral of πl over the distance from $z_n + \Delta z$ to z_T. Thus, the energy of the surroundings at the final conditions, $U_{\text{surr, 2}}$, is given by

$$U_{\text{surr, 2}} = U_{\text{surr, 1}} + \int_{z_n}^{z_n + \Delta z} \pi l \, dz \tag{14-4}$$

Since, by the first law of thermodynamics, the energy of the universe is constant, it follows that at the final conditions

$$\int_0^{z_n + \Delta z} \gamma l \, dz + \int_{z_n + \Delta z}^{z_T} \gamma_0 l \, dz + U_{\text{surr, 1}} + \int_{z_n}^{z_n + \Delta z} \pi l \, dz = \mathscr{U} \tag{14-5}$$

Elimination of $\mathscr{U}$ from Eqs. (14-2) and (14-5) followed by the consolidation of the integrals yields

$$\int_{z_n}^{z_n + \Delta z} (\gamma_0 - \gamma - \pi) l \, dz = 0 \tag{14-6}$$

Observe that Eq. (14-6) holds for each choice of z_n and Δz which satisfies both of the inequalities: $0 < z_n < z_T$ and $0 < z_n + \Delta z < z_T$. Since the integral is zero for each set $(z_n, \Delta z)$ so selected, it follows that the integrand is zero for all z in the open interval $(0 < z < z_T)$, and thus the spreading pressure is related to the surface tensions of the pure and contaminated liquid surfaces as follows:

$$\pi = \gamma_0 - \gamma \tag{14-7}$$

14-1 THERMODYNAMIC FUNCTIONS REQUIRED TO DESCRIBE THE PHYSICAL ADSORPTION OF A MULTICOMPONENT MIXTURE

The treatment that follows is restricted to the case of the interaction of a gas phase composed of a multicomponent mixture, an adsorbed phase, and a solid adsorbent. Following Guggenheim(7,8), Hill(9), and more recently Myers and Prausnitz(13), it is assumed that the adsorbent is inert, that is, all of its thermodynamic properties are the same in the presence as in the absence of the adsorbate molecules. As pointed out by Hill(9), this approximation may well be inaccurate for the chemisorption of gases by solids. Secondly, it is assumed that the surface area associated with each adsorption site is independent of temperature and pressure. As discussed in a subsequent section, this assumption differs slightly from the classical assumption regarding the surface area and the number of adsorption sites.

The thermodynamic functions for the gas phase are precisely those available from classical thermodynamics; see, for example, Refs. 2, 7, 8. These equations are stated without proof:

$$dU^V = T\,dS^V - P\,dV^V + \sum_{i=1}^{c} \bar{G}_i^V\,dn_i^V \tag{14-8}$$

$$dH^V = T\,dS^V + V^V\,dP + \sum_{i=1}^{c} \bar{G}_i^V\,dn_i^V \tag{14-9}$$

$$dA^V = -S^V\,dT - P\,dV^V + \sum_{i=1}^{c} \bar{G}_i^V\,dn_i^V \tag{14-10}$$

$$dG^V = -S^V\,dT + V^V\,dP + \sum_{i=1}^{c} \bar{G}_i^V\,dn_i^V \tag{14-11}$$

where A^V = Hemholtz free energy function for the vapor phase
G^V = Gibbs free energy function of the vapor phase
$\bar{G}_i^V$ = the partial molar free energy for component i in the vapor phase (the symbol μ_i^V, called the *Gibbs chemical potential*, is also used to denote this quantity)
H^V = enthalpy of the vapor phase
S^V = entropy of the vapor phase
U^V = internal energy of the vapor phase
V^V = volume of the vapor phase

$$\bar{G}_i^V = \left(\frac{\partial G^V}{\partial n_i}\right)_{P,\,T,\,n_{j\neq i}^V} = \left(\frac{\partial U^V}{\partial n_i}\right)_{S^V,\,V^V,\,n_{j\neq i}^V} = \left(\frac{\partial H^V}{\partial n_i^V}\right)_{S^V,\,P,\,n_{j\neq i}^V} = \left(\frac{\partial A^V}{\partial n_i^V}\right)_{T,\,V^V,\,n_{j\neq i}^V}$$

n_i^V = moles of component i in the gas phase; $n_{j\neq i}^V$ as a subscript means all of the n_i^V's are held fixed except the particular n_i^V with which the partial derivative is taken

Equation (14-8) represents the first and second laws of thermodynamics for the variation of the internal energy of a multicomponent mixture as a function of the independent variables S^V, V^V, n_1^V, n_2^V, ..., n_c^V. Equations (14-9) through (14-11) follow from Eq. (14-8) as consequences of the definitions of H^V, A^V, and G^V.

The internal energy U^σ of the adsorbed phase is a function not only of S^σ, V^σ, n_1^σ, n_2^σ, ..., n_c^σ, but also of the additional variable $\mathscr{A}$, the surface area covered by adsorbed gases. (Note that in Fig. 14-1, an element of contaminated area is given by $l\,dz = d\mathscr{A}$.) The spreading pressure π and the surface area $\mathscr{A}$ play analogous but more significant roles than P and V^σ in surface phenomenon. In addition to the PV-work term $P\,dV^\sigma$, there is a surface work term $\pi\,d\mathscr{A}$. Then for the adsorbed phase, the first and second laws of thermodynamics are represented as follows:

$$dU^\sigma = T\,dS^\sigma - P\,dV^\sigma - \pi\,d\mathscr{A} + \sum_{i=1}^{c} \left(\frac{\partial U^\sigma}{\partial n_i^\sigma}\right)_{S^\sigma,\,V^\sigma,\,\mathscr{A},\,n_{j\neq i}^\sigma} dn_i^\sigma \tag{14-12}$$

which implies that the independent variables have been selected as indicated by the functional notation

$$U^\sigma = U^\sigma(S^\sigma,\, V^\sigma,\, \mathscr{A},\, n_1^\sigma,\, n_2^\sigma,\, \ldots,\, n_c^\sigma).$$

Then, the total differential of U^σ is given by

$$dU^\sigma = \left(\frac{\partial U^\sigma}{\partial S^\sigma}\right)_{V^\sigma,\,\mathscr{A},\,n_i^\sigma} dS^\sigma + \left(\frac{\partial U^\sigma}{\partial V^\sigma}\right)_{S^\sigma,\,\mathscr{A},\,n_i^\sigma} dV^\sigma + \left(\frac{\partial U^\sigma}{\partial \mathscr{A}}\right)_{S^\sigma,\,V^\sigma,\,n_i^\sigma} d\mathscr{A} + \sum_{i=1}^{c} \left(\frac{\partial U^\sigma}{\partial n_i^\sigma}\right)_{S^\sigma,\,V^\sigma,\,\mathscr{A},\,n_{j\neq i}^\sigma} dn_i^\sigma \tag{14-13}$$

where the subscript n_i^σ on a partial derivative means that all of the n_i^σ's are to be held fixed in taking the partial derivative. Comparison of Eqs. (14-12) and (14-13) shows that

$$T = \left(\frac{\partial U^\sigma}{\partial S^\sigma}\right)_{V^\sigma,\,\mathscr{A},\,n_i^\sigma} \qquad -P = \left(\frac{\partial U^\sigma}{\partial V^\sigma}\right)_{S^\sigma,\,\mathscr{A},\,n_i^\sigma} \qquad -\pi = \left(\frac{dU^\sigma}{\partial \mathscr{A}}\right)_{S^\sigma,\,V^\sigma,\,n_j^\sigma} \tag{14-14}$$

The state functions (or extensive properties) U^σ, H^σ, A^σ, S^σ, V^σ, and $\mathscr{A}$ are all homogeneous functions of degree one (see App. 1A). Such functions have the property that the internal energy, for example, of two pound moles of adsorbed material is twice that of one pound mole of adsorbed material of the same composition at the same temperature T, pressure P, and spreading pressure π. Furthermore, the intensive properties or functions T, P, and π are known from experiment to be independent of the total amount of material in the system. More precisely, at a given set of values for T, P, and π, it follows from the definition of a homogeneous function of degree one that

$$U^\sigma(\lambda S^\sigma,\, \lambda V^\sigma,\, \lambda\mathscr{A},\, \lambda n_1^\sigma,\, \lambda n_2^\sigma,\, \ldots,\, \lambda n_c^\sigma) = \lambda U^\sigma(S^\sigma,\, V^\sigma,\, \mathscr{A},\, n_1^\sigma,\, n_2^\sigma,\, \ldots,\, n_c^\sigma) \tag{14-15}$$

where λ is any positive number.

Since U^σ is homogeneous of degree one, it follows from Euler's theorem (App. 1A) that for a given set of values for T, P, and π

$$U^\sigma = S^\sigma\left(\frac{\partial U^\sigma}{\partial S^\sigma}\right)_{V^\sigma, \mathscr{A}, n_i^\sigma} + V^\sigma\left(\frac{\partial U^\sigma}{\partial V^\sigma}\right)_{S^\sigma, \mathscr{A}, n_i^\sigma} + \mathscr{A}\left(\frac{\partial U^\sigma}{\partial \mathscr{A}}\right)_{S^\sigma, V^\sigma, n_i^\sigma} + \sum_{i=1}^{c} n_i^\sigma\left(\frac{\partial U^\sigma}{\partial n_i^\sigma}\right)_{S^\sigma, V^\sigma, \mathscr{A}, n_{j\neq i}^\sigma} \quad (14\text{-}16)$$

When the partial derivatives appearing in the first three terms on the right-hand side of Eq. (14-16) are replaced by their equivalents as given by Eq. (14-14), the following result is obtained:

$$U^\sigma = TS^\sigma - PV^\sigma - \pi\mathscr{A} + \sum_{i=1}^{c} n_i^\sigma\left(\frac{\partial U^\sigma}{\partial n_i^\sigma}\right)_{S^\sigma, V^\sigma, \mathscr{A}, n_{j\neq i}^\sigma} \quad (14\text{-}17)$$

Except for the enthalpy function, which includes the $\pi\mathscr{A}$ product as well as the PV^σ product, the remaining thermodynamic functions are defined in the usual way, that is,

$$H^\sigma = U^\sigma + PV^\sigma + \pi\mathscr{A} \quad (14\text{-}18)$$

$$A^\sigma = U^\sigma - TS^\sigma \quad (14\text{-}19)$$

$$G^\sigma = H^\sigma - TS^\sigma \quad (14\text{-}20)$$

From these definitions, it follows immediately that

$$G^\sigma = U^\sigma + PV^\sigma + \pi\mathscr{A} - TS^\sigma \quad (14\text{-}21)$$

Then,

$$dG^\sigma = dU^\sigma + P\,dV^\sigma + V^\sigma\,dP + \pi\,d\mathscr{A} + \mathscr{A}\,d\pi - T\,dS^\sigma - S^\sigma\,dT \quad (14\text{-}22)$$

Elimination of dU^σ from Eqs. (14-12) and (14-22) yields

$$dG^\sigma = -S^\sigma\,dT + V^\sigma\,dP + \mathscr{A}\,d\pi + \sum_{i=1}^{c}\left(\frac{\partial U^\sigma}{\partial n_i^\sigma}\right)_{S^\sigma, V^\sigma, \mathscr{A}, n_{j\neq i}^\sigma} dn_i^\sigma \quad (14\text{-}23)$$

The independent variables in this expression are seen to be T, P, π, and n_1^σ, n_2^σ, ..., n_c^σ. Thus, the total differential of G^σ may be stated as follows:

$$dG^\sigma = \left(\frac{\partial G^\sigma}{\partial T}\right)_{P, \pi, n_i^\sigma} dT + \left(\frac{\partial G^\sigma}{\partial P}\right)_{T, \pi, n_i^\sigma} dP + \left(\frac{\partial G^\sigma}{\partial \pi}\right)_{P, T, n_i^\sigma} d\pi + \sum_{i=1}^{c}\left(\frac{\partial G^\sigma}{\partial n_i^\sigma}\right)_{P, \pi, T, n_{j\neq i}^\sigma} dn_i^\sigma \quad (14\text{-}24)$$

Comparison of Eqs. (14-23) and (14-24) shows that

$$-S^\sigma = \left(\frac{\partial G^\sigma}{\partial T}\right)_{P, \pi, n_i^\sigma} \qquad V^\sigma = \left(\frac{\partial G^\sigma}{\partial P}\right)_{T, \pi, n_i^\sigma}$$

$$\mathscr{A} = \left(\frac{\partial G^\sigma}{\partial \pi}\right)_{P, T, n_i^\sigma}$$

$$\left(\frac{\partial U^\sigma}{\partial n_i^\sigma}\right)_{S^\sigma, V^\sigma, \mathscr{A}, n_{j\neq i}^\sigma} = \left(\frac{\partial G^\sigma}{\partial n_i^\sigma}\right)_{P, \pi, T, n_{j\neq i}^\sigma} \qquad (\text{for } i = 1, 2, \ldots, c) \quad (14\text{-}25)$$

The partial derivatives of G^σ with respect to each n_i^σ with P, π, T, and the remaining n_i^σ's being held fixed were given the name of *chemical potentials* by Gibbs and denoted by the symbol μ_i^σ. This same derivative is also called the partial molar value of G^σ and denoted by the symbol $\bar{G}_i^\sigma$, that is,

$$\mu_i^\sigma = \bar{G}_i^\sigma = \left(\frac{\partial G^\sigma}{\partial n_i^\sigma}\right)_{P, \pi, T, n_{j\neq i}^\sigma} \qquad (i = 1, 2, \ldots, c) \quad (14\text{-}26)$$

In the remaining developments, $\bar{G}_i^\sigma$ is used instead of μ_i^σ because it provides a distinction between the partial molar value of G^σ and the free energy per mole of pure component i, denoted by G_i^σ. Such a distinction is not always obvious when the single symbol μ_i^σ is employed.

By use of the last equality of Eq. (14-25), the expressions given by Eqs. (14-12) and (14-23) may be restated in terms of the $\bar{G}_i^\sigma$ as follows:

$$dU^\sigma = T\,dS^\sigma - P\,dV^\sigma - \pi\,d\mathscr{A} + \sum_{i=1}^{c} \bar{G}_i^\sigma\,dn_i^\sigma \quad (14\text{-}27)$$

$$dG^\sigma = -S^\sigma\,dT + V^\sigma\,dP + \mathscr{A}\,d\pi + \sum_{i=1}^{c} \bar{G}_i^\sigma\,dn_i^\sigma \quad (14\text{-}28)$$

In an analogous manner, it is readily shown that

$$dH^\sigma = T\,dS^\sigma + V^\sigma\,dP + \mathscr{A}\,d\pi + \sum_{i=1}^{c} \bar{G}_i^\sigma\,dn_i^\sigma \quad (14\text{-}29)$$

$$dA^\sigma = -S^\sigma\,dT - P\,dV^\sigma - \pi\,d\mathscr{A} + \sum_{i=1}^{c} \bar{G}_i^\sigma\,dn_i^\sigma \quad (14\text{-}30)$$

Furthermore, Eq. (14-17) becomes

$$U^\sigma = TS^\sigma - PV^\sigma - \pi\mathscr{A} + \sum_{i=1}^{c} \bar{G}_i^\sigma n_i^\sigma \quad (14\text{-}31)$$

When the expression given by Eq. (14-31) is used to eliminate U^σ from Eqs. (14-18), (14-19), and (14-21), the following relationships are obtained:

$$G^\sigma = \sum_{i=1}^{c} \bar{G}_i^\sigma n_i^\sigma \tag{14-32}$$

$$H^\sigma = TS^\sigma + \sum_{i=1}^{c} \bar{G}_i^\sigma n_i^\sigma \tag{14-33}$$

$$A^\sigma = -PV^\sigma - \pi\mathscr{A} + \sum_{i=1}^{c} \bar{G}_i^\sigma n_i^\sigma \tag{14-34}$$

The expression corresponding to the Gibbs–Duhem equation for a conventional vapor or liquid phase is obtained by first taking the total differential of Eq. (14-32) to obtain

$$dG^\sigma = \sum_{i=1}^{c} \bar{G}_i^\sigma \, dn_i^\sigma + \sum_{i=1}^{c} n_i^\sigma \, d\bar{G}_i^\sigma \tag{14-35}$$

Elimination of dG^σ from Eqs. (14-28) and (14-35) gives

$$0 = S^\sigma \, dT - V^\sigma \, dP - \mathscr{A} \, d\pi + \sum_{i=1}^{c} n_i^\sigma \, d\bar{G}_i^\sigma \tag{14-36}$$

At constant temperature, this expression reduces to the well-known formula which is commonly called *Gibbs' adsorption formula*

$$0 = -V^\sigma \, dP - \mathscr{A} \, d\pi + \sum_{i=1}^{c} n_i^\sigma \, d\bar{G}_i^\sigma \qquad \text{(at constant } T\text{)} \tag{14-37}$$

The Phase Rule for the Adsorption of a Gas Mixture by an Inert Solid

Consider the particular system consisting of a gas phase and an adsorbed phase. The composition of each phase is fixed by specifying $c - 1$ mole fractions for each phase, where c is equal to the total number of components. (Note: the adsorbent is not counted because it is regarded as an inert.) Thus, there are $2(c - 1)$ independent composition variables, where it is understood, of course, that the definition of the mole fraction is to be used to compute the cth mole fraction in each phase. Additional variables are the temperatures T^V and T^σ of the respective phases, the pressure P, and the spreading pressure π. The total number of variables is then given by

$$\text{Number of variables} = 2(c - 1) + 4 = 2(c + 1)$$

At equilibrium, the variables are related by the following $(c + 1)$ equations:

$$\begin{aligned} T^V &= T^\sigma \\ \bar{G}_i^V &= \bar{G}_i^\sigma \qquad (i = 1, 2, \ldots, c) \end{aligned} \tag{14-38}$$

The number of degrees of freedom or variance $\mathscr{V}$ is equal to the number of variables which must be fixed in order to obtain an equality between the number of unspecified variables and the number of equations. Then

$$\mathscr{V} = 2(c + 1) - (c + 1) = c + 1 \tag{14-39}$$

Note that for a state of equilibrium to exist between an ordinary vapor and liquid phase, the Gibbs' phase rule (Ref. 6) ($\mathscr{P} + \mathscr{V} = c + 2$, where $\mathscr{P}$ is the number of phases) gives

$$\mathscr{V} = c + 2 - \mathscr{P} = c + 2 - 2 = c \tag{14-40}$$

Then relative to the conventional vapor–liquid equilibria, one additional degree of freedom exists in the adsorption process. For example, for a pure component in equilibrium with its vapor and liquid phases, $c = 1$ in Eq. (14-40). Thus if one specifies the temperature T of the system, the pressure is uniquely determined and is equal to the vapor pressure of the pure component i at the temperature T. On the other hand, consider the adsorption of component i on a unit mass of adsorbent at the temperature T. In this case $c + 1$ in Eq. (14-39) is equal to 2. If the temperature T is regarded as fixed for such a system, then infinitely many equilibrium adsorption pressures may be specified. Thus there exists infinitely many equilibrium states for the adsorption of a pure component on a given amount of adsorbent at a specified temperature. These states are commonly represented in the form of adsorption isotherms.

Simplified Formula

As described at the beginning of this chapter, the thermodynamic model employed by Gibbs for the adsorption process regarded the adsorbed phase as a surface with, of course, no volume. Consequently, his final thermodynamic functions were simpler than those stated above because they contained neither the PV^σ product nor its derivatives.

However, in the thermodynamic expressions obtained for the adsorbed phase, the PV^σ product and its differentials are negligible until infinitely many adsorbed layers have appeared on the solid surface and the adsorbed phase becomes a conventional liquid phase. Then except in the limit as the adsorption system approaches a conventional vapor–liquid equilibrium system, the PV^σ product and its differentials may be neglected in the final results, Eqs. (14-27) through (14-31), (14-34), and (14-37), to give the same set of thermodynamic expressions obtained by Gibbs. The best-known of these is the reduced form of Eq. (14-37), namely,

$$\mathscr{A} \, d\pi = \sum_{i=1}^{c} n_i^\sigma \, d\bar{G}_i^\sigma \qquad \text{(at constant } T\text{)} \tag{14-41}$$

or in terms of the kinetic model for adsorption

$$\mathscr{A} \, d\pi = \sum_{i=1}^{c} C_i \, d\bar{G}_i^\sigma \qquad \text{(at constant } T\text{)} \tag{14-42}$$

where C_i = concentration of component i in the adsorbed phase, moles of component i adsorbed per unit mass of adsorbent. This relationship (Eq. (14-41) or (14-42)) is perhaps best known as *Gibbs' adsorption formula*, but it is also called *Gibbs' adsorption equation*, *Gibbs' equation*, and *Gibbs' adsorption isotherm*.

The Fugacity

In the analysis of thermodynamic systems, it has been found that a new variable called fugacity is more convenient to use than is free energy. The fugacity of pure component i at the temperature T and pressure P in a vapor phase composed of pure component i is defined by

$$d\bar{G}_i^V(P, T) = RT\, d \ln f_i^V \qquad \text{(at constant } T\text{)} \tag{14-43}$$

and

$$\lim_{P \to 0} \frac{f_i^V}{P} = 1$$

(Note that in the remainder of this development, the symbols G_i and $\bar{G}_i$ are used to denote the free energy per mole of pure component i and the partial molar free energy of component i, respectively, rather than μ_i.) The second condition of Eq. (14-43) is equivalent to the statement of the experimental fact that an actual gas approaches a perfect gas in the limit as the pressure goes to zero (see Ref. 10).

The fugacity of component i in a vapor phase of a multicomponent mixture is defined by

$$d\bar{G}_i^V(P, T, y_1, y_2, \ldots, y_c) = RT\, d \ln \hat{f}_i^V \qquad \text{(at constant } T\text{)}$$

and

$$\lim_{P \to 0} \frac{\hat{f}_i^V}{p_i} = 1 \tag{14-44}$$

where p_i is the partial pressure of component i.

The fugacity of pure component i at the temperature T and at the spreading pressure π in an adsorbed phase composed of pure component i is defined by

$$dG_i^\sigma(\pi, T) = RT\, d \ln f_i^\sigma \qquad \text{(at constant } T\text{)}$$

and

$$\lim_{\pi \to 0} \frac{f_i^\sigma}{\pi} = 1 \tag{14-45}$$

The second condition is equivalent to the statement that the behavior of the adsorbed phase approaches that of a perfect two-dimensional gas (discussed in a subsequent section) in the limit as the spreading pressure goes to zero.

The fugacity of component i in an adsorbed phase composed of a multicomponent mixture is defined by

$$d\bar{G}_i^\sigma(\pi, T, x_1, x_2, \ldots, x_c) = RT\, d \ln \hat{f}_i^\sigma \qquad \text{(at constant } T\text{)} \tag{14-46}$$

If the standard state of component i in the vapor phase is taken to be the pure component at the pressure P and at the temperature T of the mixture, then Eq. (14-44) may be integrated at constant temperature to give

$$\bar{G}_i^V(P, T, y_1, y_2, \ldots, y_c) = G_i^V(P, T) + RT \ln \frac{\hat{f}_i^V}{f_i^V} \tag{14-47}$$

where $G_i^V(P, T)$ = free energy of one mole of a vapor phase composed of pure component i at the pressure P and at the temperature T. For the general case of an actual three-dimensional gas, it can be shown (Ref. 10) that

$$\hat{f}_i^V = \gamma_i^V f_i^V y_i \tag{14-48}$$

where f_i^V = fugacity of pure component i evaluated at the temperature T and total pressure P of the mixture

γ_i^V = the thermodynamic activity coefficient for component i in the vapor phase, $\gamma_i^V = \gamma_i^V(P, T, y_1, y_2, \ldots, y_c)$

Many mixtures of three-dimensional gases can be adequately described by taking γ_i^V equal to unity. Such a gas is said to form an ideal solution.

Perfect Three-Dimensional Gases

A *perfect gas* is one that obeys the *perfect gas law*

$$PV^V = n_T^V RT \tag{14-49}$$

where V^V is the volume of n_T^V moles, T is the absolute temperature, P is the absolute pressure, and R is the gas constant in appropriate units. The partial pressure p_i of component i in any gaseous mixture is defined by

$$p_i = Py_i \tag{14-50}$$

A perfect gas mixture is one in which each member of the mixture behaves as a perfect gas, that is, multiplication of both sides of Eq. (14-49) by y_i gives the following relationship which holds for each component i of the mixture:

$$p_i V^V = n_i^V RT \qquad \text{or} \qquad Pv_i = n_i^V RT \tag{14-51}$$

where $v_i = V^V y_i$, the partial volume of component i.

The thermodynamic relationships for a pure component in a closed system are obtained by omitting the summation terms in Eqs. (14-8) through (14-11).

Also, for a pure component, it is to be observed that $\bar{G}_i^V$ becomes equal to G_i^V.† At constant temperature, Eq. (14-11) reduces to

$$dG^V = V^V\,dP \qquad \text{(at constant } T\text{)} \tag{14-52}$$

For one mole of a perfect gas, this expression becomes

$$dG_i^V = \frac{RT}{P}\,dP = RT\,d\ln P \qquad \text{(at constant } T\text{)} \tag{14-53}$$

Comparison of this expression with Eq. (14-43) shows that for a perfect gas, the fugacity is equal to the pressure, that is, $f_i^V = P$. For the case of a gaseous mixture, an analogous relationship exists (Ref. 10), which is stated here without proof. That is, the fugacity of component i in a perfect gas mixture is equal to its partial pressure,

$$\hat{f}_i^V = p_i \tag{14-54}$$

Interpretation of the Area Term $\mathscr{A}$ in the Thermodynamic Functions and in the Equation of State for a Perfect Two-Dimensional Gas

An adsorbed phase composed of a continuous film is said to be a perfect two-dimensional gas if it obeys the *two-dimensional perfect gas law*

$$\pi\mathscr{A} = n_T^\sigma RT \tag{14-55}$$

where $\mathscr{A}$ is the surface area covered by n_T^σ moles, T is the absolute temperature, and R is the same constant that appears in the perfect gas law for three-dimensional gases.

The area term which appears in the above equation as well as the thermodynamic relationships is seen to have a very definite meaning for an adsorbed film on the surface of a liquid as demonstrated in Fig. 14-1. However, as observed by Hill(9), a unique definition of $\mathscr{A}$ does not necessarily exist for a porous adsorbent. In the thermodynamic analysis of the kinetic models presented in Chap. 11 for multicomponent adsorption, let $\mathscr{A}$ be defined as the area covered when each adsorption site of the set C_T available at a given temperature and pressure is filled. By this definition, $\mathscr{A}$ becomes the same function of temperature and pressure as C_T. Thus, this interpretation of $\mathscr{A}$ and C_T gives the following relationship:

$$\frac{\mathscr{A}}{C_T} = \text{const} \qquad \text{(for all } T \text{ and } P\text{)} \tag{14-56}$$

† Since G^V denotes the free energy for the system under consideration ($G^V = n_i^V G_i^V$), it follows that

$$\bar{G}_i^V = \left(\frac{\partial G}{\partial n_i^V}\right)_{P,\,T,\,n_{j\neq i}^V} = \left(\frac{\partial (n_i^V G_i^V)}{\partial n_i^V}\right)_{P,\,T,\,n_{j\neq i}^V} = G_i^V$$

In the correlation of some experimental results it was found by Gonzales and Holland(3,4,5) that the total number of sites C_T available for adsorption decreased with increasing temperatures. With the above definition for $\mathscr{A}$, however, the ratio $\mathscr{A}/C_T$ remains constant for all T and P. On the basis of this interpretation of $\mathscr{A}$ and C_T for the kinetic model, the analysis of a perfect gas in the adsorbed state is continued.

In a manner analogous to that employed in the definition of a perfect gas mixture (three-dimensional), a two-dimensional perfect gas mixture is one which obeys the relationships

$$\mathscr{P}_i\mathscr{A} = n_i^\sigma RT \qquad \text{or} \qquad \pi a_i = n_i^\sigma RT \tag{14-57}$$

The quantities $\mathscr{P}_i$ and a_i are defined by

$$\mathscr{P}_i = \pi x_i \qquad a_i = \mathscr{A} x_i \tag{14-58}$$

Fugacities Relationships for Two-Dimensional Gases

For the case of a pure component in a closed system at the constant temperature T, Eq. (14-28) reduces to

$$dG^\sigma = \mathscr{A}\,d\pi \qquad \text{(at constant } T\text{)} \tag{14-59}$$

In keeping with the concept of a film as discussed in the development of Eq. (14-41), the term $V^\sigma\,dP$ has been neglected. For one mole of a perfect two-dimensional gas (Eq. (14-57)), Eq. (14-59) reduces to

$$dG_i^\sigma = \frac{RT}{\pi}\,d\pi = RT\,d\ln\pi \tag{14-60}$$

Comparison of the first expression of Eq. (14-45) and Eq. (14-60) shows that for the case of a pure component which is a perfect two-dimensional gas

$$f_i^\sigma = \pi \tag{14-61}$$

The standard state of component i in an adsorbed phase is taken to be an adsorbed phase composed of one mole of pure component i at the spreading pressure π and at the temperature T of the adsorbed mixture. On this basis, Eq. (14-46) may be integrated to give

$$\bar{G}_i^\sigma(\pi, T, x_1, x_2, \ldots, x_c) = G_i^\sigma(\pi, T) + RT\ln\frac{\hat{f}_i^\sigma}{f_i^\sigma} \tag{14-62}$$

where $G_i^\sigma(\pi, T)$ = the free energy of pure component i in an adsorbed phase composed of component i alone and at the spreading pressure π and temperature T of the mixture.

In the development that follows, the hypothetical state of an adsorbed phase at zero pressure is encountered. Although hypothetical states are perfectly permissible for state functions, it is necessary to define the properties of the

mixture in this state because they cannot be determined experimentally. Although the definition of a hypothetical state is arbitrary, once selected, it must be retained for all subsequent developments. Then by definition, the properties of an adsorbed phase at zero pressure are taken to be the same as those of a perfect two-dimensional gas.

To show that the fugacity $\hat{f}_i^\sigma$ for component i in any adsorbed phase approaches the partial spreading pressure $\mathscr{P}_i$ in the limit as π goes to zero, one may begin by making use of the fact that the cross-partials of Eq. (14-28) are equal, that is,

$$\left(\frac{\partial \bar{G}_i^\sigma}{\partial \pi}\right)_{T,\, n_i^\sigma} = \left(\frac{\partial \mathscr{A}}{\partial n_i^\sigma}\right)_{\pi,\, T,\, n_{j\neq i}^\sigma} \tag{14-63}$$

For a perfect two-dimensional gas mixture

$$\left(\frac{\partial \mathscr{A}}{\partial n_i^\sigma}\right)_{\pi,\, T,\, n_{j\neq i}^\sigma} = \left(\frac{\partial[(n_1^\sigma + n_2^\sigma + \cdots + n_c^\sigma)(RT/\pi)]}{\partial n_i^\sigma}\right)_{\pi,\, T,\, n_{j\neq i}^\sigma} = \frac{RT}{\pi} \tag{14-64}$$

Then at constant temperature, Eq. (14-63) becomes

$$d\bar{G}_i^\sigma = \frac{RT}{\pi}\, d\pi \tag{14-65}$$

which holds for each component i in a perfect two-dimensional gas mixture. Integration of Eq. (14-65) at constant temperature from the standard state of pure component i at the temperature T to the final state of component i in a mixture at the two-dimensional partial pressure $\mathscr{P}_i$ and spreading pressure π gives

$$[\bar{G}_i^\sigma(\pi, T, x_1, x_2, \ldots, x_c)]_{\text{perfect gas mixture, 2-dimensional}} = [G_i^\sigma(\pi, T)]_{\text{perfect gas, 2-dimensional}} + RT \ln \frac{\mathscr{P}_i}{\pi} \tag{14-66}$$

Since two-dimensional gases approach perfect two-dimensional gases in the limit as the spreading pressure π goes to zero, it follows that upon subtracting Eq. (14-62) from (14-66) and taking the limit as π goes to zero, one obtains the result

$$\lim_{\pi \to 0} \frac{\mathscr{P}_i}{\bar{f}_i^\sigma} = 1 \tag{14-67}$$

upon making use of the second expression given by Eq. (14-45).

For the case of vapor–liquid equilibria, only one equilibrium state exists for a pure component at a given temperature T. However, as shown previously by the phase rule for the heterogeneous adsorption of a pure component i, infinitely many equilibrium states exist at a given temperature. That is, for a given temperature T, there exist infinitely many equilibrum pairs π_i and P_i for pure component i. Let the set of all equilibrium states π_i and P_i at a given temperature T for pure component i be denoted by $\{\pi_i, P_i\}$.

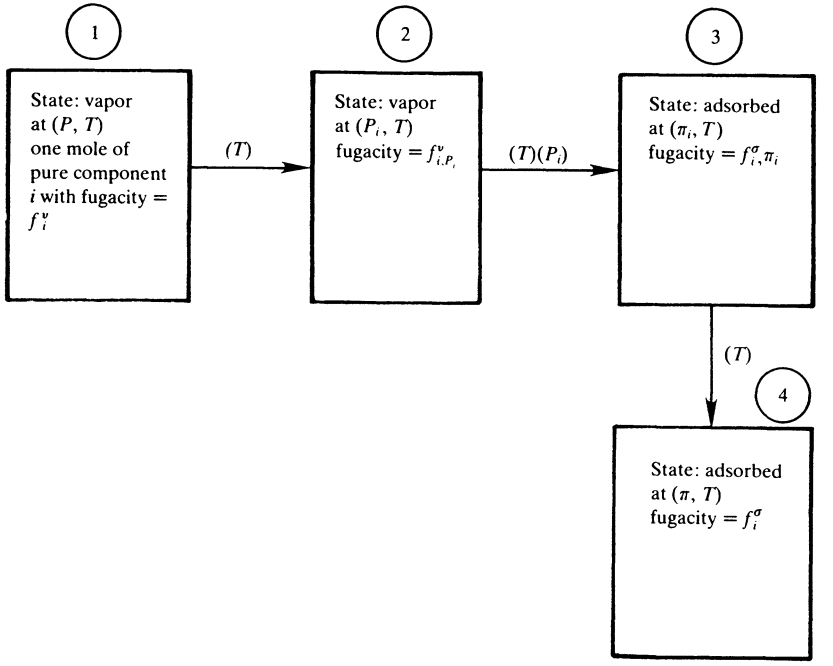

Figure 14-2 Path used to go from the standard state of a pure component in the vapor phase to the standard state of the same component in the adsorbed phase.

The free energies at the standard states for the vapor and the adsorbed phases may be related by use of the path shown in Fig. 14-2. In the following development, P_i and π_i denote a particular set of equilibrium pressures for component i at the temperature T. The change in free energy in going from state (1) to state (2) in Fig. 14-2 is given by the integration of the first expression of Eq. (14-43), that is,

$$G_i^V(P_i, T) - G_i^V(P, T) = RT \ln \frac{f_{i,P_i}^V}{f_i^V} \tag{14-68}$$

Since the change in free energy in going from state (2) to state (3) is zero (see Eq. (4-38)), it follows that

$$G_i^\sigma(\pi_i, T) - G^V(P_i, T) = 0 \tag{14-69}$$

The change in free energy in going from state (3) to state (4) is found by integration of the first expression of Eq. (14-45), namely,

$$G_i^\sigma(\pi, T) - G_i^\sigma(\pi_i, T) = RT \ln \frac{f_i^\sigma}{f_{i,\pi_i}^\sigma} \tag{14-70}$$

Addition of the corresponding members of Eqs. (14-68), (14-69), and (14-70) yields the desired relationship

$$G_i^\sigma(\pi, T) - G_i^V(P, T) = RT \ln \left(\frac{f_{i,P_i}^V}{f_{i,\pi_i}^\sigma}\right)\left(\frac{f_i^\sigma}{f_i^V}\right) \tag{14-71}$$

Since the particular equilibrium pair π_i and P_i at the given T was arbitrarily selected, Eq. (14-72) holds for all equilibrium states $\{\pi_i, P_i\}$ for component i at temperature T. Thus, the ratio $f_{i,P_i}^V/f_{i,\pi_i}^\sigma$ must be equal to a constant for all choices of equilibrium states $\{\pi_i, P_i\}$ at the temperature T. As shown below, this ratio of fugacities can be evaluated at the limiting condition of $P_i = 0$ and $\pi_i = 0$. For convenience, let

$$\lim_{P_i \to 0} \frac{f_{i,\pi_i}^\sigma}{f_{i,P_i}^V} = \Phi_i(T) \tag{14-72}$$

Since the ratio $f_{i,\pi_i}^\sigma/f_{i,P_i}^V$ is constant at a given T, it follows that for any given equilibrium state π_i and P_i of the set $\{\pi_i, P_i\}$, the corresponding fugacities are related as follows:

$$f_{i,\pi_i}^\sigma = \Phi_i(T) f_{i,P_i}^V \tag{14-73}$$

The fugacities of component i in the presence of other components in the vapor and adsorbed phases at the equilibrium state T, P, and π are related in the following manner. Since at equilibrium, $\bar{G}_i^V = \bar{G}_i^\sigma$, it follows that upon subtracting Eq. (14-62) from (14-47) one obtains

$$0 = \bar{G}_i^V - \bar{G}_i^\sigma = G_i^V(P, T) - G_i^\sigma(\pi, T) = RT \ln \left(\frac{\hat{f}_i^V}{\hat{f}_i^\sigma}\right)\left(\frac{f_i^\sigma}{f_i^V}\right) \tag{14-74}$$

When Eqs. (14-71), (14-73), and (14-74) are combined, the following result is obtained:

$$\hat{f}_i^\sigma = \Phi_i(T) \hat{f}_i^V \tag{14-75}$$

Comparison of Eqs. (14-73) and (14-75) shows that the same function which relates the fugacities f_i^σ and f_i^V of the pure component also relates the fugacities $\hat{f}_i^\sigma$ and $\hat{f}_i^V$ of component i in a mixture.

Evaluation of $\Phi_i(T)$ for the Kinetic Adsorption Models

Since $\Phi_i(T)$ is the same function for a pure component as for a mixture, it will be evaluated for the kinetic model for a pure component. For a pure component, Eq. (11-18) (the model for one-layer adsorption of multicomponent mixtures) reduces to the Langmuir isotherm

$$C_i = \frac{C_T K_{1i} P_i}{1 + K_{1i} P_i} \tag{14-76}$$

The final expression obtained for $\Phi_i(T)$ (Eq. (14-81)) holds for the general kinetic models for multilayer adsorption of multicomponent mixtures developed in Chap. 11; see Probs. 14-7 and 14-8.

To evaluate the limit of the ratio $f_{i,\pi_i}^\sigma/f_{i,P_i}^V$ (where π_i and P_i constitute equilibrium sets of pressures at the temperature T) as P_i approaches zero, use is made of the supposition that the adsorbed phase approaches a perfect two-dimensional gas as P_i approaches zero. Thus, it follows that for small values of P_i, the adsorbed phase may be represented approximately by the perfect two-dimensional gas law

$$\pi_i \mathscr{A} = C_i RT$$

where C_i is the moles of component i adsorbed per unit mass of adsorbent, and $\mathscr{A}$ is the area covered when all of the adsorption sites C_T are filled. (It should be observed that the symbols C_i and n_i^σ have precisely the same meaning.) Now, consider the equilibrium set π_i and P_i at a given T and note that

$$\lim_{P_i \to 0} \frac{\pi_i}{P_i} = \lim_{P_i \to 0} \left(\frac{C_i}{P_i}\right)\left(\frac{RT}{\mathscr{A}}\right) \tag{14-77}$$

Use of the perfect two-dimensional gas law to eliminate C_i/P_i from Eq. (14-77) yields

$$\lim_{P_i \to 0} \frac{\pi_i}{P_i} = \lim_{P_i \to 0} \left(\frac{C_T K_{1i}}{1 + K_{1i} P_i}\right)\left(\frac{RT}{\mathscr{A}}\right) = \frac{K_{1i} C_T RT}{\mathscr{A}} \tag{14-78}$$

Since the right-hand side of Equation (14-78) is finite, it is evident that in the limit as P_i approaches zero, π_i also approaches zero.

It remains to be shown that $\Phi_i(T)$ is equal to the right-hand side of Eq. (14-78). First, observe that since π_i approaches zero as P_i approaches zero, it follows from the second expression of Eq. (14-45) that

$$\lim_{P_i \to 0} \frac{f_{i,\pi_i}^\sigma}{\pi_i} = 1 \tag{14-79}$$

From the second expression of Eq. (14-43), it is evident that

$$\lim_{P_i \to 0} \frac{f_{i,P_i}^V}{P_i} = 1 \tag{14-80}$$

Then from Eqs. (14-78) through (14-80), it follows that

$$\Phi_i(T) = \lim_{P_i \to 0} \frac{f_{i,\pi_i}^\sigma}{f_{i,P_i}^V} = \lim_{P_i \to 0} \left(\frac{f_{i,\pi_i}^\sigma/\pi_i}{f_{i,P_i}^V/P_i}\right)\left(\frac{\pi_i}{P_i}\right) = \lim_{P_i \to 0} \frac{\pi_i}{P_i} = \frac{K_{1i} C_T RT}{\mathscr{A}} \tag{14-81}$$

Definition of an Ideal Adsorbed Solution

An ideal solution of a three-dimensional gas mixture may be defined simply as one which obeys Amagat's law of additive volumes. That is, the volume of an ideal solution at a given temperature and pressure is equal to the sum of the

volumes of its pure constituents at the same temperature and pressure.

$$V^V = n_1^V v_1 + n_2^V v_2 + n_3^V v_3 + \cdots + n_c^V v_c \tag{14-82}$$

where v_i = volume of one mole of component i at the temperature T and pressure P.

Among other characteristics (Refs. 2, 7, 8, 10), an ideal solution of a three-dimensional gas mixture has the property that $\gamma_i^V = 1$ (see Eq. (14-48)) for each component i of the mixture.

Let an ideal solution of an adsorbed phase be defined in a manner analogous to that given by Eq. (14-82) for a three-dimensional gas, that is, the total surface covered at a given spreading pressure and temperature is equal to the sum of the areas covered by the individual components at the same spreading pressure and temperature. More specifically

$$\mathscr{A} = n_1^\sigma a_1 + n_2^\sigma a_2 + n_3^\sigma a_3 + \cdots + n_c^\sigma a_c \tag{14-83}$$

where a_i = surface area covered by one mole of component i at the spreading pressure π and temperature T.

When Eq. (14-83) is differentiated with respect to a particular n_i^σ with the remaining n_i^σ's held fixed, the result so obtained may be combined with Eq. (14-63) to give the following relationship for an ideal adsorbed solution:

$$\left(\frac{\partial \bar{G}_i^\sigma}{\partial \pi}\right)_{T,\, n_i^\sigma} = a_i \tag{14-84}$$

The left-hand side of this expression may be evaluated by first taking the partial derivative of Eq. (14-62) with respect to π, that is,

$$\left(\frac{\partial \bar{G}_i^\sigma}{\partial \pi}\right)_{T,\, n_i^\sigma} = \left(\frac{\partial \bar{G}_i^\sigma(\pi, T)}{\partial \pi}\right)_T + RT\left(\frac{\partial \ln \hat{f}_i^\sigma / f_i^\sigma}{\partial \pi}\right)_{T,\, n_i^\sigma} \tag{14-85}$$

For one mole of a pure component, the third equality of Eq. (14-25) reduces to

$$\left(\frac{\partial G_i^\sigma(\pi, T)}{\partial \pi}\right)_T = a_i \tag{14-86}$$

When Eqs. (14-84), (14-85), and (14-86) are combined, the following result is obtained:

$$\left(\frac{\partial \log \hat{f}_i^\sigma / f_i^\sigma}{\partial \pi}\right)_{T,\, n_i^\sigma} = 0 \tag{14-87}$$

This expression shows that when the temperature and composition are held fixed, the ratio $\hat{f}_i^\sigma / f_i^\sigma$ for an ideal solution is independent of the spreading pressure. At any given temperature, the general solution of Eq. (14-87) is

$$\hat{f}_i^\sigma / f_i^\sigma = \theta_i(x_1, x_2, \ldots, x_c) \tag{14-88}$$

By use of Eqs. (14-45), (14-57) and the definition of $\mathscr{P}_i$ given by Eq. (14-58), it follows that

$$\lim_{\pi \to 0} \frac{\hat{f}_i^\sigma}{f_i^\sigma} = \lim_{\pi \to 0} \left(\frac{\hat{f}_i^\sigma}{\mathscr{P}_i}\right)\left(\frac{\mathscr{P}_i}{\pi}\right)\left(\frac{\pi}{f_i^\sigma}\right) = \lim_{\pi \to 0} \left(\frac{\hat{f}_i^\sigma}{\mathscr{P}_i}\right)\left(\frac{\pi}{f_i^\sigma}\right) x_i = x_i \tag{14-89}$$

Since θ_i is independent of π, it follows upon comparison of Eqs. (14-88) and (14-89) that for all π, $x_i = \theta_i$. Therefore at any π, Eq. (14-88) reduces to the final expression for an ideal adsorbed solution

$$\hat{f}_i^\sigma = f_i^\sigma x_i \tag{14-90}$$

For a nonideal solution, the right-hand side of Eq. (14-84) is no longer equal to a_i. In a manner analogous to that demonstrated in Ref. 10 it can be shown the fugacity $\hat{f}_i^\sigma$ for component i in a nonideal solution of the adsorbed phase is related to $f_i^\sigma x_i$ as follows:

$$\hat{f}_i^\sigma = \gamma_i^\sigma f_i^\sigma x_i \tag{14-91}$$

where

$$\gamma_i^\sigma = \gamma_i^\sigma(\pi, T, x_1, x_2, \ldots, x_c).$$

Since $\hat{f}_i^\sigma = \Phi_i(T)\hat{f}_i^V$ at equilibrium, it follows from Eqs. (14-46) and (14-91) that

$$\Phi_i(T)\gamma_i^V f_i^V y_i = \gamma_i^\sigma f_i^\sigma x_i \tag{14-92}$$

When adsorbed phase forms an ideal solution and the vapor phase forms a perfect gas mixture, then Eq. (14-92) may be further reduced as follows:

$$y_i = \left(\frac{f_i^\sigma}{\Phi_i(T) f_i^V}\right) x_i = \frac{f_{i,\, P_{i,\pi}}^\sigma}{f_i^V} x_i = \frac{P_{i,\pi}}{P} x_i \tag{14-93}$$

where $P_{i,\pi}$ is equal to that pressure which must be applied to a vapor phase composed of pure component i (at the temperature T of the mixture under consideration) in order for the equilibrium adsorbed phase (composed of pure component i) to take on a spreading pressure π equal to that of the mixture under consideration. The symbol $f_{i,\, P_{i,\pi}}^V$ denotes the fugacity of pure component i evaluated at the pressure $P_{i,\pi}$ and at the temperature T of the mixture under consideration.

14-2 CHARACTERISTICS OF THE EQUATION OF STATE FOR KINETIC ADSORPTION MODELS

Equations of state corresponding to the kinetic adsorption models are developed below. These equations of state are then shown to be consistent with Gibbs' formula.

Thermodynamic Consistency of Adsorption Models

An expression for the adsorption of either a pure component or a multicomponent mixture by an adsorbent is said to be thermodynamically consistent if it satisfies Gibbs' formula, Eq. (14-42). The use of Gibbs' formula for checking the consistency of adsorption models is analogous to the use of the Gibbs–Duhem equation for checking the consistency of models for the description of vapor–liquid equilibria.

In the following analysis, it is supposed that a state of equilibrium exists between the vapor and the adsorbed phases. Thus $\bar{G}_i^V = \bar{G}_i^\sigma$, and furthermore for all changes in the independent variables which represent a transition from one equilibrium state to another, it follows that $d\bar{G}_i^V = d\bar{G}_i^\sigma$. Thus, Eqs. (14-42) and (14-44) may be combined to give

$$\frac{\mathscr{A}\, d\pi}{RT} = \sum_{i=1}^{c} C_i\, d \ln \hat{f}_i^V \qquad \text{(at constant } T\text{)} \tag{14-94}$$

If the gas phase is a perfect gas mixture, then

$$\frac{\mathscr{A}\, d\pi}{RT} = \sum_{i=1}^{c} C_i\, d \ln p_i = \sum_{i=1}^{c} C_i \frac{dp_i}{p_i} \qquad \text{(at constant } T\text{)} \tag{14-95}$$

For a pure component, this expression reduces to

$$\frac{\mathscr{A}\, d\pi}{RT} = C \frac{dP}{P} \qquad \text{(at constant } T\text{)} \tag{14-96}$$

The Langmuir Isotherm

First it will be shown that the following proposed equation of state

$$\frac{\pi \mathscr{A}}{C_T RT} = \ln (1 + bP) \tag{14-97}$$

(where b is a function of temperature alone) and Langmuir's adsorption isotherm

$$C = \frac{C_T bP}{1 + bP} \tag{14-98}$$

satisfy the Gibb's formula for a pure component (Eq. (14-96)). If it is supposed that at constant temperature, the ratio $\mathscr{A}/C_T$ is independent of pressure, then the change in π with respect to P given by the proposed equation of state is

$$\frac{\mathscr{A}}{C_T RT} \frac{d\pi}{dP} = \frac{b}{1 + bP} \tag{14-99}$$

Elimination of $b/(1 + bP)$ from Eq. (14-99) by use of Eq. (14-98) gives

$$\frac{\mathscr{A}\, d\pi}{RT} = C \frac{dP}{P} \tag{14-100}$$

which is recognized as Gibbs' formula for a pure component.

It should be mentioned that de Boer(1) states that in 1908, von Szyszokowski found that the spreading pressure for the adsorption of gases on the surfaces of many liquids could be represented over a wide range of concentrations by use of the form given by Eq. (14-97). Also, it should be pointed out that Volmer(15) obtained the Langmuir isotherm by commencing with Gibbs' formula and a two-dimensional equation of state.

Adsorption of Multicomponent Mixture in a Unimolecular Layer

The development of the thermodynamic relationships for an adsorbed phase did not involve any consideration of the mechanism by which the adsorption process takes place. However, the kinetic development of Eq. (11-18) was based on a postulated mechanism. Thus, if it can be shown that an equation of state for which concentrations are given by Eq. (11-18) satisfy the Gibbs' formula, the proposed mechanism will not have been verified, but the thermodynamic consistency of the equation of state and the adsorption expression (Eq. (11-18)) will have been verified. That is, the thermodynamics is not concerned with the model proposed to develop an adsorption expression, but it is concerned only with the final expressions obtained for the adsorption process.

It will now be shown that the combination of the following model for the spreading pressure

$$\pi = \left(\frac{C_T RT}{\mathscr{A}}\right) \ln \left(1 + \sum_{i=1}^{c} K_i p_i\right) \tag{14-101}$$

and the expression for the surface concentration given by Eq. (11-18) satisfy the Gibbs' formula. Again it is supposed that $C_T/\mathscr{A}$ is independent of both temperature and pressure, although both C_T and $\mathscr{A}$ depend on temperature as discussed previously. Then at constant temperature, the total differential of Eq. (14-101) is given by

$$\begin{aligned} \frac{\mathscr{A}\, d\pi}{RT} &= C_T \left(\frac{\sum_{i=1}^{c} K_i\, dp_i}{1 + \sum_{i=1}^{c} p_i K_i}\right) \\ &= \left[\left(\frac{C_T p_1 K_1}{1 + \sum_{i=1}^{c} p_i K_i}\right)\left(\frac{dp_1}{p_1}\right) + \left(\frac{C_T p_2 K_2}{1 + \sum_{i=1}^{c} p_i K_i}\right)\left(\frac{dp_2}{p_2}\right)\right. \\ &\qquad \left. + \cdots + \left(\frac{C_T p_c K_c}{1 + \sum_{i=1}^{c} p_i K_i}\right)\left(\frac{dp_c}{p_c}\right)\right] \end{aligned} \tag{14-102}$$

When the first factor of each term of Eq. (14-102) is replaced by its equivalent as given by Eq. (11-18), the following result is obtained

$$\mathscr{A}\frac{d\pi}{RT} = \sum_{i=1}^{c} C_i \frac{dp_i}{p_i}$$

which is recognized as Gibbs' formula.

Equations of State for Adsorption Models I and II for Adsorption in any Number of Layers n

Gonzales(3,4,5) found that many adsorption isotherms could be represented with good accuracy by taking $(1 + v\phi_j) \simeq 1$ which corresponds to the case where the adsorption is relatively small. For this case, Eq. (11-28) reduces to

$$\frac{C_i}{K_{1i}p_i C_T} = \sum_{j=1}^{n} \frac{v^{j(j-1)/2}\phi_1^{j-1}}{1 + \phi_1} \tag{14-103}$$

which is called Adsorption Model I while the exact relationship given by Eq. (11-28) is called Adsorption Model II.

For model I as well as model II, it is evident that the ratio $C_i/(K_{1i}p_i C_T)$ is the same for all i since it is a function of ϕ_1 alone. Also, from the definition of ϕ_1 given by Eq. (11-21), it is evident that $\partial\phi_1/\partial p_i = K_{1i}$, a function of i alone. The equations of state based on model I or II which satisfy Gibbs' formula are readily obtained by use of the following integral equation:

$$\frac{\mathscr{A}\pi}{C_T RT} = \int_0^{\phi_1} \frac{C_i d\phi_1}{K_{1i}p_i C_T} \tag{14-104}$$

For adsorption in one layer by model I, Eq. (14-104) is readily shown to reduce to Eq. (14-101). Substitution of the expression for $C_i/(K_{1i}p_i C_T)$ as given by Eq. (14-103) followed by integration yields

$$\frac{\mathscr{A}\pi}{C_T RT}\int_0^{\phi_1} \frac{d\phi_1}{1 + \phi_1} = \ln(1 + \phi_1) \tag{14-105}$$

which is seen to be an equivalent form of Eq. (14-101). By carrying out the integrations for $j = 2, 3, \ldots, n$ for model I, the results so obtained may be represented by the following recurrence formula which is the equation of state for model I.

$$\frac{\mathscr{A}\pi}{C_T RT} = \sum_{j=1}^{n} \chi_j \tag{14-106}$$

where

$$\chi_1 = \ln(1 + \phi_1) \qquad \chi_2 = -v\chi_1 + v\phi_1$$

$$\chi_3 = -v^2\chi_2 + \frac{v^3\phi_1^2}{2} \qquad \chi_4 = -v^3\chi_3 + \frac{v^6\phi_1^3}{3}$$

$$\chi_5 = -v^4\chi_4 + \frac{v^{10}\phi_1^4}{4} \quad \cdots \quad \chi_n = -v^{n-1}\chi_{n-1} + \left(\frac{1}{n-1}\right)v^{[(n-1)n]/2}\phi_1^{n-1}$$

For model II (Eq. (11-28)), the integrated form of the equation of state is obtained by substituting the expression given by Eq. (11-28) for C_i into Eq. (14-104) and integrating for $j = 1, 2, \ldots, n$ adsorbed layers.

The fact that the equations of state given by Eq. (14-104) for models I and II for the general case of n layers satisfies Gibbs' formula is readily demonstrated in the following manner. Since the integral on the right-hand side of Eq. (14-104) is a function of ϕ_1 alone, let it be denoted by $F(\phi_1)$. Then for the case where $\mathscr{A}/C_T$ is regarded as a constant, the total differential of π as given by Eq. (14-104) may be stated as follows:

$$\mathscr{A}\frac{d\pi}{RT} = C_T\left[\frac{\partial F(\phi_1)}{\partial\phi_1}\frac{\partial\phi_1}{\partial p_1}dp_1 + \frac{\partial F(\phi_1)}{\partial\phi_1}\frac{\partial\phi_1}{\partial p_2}dp_2 + \cdots + \frac{\partial F(\phi_1)}{\partial\phi_1}\frac{\partial\phi_1}{\partial p_c}dp_c\right] \tag{14-107}$$

Since

$$C_T\frac{\partial F(\phi_1)}{\partial\phi_1}\frac{\partial\phi_1}{\partial p_i}dp_i = C_T\left(\frac{C_i}{K_{1i}p_i C_T}\right)(K_{1i})\left(p_i\frac{dp_i}{p_i}\right) = C_i\frac{dp_i}{p_i} \tag{14-108}$$

it follows that Eq. (14-107) reduces to Gibbs' formula, Eq. (14-95).

Proof that the Equations of State for Models I and II Form Ideal Solutions

By comparison of Eqs. (14-90) and (14-91) it is evident that if it can be shown that for each component i, $\gamma_i^\sigma = 1$ for a given adsorption model, then it will have been shown that the given adsorption model is an ideal solution. The formulation of the proof that the equation of state for the two-layer version of model I satisfies the condition that $\gamma_i^\sigma = 1$ for all i follows. The proofs for the general case of n adsorbed layers for models I and II are carried out in the same manner as demonstrated below for the special case, $n = 2$ for model I.

The mole fraction x_i of component i (in the adsorbed phase), which appears in Eq. (14-91) may be stated in terms of the expression for C_i as given by the two-layer version of model I (Eq. (11-27)) as follows:

$$x_i = \frac{C_i}{\sum_{i=1}^{c} C_i} = \frac{\hat{f}_i^V K_{1i}}{\phi_1} \tag{14-109}$$

Since $\hat{f}_i^\sigma = \Phi_i(T)\hat{f}_i^V$ at equilibrium, it follows from Eqs. (14-91) and (14-109) that

$$\gamma_i^\sigma = \frac{\phi_1\Phi_i(T)}{f_i^\sigma K_{1i}} \tag{14-110}$$

Also, when an equilibrium state exists between a pure component in an adsorbed phase (composed of that component alone) at the spreading pressure of the mixture π and a vapor phase composed of pure component i at the corresponding equilibrium pressure $P_{i,\pi}$, the corresponding fugacities are

related by Eq. (14-73), namely,

$$f_i^\sigma = \Phi_i(T) f^V_{i,P_{i,\pi}}$$

Thus, Eq. (14-110) reduces to

$$\gamma_i^\sigma = \frac{\phi_1}{f^V_{i,P_{i,\pi}} K_{1i}} \tag{14-111}$$

The first step in the evaluation of $f^V_{i,P_{i,\pi}}$ at any given temperature is the determination of the spreading pressure π for the given adsorbed mixture. For any such mixture, every term on the right-hand side of the equation of state for the mixture (Eq. (14-106)) may be evaluated. Thus, a number value for the spreading pressure may be computed in this way and represented as follows:

$$\pi = N_1 \tag{14-112}$$

The next step is to find that adsorption pressure $P_{i,\pi}$ which must be placed on pure component i in the gas phase in order for its adsorbed phase to take on a spreading pressure equal to N_1. Thus, the desired value of $P_{i,\pi}$ is the one which satisfies the following equation:

$$\left(\frac{C_T RT}{\mathscr{A}}\right)[\ln(1 + K_{1i} f_i^V) + \nu[K_{1i} f_i^V - \ln(1 + K_{1i} f_i^V)]] - N_1 = 0 \tag{14-113}$$

Since N_1 is of the same form as the first term of Eq. (14-113) it is possible to rearrange this equation to the following form.

$$\left(\frac{C_T RT}{\mathscr{A}}\right)\left[\ln\frac{(1 + K_{1i} f_i^V)}{(1 + \phi_1)} + \nu(K_{1i} f_i^V - \phi_1) - \nu \ln\frac{(1 + K_{1i} f_i^V)}{(1 + \phi_1)}\right] = 0 \tag{14-114}$$

where ϕ_1 for the mixture, C_T, K_{1i}, and ν are all regarded as fixed for any given determination of $P_{i,\pi}$. Obviously, the pressure $P_{i,\pi}$ at which f_i^V must be evaluated in order to satisfy Eq. (14-114) is the one which produces the following equality:

$$K_{1i} f^V_{i,P_{i,\pi}} = \phi_1 = \sum_{i=1}^{c} K_{1i} f_i^V \tag{14-115}$$

Use of this result in Eq. (14-111) leads to the result

$$\gamma_i^\sigma = 1 \tag{14-116}$$

for all components i. This result may be generalized for the case of any number of adsorbed layers n for both models I and II.

Enthalpy of a pure component in the adsorbed phase The fact that the adsorbed phase forms an ideal solution when described by the equation of state for the kinetic model leads to the further simplification that the partial molar enthalpy $\bar{H}_i^\sigma$ is equal to the enthalpy H_i^σ of one mole of pure component i in an adsorbed phase composed of component i alone. An outline of the proof of the equality $\bar{H}_i^\sigma = H_i^\sigma$ follows.

As in the classical thermodynamics of vapors and liquids (Refs. 2, 7, 8, 10) the partial molar enthalpy $\bar{H}_i^\sigma$ of component i in the adsorbed phase is defined by

$$\bar{H}_i^\sigma = \left(\frac{\partial H^\sigma}{\partial n_i^\sigma}\right)_{\pi, T, n_{j\neq i}^\sigma} \tag{14-117}$$

At any π and T, the function H^σ like U^σ (see Eq. (14-15)) is homogeneous of degree one. Thus, it follows from Euler's theorem (App. 1A) that

$$H^\sigma = \sum_{i=1}^{c} n_i^\sigma \bar{H}_i^\sigma \tag{14-118}$$

In a manner analogous to that commonly presented in treatments of the classical thermodynamics of vapor and liquid mixtures (Refs. 2, 7, 8), the partial molar enthalpy $\bar{H}_i^\sigma$ is related to the activity coefficient γ_i^σ of component i in the adsorbed phase as follows:

$$-\left(\frac{\bar{H}_i^\sigma - H_i^\sigma}{RT^2}\right) = \left(\frac{\partial \ln \gamma_i^\sigma}{\partial T}\right)_{\pi, n_i^\sigma} \tag{14-119}$$

The development of the relationship given by Eq. (14-119) is outlined in Probs. (14-4) and (14-5).

Since $\gamma_i^\sigma = 1$ (see Eq. (14-116)) for the kinetic model for adsorption, it follows from Eq. (14-119) that

$$\bar{H}_i^\sigma = H_i^\sigma \tag{14-120}$$

and Eq. (14-118) reduces to the usual form for ideal solutions.

NOTATION

(see also Chap. 11)

a_i = area covered per mole of component i at the spreading pressure π and temperature T

$\mathscr{A}$ = total area covered by the molecules in an adsorbed film (on, say, the surface of a liquid); total surface area of an adsorbent per unit mass (Langmuir-type models), and the surface area covered per unit mass of adsorbent when all of the available adsorption sites C_T are filled at a given temperature (kinetic model for adsorption)

$\bar{\mathscr{A}}_i$ = partial molar value of the area $\mathscr{A}$ (defined by Eq. (B) of Prob. 14-3)

A^V, A^σ = Helmholtz free energy functions for the vapor and adsorbed phases, respectively

$f_i^V, \hat{f}_i^V$ = fugacity of pure component i in the vapor state and the fugacity of component i in a mixture of vapors, respectively, pressure units

$f_i^\sigma, \hat{f}_i^\sigma$ = fugacity of pure component i in the adsorbed phase and the fugacity of pure component i in an adsorbed phase consisting of a mixture of adsorbed components, respectively, pressure per unit length

G^V, G^σ = total free energy of the vapor and adsorbed phases, respectively

$G_i^\sigma, \bar{G}_i^\sigma$ = free of pure component i in an adsorbed phase consisting of pure component i at π and T and the partial molar free energy of component i at π and T, respectively

H^V, H^σ = enthalpy of the vapor and adsorbed phases, respectively

$H_i^\sigma, \bar{H}_i^\sigma$ = enthalpy of one mole of pure component i and the partial molar enthalpy of component i at a given π and T, respectively

l = width of surface (see Fig. 14-1)

n_i^V = moles of component i in the gas phase

n_i^σ = moles of component i in the adsorbed phase, moles adsorbed per unit mass of adsorbent

$\mathscr{P}_i$ = partial pressure of component i in the adsorbed phase (defined by Eq. (14-58))

$\mathscr{P}$ = number of phases

P = total pressure

P_i^0 = vapor pressure (vapor–liquid equilibria) of pure component i at the temperature T

P_i = gas phase pressure at which component i has an equilibrium spreading pressure π_i in the adsorbed phase at the temperature T

$P_{i,\pi}$ = that pressure which must be applied on a vapor phase (at the temperature T of the mixture) composed of pure component i in order for the adsorbed phase (composed of pure component i) to take on equilibrium spreading pressure π equal to that of the given mixture under consideration

R = conventional gas constant (for a perfect three-dimensional gas, $R = PV^V/T$)

S^V, S^σ = entropy of the vapor and adsorbed phases, respectively

$S_i^\sigma, \bar{S}_i^\sigma$ = entropy per mole of pure component i and the partial molar entropy of component i in an adsorbed mixture, respectively

T^V, T^σ = temperature of the vapor and adsorbed phases, respectively

$\mathscr{U}$ = energy of the universe

U_{sys}, U_{surr} = total energy of the system and the surroundings, respectively

U^V, U^σ = internal energy of the vapor and adsorbed phases, respectively

$\mathscr{V}$ = degrees of freedom

V^V, V^σ = volumes of the vapor and adsorbed phases, respectively

x_i = total mole fraction of component i in the adsorbed phase

y_i = mole fraction of component i in the vapor phase

$\mathscr{Z}_i$ = compressibility factor for component i

z = length; z_T = total length

Greek letters

γ_0, γ = surface tension of a pure liquid surface and of a contaminated liquid surface, force per unit length

$\gamma_i^V, \gamma_i^\sigma$ = activity coefficients for component i in a nonideal mixture in the vapor phase and in the adsorbed phase, respectively

ν = parameter in the kinetic model for multilayer adsorption

π = spreading pressure for the adsorbed phase, force per unit length

ϕ_j = $\sum_{i=1}^{c} K_{ji} p_i$, $(1 \le j \le n)$

χ_j = functions $(1 \le j \le n)$ in the generalized equation of state for the adsorption of multicomponent mixtures in n layers

$\Phi_i(T)$ = function defined by Eq. (14-72)

REFERENCES

1. J. H. de Boer: *The Dynamical Character of Adsorption*, Oxford University Press, New York, 1953.
2. Kenneth Denbigh: *The Principles of Chemical Equilibrium*, Cambridge University Press, New York, 1955.
3. A. J. Gonzalez: Ph.D. dissertation, "Adsorption Equilibria of Multicomponent Mixtures," Texas A&M University, 1969.
4. A. J. Gonzalez and C. D. Holland: "Adsorption of Multicomponent Mixtures by Solid Adsorbents," *AIChE J.*, **16**:718 (1970).
5. A. J. Gonzalez and C. D. Holland: "Adsorption Equilibria of Light Hydrocarbon Gases on Activated Carbon and Silica Gel," *AIChE J.*, **17**:470 (1970).
6. R. J. Grant, M. Manes, and S. B. Smith: "Adsorption of Nornam Paraffins and Sulfur Compounds on Activated Carbon," *AIChE. J.*, **8**:403 (1962).
7. E. A. Guggenheim: *Thermodynamics*, New York Interscience Publishers Inc., 1949.
8. E. A. Guggenheim: *Mixtures, The Theory of the Equilibrium Properties of Some Simple Classes of Mixtures Solutions and Alloys*, Oxford University Press, New York, 1952.
9. T. L. Hill: "Thermodynamics and Heat of Adsorption," *J. Chem. Phys.*, **17**:520 (1949).
10. C. D. Holland: *Fundamentals of Multicomponent Distillation*, McGraw-Hill Book Company, New York, 1981.

11. A. J. Kidnay and A. L. Myers' "A Simplified Method for the Prediction of Multicomponent Adsorption Equilibria from Single Gas Isotherms," *AIChE J.*, **12**:981 (1966).
12. I. Langmuir: "Oil Lenses on Water and the Nature of Nonomolecular Expanded Films," *J. Chem. Phys.*, **1**:756 (1953).
13. A. L. Myers and J. M. Prausnitz: "Thermodynamics of Mixed-Gas Adsorption," *AIChE J.*, **11**:121 (1965).
14. R. K. Schofield and E. K. Rideal: "The Kinetic Theory of Surface Films. Part I—The Surfaces of Solutions," *Proc. R. Soc. London*, **A109**:57 (1925).
15. M. Volmer: "Thermodynamische der Zustansgleichung fur Adsorbierte Stoffe," *Z. Phys. Chem.*, **115**:253 (1925).

PROBLEMS

14-1 Verify the results given by Eqs. (14-29) and (14-30).

14-2 Show that the equation of state obtained by substituting the expression for C_i for model II (Eq. (11-28)) into Eq. (14-104) is consistent with Gibbs' formula.

14-3 Analogous to the expression for the volume of a liquid that forms a nonideal solution (Refs. 7, 8, 10), the surface covered by a nonideal adsorbed solution may be expressed in terms of the partial molar areas as follows:

$$\mathscr{A} = n_1^\sigma \bar{\mathscr{A}}_1 + n_2^\sigma \bar{\mathscr{A}}_2 + \cdots + n_c^\sigma \bar{\mathscr{A}}_c \tag{A}$$

where the $\bar{\mathscr{A}}_i$'s are the partial molar areas, which are defined by

$$\bar{\mathscr{A}}_i = \left(\frac{\partial \mathscr{A}}{\partial n_i^\sigma}\right)_{\pi, T, n_{j\neq i}^\sigma} \tag{B}$$

(*a*) By use of Eqs. (B), (14-62), (14-63), and (14-86), show that

$$\bar{\mathscr{A}}_i - a_i = RT\left(\frac{\partial \ln \hat{f}_i^\sigma / f_i^\sigma}{\partial \pi}\right)_{T, n_i^\sigma} \tag{C}$$

(*b*) Use Eq. (C) to verify the result given by Eq. (14-91).

(*c*) Show that when the temperature T and all of the n_i^σ's are held fixed, Eq. (C) may be integrated to give

$$\ln \gamma_i^\sigma = \frac{1}{RT}\int_0^\pi (\bar{\mathscr{A}}_i - a_i)\, d\pi$$

14-4 Partial differentiation of both sides of Eq (14-20) with respect to n_i^σ at constant π and T gives

$$\mu_i^\sigma = \bar{G}_i^\sigma = \bar{H}_i^\sigma - T\bar{S}_i^\sigma \tag{A}$$

where

$$\bar{H}_i^\sigma = \left(\frac{\partial H^\sigma}{\partial n_i^\sigma}\right)_{\pi, T, n_{j\neq i}^\sigma} \qquad \bar{S}_i^\sigma = \left(\frac{\partial S^\sigma}{\partial n_i^\sigma}\right)_{\pi, T, n_{j\neq i}^\sigma}$$

(*a*) Show that

$$\left(\frac{\partial S^\sigma}{\partial n_i^\sigma}\right)_{\pi, T, n_{j\neq i}^\sigma} = -\left(\frac{\partial \bar{G}_i^\sigma}{\partial T}\right)_{\pi, T, n_j^\sigma} \tag{B}$$

Hint: Make use of Eq. (14-28).

(*b*) By use of the results given by Eqs. (A) and (B), show that

$$\left(\frac{\partial \bar{G}_i^\sigma / T}{\partial T}\right)_{\pi, n_i^\sigma} = -\frac{\bar{H}_i^\sigma}{T^2} \tag{C}$$

14-5 Show that for the general case of a nonideal adsorbed solution,

$$-\left(\frac{\bar{H}_i^\sigma - H_i^\sigma}{RT^2}\right) = \left(\frac{\partial \ln \bar{f}_i^\sigma / f_i^\sigma}{\partial T}\right)_{\pi, n_i^\sigma} = \left(\frac{\partial \ln \bar{f}_i^\sigma / (f_i^\sigma x_i^\sigma)}{\partial T}\right)_{\pi, n_i^\sigma}$$
$$= \left(\frac{\partial \log \gamma_i^\sigma}{\partial T}\right)_{\pi, n_i^\sigma}$$

14-6 For one mole of a pure component in a closed system at constant temperature, Eq. (14-11) reduces to

$$dG_i^V = V_i^V\, dP \tag{A}$$

The volume per mole of an actual gas is given by

$$V_i^V = \mathscr{Z}_i \frac{RT}{P} \tag{B}$$

where the compressibility factor $\mathscr{Z}$ has the property

$$\lim_{P\to 0} \mathscr{Z}_i = 1 \tag{C}$$

Equations (A) and (B) may be combined to give

$$dG_i^V = \mathscr{Z}_i RT d \ln P \qquad \text{(at constant } T\text{)} \tag{D}$$

By use of Eqs. (C), (D), (14-43), show that

$$\lim_{P\to 0} \frac{\partial f_i^V}{\partial P} = 1 \qquad \text{(at constant } T\text{)}$$

14-7 Show that the result given by Eq. (14-78) is also obtained for the general case of n adsorbed layers for both models I and II.

14-8 Show that the expression given for $\Phi_i(T)$ by Eq. (14-81) is also obtained for the general case of n layers for both models I and II.

INDEX

Absorbers, 217, 235–247, 253–268
  field tests, 258–260
  fractional response, 265
  packed absorbers, 253–258
Acrivos, A., 356
Activity coefficients, 43, 128, 129
Adiabatic adsorbers, 404–414
Adsorbers:
  breakthrough curves, 378, 392, 393
  countercurrent operation, 415, 416
  fixed-beds, 374–384, 389–414
    periodic operation, 414–416
Adsorption:
  chemical adsorption, 363, 364
  physical adsorption, 363–372
  thermodynamics of physical adsorption, 439–463
Adsorption isotherms:
  of mixtures, 369–372, 398
  of pure components, 364–369, 427
Allen, R. H., 19
Anzelius, A., 378
Arnold, J. R., 369

Balzli, M. W., 392
Barb, D. K., 183, 207
Bassyoni, A. A., 254–255, 262, 264
Batch-distillation, 177–207
  comparison of model predictions with experimental results, 199–202
  cyclic operation, 195–197
  optimization of, 202–207
Bennett, J. M., 67, 167
Benton, A., 369, 371
Bernouli's theorem, 270, 271
BET isotherm, 367–369
Bolles, W. L., 273, 274
Bonilla, C. F., 73
Breakthrough curves (*see* Adsorbers)
Broyden, C. G., 71, 167
Broyden–Bennett algorithm, 162
Broyden's method, 63–67, 162
Brunauer, S., 364, 366, 369
Bullington, L. A., 272
Burdett, J. W., 71, 73, 81, 86, 92
Buron, A. G., 274
Butcher, J. C., 19

Caillaud, J. B., 19, 217, 218, 304
Calahan, D. A., 19
Carnahan, B., 336
Carslaw, H. S., 82
Characteristics (*see* Method of characteristics)
Chemical potential, 442, 445
Chilton, C. H., 103
Chua, L. O., 309
Churchill, R. V., 84, 114
Clenshaw, C. W., 341
Conte, S. D., 31, 337
Control valves, 279, 282–285
Controllers:
  for distillation columns, 279–281, 282–285
  proportional-integral controller, 281
  proportional-integral-rate controller, 281

Convective mass transport, 372–373
Cooke, C. E., Jr., 369
Crank, J., 348
Crank–Nicolson method, 348, 356, 432, 433
Crosser, O. K., 408
Countercurrent operation (*see* Adsorbers)
Coupled differential and algebraic equations, 218–235, 321–326
  Gear's *k*th-order algorithms, 222–229
  Michelsen's algorithms, 218–222
  semi-implicit Runge–Kutta algorithms, 222–229

Dahlquist, G., 31
Damköhler, G., 382, 384
D'Arcy equation, 427
de Boer, J. H., 439, 440
de Boor, C., 31, 337
Deming, L. S., 364
Deming, W. E., 364
Denbigh, K., 42, 442, 456
Departure functions, 127
Desalination plant, 73–77, 88–111
  comparisons of model predictions with experimental data, 109, 110
  equipment parameters, 103–105
  of Freeport, 73, 88–111
Diffusion:
  axial diffusion, 394
  coefficients, 380, 382
  Knudsen diffusion, 427
  in pores, 379–384, 395, 427
  solid diffusion, 395
  surface diffusion, 382
Distillation:
  batch distillation (*see* Batch distillation)
  continuous distillation, 123–164, 269–285
  examples, 138–143, 147–153, 285–292
  control of distillation columns, 279–281, 282–285
  equilibrium relationships, 128, 129
Dühring lines, 43
Dukler, A. E., 73
Dusty-gas model, 427
Dykstra, D. I., 77
Dynamics of sieve trays, 270–276

Eckert, C. A., 286
Emmett, P. H., 367, 369
Energy balances, 5–12
Enthalpy, 6
Evans, R. B., 427
Evaporation, 37–45
Evaporators:
  boiling point elevation, 42, 45
  of multiple-effect, 41, 68, 69, 72
  of single-effect, 40, 41, 46–57
    control of mass holdup, 101, 102
    steam consumption, 42
    Swenson type, 38–40
Euler's method, 13, 14
Euler's theorem, 34, 444

Feng, An, 248, 268
Fick's law, 379
Film resistance and diffusion model, 394–404
Finite-difference methods, 348–356
  explicit methods, 351–354
  implicit methods, 354–356
Finlayson, B. A., 341, 344
Fluid flow in pipes, 6–12
Foam factor, 274
Fowler, R. H., 366
Franke, F. R., 153
Freeze-drying, 420–435
  adsorbed water, 426, 427
  models, 421–429
  model solutions, 429–435
Freundlich isotherm, 365
Friction factor, 275
Friedly, J., 356
Fritz, W., 372
Fritz–Schluender isotherm, 372
Fugacity, 42, 43, 448, 451–454
Furnas, C. C., 378

Gallun, S. E., 248, 281, 285
Gear, C. W., 30, 248, 285, 309
Gear's integration algorithm, 276–279
Gear's method of integration, 22–24, 269, 285, 315–326
Generalized theorem of integral calculus, 33, 79
Gentzler, G. L., 421
Gerlack, A., 45
Gibb's adsorption formula, 447, 448
Gill, S., 17, 304
Glueckauf, E., 375, 376, 387
Glueckauf model, 375–379, 389–393
Gonzalez, A. J., 369, 372, 451, 460
Greenfield, P. G., 431
Groves, D. M., 268
Guggenheim, E. A., 439, 442, 456
Gunn, R. D., 427, 430

Hamming, R. W., 337
Hanson, D. T., 407, 408, 413, 414
Harper, J. C., 422

Harwell, J. H., 407, 408, 413, 414
Heat, 5
Heat transfer models, 77–88
  errors in the predictions, 85, 86
Henrici, P., 301
Henry's law, 365
Hildeband, F. B., 334
Hill, T. L., 369, 439, 450
Hlávaček, V., 293
Holland, C. D., 67, 71, 76, 81, 84, 86, 91, 92, 126, 167, 208, 248, 264, 291, 369, 448, 456, 463
Holmes, M. J., 300
Holmes, R. E., 378, 379
Horvay, G., 341
Hougen, O. A., 378
Householder, A. S., 293
Huang, C. J., 73
Huckaba, C. E., 153, 208
Hugmark, G. A., 275
Hutchinson, M. H., 274
Hwang, M., 32
Hydraulic gradient, 271, 275
Hydraulic radius, 275, 276

Ideal adsorbed solution, 455–457
Integration of differential equations (*see* Numerical methods of integration)
Interface (*see* Phase interface)
Interfacial area, 373, 426
Internal energy, 6
Isotherms for adsorption, 364–372, 398, 427, 439–463
Itahara, S., 73

Jacobian matrix, 19, 53, 54
Jaeger, J. C., 82

K_b method, 136
Kelley, R. E., 272
Kinetic energy, 6
King, C. J., 421, 426, 430
Kirkpatrick, S. D., 103
Krylov, V. I., 361
Kubiček, M., 293
Kubiček's algorithm for matrices, 291, 293, 294

Lam, W. K., 426, 433
Lanczos, C., 341
Langmuir, I., 364, 366, 440, 458
Langmuir isotherm, 365
Lapidus, L., 32, 167
Lee, H. M., 73
Leibson, I., 272
Leland, T. W., Jr., 378, 379
Liapis, A. I., 392, 396, 402, 404, 408, 414, 421, 427, 431, 435
Lin, Pen-Min, 309
Liquid surface, 440
Litchfield, R. J., 396, 407, 414, 421, 430
Lord, R. C., 279
Lugin, V. V., 361
Luther, H. A., 327, 336

McBain, J. W., 364
McCabe, W. L., 44
McDaniel, R., 248, 258, 262, 264
Markham, E. C., 369, 371
Markham–Benton isotherms, 369, 371
Marshall, W. R., 167, 377, 378
Mason, E. A., 427
Mason, J., 369
Mass transfer coefficients, 373, 374, 426
Material balances, 2–5
May, R. B., 153
Mean-value theorem of differential calculus, 4, 5, 33
Meo, D., 430
Method of characteristics, 356–360, 390, 408
Method of weighted residuals, 340, 341
Michelsen, M. L., 19, 218, 248, 308, 341, 342, 344
Michelsen's method of integration, 18, 308, 398, 403
Mickley, H. W., 377
Mijares, G., 164
Miller, B. P., 274
Milne, W. E., 32
Minton, P. E., 279
Modeling:
  fundamentals of, 1–12
    energy balances, 5–12
    material balances, 2–5
    rate expressions, 7, 8, 373, 374, 379, 382, 394, 405–407, 427
Moffert, H. T., 421
Moving-boundary problem, 429
  solution of, 430, 431
Multicomponent adsorbers, 389–416
Multistep integration methods, 308–326
  of Adams–Bashforth, 311, 312
  of Adams–Moulton, 312
  Gear's, 312–326
Myers, A. L., 439, 442

Newton–Raphson method, 53–55, 102, 134, 346, 348, 409, 412
  the 2*N*, 160–164, 192–195
Nicolson, P., 348

Nonlinear algebraic equations:
  solution of (*see* Newton-Raphson method)
Nordsieck vector, 22, 317-319
Norton, H. T., 341
Numerical methods of integration:
  of ordinary differential equations, 13-24, 308-326
    Euler's method, 13
    Gear's methods, 22-24, 269, 276-279, 285, 315-326
    Michelsen's method, 18, 308, 398, 403
    multistep methods, 308, 398, 403
    point-slope predictor, 15, 16
    Runge-Kutta methods (*see* Runge-Kutta methods)
    trapezoidal corrector, 19
    two-point implicit method, 21, 52, 94, 129, 160, 179
  of partial differential equations, 348-360, 390-393, 400-404, 408-413, 431-433
    finite-difference methods (*see* Finite-difference methods)
    method of characteristics (*see* Method of characteristics)
    orthogonal collocation method (*see* Orthogonal collocation)

O'Connell, H. E., 275
O'Connell, J. P., 286
Open-boundary system, 11, 12
Orthogonal collocation:
  method of, 331-348, 398, 400-403
  applications, 341-348, 400-403
Orthogonal polynomials, 332-336, 402, 403
  Chebyshev, 333
  Hermite, 333, 334
  Jacobi, 334-336
  Laguerre, 332, 333
  Legendre, 332
Orye, R. V., 286

Padmanabhan, L., 19, 217, 304
Partial molar enthalpies, 127
Peck, R. E., 421
Percolation processes, 362
Perfect gases, 449-451
  three-dimensional gases, 449, 450
  two-dimensional gases, 450, 451
Perfect mixer, 3-5, 11, 12
Periodic operation (*see* Adsorbers)
Perry, R. H., 103
Peters, W. A., Jr., 260
Phase interface, 373
Phase rule, 446, 447
Pigford, R. L., 167, 377
Point-slope predictor, 15, 16
Pore diffusion (*see* Diffusion)
Potential energy, 6
Prausnitz, J. M., 286, 439, 442
Prochaska, F., 293

Quadratures, 336-340
  gaussian quadrature, 336, 337
  Gauss-Jacobi quadrature, 337-340

Rayleigh, Lord, 208
Reed, C. E., 377
Reid, R. C., 300
Residuals (*see* Method of weighted residuals)
Reynolds number, 275
Richtmyer, R. D., 353, 356
Rippin, D. W. T., 392, 402, 403, 404, 415, 416
Rosenbrock, H. H., 19, 308
Runge-Kutta methods, 17-19, 301-308
  explicit, 17, 302-304
  of fourth-order, 17
  Michelsen's, 18
  of Runge-Kutta-Gill, 17
  semi-implicit, 18, 19, 218-229, 265, 304-308, 393

Sandall, O. C., 426, 430, 433
Scaling procedures, 57-63
  column scaling, 62, 63
  row scaling, 60-63
  variable scaling, 60-62
Schluender, E. U., 372
Schmidt, F. W., 421
Secrest, D., 335
Seinfeld, J. H., 32
Semi-implicit Runge-Kutta methods, 18, 19, 218-229, 265, 304-308, 393
  generalized algorithm, 222-229
Separation by sublimation (*see* Freeze-drying)
Shapiro, A. H., 356
Sheng, T. R., 421
Sherwood, T. K., 300, 377
Sieve trays (*see* Dynamics of sieve trays)
Simultaneous differential and algebraic equations (*see* Coupled differential and algebraic equations)
Single-component adsorbers, 374, 384
Sips II isotherm, 427
Slusser, R. P., 279
Smith, B. D., 274, 275
Solid diffusion (*see* Diffusion)
Spiess, F. N., 341
Spreading, 439

Spreading pressure, 441
Stability of numerical integration methods:
  for ordinary differential equations, 25-30
  for partial differential equations, 353-356
    explicit methods, 353, 354
    implicit methods, 355, 356
  for stiff differential equations, 29, 30
Stewart, W. E., 341
Stiel, L. I., 73
Stiff ordinary differential equations, 29, 30
Stroud, A. H., 335
Sublimation interface, 422, 428, 429
Surface diffusion (*see* Diffusion)
Surface tension, 441
System with open boundary, 11, 12

Taylor's theorem, 33
Teller, E., 364, 369
Temperature:
  bubble-point, 129
  dewpoint, 129
Tetlow, N. J., 268
Tewarson, R. P., 248
Theta method, 124, 132, 137, 156-159, 183-188
  exact solution, 157-159
  modified, 156, 157
Thomas algorithm, 131, 132
Trapezoidal corrector, 20
Trapezoidal rule, 359, 360, 409, 410

Van Winkle, J., 300
Van Winkle, M., 274
Vichnevetsky, R., 344
Villadsen, J., 341, 342, 344
Viscous flow, 427
Volmer, M., 366, 439, 459

Waggoner, R. C., 153, 208
Watson, G. M., 427
Wetting, 439, 440
Wicke, E., 384
Wilke, C. R., 430
Wilkes, J. O., 327, 336
Wright, K., 341

Yanovich, L. A., 361

Zoller gas plant, 254, 255, 258